Synthesis and Network Analysis of Substituted Bullvalenes
and
the Total Synthesis of Endiandric Acid J and Beilcyclone A

Ossama Yahiaoui

A thesis by publication submitted to attain the degree of

Doctor of Philosophy

THE UNIVERSITY *of* ADELAIDE

SUB CRUCE LUMEN

May 2020

School of Physical Science

Department of Chemistry

TABLE OF CONTENT

Abstract

This thesis is divided into two topics, 1) the synthesis and analysis of bullvalene and substituted bullvalene, 2) and the synthesis of endiandric acid J and beilcyclone A.

Bullvalene is the epitome of fluxional molecules. This $C_{10}H_{10}$ hydrocarbon undergoes an infinite succession of fast sigmatropic Cope rearrangements and exists as an ensemble of 1, 209, 600 degenerate isomers. Substituents on this core structure will explore all possible non–degenerate isomers. Mono substituted bullvalene for instance exists between 4 isomers and disubstituted bullvalene with unidentical substituents interconverts between 30 isomers. With more substituents, the complexity of the molecular system rapidly escalates.

Chapter 1 presents a comprehensive history of the synthetic chemistry of bullvalene, written in a review format.

In **chapter 2** we demonstrate a new method to access bullvalene, as well as mono– and disubstituted bullvalenes in two–steps. A cobalt catalysed [6+2] cycloaddition reaction between cyclooctatetraene and substituted alkynes followed by a photorearrangement gives the desired products. The isomer distribution of these substituted bullvalenes were elucidated using low temperature NMR spectroscopy. Our collaborator Lukáš F. Pašteka developed a computational toolbox to predict the isomer distribution of substituted bullvalenes and reaction graphs display their interconversion network. Despite the efficiency of this method, intrinsic limitations in alkyne substitution patterns prevent access to trisubstituted bullvalenes.

Chapter 3 continues the narrative of chapter 2, where we overcome the limitation of our method by introducing a trimethylsilyl group to cyclooctatetraene to access trisubstituted bullvalenes. Surprisingly, all trisubstituted bullvalenes share a kinetically metastable major isomer which is in slow exchange with the rest of the network. Using DFT calculations as well as kinetic simulations we gain a deeper insight on the interconversion network of substituted bullvalenes.

In **chapter 4** we expand the dynamic behaviour of bullvalene by introducing one or two elements of stereogenicity into the substituents of disubstituted bullvalenes. This leads to the

creation of a chemical library which is defined by structure. In this chemical library some isomers show mutating helicity on their bullvalene core by a fast Cope rearrangement, while the stereocentre of their substituent is fixed. The coupling of two disubstituted bullvalenes by a stereogenic tether leads to a structure with three mutating stereogenic elements, where the tethers' configuration is mutated by the dynamic ensemble of exchanging isomers of the bullvalenes attached to it.

Chapter 5 is an introduction to the endiandric acid natural product. Here, we explore the previous syntheses of these natural products and showcase alternative strategies to access these structures.

In **chapter 6** we demonstrate the total synthesis of endiandric acid J and beilcyclone A in six and five steps, respectively. The natural products are isolated from the roots of *Beilschmiedia erythrophloia* as racemates. Our strategy is based on an overall anti–vicinal difunctionalisation of COT through an alkylative *anti*–SN_2' addition of COT–oxide, followed by a cascade Claisen rearrangement/ 6π electrocyclization reaction. A Wittig olefination and intramolecular Diels Alder reaction afford the natural products.

Publications

1. O. Yahiaoui, L. F. Pašteka, B. Judeel, T. Fallon, *Angew. Chem, Int. ed.* **2018**, *57*, 2570–2574.

2. O. Yahiaoui, L. F. Pašteka, C. J. Blake, C. G. Newton, T. Fallon, *Org. Lett.* **2019**, *21*, 9574–9578.

Declaration

I certify that this work contains no material which has been accepted for the award of any other degree or diploma in my name , in any university or other tertiary institution and, to the best of my knowledge and belief, contains no material previously published or written by another person, except where due reference has been made in the text. In addition, I certify that no part of this work will, in the future, be used in a submission in my name, for any other degree or diploma in any university or tertiary institution without the prior approval of the University of Adelaide and where applicable, any partner institution responsible for the joint–award of this degree.

I acknowledge that copyright of published works contained within this thesis resides with the copyright holder of those works.

I acknowledge the support I have received for my research through the provision of an Australian Government Research Training Program Scholarship.

Sign   Date: 22.05.2020

Acknowledgements

I would like to thank Dr. Thomas Fallon who was an excellent supervisor during my PhD. His tremendous help, support, and guidance during these three and half years made this journey easier. You were not only my supervisor but also a close friend with whom I have shared good moments and great achievements. Your dedication for chemistry has motivated me to work harder and overcome problems.

Thank you Harshal for joining our group in New Zealand and keeping me company in that empty laboratory. Your corrections helped me tremendously and I still owe you. The change of countries led us become friends rather than work colleagues. I am proud of your development during these two years, you became a talented chemist with a lot of passion for chemistry.

I would like to thank Dr. Jonathan George for his immense support since the day we arrived in Adelaide. All the chemicals that we took from your lab helped me enormously. You are a generous person and will become soon one of the greatest chemists in Australia. Laura (TD), I enjoyed your company and having coffee with you. Aaron (SD), you were really helpful since the first day I arrived in Adelaide.

Rouven, I shared many happy meals with you, and you gave me advice when life brought me down to my knees. Jenny, for being a such good friend and for your delicious food.

My thanks go also to Dr. Chris for his difficult questions during group meetings and his extraordinary help to complete my second project.

Thank you Dr. Lukáš for your contribution and your hard work. I would also like to thank my co–supervisor Pro. Pyke.

This thesis is dedicated to my family

Abbreviation

%	percentage
Δ	heat
ºC	degree/s Celsius
aq.	Aqueous
BDT	bicyclo[4.2.2]deca–2,4,7,9– tetraene
bn	benzyl
br	broad
ca	circa
cm^{-1}	wave number
COSY	correlated spectroscopy
COT	Cyclooctatetraene
COT–Br	Cyclooctatetraene bromide
COT–Me	Cyclooctatetraene methyl
COT–TMS	cyclooctatetraene trimethylsislyl
δ	chemical shift
DEBT	distortionless enhancement by polarisation transfer
CIP	Cahn–Ingold–Prelog
D_2O	deuterium oxide
DCE	1,2–dichloroethane
DFT	Density functional theory
DMSO	dimethyl sulfoxide
Dppe	1,2–bis(diphenylphosphanyl)ethane
Equiv.	equivalent
h	hour
^{1}H	proton
HMBC	heteronuclear multiple bond
HRMS	high–resolution mass spectroscopy
HSQC	heteronuclear single quantum coherence
Hz	hertz
IR	infrared
IUPAC	international union of pure and applied chemistry '

J	coupling constant
J	joule(s)
M	molar or molecular ion
M	multiplet
Me	methyl
MHz	megahertz
Mol	mole(s)
m.p.	melting point
m/z	mass to charge ratio
IMDA	intramolecular Diels Alder
M	minus
n–Buli	*n*–butyllithium
NMR	nuclear magnetic resonance
P	positive
Ph	phenyl
q	quartet
R_f	retention factor
rt	Room temperature
t	tertiary
t	triplet
TBS	*tert*–butyldimethylsilyl
TBSCl	*tert*–butyldimethylsilyl chloride
TCNE	tetracyanoethylene
TFE	2,2,2–trifluroethanol
THF	tetrahydrofuran
TMS	trimethylsilyl
TS	transition state
UV	ultraviolet
VT–NMR	Variable Temperature nuclear magnetic resonance

Chapter 1

1. Introduction

This chapter details a comprehensive review of bullvalene chemistry. The history of this area dates back to 1963, with the most recent comprehensive review appearing in 1967 by Schröder.[1] In its early decades, bullvalene's chemistry was mostly investigated by German scientists. Most of their work was published in the German language, which has made this body of work more unavailable to the community. Therefore, we sumarised these works in this review, increasing accessibility for future purposes.

Recent reviews in bullvalene chemistry were published early last year by Echavarren[2] and McGonigal.[3] Echavarren reviewed the synthesis of bullvalene and substituted bullvalenes, while McGonigal discussed the applications of shapeshifting molecules. We sought to write this review by including all the scientific papers that were not mentioned in both reviews and provide a comprehensive synthetic summary.

The review includes following chapters: (i) the synthesis of bullvalene, substituted bullvalene, and azabullvalene (i) reactions of bullvalene such as 1,2– and 1,6–, addition, complexation with metals, and reduction etc. (iii) applications of substituted bullvalene (iv) isomer distributions of all synthesised substituted bullvalene tabularised. The review evokes all forgotten work from various scientists in this field and gives better insight about bullvalene chemistry.

Statement of Authorship

Title of Paper	A Brief History of Bullvalene
Publication Status	☐ Published ☐ Accepted for Publication ☐ Submitted for Publication ☑ Unpublished and Unsubmitted work written in manuscript style
Publication Details	O. Yahiaoui, H. D. Patel, and T. Fallon

Principal Author

Name of Principal Author (Candidate)	Oussama Yahiaoui
Contribution to the Paper	Wrote the review.
Overall percentage (%)	90%
Certification:	This paper reports on original research I conducted during the period of my Higher Degree by Research candidature and is not subject to any obligations or contractual agreements with a third party that would constrain its inclusion in this thesis. I am the primary author of this paper.
Signature	Date 19-05-20

Co-Author Contributions

By signing the Statement of Authorship, each author certifies that:

i.   the candidate's stated contribution to the publication is accurate (as detailed above);

ii.   permission is granted for the candidate in include the publication in the thesis; and

iii.   the sum of all co-author contributions is equal to 100% less the candidate's stated contribution.

Name of Co-Author	Harshal D. Patel
Contribution to the Paper	Revised the manuscript and wrote the chapter about the application of bullvalene.
Signature	Date 19 May 2020

Name of Co-Author	Thomas Fallon
Contribution to the Paper	Corresponding author, revised manuscript.
Signature	Date 19-05-20

1.1. Introduction

Shapeshifting molecules are dynamic frameworks that interconvert between a number of constitutional isomers through low–energy rearrangements.[2,4] This process occurs via valence tautomerization, where single or double bonds form and break without migration of atoms or groups. Through a fast Cope rearrangement, bullvalene it exists within an ensemble of 1, 209, 600 degenerate isomers (Figure 1.1a). This hydrocarbon has a C_3 symmetric axis and can be viewed as a 3,4–homotropilidene **2** moiety which is connected on both vertices by an ethene unit (Figure 1.2b). 3,4–homotropilidene exhibits fluxional properties and exists between two degenerate isomers through a Cope rearrangement.
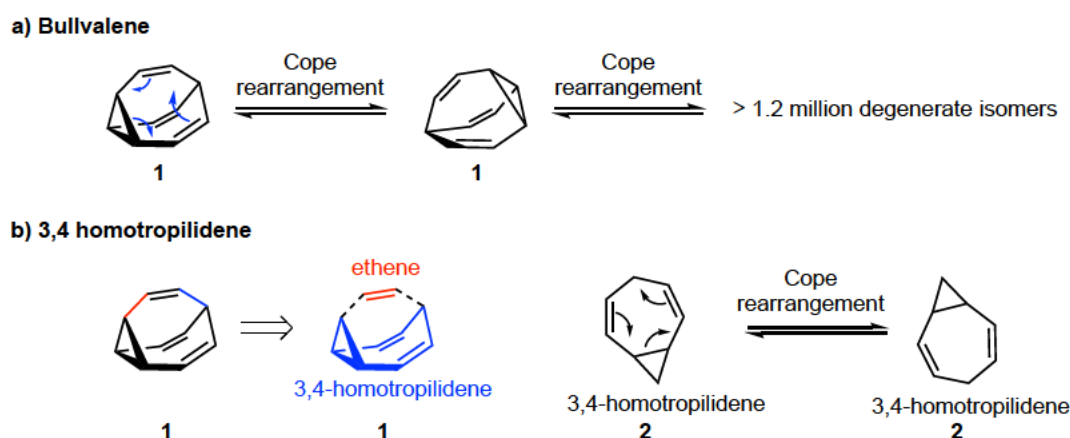
Figure 1.1: a) Fluxional isomerism of bullvalene, b) fluxional isomerism of 3,4–homotropilidene.

Other fluxional caged molecules share the same 3,4–homotropilidene unit; they include the barbaryl cation **3**,[5,6] barbaryl radical **4**,[7] barbaralene **5**,[8] bullvalone **6**,[9] barbaralone **7**[9], and semibullvalene **8**.[10] The number of possible isomers within these molecules is shown in Figure 1.2.

1	3	4	5	6	7	8
1 209 400	181 400	181 400	2	2	2	2
bullvalene	barbaryl cation	barbaryl cation	barbaralene	bullvalone	barbaralone	semibullvalene
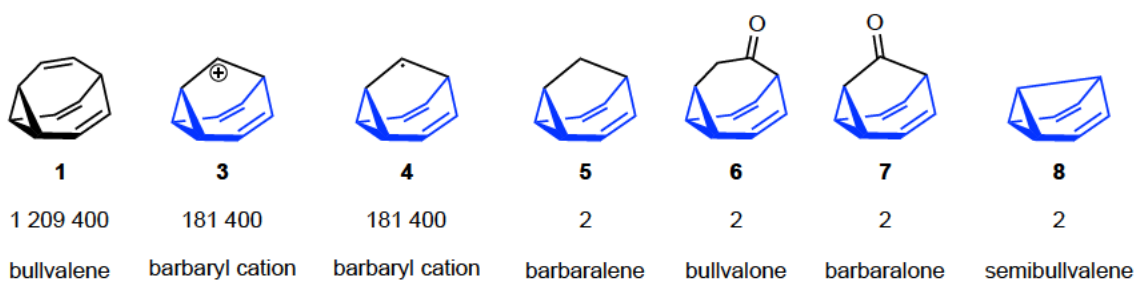
Figure 1.2: Fluxional molecules containing a 3,4–homotropilidine moiety.

In this review we will predominantly focus on bullvalene and will not discuss other fluxional molecules.

The dynamic behaviour of bullvalene is reflected in its ^{1}H NMR spectra at different temperatures (Figure 1.3). At room temperature all carbon and hydrogen atoms are equivalent on the NMR timescale, which is represented by a broad peak. At 100 ℃, a sharp singlet peak is obtained from total degeneracy of all the protons. By cooling the sample down to –50 ℃, the Cope rearrangement becomes very slow and we obtain well resolved NMR spectra. Only at this temperature can we reveal the structure of the molecule.
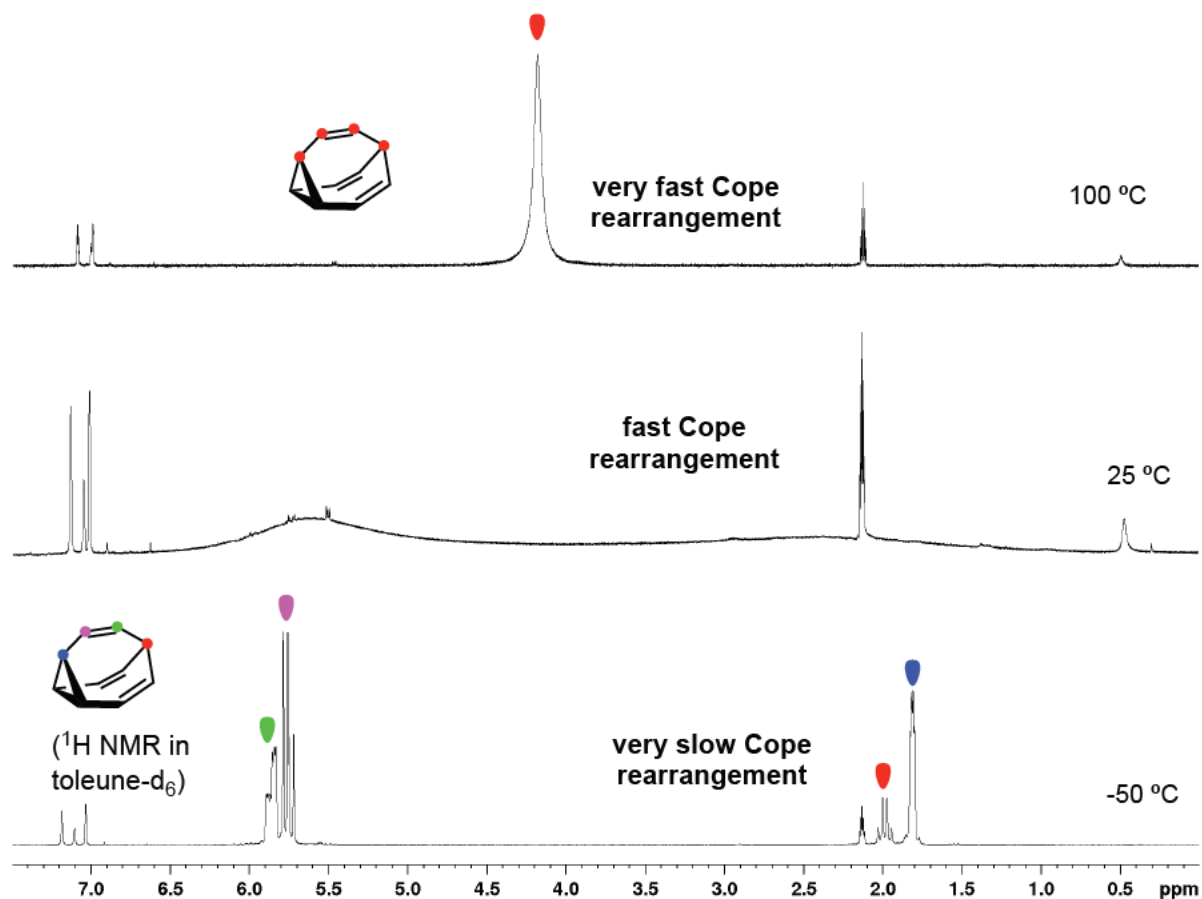
Figure 1.3: ^{1}H NMR spectra of bullvalene at 100 °C, 25 °C, and −50 °C.

Substituents on this core structure will explore all possible non–degenerate isomers. Mono substituted bullvalene for instance exists between four possible non–degenerate isomers. Disubstituted bullvalene interconverts either between 30 isomers (unidentical substituents) or 15 isomers (identical substituents). With further substitution, the number of possible isomers of bullvalene rises exponentially.

Doering theorized the existence of bullvalene in 1963 and in the same year Schröder synthesised the molecule in two steps.[4,11] The era of bullvalene began in that year, and since then, the organic synthetic community was intrigued by this dynamic molecule. We will begin our story by introducing all the syntheses of bullvalene chronologically. Afterwards we will demonstrate the reactivity of bullvalene, followed by the synthesis of substituted bullvalenes, and at last, we will illustrate applications of bullvalene.

1.2. Synthesis of bullvalene

In 1963, the same year of its conception as a hypothetical molecule,[12] Schröder fortuitously synthesised bullvalene in two steps. The thermal dimerisation of cyclooctatetraene (COT) **9** gave various products and among these, a COT dimer **10** in 10% yield.[13] Photolysis of **10** in ether delivered bullvalene **1** in 75% yield. Despite an overall yield of 5.6%, Schröder's methodology remained the highest yielding and most scalable for the next half–century.[14] Other research groups continued to investigate synthetic routes to bullvalene; the work of these chemists inspired methods utilised in the 21st century.
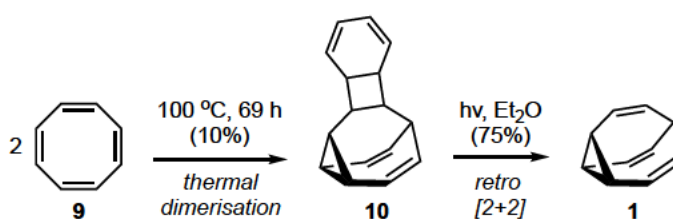
Figure 1.4: Synthesis of bullvalene by Schröder.

Following the synthesis of bullvalene, numerous research groups began investigations into the thermal and photochemical rearrangements of bullvalene and other related $C_{10}H_{10}$ hydrocarbons. 1967: Jones and Scott were the first to synthesise bicyclo[4.2.2]deca–2,4,7,9– tetraene (BDT) **12** and demonstrate its clean photorearrangement to bullvalene.[15] Cyclooctatetraene was transformed in five steps to tosyl hydrazone derived sodium salt **11**.[16] Pyrolysis of the sodium salt **11** delivered **12** in 38% yield[17] and the photorearrangement of **12** using UV light gave bullvalene in 64%.

1968: Nakatsuka and co–worker replicated the pyrolysis of **11**, as conducted by Jones and Scott (Figure 1.5), and were able to isolate pyrazoline **13** amongst other products.[18] They showed that **13** can be converted to bullvalene **1** and BDT **12** through pyrolysis or photolysis. BDT **12** is considered to be an intermediate during the photolysis of **13** to deliver bullvalene.

1966: Doering and co–worker attempted to synthesise bullvalene from the thermal rearrangement of Nenitzescu's hydrocarbon **14**, but obtained 9,10–dihydronaphtalene **15** amongst other compounds instead.[19] UV irradiation of **15** delivered bullvalene **1**, naphthalene,

and two other unidentified compounds. One these was BDT 12, isolated in 26% yield.[20] Doering also showed the photorearrangement of **12** cleanly delivered bullvalene, in 66%.
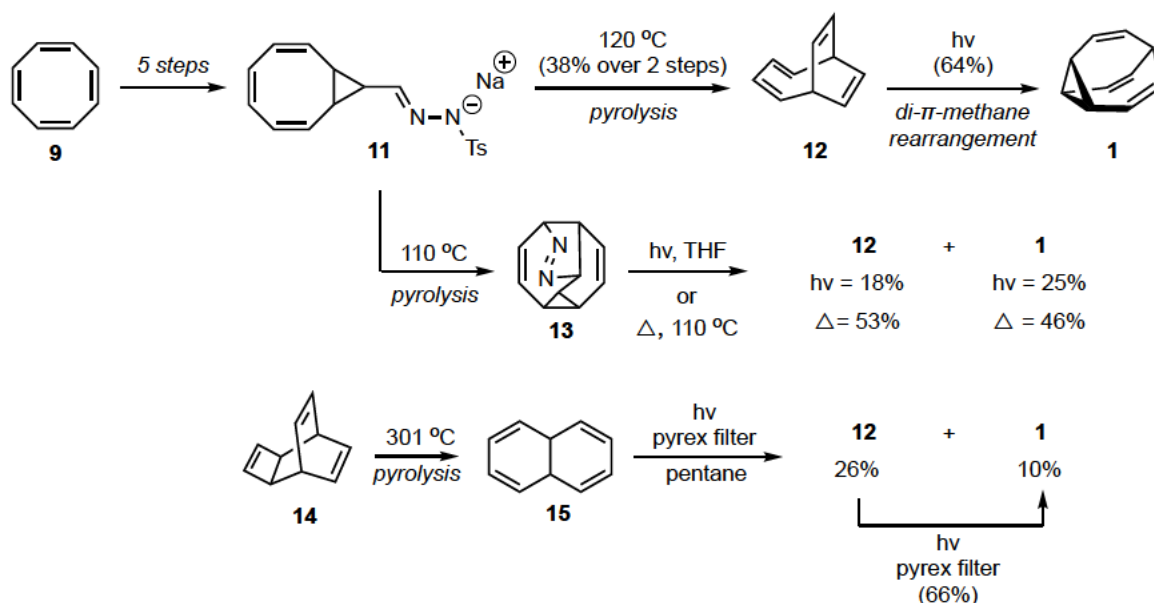
Figure 1.5: Methods to access BDT **12** and bullvalene 1.

1967: Doering and co–worker presented a stepwise synthesis of bullvalene,[21] thus providing alternate proof of its structure (Figure 1.6). Benzene **16** was turned into diazomethyl ketone **17** in four steps. A copper catalysed intramolecular cyclopropanation of **17** delivered barbaralone **7**. One carbon homologation of **7** with diazomethane gave bullvalone **6**. Reduction, acetylation, and pyrolysis from bullvalone **6** delivered bullvalene.
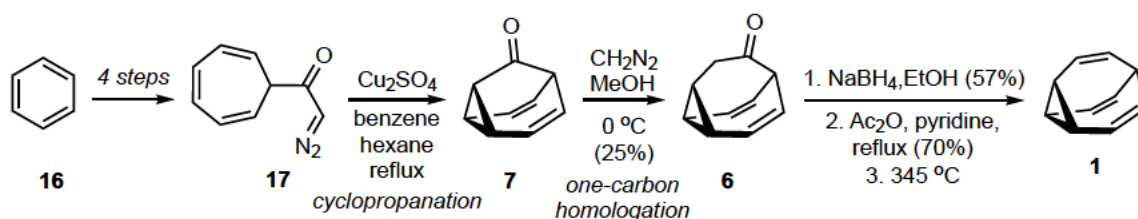
Figure 1.6: Synthesis of bullvalene by Doering.

1972: Serratosa carried out another synthesis of bullvalene but with a new approach, relying on the trimerization of α–diazoketones **18** to forge the cyclopropane ring **20** (Figure 1.7).[22] Attempting to form all three bonds of the cyclopropane ring in a single step represents a stark contrast to other bullvalene syntheses such as those that rely on single carbene generation to

form two bonds of a cyclopropane ring. Tri(3–diazo–2–oxopropyl)methane **19** was synthesised in four steps from diethyl glutarate **18**. Unfortunately, the intramolecular trimerization of **19**, catalysed by a copper chelate, delivered the triketone **20** in very poor yield (4%). The low yield of the reaction is expected, due to its inherent difficulty. Formation of tosylhydrazone **21** followed by Shapiro reaction with methyl lithium delivered bullvalene.
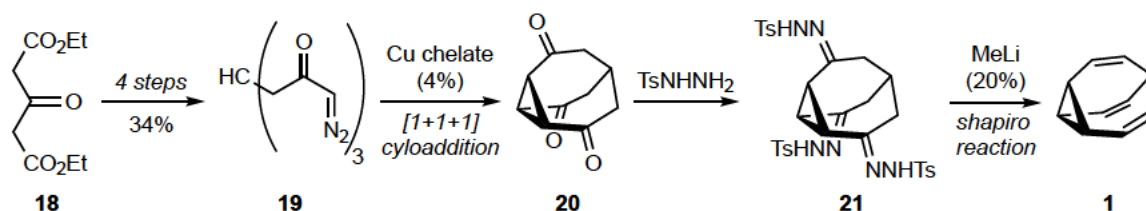
Figure 1.7: Synthesis of bullvalene by Serratosa.

1974: Löffler showed that the photochemical reaction of butadiene **22** with benzene **16** gives rise to bicyclodecatriene **23** (Figure 1.8). Dibromination of this molecule with NBS followed by reduction with zinc gave BDT **12** along with small amounts of bullvalene.[23] **24** was not isolated but is thought to have given rise to bullvalene. Löffler noted that zinc bromide produced during the reduction may also be converting bullvalene back to BDT **12**[24] and so, the amount of **25** produced could not be established.
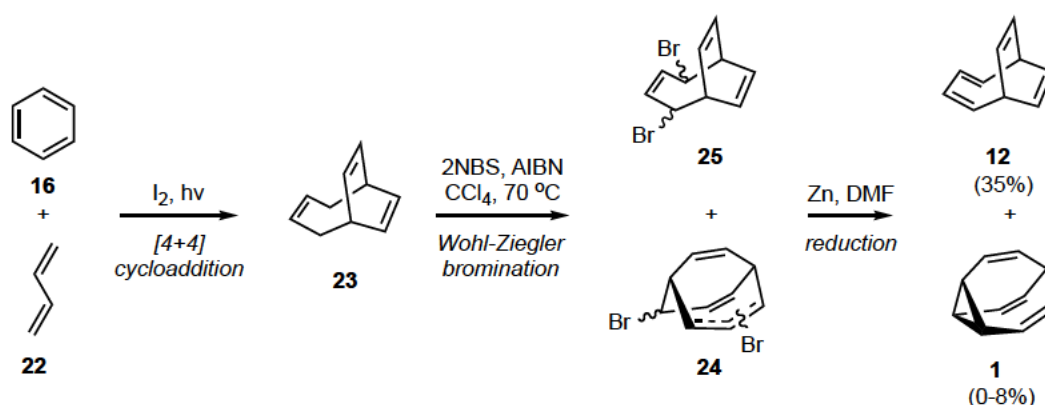
Figure 1.8: Synthesis of bullvalene by Löffler.

1977: Serratosa's group created another route to bullvalene intercepting Doering's work (Figure 1.6).[25] After synthesising bullvalone **6** in a manner analogous to Doering (Figure 1.9), formation of the tosylhydrazone from bullvalone **6** under acidic conditions gave a surprising

rearrangement to tosylhydrazone **26**. Shapiro reaction of **26** gives BDT **12**, which undergoes facile photochemical conversion to bullvalene.
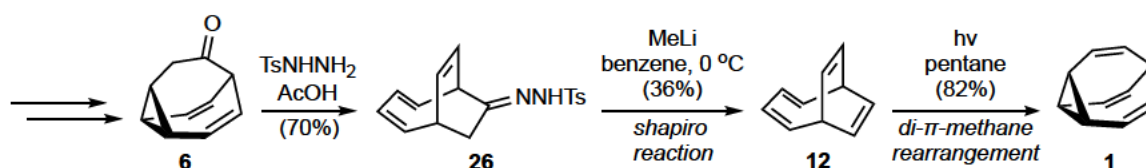
Figure 1.9: Synthesis of bullvalene by Serratosa.

2016: Echavarren's synthesis of bullvalene represents the first modern approach to the parent molecule. The approach imitates the cyclopropanation strategies of Doering (Figure 5) and Serratosa (Figure 6). Echavarren's synthesis[26] begins with the addition of ethynylmagnesium bromide **28** to tropylium tetrafluoroborate **27** to give ethynylcycloheptatriene **29**. The next key step, a Au(I) catalysed oxidative cyclisation of ethynylcycloheptatriene **29**, gave barbaralone **7**. One carbon homologation of barbaralone **6** gave bullvalone **6**, which was then converted into the corresponding enol triflate **30**. The crude of this reaction was used immediately and reduced under palladium catalysis to give bullvalene in a total of 5 steps with an overall yield of 11%.
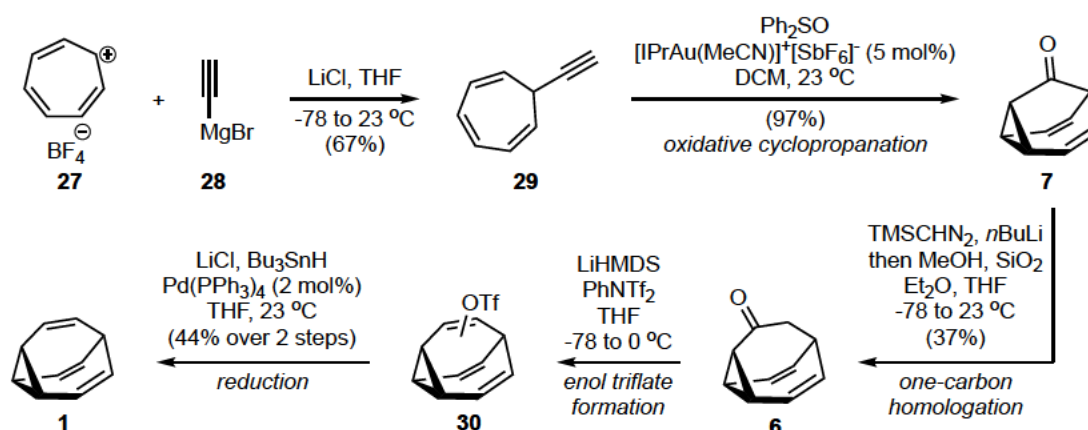
Figure 1.10: Echavarren's bullvalene synthesis.

2018: Fallon's bullvalene route[27] recognises the value of the photochemical conversion of BDT **12** to bullvalene, as first reported by Jones (Figure 1.5). They noted that Buono had reported the [6+2] cycloaddition of COT **9** with substituted alkynes[28] **31** to give substituted BDTs **12** and adapted it to synthesise BDT **12**. A cobalt catalysed [6+2] cycloaddition of cyclooctatetraene **9** and acetylene gas gives BDT **12**. This undergoes a photochemical di–π–

methane rearrangement to give bullvalene. With this two–step route, Fallon was able to synthesise bullvalene with an overall yield of 60%, moreover, they demonstrated the scalability of both steps by synthesising 8g of bullvalene in a single run.
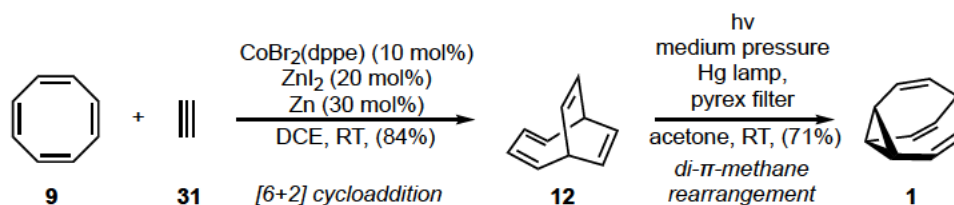
Figure 1.11: Fallon synthesis of bullvalene.

1.3. Reactions of bullvalene

Bullvalene displays a range of unique reactivity which may be attributed to its structure: it is a caged tri–olefinic hydrocarbon containing vinyl–cyclopropane motifs as well as 1,4–diene motifs. The molecule undergoes an interesting range of thermal and photochemical rearrangements. It is able to complex with various metals, and in certain circumstances, these metals induce structural rearrangements. Bullvalene olefins can be oxidised, reduced, and participate in cycloaddition reactions, leading to a wide range of synthesis possibilities. In addition, bullvalene also displays 1,4–addition reactivity with electrophiles across the vinyl cyclopropane fragment.

In this section we will show that the BDT system is the common product when bullvalene is in the presence of metals such as $PdCl_2$, $HgBr_2$, or chromium after heating. The complexation of bullvalene with a metal is only observed with tungsten, chromium, molybdenum, and silver. This feature shows that bullvalene can be used as a ligand if needed. The reaction of bullvalene with $Fe(CO)_5$, and $Fe_2(CO)_9$ gave the most complicated products which should be reinvestigated.

1.3.1 Thermal– and Photo–rearrangements of bullvalene

Jones, Scott, Doering, and Schröder studied the photo– and thermal– rearrangements of bullvalene.[11,19,29,30] Bullvalene is thermally stable and decomposes at 400 ºC to 1,9–dihydronaphtalene **15** (Figure 1.12). Its photorearrangement gives lumibullvalene **32**, BDT **12**,

Nenitzescu's hydrocarbons **14**, and **33**. The $C_{10}H_{10}$ hydrocarbons (**1, 12, 14, 15, 32** and **33**) can interconvert through thermal or irradiation reactions.
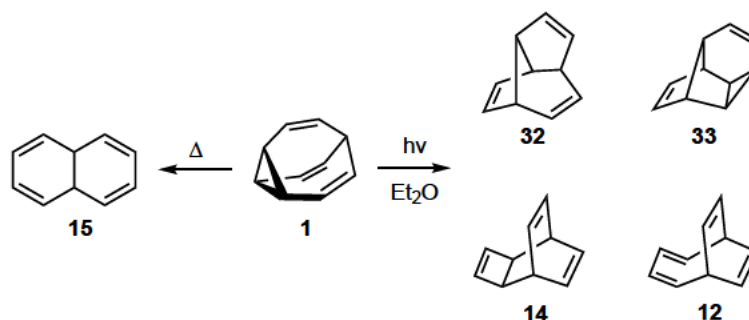
Figure 1.12: Thermal– and photo–rearrangement of bullvalene by Jones and Scott.

1.3.2. Complexation of bullvalene with metals

The introduction of $AgBF_4$ to bullvalene generates a silver bullvalene complex **34** in which, following recrystallisation, silver can be surrounded by one,[31] two,[32] or three[33] bullvalene units (Figure 1.13). NMR experiments at different temperatures (50 – 80 °C) in a D_2O solution containing $AgNO_3$ and bullvalene in a 1:3 ratio respectively showed that the Cope rearrangement is decreased by a factor of 10.[32]
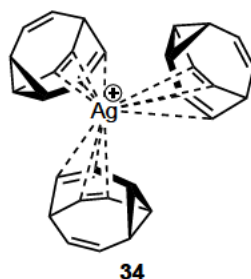
Figure 1.13: X–ray structure of bullvalene and silver.

Aumann prepared stable bullvalene–$M(CO)_4$ complexes[34] by the reaction of bullvalene with $(MeCN)_3M(CO)_3$ complexes in dioxane; the metals used were chromium, molybdenum, and tungsten (Figure 1.14). NMR studies indicated the absence of a degenerate Cope rearrangement. Upon heating, **35b** and **35c** gave undetermined paramagnetic products whereas **35a** gave complexed BDT **36a** at above approximately 80 °C. Decomplexation of chromium from BDT **36a** occurred in the presence of ammonia to give BDT **12**.
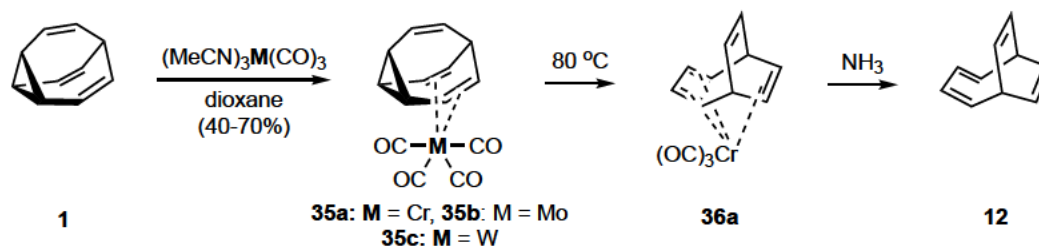
Figure 1.14: Complexation of bullvalene with Cr, Mo, and W. Rearrangement of chromium bullvalene complex to the tetraene.

Vedjes demonstrated that in the presence Pd(C$_6$H$_5$CN)$_2$Cl$_2$, bullvalene rearranges to form BDT palladium complex **37** (detailed mechanism).[35] Palladium was decomplexed from the BDT using pyridine (Figure 1.15).
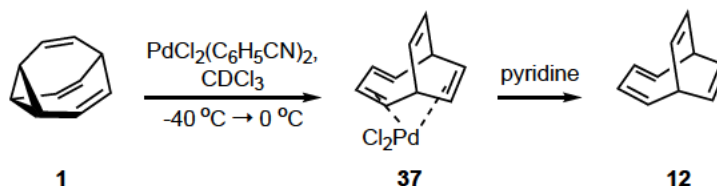
Figure 1.15: Palladium catalysed rearrangement of bullvalene to BDT.

Auman studied the reaction between bullvalene and Fe(CO)$_5$ or Fe$_2$(CO)$_9$.[36–38] Irradiation of bullvalene with Fe(CO)$_5$ in benzene forms **38** and **39** in moderate yield (Figure 1.16). In both complexes iron forms a π–allyl complex and a sigma bond to a carbonyl **38** or a carbinol **39**.
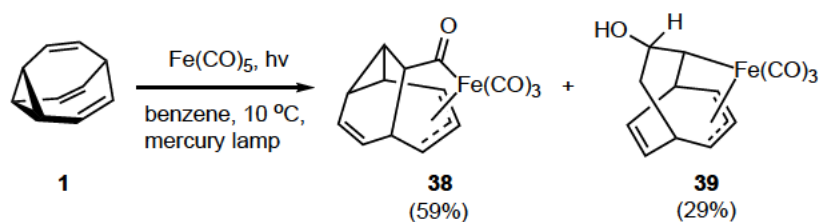
Figure 1.16: Reaction of Fe(CO)$_5$ and bullvalene.

The reaction of bullvalene and Fe$_2$(CO)$_9$ was first done by Schrauzer who studied the thermal rearrangement of an iron bullvalene complex and suggested that the formation of 1,9–dihydronaphtalene **15** occurs through intermediate **43**. [39,40] Auman repeated the experiment and isolated three additional diiron complexes (**40–43**) (Figure 1.17). **40** and **43** are generated

from **38** through the addition of another $Fe(CO)_3$ into the cyclopropyl unit or to the vinyl group. **41** and **42** are products from an intermediate that forms **39**.
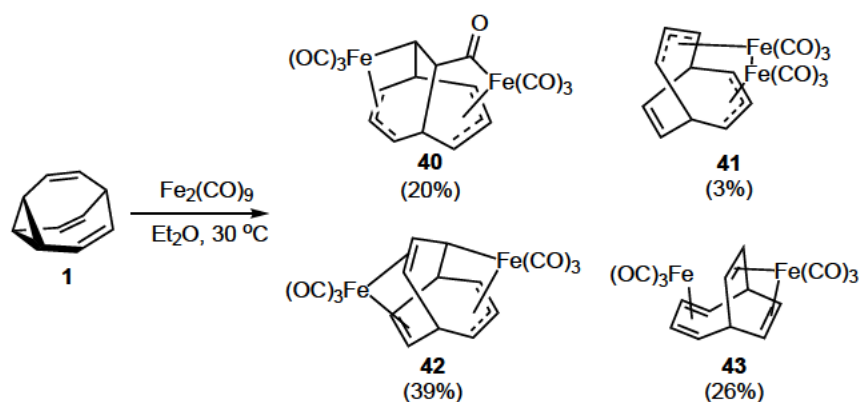
Figure 1.17: Reaction of bullvalene and $Fe_2(CO)_9$

Schröder treated bullvalene **1** with $HgBr_2$ in ether and obtained the rearrangement product BDT **12** in high yield (98%).[24] The same reaction was performed with different heavy–metal salts (HgX_2, X = Br, Cl , I), $ZnBr_2$ (in CH_3OH, 36 h at 20 °C, 34%), and $SbBr_3$ (in CS_2, 14 h at 0 °C, 12%). This rearrangement was also observed, when Vedjes reacted bullvalene with palladium (Figure 1.15).[35] Monosubtituted bullvalenes **44** (where R = F, Br, or COOMe) reacted with $HgBr_2$ to deliver the mono substituted tetraene (**12a–d**) (Figure 1.18). The addition of mercury(II)acetate to bullvalene **1** in methanol leads to the formation of a 1,6–addition product **45**.[41] The formation of the product indicates that the bullvalene does not rearrange to a BDT **12** system like HgX_2.
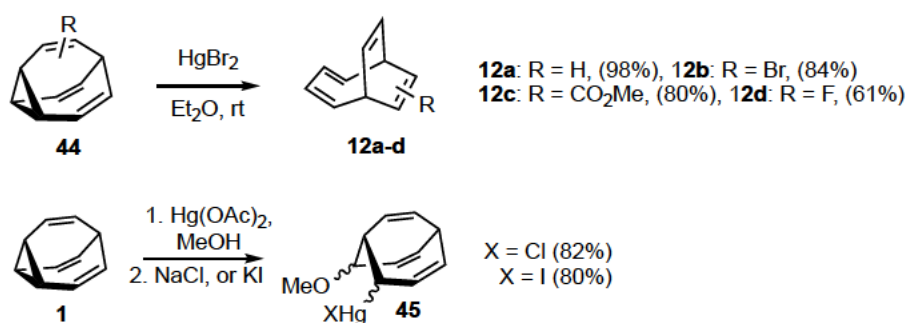
Figure 1.18: Reaction of mono–and unsubtituted bullvalene with $HgBr_2$ and the 1,6–addition of mercury(II)acetate to bullvalene.

1.3.3. Oxidation of bullvalene

The reaction of bullvalene and Pb(OAc)$_4$ gives bicyclo[4.3.1]decatriene diacetate **46** (Figure 1.19).[42] Schröder suggested that bullvalene first undergoes a rearrangement to the BDT **12**, then oxidation, generating bishomotropylium–ion **47**; then and a second nucleophilic attack occurs to give the product **46**.
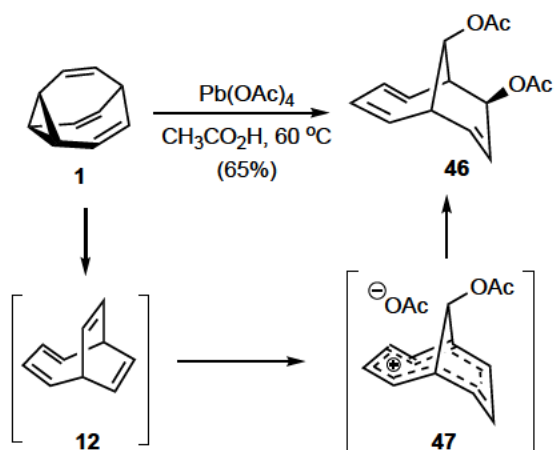
Figure 1.19: Reaction of bullvalene and Pb(OAc)$_4$.

The ozonolyis of bullvalene was done by Schröder in the 60s. The product can be used as a precursor for the synthesis of hetero peristylanes **49** (Figure 1.20a).[11,43,44] These building blocks are endowed with two chemically distinct surfaces composed of a hydrophobic base and a hydrophilic rim and are expected to exhibit many interesting properties such as selectivity for metal ions.[45,46] The epoxidation of bullvalene with oxone delivered a racemic tris–epoxide **rac–50** and the structure was revealed by X–ray crystallography (Figure 1.20b).[47] Treatment of racemic tris–epoxide **rac–50** with BF$_3$.Et$_2$O or MgSO$_4$ resulted in the formation of racemic tris ether **rac–51**. Schröder also performed the OsO$_4$ mediated dihydroxylation of bullvalene to give the 1,2–diol **52** (Figure 1.20c).[14]

a)

b)

c)
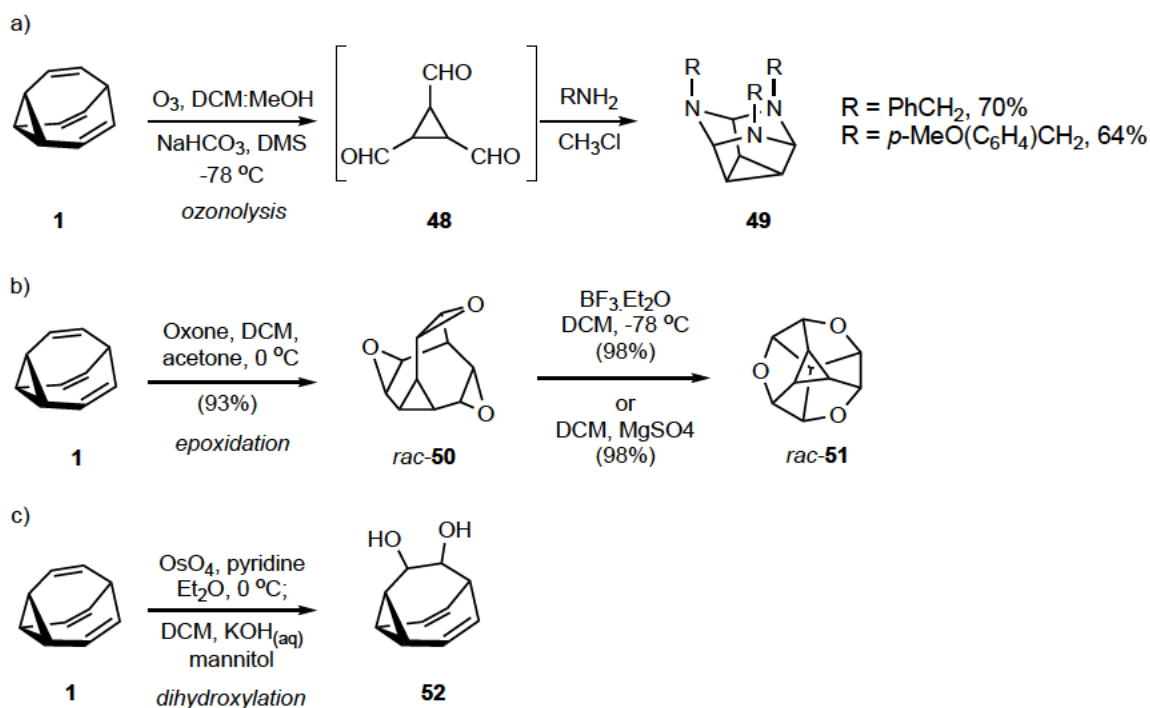
Figure 1.20: Oxidation of bullvalene: (a) ozonolysis leading to the formation of hetero peristylanes, (b) epoxidation and formation of tris–ether, and (c) dihydroxylation of bullvalene.

1.3.4. Reduction of bullvalene

The reduction of bullvalene was done early in 1964 by Schröder (Figure 1.21). Bullvalene **1** can be reduced using hydrazine with a copper catalyst (**53**), sodium and liquid ammonia in methanol (**54**), or hydrogenation with Pd/C (**55**) (Figure 1.21).[11] The formation of an anionic species of bullvalene can be observed by treating bullvalene in THF with a sodium–potassium alloy.[48,49] Single electron transfer occurs from a dianion **56**, which can be observed in the ^{1}H NMR spectra. The proof of the existence of the molecule is assured by its oxidation with iodine to regenerate bullvalene (92%) and the addition of an acid to form isomeric bicyclic trienes **57** and **58**.
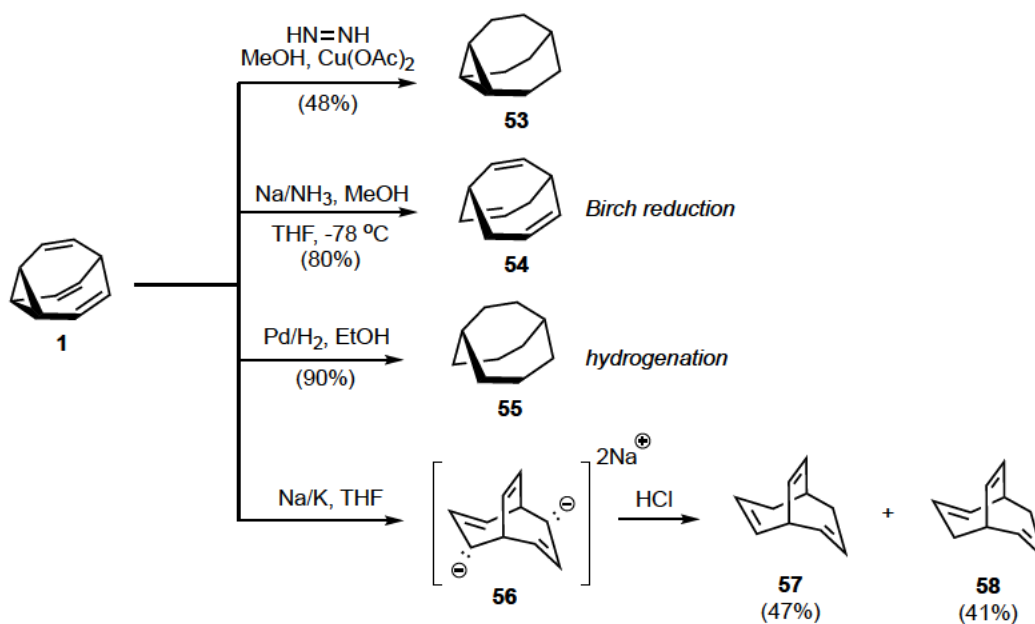
Figure 1.21: Reduction of bullvalene.

1.3.5 Cycloaddition of bullvalene

Paquette observed a competitive 1,2– and 1,6–electrophilic cycloaddition to bullvalene using chlorosulfonyl isocyanate (CSI) (Figure 1.22).[50] The 1,2 cycloaddition resulted in the formation of a ß–lactam **61**–**62**, which exists between two fluxional isomers containing the homotropilidene skeleton. The 1,6–addition led to the formation of a lactam **63** or product **60**.
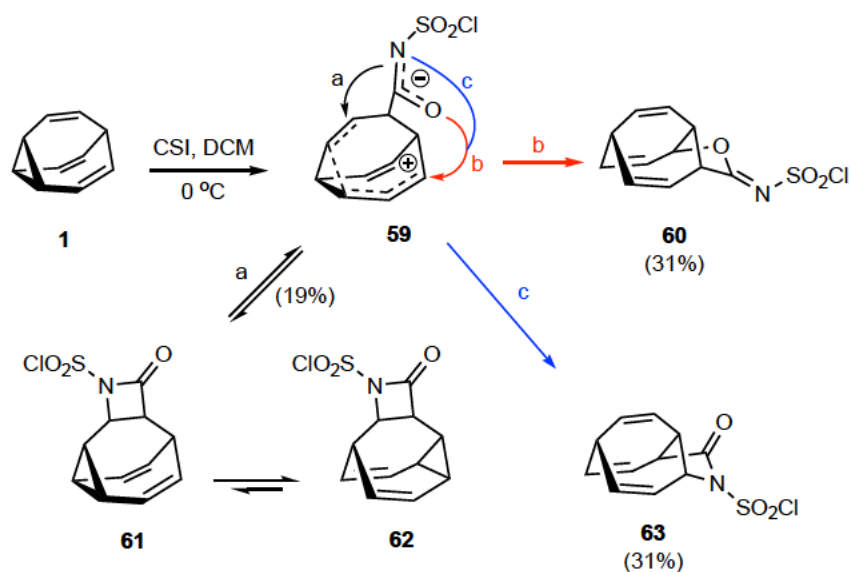
Figure 1.22: Competitive 1,2– and 1,6–cycloaddition of CSI with bullvalene.

Erden showed the reaction of bullvalene and trichloroacetyl chloride **64** leads to the formation of a 1,2–cycloaddition product **65**.[51] Prolonged exposure to silica gel or zinc chloride results in a rearrangement to generate the 1,6 cycloaddition product **66**. In three steps **66** can be converted to the hydrocabon **67**.[52,53]
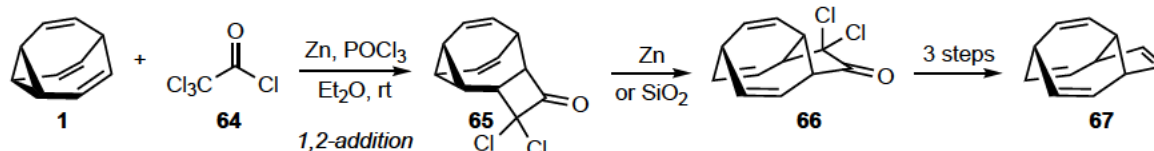
Figure 1.23: 1,2–cycloaddition of dichloroketene with bullvalene.

Gandolfi performed 1,3–dipolar cycloadditions to bullvalene using various nitrile oxides as dipoles (Figure 1.24). The formed products are isoxazole **67** and oxazonine **68–69**.[54] The isoxazole **68–69** exists between two isomers, due to the presence of the homotropilidene skeleton.

XX: R = Me, (55%)
XX: R = *t*-Bu, (53%)
XX: R = Ph, (83%)
XX: R = *p*-NO$_2$(C$_6$H$_5$), (95%)
XX: R = *p*-MeO(C$_6$H$_5$), (89%)

XX: R = 2,6-Cl$_2$(C$_6$H$_3$), (78%)
XX: R = 2,4,6-Me$_3$(C$_6$H$_2$), (82%)
XX: R = 2,4,6-(MeO)$_3$(C$_6$H$_2$), (84%)
XX: R = 2,4,6-Me$_3$-3,5-Cl$_2$(C$_6$), (90%)
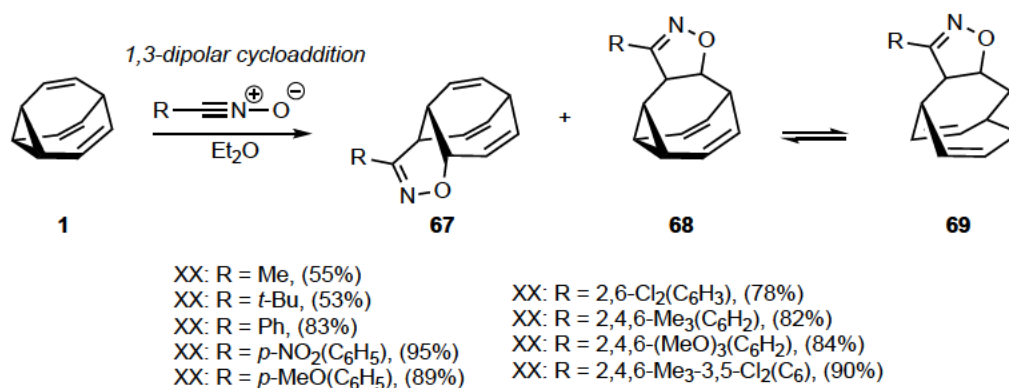
Figure 1.24: 1,3–dipole cycloaddition of bullvalene with nitrile oxide.

Schröder could not identify the products from the cycloaddition reaction between bullvalene and tetracyanoethylene (TCNE).[55,56] Gandolfi and co–worker repeated the reaction and isolated three products **70–72** (Figure 1.25).**70** is formed through a homo Diels–Alder reaction, **72** is obtained through a bishomotropylium ion intermediate **47**, [42] and **71** likely through a rearrangement.
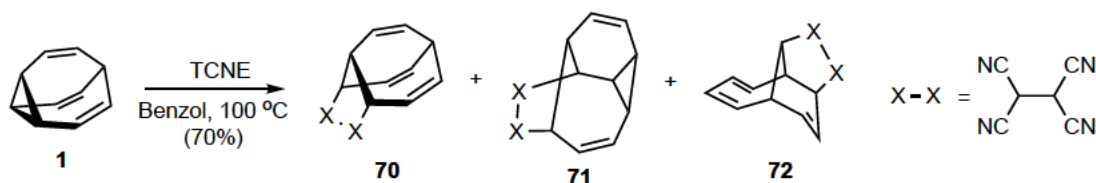
Figure 1.25: Cycloaddition of bullvalene and TCNE.

Cyclopropanations of bullvalene using dichlorocarbene or diazomethane are not chemoselective. Mono–, di–, and– tri addition products were obtained by De Meijere and Okamura using dichlorocarbene **73a–d** or diiodomethane **74a–d**.[11,57,58]
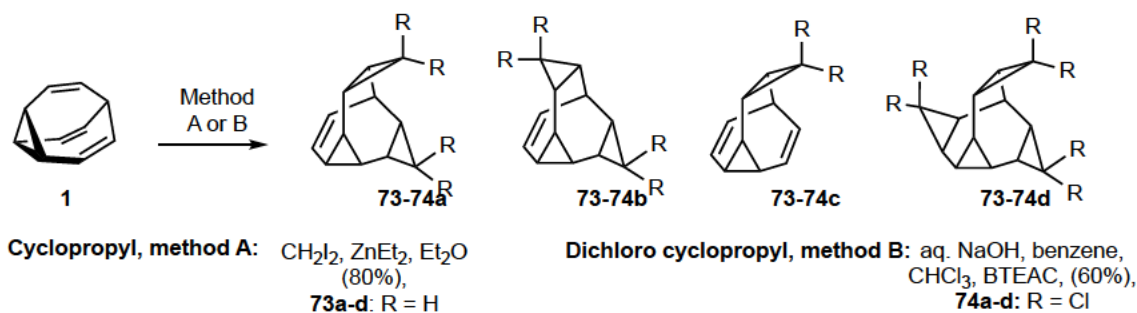
Figure 1.26: Cyclopropanation of bullvalene with dichlorocarbene or diiodomethane.

1.3.6. 1,4–addition

Bromo– **77** and chlorobullvalene **78**, are synthesised by the addition of bromine or thionyl chloride to bullvalene at the 1,4–position of the vinyl cyclopropyl group (Figure 1.27).[59,60] Schröder also showed that methanol under acidic conditions also adds in a 1,4 fashion, deuterium labelling studies aided the understanding of this addition.[61] The first halogen is added to the vinyl group generating a carbocation **74**, where the empty p–orbital of the cation is parallel to the carbon **a** and **b**. The second attack occurs along a path to deliver the *cis* product **75**, which is more stable than the trans product **76**.[61] A transannular 1,4–elimination of HBr with potassium *tert*–butoxide generates the bromo– **77** or bromo–bullvalene **78**. Bromo–bullvalene 77 plays a central role in the synthesis of substituted bullvalene.
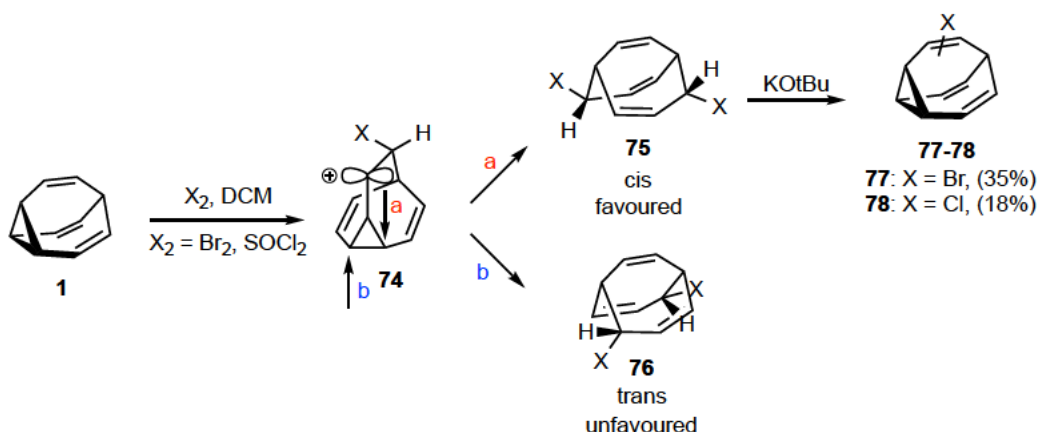
Figure 1.27: Synthesis of bromo– and chloro– bullvalene.

1.4. Synthesis of substituted bullvalenes – Molecules derived from bullvalene

Among all the researchers who were interested in the synthesis of substituted bullvalenes, Schröder did a tremendous volume of work using bromo–substituents **77**, **79**, **80** to perform functional group transformations to access other substitution patterns.[59,60,62,63] Sequential bromination elimination sequences, to install bromo–substituents, allowed access to higher orders of substitution onto the bullvalene core (Figure 1.28). Paquette was also active in this field and did much work concerning substituted bullvalenes and azabullvalenes.[64]
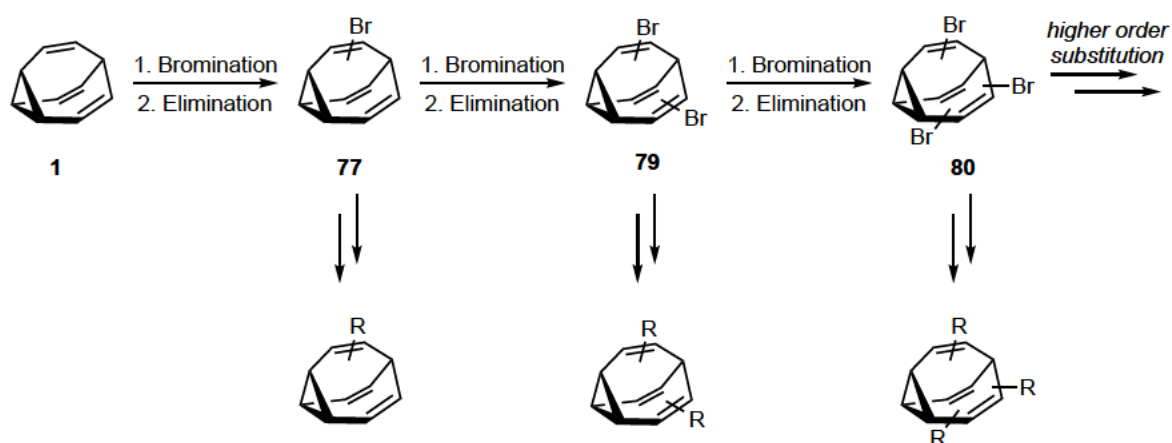
Figure 1.28: Strategy to of accessing substituted bullvalene by Schröder.

1.4.1. Monosubstituted

Grignard bullvalene **81** is generated from the reaction of bromo–bullvalene **77** and magnesium (Figure 1.29). The addition of dry ice, iodine, or bromo–bullvalene **77** with cobalt chloride to (Grignard) **81** delivered carboxylic acid–**82** iodo– **83** and bi–bullvalene **84,** respectively.[63] Iodo–bullvalene **83** can be converted to fluoro–bullvalene **85** by halogen exchange using silver fluoride.[65] The esterification of **82** using diazomethane formed methyl ester **86**.[63] Alkoxy– bullvalenes **87** are generated from the reaction between bromo–bullvalene **77** and an alkoxide via dehydrobullvalene as the intermediate.[60] Phenyl bullvalene **88** was obtained by reaction of bromo–bullvalene **77** with the corresponding in situ generated Gilman cuprate.[66] Kharasch coupling of **77** with methyl magnesium iodide produced methyl bullvalene **89**.[63] Treating **77** with sodium cyanide and copper cyanide delivered cyano bullvalene **90**, which was reduced with DIBAL to obtain aldehyde bullvalene **91**.[64] Aldehyde **91** was reduced to give alcohol **100**; acetylation of the alcohol gave **101**. Condensation reactions with aldehyde **91** gave oxime **102** and tosylhydrazone **103**
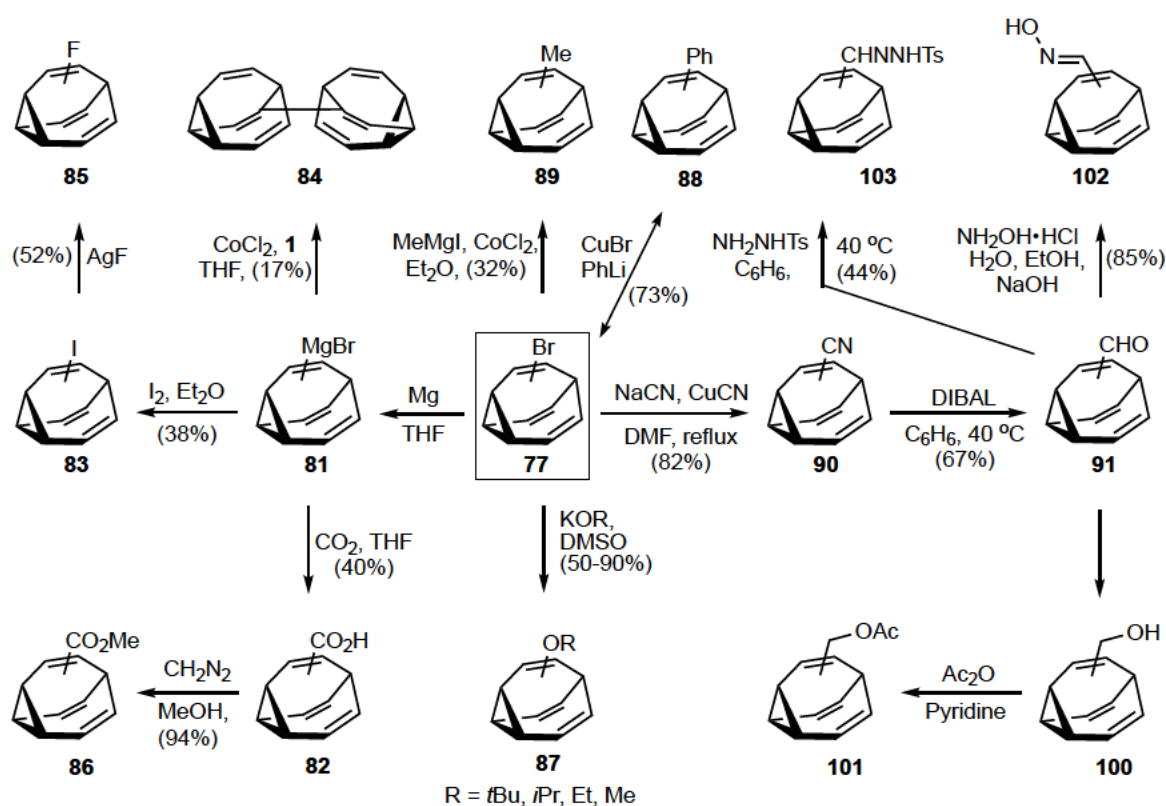
Figure 1.29: Synthesis of mono–substituted bullvalene by Schröder.

1.4.2. Disubstituted

Dibromo bullvalene **77** was used as a precursor for the synthesis of many disubstituted bullvalenes (Figure 1.30). The bromination of bromobullvalene followed by an 1,4–elimination with potassium *tert*–butoxide gave dibromo bullvalene **79** in low yield. Dimethyl **104** and diphenyl bullvalene **105** were obtained by treating **79** with the corresponding Gilman cuparate, which was generated in situ.[67] The addition of sodium cyanide and copper cyanide to **79** gave the dicyano bullvalene **106**. The latter was either reduced to the aldehyde **107**,[68] oxidized to the dicarboxylic acid bullvalene **108** and the mono acid–carboxamide bullvalenes **109**. Dimethanol bullvalene **110** can be obtained by reducing the dialdehyde **107**. The dimenthol bullvalene can be methylated **111** or acetylated **112**.[67] The formation of cyano–bromo bullvalene **113** was achieved by using the same condition as for the synthesis of dicyano bullvalene **106**. The former 113 was reduced to the aldehyde–bromo bullvalene **114**. Aldehyde–bromo bullvalene **114** was reduced to the alcohol **115** and protected with acetate **116**. Introduction a cyano group **117** was achieved by treating **116** with sodium cyanide and copper cyanide.[67] The bromination and the 1,4–elimination of methyl bullvalene **118** gave the disubstituted bromo–methyl bullvalene **119**.[67] The latter **119** was converted to the cyano–methyl bullvalene **120** and then oxidized and esterified to the methylester–methyl bullvalene **121**.
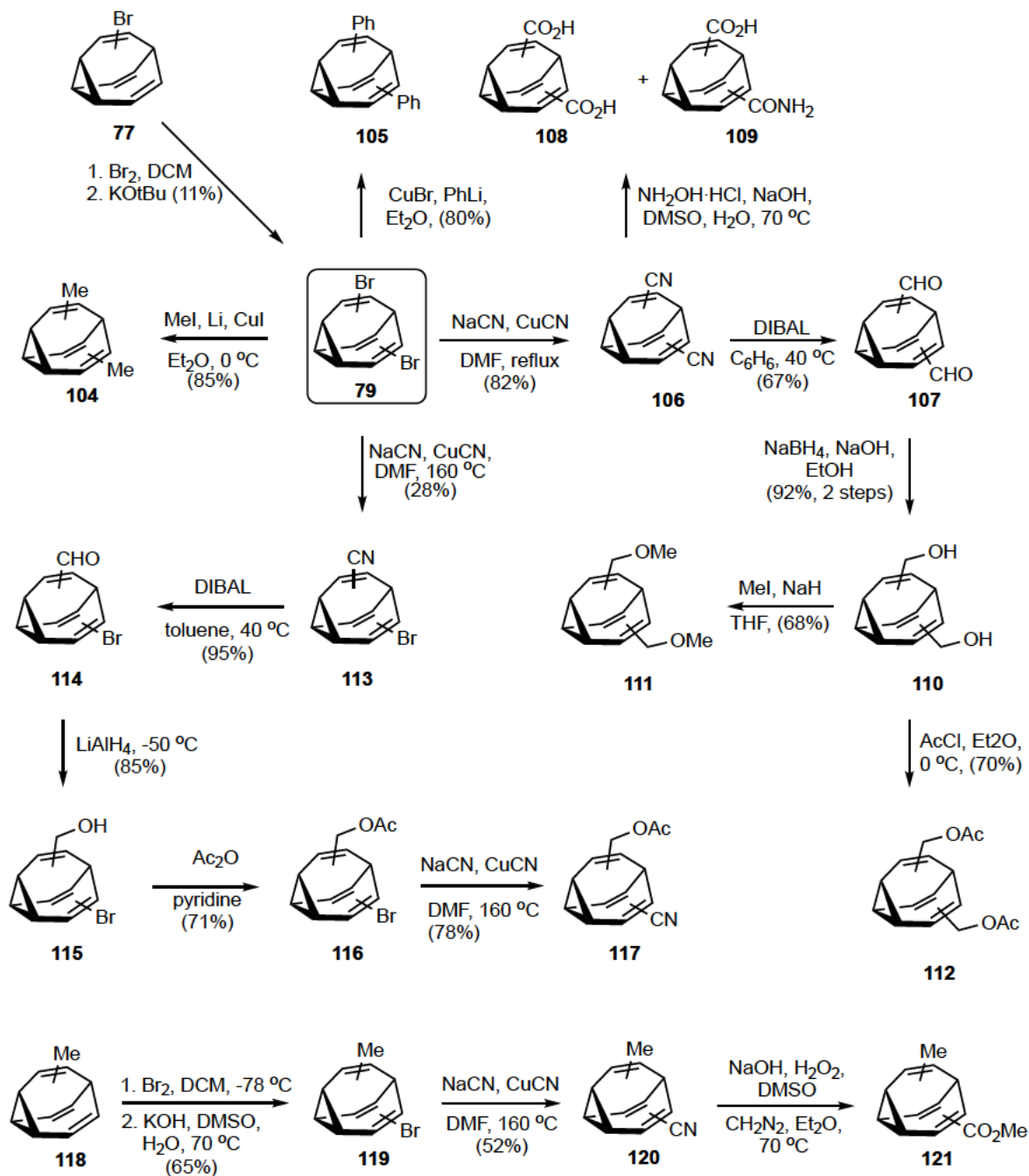
Figure 1.30: Synthesis of disubstituted bullvalenes.

1.4.3. Annulated bullvalene

Annulated bullvalenes show that the Cope rearrangement can be decreased or even frozen. The isomer distribution of these molecules will be discussed in the following sections.

Bromo bullvalene **77** acted again as a precursor to synthesise three annulated bullvalenes **123**–**125** (Figure 1.31). The elimination of HBr from bromo bullvalene **77** generated

dehydrobullvalene **122** as the intermediate which underwent a Diels–Alder reaction with three dienes to give annulated products.
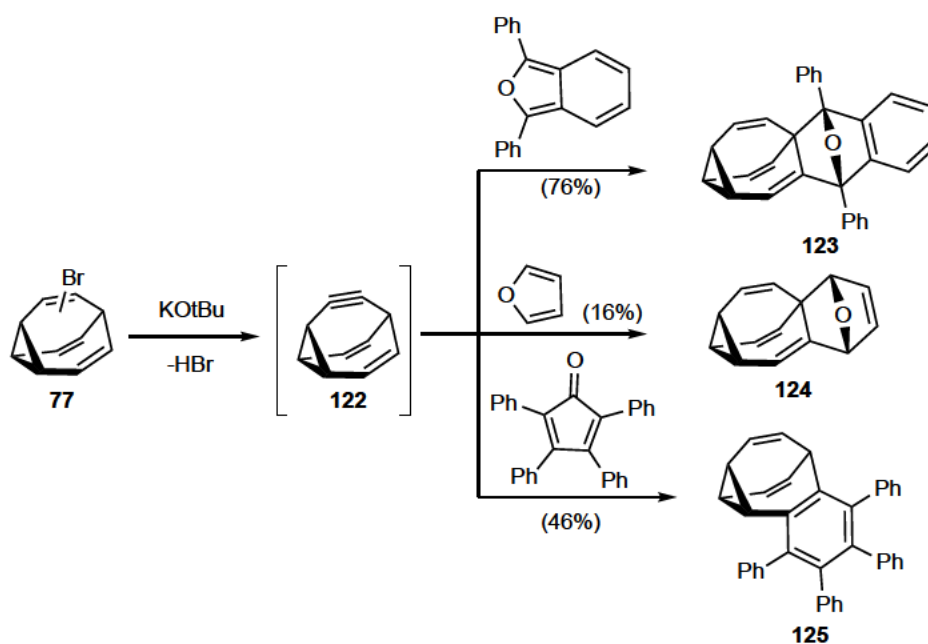
Figure 1.31: Synthesis of annulated bullvalene though the dehydrobullvalene **122** intermediate.

Other annulated bullvalene were synthesized from disubstituted bullvalenes (Figure 1.32). Pyrazole bullvalene **127** was formed from the pyrolysis of tosylhydrazine bullvalene **126** under neat conditions. The reaction of the dialdehyde bullvalene **107** with an oxime gave the pyrrolidine dioxme **128**. The carboxylic acid–amide bullvalene **109** was treated with hydroxylamine and then with acetic anhydride to give the pyrrolidinedione bullvalene **129**. Dicarboxylic acid bullvalene **108** was converted to the anhydride bullvalene **130**. The anhydride was reduced and treated with acid to give lacton bullvalene **131**. The lacton is reduced to the furan bullvalene **132**.[69]
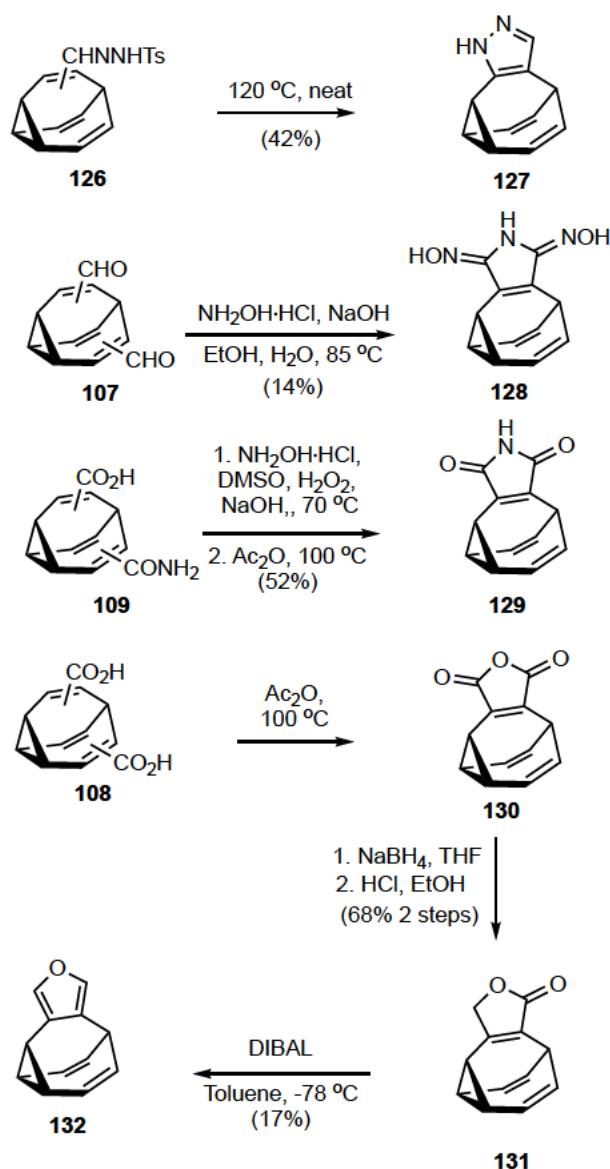
Figure 1.32: Synthesis of annulated bullvalene.

Schröder synthesised a range of crown ether bullvalenes (Figure 1.33).[70,71] Treatment of dimethanol bullvalene **110** with base and the appropriate ethylene glycol ditosylate resulted in the synthesis of a range of crown ether bullvalenes **132a–e** of varying ring sizes. Schröder explored the ability of these molecules to adaptively bind cations, the results of this work will be discussed later.
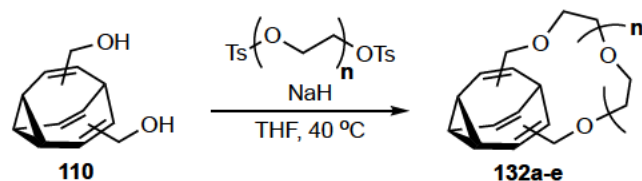
Figure 1.33: Synthesis of crown ether bullvalene.

1.4.4. Tri–, tetra–, penta– and hexa– substituted bullvalenes

The synthesis of tri–, tetra–, penta–, and hexa–substituted bullvalenes was performed by Schröder (Figure 1.34).[72–74] Bromination of dibromo bullvalene **79** followed by the elimination of HBr gave tribromo bullvalene **79**. This method is repeated to deliver tetra– **135**, penta– **137**, and hexa– bromo bullvalenes **139**, **141**.[72] Tri– (**133**, **134**), tetra– (**136**, **137**), penta– **138**, and hexa– (**140**, **142**) methyl or phenyl bullvalene are synthesised by adding the Gilman cuprate to the corresponding bromo bullvalene. When synthesising tetramethyl bullvalene **137**, hexamethylbibullvalene **136** was also isolated.
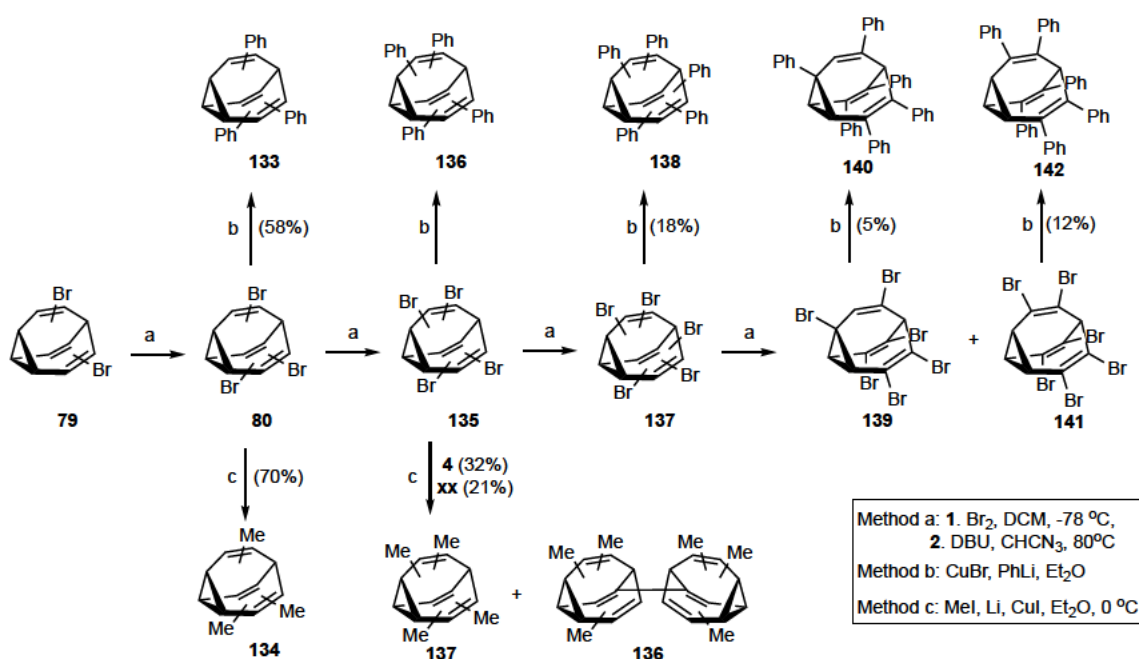
Figure 1.34: Synthesis of tri–, tetra–, penta–, and hexasubstituted bullvalenes.

1.5. Synthesis of substituted bullvalenes – Bullvalenes derived from alternate precursors

Numerous preparations of substituted bullvalenes exist without the requirement of bullvalene as an intermediate. The work here highlights the ability to access substituted bullvalenes from other building blocks, without the need for multi–step transformations from bullvalene as done by Schroder and Paquette. Work by Bode, Echavarren, and Fallon takes this approach and represents bullvalene chemistry in the 21st century.

1.5.1 Miscellaneous

Schröder demonstrated that the COT dimer **10** when treated with strong base rearranges to give phenyl substituted bicyclodecatetraene **143**. Dibromination followed by zinc reduction furnishes phenylbullvalene **88** (Figure 1.35).[75]
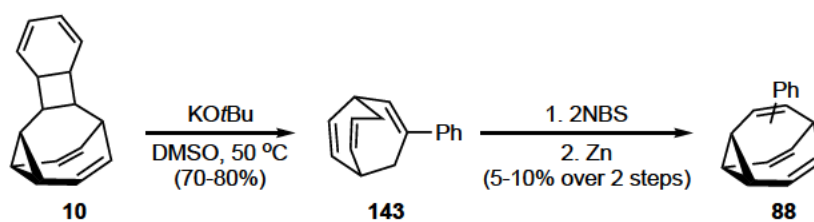
Figure 1.35: Synthesis of phenylbullvalene.

Doering has also shown that from bullvalone, addition of methyl lithium or phenylmagnesium bromide to bullvalone **6**, followed by elimination of the resultant tertiary alcohol, can give rise to methylbullvalene **89** and phenylbullvalene **88**, respectively.[9]
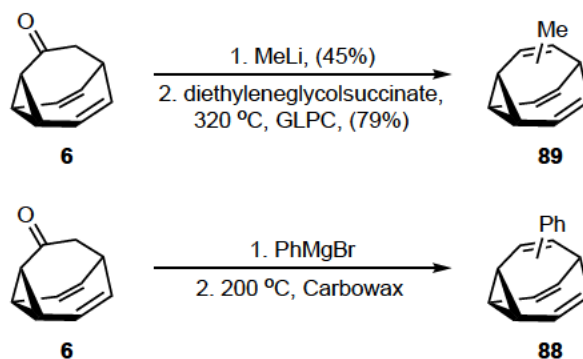
Figure 1.36: Synthesis of methyl– and phenyl bullvalene from bullvalone.

Vogel was the first to synthesise disubstituted bullvalenes. Irradiation of *cis* dimethyl ester 1,9–dihydronaphtalene **144** delivered the desired diemthyl ester bullvalene **145** in low yield (Figure 1.37).[76] On the other hand, the irradiation of anhydride 1,9–dihydronaphtalene **146** gave the corresponding bullvalene anhydride **130** in high yield.
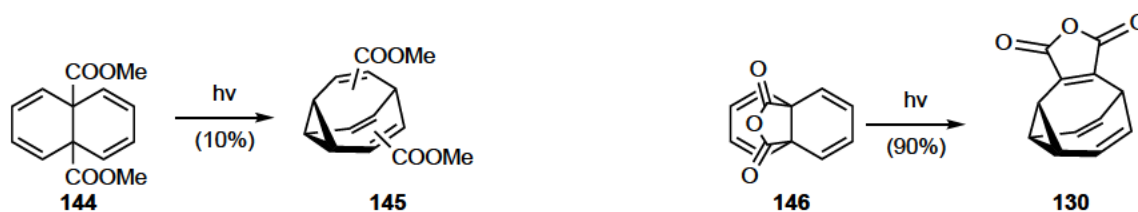
Figure 1.37: Synthesis of disubstituted bullvalene by Vogel.

Schröder synthesized disubstituted bullvalenes using COT **9** as a precursor (Figure 1.38). The thermal 1,2–cycloaddition of 1,1–dichloro–2,2–difluoroethene **147** and COT **9** followed by a reduction with methyl lithium gave **148**.[77] Irradiation of **148** at –40 °C through a quartz cylinder with a UV lamp (200 mA) in dry ether delivered chloro–fluoro BDT **149**. The photorearrangement of **149** at –20 °C under the same condition as described before, gave chloro–fluoro bullvalene **150** in moderate yield.[78] This synthesis is interesting as we might expect that the irradiation leads to the decomposition of the product, since the di–π–methane rearrangement will eliminate either the chloride or the fluoride.
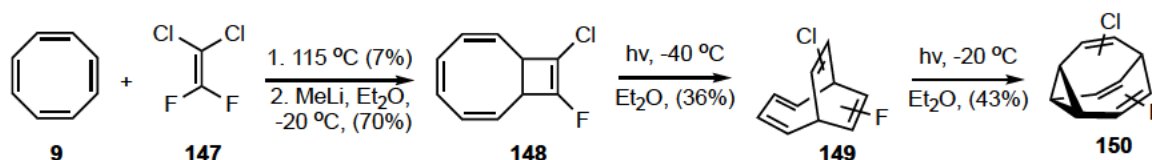
Figure 1.38: Synthesis of chloro– fluro– bullvalene from COT.

Krüecke synthesised diphenyl bullvalene **105**, but was not able to isolated.[79] A [6+2] cycloaddition reaction between COT iron tricarbonyl **151** and substituted acetylene under harsh condition gave the corresponding BDT **152a–c** in low yield (Figure 1.39). Milder photochemical conditions to synthesise the BDT frame have been reported.[80] The irradiation of the diphenyl diiron BDT complex **152a** gave the bullvalene **105**, which could not be isolated but fluxional characteristics were observed in the ^{1}H NMR spectra.

152a: $R_1 = R_2 = Ph$, 35%
152b: $R_1 = Ph$, $R_2 = COOMe$, 10%
152c: $R_1 = Ph$, $R_2 = TMS$, 15%

105
could not be isolated
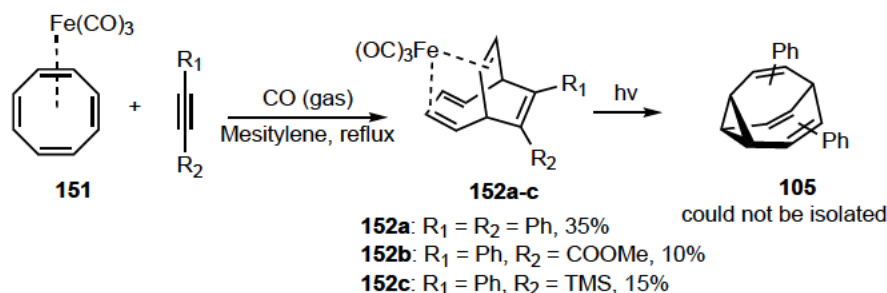
Figure 1.39: Attempt to synthesise diphenyl bullvalene.

1.5.2. Bode's synthesis of tetrasubstituted bullvalene

Bode's synthesis of highly complex tetrasubstituted bullvalenes relied on triketone **156**, from which diversification allowed the introduction of a range of functionalised substituents allowing his group to explore bullvalenes in a range of supramolecular settings. This approach takes inspiration from Serratosa's triketone bullvalene (Figure 1.7) envisioning functionalisations of each ketone to synthesise the bullvalene core. Coupling of **153**[81] with sulphur ylide **154** gave **155**, which underwent a scandium triflate catalysed intramolecular cyclopropanation to give key triketone **156** (Figure 1.40).[82]
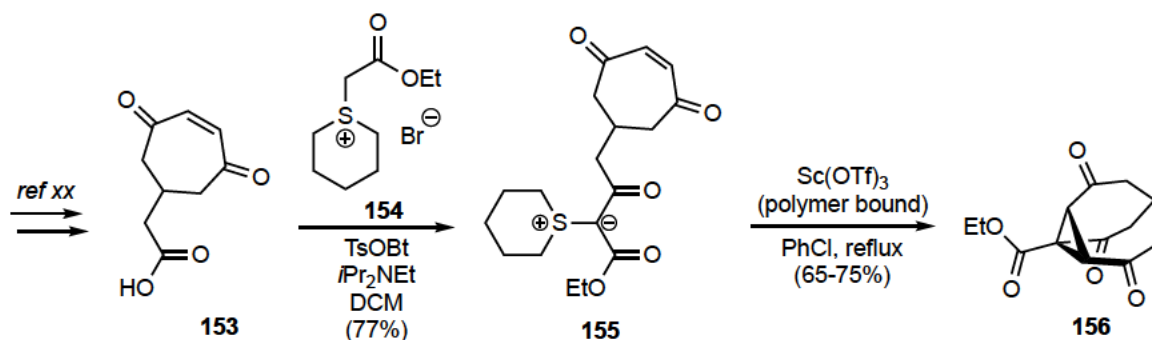
Figure 1.40: Bode's syntesis of key ketone **156**.

Bode group's method of functionalisation of ketone groups in **156** to give a tetrasubstituted bullvalene is typical: Grignard addition followed by elimination, and base mediated enolate formation with conversion to an enol carbonate (Figure 1.41). As an example, the synthesis of bisallyl bullvalene **160** is shown.[83] Addition of allylmagnesium bromide to triketone **156** gives *meso* and *chiral* diols **157** and **158**, respectively. The desymmetrisation of the ester moiety leads to ketone differentiation. Thionyl chloride mediated elimination of *meso* **157** and *chiral* **158** diols gives bisallyl bullvalone **159**. Subsequent enol carbamate formation furnishes tetrasubstituted bullvalene **160**.
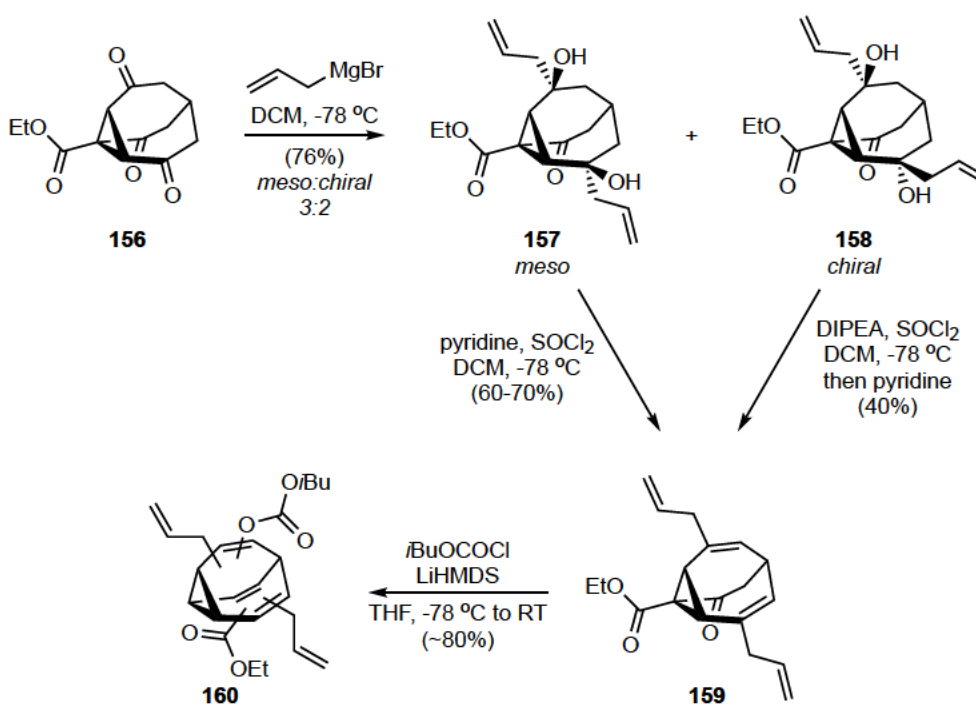
Figure 1.41: Bode's synthesis of tetrasubstituted bullvalene.

Supramolecular applications of Bode's tetrasubstituted bullvalenes will be discussed in later section along with the relevant syntheses from triketone **156**.

1.5.3. Echavarren synthesis of substituted bullvalenes

Echavarren demonstrated that his strategy to access bullvalene was also adaptable to synthesise phenylbullvalene **88** (Figure 1.42).[26] Addition of the lithium acetylide of phenyl acetylene **161** to tropylium tetrafluoroborate **27** gave **162**. Gold catalysed oxidative cyclisation and one carbon homologation gave phenyl bullvalone **164**. Transformation of the ketone to a triflate **165**, followed by its reduction under palladium catalysis gave phenylbullvalene **88**.
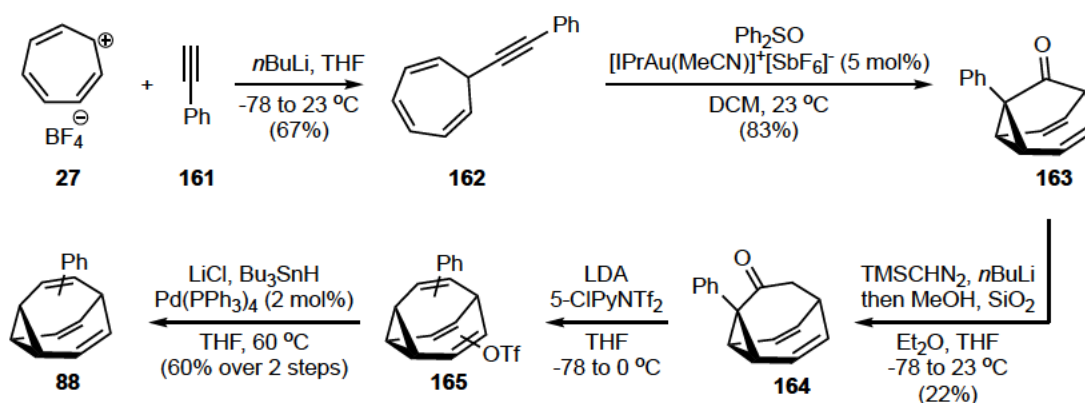
Figure 1.42: Synthesis of phenylbullvalene by Echavarren.

Echavarren showed that the triflate group on **165** generated from phenyl bullvalone **164** is able to participate in Stille cross couplings giving diphenylbullvalene **105** and two other hetero–disubstituted bullvalenes **166b–c** (Figure 1.43).[26]
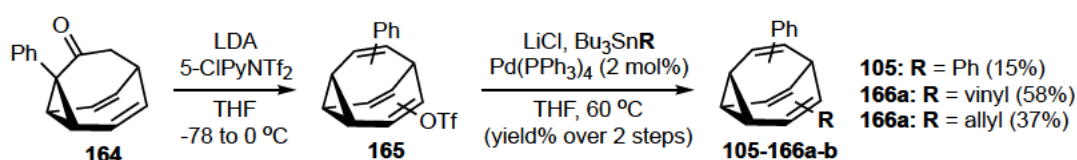
Figure 1.43: Synthesis of disubstituted bullvalene by Echavarren.

1.5.4. Fallon's substituted bullvalenes

Fallon demonstrated that with substituted alkynes, their two step route to bullvalene is also able to access monosubstituted bullvalenes (Figure 1.44).[27] Cobalt catalysed cycloaddition of COT and substituted alkynes, followed by photochemical rearrangement of the subsequent BDT **167a–f** gave bullvalenes **168a–e**. When phenyl acetylene was used to synthesise the phenyl BDT **167f** the subsequent step gave rise to phenyl–lumibullvalene **168f** through an alternate di–π–methane rearrangement.

167a: R = Me (70%)
167b: R = *n*-hex (90%)
167c: R = CH$_2$OH (86%)
167d: R = Bn (91%)
167e: R = SiMe$_3$ (100%)
167f: R = Ph (63%)

168a: (40%)
168b: (81%)
168c: (63%)
168d: (42%)
168e: (70%)
168f: (67%)
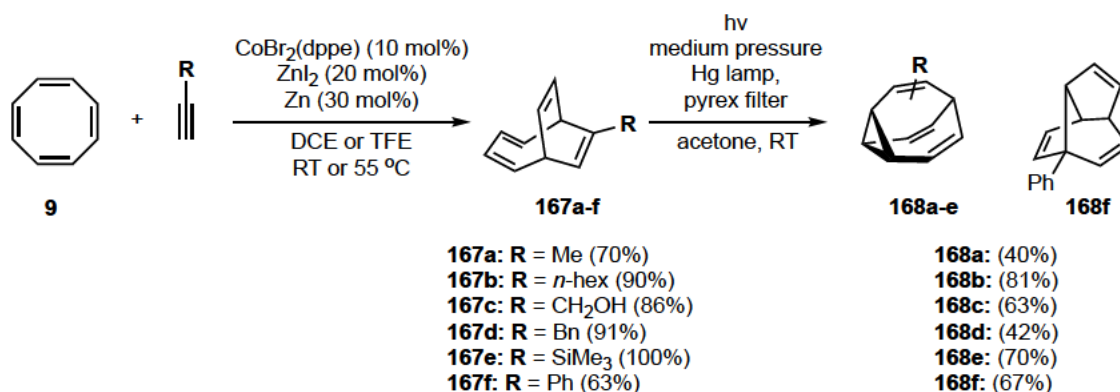
Figure 1.44: Synthesis of monosubstituted bullvalene by Fallon group.

By using a disubstituted alkyne,[27] or a monosubstituted alkyne and a monosubstituted COT **171** or COT **9**,[84] Fallon group were able to employ their same synthetic strategy, consisting of a cobalt catalysed cycloaddition followed by a photochemical di–π–methane rearrangement, to synthesise disubstituted bullvalenes **170a–b** and **173a–e** respectively (Figure 1.45).
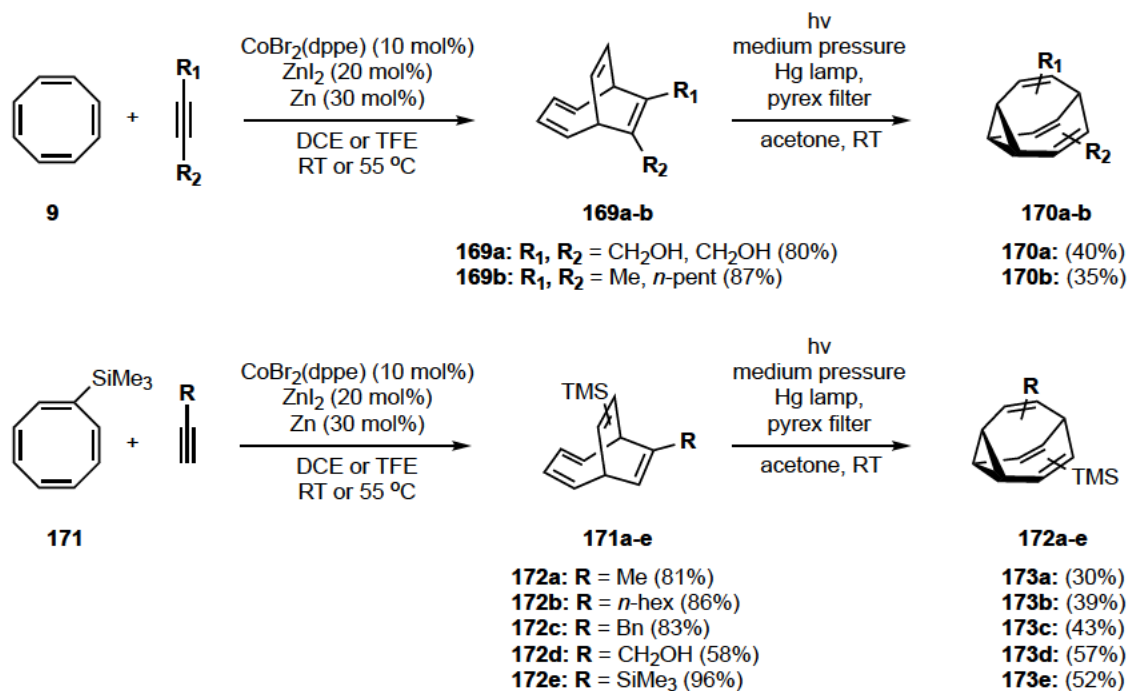
Figure 1.45: Synthesis of mono– and disubstituted bullvalene by the Fallon group.

By performing a cycloaddition reaction with a 1,4–butynediol **174** and a TMS substituted COT **171**, followed by a photorearrangement; Fallon group were able to access trisubstituted bullvalene **176** (Figure 1.46).[84] Swern oxidation of this molecule gave dialdehyde **178**. By taking tetraene **175**, they were able to selectively functionalise one of the alcohols into silyl ether **177**. This was then converted into the corresponding bullvalene **179** and oxidation of the unprotected alcohol gave bullvalene **180**.
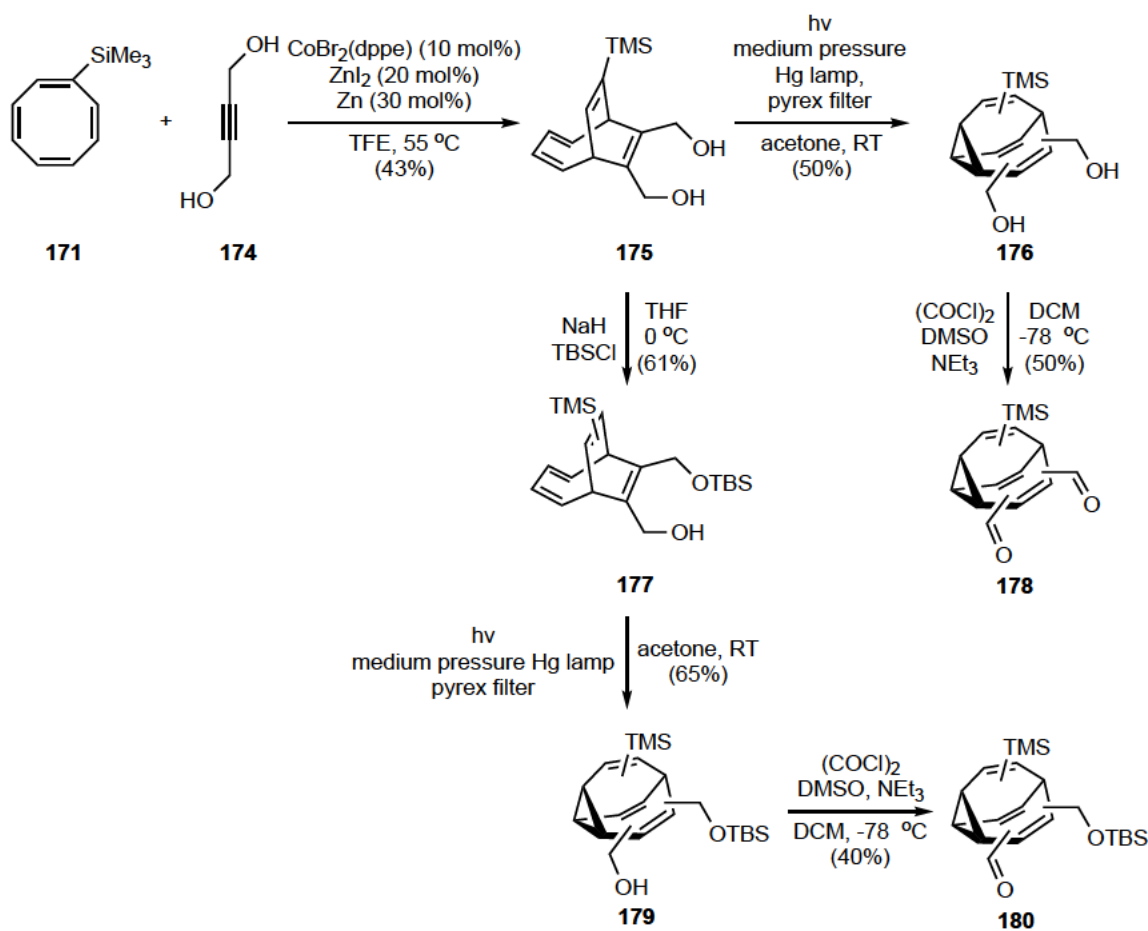
Figure 1.46: Synthesis of trisubstituted bullvalenes by the Fallon group.

Fallon showed that a cobalt catalysed cycloaddition of a Bpin substituted acetylene **181** with COT **9** can be used to make Bpin BDT **182** (Figure 1.47).[85] With a modified photochemical procedure involving 9*H*–thioxanthen–9–one as a sensitiser[86] they were able to synthesise Bpin–bullvalene **183**. This molecule opens up many opportunities for diversification as demonstrated through Suzuki cross–couplings to give **186a–g**, simple oxidation to furnish bullvalone **6**, Chan–Lam coupling to produce **189**, and rhodium catalysed 1,2– and 1,4– additions to give **187** and **188** respectively.
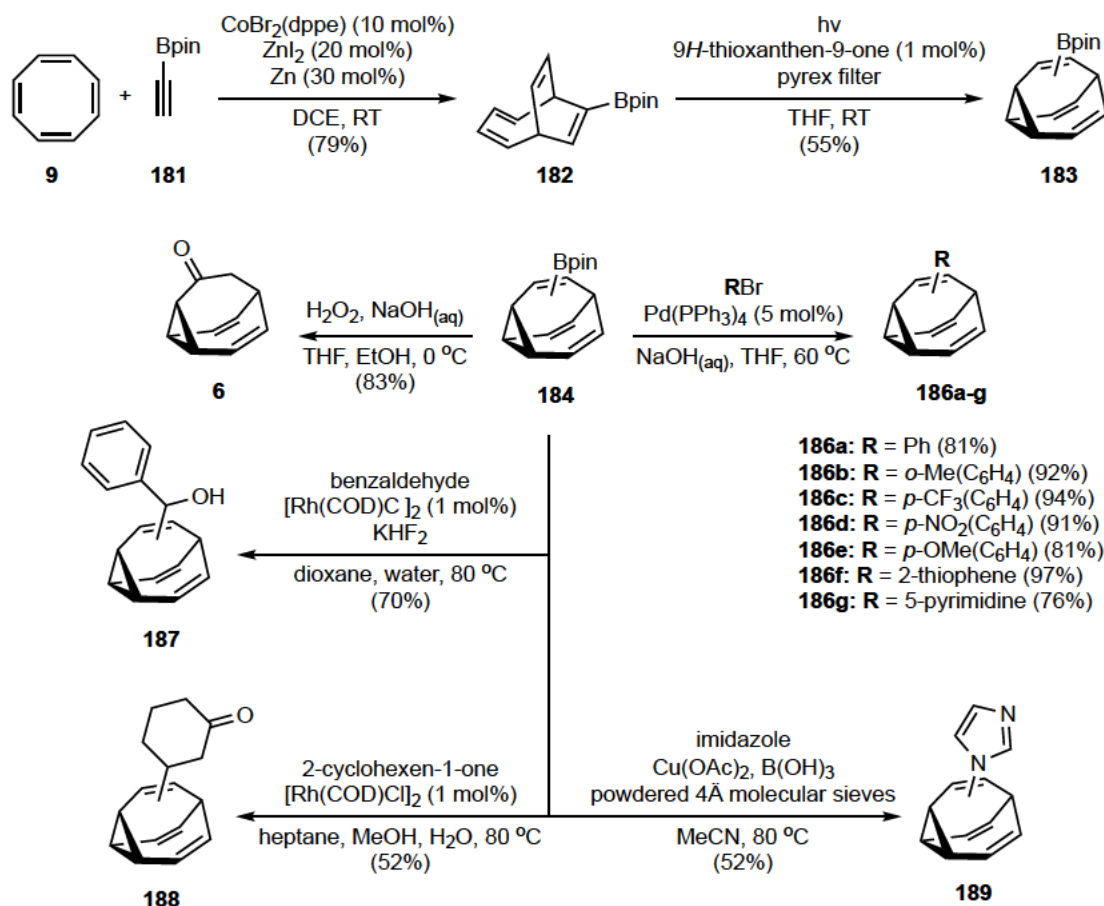
Figure 1.47: Synthesis of mono Bpin bullvalene, its Suzuki coupling and functionalization.

Now using a double Bpin alkyne **190**, the Fallon group were able to synthesise the corresponding bullvalene **192** and demonstrate its utility in Suzuki cross–coupling reactions by synthesising **193a–g** (Figure 1.48).[85]
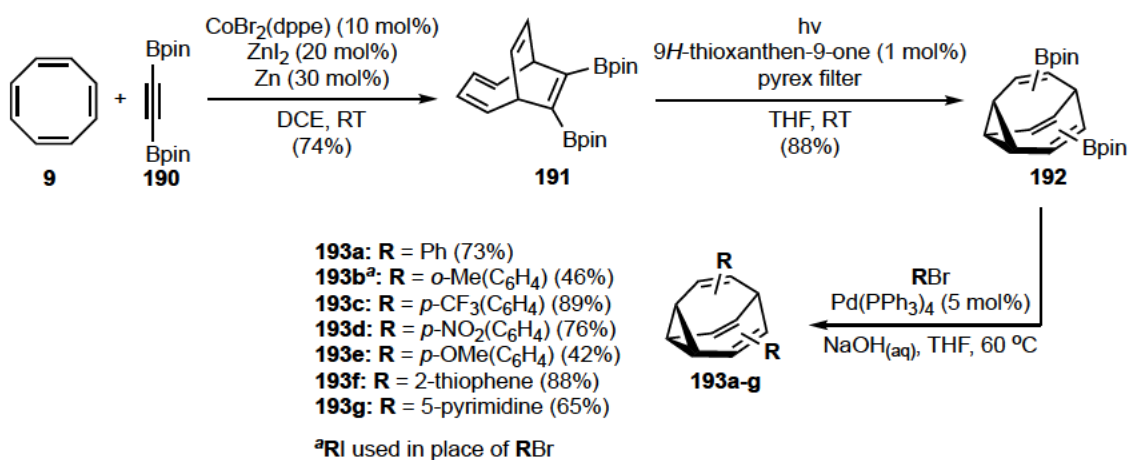
Figure 1.48: Synthesis of BisBpin bullvalene and its Suzuki coupling.

By condensing a MIDA group onto BDT **191**, Fallon group were able to make BDT **194** which was converted to bullvalene **195** (Figure 1.49).[85] By incorporating two different functional handles, Bpin and B$_{MIDA}$, they were able to demonstrate differential coupling of substituents onto the bullvalene to give hetero–disubstitued bullvalenes. First the Bpin functional handle was coupled under anhydrous conditions to give **196**. The subsequent hydrous conditions coupled the B$_{MIDA}$ group to give **197a–c**.
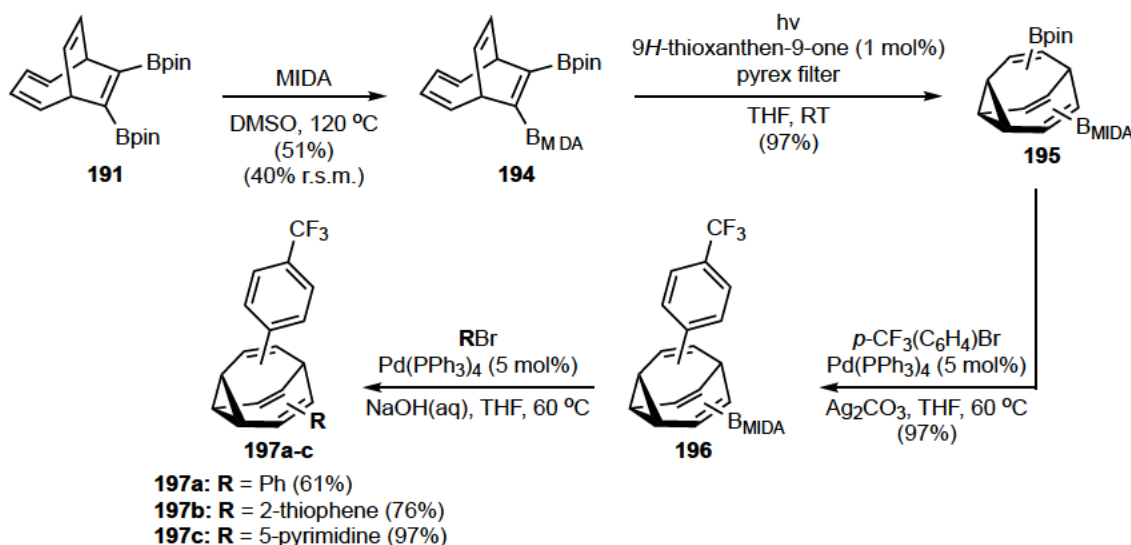
Figure 1.49: Synthesis of B$_{MIDA}$–Bpin–bullvalene and its Suzuki coupling.

By substituting COT with a Bpin group **198** and carrying out a cycloaddition with **190**, followed by photorearrangement, the Fallon group were able to synthesise a bullvalene with three Bpin substituents **200** and demonstrated its ability to participate in Suzuki cross–coupling reactions by synthesising triphenylbullvalene **201** (Figure 1.50).[85]
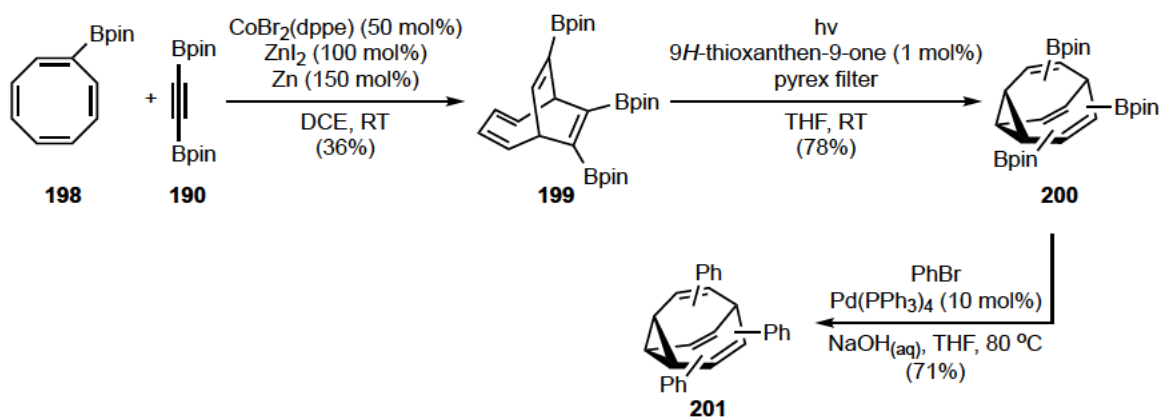
Figure 1.50: Synthesis of tri–Bpin bullvalene and triphenyl bullvalene.

1.5.5. Paquette azabullvalene

Paquette's contribution to the chemistry of bullvalene is prestigious with a focus on synthesising a derivative of bullvalene, namely azabullvalene. While Paquette did not succeed to synthesize azabullvalenes, he developed a three–step method to obtain mono–, di–, and annulated azabullvalenes in moderated yields (Figure 1.51). A 1,2–cycloaddition of CSI to COT **9** followed by a reductive etherification gave **203**. The latter **203** was subjected to irradiation to deliver the methoxy azabullvalene **204** in good yield.[87,88] **202** can be converted to the thioamide **206**, upon reductive etherification. The photorearrangement of **206** gave the methylthio– azabullvalene **207**.[88] Methoxy–methyl–azabullalene **208** was formed from the irradiation of **209** in high yield.[88] Paquette synthesized methoxy benzazabullvalene **212** though a 1,2–cycloaddition between CSI and **9**, followed by reductive etherification and irradiation.[89] Heating the product lead to the irreversible formation of **212**.
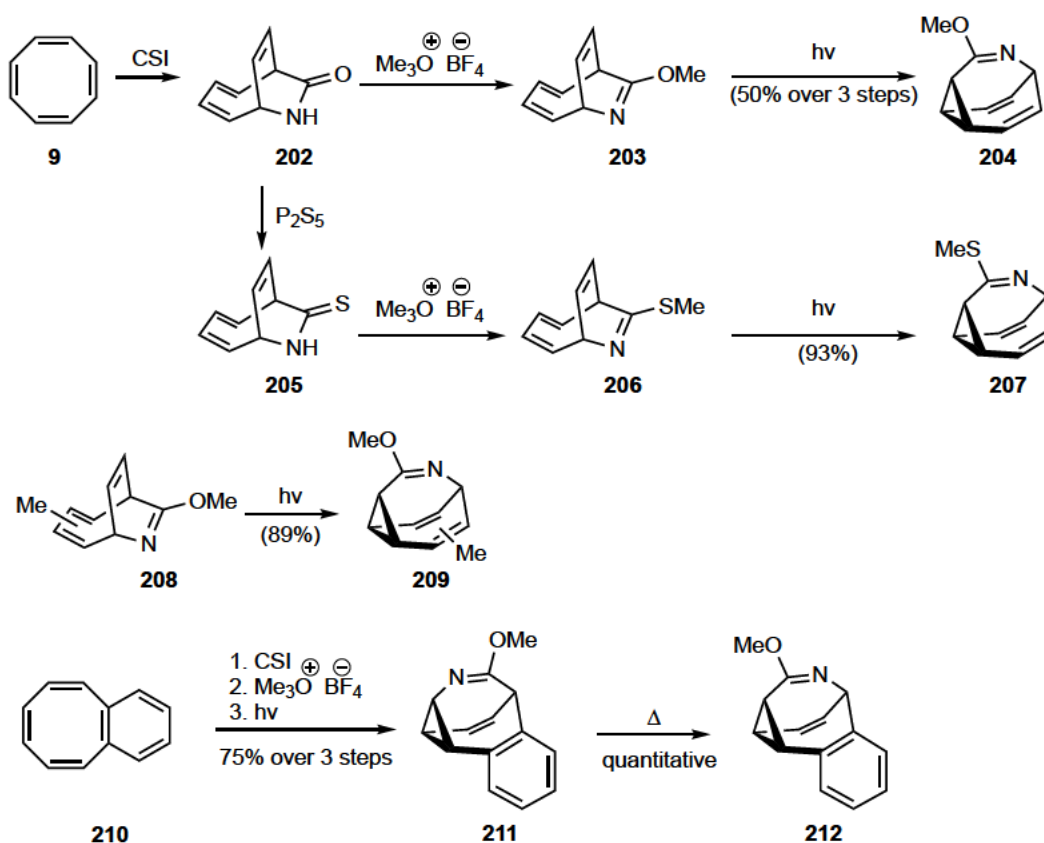
Figure 1.51: Synthesis of phenyl– methoxy– azabullvalene.

Under the same irradiation conditions for the photorearrangement of bullvalene (Figure 1.12), Paquette's methoxy–azabullvalene gives similar products (Figure 1.52).[90] Except here,

methoxy–aza–BDT (**212**, **215**) and the Nenitzescu's hydrocarbon (**213**, **216**) were separated as two isomers. Methoxy–aza–lumibullvalene **214** was also separated, but a methoxy–aza equivalent of compound **33** is absent.
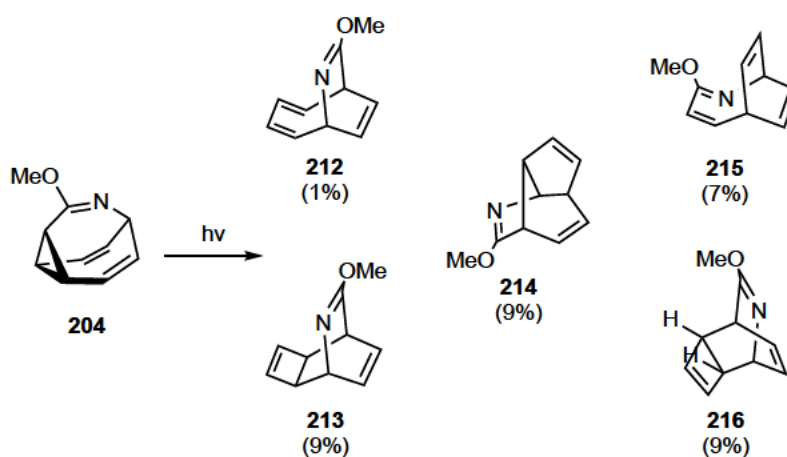
Figure 1.52: Photorearrangement of methoxy–azabullvalene.

1.6. Supramolecular Applications of Bullvalene (written by Harshal Patel)

The dynamic behaviour of bullvalene could be promising for many applications, such as sensor, supramolecular chemistry, catalysis, drug delivery, etc. Yet, only Bode has used his tetrasubstituted bullvalenes as a sensor, showing great results. This field remains under explored due to the low and/or lengthy synthesis of bullvalene.

A recent comprehensive review on the application of shapeshifting molecules was reported by Mcgonigal.[3] We will represent the tremendous work by Bode and co–worker and one example from Schröder.

The earliest exploration of bullvalene in a supramolecular setting was conducted by Schröder by synthesising crown ether bullvalenes **132a–e** (Figure 1.53).[70,71] They assessed the binding activity of bullvalene crown ethers **132a–e** against a range of alkali picrates and ammonium picrates, in the hope of observing bullvalene adapting its shape to better accommodate the guest ion. Overall, they determined that the rate constants showed weak host–guest interactions, they did not observe the adaptive binding that was expected and concluded that ion

complexation/decomplexation is significantly faster than the intramolecular Cope rearrangement.

alkali picrate: Li⁺, Na⁺, K⁺, Rh⁺, Cs⁺
K_a = 0.33-31.54 x10⁻⁴ (l/mol)

ammonium picrate: NH₄⁺, MeNH₃⁺, tBuNH₃⁺
K_a = 0.02-18.05 x10⁻⁴ (l/mol)

xxa-e

132a: n = 1
132b: n = 2
132c: n = 3
132d: n = 4
132e: n = 5
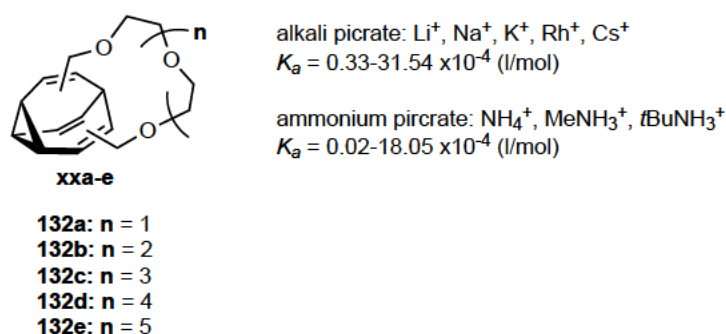
Figure 1.53: Crown ether bullvalene and its binding constant to alkali prircrate and ammonium pircrate.

Bode's triketone **156** was a key molecule to synthesise a whole range of functionalised bullvalenes in order to explore shapeshifting molecules in supramolecular settings. In their earliest paper, the research team were acquainting themselves with the synthesis of bullvalene.[81] From bis allyl bullvalone **159**, the group wanted to demonstrate that the molecule was stimuli responsive and that rearrangement of the molecule in its entirety would occur (Figure 1.54). Under basic conditions, bullvalone **159** was transformed into deuterated molecule **218**. The ethyl ester was transesterified with CD_3O^- and each proton on the bullvalone was exchanged with deuterium indicating bullvalene type fluxionality under these conditions. Resubjection of deuterated **217** to non–deuterated analogous conditions gave back non deuterated bullvalone **217**.
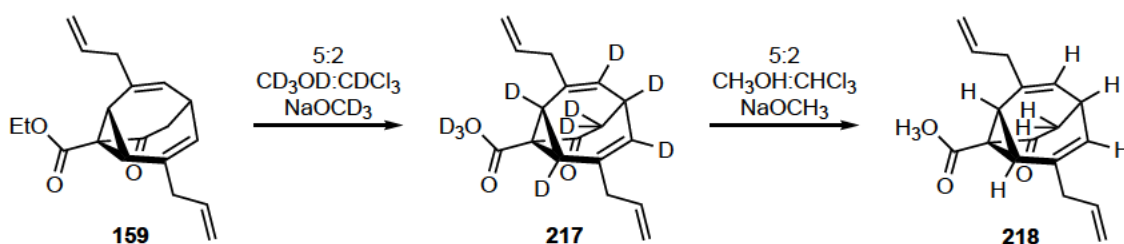
Figure 1.54: Deuterated bullvalone.

From bullvalene **160** Bode's group functionalised the molecule with porphyrin rings through a Grubbs metathesis to give bullvalene **219** and demonstrated its ability to adapt shape to better complex a substrate (Figure 1.55).[83] Addition of a C60 fullerene complexed the bisporphyrin

bullvalene; they concluded that bullvalene formed a network of two or more interconverting complexes upon addition of C60.
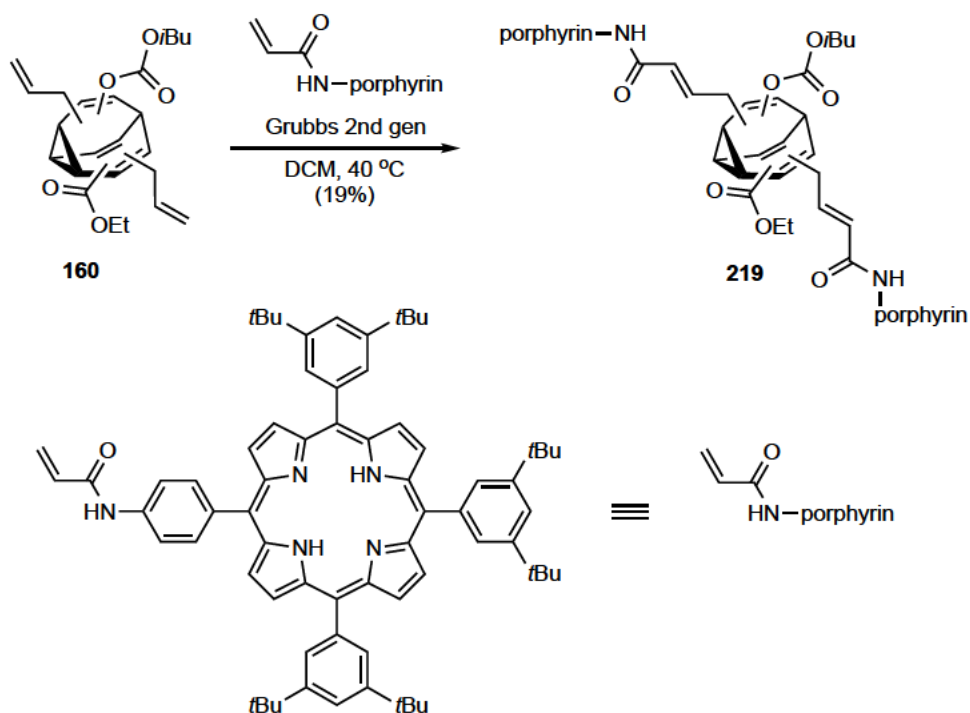
Figure 1.55: Tetrasubstituted bullvalene with porphyrin rings used as C60 fullerene sensor.

In their next piece, Bode introduced a photolabile NVOC carbonate onto bullvalene **220**, followed by introduction of porphyrin rings by Grubbs metathesis to give bullvalene **221** (Figure 1.56).[91] Now, photocleavage of the NVOC carbonate would result in the formation of static bullvalone isomers. Introduction of C60 fullerene showed a change in isomer distribution to those that more tightly bound C60. Upon UV irradiation, the NVOC carbonate was photolysed yielding a static set of bullvalone isomers which displayed favourable binding properties.
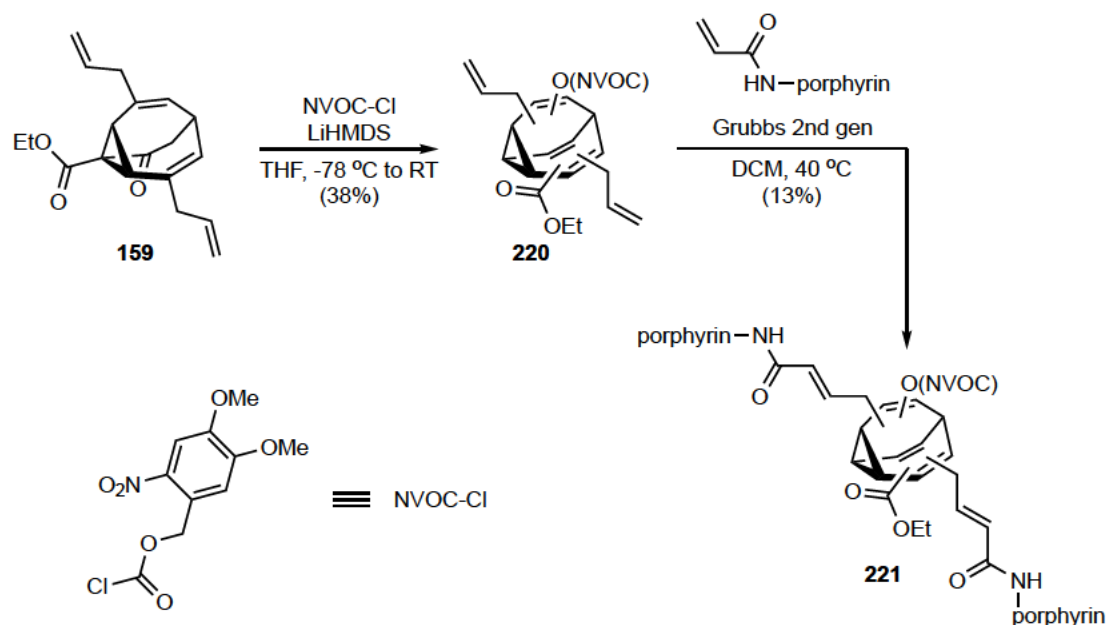
Figure 1.56: Tetrasubstituted bullvalene with porphyrin rings and a photolabile NVOC.

Bode took triketone **156**, and through two addition/elimination steps, and an enol carbonate formation, synthesised tetrasubstituted bullvalene **226** (Figure 1.57).[92] The fluxional characteristics of this bullvalene were shown through its behaviour through a HPLC column. The tetra–substituted bullvalene was separated by numerous peaks on its HPLC trace. Each fraction collected was then individually separated again on the column, and the homology between the new and original traces demonstrated the tendency for bullvalene to re–equilibrate to a more thermodynamically and kinetically stable population. However, one of the fractions took much longer to re–equilibrate than the others, indicating the presence of a transient metastable isomer with a half–life of 46 h at room temperature.
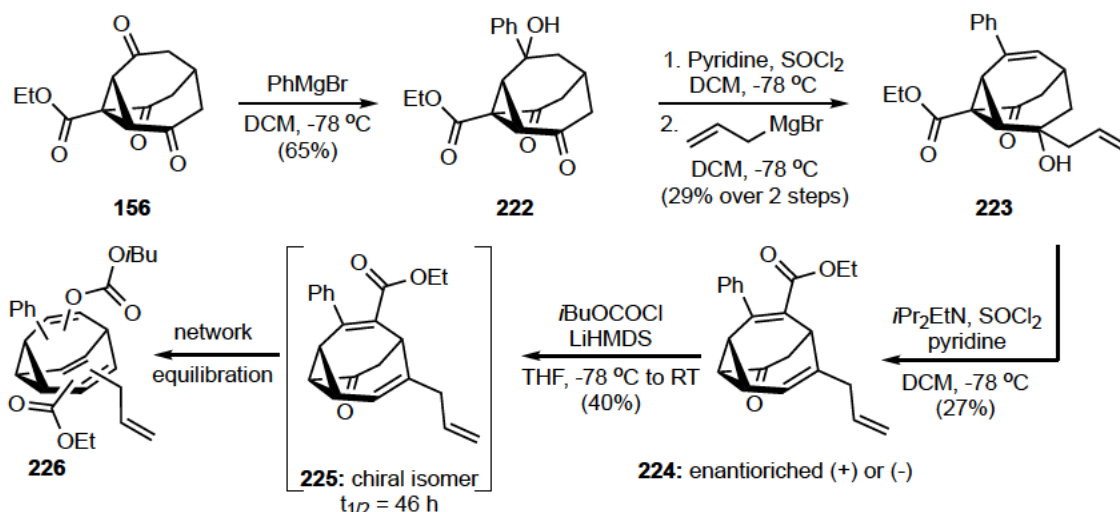
Figure 1.57: Isolation of chiral isomer through HPLC.

13C–labelled bisporphyrin bullvalene **227** was synthesised by incorporating a 13C label into their existing synthetic methodology (Figure 1.58).[82] Fullerene analytes were introduced to the system. Upon introduction, the peak patterns of ^{13}C NMR spectra changed, due to the interactions between the analytes and bullvalene's porphyrin recognition elements. It was suggested from these findings that the C13–labelled bullvalene core could function as a reporter for different analyte classes, depending on the recognition domains connected to it.
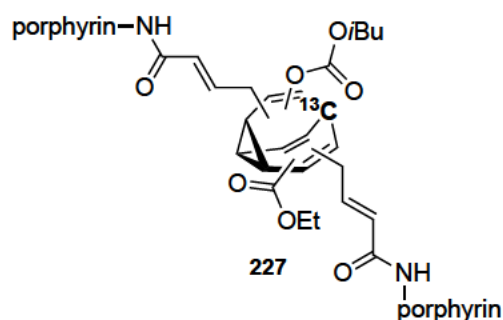
Figure 1.58: Synthesis of 13C–labeled tetrasubstituted bullvalene.

Bode synthesised 13C labelled bis–boronic acid bullvalene **234** and demonstrated its use in sensor arrays for polyhydroxylated compounds.[93] First, 13C labelled bullvalone **228** underwent a sequence of Grubbs methathesis **229**, enol carbonate formation **230**, azide substitution **231**, and alkyne–azide click reaction to give Bpin substituted bullvalene **232**. The Bpin functionality was transformed into a BF$_3$K group **233**, and then to a boronic acid to give bullvalene **234**. They showed that each analyte that bound bis–boronic acid bullvalene **234**

changed the ^{13}C NMR peak pattern in a unique way, leading to such patterns being transformed into a novel, easy–to–read barcode.
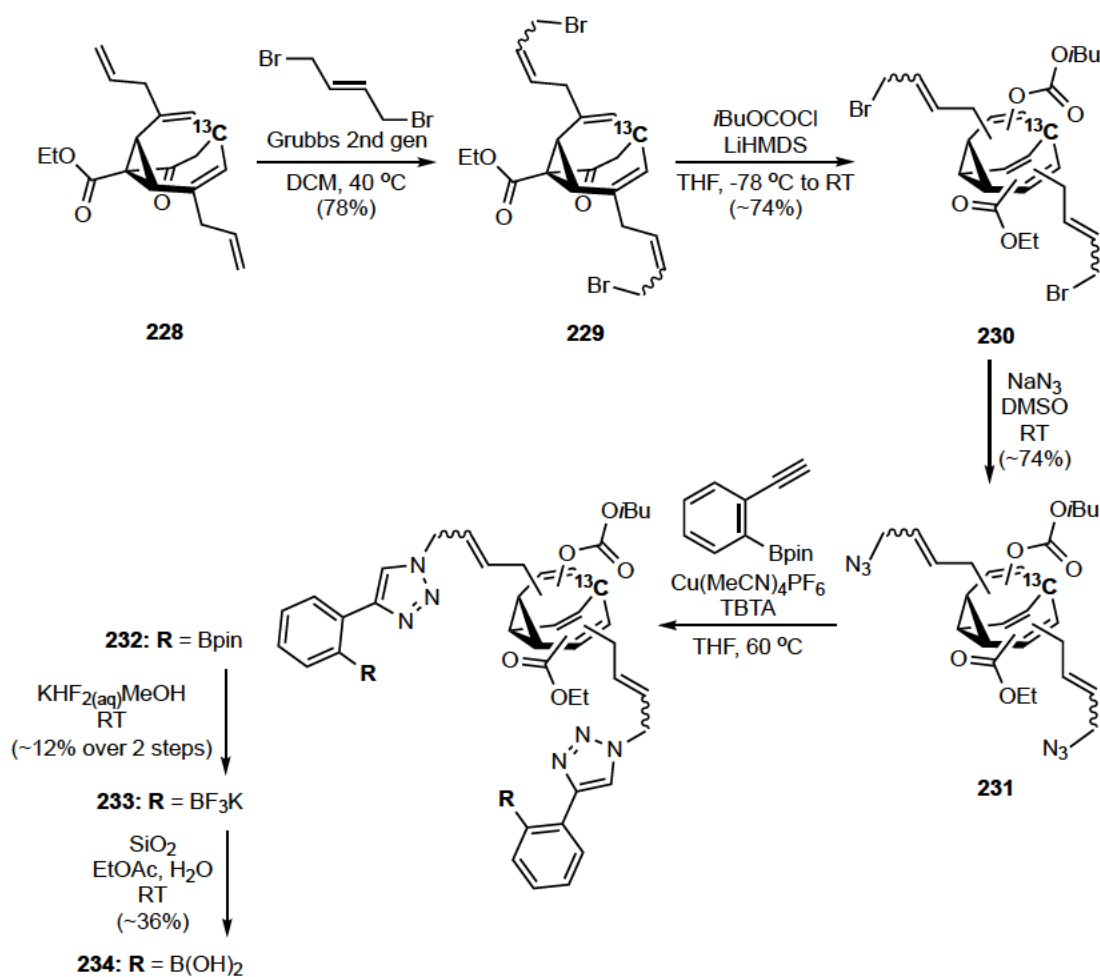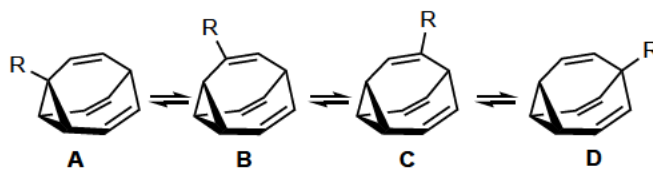
Figure 1.59: Synthesis of 13C–labeled bis–boronic acid bullvalene.

1.7. Isomer distribution

As a dynamic ensemble of exchanging isomers, the elucidation of the most populated isomers of substituted bullvalene is very challenging and can be, in a few cases, elusive. Monosubstituted bullvalene for instance exists between four possible isomers. Disubstituted bullvalenes exist either between 30 isomers (unidentical substituents) or 15 isomers (identical substituents). With further substitution, the number of possible isomers of bullvalene rises exponentially. Low temperature NMR spectroscopy is the only analytic method that reveals the distribution of isomers for substituted bullvalenes. In this section, we tabularized the most populated isomers for all synthesised substituted bullvalenes.

1.7.1. Monosubstituted bullvalene

The elucidation of the isomer distribution of monosubstituted bullvalenes is easy because the number of possible isomers is four (Figure 1.60). In most cases the number of major isomers is two, whereby the substituents are attached to the olefinic carbons and rarely to the cyclopropyl or the bridgehead carbons. The only exception is flurobullvalene in which the substituent for the major isomer is attached to the bridgehead carbon. The fluorine substituent prefers the bridgehead carbon as it requires maximum satisfaction of its electronegativity requirements, and because the bond to the bridgehead carbon (sp^3) is endowed with less s character and is therefore less electronegative than that the cyclopropyl carbon (sp^2).[88]

R	A		B		C		D
R = Br[57]	-	:	45	:	55	:	-
R = OtBu[57]	-	:	45	:	55	:	-
R = OMe[58]	-	:	45	:	55	:	-
R = OEt[58]	-	:	45	:	55	:	-
R = OiPr[58]	-	:	45	:	55	:	-
R = F[63]	-	:	7	:	15	:	78
R = I[63]	-	:	45	:	55	:	-
R = Cl[63]	-	:	45	:	55	:	-
R = COOH[60]	-	:	55	:	54	:	-
R = COOMe[60]	-	:	55	:	45	:	-
R = Me[24]	-	:	42	:	58	:	-
R = CH$_2$OH[24]	18	:	25	:	57	:	-
R = CH$_2$OAc[93]	20	:	20	:	40	:	20
R = CH$_2$OMe[93]	20	:	20	:	40	:	20
R = n-hex[24]	7	:	25	:	68	:	-
R = Bn[24]	-	:	24	:	76	:	-
R = TMS[24]	-	:	7	:	93	:	-
R = Bpin[83]	-	:	28	:	72	:	-
R = Ph[83]	-	:	20	:	80	:	-
R = o-Me(C$_6$H$_4$)[83]	-	:	28	:	72	:	-
R = p-CF$_3$(C$_6$H$_4$)[83]	-	:	22	:	78	:	-
R = p-NO$_2$(C$_6$H$_4$)[83]	-	:	21	:	79	:	-
R = p-OMe(C$_6$H$_4$)[83]	-	:	21	:	79	:	-
R = 2-thiophene[83]	-	:	16	:	84	:	-
R = 5-pyrimidine[83]	-	:	28	:	72	:	-

Figure 1.60: Isomer distribution of monosubstituted bullvalene.

1.7.2. Disubstituted bullvalene

The elucidation of the isomer distribution for disubstituted bullvalenes is more difficult. For unidentical substituents the number of possible isomers is 30 and for identical 15. For most disubstituted bullvalenes, the substituents are attached to the olefinic carbons, except for fluoro substituents.
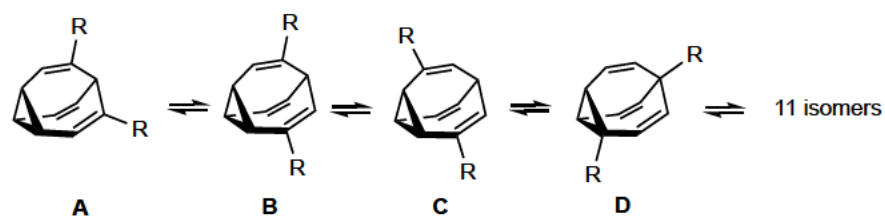
	A		B		C		D		
R = CO$_2$Me[74]	75	:	25	:	-	:	-	:	-
R = CN[64]	72	:	28	:	-	:	-	:	-
R = CHO[65]	68	:	32	:	-	:	-	:	-
R = Br[65]	14	:	59	:	27	:	-	:	-
R = F[65]	1	:	16	:	12	:	71	:	-
R = OtBu[65]	-	:	50	:	50	:	-	:	-
R = Me[65]	25	:	55	:	20	:	-	:	-
R = Ph[83]	51	:	39	:	10	:	-	:	-
R = CH=N-OH[65]	40	:	60	:	-	:	-	:	-
R = CH$_2$OMe[65]	60	:	30	:	-	:	-	:	10
R = CH$_2$OAc[65]	60	:	30	:	-	:	-	:	10
R = TMS[82]	70	:	30	:	-	:	-	:	-
R = p-CF$_3$-(C$_6$H$_5$)[83]	52	:	40	:	8	:	-	:	-
R = p-OMe-(C$_6$H$_5$)[83]	60	:	40	:	-	:	-	:	-
R = 2-thiophene[83]	66	:	29	:	5	:	-	:	-
R = 5-pyrimidine[83]	37	:	53	:	10	:	-	:	-
R = Bpin[83]	18	:	74	:	8	:	-	:	-

Figure 1.61: Isomer distribution for disubstituted bullvalene with identical substituents.

R_1/R_2-substituted bullvalene equilibrium:
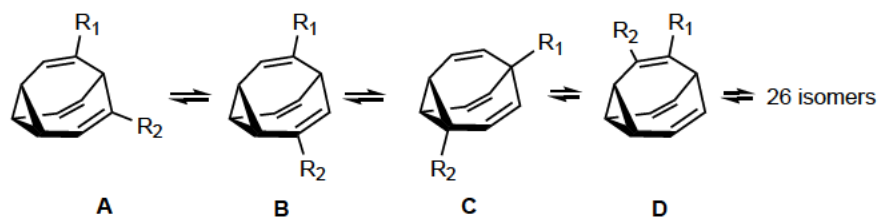
A ⇌ **B** ⇌ **C** ⇌ **D** ⇌ 26 isomers

	A	B	C	D	
R_1 = F, R_2 = Cl[65]		56[a]	44 (R_1=F)	-	-
R_1 = F, R_2 = Br[65]		50[a]	50 (R_1=F)	-	-
R_1 = CH_2OH, R_2 = Br[65]	-	40	-	48[b]	12
R_1 = CH_2OAc, R_2 = Br[65]	-	40	-	48[b]	12
R_1 = Me, R_2 = CN[65]		50	-	50[b]	-
R_1 = CH_2OAc, R_2 = CN[65]	67	-	-	19[b]	14
R_1 = Me, R_2 = CO_2Me[65]	52	30	-	18	-
R_1 = CH_2OH, R_2 = CO_2Me[65]	70	-	-	18[b]	12
R_1 = Br, R_2 = CN[65]	-	100	-	-	-
R_1 = CH_2OH, R_2 = CHO[65]	30	62[b]	-	8[b]	-
R_1 = SEt, R_2 = CN[65]	-	100	-	-	-
R_1 = TMS, R_2 = Me[82]	66	34	-	-	-
R_1 = TMS, R_2 = hexyl[82]	67	24	-	-	-
R_1 = TMS, R_2 = Bn[82]	75	25	-	-	-
R_1 = TMS, R_2 = CH_2OH[82]	76	24	5	-	-
R_1 = TMS, R_2 = Me[82]	37	53	10	-	-

(a) isomer A and B could not be distinguished   **(b) R_1 and R_2 could not be distinguished**

Figure 1.62: Isomer distribution of disubstituted bullvalenes with unidentical substituents.

	A		B		C		D		E
R_1 = Me, R_2 = n-pent[24]	42	:	30	:	17	:	11	:	-
R_1 = Me, R_2 = Br[65]	25	:	45	:	-	:	25	:	5
R_1 = p-CF$_3$(C$_6$H$_5$), R_2 = 2-thiophene[83]	64	:	36[a]	:		:	-	:	-
R_1 = p-CF$_3$(C$_6$H$_5$), R_2 = 5-pyrimidine[83]	48	:	44[a]	:		:	8	:	-
R_1 = p-CF$_3$(C$_6$H$_5$), R_2 = Ph[83]	59	:	41[a]	:		:	-	:	-
R_1 = Ph, R_2 = (allyl)[23]	68	:	-	:	19	:	13	:	-
R_1 = Ph, R_2 = (butenyl)[23]	59	:	-	:	33	:	14	:	-

(a) isomers B and C could not be distinguished
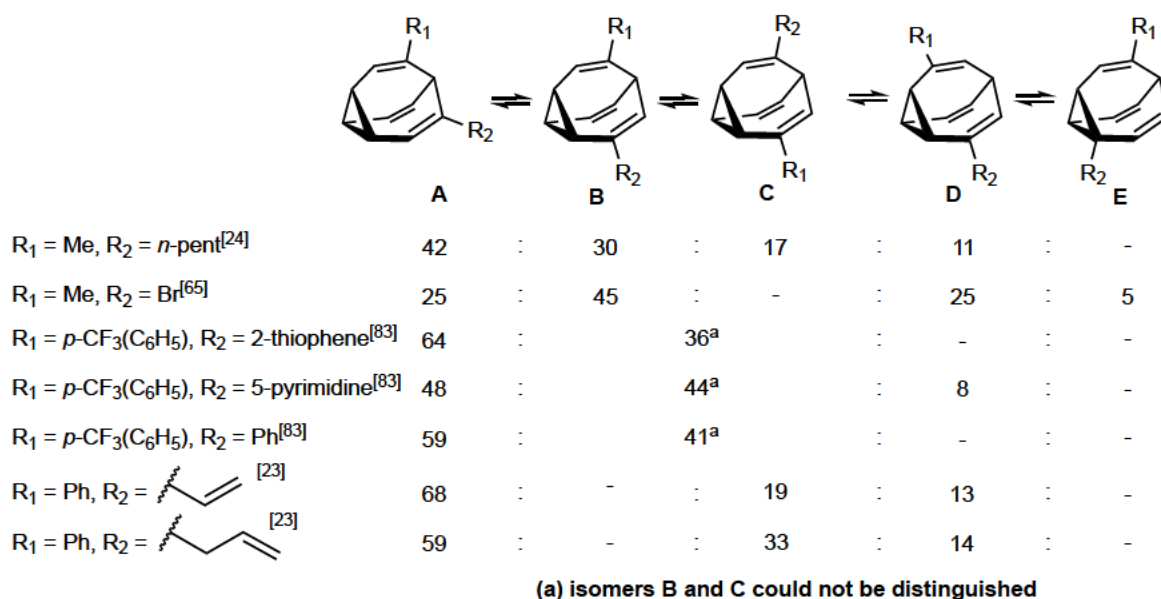
Figure 1.63: Isomer distribution of disubstituted bullvalenes with unidentical substituents.

1.7.3. Trisubstituted bullvalene

Trisubstituted bullvalenes with three different substituents interconvert between 240 isomers, with two un–identical substituents, 120 isomers; and with three identical substituents, 42 isomers. For all trisubstituted bullvalenes, the substituents are attached to the olefinic carbons. The tri– methyl, tri– bromo, and tri– Bpin bullvalenes do not possess a kinetically metastable isomer (Figure 1.64).[72–74,85] Triphenylbullvalene **133** and **176, 179–180** trisubstituted bullvalenes have a kinetically metastable isomer as the major isomer (Figure 1.65).[66,84] In order to communicate with the rest of the of the network, any isomer of this type must pass through two generations of relatively high–energy isomers accompanied with high–energy barriers.[84]
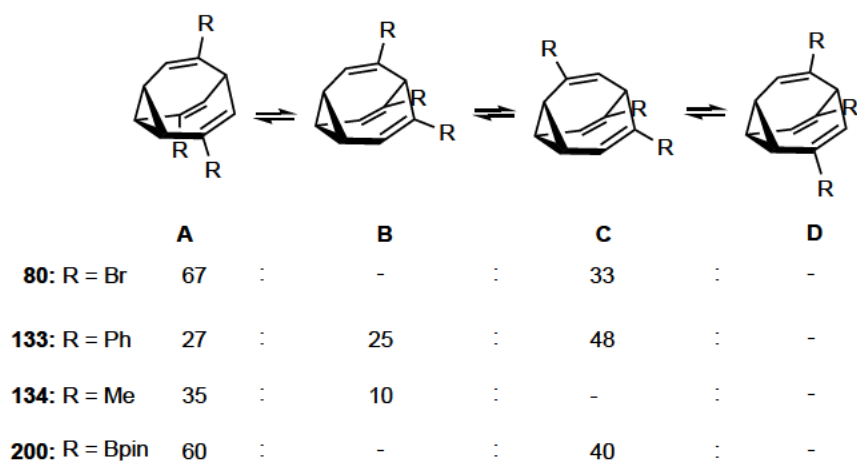
Figure 1.64: Isomer distribution of trisubstituted bullvalene with identical substituents.

	A		B		C		D
80: R = Br	67	:	-	:	33	:	-
133: R = Ph	27	:	25	:	48	:	-
134: R = Me	35	:	10	:	-	:	-
200: R = Bpin	60	:	-	:	40	:	-

176, R = OH
179, R = OTBS
178
180

	A		B		C		D		E		F
176	71	:	29	:	-	:	-	:	-	:	-
$t_{1/2}$	0.67 s										
179	77	:	23	:	-	:	-	:	-	:	-
$t_{1/2}$	0.57 s										
178	64	:	21	:	4	:	5	:	3	:	3
$t_{1/2}$	1.8 h										
180	47	:	35	:	1	:	9	:	2	:	0
$t_{1/2}$	2.9 min										
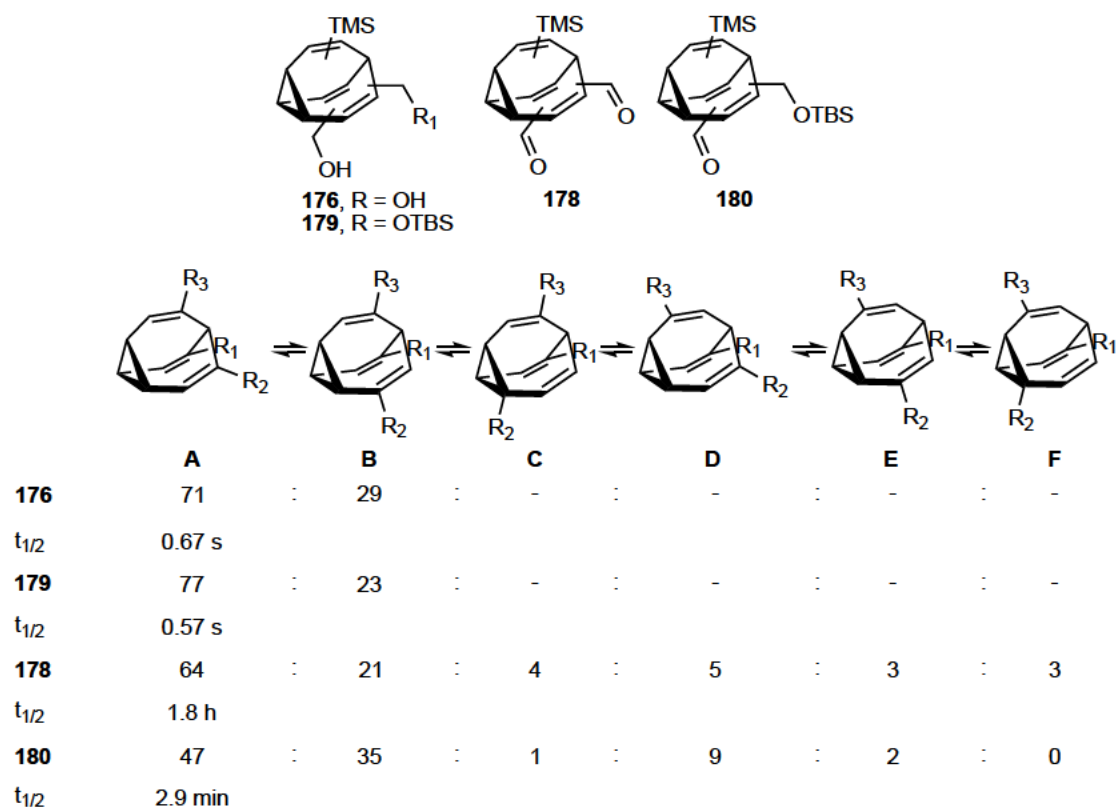
Figure 1.65: Isomer distribution of trisubstituted bullvalenes

1.7.4 Tetrasubstituted bullvalene

Schöder synthesised tetra bromo–, phenyl–, and methyl bullvalene **135–137** and noticed that tetramethyl bullvalene **136** does not possess a kinetically metastable isomer like **135** and **137** (Figure 1.66). The absence of a metastable isomer is due to the small energy differences between isomers containing substituents attached to the cyclopropyl or the apex carbons and the olefinic carbons.

135, R = Br
136, R = Me
137, R = Ph

	A		B		C		D		E		F
135	49	:	8	:	23	:	-	:	-	:	-
$t_{1/2}$/T			90min/40 °C		60min/10 °C						
136	-	:	-	:	-	:	35	:	10	:	55
137	-	:	-	:	-	:	38	:	9	:	53
$t_{1/2}$/T					12.5h/rt						
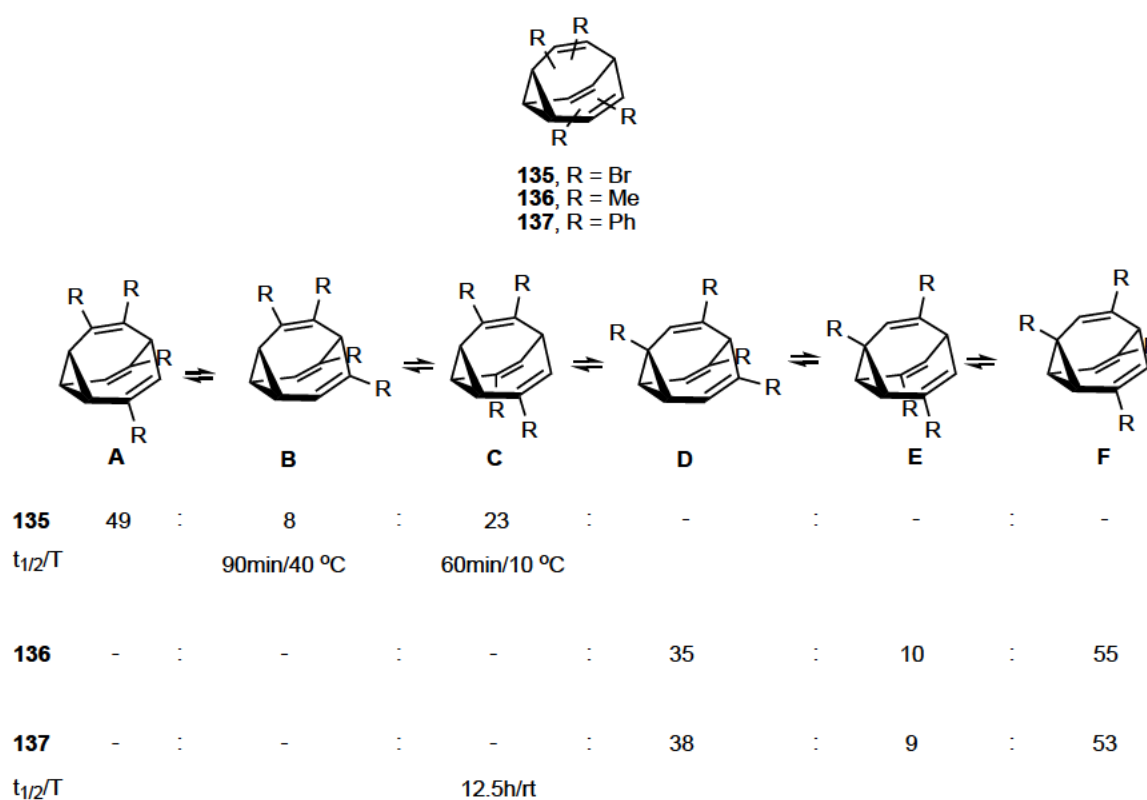
Figure 1.66: Tetrasubstituted bullvalenes.

Bode isolated metastable tetrasubstituted bullvalene **225** by HPLC and determined its half–life as 265 minutes (Figure 1.67).

225

$t_{1/2}/T$ 265min/23 °C
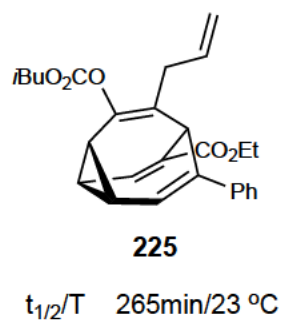
Figure 1.67: Chiral tetrasubstituted bullvalene isolated by Bode.

1.7.5. Penta substituted bullvalene

Pentaphenyl bullvalene exists between two isomers and both have the same half–life (Figure 1.68). Pentabromo bullvalene **137** exists between five isomers. The kinetically metastable isomer **137b** is the slowest and isomer **137e** the fastest to undergo the Cope rearrangement.

137, R = Br
138, R = Ph

	A		B		C		D		E
137	49	:	24	:	54	:	9	:	13
$t_{1/2}/T$			30h/55 °C						
138	40	:	-	:	-	:	60	:	-
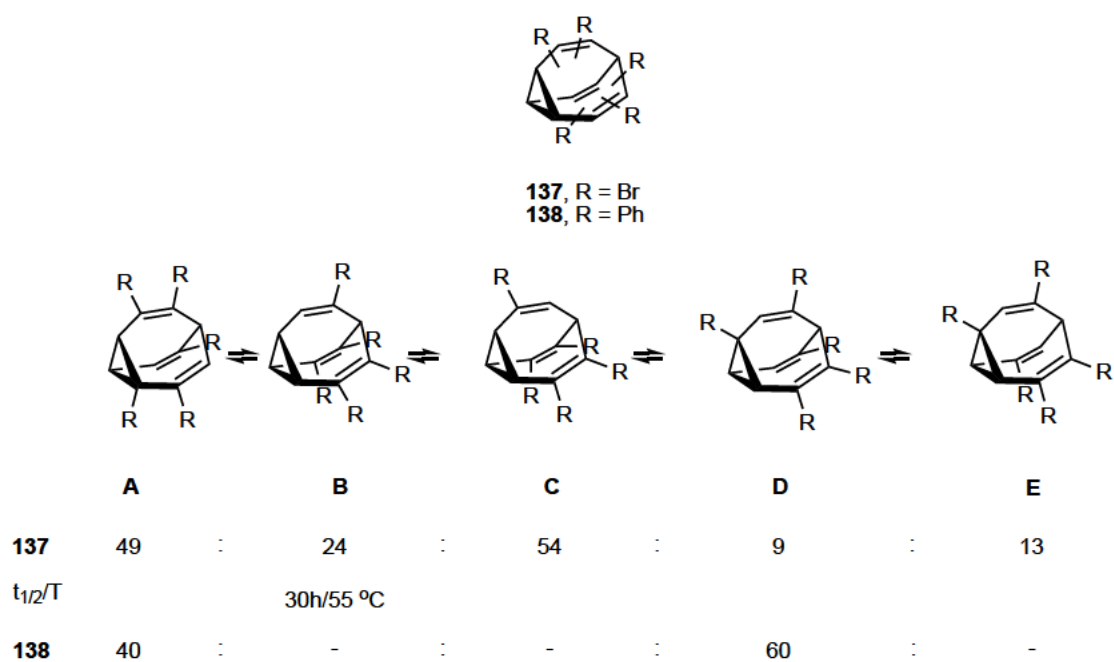
Figure 1.68: Tetrasubstituted bullvalene.

1.7.6. Hexasubstituted bullvalene

Fluxional properties are lost when it comes to hexasubstituted bullvalenes (Figure 1.69). The synthesis of hexabromo bullvalene **141–139** from penta bromobullvalene **137** leads to the isolation of two isomers which cannot be converted into each other. Each hexaphenyl isomer **142–141** that can be formed has the same substitution pattern as hexabromo bullvalene isomers. Here the fluxional behaviour is also lost and the isomers cannot be converted to one another.
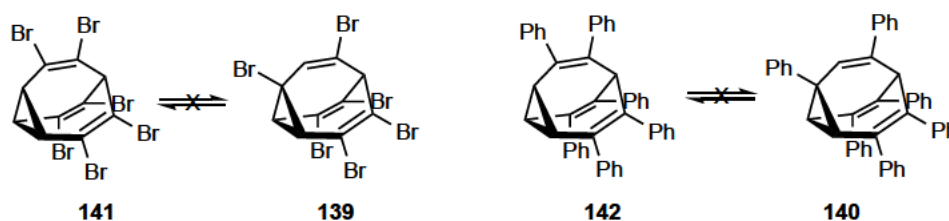
Figure 1.69: Static hexasubstituted bullvalenes.

1.7.7 Annulated bullvalene

Annulated bullvalenes decrease or cease the Cope rearrangement. In most cases the annulated bullvalenes exist between two isomers[94] (Figure 1.70).
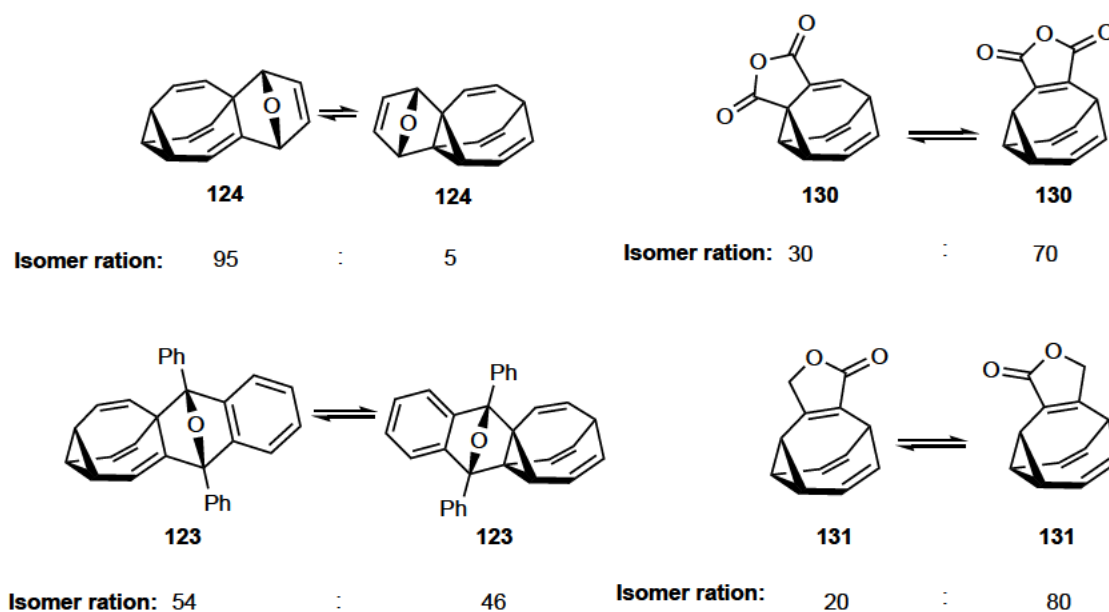
Figure 1.70: Isomer distribution of annulated bullvalenes.

If an aromate is fused to bullvalene, the double bond does not participate in the Cope rearrangement. Therefore, the molecule loses its fluxional property and becomes a static compound (Figure 1.71).[69,87,94]
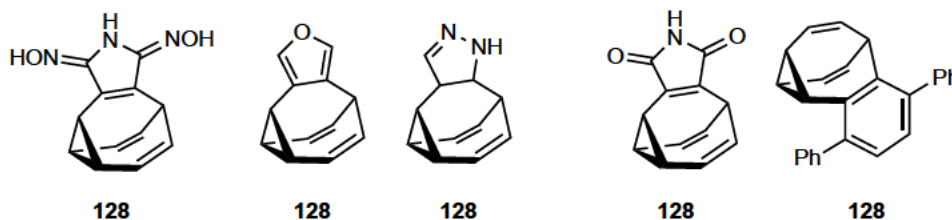
Figure 1.71: Frozen annulated bullvalenes.

As the ring size of the annulated groups increases, conformational flexibility is somewhat restored and bullvalenes are able to access other isomers as demonstrated in a series of crown ether bullvalenes made by Schroder (Figure 1.72).[70,71]

n	A		B		C
132a	95-96	:	-	:	4-5
132b	85-87	:	5	:	6-8
132c	72-74	:	18-20	:	8-10
132d	60-62	:	28-30	:	10
132e	60-65	:	25-30	:	10
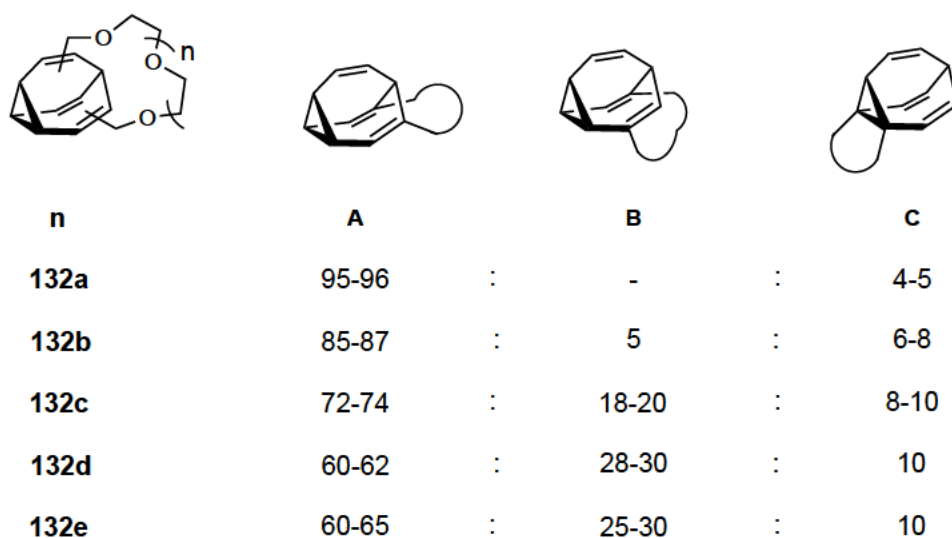
Figure 1.72: Crown ether bullvalene isomer distribution.

1.7.7. Substituted azabullvalene

The number of degenerate isomers of azabullvalene is 28 and not 1.2 million like bullvalene. This is due to the preference of the nitrogen atom for participation in a double bond, thus circumventing its participation in any rearrangement that places the hetero atom in the three–membered ring (Figure 1.73).[87] For instance **204**, **207**, and **212** are static molecules, while the disubstituted azabullvalene **209** exist between 2 isomers.
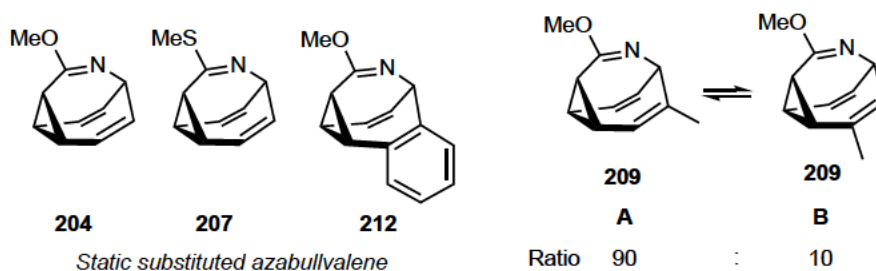
Figure 1.73: Static substituted azabullvalene and fluxional methyl–methoxy–azabullvalene.

Isomer distributions follow predictable patterns whereby substituents typically occupy olefinic positions, with a few exceptions such as fluro groups. As orders of substitution increase, substitution patterns are adopted that minimise steric clash, thus avoiding high energy isomers. This is also reflected by the appearance of metastable isomers, but also the slowing down of the Cope rearrangement when high degrees of substitution are present. This can be to the extreme of the Cope rearrangement stopping as with hexa– substituted bullvalenes. In addition, annulation restricts the Cope rearrangement. However, as overall annulated ring size increases conformational flexibility is restored making it possible to access other isomers.

1.8. Conclusion

Following its initial conception as a unique hypothetical molecule, bullvalene chemistry has witnessed considerable evolution. Initial syntheses of bullvalene and its substituted derivatives were tedious and low yielding, but still, these chemists explored the reactivity of the molecule, undertook detailed NMR analysis to understand its dynamic behaviour both in solution and the solid state, and have contributed a great deal to our modern understanding and interpretation of bullvalenes. Syntheses of the parent hydrocarbon have changed dramatically, with modern catalytic methods providing the ability to access large quantities of bullvalene efficiently. Moreover, modern synthetic methods have allowed for facile access to substituted analogues, opening the possibilities to explore this constitutionally rich hydrocarbon in a range of settings.

Chapter 2

2.1. Introduction

Chapter 2 is a published document: O. Yahiaoui, L. F. Pašteka, B. Judeel, T. Fallon, *Angew. Chem, Int. ed.* **2018**, *57*, 2570–2574.

The shapeshifting ability of bullvalene was theorized by Doering in 1963 and in the same year, Schröder synthesised the molecule in two steps. Schröder's synthesis remained the best despite the poor overall yield (5.6%). Over the years, several groups attempted to optimise the synthesis of bullvalene, but their methods were lengthy and low yielding.

Through a rapid Cope rearrangement bullvalene exists between over 1.2 million degenerate isomers. Substituents on this core structure will explore all possible non–degenerate isomers. Mono substituted bullvalene exists between four isomers and disubstituted bullvalene with unidentical substituents between 30 isomers. The fluxional property of bullvalene is unique and can be advantageous in applications like a molecular sensors, supramolecular chemistry, catalysis etc. Bode and co–workers were the only group to show the benefit of this feature by using diverse tetrasubstituted bullvalenes as a sensor. However, bullvalene is an under explored system, due to its low yielding and/or lengthy synthesis.

We uncovered a hidden strategy for the synthesis of bullvalene and substituted bullvalene, by combining two ideas (Figure 2.1). The first idea dates back to the 1970s where Jones and Scott investigated the photorearrangement of bullvalene and discovered the high conversion and clean reaction of a tetraene **4** ($R_1 = R_2 = H$) to bullvalene. The second idea is based on the work of Buono who synthesised substituted tetraenes **4** though a [6+2] cobalt catalysed cycloaddition reaction between substituted alkynes and COT. The combination of both ideas was the key strategy for the synthesis of bullvalene, as well as mono– and disubstituted bullvalene, in only two steps. Our collaborator Lukáš F. Pašteka developed a toolbox to predict the isomer distribution of substituted bullvalenes and a reaction graph to gain insight into their dynamic behaviour.
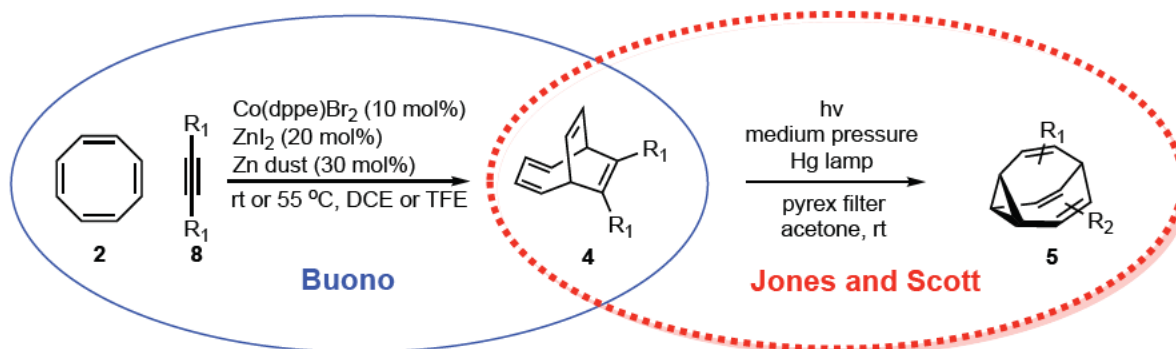
Figure 2.1: Our strategy for the synthesis of bullvalene, mono–, and di– substituted bullvalene based on Jones and Scott, and Buono's methods.

Statement of Authorship

Title of Paper	Synthesis and Analysis of Substituted Bullvalenes
Publication Status	☑ Published ☐ Accepted for Publication ☐ Submitted for Publication ☐ Unpublished and Unsubmitted work written in manuscript style
Publication Details	O. Yhaioaui, Lukáš F. Pašteka, Bernadette Judeel, and Thomas Fallon, Synthesis and Analysis of Substituted Bullvalenes, Angew. Chem. Int. ed. 2018, 57, 2570-2574.

Principal Author

Name of Principal Author (Candidate)	Oussama Yahiaoui
Contribution to the Paper	Performed all the experiments and characterisation of compounds, wrote also the experimental section.
Overall percentage (%)	30%
Certification:	This paper reports on original research I conducted during the period of my Higher Degree by Research candidature and is not subject to any obligations or contractual agreements with a third party that would constrain its inclusion in this thesis. I am the primary author of this paper.
Signature	Date 19-05-20

Co-Author Contributions

By signing the Statement of Authorship, each author certifies that:

i.   the candidate's stated contribution to the publication is accurate (as detailed above);

ii.   permission is granted for the candidate in include the publication in the thesis; and

iii. the sum of all co-author contributions is equal to 100% less the candidate's stated contribution.

Name of Co-Author	Lukáš F. Pašteka.
Contribution to the Paper	Performed all the DFT calculations. A corresponding author
Signature	Date 14 May 2020

Name of Co-Author	Bernadette Judeel
Contribution to the Paper	Performed the big scale bullvalene synthesis.
	Bernadette was an intern in the group under the supervision of O.T. at Massey University in NZ. Unfortunately we are unable
Signature to contact her at this time.	Date 19.05-20

Name of Co-Author	Thomas Fallon		
Contribution to the Paper	Supervised the project and wrote the manuscript. A corresponding author.		
Signature		Date	19-5-20

Fluxional Molecules

Synthesis and Analysis of Substituted Bullvalenes

Oussama Yahiaoui, Lukáš F. Pašteka,* Bernadette Judeel, and Thomas Fallon*
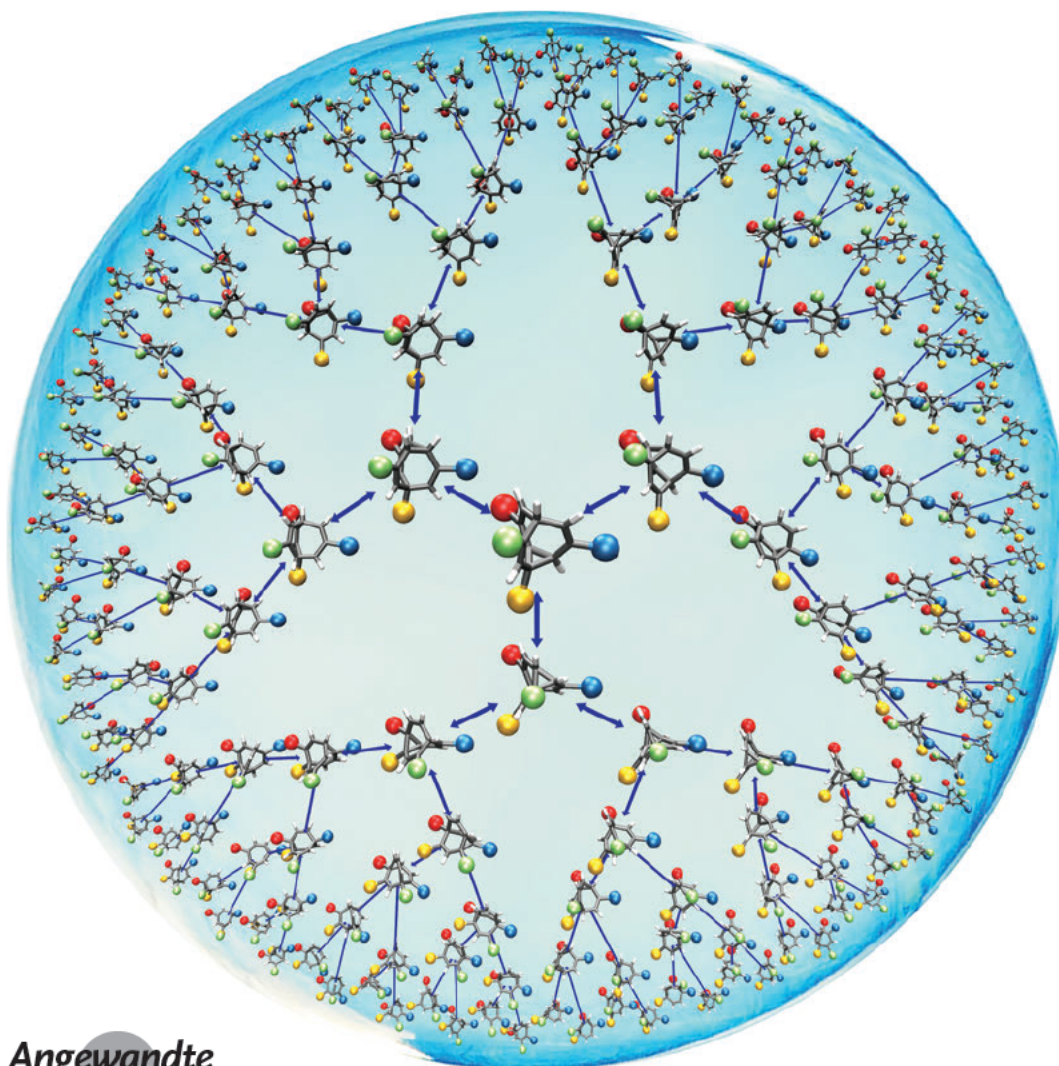
Angewandte
Chemie

© 2018 Wiley VCH Verlag GmbH & Co. KGaA, Weinheim

GDCh

Communications

Angewandte *Chemie*
International Edition

Abstract: Herein we detail a practical synthesis of bullvalene and a variety of mono- and disubstituted analogues through cobalt-catalysed [6+2] cycloaddition of cyclooctatetraene to alkynes, followed by photochemical di-π-methane rearrangement. The application of isomer-network analysis, coupled with quantum-chemical calculations, provides a powerful automated tool for predicting the properties of bullvalene isomer networks.

Bullvalene (**1**) is the archetypal fluxional molecule. By virtue of rapid Cope rearrangements it exists within an ensemble of more than 1.2 million degenerate isomers (Scheme 1a). With the exception of the barbaralyl cations,[1]
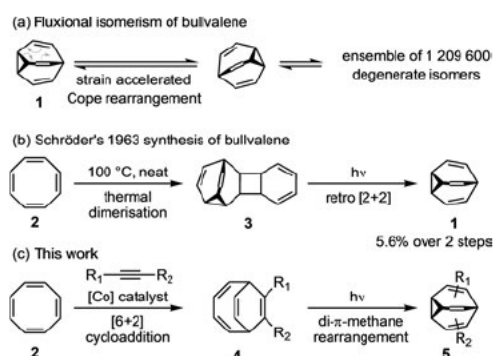
Scheme 1. a) Fluxional isomerism of bullvalene. b) Schröder's original synthesis of bullvalene. c) This study.

this property of total degeneracy is unique. Substituents bound to this core structure will explore all possible structural isomers. This geometrically rich fluxional behaviour gives substituted bullvalenes a potentially significant place within the rapidly developing context of dynamic covalent chemistry.[2]

Doering and Roth first predicted bullvalene in 1963.[3] Later that year, Schröder serendipitously encountered the structure while studying the photochemistry of cycloocta-

[*] O. Yahiaoui, B. Judeel, Dr. T. Fallon
Institute of Natural and Mathematical Sciences, Massey University
1/5 University Avenue, Albany, Auckland 0632 (New Zealand)
E-mail: t.fallon@massey.ac.nz

Dr. L. F. Pašteka
Centre for Theoretical Chemistry and Physics, NZIAS, Massey University, Oaklands Road, Albany, Auckland 0632 (New Zealand)
and
Department of Physical and Theoretical Chemistry, Faculty of Natural Sciences, Comenius University, Ilkovičova 6, Bratislava (Slovakia)
E-mail: lukas.f.pasteka@gmail.com

Dr. L. F. Pašteka
Centre for Advanced Study, Norwegian Academy of Science and Letters, Drammensveien 78, NO-0271 Oslo (Norway)

Supporting information and the ORCID identification number(s) for the author(s) of this article can be found under:
https://doi.org/10.1002/anie.201712157.

tetraene (COT) dimers (Scheme 1b).[4] Despite the low overall yield (5.6%), this first synthesis has remained the best. It formed the basis of extensive studies into bullvalene chemistry by Schröder and co-workers, and the preparation of many substituted examples.[5] Rational synthetic strategies towards bullvalene have also been devised by the research groups of Doering[6] and Serratosa,[7] both employing a trans-annular cyclopropanation as a key step. Recently, Ferrer and Echavarren introduced a new approach based on the gold-catalysed synthesis of barbaralones.[8] Bode and co-workers developed a synthesis of tetrasubstituted bullvalenes and demonstrated supramolecular opportunities, including adaptive binding and sensing.[9] This exciting new work is, however, limited by the lengthy synthetic route to these heavily substituted bullvalenes.

The photochemical di-π-methane rearrangement[10] of bicyclo[4.2.2]deca-2,4,7,9-tetraene (BDT) systems is a rare class of transformations. The parent hydrocarbon **4a** was first prepared by Jones and Scott through a low-yielding photo-isomerisation of bullvalene.[11] It was found, however, that **4a** slowly but cleanly photoisomerises back to bullvalene when irradiated with a medium-pressure mercury lamp behind a Pyrex filter. This type of di-π-methane rearrangement was instrumental in the classic synthesis of substituted azabullvalenes by Paquette et al.,[12] as well as an attempted synthesis of diazabullvalene.[13]

Cobalt(I)-catalysed formal cycloaddition reactions are powerful transformations in organic synthesis.[14,15] In 2006, Buono and co-workers reported that cyclooctatetraene undergoes [6+2] cycloaddition reactions with alkynes to give substituted BDTs in the presence of a CoI$_2$(dppe)/ZnI$_2$/Zn catalyst system.[16] This reaction has recently been reevaluated, revealing that a variety of Co^{II} salts are viable precatalysts.[17]

With access to substituted BDTs, we foresaw a rapid two-step synthetic path to mono- and disubstituted bullvalenes. A range of BDTs were prepared by adaptation of the reported protocols (Scheme 2). Interestingly, acetylene gas also participates in this reaction to give the parent hydrocarbon (84% yield, 12 g scale).[18]

With BDT precursors in hand, we investigated photo-isomerisation to the corresponding bullvalenes. Irradiation of solutions of **4a–h** in acetone (150 W medium-pressure mercury lamp, Pyrex glassware) led to the corresponding bullvalenes in fair to very good yield (Scheme 3). In some cases long reaction times were needed. The synthesis of

4a: R$_1$, R$_2$ = H, H, 84%
4b: R$_1$, R$_2$ = Me, H, 70%
4c: R$_1$, R$_2$ = n-Hex, H, 90%
4d: R$_1$, R$_2$ = CH$_2$OH, H, 86%
4e: R$_1$, R$_2$ = Bn, H, 91%
4f: R$_1$, R$_2$ = SiMe$_3$, H, quant.
4g: R$_1$, R$_2$ = CH$_2$OH, CH$_2$OH, 80%
4h: R$_1$, R$_2$ = Me, n-pent, 87%
4i: R$_1$, R$_2$ = Ph, H, 63%

Scheme 2. Cobalt-catalysed synthesis of bicyclo[4.2.2]deca-2,4,7,9-tetraenes. Bn = benzyl, dppe = 1,2-bis(diphenylphosphanyl)ethane.

Scheme 3. Photochemical synthesis of bullvalenes.

Figure 1. Monosubstituted bullvalene network analysis and populated isomers.

bullvalene itself proceeded in 71% yield (8 g isolated, 60% yield from COT). This procedure avoids the low-yielding thermal dimerization of COT, and provides practical access to the parent hydrocarbon. A variety of monosubstituted bullvalenes **5b–f** were prepared, as well as the bis(methylenehydroxy)bullvallene **5g** and methyl(*n*-pentyl)bullvalene **5h**.

Interestingly, when phenyl-substituted BDT **4i** was irradiated under the standard conditions, phenyl "lumibullvalene" **6** was isolated in 63% yield (Scheme 4). None of the

Scheme 4. Synthesis of phenyl-substituted lumibullvalene **6**.

expected phenylbullvalene could be detected in the reaction mixture. Presumably, the di-π-methane rearrangement proceeds, but through an alternate path to give phenyl-substituted "isolumibullvalene" **7**, which would rapidly undergo a cyclopropane-accelerated Cope rearrangement to give phenyl lumibullvalene.[19] This switch in reactivity is not yet understood, and may preclude the use of our strategy for the synthesis of aryl-substituted bullvalenes. However, access to substituted lumibullvalene frameworks may prove useful.

As dynamic ensembles of exchanging isomers, bullvalenes represent a conceptually intriguing and challenging analytical problem. Monosubstituted bullvalenes have four possible isomers; disubstituted networks have either 15 isomers (identical substituents) or 30 isomers (unique substituents). With further substitution the level of complexity rapidly escalates.[20]

Substituted bullvalenes represent closed reaction graphs.[21] Bode introduced a convenient isomer coding system (Figure 1) and algorithm that enumerates the inter-

connections of any bullvalene substitution pattern.[9] Building on this method, we have developed a program that evaluates any possible substituted bullvalene network and performs quantum-chemical energy calculations on all objects within the reaction graph.

Using the required substituent geometries as input, our newly developed algorithm generates the full rearrangement network with corresponding codes for all isomers and interconnecting transition states. Furthermore, enantiomeric pairs are identified, and starting geometries for all non-degenerate species are produced. These geometries are subsequently optimized in two steps with an increasing level of theory through the interface to the program package ORCA 4.0.[22] In the first step, large-scale screening of rotamers is performed and the lowest-energy rotamer is chosen for each isomer by employing a combination of inexpensive semiempirical and density functional theory (DFT) methods. In the second step, geometries of all isomers are fully optimized using DFT. Finally, for the optimized structures, single-point energies are calculated using the highest level of theory with or without a solvation model. A detailed account of the computational methods used to obtain the presented results can be found in the Supporting Information.

Experimental isomer ratios were determined on the basis of low-temperature NMR measurements. For monosubstituted bullvalenes **5b–f** the analysis is routine (Figure 2). In all cases, the computationally predicted ratios are consistent with experiment.[23]

For disubstituted bullvalenes **5g** and **5h**, the complexity of the mixtures and signal overlap necessitated the careful interpretation of 2D NMR experiments. The analysis of bis(methylenehydroxy)bullvalene **5g** proved to be most challenging and revealed a dynamic ensemble of six populated isomers (Figure 2a).[24] For this system, the isomer distribution is remarkably flat.[5f] In fact, all possible isomers that do not have a vicinal arrangement of substituents, or a substituent at the apex position, were found to be populated. In the case of methyl(*n*-pentyl)bullvalene **5h**, the four possible isomers which retain the substituents connected to alkenes were found to be populated (Figure 2b). These experimental ratios are all consistent with a computational survey of isomer stability.

(a) Populated isomers of bis(methylenehydroxy)bullvalene **5g**

| | | | | | | |
experimental: 44 : 23 : 14 : 9 : 6 : 5
calculated: 91 : 7 : 0 : 2 : 0 : 0   6 other unique isomers

(b) Populated isomers of methyl(n-pentyl)bullvalene **5h**

experimental: 42 : 30 : 17 : 11
calculated: 79 : 11 : 6 : 3   26 other isomers

(c) Reaction graph of methyl(n-pentyl)bullvalene **5h**
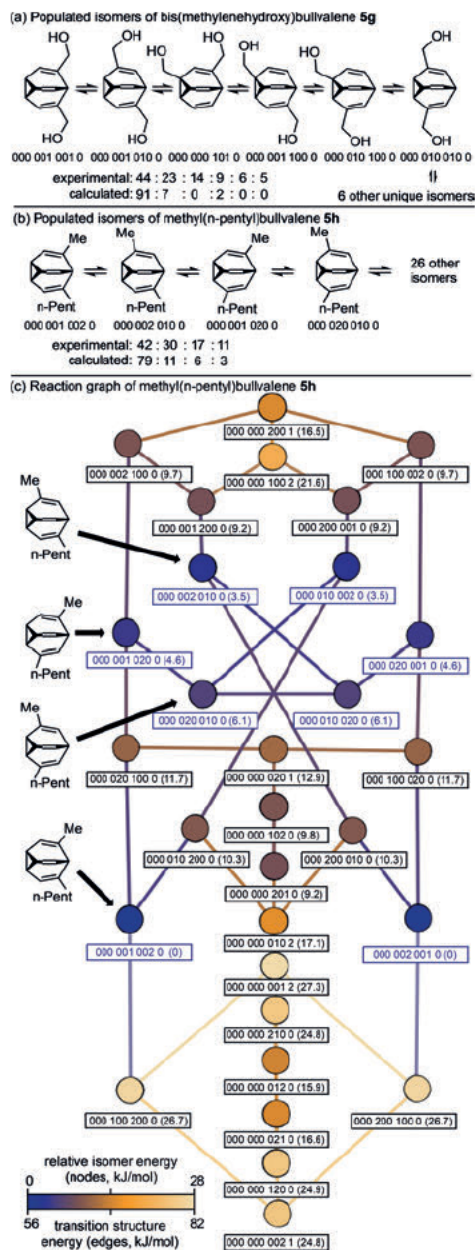
Figure 2. a) Experimental and computationally predicted populated isomers of bis(methylenehydroxy)bullvalene **5g**. b) Experimental and computationally predicted populated isomers of methyl(n-pentyl)bullvalene **5h**. c) Reaction graph of **5h**. The nodes shaded blue correspond to the populated isomers. A mirror plane of symmetry bisects the graph vertically and relates the enantiomer pairs.

Our computational toolbox also allows for the generation of reaction graph diagrams. This is a convenient method to visualise the interconnectivity, and energy profile, of any given bullvalene network. An example is shown for the 30 possible isomers of bullvalene **5h** (Figure 2c). Nodes represent isomers, and edges transition structures. A vertical plane of symmetry bisects the diagram and relates enantiomers. This technique aids in highlighting the nonpopulated but low-lying isomers, as well as giving an overview of the kinetic parameters of rearrangement. In future, these features will become valuable in the analysis of bullvalene ensembles in response to external stimuli.

To conclude, we have developed a two-step synthesis of bullvalene itself and substituted derivatives: the shortest synthesis of any substituted bullvalenes, and the most practical method for the preparation of the parent structure. Our network analysis algorithm enables rapid assessment of the energy landscape and interconnections of any bullvalene isomer ensemble. DFT calculations predicted the ratios of populated isomers in good agreement with experiment.

Conflict of interest

The authors declare no conflict of interest.

[1] a) P. Ahlberg, D. L. Harris, S. Winstein, J. Am. Chem. Soc. 1970, 92, 2146–2147; b) P. Ahlberg, J. B. Grutzner, D. L. Harris, S. Winstein, J. Am. Chem. Soc. 1970, 92, 3478–3480; c) P. Ahlberg, D. L. Harris, S. Winstein, J. Am. Chem. Soc. 1970, 92, 4454–4456; d) C. Engdahl, P. Ahlberg, J. Phys. Org. Chem. 1990, 3, 349–357.
[2] For recent reviews, see: a) S. J. Rowan, S. J. Cantrill, G. R. L. Cousins, J. K. M. Sanders, J. F. Stoddart, Angew. Chem. Int. Ed. 2002, 41, 898–952; Angew. Chem. 2002, 114, 938–993; b) P. T. Corbett, J. Leclaire, L. Vial, K. R. West, J.-L. Wietor, J. K. M. Sanders, S. Otto, Chem. Rev. 2006, 106, 3652–3711; c) Y. Jin, C. Yu, R. J. Denman, W. Zhang, Chem. Soc. Rev. 2013, 42, 6634–6654.
[3] W. von E. Doering, W. R. Roth, Tetrahedron 1963, 19, 715–737.

Communications

[4] G. Schröder, *Angew. Chem. Int. Ed. Engl.* **1963**, *2*, 481–482; *Angew. Chem.* **1963**, *75*, 722–722.

[5] For an early review, see: a) G. Schröder, J. F. M. Oth, *Angew. Chem. Int. Ed. Engl.* **1967**, *6*, 414–423; *Angew. Chem.* **1967**, *79*, 458–467; For further highlights of Schröder's synthetic campaign, see: b) G. Schröder, *Chem. Ber.* **1964**, *97*, 3140–3149; c) J. F. M. Oth, R. Merenyi, J. Nielsen, G. Schröder, *Chem. Ber.* **1965**, *98*, 3385–3400; d) J. F. M. Oth, R. Merényi, G. Engel, G. Schröder, *Tetrahedron Lett.* **1966**, *7*, 3377–3382; e) J. F. M. Oth, E. Machens, H. Roettele, G. Schröder, *Justus Liebigs Ann. Chem.* **1971**, *745*, 112–123; f) K. Sarma, W. Witt, G. Schröder, *Chem. Ber.* **1986**, *119*, 2339–2349.

[6] W. von E. Doering, B. M. Ferrier, E. T. Fossel, J. H. Hartenst, M. Jones, Jr., G. Klumpp, R. M. Rubin, M. Saunders, *Tetrahedron* **1967**, *23*, 3943–3963.

[7] J. Font, F. Lopez, F. Serratosa, *Tetrahedron Lett.* **1972**, *13*, 2589–2590.

[8] S. Ferrer, A. M. Echavarren, *Angew. Chem. Int. Ed.* **2016**, *55*, 11178–11182; *Angew. Chem.* **2016**, *128*, 11344–11348.

[9] a) A. R. Lippert, V. L. Keleshian, J. W. Bode, *Org. Biomol. Chem.* **2009**, *7*, 1529–1532; b) A. R. Lippert, A. Naganawa, V. L. Keleshian, J. W. Bode, *J. Am. Chem. Soc.* **2010**, *132*, 15790–15799; c) M. He, J. W. Bode, *Proc. Natl. Acad. Sci. USA* **2011**, *108*, 14752–14756; d) K. K. Larson, M. He, J. F. Teichert, A. Naganawa, J. W. Bode, *Chem. Sci.* **2012**, *3*, 1825–1828; e) J. F. Teichert, D. Mazunin, J. W. Bode, *J. Am. Chem. Soc.* **2013**, *135*, 11314–11321; f) M. He, J. W. Bode, *Org. Biomol. Chem.* **2013**, *11*, 1306–1317.

[10] For early studies, see: a) H. E. Zimmerman, G. L. Grunewald, *J. Am. Chem. Soc.* **1966**, *88*, 183–184; b) H. E. Zimmerman, R. W. Binkley, R. S. Givens, M. A. Sherwin, *J. Am. Chem. Soc.* **1967**, *89*, 3932–3933; c) H. E. Zimmerman, P. S. Mariano, *J. Am. Chem. Soc.* **1969**, *91*, 1718–1727.

[11] a) M. Jones, L. T. Scott, *J. Am. Chem. Soc.* **1967**, *89*, 150–151; b) M. Jones, S. D. Reich, L. T. Scott, *J. Am. Chem. Soc.* **1970**, *92*, 3118–3126.

[12] L. A. Paquette, J. R. Malpass, R. Krow, T. J. Barton, *J. Am. Chem. Soc.* **1969**, *91*, 5296–5306.

[13] A. B. Evnin, R. D. Miller, G. R. Evanega, *Tetrahedron Lett.* **1968**, *9*, 5863–5865.

[14] For pioneering reports, see: a) G. Hilt, T. J. Korn, *Tetrahedron Lett.* **2001**, *42*, 2783–2785; b) W. Hess, J. Treutwein, G. Hilt, *Synthesis* **2008**, 3537–3562; c) G. Hilt, K. I. Smolko, *Angew. Chem. Int. Ed.* **2003**, *42*, 2795–2797; *Angew. Chem.* **2003**, *115*, 2901–2903.

[15] For reviews of this class of catalysis, see: a) P. Gandeepan, C.-H. Cheng, *Acc. Chem. Res.* **2015**, *48*, 1194–1206; b) W. Hess, J. Treutwein, G. Hilt, *Synthesis* **2008**, 3537–3562; c) P. Röse, G. Hilt, *Synthesis* **2016**, *48*, 463–492.

[16] M. Achard, M. Mosrin, A. Tenaglia, G. Buono, *J. Org. Chem.* **2006**, *71*, 2907–2910.

[17] V. A. D'yakonov, G. N. Kadikova, L. U. Dzhemileva, G. F. Gazizullina, I. R. Ramazanov, U. M. Dzhemilev, *J. Org. Chem.* **2017**, *82*, 471–480.

[18] We could find only one report of acetylene used in a cobalt-catalysed cycloaddition reaction: I.-F. Duan, C.-H. Cheng, J.-S. Shaw, S.-S. Cheng, K. F. Liou, *J. Chem. Soc. Chem. Commun.* **1991**, 1347–1348.

[19] a) S. Masamune, K. Hojo, R. T. Seidner, *J. Am. Chem. Soc.* **1970**, *92*, 6641–6642; b) J. Dressel, P. D. Pansegrau, L. A. Paquette, *J. Org. Chem.* **1988**, *53*, 3996–4000.

[20] In fact, for two or more unique substituents, N_{sub}, the total numbers of isomers, N_{iso}, and interconnecting transition states, N_{TS}, follow the relations: $N_{iso} = \frac{1}{3}\frac{10!}{(10-N_{sub})!}$, $N_{TS} = \frac{1}{2}\frac{10!}{(10-N_{sub})!}$

[21] J. Brocas, *J. Math. Chem.* **1994**, *15*, 389–395.

[22] F. Neese, *WIREs Comput. Mol. Sci.* **2012**, *2*, 73.

[23] For the disubstituted bullvalenes **5g** and **5h** our ratio of isomers was determined by a comparison of like ^{13}C signals and should be regarded as indicative rather than quantitative.

[24] This analysis included a range of high-resolution heteronuclear correlation experiments, including HSQC-TOCSY, H2BC, and HMBC, as well as a very high resolution HSQC spectrum from which high-quality carbon-resolved 1D proton spectra of each isomer could be extracted and reconstructed (see the Supporting Information for details).

2.2 Conclusion and outline

Our strategy for the synthesis of bullvalene and substituted bullvalenes, alongside the design of a toolbox to predict isomer distribution and draw reaction graphs, is an enormous innovation in this field.

Easy synthetic access to these molecules will open up new concepts in dynamic covalent chemistry. The ability to make substituted bullvalene libraries, whereby each member is itself a dynamic library of structures, will allow the exploration of large areas of chemical space. In Figure 2.2, the hydroxyl group of **5g** can be converted to three different functional groups, oxidation to the aldehyde **6**, activation by conversion to a leaving group **7**, or performing a direct conjugation **8**.
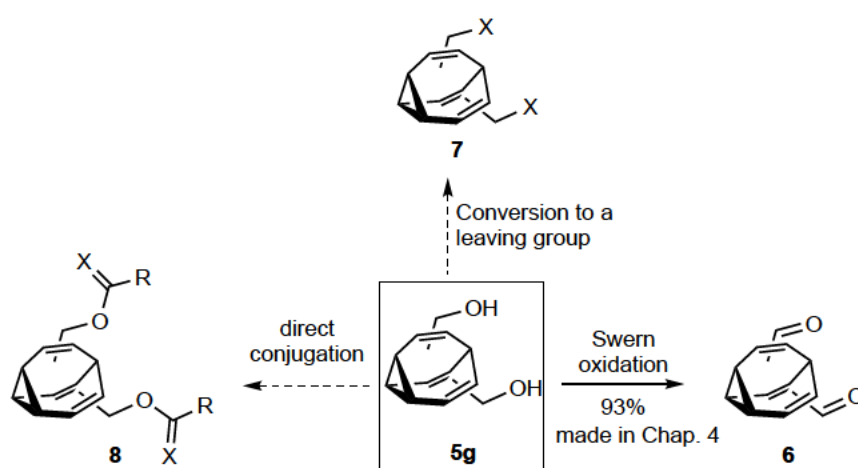
Figure 2.2: Functionalization of diol–bullvalene **5g**.

Despite the efficiency of our method, a limitation emerges in the synthesis of trisubstituted bullvalenes. Heterogenous trisubstituted bullvalenes exist between 240 isomers and the study of their isomer distribution is intriguing. As shown in the introduction, triphenyl–, trimethyl–, and tribromo bullvalene are the only trisubstituted bullvalenes previously reported.[72–74] Interestingly, triphenyl bullvalene possess a major kinetically metastable isomer, which is in slow exchange with the other isomers.

In the next chapter we extend our synthetic methods to trisubstituted bullvalene and explore their intriguing kinetic properties.

Chapter 3

3.1. Introduction

Chapter 3 is a published document: O. Yahiaoui, L. F. Pašteka, C. J. Blake, C. G. Newton, T. Fallon, *Org. Lett.* **2019**, *21*, 9574–9578.

In the previous chapter, we claimed a limitation in our method for the synthesis of trisubstituted bullvalenes; that is the intrinsic limitation in the number of substituents on acetylene. Hence, we overcome this problem by introducing a trimethyl silyl group to COT to procure COT–TMS. Using our synthetic strategy and with COT–TMS in hand, we synthesised analogous disubstituted bullvalenes and for the first time heterogenous trisubstituted bullvalenes. The appearance of a kinetically metastable major isomer among all trisubstituted bullvalenes was investigated using DFT calculations and kinetic simulations. Furthermore, we explored a survey of the thermodynamic and kinetic landscapes through computational studies.

An additional discussion section of unreported results from this project is included after the manuscript.

Statement of Authorship

Title of Paper	Network Analysis of Substituted Bullvalenes
Publication Status	☑ Published ☐ Accepted for Publication ☐ Submitted for Publication ☐ Unpublished and Unsubmitted work written in manuscript style
Publication Details	O. Yahiaoui, L. F. Pašteka, C. J. Blake, C. G. Newton, T. Fallon, Network Analysis of Substituted Bullvalenes org. Lett. 2019, 21, 9574-9578.

Principal Author

Name of Principal Author (Candidate)	Oussama Yahiaoui
Contribution to the Paper	Performed all the experiments and characterisation of compounds.
Overall percentage (%)	40%
Certification:	This paper reports on original research I conducted during the period of my Higher Degree by Research candidature and is not subject to any obligations or contractual agreements with a third party that would constrain its inclusion in this thesis. I am the primary author of this paper.
Signature	Date 18-05-20

Co-Author Contributions

By signing the Statement of Authorship, each author certifies that:

    i.   the candidate's stated contribution to the publication is accurate (as detailed above);

    ii.   permission is granted for the candidate in include the publication in the thesis; and

    iii.   the sum of all co-author contributions is equal to 100% less the candidate's stated contribution.

Name of Co-Author	Lukáš F. Pašteka.
Contribution to the Paper	Performed all the DFT calculations. A corresponding author
Signature	Date 14 May 2020

Name of Co-Author	C. G. Newton
Contribution to the Paper	Revised manuscript
Signature	Date 19-5-2020

Name of Co-Author	C J Blake		
Contribution to the Paper	Used NMR machine to measure samples		
Signature		Date	14 May 2020

Name of Co-Author	Thomas Fallon		
Contribution to the Paper	Supervised the project and wrote the manuscript. A corresponding author.		
Signature		Date	19-5-20

Network Analysis of Substituted Bullvalenes

Oussama Yahiaoui,[†,‡] Lukáš F. Pašteka,*[,§] Christopher J. Blake,[‖] Christopher G. Newton,[†] and Thomas Fallon*[,†,‡]

[†]Department of Chemistry, The University of Adelaide, Adelaide, SA 5005, Australia
[‡]Institute of Natural and Mathematical Sciences, Massey University, Auckland 0632, New Zealand
[§]Department of Physical and Theoretical Chemistry, Faculty of Natural Sciences, Comenius University, Bratislava, Slovakia
[‖]Research School of Chemistry, Australian National University, Canberra, ACT 0200, Australia

● *Supporting Information*

ABSTRACT: Substituted bullvalenes are dynamic shape-shifting molecules that exist within complex reaction networks. Herein, we report the synthesis of di- and trisubstituted bullvalenes and investigate their dynamic properties. Trisubstituted bullvalenes share a common major isomer which shows kinetic metastability. A survey of the thermodynamic and kinetic landscapes through computational analysis together with kinetic simulation provides a map of the internal dynamics of these systems.
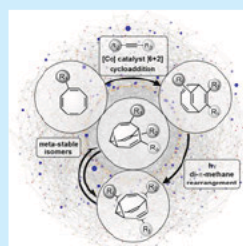
More than half a century since its prediction and initial preparation,[1,2] bullvalene (**1**) remains a source of continued intrigue. This archetypal fluxional molecule exists as an ensemble of 1 209 600 degenerate isomers through rapid Cope rearrangements (Scheme 1a). This property of *total*

Scheme 1. (a) Total Degeneracy of Bullvalene and (b) Our Synthetic Route to Trisubstituted Bullvalenes
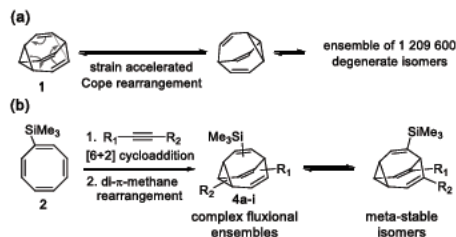
degeneracy is unique among stable organic structures.[3] Substituted bullvalenes are particularly interesting, as degeneracy is lost and substituents will spontaneously explore all possible structural arrangements.

Within the rapidly advancing context of dynamic covalent chemistry,[4] the unimolecular shape-shifting nature of bullvalene suggests a range of potential applications in medicinal chemistry and molecular devices. In a series of reports, the Bode group has explored these concepts,[5] most notably in the construction of a fluxional polyol sensing array.[5e] However, the

rational design of applications built on fluxional molecules remains underdeveloped.

Heavily substituted bullvalenes represent enormous reaction networks with hundreds or even thousands of unique isomers. However, the overall structure and dynamics of such systems will ultimately be governed by a small subset of low-energy isomers and isomerization pathways. A more detailed understanding of the internal dynamics of bullvalene networks will help to advance these systems toward viable applications.

The activation energy of bullvalene isomerization was first determined by Saunders at 49.4 ± 0.4 kJ/mol using VT-NMR measurements.[6] Substituted bullvalenes present increasingly complex kinetic landscapes. The only detailed kinetic study of a substituted bullvalene was by Luz who experimentally determined the kinetic parameters of all reactions within the network of fluorobullvalene.[7]

A picture of the internal energy landscapes of substituted bullvalenes has generally come from measuring the distributions of populated isomers using low-temperature NMR studies and assuming rapid equilibration at room temperature. Occasionally metastable isomers have been observed and even isolated by recrystallization[8] or chromatography.[5c] Foremost of these is a tetrasubstituted bullvalene encountered by Bode. The stability of this structure was rationalized through a computational analysis of the local network environment.[5f]

The synthesis of substituted bullvalenes has seen renewed interest with important contributions from the Bode[5] and

Echavarren[9] groups. We recently reported an efficient two-step synthetic protocol for the synthesis of mono- and di-substituted bullvalenes.[10] The method employs cobalt-catalyzed [6 + 2] cycloaddition reactions of cyclooctatetraene[11] followed by photochemical di-π-methane rearrangement.[12] Alongside our synthetic work, we developed a computational toolbox to automate the network analysis of substituted bullvalenes and generate input structures for quantum chemical calculations for all objects in any given network. This provides a global picture of bullvalene energy landscapes.

In this paper, we extend our synthetic protocol to the preparation of trisubstituted bullvalenes through the use of a substituted cyclooctatetraene (Scheme 1b). This includes the first synthesis of heterogeneously trisubstituted bullvalenes, objects of considerable dynamic complexity, that surprisingly all share a common metastable isomer. Computational analysis coupled with kinetic simulations help rationalize this general kinetic feature.

The synthesis employs a cobalt-catalyzed [6 + 2] cyclo-addition of trimethylsilylcyclooctatetraene 2[13] and a range of substituted alkynes (Scheme 2). The bicyclo[4.2.2]deca-

relatively simple networks.[15] In all cases the major isomer is observed, whereby both substituents flank the bridgehead position (4a-e:A), together with a minor isomer 4a-e:B (Figure 1a). Room-temperature NMR analysis of trisubstituted bullvalenes 4f i revealed a major isomer that is not in rapid exchange with the ensemble, isomer 4f-i:A, together with broad signals characteristic of dynamic bullvalene ensembles (Figure 1b). Low-temperature NMR measurements revealed a minor isomer 4f-i:B, along with several others. In all cases, ^{1}H

Scheme 2. Synthesis of Substituted Bullvalenes[a]

	3 yield	4 yield
R = CH₃	3a, 81%	4a, 30%
R = (hexyl)	3b, 86%	4b, 39%
R = Bn	3c, 83%	4c, 43%
R = CH₂OH	3d, 58%[b]	4d, 57%
R = SiMe₃	3e, 96%	4e, 52%
	3f, 43%[b]	4f, 50%
	3g, 61%	4g, 65%
		4h, 50%
		4i, 40%

[a]Reagents and conditions: (a) NaH (3 equiv), TBSCl (1 equiv), THF, 0 °C, 16 h. (b) Photochemical reaction conditions as above. (c) (COCl)₂ (2.4 equiv), DMSO (5 equiv), Et₃N (10 equiv), CH₂Cl₂ −78 °C, 1 h. (d) (COCl)₂ (1.3 equiv), DMSO (2.6 equiv), Et₃N (5 equiv), CH₂Cl₂ −78 °C, 1 h. [b]Reaction run with 2,2,2-trifluoroethanol as solvent at 55 °C.

2,4,7,9-tetraene (BDT) intermediates 3a g were isolated as inconsequential mixtures of constitutional isomers.[14] A simple TBS protection of 3f gave 3g, which structurally differentiates the three substituents. Photochemical di-π-methane rearrangement of the BDT intermediates proceeded smoothly to give the corresponding bullvalenes in moderate yields. The alcohol 4g and diol 4f were oxidized under Swern conditions to give the corresponding aldehydes.

With this collection of bullvalenes in hand, we began to study their dynamic behavior. Population distributions of the ensembles were determined using low-temperature NMR experiments. Disubstituted bullvalenes 4a e exist within

(a) Disubstituted isomer distributions

		4a-e:A	4a-e:B	c
4a: R = Me	exp:	66	34	-
	calc:	77	18	5
4b: R = hexyl	exp:	76	24	-
	calc:	35	52	13
4c: R = Bn	exp:	75	25	-
	calc:	81	10	9
4d: R = CH₂OH	exp:	76	24	-
	calc:	67	19	14
4e: R = SiMe₃	exp:	70	30	-
	calc:	50	41	9

(b) Trisubstituted isomer distributions

4f (OH, OH); 4g (CH₂OH, OTBS); 4h (CHO, CHO); 4i (CHO, OTBS)

Isomer:		A	B	C	D	E	F	G
4f	exp:	71	29	-	-	-	-	-
	calc:	90	3	1	2	0	0	4
4g	exp:	77	23	-	-	-	-	-
	calc:	33	53#	2	0	2	0	10
4h	exp:	64	21	4	5	3	3	-
	calc:	97	0	0	2	0	0	1
4i	exp:	45	27	16	12	-	-	-
	calc:	47	35	1	9	2	0	6

(c) Meta-stability of trisubstituted bullvalenes
$5:A \;\; \underset{k_{-1st\,gen}}{\overset{k_{1st\,gen}}{\rightleftharpoons}} \;\; \underset{k_{-2nd\,gen}}{\overset{k_{2nd\,gen}}{\rightleftharpoons}} \;\; \rightleftharpoons$

(d) Predicted half-lives of trisubstituted bullvalenes

4f:A	4g:A	4h:A	4i:A
$t_{1/2}$ = 0.67s	$t_{1/2}$ = 0.57s	$t_{1/2}$ = 1.8h	$t_{1/2}$ = 2.9min

Figure 1. (a) Disubstituted isomer distributions. (b) Trisubstituted isomer distributions. Experimental and computational analysis of isomer distributions. (c) Meta-stability of trisubstituted bullvalenes. (d) Predicted half-lives of trisubstituted bullvalenes. VT-NMR experiments conducted-60 °C. Indicative experimental isomer ratios are reported as a fraction of the sum of those identified. Single-point DFT calculations at B3LYP-D3BJ/Def2-TZVPPD/CPCM solvent (chloroform) performed in Orca.[18] #Predicted population reported as the sum of R₁/R₂ and R₂/R₁ isomers.
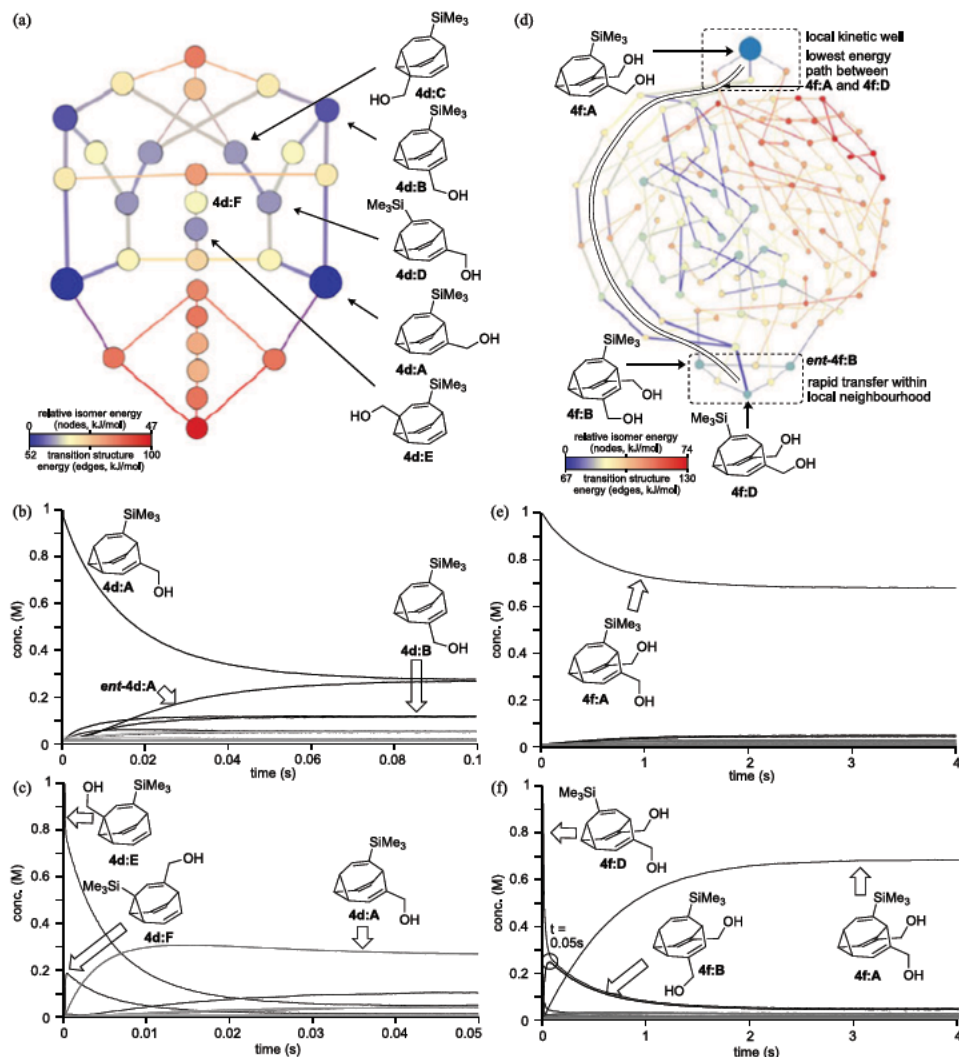
Figure 2. (a) Network graph of **4d**. (b) Simulation starting from **4d:A**. (c) Simulation starting from **4d:E**. (d) Network graph of **4f**. (e) Simulation starting from **4f:A**. (f) Simulation starting from **4f:D**.

and ^{13}C NMR spectra indicated a range of other minor isomers which could not be structurally elucidated.

Density functional theory calculations were run for all ground states and transition structures for all the ensembles studied (see SI for full details). The predicted population distributions are presented in Figure 1a,b. In all cases, the calculated population distributions are in fair agreement with experiment.

The metastability of bullvalene isomers **4f–i:A** can be rationalized by considering the local network environment of

a general trisubstituted bullvalene **5:A** (Figure 1c). In order to communicate with the rest of the network, any isomer of this type must pass through two generations of relatively high-energy isomers accompanied by high-energy barriers. This combines to form a local kinetic well. Conjugating and/or sterically demanding substituents will tend to provide increased kinetic stability. This appears to be a general feature across heavily substituted bullvalenes.[16]

The local kinetic wells around bullvalenes **4f–i:A** were assessed by estimating the first- and second-generation rate

constants using the Eyring equation and modeling the kinetics using the *KinTek Explorer* software package.[17] This predicts room-temperature half-lives ranging from 0.57 s to 1.8 h (Figure 1d).

Reaction network diagrams provide a powerful visual tool to explore the connectivity and thermodynamic/kinetic landscapes of substituted bullvalenes. The network graphs of disubstituted bullvalene **4d** and trisubstituted bullvalene **4f** are shown in Figure 2. Nodes represent individual isomers and the edges transition structures, each color coded according to relative energy. Bullvalene **4d** exists as an ensemble of 30 isomers connected by 46 transition states. The predicted populated isomers **4d:A–E** are shown (though only **4d:A** and **4d:B** have been identified experimentally). This visualization reveals that the populated isomers reside within a local group connected by a set of relatively low-energy isomerization pathways. The "southern" region of the network will essentially remain unpopulated.

A complete kinetic model of **4d** was constructed by estimating all 92 first-order rate constants. Stochastic Monte Carlo simulations were run using the *Kinetiscope* software package.[19] Figure 2b shows a simulation from an initial population of the major isomer **4d:A**. The system rapidly equilibrates within 0.1 s. Initiating the simulation from the minor isomer **4d:E** illustrates the path-dependent passage of material through the system (Figure 2c).

The reaction graph of trisubstituted bullvalene **4f** is presented in Figure 2d showing all 120 isomers and 184 transition states. The major isomer **4f:A** is relatively isolated from the other populated isomers and resides within its shallow local kinetic well. Several populated isomers (calculated), **4f:B**, *ent*-**4f:B**, and **4f:D**, all reside within a local group, mutually accessible via two-step isomerizations. The lowest-energy pathway between these two regions of the network is highlighted.

A kinetic simulation from an initial population of isomer **4f:A** shows that the system reaches equilibrium within ~1.5 s (Figure 2e). A simulation from an initial population of the minor populated isomer **4f:D** is shown in Figure 2f. In this scenario the system rapidly equilibrates toward a ~1:1:1 mixture of **4f:D:4f:B:***ent*-**4f:B** within a period of ~0.05 s. From here the ensemble slowly generates the major isomer **4f:A** over a period of ~2 s.

More heavily substituted bullvalenes represent a major jump in complexity, as well as a considerable synthetic challenge. However, the thermodynamic and kinetic properties of these large systems may be anticipated. To demonstrate, we ran a computational analysis of the (hypothetical) tetrasubstituted bullvalene **6** (Figure 3). With this substitution pattern there are 1640 unique isomers (852 discounting enantiomers) and 2520 transition structures. A full DFT analysis of the ground-state energies predicts only 16 isomers to be populated at room temperature with a relative abundance of greater than 1% (**6:A-P**, Figure 3). All these isomers (excepting **6:N**) have 2–3 substituents adjacent to the bridgehead, analogous to the dominant isomers of **4a–i**. Intriguingly, the global minimum isomer **6:A** does not have an arrangement analogous to that of **4f-i:A** and benefits from a specific intramolecular hydrogen bond, as do isomers **6:D** and **6:L**.

The full computation analysis of all transition structures represents an arduous and impractical exercise. However, surveying the likely local kinetic wells would provide useful insights. There are 28 possible isomers of **6** that maintain three

substituents adjacent to the bridgehead. Of these, only five reside within the pool of 16 populated isomers shown in Figure 3, **6:B-E,L**. For each of these, the first- and second-generation
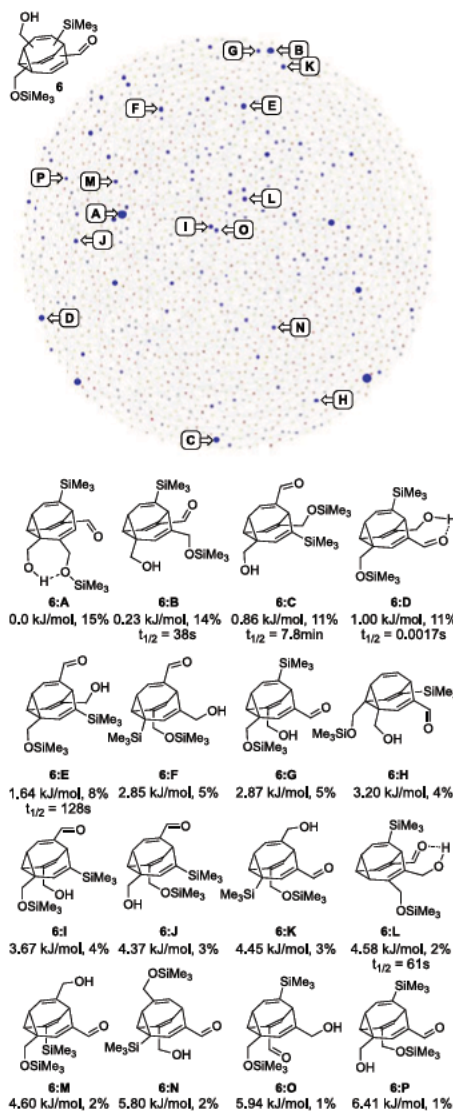
Figure 3. Network analysis of (hypothetical) tetrasubstituted bullvalene **6**. The relative stability of the predicted populated isomers **6:A-P** is shown based on single-point DFT calculations at the B3LYP-D3BJ/Def2-TZVPPD/CPCM solvent (chloroform). The predicted half-lives for isomers **6:B-E,L** is shown based on the local first- and second-generation transition structures calculated at B3LYP-D3BJ/Def2-TZVPPD(chloroform).

transition structure energies were calculated, and the local kinetics modeled. The predicted half-lives range between 0.0017 s and 7.8 min. Isomer **6:D** has a surprisingly short half-life which is traced to an intramolecular hydrogen bond, stabilizing one of the first-generation transition structures (see SI for full details).

In summary, we demonstrated the synthesis of a range of disubstituted bullvalenes and the first synthesis of differentially trisubstituted bullvalenes. Low-temperature NMR experiments reveal the populated isomer distributions, in broad agreement with DFT calculations. Kinetic simulations provide a new window into the rich dynamic nature of these systems and help rationalize the meta-stability of trisubstituted bullvalene major isomers. The anticipation of kinetic and thermodynamic features within heavily substituted bullvalenes provides a framework through which to navigate these complex systems and design future shape-selective molecular devices.

■ ASSOCIATED CONTENT

● Supporting Information

The Supporting Information is available free of charge on the ACS Publications website at DOI: 10.1021/acs.orglett.9b03737.

> Experimental details and characterization data for all new compounds. Details of computational methods and analysis (PDF)
>
> List of computational results (PDF)

■ AUTHOR INFORMATION

Corresponding Authors

*E-mail: thomas.fallon@adelaide.edu.au.
*E-mail: lukas.f.pasteka@gmail.com.

ORCID ●

Lukáš F. Pašteka: 0000 0002 0617 0524
Christopher G. Newton: 0000 0002 8962 5917
Thomas Fallon: 0000 0002 6495 5282

Notes

The authors declare no competing financial interest.

■ REFERENCES

(1) von E. Doering, W.; Roth, W. R. *Tetrahedron* **1963**, *19*, 715−737.
(2) (a) Schröder, G. *Angew. Chem., Int. Ed. Engl.* **1963**, *2*, 481−482. (b) Schröder, G. *Angew. Chem.* **1963**, *75*, 722−722.
(3) The barbaryl cation and radical represent the other totally degenerate cage hydrocarbons: (a) Ahlberg, P.; Harris, D. L.; Winstein, S. *J. Am. Chem. Soc.* **1970**, *92*, 2146−2147. (b) Ahlberg, P.; Grutzner, J. B.; Harris, D. L.; Winstein, S. *J. Am. Chem. Soc.* **1970**, *92*, 3478−3480. (c) Ahlberg, P.; Harris, D. L.; Winstein, S. *J. Am. Chem. Soc.* **1970**, *92*, 4454−4456. (d) Engdahl, C.; Ahlberg, P. J. *J. Phys. Org. Chem.* **1990**, *3*, 349−357.
(4) For recent reviews, see: (a) Rowan, S. J.; Cantrill, S. J.; Cousins, G. R. L.; Sanders, J. K. M.; Stoddart, J. F. *Angew. Chem., Int. Ed.* **2002**, *41*, 898−952. (b) Corbett, P. T.; Leclaire, J.; Vial, L.; West, K. R.; Wietor, J.-L.; Sanders, J. K. M.; Otto, S. *Chem. Rev.* **2006**, *106*, 3652−3711. (c) Jin, Y.; Yu, C.; Denman, R. J.; Zhang, W. *Chem. Soc. Rev.* **2013**, *42*, 6634−6654.
(5) (a) Lippert, A. R.; Keleshian, V. L.; Bode, J. W. *Org. Biomol. Chem.* **2009**, *7*, 1529−1532. (b) Lippert, A. R.; Naganawa, A.; Keleshian, V. L.; Bode, J. W. *J. Am. Chem. Soc.* **2010**, *132*, 15790−15799. (c) He, M.; Bode, J. W. *Proc. Natl. Acad. Sci. U. S. A.* **2011**, *108*, 14752−14756. (d) Larson, K. K.; He, M.; Teichert, J. F.; Naganawa, A.; Bode, J. W. *Chem. Sci.* **2012**, *3*, 1825−1828. (e) Teichert, J. F.; Mazunin, D.; Bode, J. W. *J. Am. Chem. Soc.* **2013**, *135*, 11314−11321. (f) He, M.; Bode, J. W. *Org. Biomol. Chem.* **2013**, *11*, 1306−1317.
(6) Saunders, M. *Tetrahedron Lett.* **1963**, *4*, 1699−1702.
(7) Poupko, R.; Zimmermann, H.; Muller, K.; Luz, Z. *J. Am. Chem. Soc.* **1996**, *118*, 7995−8005.
(8) Rebsamen, K.; Roettele, H.; Schroeder, G. *Chem. Ber.* **1993**, *126*, 1429−33.
(9) (a) Ferrer, S.; Echavarren, A. M. *Angew. Chem., Int. Ed.* **2016**, *55*, 11178−11182. (b) McGonigal, P. R.; de León, C.; Wang, Y.; Homs, A.; Solorio-Alvarado, C. R.; Echavarren, A. M. *Angew. Chem., Int. Ed.* **2012**, *51*, 13093−13096.
(10) Yahiaoui, O.; Pašteka, L. F.; Judeel, B.; Fallon, T. *Angew. Chem., Int. Ed.* **2018**, *57*, 2570−2574.
(11) (a) Achard, M.; Mosrin, M.; Tenaglia, A.; Buono, G. *J. Org. Chem.* **2006**, *71*, 2907−2910. (b) D'yakonov, V. A.; Kadikova, G. N.; Dzhemileva, L. U.; Gazizullina, G. F.; Ramazanov, I. R.; Dzhemilev, U. M. *J. Org. Chem.* **2017**, *82*, 471−480.
(12) (a) Jones, M.; Scott, L. T. *J. Am. Chem. Soc.* **1967**, *89*, 150−151. (b) Jones, M.; Reich, S. D.; Scott, L. T. *J. Am. Chem. Soc.* **1970**, *92*, 3118−3126.
(13) de Meijere, A.; Lee, C.-H.; Bengtson, B.; Pohl, E.; Kozhus, S. I.; Schreiner, P. R.; Boese, R.; Haumann, T. *Chem. - Eur. J.* **2003**, *9*, 5481−5488.
(14) In principle these cycloadditions could proceed in any of eight distinct modes, leading to eight regioisomers. In practice the trimethylsilyl group is primarily directed to the bridging alkene. See Supporting Information for full details.
(15) Disubstituted bullvalenes exist as ensembles of either 15 isomers (R_1, R_1) or 30 isomers (R_1, R_2), respectively. Trisubstituted systems will exist as ensembles of 42 (R_1, R_1, R_1), 120 (R_1, R_1, R_2), or 240 isomers (R_1, R_2, R_3), respectively.
(16) This feature was previously described by Bode, ref 5f.
(17) https://kintekcorp.com/, accessed Nov 19, 2019.
(18) (a) Becke, A. D. *J. Chem. Phys.* **1993**, *98*, 5648. (b) Lee, C.; Yang, W.; Parr, R. G. *Phys. Rev. B: Condens. Matter Mater. Phys.* **1988**, *37*, 785. (c) Rappoport, D.; Furche, F. *J. Chem. Phys.* **2010**, *133*, 134105. (d) Barone, V.; Cossi, M. *J. Phys. Chem. A* **1998**, *102*, 1995. (e) Cossi, M.; Rega, N.; Scalmani, G.; Barone, V. *J. Comput. Chem.* **2003**, *24*, 669. (f) Neese, F. *WIREs Comput. Mol. Sci.* **2012**, *2*, 73.
(19) (a) http://hinsberg.net/kinetiscope/, accessed Nov 19, 2019. (b) https://github.com/sbednarz/chemical-kinetics-simulator, accessed Nov 19, 2019.

In this section we discuss all the unpublished results that were not included into the manuscript.

3.2. Synthesis of substituted cyclooctatetraene

The synthesis of trisubstituted bullvalene required the introduction of a substituent into the COT core **1**. Therefore, four substituted COTs were synthesized such as bromo– **2**, trimethylsilyl – **3**, hydroxymethylene– **4**, and methyl–cyclooctatetraene **5** using COT as starting material. The bromination of COT followed by an in–situ elimination with potassium *tert*–butoxide delivered COT–Br **2** in high yield.[95] The latter was the key molecule for the synthesis of the substituted COTs in one or two steps. The treatment of COT–Br **2** with *n*–butyllithium generated the organo lithium species, which was reacted with the corresponding electrophile to give the desired product as shown in Figure 3.1.
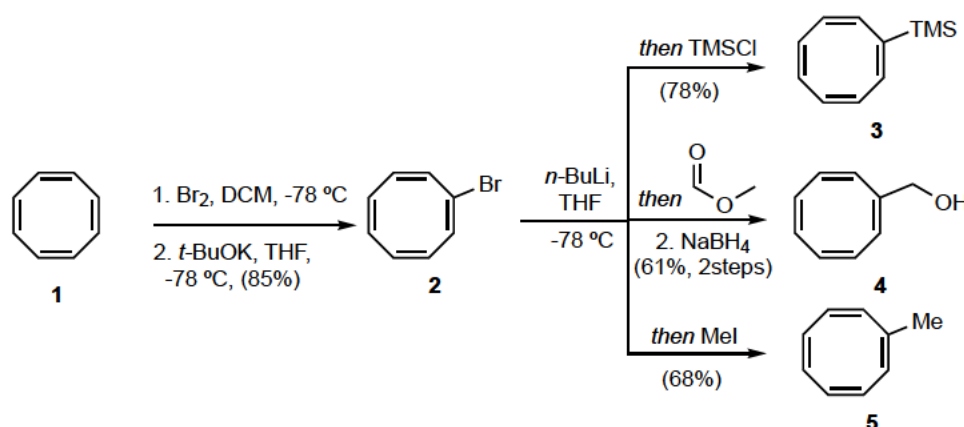
Figure 3.1: Synthesis of substituted COTs.

3.2.1. Reactivity of substituted COT

The reactivity of the substituted COTs **2**–**5** was examined in the cobalt catalysed [6+2] cycloaddition reaction (Table 1). We chose TMS–acetylene **6** as the alkyne due to its high reactivity with COT **1**.[96] The [6+2] cycloaddition reaction occurred at room temperature between the substituted COTs **2**–**5** and the alkyne **6** in DCE as the solvent (entry 1, 2, 3, 5). Only COT–Me **5** and COT–TMS **3** (entry 1 – 2) showed reactivity, while **2** and **4** gave starting material (entry 3 – 5). Repeating the unsuccessful reactions at 60 °C was also unsuccessful (entry 3 – 5). Changing the solvent to TFE and performing the reaction under the previous conditions was fruitless as well (entry 4, 6).

7a: R$_1$ = TMS, 96%, **7b**: R$_1$ = Me, 56%
7c: R$_1$ = Br, no conversion,**7d**: R$_1$ = CH$_2$OH, no conversion
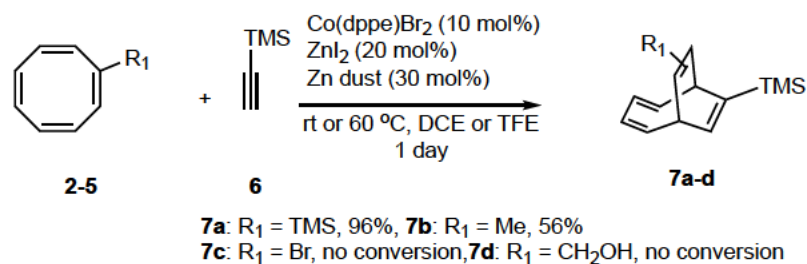
Figure 3.2: [6+2] cycloaddition of substituted COTs **2–5** and TMS–acetylene.

Table 1: Cobalt catalysed [6+2] cycloaddition of sub–COTs and ethynyltrimethylsilane.

Entry	Substituted COT	Alkyne	Temperature	Solvent	Yield
1	COT–TMS	TMS–acetylene	rt	DCE	96%
2	COT–Me	TMS–acetylene	rt	DCE	56%
3	COT–Br	TMS–acetylene	rt or 60 °C	DCE	No conversion
4	COT–Br	TMS–acetylene	rt or 60 °C	TFE	No conversion
5	COT–CH$_2$OH	TMS–acetylene	rt or 60 °C	DCE	No conversion
6	COT–CH$_2$OH	TMS–acetylene	rt or 60 °C	TFE	No conversion

The reactivity pattern of substituted COTs (**2** and **4**) in Cobalt catalysed [6+2] reactions remains unclear. Our results represent the first examples of such reactions, and it seems that the substrate scope is limited. Cobalt catalysed [4+2] cycloaddition reactions have been more extensively studied by Hilt and also display severe substrate limitations.[97]

3.3. Synthesis of substituted bullvalenes from COT–Me

The synthesis of BDTs deriving from COT–TMS are described in the manuscript.

COT–Me underwent the [6+2] cycloaddition with various alkynes to deliver di– and trisubstituted BDTs in moderate yield (Figure 3.3). The reactions occurred at room temperature in DCE or in TFE at 55 °C. The products were easily obtained as inconsequential mixtures of constitutional isomers.

8a: R_1 = Me, R_2 = H, 75%, **8b**: R_1 = hex, R_2 = H, 40%
8c: R_1 = Bn, R_2 = H, 59%, **8d**: R_1 = CH_2OH, R_2 = H, 45%
8e: R_1 = CH_2OH, R_2 = CH_2OH, 50%
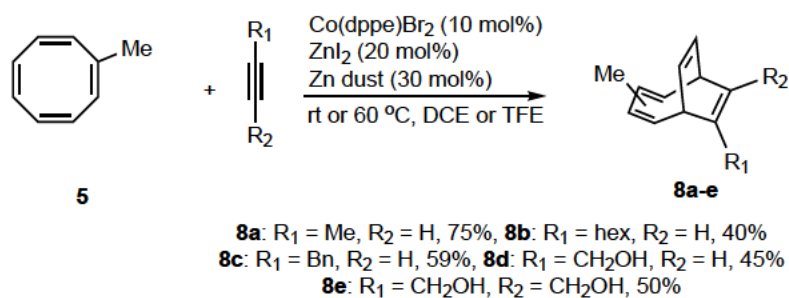
Figure 3.3: Synthesis of substituted BDTs **8a–e** with COT–Me.

The irradiation of the BDTs **8a–e** in acetone for 3 – 8h with a 150 W medium–pressure mercury lamp containing a Pyrex filter delivered the desired bullvalenes **9a–e** in moderate yield (Figure 3.4).

9a: R_1 = Me, R_2 = H, 70%, **9b**: R_1 = hex, R_2 = H, 37%
9c: R_1 = Bn, R_2 = H, 33%, **9d**: R_1 = CH_2OH, R_2 = H, 61%
9e: R_1 = R_2 = CH_2OH, 41%
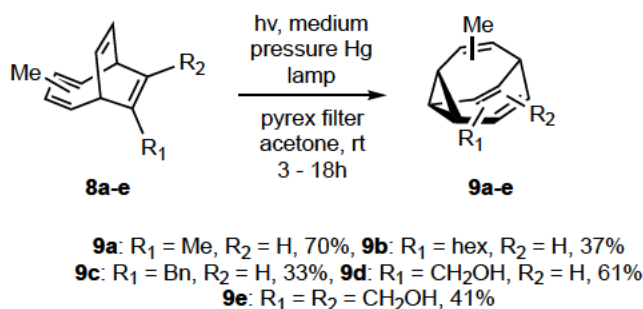
Figure 3.4: Synthesis of substituted bullvalenes **9a–e**.

The structural elucidation of complex bullvalene ensembles is challenging, requiring very high–resolution low temperature NMR data sets. Key to the analysis are the proton and carbon signals at the bridgehead of each isomer. Good resolution of these signals is critical. Unfortunately, the COT–Me derived bullvalenes showed significant overlap of the key signals, making NMR analysis unfeasible. This was compounded with the low stability of this series of molecules, and the need to use remote NMR services. The ^{1}H NMR of methylhydroxy–methyl bullvalene **9d** shown in Figure 3.5 exhibits this overlap of key signals in the methine region. At this point, we decided not to investigate further the isomer distribution of **9a–e**. Interestingly, the room temperature ^{1}H NMR of trisubstituted bullvalene **9e** indicated the kinetic metastable isomer which is not in rapid exchange with the other isomers (Figure 3.6). This major isomer is identical to the other trisubstituted bullvalenes that are outlined in the manuscript.
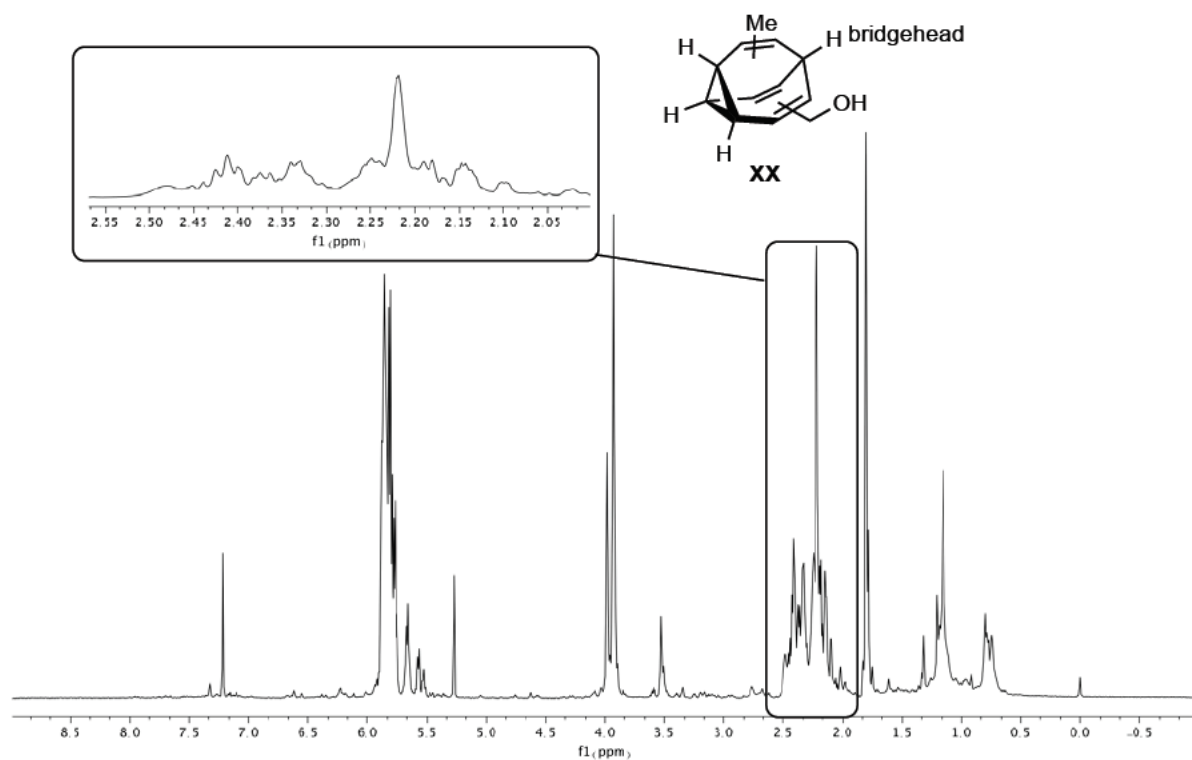
Figure 3.5: ^{1}H NMR spectra of hydroxymethylene–methyl–bullvalene at –60 ℃.
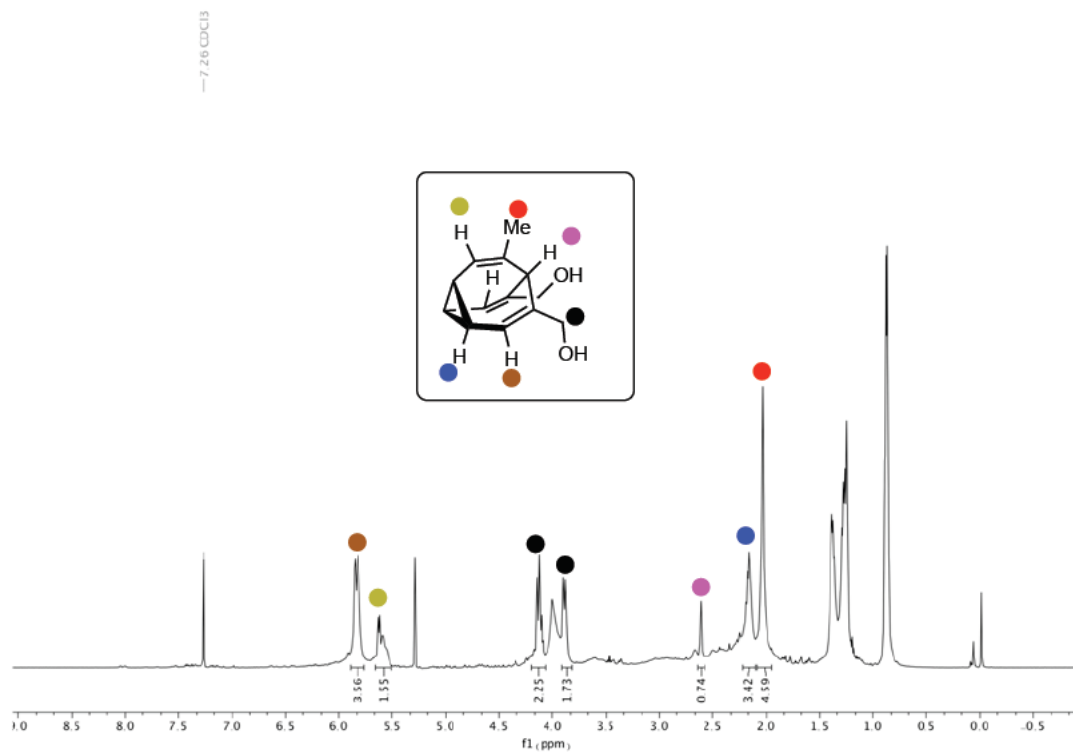
Figure 3.6: ^{1}H NMR spectra of dimethylhydroxy–methyl–bullvalene at room temperature.

3.4 Cobalt catalysed [6+2] cycloaddition reaction between differently disubstituted alkynes and COT–TMS

We discontinued the analysis of the substituted bullvalenes **9a–e** deriving from COT–Me. Therefore, we shifted our focus toward the synthesis of differentially trisubstituted bullvalene with COT–TMS. As outlined in the manuscript, the synthesis of a trisubstituted bullvalene with unidentical substituents required an additional step to give the desired product. As the cobalt catalysed reaction between COT–TMS **3** and 2,4–butynediol gave a symmetrical BDT **10**. A desymmetrization of the latter through a mono protection of the alcohol with a TBS group gave the suitable precursor **11** for the synthesis of the bullvalene **12** (Figure 3.7). This approach was outlined in the manuscript. We sought to synthesise an unsymmetrical BDT moiety to decrease the number of steps. Therefore, a disubstituted alkyne with different substituents is required.
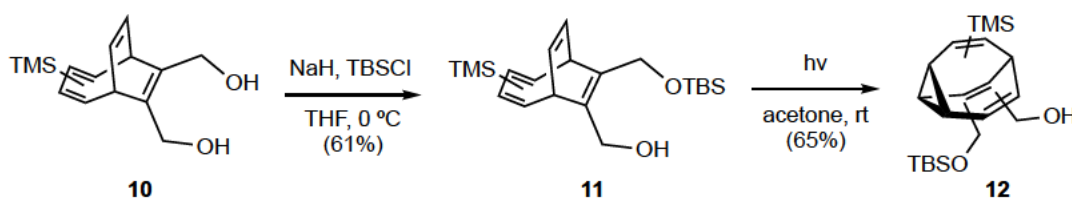
Figure 3.7: Synthesis of trisubstituted bullvalenes with three non–identical substituents.

We started our investigation by performing the cobalt catalysed [6+2] cycloaddition reaction between COT–TMS **3** and oct–2–yne **13a** at different temperatures (rt or 60 °C) and solvents (TFE or DCE) without any success (Figure 3.8).We arbitrarily changed the alkyne to non–2–yn–1–ol[98] **13b** and the [6+2] cycloaddition reaction was fruitless. We thought that the protection of latter alkyne with a *tert*–butyldimethylsilyl group[98] **13c** might improve the reactivity. Unfortunately, our attempts were unsuccessful.

13a: R_1 = hex, R_2 = CH$_2$OH
13b: R_1 = hex, R_2 = CH$_2$OTBS
13c: R_1 = pent, R_2 = Me
13d: R_1 = Bn, R_2 = TMS
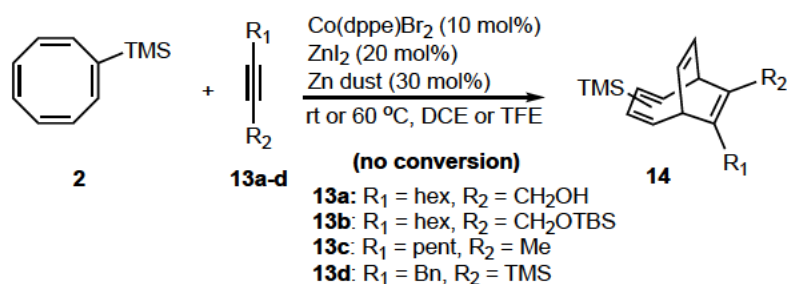
Figure 3.8: Cobalt catalysed [6+2] cycloaddition of COT–TMS with various alkyne.

COT–TMS showed no reactivity in the [6+2] cycloaddition reaction with heterogenous alkynes. However, an alternative solution to this issue was the desymmetrization of the BDT **4**

3.5 Conclusion and outline

In this chapter we overcome the limitations of our previous method by synthesizing differentially trisubstituted bullvalenes for the first time. Furthermore, the calculation of the rate constants accompanied with DFT calculation clarified the complex behaviour of di–, tri–, and tetra– substituted bullvalenes.

The synthesis of higher substituted bullvalenes such as tetra–, penta–, and onward could be achieved by introducing further substituents to COT. With further substitution, the number of possible isomers of bullvalene rises exponentially. However, only a small subset of isomers will be populated, and the internal kinetics of the system will impose limitations. For instance, Schröder showed the hexaphenyl– **15a–b** and hexabromo bullvalene **16a–b** exist as only two static isomers (Figure 3.9).
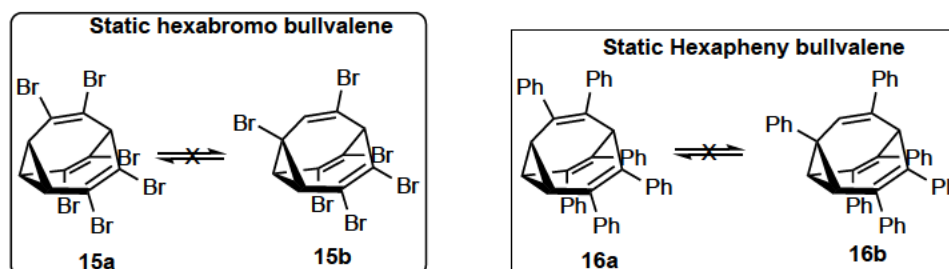
Figure 3.9: Hexabromo–, and hexaphenyl bullvalenes.

Tetrasubstituted bullvalenes show considerable complexity, as explored by the Bode group. Our calculations of all possible isomers of tetrasubstituted bullvalene (molecule nr. **6** in manuscript) showed that only 16 isomers are likely to be populated, and these 16 are predicted to be metastable.

In the next chapter we will expand the dynamic behaviour of bullvalene by introducing a stereogenic centre to the substituents of bullvalene.

Chapter 4

4.1. Introduction

4.1.1. Helical chirality

Chirality is the property whereby a structure is non–superimposable with its mirror image. This property must arise from one or more elements of stereogenicity. Most commonly this is a tetrahedral centre bearing four unidentical substituents. For instance (*S*)–bromochlorofluromethane **1** has four unique substituents and cannot be superimposed to its mirror image (*R*)– bromochlorofluromethane **2** (Figure 4.1.a). **1** and **2** are enantiomers to one another and their configuration is determined with the Cahn–Ingold–Prelog (CIP) rules.[99] The presence of two or more stereocentres in a molecule leads to stereoisomerism in the form of diastereomers and meso compounds. Diastereomers are not mirror images and cannot be superimposed onto one another like ephedrine **3** and pseudoephedrine **4** (Figure 4.1b). A meso compound such as (2*R*,3*S*)-butane-2,3-diol **5** contains two stereogenic centres and a plane of symmetry. It is considered achiral because it can be superimposed to its mirror image (Figure 4.1c).
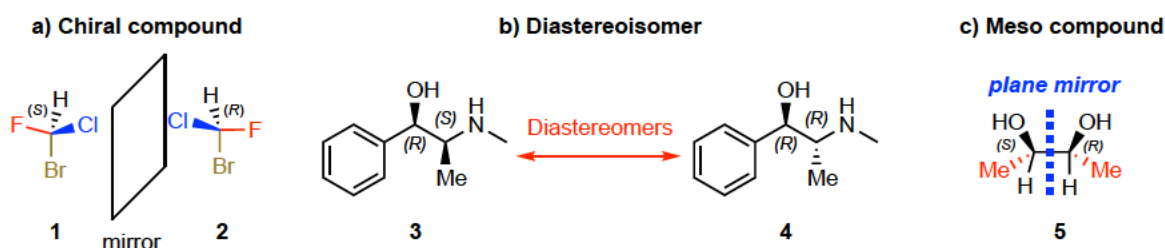
Figure 4.1: (a) chiral compound, (b) (c) ephedrine and pseudoephedrine diastereomers, and (d) meso compound.

A stereogenic centre is not always necessary for a molecule to be chiral. Some molecules are chiral, due to the presence of an axis of chirality. For instance, biphenyl ligands **7** and **8** have C_2 symmetry and an axis of chirality which arises from a restricted rotation around a single bond (Figure 4.2).[100] This restricted rotation is called atropisomerism. The configuration of these molecules is also called helicity and is determined following these rules: the substituents with a higher atomic number has the highest priority (A>B and C>D) and the plane that is nearer to the viewer has the highest rank.[99] The molecule is observed along its axis and if the rotation is clockwise then the helicity is *P* (positive) and if counterclockwise *M* (Minus).
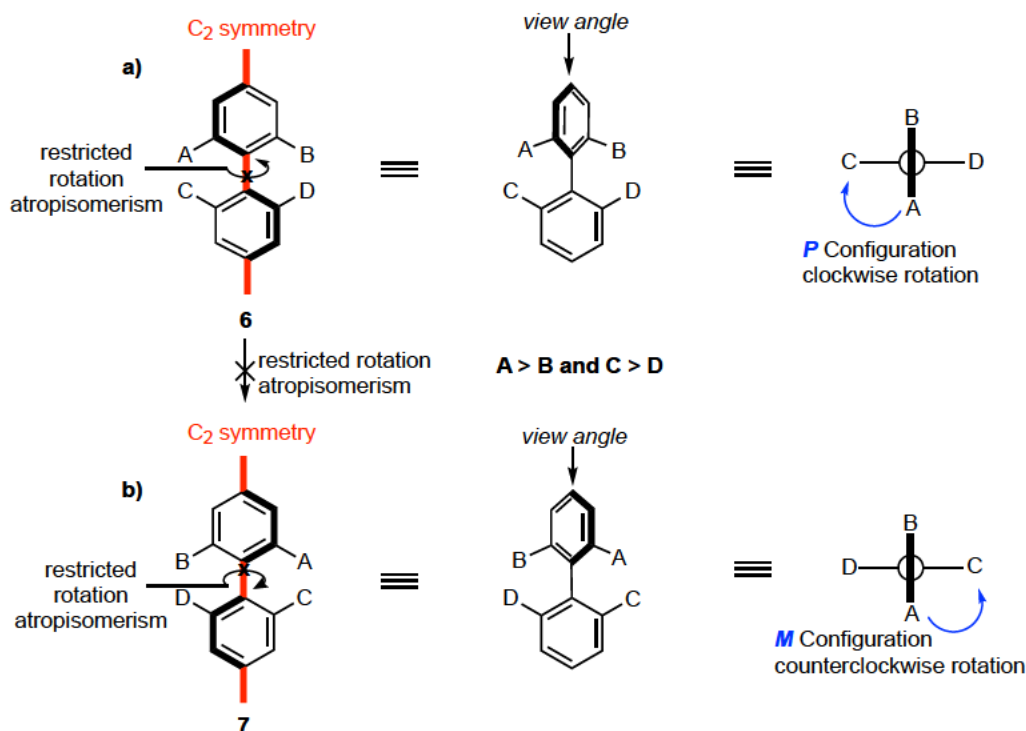
Figure 4.2: Axial of chirality configuration and atropisomers (a) *P* configuration and (b) *M* configuration.

Atropisomers may interconvert if the energy barrier to rotation is surmounted. BINOL **8** is the most used ligand for enantioselective reactions. It has C_2 symmetry, exhibits atropisomerism, and a half–life racemization at room temperature of $t_{1/2}$ = 2 million years.[101] Irradiation of (*P*)–BINOL **8** with a 500–W Hg–Ne lamp for 3 hours leads to racemization through formation of the (*M*) enantiomer **9**. HPLC analysis indicated a decrease of enantiomeric excess from 99% to 44% ee.[102]
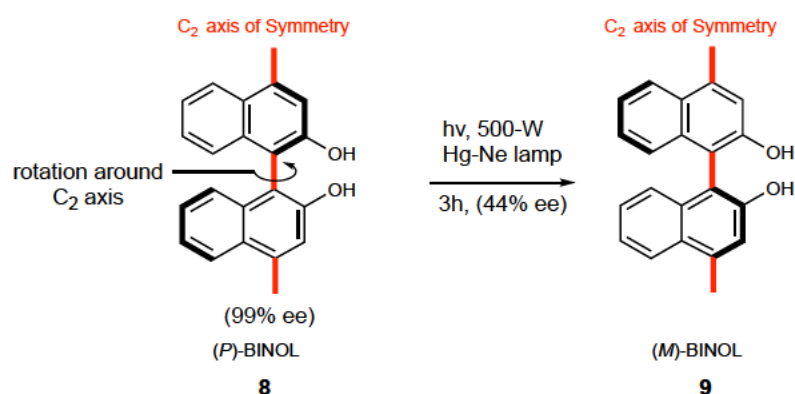
Figure 4.3: Racemization of (*P*)–BINOL through irradiation to (*M*)–BINOL.

Molecules with C_3 symmetry typically offer large orientational freedom for the substituents to rotate around the central axis, thus circumventing atropisomerism.[103] Ortho–substituted phosphine oxide **10**, however, displays intramolecular repulsive interactions and restricted rotations about the P–C bonds.[104] C_3 symmetric molecules such as **10** are often described as propeller–type structures
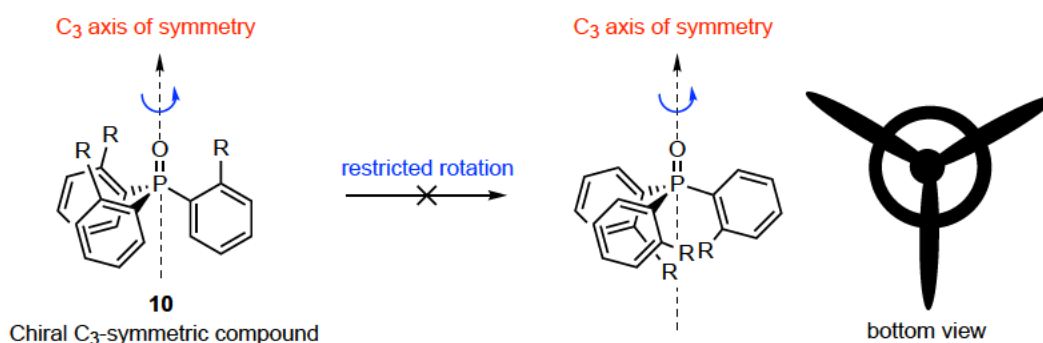
Figure 4.4: Ortho–substituted phosphine oxide with C_3 symmetry and atropisomerism.

4.1.2. Stereomutation

As shown in Figure 4.3, the helicity of a molecule can be changed from (*P*) to (*M*). The configuration of a chiral stereocentre can also be modified from (*S*) to (*R*). This change in configuration of a stereogenic centre is called stereomutation. The stereomutation of sugar is perhaps the earliest recognized example and occurs through a dynamic covalent process (Figure 4.5). Epimers like D–glucose **11** and D–mannose **13** are found in nature and under mild basic conditions, the hydroxy group in D–glucose **11** epimerises to form D–Mannose **13** through enediol intermediate **12**. Another example of stereomutation is the epimerization of D–alanine **14** to *L*–alanine **16** through the formation of a planar carbanion intermediate **15**.
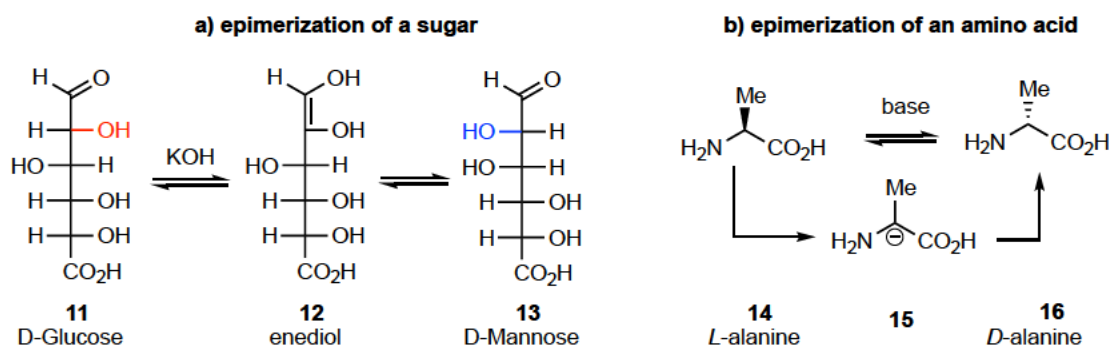
Figure 4.5: a) Epimerization of D–Glucose to D–Mannose, b) epimerization of the amino acid alanine.

Stereomutation may also arise through valence isomerism. In chlorophosphonium barbaralane **17**, two stereomutations occur simultaneously: a fast Cope rearrangement of the barbaralane core (highlighted in blue), as well as Walden inversion of the phosphorous stereocentre (centre highlighted in red), causes the inversion of the phosphorus stereocentre (Figure 4.6).[105]
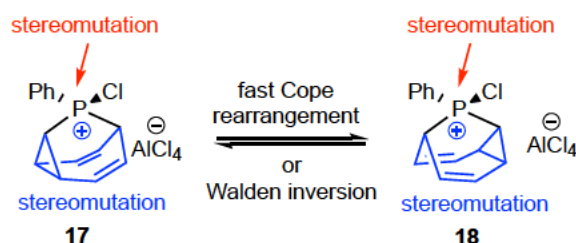
Figure 4.6: Chlorophosphonium barbaralane **18** exhibiting two stereomutations.

There is only one previous report that explored stereomutation in substituted bullvalenes. In this work, Bode demonstrate that an enantiomerically enriched precursor **19** to bullvalene **20** could be prepared.[106,107] Time–resolved CD spectra showed that chiral bullvalene **20** loses optical activity over 42 h at room temperature and equilibrates to the bullvalene network **21**..
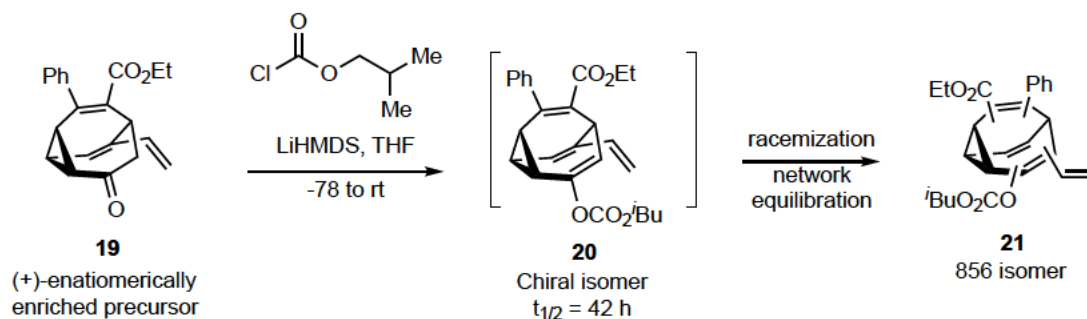
Figure 4.7: Bode isolating a chiral tetrasubstiuted bullvalene **20**.

To graphically visualize the dynamic interconversion network of bullvalene **21**, Bode and He developed a numeric code to quickly identify all possible isomers, and integrated this code with computational data handling methods. In the next section we will introduce this numeric code and apply it to stereochemically challenging concepts in bullvalene chemistry.

4.1.3. Code system of bullvalene

Bullvalene **22** has a propeller–type structure bearing a C_3 symmetric axis that goes through the cyclopropyl group and the bridgehead carbon (Figure 4.8). The structure also possesses an internal mirror plane of symmetry and is achiral. Simple monosubstituted bullvalenes are also achiral. Methyl bullvalene **23a–d** for instance, exists between four possible isomers, which all preserve an internal mirror plane (Figure 4.8).
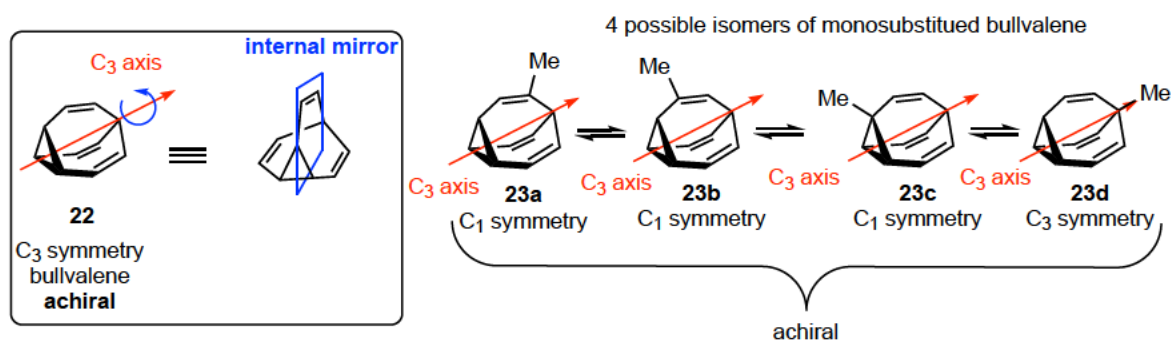
Figure 4.8: Achiral bullvalene **22** and methylbullvalene **24a–d**.

Disubstituted bullvalenes however, exist between isomers that are either achiral **24a–b** or chiral **24c–d** (Figure 4.9). **24c** and **24d** are an enantiomer pair, each with four stereocentres. To distinguish enantiomers from each other, one has to determine the stereochemical configuration of all four stereocentres, which can be difficult and inconvenient.
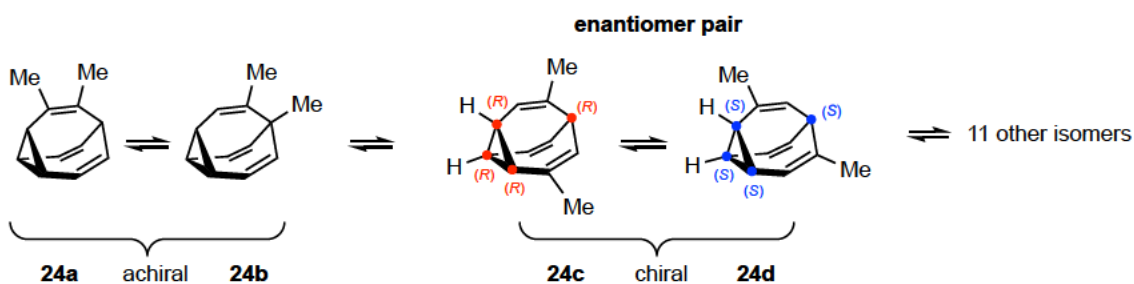
Figure 4.9: Achiral and chiral dimethyl bullvalene isomers.

An easy way to differentiate these enantiomers from each other is by defining the helical chirality of bullvalene. Bullvalene has a propeller–type structure and a C_3 symmetric axis **22** as presented in Figure 4.10. The propeller blades can be seen as the cyclopropyl–vinyl groups, which we describe as the arms of bullvalene. By ranking the arms, one can determine the

helicity of the molecule. Therefore, a few rules need to be clarified to assign the priorities of the arms if the molecule is substituted.
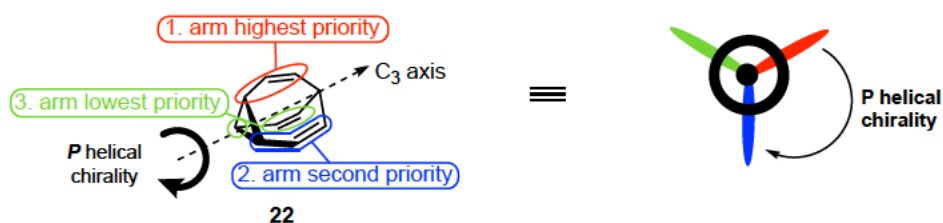
Figure 4.10: Presentation of bullvalene's arm.

Rule 1: Regardless of the Cahn Ingold Prelog (CIP) rule, the arm in which the substituent is closer to the start of the arm or the cyclopropyl group has the highest priority (Figure 4.11). Bromo–methyl– bullvalene **25** for example has *M* helicity
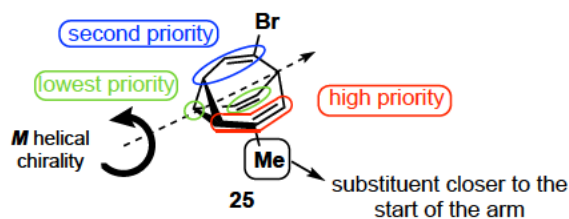
Figure 4.11: Rule 1 to determine the priority of the arms of bullvalene.

Rule 2: If two arms have the substituents on the same position, the ranking of the substituents is decided by the CIP rule. The arm with the highest–ranking substituent has the highest priority (Figure 4.12). **15** has a *P* helicity.
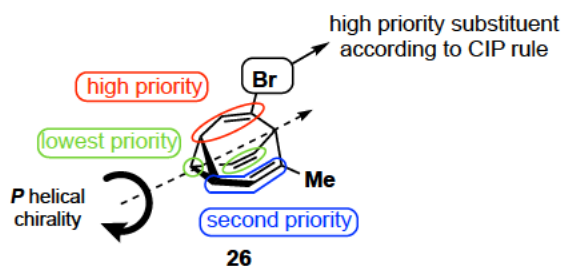
Figure 4.12: Rule 2 to determine the priority of the arm of bullvalene.

As mentioned before, to differentiate enantiomer **24c** from **24d** we have to determine their stereochemical configuration, which can be difficult and inconvenient. But, the identification of their helicity considerably simplifies the distinction of both enantiomers (Figure 4.13).
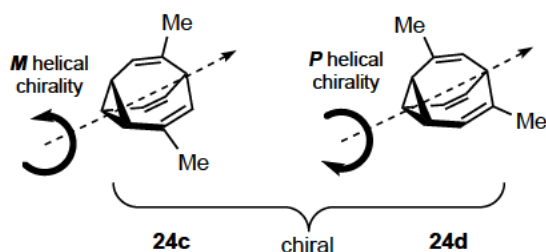
Figure 4.13: (*P*) and (*M*) helical bullvalenes.

To further simplify the identification of helicity we can utilise a barcode system for bullvalene, which was developed by Bode,[108] expanded by our group,[27] and detailed in chapter 2. The barcode contains 10 digits, every 3 digit–block defines an arm and each digit represents a carbon atom (Figure 4.14).
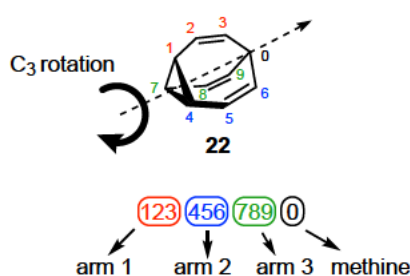
Figure 4.14: The rotational directionality of the isomer coding system.

Substituents are numbered following CIP rules. For example, a carbon with a digit "2" has a substituent with the highest priority, "1" for a lower priority, and "0" for lowest priority. In Figure 4.15 the carbon atoms on the bullvalene core that carry a substituent are presented as "2" for a bromide group, "1" for a methyl group, and "0" for a hydrogen group. The sequence of 3–digit blocks is clockwise with respect to the C_3 axis of symmetry. Bullvalene **27** for instance can be presented by three equivalent codes, and we choose the code with the lowest number sequence.
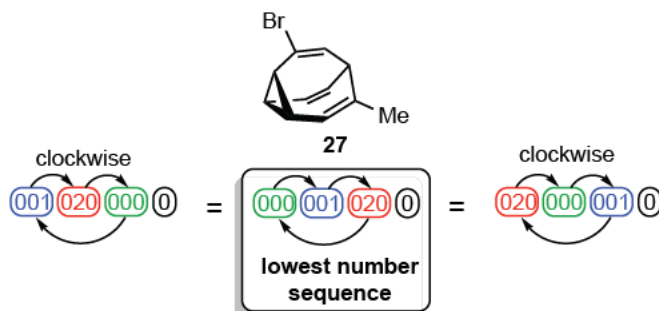
Figure 4.15: Code of bromo–methyl bullvalene 27.

The first benefit of using the code system is the identification of chiral and achiral molecules. For instance, in Figure 4.16 an isomer is chiral if the arms are distinct from each other **28** and achiral if they are identical **29**.
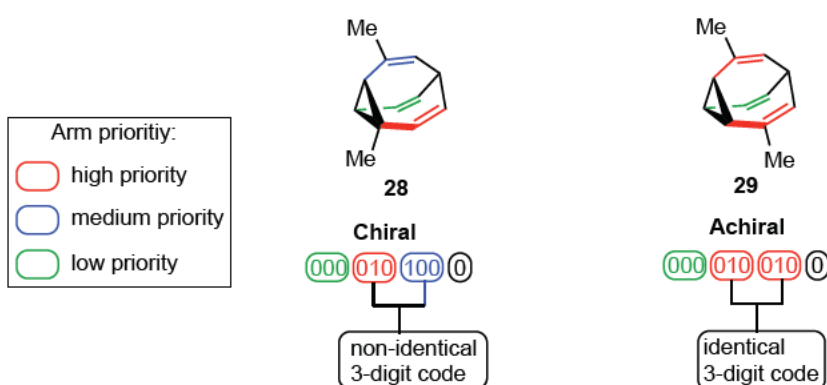
Figure 4.16: Identification of chiral and achiral isomers with the coding system.

The second advantage of the code is the determination of helicity. Here, we need to apply rule 1 and 2 to the coding system. In Figure 4.17a, the 3–digit block that contains a substituent that is near the start of the arm has the highest priority (rule 1). If two 3–digit blocks have the substituents on the same position of their arms, the priority of the substituents is determined with the CIP rule (Figure 4.17b).
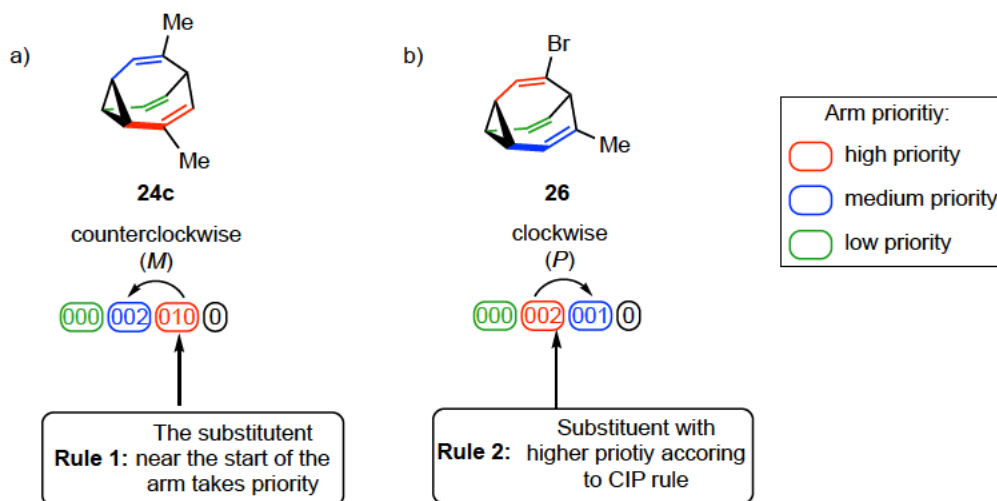
Figure 4.17: Identification of helicity using the code system.

4.2. Result and discussion

4.2.1. Aim

In this project we further explore the fluxional stereochemistry of bullvalene by synthesizing and analysing bullvalene targets 1–3 shown in (Figure 4.18). Introduction of one (Target 1) or two (Target 2) elements of point–chirality to the substituents of disubstituted bullvalenes leads to the formation of a molecule in which one or two stereogenic centres are fixed, while the axial chirality of the bullvalene is mutating. Furthermore, two disubstituted bullvalenes are linked together by a chiral bridge (Target 3), thus presenting a novel example of stereomutation in which the bridge's configuration is mutating due to the fluxional properties of the attached bullvalenes.
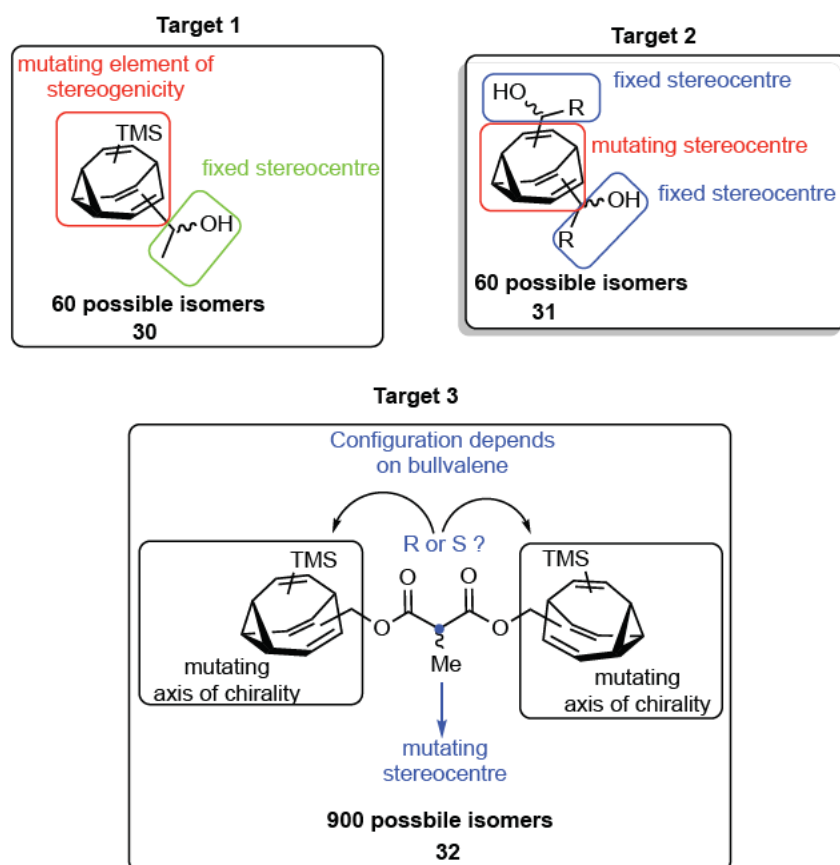
Figure 4.18: Target molecules.

4.2.2. Introduction of one stereogenic centre

4.2.2.1. Synthesis

In the previous chapter we synthesised methylhydroxy–TMS–bullvalene[84] **31** in three steps. The oxidation of **31** under Swern conditions gives aldehyde–TMS–bullvalene **32** in poor yield (12%). The sensitivity of the product towards acid during work up led to the poor yield. With aldehyde **32** a 1,2–addition with methyllithium gave ethanol–TMS bullvalene **30** in high yield (93%).
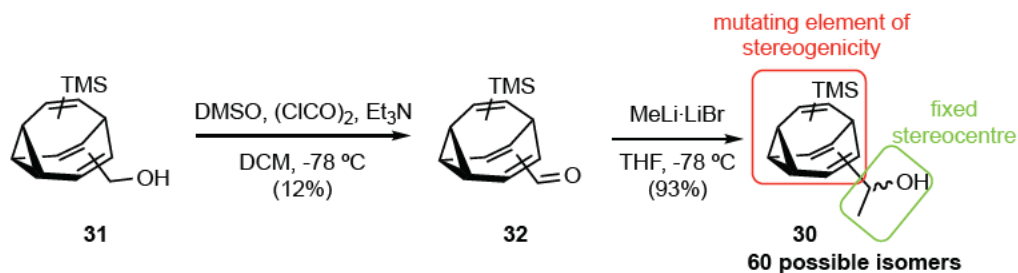
Figure 4.19: Synthesis of bullvalene **30**.

Low temperature ^{1}H NMR of bullvalene **30** was able to reveal the major isomer **30a** (Figure 4.20). A distinctive doublet in the methine region is characteristic of an apex proton signal being flanked by its substituents. In the previous chapter, we became knowledgeable in the analysis of di– and tri–substituted bullvalenes containing a TMS group and here we observe a characteristically downfield alkenic signal representing a proton adjacent to the TMS group. This allows for the assignment of major isomer **30a** by analogy.
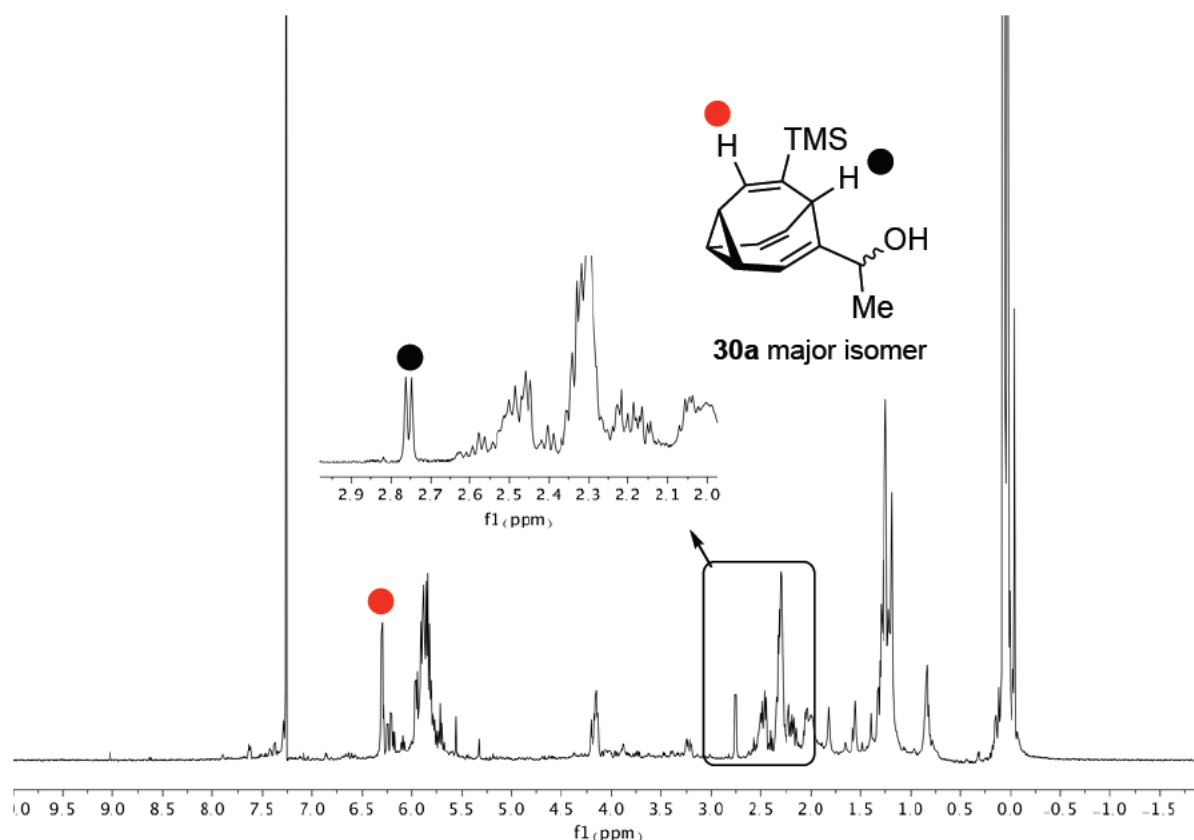
Figure 4.20: Low temperature of **30**.

We were interested in whether the existence of an additional element of stereogenicity will have an impact on the total number of isomers. To predict this number, we will consider arbitrary isomer **30a**. Isomer **30a** is chiral and exist as an enantiomer pair of **ent–31a** and **ent–32a** (Figure 4.21). **Ent–31a** and **ent–3ab** undergo the Cope rearrangement to generate **31b** and **32b**, respectively. The Cope rearrangement occurs and maintains the stereochemical information of the substituent, which means that **ent–31a** and **en**t–**32b** are not interconverting between each other and exist in two separate pools of structures. Consequently, each enantiomer (e.g **ent–31a** or **ent–32a**) exists between an ensemble of 30 isomers. This means **30** exists as a pool of 60 possible isomers. As a result, the addition of one chiral stereocentre to a disubstituted bullvalene, doubled the number of total isomers.
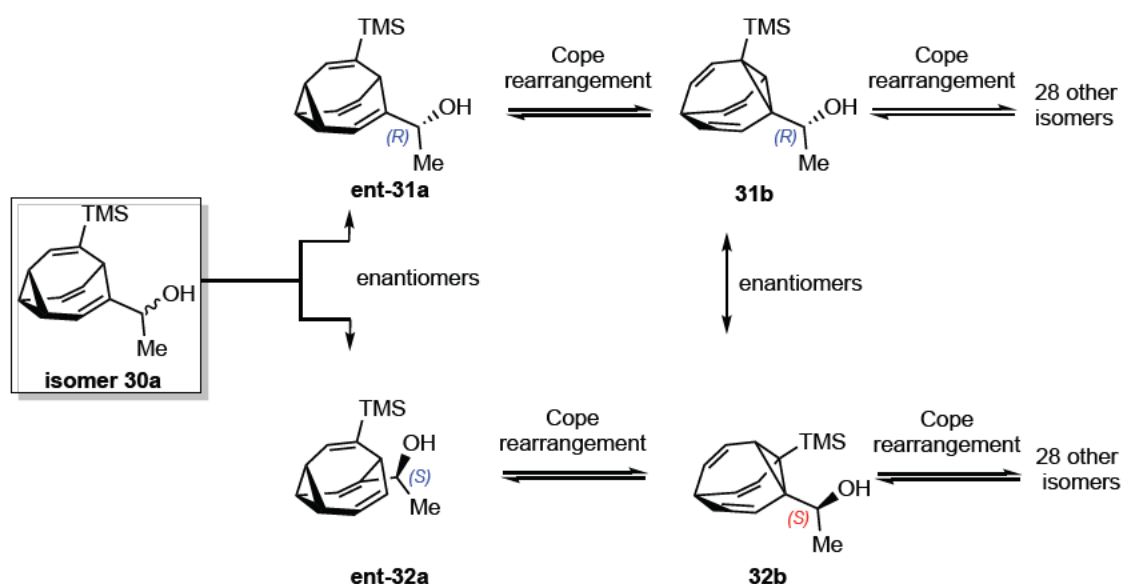
Figure 4.21: Possible number of isomers for **30.**

4.2.2.2. Determination of helicity
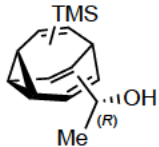
Bullvalene **30** exists between 60 isomers, divided into two enantiomeric pools. Each pool contains isomers that have one or two elements of stereogenicity. Isomers with two elements of stereogenicity possess an axis of chirality and a chiral substituent, whereas isomers with one element of stereogenicity only possess a chiral substituent. We were interested in the analysis of each pool to distinguish the isomers with one or two elements of stereogenicity and determine their helicity with our coding system. Each pool can be regarded as a disubstituted bullvalene with non–identical substituents. Our analysis in Figure 4.22 showed that each pool

contains 18 isomers with two elements of stereogenicity which interconvert between helicity *P* and *M*. Furthermore, 12 isomers possess only one stereocentre.

Figure 4.22: Helicity determination with code system of **30**.

4.2.3. Introduction of two stereogenic centres

4.2.3.1. Synthesis

Our next aim is the installation of two chiral centres into the substituents of a disubstituted bullvalene. For this task we first synthesised dialdehyde bullvalene **34** in high yield (93%) from diol–bullvalene **33**[27] using Swern conditions. Dialdehyde bullvalene **34** is an excellent molecule for further derivatisation such as imine condensation, reductive amination, and Wittig olefination. In this study we performed a double nucleophilic addition to the dialdehyde **34** with lithiated methyl, anisole, and 4,3–dimethoxybenzene to give the corresponding diol **35–37** in moderate yields. The ^{1}H NMR of **35–37** at room temperature displays broad signals which are characteristic of the fluxional behaviour of the molecule. Despite using low temperature

NMR spectroscopy, it remained difficult to elucidate the isomer distribution. High–resolution mass spectrometry affirmed the existence of the products (e.g. **35** measured for ([M+NH$_4$]$^+$) C$_{14}$H$_{22}$O$_2$N$^+$ 236.1645, found 236.1647).
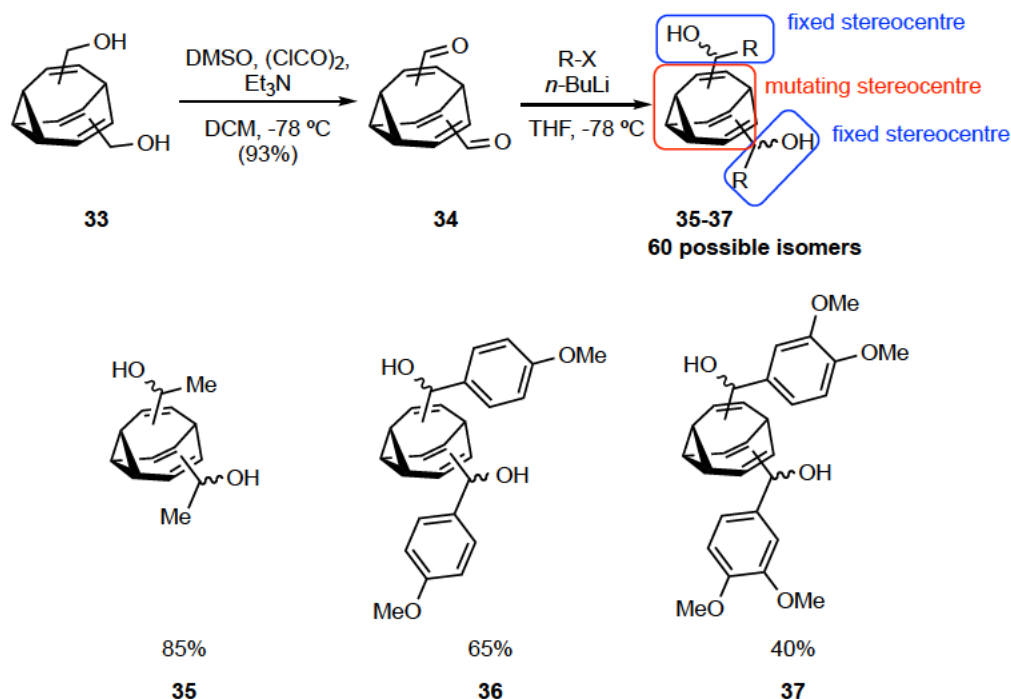
Figure 4.23: Synthesis of diol–bullvalene **35–37**.

The low temperature ^{1}H NMR of the dialdehyde bullvalene **34** however indicated two major isomers **a** and **b** in a ratio of 73:27, respectively.
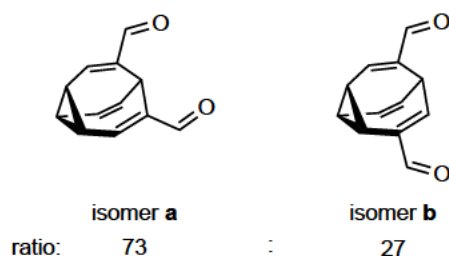
Figure 4.24: Major isomers of **34**.

The products **35–37** each have 60 possible isomers which exist in three separate pools. The first 1,2–addition on the aldehyde gives a chiral bullvalene that exist as two enantiomers ent–**2** and ent–**3**. The latter undergo a further 1,2–addition to deliver diasteromer **40a**, ent–**40b**, and ent–**40c** (Figure 4.25a). Diastereomer–**40a** interconverts between 30 possible isomers, because

it is a disubstituted bullvalene with two unidentical substituents. Ent–**40b** and ent–**40c** interconvert individually between 15 isomers, because both molecules are disubstituted bullvalenes with identical substituents (Figure 4.25b).

Figure 4.25: (a) Stepwise 1,2–addition (b) **35–37** exist between 60 isomers which are divided in three pools of stereoisomers.
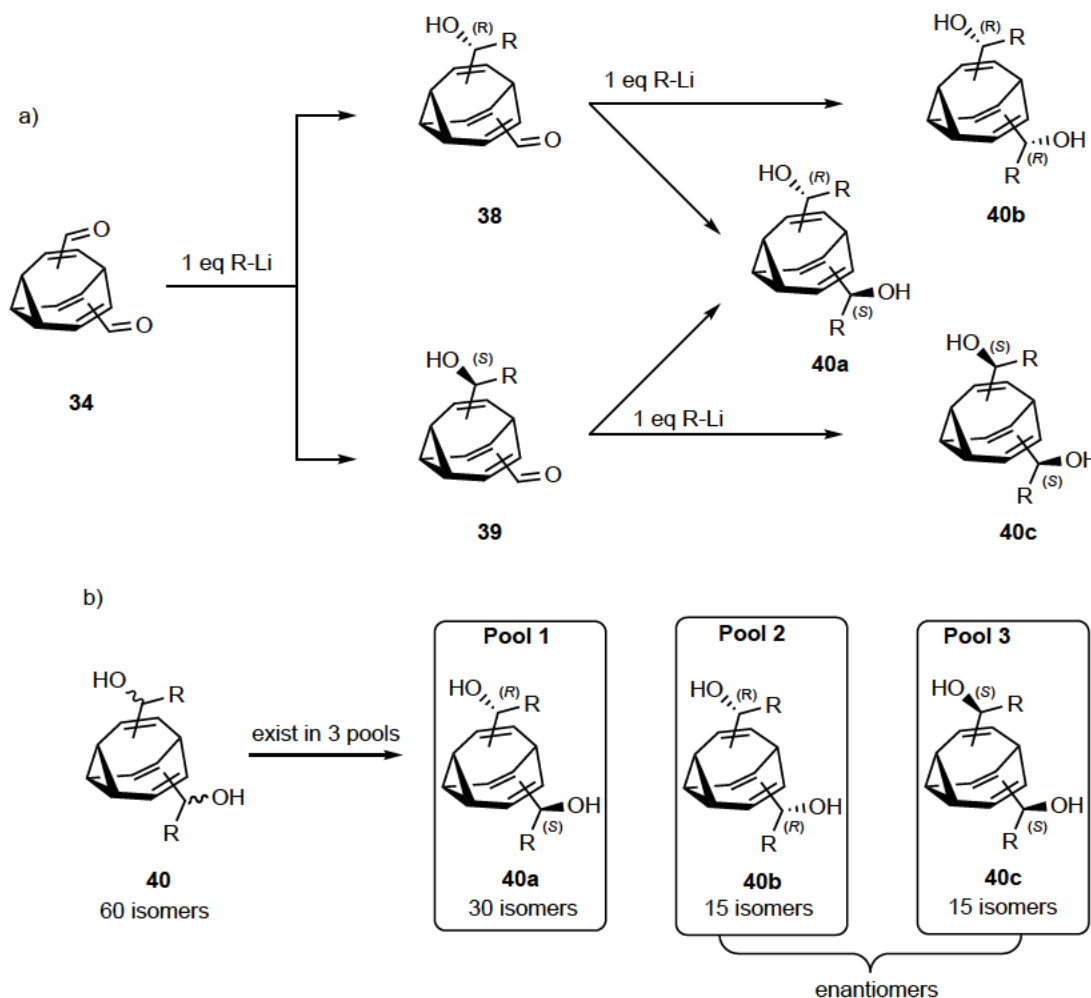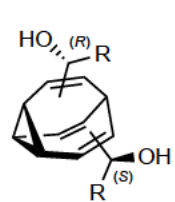
4.2.3.2. Determination of helicity

Pool 1 contains isomers with either two or three elements of stereogenicity. Isomers with two elements of stereogenicity possess two stereogenic centres on the substituents of the bullvalene, whereas isomers with three elements of stereogenicity have one axis of chirality and two stereogenic centres on the substituents. As pool 1 can be regarded as a disubstituted bullvalene with non–identical substituents, our isomer codes used here are the same as those used

previously in Figure 4.22. Pool 1 exists as 18 isomers with three stereogenic isomers and 12 isomers with two stereogenic centres.

Figure 4.26: Determination of helicity for pool 1.

Enantiomeric pools 2 and 3 include disubstituted bullvalenes with identical substituents that also have either two or three elements of stereogenicity. The analysis of the coding system for each enantiomer pool reveals six isomers bearing three elements of stereogenicity, and nine isomers with two stereocentres on its substituents.

				two stereocentres
three elements of stereogenicity				000 000 100 1
				000 010 000 0
enantiomer pairs				000 000 011 0
	mirror			000 000 110 0
Isomer		**Isomer**		000 000 001 1
000 100 001 0 P		000 001 100 0 M		000 100 100 0
				000 001 001 0
000 010 001 0 P		000 001 010 0 M		000 000 010 1
				000 000 100 0
000 100 010 0 P		000 010 100 0 M		

Pool 2	Pool 3
40b	**40c**
15 possible isomers:	**15 possible isomers:**
- 6 with three elements of stereogenicity	- 6 with three elements of stereogenicity
- 3 P isomers	- 3 P isomers
- 3 M isomers	- 3 M isomers
- 9 with two stereocentres	- 9 with two stereocentres

Figure 4.27: Determination of pool 2 and 3 helicity.

Aromatic rings like anisole and 3,4–dimethoxy benzene serve as simple models for aromatic medicinal chemistry fragments. Our synthesised bis((4–methoxyphenyl)methanol) bullvalene **36** and bis((4,3dimethoxypheny)methanol) bullvalene **37** represent a chemical library with 60 possible isomers that are distinguished by shape rather than functionality (Figure 4.28).
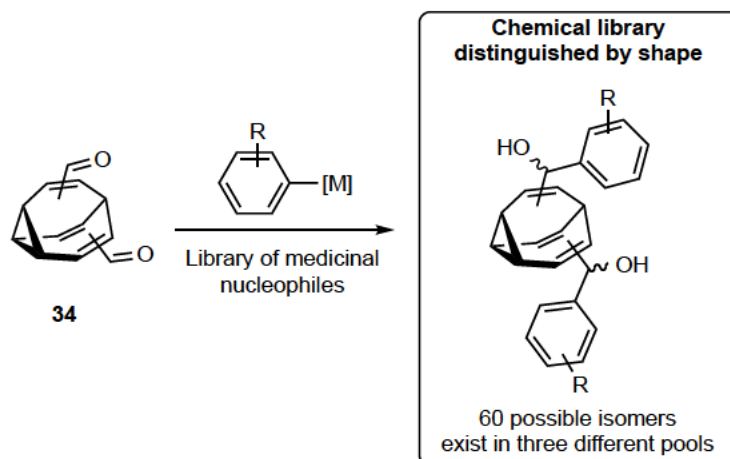
Figure 4.28: Creation of chemical library in one reaction.

4.2.4. Bis(TMS) methylmalonic diester bibullvalene

Schröder previously synthesised dibullvalene[62] **43** and hexamethylbibullvalene[73] **45** from bomo bullvalene **41** and tetrabromo bullvalene **44**, respectively. Dibullvalene **43** exists between three isomers within an ensemble of 10 possible isomers. The low temperature NMR analysis of hexamethyl bibullvalene **45** is lacking detail, but the bullvalenes are attached to each other through the olefinic carbons.
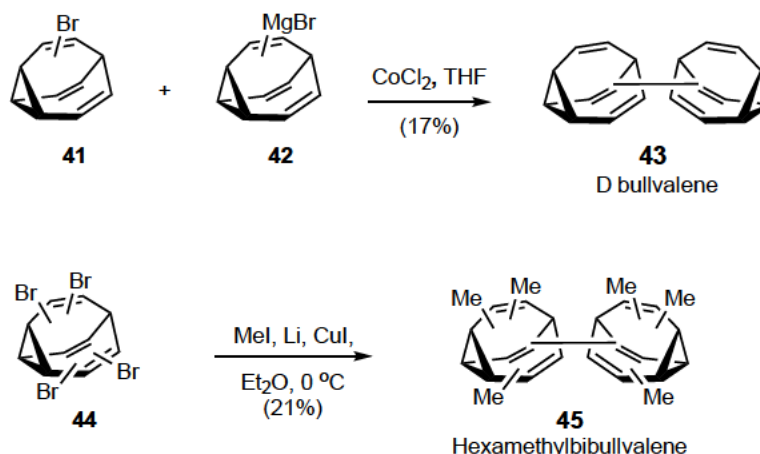
Figure 4.29: Synthesis of dibullvalene and hexamethyl dibullvalene.

The conjoining of bullvalene units into dimers, oligomers, or even polymers has the potential to dramatically expand the number of possible isomers. We envisaged to synthesise a dibullvalene **32** by linking two disubstituted bullvalenes through a chiral bridge (Figure 4.30). Therefore, the molecule will have three elements of stereogenicity: two of these belongs to

bullvalenes which have a mutating axis of chirality, and the third central stereocentre which would stereomutate depending on the isomer identity of the adjacent bullvalenes.
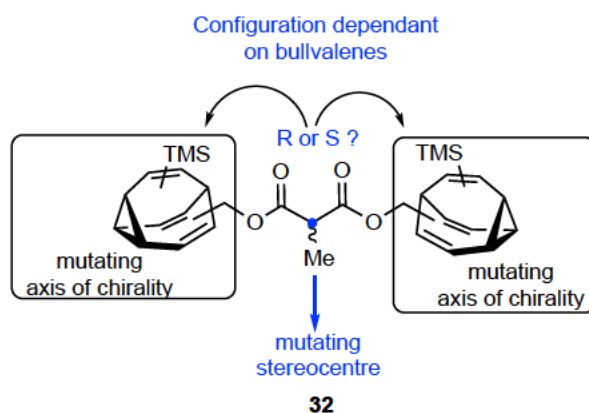
Figure 4.30: Dibullvalene representation.

4.2.4.1. Synthesis

Steglich diesterification of 2–methylmalonic acid[109] **1** with TMS–menthol–bullvalene **4** gave bis(TMS)–methymalonic diester dibullvalene **2** in moderate yield (34%) (Figure 4.31).
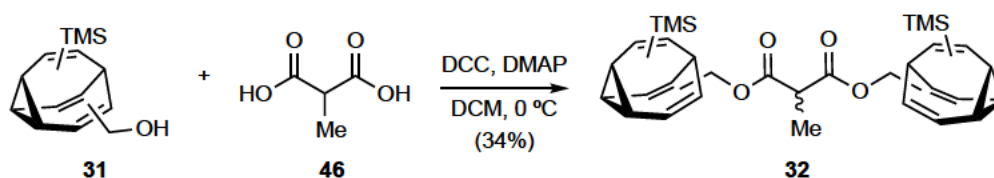
Figure 4.31: Synthesis of Bis(–TMS)–methylmalonic diester dibullvalene.

The low temperature ^{1}H NMR of bis(TMS) methylmalonic diester dibullvalene **32** indicated a major isomer in which the substituents are flanking the bridgehead carbon (Figure 4.32). A distinctive doublet in the methine region is a characteristic signal of a bridgehead proton flanked by two substituents. The downfield alkenic signal is characteristic of a proton adjacent to the TMS group. These same analytical observations were seen in the major isomer **a** (Figure 4.20).
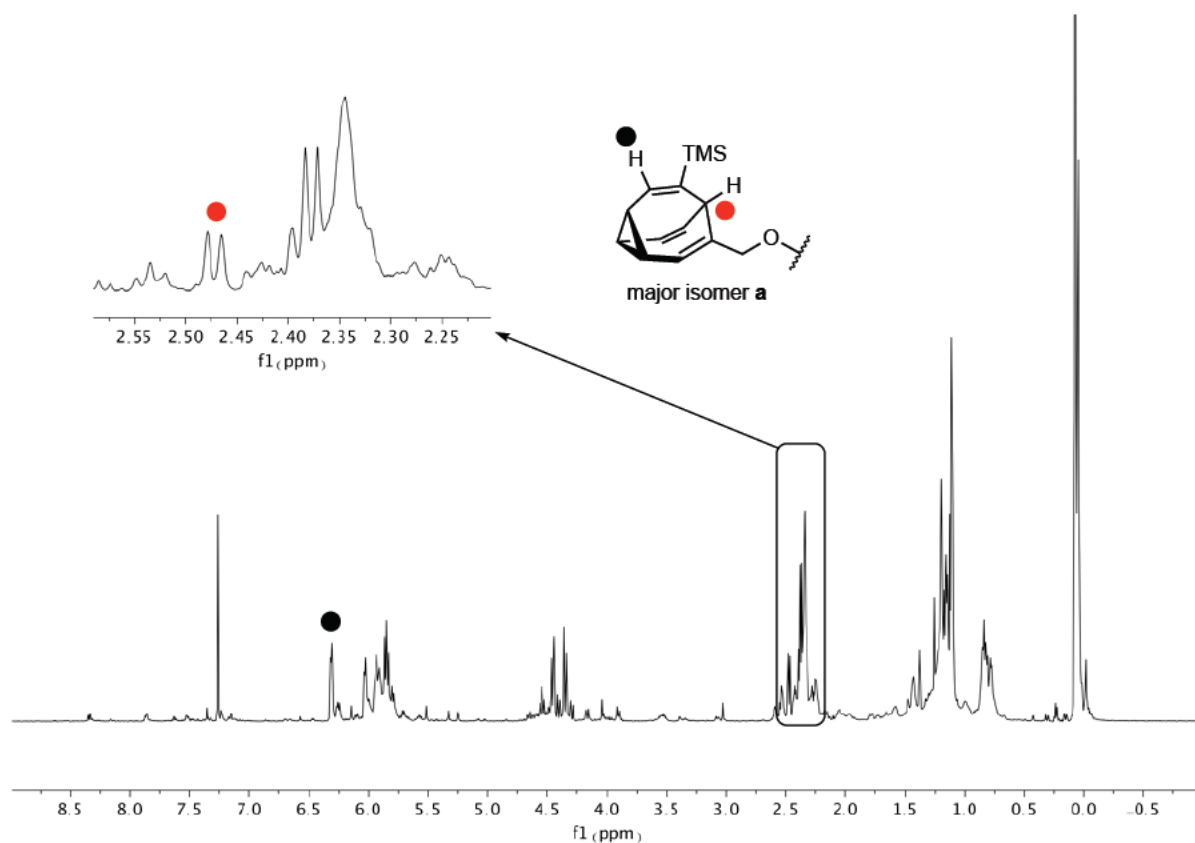
Figure 4.32: Low temperature ^{1}H NMR spectra of bis(TMS) methylmalonic diester dibullvalene revealing major isomer **a.**

Furthermore, the low temperature ^{13}C NMR indicated a set of 6 olefinic carbon signals with high intensity, indicating only one major isomer (Figure 4.33). Spectroscopically, we cannot observe distinct connections between the two bullvalene units. We expect, given the distance between the bullvalene units, that the isomer identity of one bullvalene will not significantly change the chemical environment of the other bullvalene.
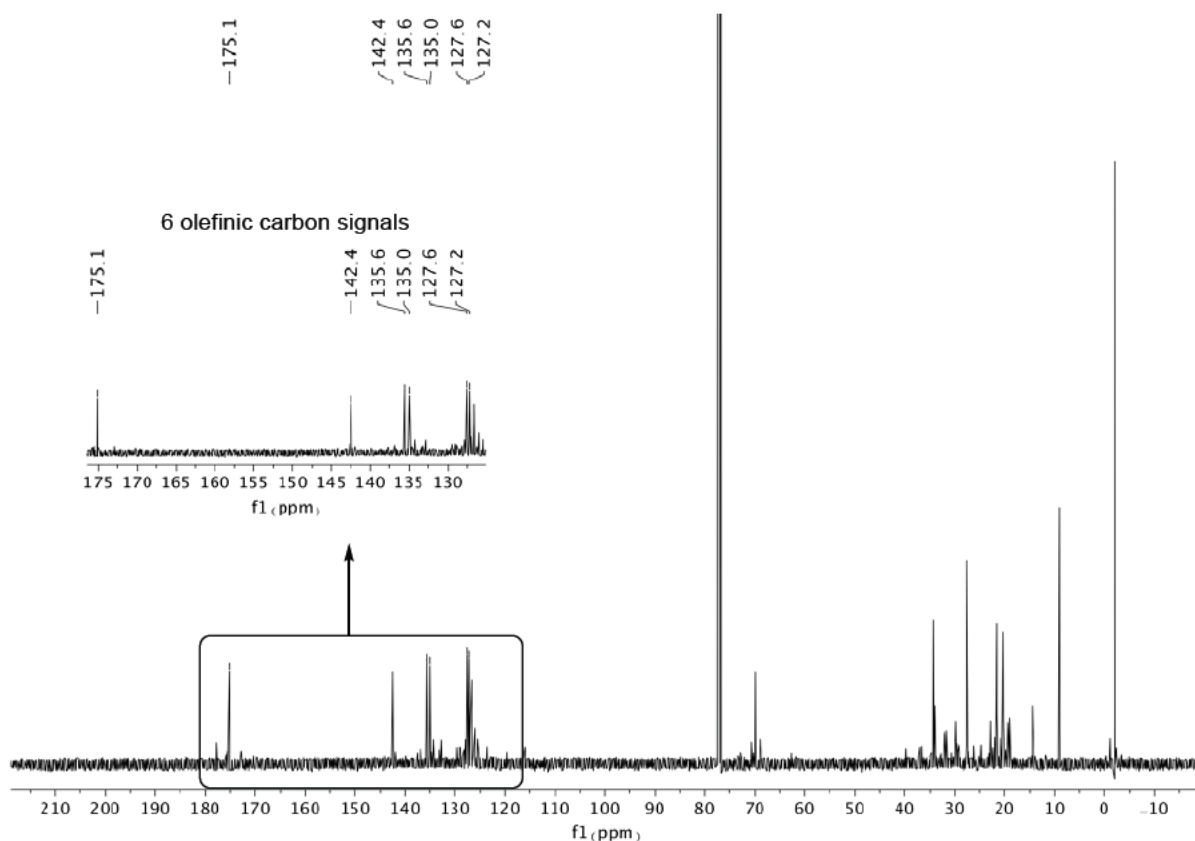
Figure 4.33: Low temperature ^{13}C NMR spectra of bis(TMS) methylmalonic diester.

4.2.4.2. Identification of the central stereocentre configuration

As mentioned in Figure 4.30, the configuration of the central element would stereomutate depending on the isomer identity of bullvalene. To determine the *R/S* configuration of the central stereocentre, one must assign Cahn–Ingold–Prelog priorities to the bullvalene isomers. For polycyclic caged systems this is not trivial, so we utilised the CIP engine within the chemdraw software to compare isomer pairs and develop a "CIP ranking" for all 30 possible isomers. This is listed in Figure 4.34, and allows for easy assignment of the configuration of the central stereocentre.

Isomer	Ranking	
000 200 100 0	30	**High**
000 100 200 0	29	
000 000 210 0	28	
000 000 001 2	27	
000 000 120 0	26	
000 000 002 1	25	
000 000 021 0	24	
000 000 012 0	23	
000 200 010 0	22	
000 010 200 0	21	
000 000 201 0	20	
000 000 010 1	19	
000 020 100 0	18	
000 100 020 0	17	
000 000 102 0	16	
000 002 001 0	15	
000 001 002 0	14	
000 000 020 1	13	
000 200 001 0	12	
000 001 200 0	11	
000 000 200 1	10	
000 000 100 2	9	
000 020 010 0	8	
000 010 020 0	7	
000 010 002 0	6	
000 002 010 0	5	
000 100 002 0	4	
000 002 100 0	3	
000 020 001 0	2	
000 001 020 0	1	**Low**

Example of isomer ranking

higher rank   lower rank

isomer: 000 000 210 0   000 200 001 0
rank: 28   12

Figure 4.34: Ranking of all 30 isomers.

The total number of possible isomers of bis(TMS) methylmalonic diester is 900 as each of the two bullvalenes are of the differentially disubstituted type with 30 possible isomers. By using an extended coding system that includes the barcode of bullvalene 1 and bullvalene 2 we can determine the *R/S* configuration of the central stereocentre as shown in Figure 4.35 (with the methyl group arbitrarily shown towards us).
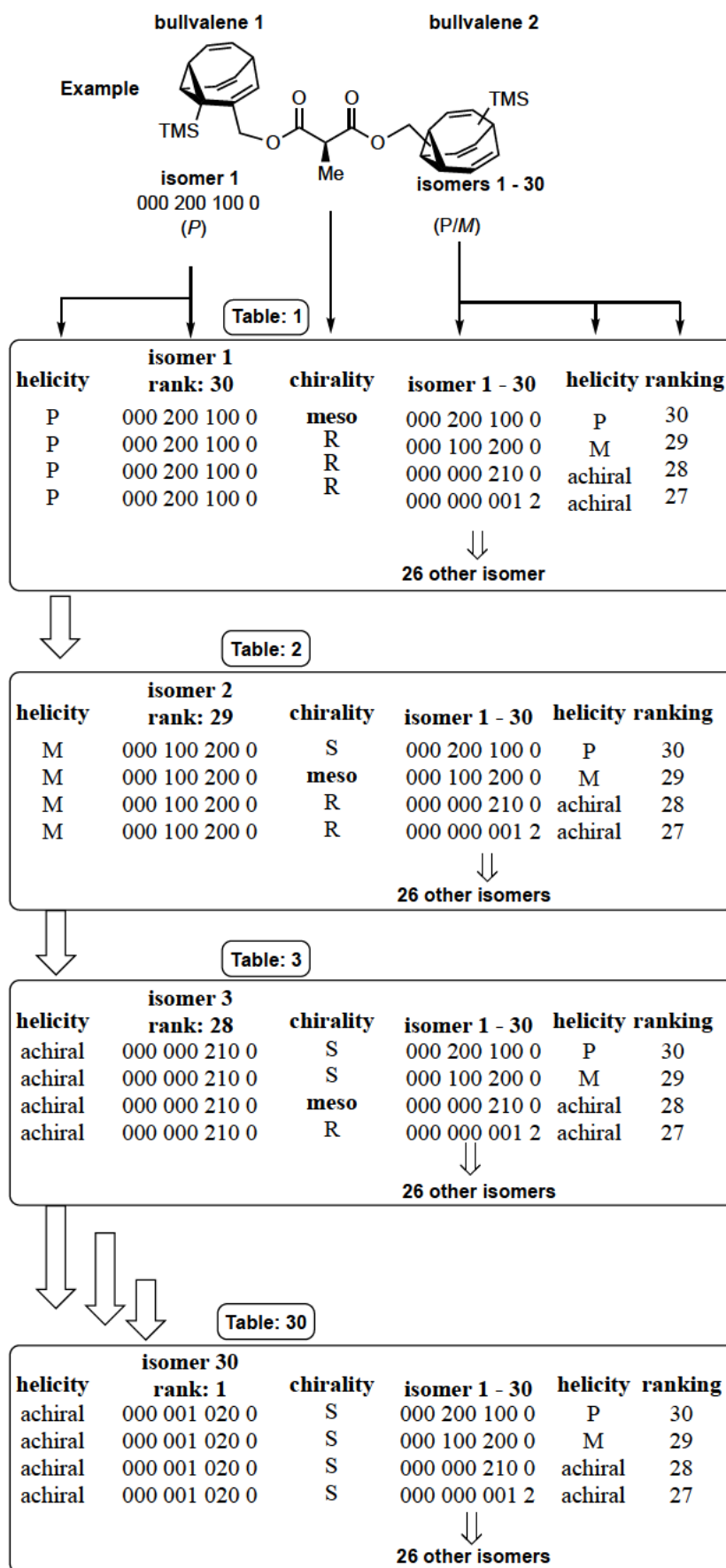
Figure 4.35: Determination of the central stereocentre configuration of all 900 possible isomers.

The analysis of the bullvalene stereocentres shows how the dynamic ensemble of exchanging isomers made the central streoreocentre mutate. The is a novel example of steromutation in which the shapeshifting property of the bullvalene is controlling the configuration of the stereocentre. Moreover, three stereomutation are occurring simultaneously.

4.3. Conclusion and future work

To conclude, we expanded the dynamic behaviour of disubstituted bullvalene by installing one or two elements of stereogenicity into their substituents. This leads to the formation of a chemical library that is distinguished by shape, in which some isomers have a stereomutation occurring on the bullvalene core while the configuration of the stereogenic centre is fixed. Dialdehyde bullvalene **34** is an exemplary molecule for further derivatisation. A further oxidation would deliver the dicarboxylic acid **47**, which can be used as a building block to form a metal organic framework **48**. Reductive amination **49** or iminium condensation **50** formation could rapidly diversify a chemical library of disubstituted bullvalenes. A Wittig olefination might lead to a product **51** that can undergo a Cope rearrangement **52** to give an "opened out" bullvalenee **53**.

The conjoining of two bullvalenes with a stereogenic tether forming bis(TMS) methylmalonic diester dibullvalene is a novel example of stereomutation in which three stereomutations are occurring side by side. Yet, the configuration of the central stereocentere is dependant on the bullvalene isomers.

This project requires DFT calculations to support our observed isomer ratios of the substituted bullvalenes and to develop a reaction graph that shows the interconversion of all possible isomers.
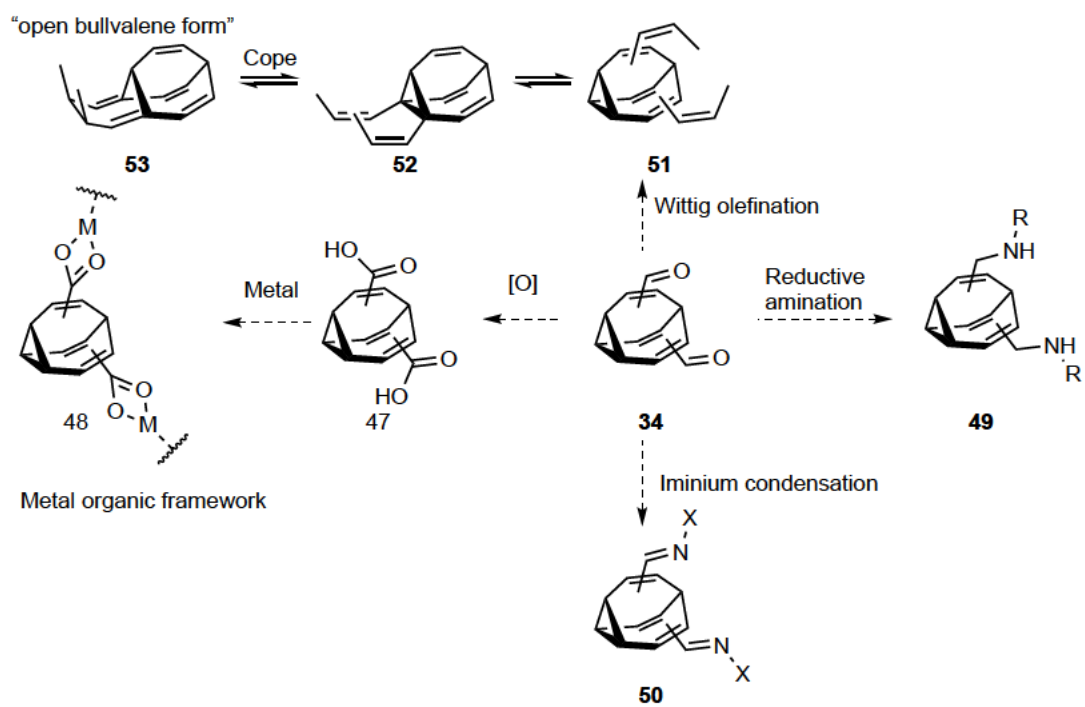
Figure 4.36: Dialdehyde as a key molecule for further functionalization.

Chapter 5

5. Endiandric acid minireview

Hitherto, a review about the synthesis of endiandric acid natural products has not been reported. Therefore, this introduction will form the basis of a future minireview. Here we cover all the strategies to access the bicyclo[4.2.0]octadiene moity that act as the key component for the synthesis of bicyclo[4.2.0]octadiene derived natural products and the synthesis of all reported endiandric acids.

Statement of Authorship

Title of Paper	Endiandric Acid minireview
Publication Status	☐ Published ☐ Accepted for Publication ☐ Submitted for Publication ☒ Unpublished and Unsubmitted work written in manuscript style
Publication Details	O. Yhaioaui, H. D. Patel, and Thomas Fallon

Principal Author

Name of Principal Author (Candidate)	Oussama Yahiaoui
Contribution to the Paper	Wrote the manuscript
Overall percentage (%)	90%
Certification:	This paper reports on original research I conducted during the period of my Higher Degree by Research candidature and is not subject to any obligations or contractual agreements with a third party that would constrain its inclusion in this thesis. I am the primary author of this paper.
Signature	Date 22.05.2020

Co-Author Contributions

By signing the Statement of Authorship, each author certifies that:

i.   the candidate's stated contribution to the publication is accurate (as detailed above);

ii.   permission is granted for the candidate in include the publication in the thesis; and

iii.   the sum of all co-author contributions is equal to 100% less the candidate's stated contribution.

iv.

Name of Co-Author	Harshal Patel
Contribution to the Paper	Revised manuscript
Signature	Date 22.05.202

Name of Co-Author	Thomas Fallon
Contribution to the Paper	Corresponding authr
Signature	Date 22.05.202

5.1. Introduction of the endiandric acid family

This family of natural products biosynthetically derived or proposed to arise, from a linear tetraene giving rise to a bicyclo[4.2.0]octadiene framework, as well as natural products derived from further reactivity of this motif.

In the 1980s, Black discovered and isolated the endiandric acids. They were all isolated as racemates and proposed to arise through a non–enzymatic cascade; the 8π–6π electrocyclization of a linear tetraene to give a bicyclo[4.2.0]octadiene[110] followed by an intramolecular Diels–Alder reaction. Following Blacks report, the biosynthesis of this family of natural products was promptly proven by Nicolaou.[111] Since then, numerous bicyclo[4.2.0]octadiene containing and derived natural products have been isolated (Figure 5.1), and their synthesis targeted by numerous research groups.
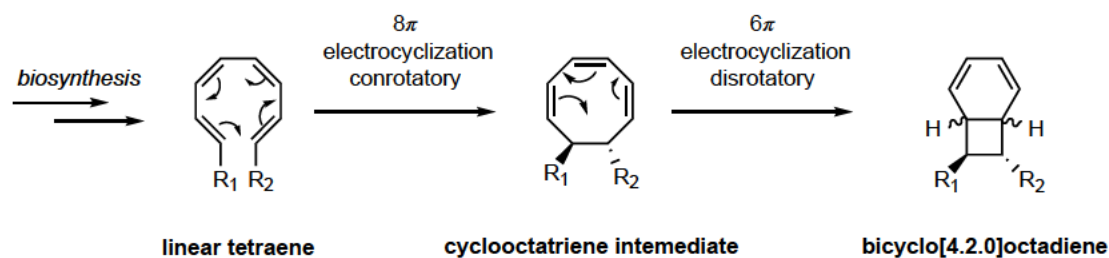
Figure 5.1: Blacks theory of a cascade reaction from a linear tetraene to give the bicyclo[4.2.0]octadiene motif.
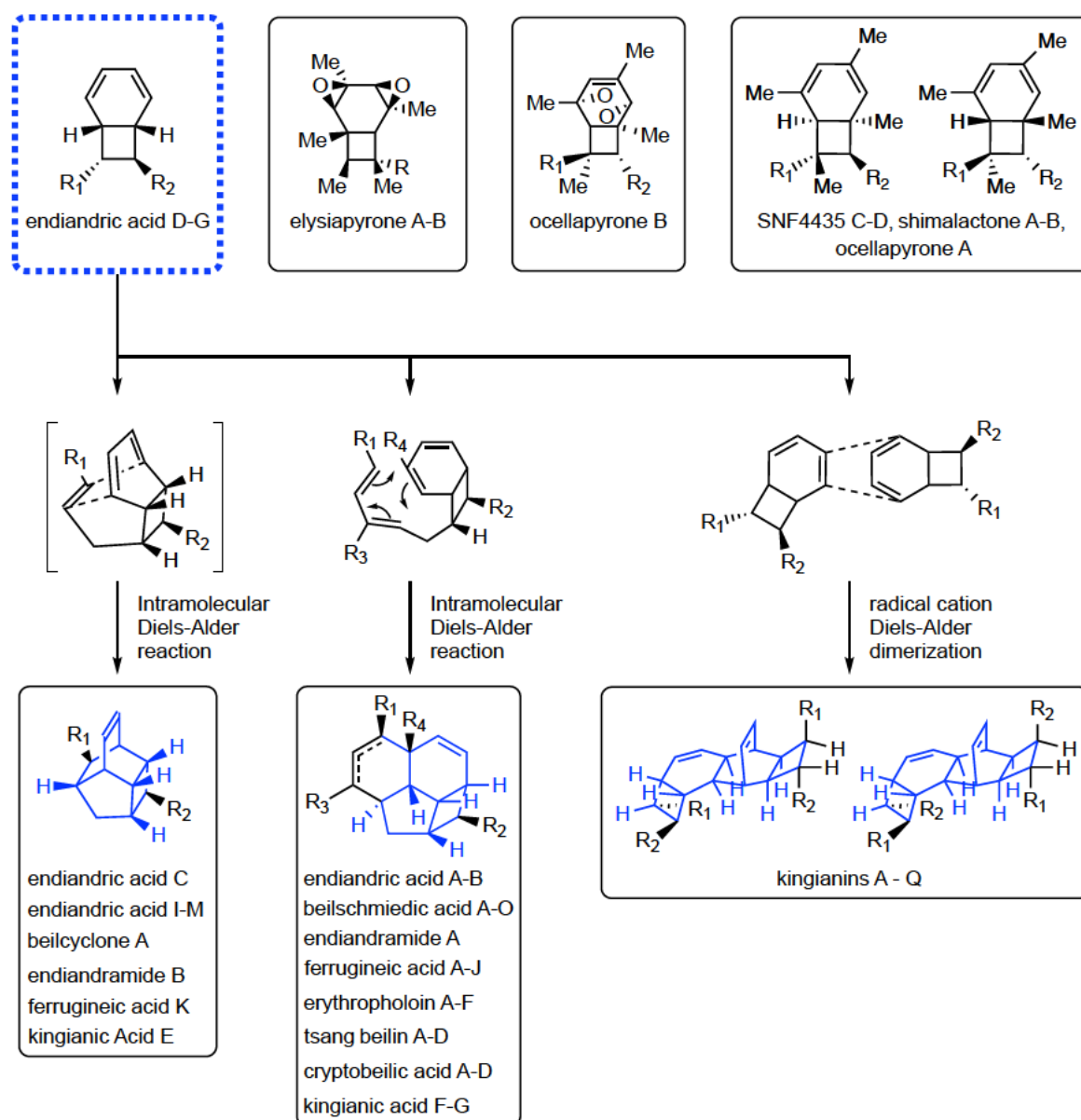
Figure 5.2: Bicyclo[4.2.0]octadiene natural products: Endiandric acid A [112–117] , Endiandric acid B [117], Endiandric acid C [115–117], Endiandric acid D, Endiandric acid E, Endiandric acid F, Endiandric acid G, Beilcyclone A [118], Kingianic acid A–E[119], The Kingianin natural product isolated from the bark of Endiandra kingiana (Lauraceae) by Litaudon and co, [120,121] SNF4436 C and D[122,123], elysiapyroneA and B[124], Ocellapyrone A and B[125], Shimalactone A and B.

Strategies that have been successful in the synthesis of bicyclo[4.2.0]octadiene natural products are highlighted in Figure 5.3. Most syntheses have relied on building block methodology to reach a linear tetraene precursor, either proceeding through semi–hydrogenation of poly–alkynes as shown by Nicolaou and Lawrence/Sherburn, or through the cross coupling of diene building blocks as demonstrated by Trauner, Parker, and Moses. Our group's approach differs

to previous strategies through interception of the 8π–6π cascade by achieving an overall 1,2–anti difunctionalisation of cyclooctatetraene.
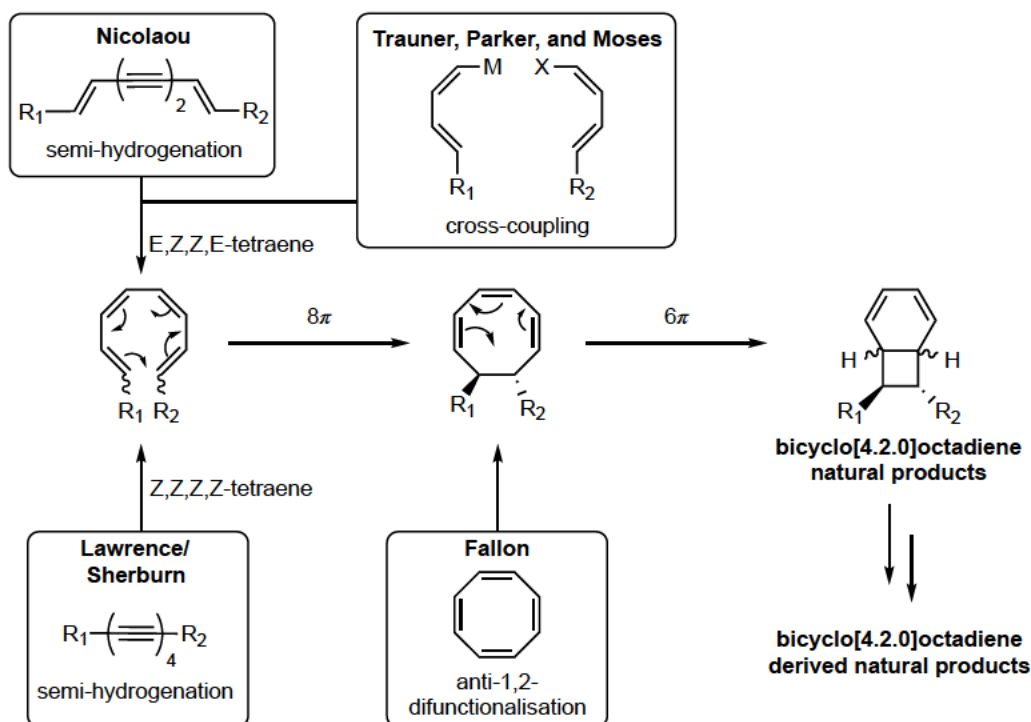
Figure 5.3: Strategies to access the bicyclo[4.20]octadiene moity.

The following sections will highlight the work achieved by the aforementioned groups, as well as considering other synthetic methodology that may allow access to the bicyclo[4.2.0]octadiene (BOD) families of natural products.

5.2. Synthesis of endiandric acid

5.2.1. Synthesis of endiandric acid A–G by Nicolaou

Nicolaou's seminal syntheses of endiandric acids A–G encompasses synthetic strategies to isolate each individual natural product, as well as the biomimetic synthesis of these molecules, thus confirming Black's biosynthetic proposal.[126,127]

Nicolaou's total synthesis campaign begins with Glasser acetylene coupling of the commercially available *trans*–pent–2–en–4–yn–1–ol **1** to give diacetylene **2** (Figure 5.4). The

latter **2** was hydrogenated with Lindlar catalyst to generate the (*E,Z,Z,E*)–tetraene intermediate **3**, which underwent spontaneous 8π conrotatory **4** and 6π disrotatory electrocyclization to afford the bicyclo[4.2.0]octadiene **5** (BOD). The BOD **5** was subjected to an iodoetherification to differentiate the hydroxy groups, giving ether **6**.
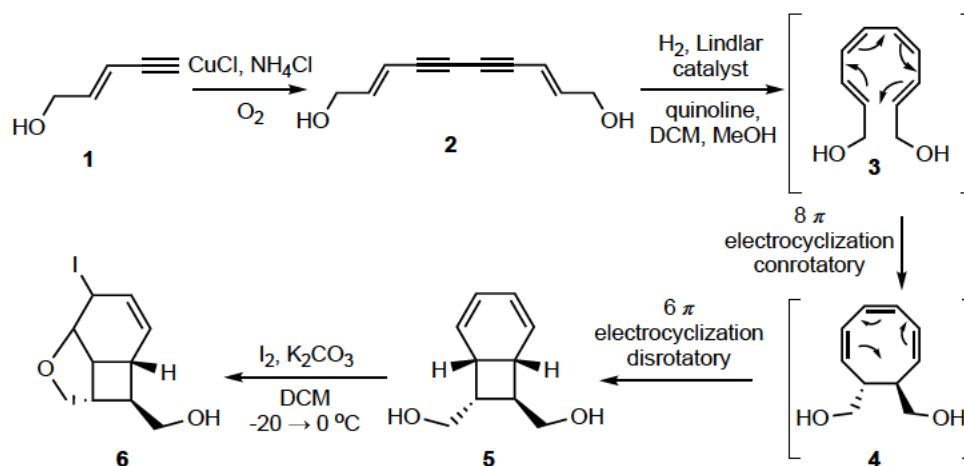
Figure 5.4: Synthesis of endiandric acid A–G by Nicolaou.

Protection of the alcohol in **6** and the conversion of the ether to the cyanide afforded **7** in four steps (Figure 5.5). This molecule acted as a point of diversification from which endiandric acids A–G were synthesised. In **7** the endo cyano group was transformed to the carboxylic acid. After deprotection and further manipulations, endiandric acid D **8** was obtained. Endiandric acid G **9** is obtained from **8** by converting the acid to a vinyl acid in four steps.

The BOD **7** was reduced to the aldehyde **10** with DIBAL. Endiandric acid C **12** was synthesized from aldehyde **10** through a Horner–Wadsworth–Emmons (HWE) reaction to give an olefin on the endo side of the BOD **11**, which undergoes an intramolecular Diels–Alder reaction and with further synthetic transformations reached the natural product **12**.

Aldehyde **10** is also used for the synthesis of endiandric acid A and B, through a HWE reaction to give a diene **13** which undergoes an intramolecular Diels–Alder reaction. **13** can be converted to either endiandric acid E or F by converting the aldehyde to the corresponding substituent.
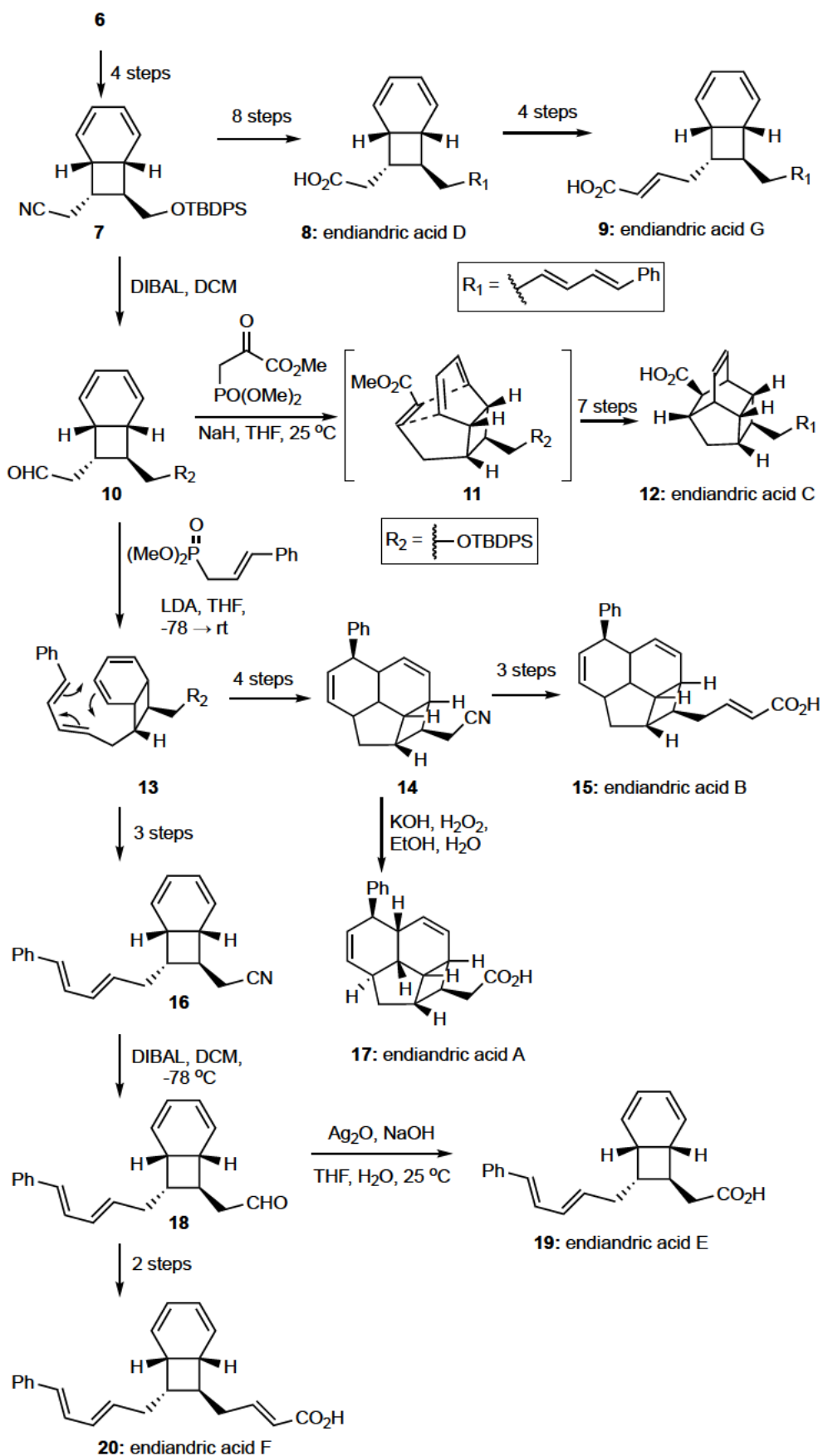
Figure 5.5: Synthesis of endiandric acid A–G by Nicolaou.

In the biomimetic synthesis of endiandric acids A–G[128,129] Nicolaou constructed precursor **21** in 13 steps (Figure 5.6). Semihydrogenation with Lindlar catalyst gave the *E,Z,Z,E*–tetraene which undergoes an 8π–6π cascade to give a mixture of endiandric acids methyl ester **22** and **23**. When both molecules were heated in toluene the intramolecular Diels–Alder afforded endiandric acid methyl ester A **24** in 30 % yield. Using the same methodology but with a different precursor **25**, endiandric acids methyl ester F and G (**26**, **27**) were synthesised. Heating in toluene gave endiandric methyl ester B and C (**28**, **29**) in a combined yield of 28% and a ratio of 4.5:1, and reflects the ability of the BOD precursors to undergo the intra–molecular Diels–Alder in one of two distinct modes.
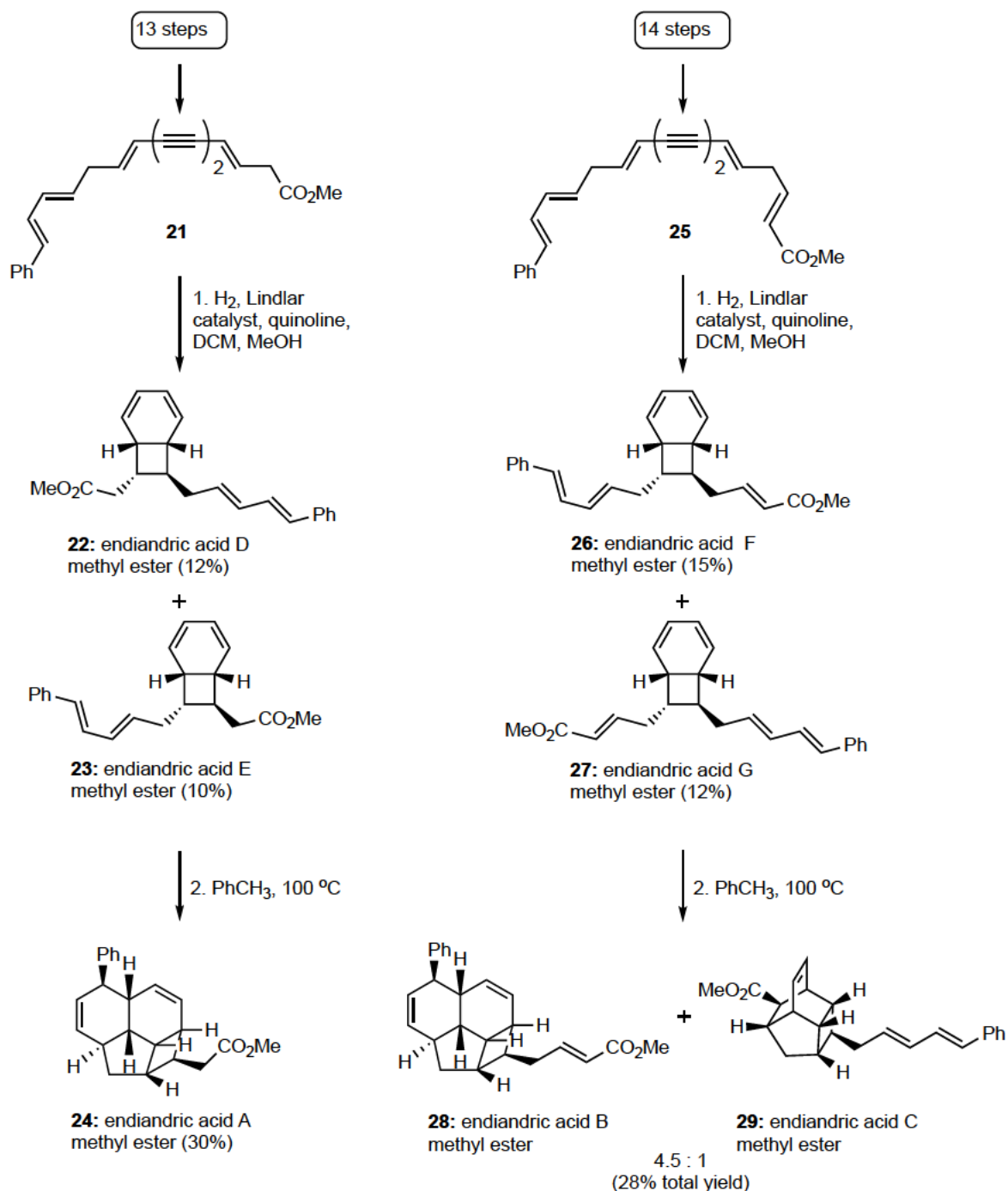
Figure 5.6: Biomimetic synthesis of Endiandric acid A–G by Nicolaou.

5.2.2. Synthesis of endiandric acid A and kingianic acid E by Sherburn and Lawrence

Where Nicolaou's syntheses proceeded through an *E,Z,Z,E* tetraene using a biomimetic approach, Sherburn's approach proceeded through a non–biomimetic *Z,Z,Z,Z* tetraene requiring heating to initiate the 8π–6π cascade (Figure 5.7).[130] Hydrogenation of tetrayne **30**

or **33** with Riecke zinc afforded the (*Z,Z,Z,Z*)–tetraene **31** or **34**. Heating **31** in DMF at 150 °C followed by an in situ deprotection and subsequent oxidation to the carboxylic acid, afforded the desired kingianic acid E **32**. Heating **34** in toluene at 150 °C followed by a deprotection in situ and an oxidation to the carboxylic acid afforded endiandric acid A **17**.
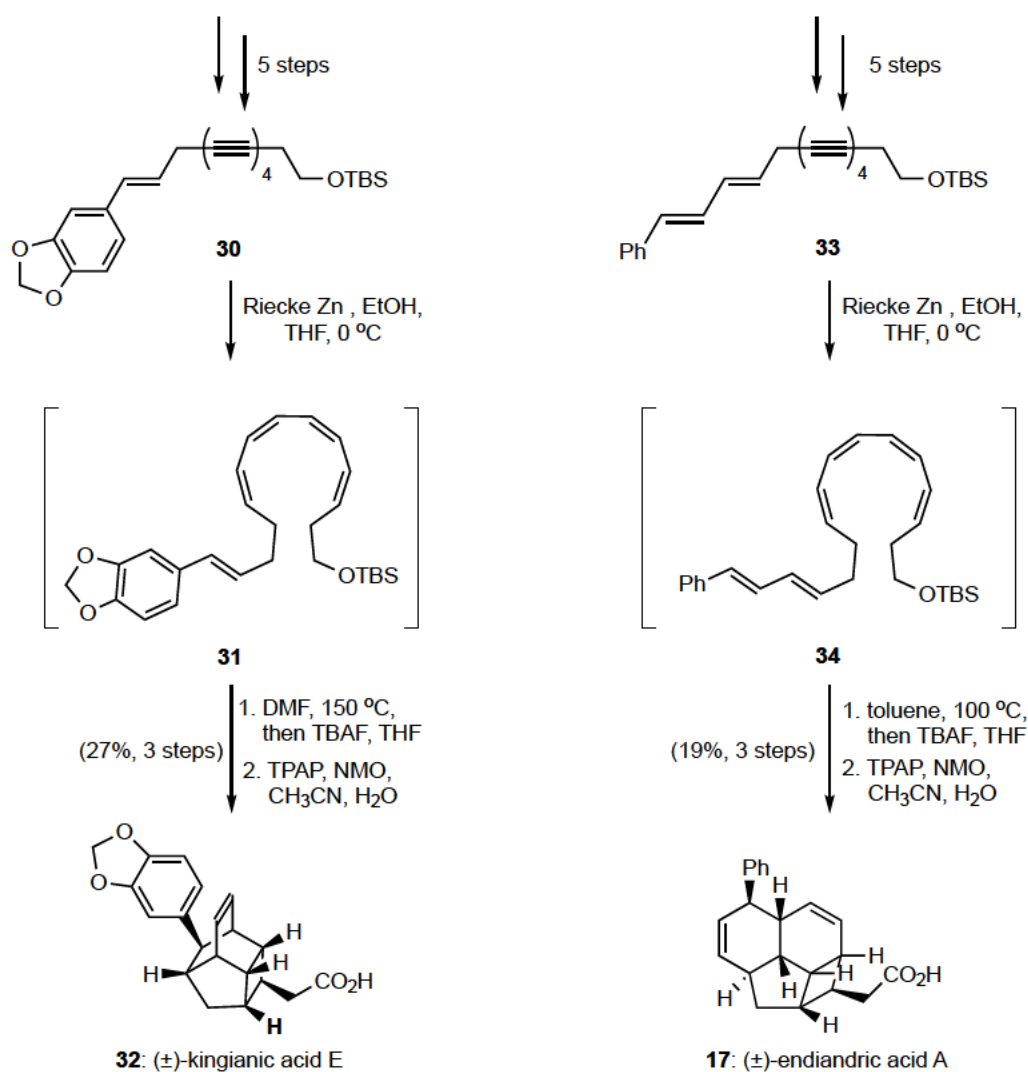
Figure 5.7: Total synthesis of endiandric acid A and kingianic acid E by Sherburn.

5.2.3. Vosburg's Synthesis of Endiandric Acid Type Natural Products

Vosburg's strategy relies on the cross–coupling of alkenyl MIDA boronate **35** and alkenyl iodide **36** precursors to access an *E,Z,Z,E* linear tetraene, which after the 8π–6π cascade give bicyclo[4.2.0]octadiene **37** (Figure 5.8).[131] Subsequent functional group manipulations provide access to endiandric acid type scaffolds **38** and **39**.
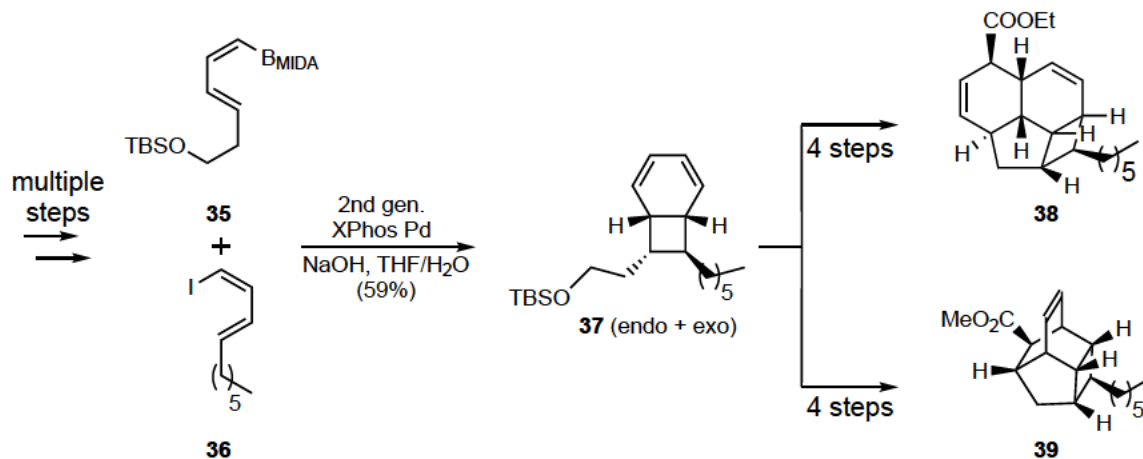
Figure 5.8: Alternative route for the synthesis of Endiandric acid–type by Vosburg.

5.3. Total synthesis of Kingianin

5.3.1. Parker's synthesis

Parker's strategy to Kingianin A begins with a Suzuki cross–coupling of pinacol boronate ester diene[132] **41** and iodo–diene **40** to generate a tetraene intermediate, which undergoes 8π/6π electrocyclization to afford the bicyclo[4.2.0]octadiene system **42** (Figure 5.9). Deprotection and a selective iodoetherification to aid purification gave **5**. Dimerisation of **43** has the ability to produce kingianins A and D. The encountered difficulties during the isolation of kingianin A from the other natural product led Parker to design an easy way to isolate the natural product. Linking two molecules of alcohol **43** with a removable tether would facilitate an intramolecular dimerization and simplify the purification. Etherification of alcohol **43** with adipoyl chloride gave racemic **44** and the C–2 symmetric substrate **45**. Treatment of **44** and **45** with the Ledwith–Weitz Salt led to a radical intramolecular Diels–Alder reaction giving an approximately equal amount of easily separable endo **47** in 34% yield and exo **46** in 30 % yield. Kingianin A was obtained from endo **47** after three steps in 72% yield.
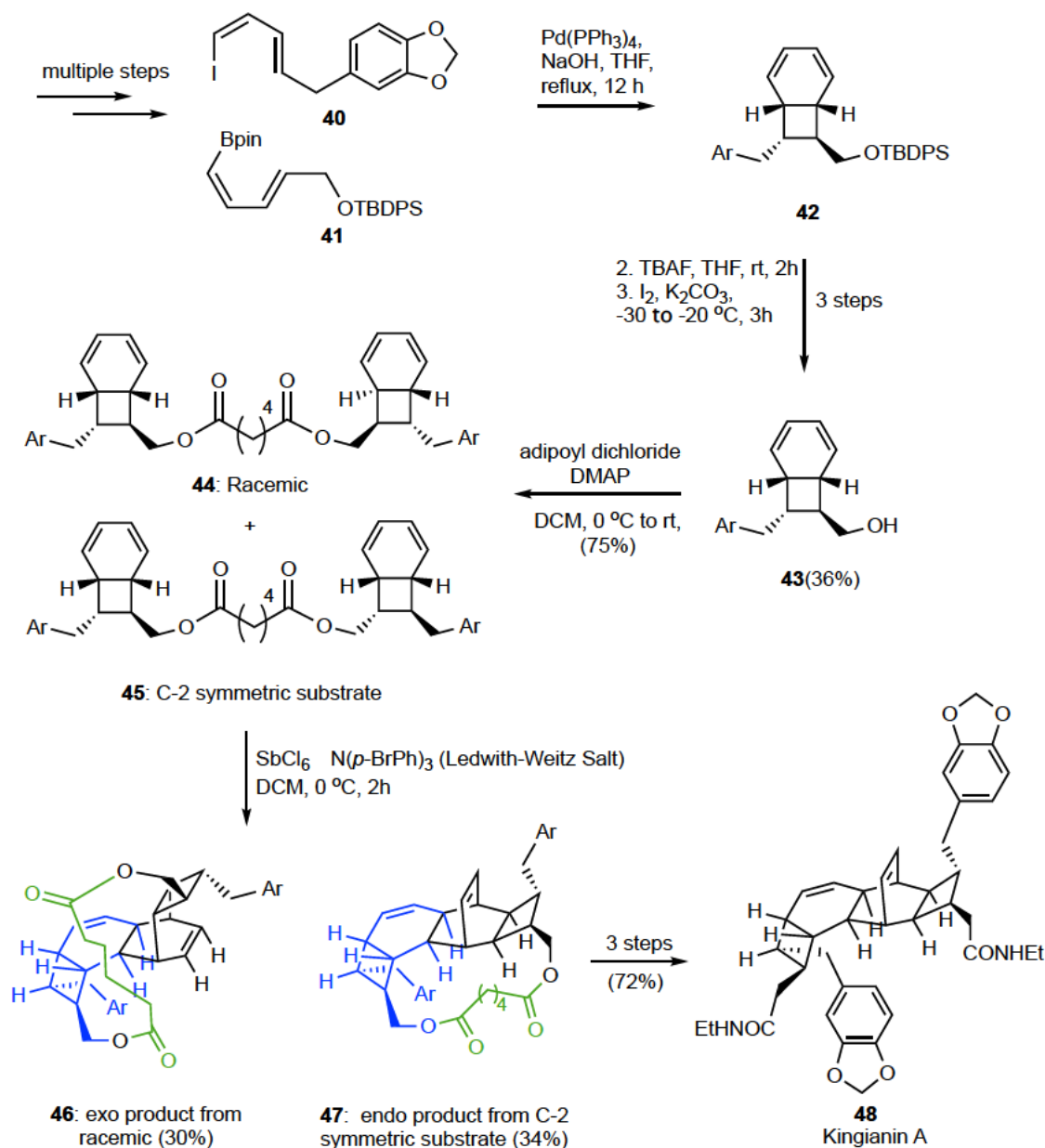
Figure 5.9: Total synthesis of Kingianin by Parker.

5.3.2. Synthesis of Kingianins A, D, and F by Sherburn and Lawrence

The Sherburn and Lawrence strategy towards the synthesis of kingianin is practical and requires a small number of steps (Figure 5.10).[133][134] Tetrayne 49[135,136] is reduced with Riecke zinc to afford a *Z,Z,Z,Z*–tetraene[137] which is heated up at 100 °C in toluene to spark the 8π/6π electrocyclization reaction.[138][134] Deprotection of the TBS group afforded the two diastereomeric alcohols 50 and 51 in combined yield of 21%. Alcohol 50 was oxidised, subjected to radical intermolecular Diels–Alder conditions using Ledwith–Weitz salt,[139,140]

and amidified to give Kingianins A **48** and D **53**. Alcohol **51** first underwent the radical intermolecular Diels–Alder, followed by oxidation and amidification to give Kingianin F **54**. The radical cation Diels–alder dimerization occurrs very selectively, since three products were obtained from thirty–two potential isomeric products that have been isolated.
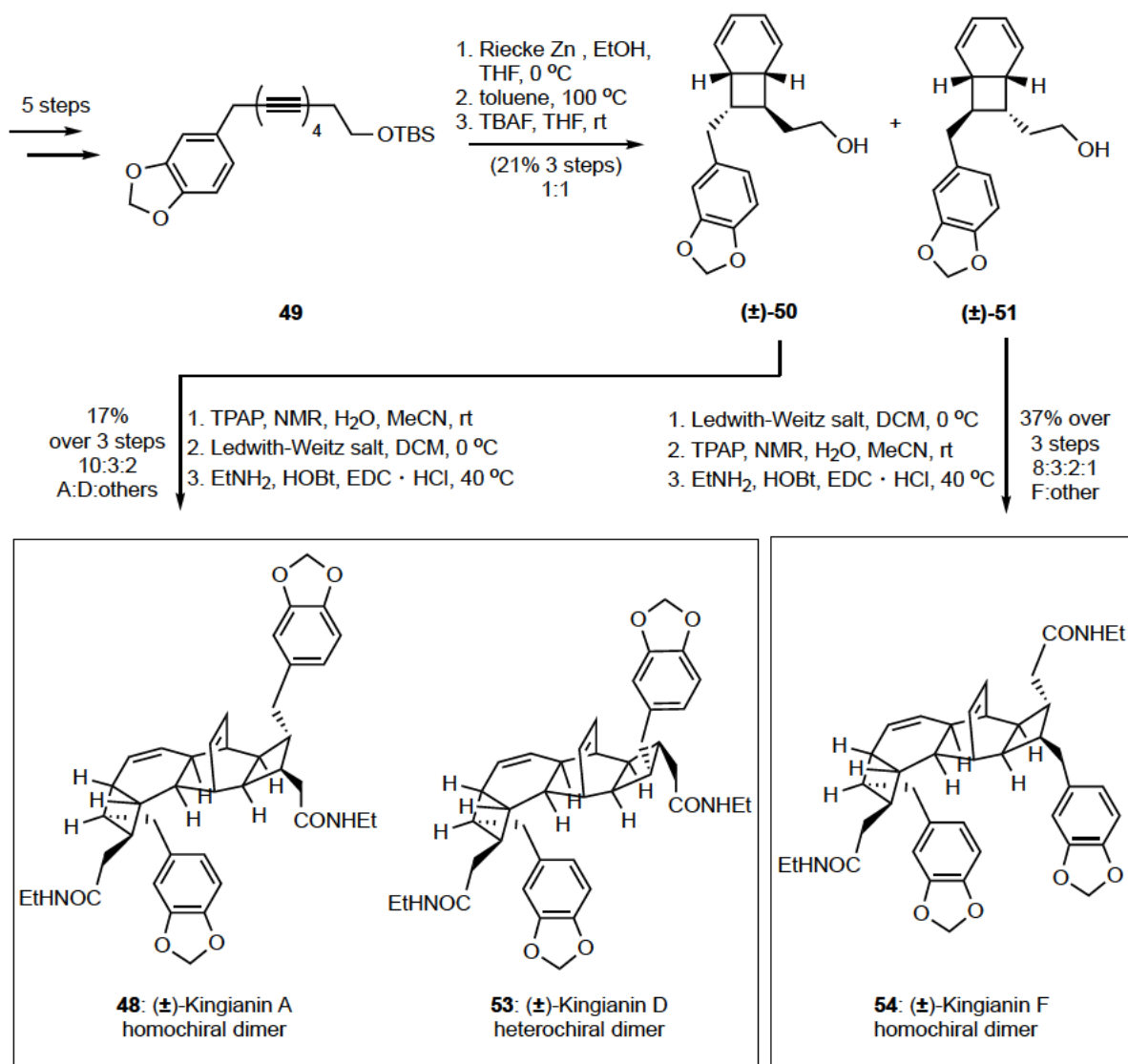
Figure 5.10: Synthesis of Kingianin A, D, and F by Sherburn and Lawrence.

5.3.3. Formal Synthesis of Kingianin A by Moses

Moses and Baldwin reported a formal synthesis of Kingianin A, Suzuki cross coupling and silyl group deprotection gave diastereomeric alcohols **57** and **58** (Figure 5.11).[141][142] Electrochemical mediated Diels–Alder dimerization[143] gave a precursor to Kingianin A.
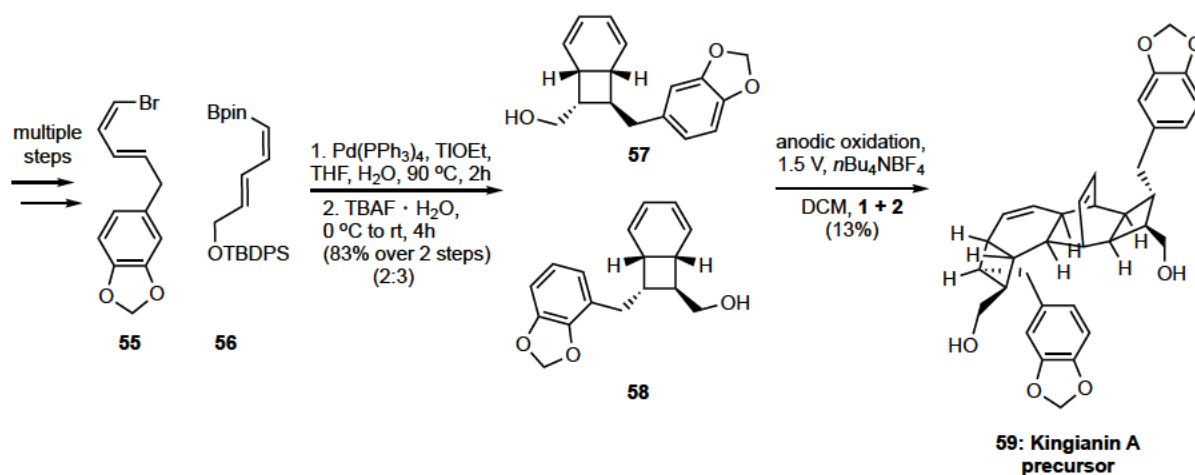
Figure 5.11: Total synthesis of kingianin Aprecursor by Moses.

5.4. SNF4435 C and SNF4436 D

5.4.1. Synthesis of SNF4436 C and SNF4436 D by Parker, Trauner, and Baldwin.

SNF4435C and SNF4435D are novel polypropionate derived metabolites from streptomyces spectabilis.[122,123] Parker was the first to synthesise SNF4436 C **62** and SNF4436 D **63** through Stille coupling of **60** and **61** (Figure 5.12).[144] Trauner also used a Stille cross coupling of **64** and **65** to give a tetraene that undergoes an 8π–6π electrocyclization to give the natural products.[145] Baldwin's biomemetic synthesis relies on a Suzuki cross–coupling of building blocks **66** and **67** to reach Spectinabilin **68** and isospectinabilin **69**.[146] Heating spectinabilin **68** led to the SNF natural products. Treating isospectinabilin **69** with palladium chloride bis(acetonitrile) gave SNF like molecules **70** and **71**.
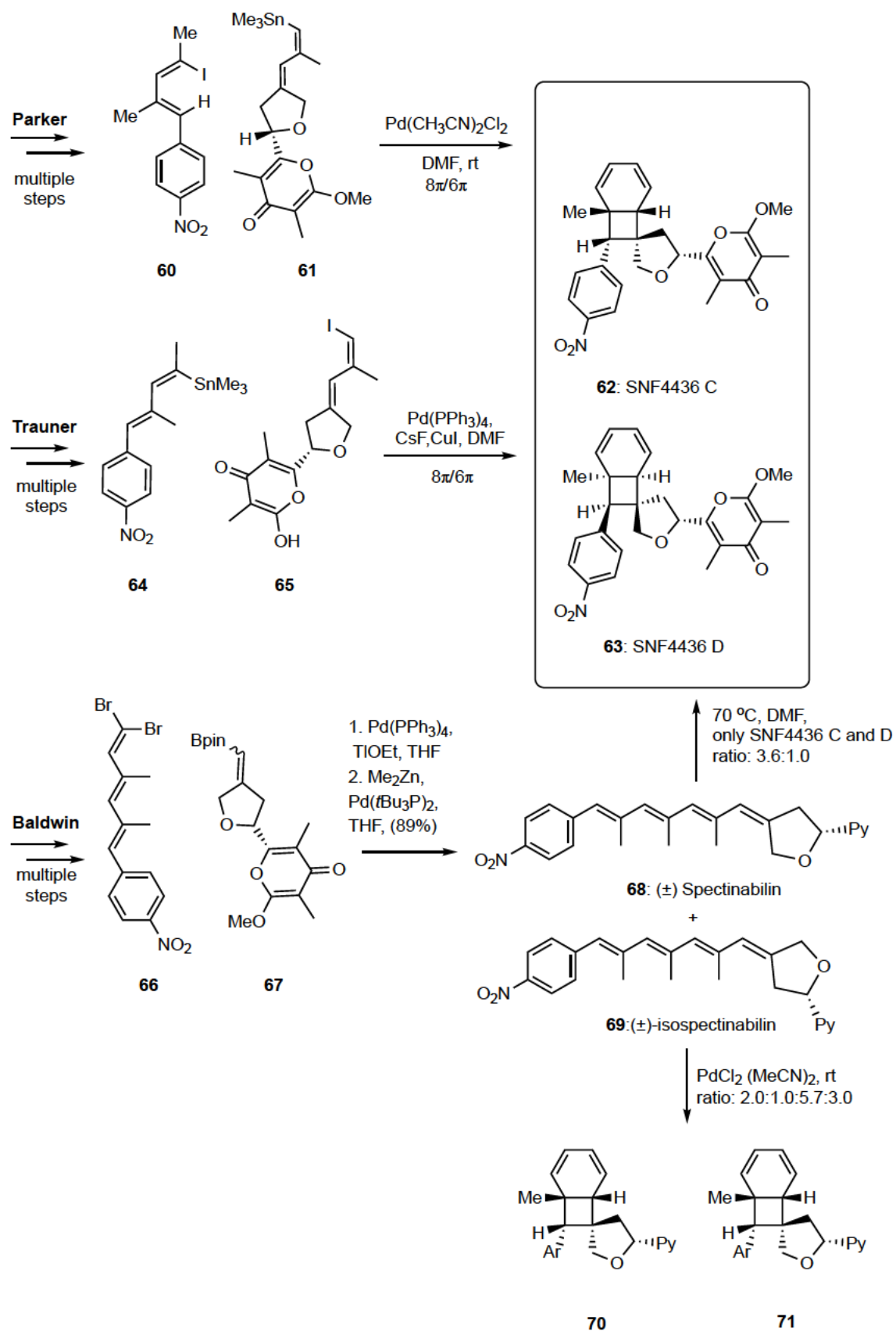
Figure 5.12: Total synthesis of (–)–SNF4435 C and (+)–SNF4435 by Parker, Trauner, and Baldwin.

5.5. Elysiapyrone A and elysiapyrone B

5.5.1 Synthesis of elysiapyrone A and B by Trauner

Elysiapyrone A and Elysiapyrone B were found in the saccoglossan mollusks *Placobranchus ocellatus* and *Elyzisa diomedea* respectively, and first synthesised by Trauner (Figure 5.13).[124][147] Stille coupling of the building blocks **72** and **73** generated a tetraene which underwent a rapid $8\pi/6\pi$ electrocyclization to give separable bicyclo[4.2.0]octadienes **74** and **75**; each isomer was reacted with singlet oxygen to afford endo peroxides which were isomerised under Noyori's ruthenium(II)–catalyzed method to elysiapyrones A **76** and B **77** respectively (Figure 5.13).[148]
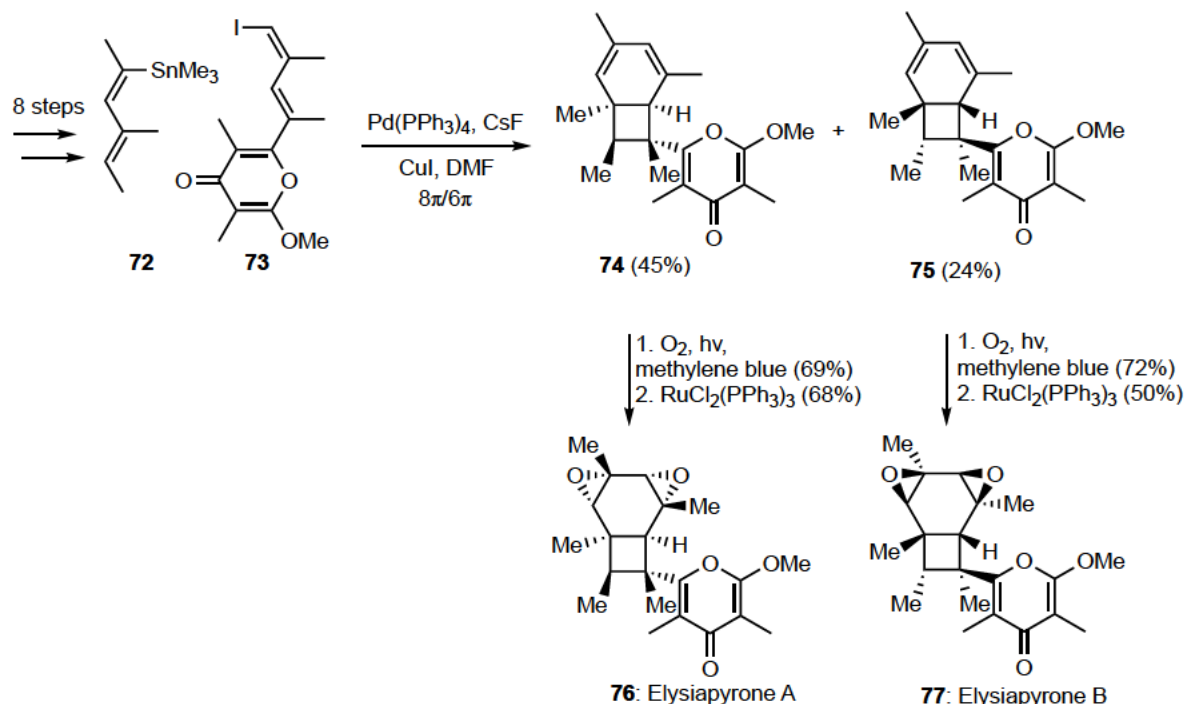
Figure 5.13: Total synthesis of elysiapyrone A and B by Trauner.

5.6. Ocellapyrone A and Ocellapyrone B

3.6.1. Total synthesis of Ocellapyrone A and B by Trauner and Baldwin

Ocellapyrones A and B were found in Placobranchus ocellatus.[125] The first synthesis of these natural products was performed by Trauner (Figure 5.14).[149] Stille coupling of vinyl stannane

78 and vinyl iodide 79[150] gave a tetraene that underwent an 8π–6πelectrocyclisation[138] to give ocellapyrone A 80 and 81. The reaction of 81 with singlet oxygen gave ocellapyrone C 85 in 89% yield. Baldwin's synthesis of Ocellapyrone A utilised Suzuki cross–coupling of 82 with 83 to give tetraene 84.[151] Heating of tetraene 84 in benzene at 120 °C gave two products: ocellapyrone A 80 as the result of an E/Z isomerisation and 8π–6π electrocyclisation, as well as 9,10–deoxytridachinone 86 from a 6π electrocyclization.
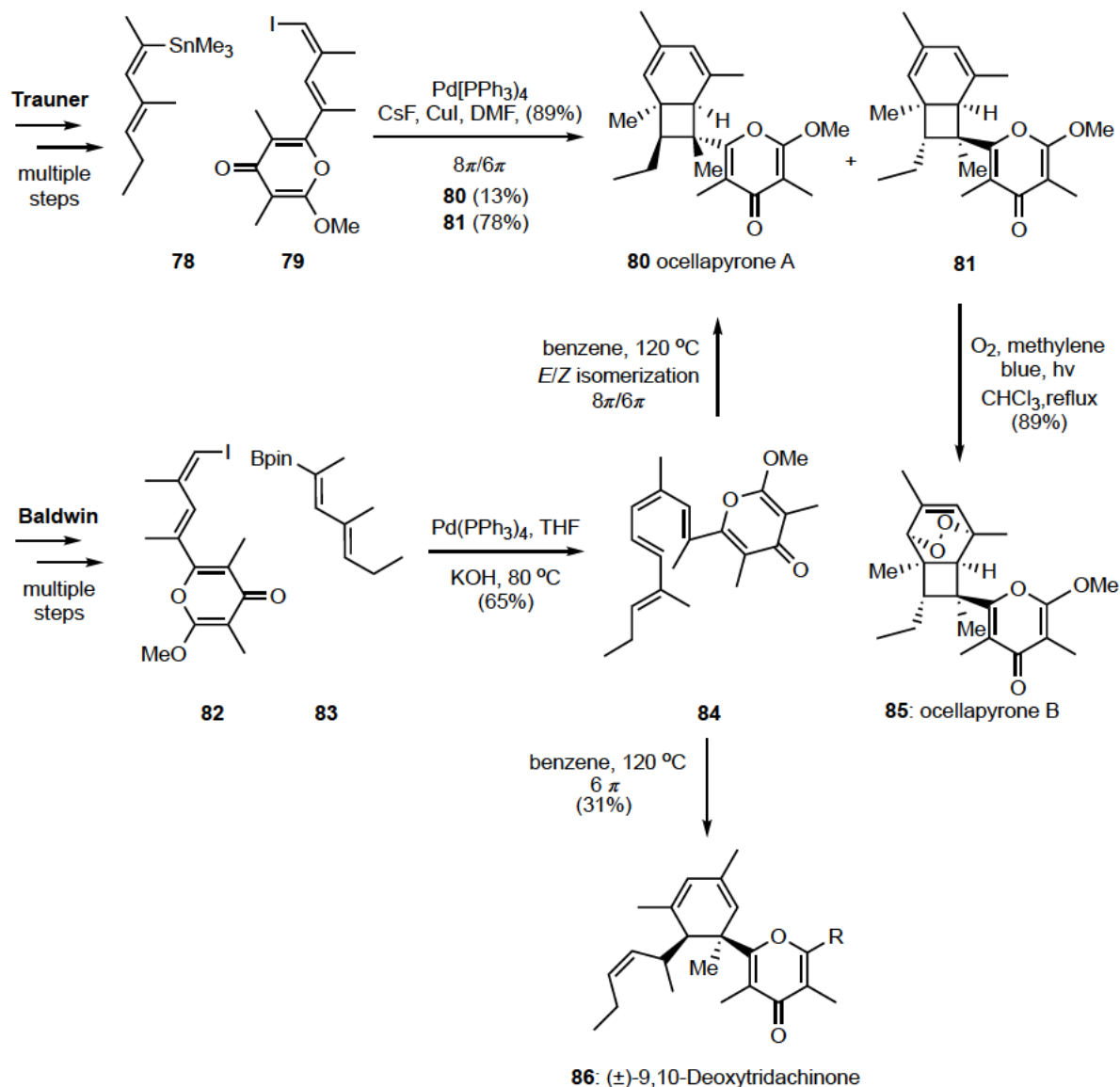
Figure 5.14: Total synthesis of Ocellapyrones A and B by Trauner and Baldwin.

5.7. Shimalactones A and Shimalactones B

5.7.1. Synthesis of Shimalactones A and B by Trauner

Shimalactone A and B were isolated from the cultured marine fungus Emericella variecolor. [152]. Stille cross–coupling of building blocks **87** and **88** gave an intermediate that underwent spontaneous 8π–6π electrocyclization to afford shimalactones A **89** and B **90** (Figure 5.15).[152]
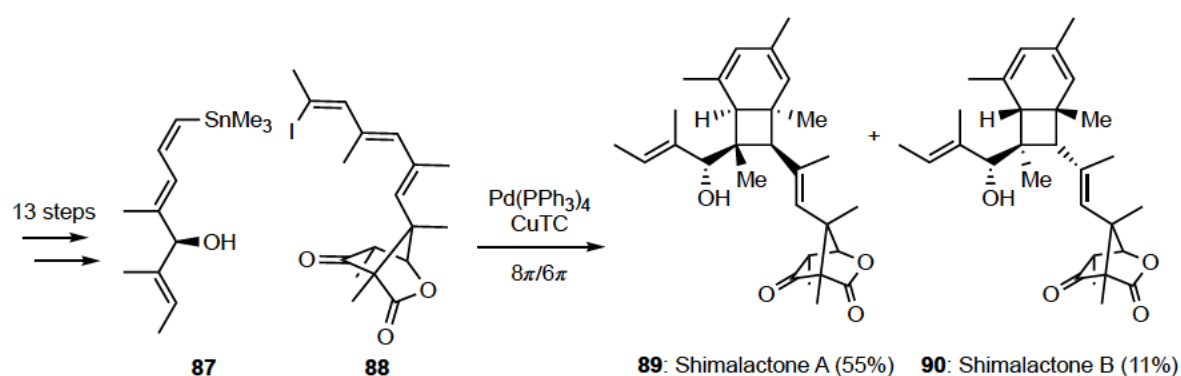
Figure 5.15: Synthesis of shimalactone A and B by Trauner.

All the aforementioned strategies have required the synthesis of linear poly–yne precursor, or substrates that are capable of cross coupling reactions, in order to access a linear tetraene that ultimately undergoes an 8π–6π cascade to arrive at a BOD framework. The following syntheses utilise tetraene precursors, some of which are readily available, in order to access the BOD product.

5.8. Syntheisis of BOD moiety

5.8.1 Craig Williams synthesis of a bicyclooctadiene

One of the first methods to steer away from linear tetraene precursor synthesis to access a BOD was adopted by Craig Williams (Figure 5.16).[153] Following the synthesis of a 1,8–disubstitued cyclooctatetraene **91**, the photochemical Diels–Alder reaction with DIAD **92** gave hydrazide **93**. This molecule can undergo cycloreversion reaction to regenerate a 1,3–diene unit.[154] Conversion of **93** in three steps to the two diastereoisomers **94** and **95**, followed by

microwave irradiation and alcohol protection with PMB gave bicyclo[4.2.0]octadienes **96** and **97**.
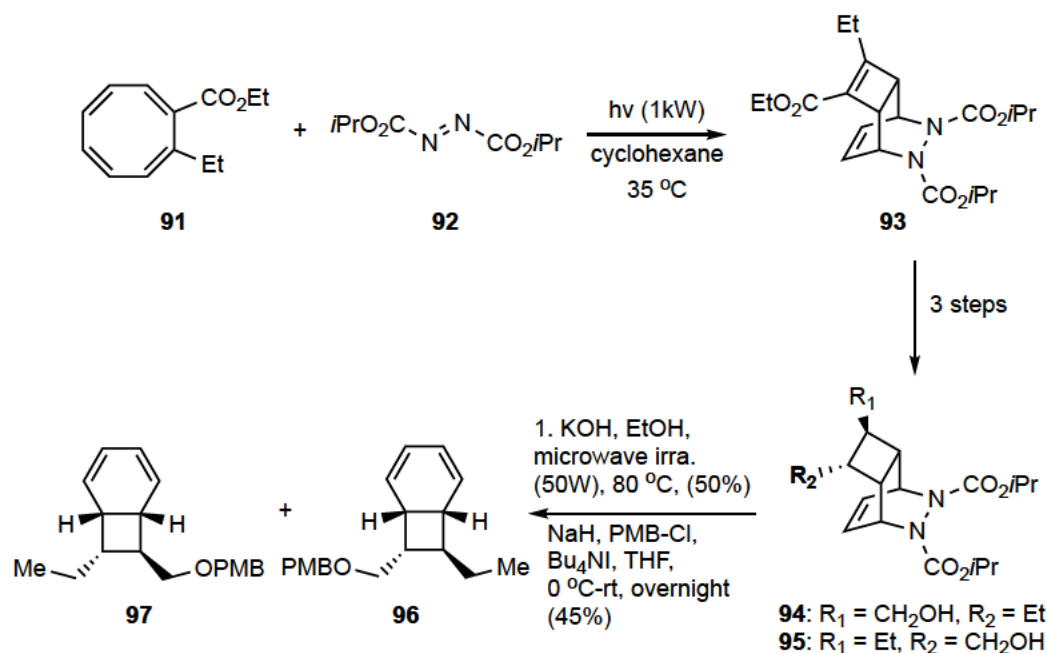
Figure 5.16: Alternative route for the synthesis of Endiandric acid–type by Williams.

5.9. Alternate Strategies Towards a BOD Framework

5.9.1. Nicolaou previous attempt

In his previous attempt to synthesise endiandric acids A–G, Nicolaou attempted to use 1,8–derivatives from COT (Figure 5.17).[155] 1,8 disubstituted cyclooctatriene **112** exists in equilibrium with the tetraene **113** and the BOD **114**. The addition of bromine, chlorine, or mercury(II)acetate to cyclooctatetraene **98** generated the corresponding BOD product **114b**–**114d**.[156,157] Unfortunately, the functionalization of the substituents was either difficult or lengthy. For instance, the exchange of the bromide to the cyanide using KCN led to the formation of the linear tetraene **113a**.

Treatment of cyclooctatetraene **98** with sodium in THF generates the dianion **111**. This dianion can react with an electrophile such as methyl iodide to form the trans dimethyl product **114a**, but in low yield.[158] Using carbon dioxide as the electrophile generates the diacid tetraene **113a** instead of the BOD.[159] Esterification of the latter **113a** delivers the diester tetraene **113c**, which can be converted to the diester BOD **114e** upon heating (80 °C). But, functional group transformations of **114e** to procure the desired natural product require multiple steps.
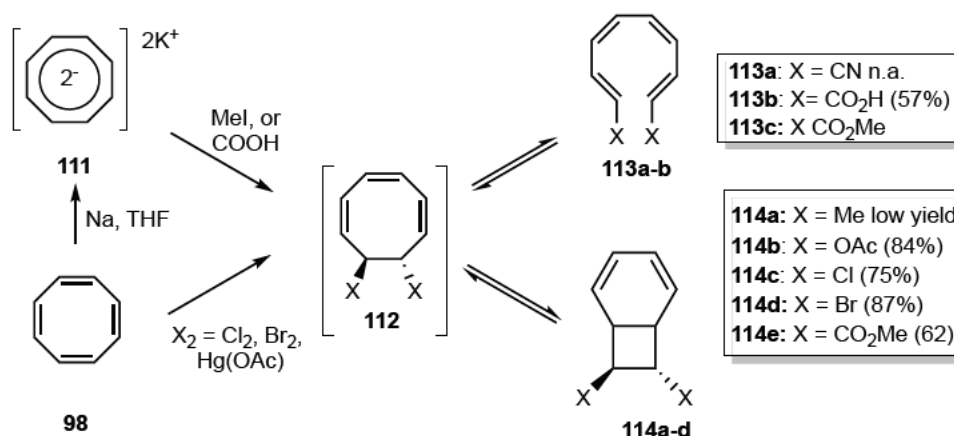
Figure 5.17: Nicolaou previous attempts using cyclooctatetraene as a precursor.

Another strategy attempted by Nicolaou was the synthesis of the BOD through a [2+2] photochemical cycloaddition reaction (Figure 5.18).[155] Acetylene gas **115** and maleic anhydride **116** undergo a photochemical [2+2] cycloaddition reaction to deliver cyclobutene adduct **114**. A Diels–Alder reaction of the cyclobutene **117** with butadiene **118** afford bicyclooctene **119**.[160] The conversion of the olefin **119** to a diene and the epimerisation of one of the carbonyl groups **120** required multiple steps.
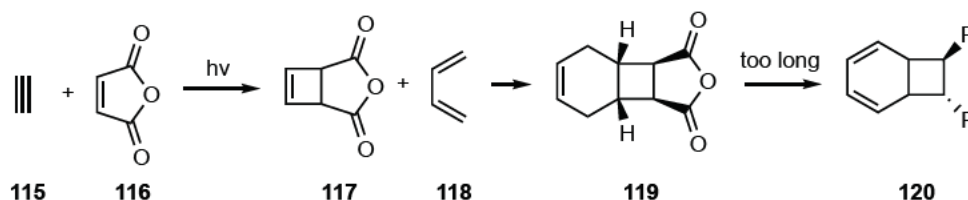
Figure 5.18: Maleic anhydride as a precursor for the synthesis of BOD.

A comparatively more ideal approach is the irradiation of benzene **121** with maleic anhydride **116**, but the generated BOD **122** reacts further with maleic anhydride **112** under a thermal Diels–Alder cycloaddition reaction **123**.[161,162]
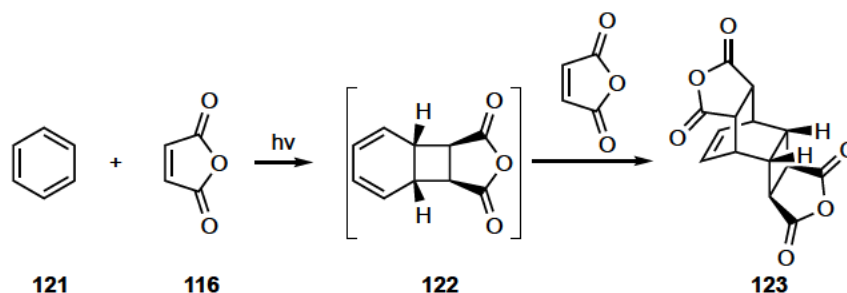
Figure 5.19: Photochemical [2+2] cycloaddition of benzene and maleic anhydride.

5.9.2. other strategy to access the BOD unit

A third photochemical reaction that delivers the BOD system is the reaction between benzene **121** or anisole **124** with acrylonitrile **125**.[163,164] The product however, is not an ideal starting material to access BOD natural products **126** because it requires multiple manipulations to install a substituent adjacent to the cyanic group.
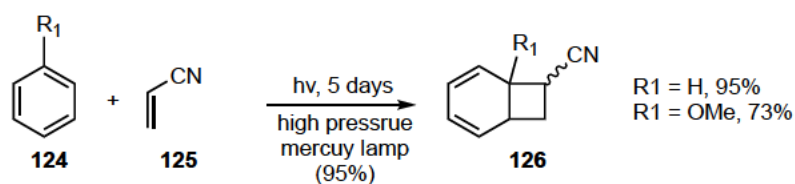
Figure 5.20: Photolytic [2+2] cycloaddition of benzene or anisole to acrylonitrile.

Brown and Reissman used a similar approach to access a bicyclo[4.2.0]octene system in the total synthesis (±)–welwitindolinone A. Reisman and co–worker performed an intermolecular [2+2] cycloaddition reaction between a cyclohexadiene **127** and a ketene **128** to obtain **129**. Reduction of the diol fragment and further manipulations might give rise to BOD systems.
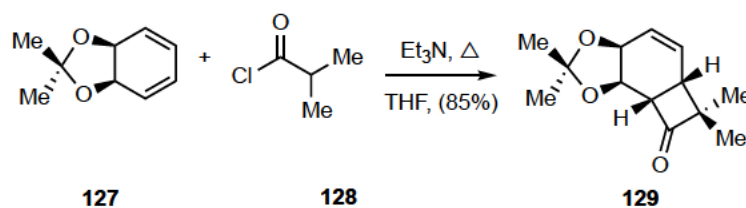
Figure 5.21: Intermolcular [2+2] cycloaddition reaction of cyclohexadieneand ketene.

In the total synthesis of (–)–cajanusine[165] Brown and co–worker used a β–γ–unsaturated alkenyl ketone **130** which was isomerized to the allenic ketone **130** with a thiourea catalyst

(Figure 5.22). Treatment of the intermediate with Bi(OTf)₃ triggered the [2+2] cycloaddition reaction **133**.[166] DBU mediated isomerisation gave **134** which could be further manipulated to give a BOD framework.
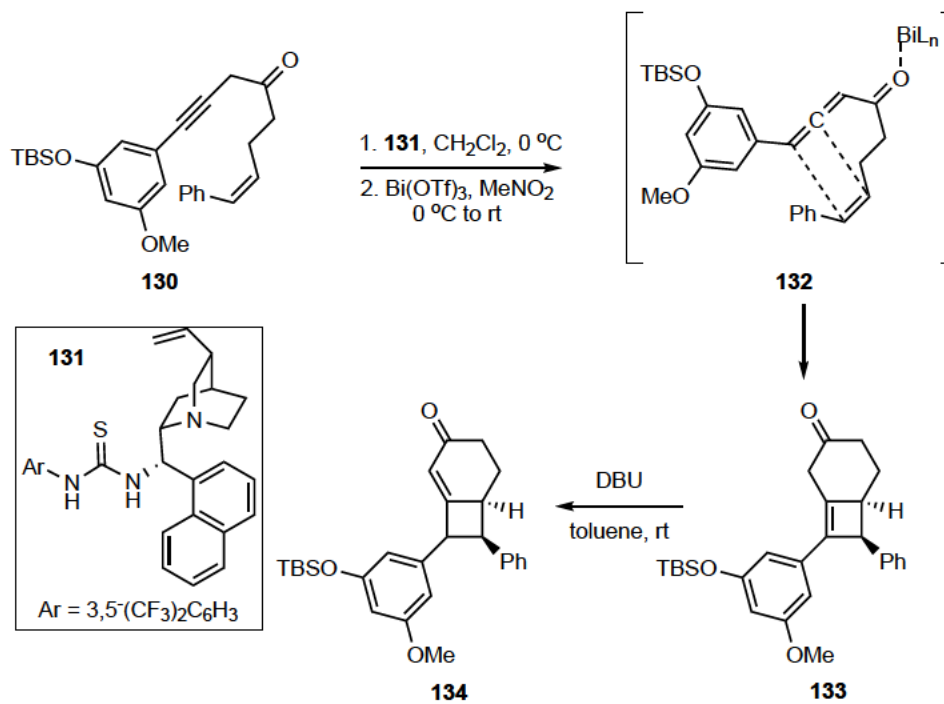
Figure 5.22: Synthesis of a BOD unit by Brown.

5.10. Conclusion

While the aforementioned strategies have never progressed into total synthesis projects, or discussed in this context, the potential is clear. In particular, photochemical cycloaddition strategies could provide a rapid and efficient entry into these natural product frameworks.

All reported synthesis of endiandric acid involve a linear tetraene that must be constructed through arduous synthetic manipulations. Due to lengthy synthetic steps and difficult functionalization, even the strategies to access the BDT moiety do not lead to the desired product. Our strategy is the shortest method to synthesise endiandric acid J and beilcyclone A. We also believe that the right nucleophile to open the COT–oxide will lead to the formation of numerous endiandric acid like endiandric acid A – G, kingianin A–F.

Hitherto, an enantioselective synthesis of endiandric acid has not been done yet.

Chapter 6

6.1. Introduction

Endiandric acids are peculiar targets and are isolated as racemates. Their Australian discoverer Black suggested that their biosynthesis involves a non–enzymatic cascade 8π conrotatory electrocyclization/6π disrotatory electrocyclization, and an intramolecular Diels–Alder reaction (IMDA) from a linear tetraene. His theory was proved by the Nicolaou group who synthesized endiandric acid A–G from a linear tetraene. Since then, all the strategies to synthesise related natural products of this family were similar. The formation of a tetraene intermediate, through cross–coupling, or semi–hydrogenation which upon heating or at room temperature undergoes a cascade 8π/6π electrocyclization reaction to deliver the natural product or the bicylo[4.2.0]octadiene precursor. Despite the efficiency of the cascade reaction, the formation of the tetraene with the correct stereoselectivity is the most challenging part of the synthesis

We developed the shortest method to synthesise endiandric acid J and beilcyclone B in 6 and 5 steps, respectively. With COT as a starting material we access the bicyclo[4.2.0]octadiene scaffold through the desymmetrisation of COT oxide through an S_N2' alkylation. A gold catalysed vinyl transfer, which upon heating undergoes a Claisen/6π electrocyclization reaction to give the bicyclooctadiene moity. A one pot Wittig olefination and an IMDA delivered the natural products. As we thought that we can enantioselectively synthesise the natural products, computational calculation proved that an enantiopure sample would racemize during the 6π or the IMDA reaction though ring opening and ring.

6.2. Conclusion and future work

Our strategy is the ideal method to synthesise other related endiandric acid natural products in few steps. For instance, endiandric acid A, D, and E are synthesized in 15 – 16 steps by Nicolaou. With our method and the corresponding nucleophile[167] to desymmetrize the COT oxide we can obtain the natural products in 6 – 7 steps. This is 10 steps less than the original synthesis. The only challenging task is the ring opening of the COT oxide with
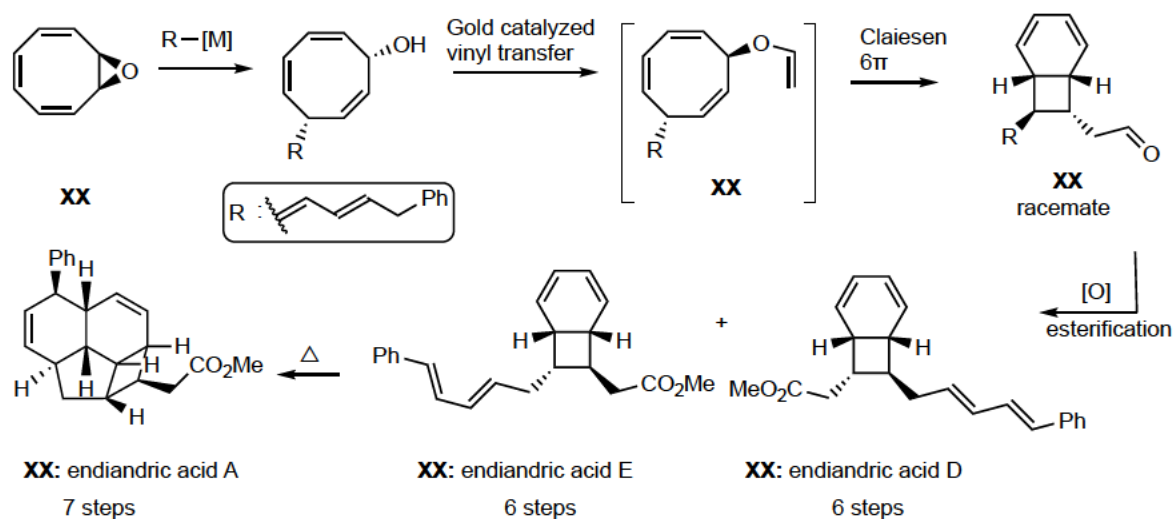
Figure 6.1: Synthesis of endiandric acid A, E, and D with our method in 6 and 7 steps.

As our DFT calculation show that an enantiopure sample would racemise under thermal conditions during the 8pi/6pi cascade, we propose that we may still be able to access the natural products enantioselectively by employing a chiral Lewis acid mediated IMDA in a dynamic kinetic resolution strategy .
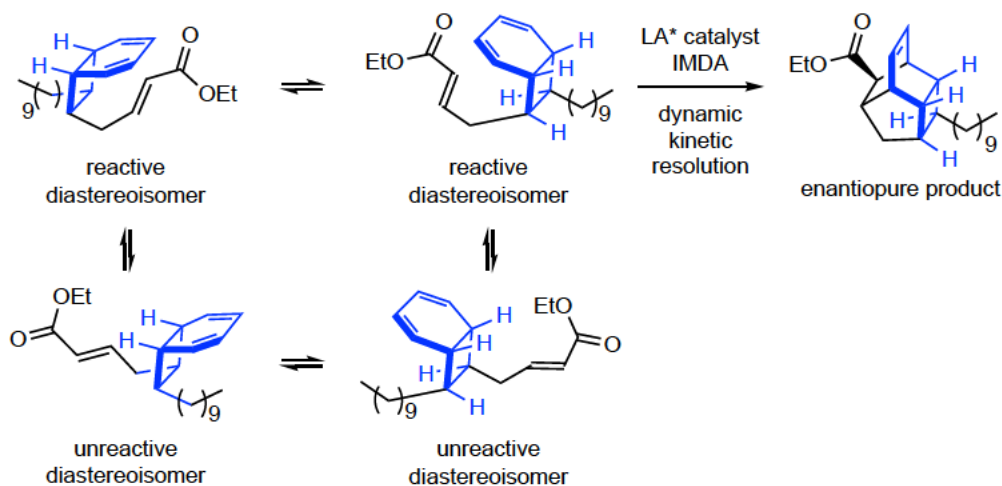
Figure 6.2: Proposed enantioselective synthesis of endiandric acid J or beilcyclone A.

Statement of Authorship

Title of Paper	Total Synthesis of Endiandric Acid J and Beilcyclone A
Publication Status	☐ Published ☐ Accepted for Publication ☐ Submitted for Publication ☑ Unpublished and Unsubmitted work written in manuscript style
Publication Details	O. Yahiaoui, A. Almass, T. Fallon, Total synthesis of endiandric acid J and beilcyclone A.

Principal Author

Name of Principal Author (Candidate)	Oussama Yahiaoui
Contribution to the Paper	Optimized all the reactions and characterised all the compounds. Made endiandric acid J Wrote the experimental section. Supervised Adrian Almass during his Honour and helped him synthesise the natural products.
Overall percentage (%)	40%
Certification:	This paper reports on original research I conducted during the period of my Higher Degree by Research candidature and is not subject to any obligations or contractual agreements with a third party that would constrain its inclusion in this thesis. I am the primary author of this paper.
Signature	Date 19-05-2020

Co-Author Contributions

By signing the Statement of Authorship, each author certifies that:

i.   the candidate's stated contribution to the publication is accurate (as detailed above);

ii.   permission is granted for the candidate in include the publication in the thesis; and

iii.   the sum of all co-author contributions is equal to 100% less the candidate's stated contribution.

Name of Co-Author	Adrian Almass
Contribution to the Paper	Optimized the gold vinyl transfer reaction. Made Beilcyclone A.
Signature	Date 18 May 2020

Name of Co-Author	Thomas Fallon
Contribution to the Paper	Supervised the project and wrote the manuscript. Corresponding author.

Signature		Date	19-05-20

COMMUNICATION

Total Synthesis of Endiandric Acid J and Beilcyclone A from Cyclooctatetraene

Oussama Yahiaoui Adrian Almass and Thomas Fallon*

Abstract: The endiandric acids are classic targets in natural product synthesis. The spectacular 8π 6π-electrocylisation Intramolecular Diels-Alder (8π 6π IMDA) reaction cascade at the heart of their biosynthesis has inspired practitioners and students of pericyclic chemistry for nearly forty years. All previous synthetic approaches have sought to prepare a linear tetraene and thereby initiate the cascade. In this communication we demonstrate the use of cyclooctatetraene as π-rich starting material from which to rapidly intercept the 8π 6π IMDA cascade at the cyclooctatriene stage. Endiandric acid J and beilcyclone A are prepared for the first time in six and five steps, respectively. The strategy features a tactical overall anti-vicinal difunctionalisation of cyclooctatetraene through S_N2 alkylation of cyclooctatetraene oxide followed by an intriguing tandem Claisen rearrangement 6π-electrocyclisation from the corresponding vinyl ether. This rapidly constructs an advanced bicyclo[4.2.0]octadiene aldehyde intermediate. Olefinations and intramolecular Diels-Alder cycloadditions completes the syntheses. This establishes a short and efficient new path to the endiandric acid natural products.

he endiandric acids are the irst o a amily o natural products characterised by the structure or intermediacy o a bicyclo[4 2 0 octadiene Black and co-workers originally isolated and structurally elucidated endiandric acids A-G and proposed their biosynthesis hat the ormation o a linear tetraene intermediate would initiate an 8 /6 -electrocyclic cascade reaction ollowed by an intramolecular Diels-Alder (MDA) reaction in either o two distinct modes to give complex tetracyclic sca olds [2] he Nicoloau group promptly proved this concept in their classic 1982 synthesis [3] his work has become perhaps the most iconic example o pericyclic cascade reactions in biomimetic total synthesis

More than 80 structurally related natural products have been solated rom the *Beilschmiedia* and *Endiandra* genera o plants [4] and a wide range o potent biological activities established Synthetic e orts in the area have ocused on the bacterial SNF4435 natural products [5] the sea mollusc bicyclo[4 2 0 octadienes natural products [6] and the kingianins [4] with elegant syntheses reported by the Parker [7] rauner [8] Baldwin and Moses [9] and Sherburn [0] groups

he common eature o all previous synthetic approaches is the construction o a linear tetraene intermediate (Scheme 1a) Nicolaou adopted the semi-hydrogenation o dienediyne intermediates Parker Baldwin/Moses and rauner all adopted cross-coupling reactions whereas Lawrence/Sherburn demonstrated the our- old semi-hydrogenation o a linear

O. Yahiaoui, A. Almass, Dr. T. Fallon
Department of Chemistry, The University of Adelaide, SA 5005 (Australia)
E-mail: thomas.fallon@adelaide.edu.au

Supporting information for this article is given via a link at the end of the document.
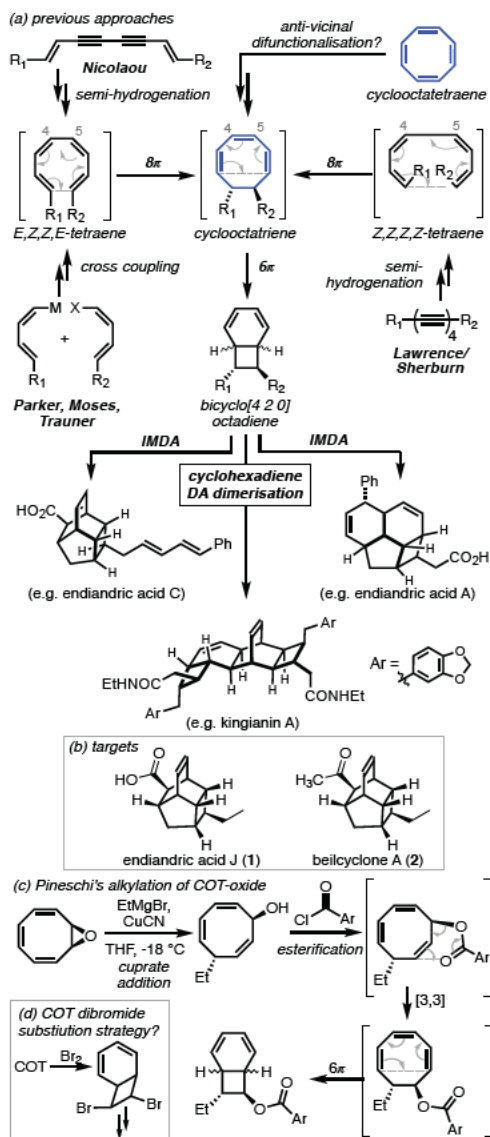
Scheme 1. a) entry to the 8π/6π/DA cascade. b) targets. c) Pineschi's precedent. d) dibromobicyclo[4.2.0]octadiene.

COMMUNICATION

Scheme 2. Synthesis of endiandric acid J and beilcyclone A
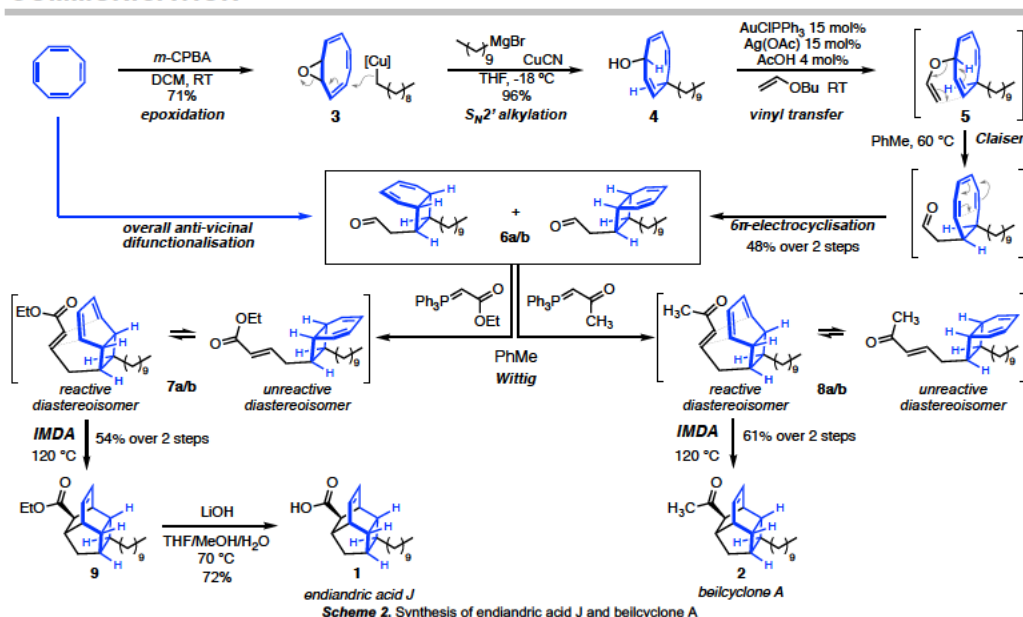
tetrayne to give Z,Z,Z,Z-tetraene intermediate All previous approaches ultimately forge the 4-5 carbon-carbon bond through some kind of coupling reaction as a key step While this is an intuitive and successful disconnection it requires the often challenging stereoselective synthesis of situatable dienyl coupling partners

he use of -rich hydrocarbons as key starting materials has been a powerful approach in natural product synthesis with reactive -bonds providing the basis of dense functionalisation patterns Annulenes have been used occasionally in this context Examples include Snapper s use of cyclobutadiene in cycloaddition/cyclopropanation/rearrangement sequences in the synthesis of pleocarpenene and pleocarpenone [2] Sarlah recently reported a dearomative six- old functionalisation of benzene in the synthesis of isocarbostyril alkaloids [3] Corey used cyclooctatetraene (CO) as the basis of his inspirational synthesis of the ladderane natural product pentacycloanammoxic acid [4]

We realised that an anti-vicinal defunctionalisation of CO would intercept the 8 /6 cascade and potentially provide a rapid entry point to advanced bicyclo[4 2 0 octadiene intermediates (Scheme 1) his concept was originally considered by the Nicolaou group via a potential dialkylation of the bromination product of CO (Scheme 1d) [5]

Our recent work on the synthesis of bullvalenes [6] prompted an appreciation of the hidden complexity and rich chemistry of CO [7] We were drawn to the work of Pineschi who established stereoselective and enantioselective anti-SN2 addition ring-opening reactions of clyclooctatetraene oxide (Scheme 1c) [8]

hey noted that esterification of the resultant cycloocta-2 4 7-trienol was occasioned by an unusual [3 3-transposition of the ester and subsequent 6 -electrocyclization to give the corresponding bicyclo[4 2 0 octadiene ester By changing out the

[3 3 ester transposition with a Claisen rearrangement a new path to the 8 /6 natural products might be forged

n this communication we demonstrate this concept through the synthesis of endiandric acid J **1** and beilcyclone A **2** (Scheme 1b 2) solated from the roots of *Beilschmiedia erythrophloia* these structures differ only in the identity of the carbonyl function [9]

Our synthesis began with epoxidation of CO to give cyclooctatetraene oxide **3** in 71% yield his is followed by anti-SN2 addition ring-opening of the epoxide using didecyl cuprate under Pineschi s conditions to give alcohol **4** in 96% yield with complete regio- and stereo-selectivity he allyl-pentadienyl-alcohol **4** is both acid sensitive and thermally unstable but could be purified by rapid flash chromatography on buffered silica gel

he synthesis of vinyl ethers is a significant challenge in organic synthesis [20] he most widely used method employs mercury( )-catalysed vinyl transfer typically from an alkyl vinyl ether solvent [2] Reaction conditions generally require high catalyst loading elevated temperatures and extended reaction times here are only several alternatives to mercury( )-catalysis Among these are palladium[22] and iridium[23] catalysed methods both of which require elevated reaction temperatures

n our hands mercury( )-catalysed vinyl transfer to alcohol **4** using either Hg(OAc)2 or Hg(FA)2 was fraught with difficulty Reactions suffered from low conversion degradation long reaction times and poor reproducibility between runs

Finally modification of a gold( )-catalysed protocol reported by okunaga[24] using AuClPPh3 led to the successful synthesis of vinyl ether **5** Warming of the sensitive crude material in toluene at 60 °C prompted a Claisen/6 cascade to give aldehyde **6a/6b** with complete regioselectivity and 1 2-anti stereospecificity as an inconsequential ~2 1 mixture of diastereoisomers in 48% yield over 2 steps his appears to be the first example of a tandem Claisen rearrangement/ 6 -electrocyclisation of a non-aromatic

COMMUNICATION
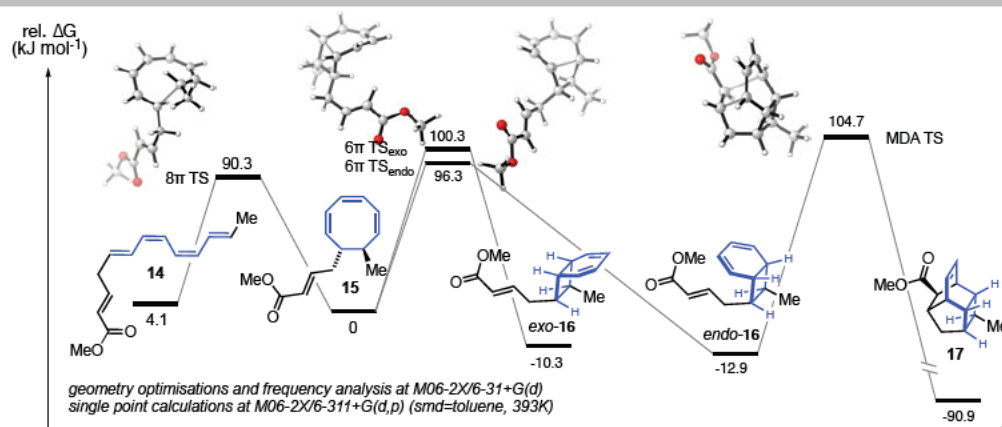
Figure 1. Computational analysis oft he 8π/6π/IMDA cascade.

substrate [25] he transposition o the S_N2 addition into this cascade represents a tactical *anti*-vicinal de unctionalisation o CO as well as setting the aldehyde as a key unctional handle or endgame operations

Wittig ole ination o **6a/6b** gave the α/β unsaturated ester **7a/7b** and ketone **8a/8b** respectively as intermediates [26] Heating o the reaction mixtures at 120 °C promoted equilibration o the diasteroisomers through 6 -electrocyclic ring opening/closing and intramolecular Diels-Alder reaction to give beilcyclone A **2** in 61% yield and tetracyclic ester **9** in 54% yield Hydrolysis o the ester gave endiandric acid J **1** in 72% yield

he 8 /6 natural products are all isolated as their racemates or as mixtures o diasteroisomers with respect to a ixed element o stereogenicity Despite this the prospect o enantioselective chemical synthesis has remained an appealing open challenge While there are a variety o good methods or enantioselective Nazarov reactions [27] as well as 6 -electrocyclic reactions [28] the question o enantioselective 8 -electrocyclic reactions is largely unsolved [29] Parker has reported a series o studies into stereoinduction o 8 /6 cascades using chiral auxiliaries but diasteroisomer ratios were generally modest [30]

By avoiding the interception o a linear tetraene our strategy should in principle be applicable to enantioselectivity ndeed Pineschi s desymmetrisation o cyclooctatetraene oxide brings an enantioselective strategy into clear view However while perusing this goal doubts grew as to the con igurational stability o bicyclo[4 2 0 octadienes generally While the dynamic relationship between *endo* and *exo* isomers through 6 -electrocyclic ring opening/closure is long known³ and would not destroy enantiopurity transient 8 -electrocyclic ring opening to the corresponding linear tetraene certainly would n a recent computational study [32] Houk predicted the 8 /6 transition state energies o the *trans-trans*-dimethyl-(*E,Z,Z,E*)-tetraene 8 /6 system at 91 kJ/mol and 95 kJ/mol relative to the cyclooctatriene respectively he inely balanced kinetics and thermodyncamics o these 8 /6 systems warrants caution

o anticipate the prospects or a success ul enantioselective synthesis o **1** and/or **2** we conducted a computational study on truncated analogues o the Claisen/8 /6 cascade o vinyl ether **5** as well as the

8 /6 / MDA cascade o involving esters **7a/b** he results o the latter analysis are presented in Figure 1 he sequence was modelled using density unctional theory calculations employing the M06-2X method and 6-311+G(d p) basis set which has been shown to give reliable thermochemistry or pericyclic reactions o organic molecules [33]

he predicted ree energies o the 8 6 endo 6 exo and MDA transition structures are predicted to be inely balanced with the 8 electrocyclic reaction having the lowest barrier at 90 3 kJ/mol Un ortunately we must conclude that under thermal reaction conditions an enantiopure sample o the *endo* isomer o **16** (i it could be prepared) would almost entirely racemise prior to intramolecular Diels-Alder reaction Conceivably a catalytic MDA reaction might address this problem However the 8 /6 cascade o aldehyde **6a/b** (not shown) is predicted to have a similar pro ile to that o **16** whereby an enantiopure sample o vinyl ether **5** would likely give rise to racemic **6a/b** under the reaction conditions o its ormation his interpretation is aided by ull kinetic modelling o these reaction sequences (see the S or ull details)

n summary this study demonstrates a rapid new entry into the 8 /6 natural products through a distinctive synthetic strategy his sets the stage or short and practical syntheses o other members o the amily as well as analogues Computational analysis o the pericyclic cascades predicts the antipodal instability the bicyclo[4 2 0 octadiene intermediates and deters the pursuit o enantioselective synthesis in this case

COMMUNICATION

[1] R. Huisgen, A. Dahmen, H. Huber, *J. Am. Chem. Soc.* **1967**, *89*, 7130 7131.

[2] a) W. M. Bandaranayake, J. E. Banfield, D. S. C. Black, *J. Chem. Soc., Chem. Commun.* **1980**, 902 903. b) W. M. Bandaranayake, J. E. Banfield, D. S. C. Black, G. D. Fallon, B. M. Gatehouse, *J. Chem. Soc., Chem. Commun.* **1980**, 162 163. c) W. M. Bandaranayake, J. E. Banfield, D. S. C. Black, G. D. Fallon, B. M. Gatehouse, *Aust. J. Chem.* **1981**, *34*, 1655 1667. d) W. M. Bandaranayake, J. E. Banfield, D. S. C. Black, *Aust. J. Chem.* **1982**, *35*, 557 565. e) W. M. Bandaranayake, J. E. Banfield, D. S. C. Black, G. D. Fallon, B. M. Gatehouse, *Aust. J. Chem.* **1982**, *35*, 567 579. f) J. E. Banfield, D. S. C. Black, S. R. Johns, R. I. Willing, *Aust. J. Chem.* **1982**, *35*, 2247 2256.

[3] a) K. C. Nicolaou, N. A. Petasis, R. E. Zipkin, J. Uenishi, *J. Am. Chem. Soc.* **1982**, *104*, 5555 5557. b) K. C. Nicolaou, N. A. Petasis, J. Uenishi, R. E. Zipkin, *J. Am. Chem. Soc.* **1982**, *104*, 5557 5558. c) K. C. Nicolaou, R. E. Zipkin, N. A. Petasis, *J. Am. Chem. Soc.* **1982**, *104*, 5558 5560. d) K. C. Nicolaou, N. A. Petasis, R. E. Zipkin, *J. Am. Chem. Soc.* **1982**, *104*, 5560 5562.

[4] a) B. Lenta, J. Chouna, P. Nkeng-Efouet, N. Sewald, B. N. Lenta, J. R. Chouna, P. A. Nkeng-Efouet, N. Sewald, *Biomolecules* **2015**, *5*, 910 942. b) A. Leverrier, M. E. T. H. Dau, P. Retailleau, K. Awang, F. Guéritte, M. Litaudon, *Org. Lett.* **2010**, *12*, 3638 3641. c) M. N. Azmi, T. Péresse, C. Remeur, G. Chan, F. Roussi, M. Litaudon, K. Awang, *Fitoterapia* **2016**, *109*, 190 195.

[5] a) K. Kurosawa, K. Takahashi, E. Tsuda, *J. Antibiot.* **2001**, *54*, 541 547. b) K. Takahashi, E. Tsuda, K. Kurosawa, *J. Antibiot.* **2001**, *54*, 548 553.

[6] a) E. Manzo, M. L. Ciavatta, M. Gavagnin, E. Mollo, S. Wahidulla, G. Cimino, *Tet. Lett.* **2005**, *46*, 465 468. b) M. Cueto, L. D'Croz, J. L. Maté, A. San-Martín, J. Darias, *Org. Lett.* **2005**, *7*, 415 418. c) H. Wei, T. Itoh, M. Kinoshita, N. Kotoku, S. Aoki, M. Kobayashi, *Tetrahedron* **2005**, *61*, 8054 8058. d) M. Kobayashi, H. Wei, T. Itoh, N. Kotoku, *Heterocycles* **2006**, *68*, 111.

[7] a) K. A. Parker, Y.-H. Lim, *J. Am. Chem. Soc.* **2004**, *126*, 15968 15969. b) H. N. Lim, K. A. Parker, *Org. Lett.* **2013**, *15*, 398 401. c) For a recent review, see: K. A. Parker, H. N. Lim, in *Strategies and Tactics in Organic Synthesis* (Ed.: M. Harmata), Academic Press, **2014**, pp. 51 78.

[8] a) C. M. Beaudry, D. Trauner, *Organic Letters* **2002**, *4*, 2221 2224. b) C. M. Beaudry, D. Trauner, *Org. Lett.* **2005**, *7*, 4475 4477. c) J. E. Barbarow, A. K. Miller, D. Trauner, *Org. Lett.* **2005**, *7*, 2901 2903. d) V. Sofiyev, G. Navarro, D. Trauner, *Org. Lett.* **2008**, *10*, 149 152. e) A. K. Miller, D. Trauner, *Angew. Chem.* **2005**, *117*, 4678-4682; *Angew. Chem. Int. Ed.* **2005**, *44*, 4602 4606.

[9] a) J. E. Moses, J. E. Baldwin, R. Marquez, R. M. Adlington, A. R. Cowley, *Org. Lett.* **2002**, *4*, 3731 3734. b) M. F. Jacobsen, J. E. Moses, R. M. Adlington, J. E. Baldwin, *Org. Lett.* **2005**, *7*, 2473 2476. c) R. Rodriguez, R. M. Adlington, S. J. Eade, M. W. Walter, J. E. Moses, *Tetrahedron* **2007**, *63*, 4500 4509. d) S. J. Eade, M. W. Walter, C. Byrne, B. Odell, R. Rodriguez, J. E. Baldwin, R. M. Adlington, J. E. Moses, *J. Org. Chem.* **2008**, *73*, 4830 4839. e) J. C. Moore, E. S. Davies, D. A. Walsh, P. Sharma, J. E. Moses, *Chem. Commun.* **2014**, *50*, 12523 12525. b)

[10] a) S. L. Drew, A. L. Lawrence, M. S. Sherburn, *Angew. Chem. Int. Ed.* **2013**, *52*, 4221 4224. b) S. L. Drew, A. L. Lawrence, M. S. Sherburn, *Chem. Sci.* **2015**, *6*, 3886 3890

[11] For a recent example, see: C. G. Newton, S. L. Drew, A. L. Lawrence, A. C. Willis, M. N. Paddon-Row, M. S. Sherburn, *Nature Chemistry* **2015**, *7*, 82 86.

[12] M. J. Williams, H. L. Deak, M. L. Snapper, *J. Am. Chem. Soc.* **2007**, *129*, 486 487.

[13] T. W. Bingham, L. W. Hernandez, D. G. Olson, R. L. Svec, P. J. Hergenrother, D. Sarlah, *J. Am. Chem. Soc.* **2019**, *141*, 657 670.

[14] V. Mascitti, E. J. Corey, *J. Am. Chem. Soc.* **2004**, *126*, 15664 15665.

[15] K. C. Nicolaou, N. A. Petasis, in *Strategies and Tactics in Organic Synthesis* (Ed.: T. Lindberg), Academic Press, **1984**, pp. 155 173.

[16] a) Fray, G. I.; Saxton, R. G. The Chemistry of Cyclo-octatetraene and its Derivatives; Cambridge University Press: New York, 1978. b) L.A. Paquette, *Tetrahedron*, **1975**, *31*, 2855 2883.

[17] a) O. Yahiaoui, L. F. Pašteka, B. Judeel, T. Fallon, *Angew. Chem. Int. Ed.* **2018**, *57*, 2570 2574. b) O. Yahiaoui, L. F. Pašteka, C. J. Blake, C. G. Newton, T. Fallon, *Org. Lett.* **2019**, *21*, 9574 9578.

[18] a) F. Del Moro, P. Crotti, V. Di Bussolo, F. Macchia, M. Pineschi, *Org. Lett.* **2003**, *5*, 1971 1974. b) M. Pineschi, F. D. Moro, P. Crotti, F. Macchia, *Eur. J. Org. Chem.* **2004**, 4614 4620.

[19] a) P.-S. Yang, M.-J. Cheng, C.-F. Peng, J.-J. Chen, I.-S. Chen, *J. Nat. Prod.* **2009**, *72*, 53 58. b) P.-S. Yang, M.-J. Cheng, J.-J. Chen, I.-S. Chen, *Helvetica Chimica Acta* **2008**, *91*, 2130 2138.

[20] D. J. Winternheimer, R. E. Shade, C. A. Merlic, *Synthesis* **2010**, *2010*, 2497 2511.

[21] W. H. Watanabe, L. E. Conlon, *J. Am. Chem. Soc.* **1957**, *79*, 2828 2833.

[22] M. Bosch, M. Schlaf, *J. Org. Chem.* **2003**, *68*, 5225 5227.

[23] Y. Okimoto, S. Sakaguchi, Y. Ishii, *J. Am. Chem. Soc.* **2002**, *124*, 1590 1591.

[24] a) A. Nakamura, M. Tokunaga, *Tetrahedron Letters* **2008**, *49*, 3729 3732. b) The addition of a catalytic amount of acetic acid was found to significantly accelerate this reaction, see: S. S. Zalesskiy, V. N. Khrustalev, A. Yu. Kostukovich, V. P. Ananikov, *Organometallics* **2015**, *34*, 5214 5224.

[25] For examples involving propargyl aryl ether substrates, see: a) R. Hesse, K. K. Gruner, O. Kataeva, A. W. Schmidt, H.-J. Knölker, *Chem. A Eur. J.* **2013**, *19*, 14098 14111. b) L. A. M. Murray, T. Fallon, C. J. Sumby, J. H. George, *Org. Lett.* **2019**, *21*, 8312 8315.

[26] Intermediates **7a/b** and **8a/b** can be isolated and fully characterised. See the Supporring Information for full details.

[27] For recent reviews, see: a) M. G. Vinogradov, O. V. Turova, S. G. Zlotin, *Org. Biomol. Chem.* **2017**, *15*, 8245 8269. b) D. R. Wenz, J. R. de Alaniz, *European Journal of Organic Chemistry* **2015**, *2015*, 23 37. c) T. Vaidya, R. Eisenberg, A. J. Frontier, *ChemCatChem* **2011**, *3*, 1531 1548.

[28] S. Thompson, A. G. Coyne, P. C. Knipe, M. D. Smith, *Chem. Soc. Rev.* **2011**, *40*, 4217 4231.

[29] Litaudon reported that two antipodes of kingianin A show striking differences in BCL-XL binding affinity assays, see: A. Leverrier, K. Awang, F. Guéritte, M. Litaudon, *Phytochemistry* **2011**, *72*, 1443 1452.

[30] a) K. Kim, J. W. Lauher, K. A. Parker, *Organic Letters* **2012**, *14*, 138 141. b) K. A. Parker, Z. Wang, *Org. Lett.* **2006**, *8*, 3553 3556.

[31] a) R. Huisgen, A. Dahmen, H. Huber, *J. Am. Chem. Soc.* **1967**, *89*, 7130 7131. b) R. Huisgen, G. Boche, A. Dahmen, W. Hechtl, *Tetrahedron Letters* **1968**, *9*, 5215 5219. c) A. C. Cope, A. C. Haven, F. L. Ramp, E. R. Trumbull, *J. Am. Chem. Soc.* **1952**, *74*, 4867 4871.

[32] A. Patel, K. N. Houk, *J. Org. Chem.* **2014**, *79*, 11370 11377.

[33] a) Y. Zhao, N. E. Schultz, D. G. Truhlar, *J. Chem. Theory Comput.* **2006**, *2*, 364 382. b) Y. Zhao, D. G. Truhlar, *J. Phys. Chem. A*, **2005**, *109*, 5656 5667. c) Y. Zhao, D. G. Truhlar, *J. Chem. Phys.* **2006**, *125*, 194101. d) Y. Zhao, D. G. Truhlar, *Theor. Chem. Acc.* **2008**, *120*, 215 241.

Chapter 7

1. Experimental section for chapter 2

Supporting Information

Synthesis and Analysis of Substituted Bullvalenes

Oussama Yahiaoui, Lukáš F. Pašteka,* Bernadette Judeel, and Thomas Fallon*

ange 201712157 sm miscellaneous information.pdf

Table of Contents

1　General Information

NMR analysis was conducted using a *Bruker Advance III-HD* 300, 500, or 700 MHz spectrometer. Chemical shifts are referenced to the residual solvent resonance as the internal standard (CHCl$_3$: δ = 7.26 ppm for ^{1}H NMR and δ = 77.16 ppm for ^{13}C NMR, acetone: δ = 2.05 ppm for ^{1}H NMR and and δ = 29.84 ppm for ^{13}C NMR, tetrahydrofuran: δ = 3.58 ppm for ^{1}H NMR and δ = 25.31 ppm for ^{13}C NMR). Data are reported as follows: chemical shift, multiplicity (br s = broad singlet, s = singlet, d = doublet, t = triplet, q = quartet, m = multiplet). High-resolution mass spectrometry was recorded using either a *VG70SE spectrometer* (ESI) or a *Micromass/Waters AutoSpec Premier* spectrometer (EI). Infra-red spectra were recorded using a *Bruker Alpha* FTIR spectrometer equipped with an attenuated total reflectance probe. Melting points were recorded using an Electrothermal IA9300 capillary melting point apparatus and are uncorrected.

Cyclooctatetraene was obtained as a generous gift from the University of Adelaide. The material was manufactured by BASF, most lkely sometime in the 1970s. Samples were purified by vacuum distillation using a short vigrex column (20 mbar/ 60 °C), and stored in a freezer under an atmosphere of argon. All other chemicals were purchased from commercial suppliers and used as received.

2   Experimental Procedures

General Procedure A: Cobalt-Catalysed Cycloaddition Reactions with Cyclooctadiene

Under an argon atmosphere, a 20 mL oven-dried sealed tube was charged with $CoBr_2$(dppe) (0.1 mmol, 0.10 eq), zinc iodide (0.2 mmol, 0.20 eq), and zinc dust (0.3 mmol, 0.30 eq). The tube was flushed with argon and evacuated under high vacuum three times. Afterwards, a solvent (either 1,2-dichlorethane or trifluoroethanol) was added and the reaction mixture stirred for 15 min at room temperature. Cyclooctatetraene **2** (112 μL, 1.00 mmol, 1.00 eq) and the substituted acetylene (1-2 eq) were added to the solution and the reaction stirred for (16 - 24 h) at either room temperature or 55 °C. After the reaction was complete, the suspension was filtered through a short pad of silica gel eluting with either hexane or dichloromethane. The solvent was evaporated using a rotary evaporator, and the desired product was purified via flash column chromatography on silica gel.

General Procedure B: Photochemical Rearrangement to Bullvalenes

A 10 mL vial was charged with **4a-i** and dry acetone. The solution was flushed with argon and transferred into an NMR tube (Pyrex ASTM type 1 class B glass, Norell item: S-5-300). The tube was placed in a water bath next to a 150 W medium pressure mercury UV lamp (ca. 3-2 cm distance). The tube was irradiated for 16 – 24 h. After the reaction was complete, the solvent was evaporated to dryness and the desired product was purified by flash column chromatography on silica gel.

Large Scale Synthesis of (2Z,4Z)-bicyclo[4.2.2]deca-2,4,7,9-tetraene (4a)

To a dry 250 mL schlenk flask was added $CoBr_2$(dppe) (7.41 g, 12.0 mmol, 0.10 eq.), zinc iodide (7.66 g, 24.0 mmol, 0.20 eq.) and zinc dust (3.14 g, 48.0 mmol, 0.40 eq.). This mixture was pump/purged with argon, and then 1,2-dichloroethane (30 mL) was added. The mixture was stirred at room temperature for 10 min. Cyclooctatetraene **2** (13.5 mL, 120 mmol, 1.00 eq.) was then added *via* syringe. The mixture was frozen in liquid nitrogen and sealed under vacuum and then warmed to room temperature. A cylinder of acetylene gas (instrument grade) was equipped with a low-pressure regulator set slightly above ambient pressure together with an overpressure release valve. The stream of gas was passed through a series of bubblers (empty, distilled water, empty, concentrated sulfuric acid, empty) and then through a cartridge of silica gel before reaching a glass manifold. This system was purged with acetylene before being connected to the reaction flask. The reaction mixture was opened to the supply of acetylene and the mixture rapidly stirred. An exotherm was observed and after 15 min the temperature had reached 40 °C (externally measured using an IR probe). The reaction flask was then placed in a room temperature water bath. After 2.5 hours the rate of gas uptake had greatly reduced. The mixture was allowed to stir for a further 2 hours. The mixture was passed through a pad of silica gel and washed with hexane. The solvent was removed *in vacuo* (down to

120 mbar/40 °C) and the residue passed through second pad of silica gel eluting with hexane. The solvent was removed *in vacuo* (down to 100 mbar/40 °C) to give the title compound **1a** as a yellow oil (12.4 g, 84% yield). **IR** (ATR): $\tilde{v}/cm^{-1}$ = 3010, 2916, 1397, 976, 947, 840, 811, 748, 732, 664, 638. **^{1}H NMR** (300 MHz, CDCl$_3$) δ = 6.26 – 6.19 (2H, m), 5.88-5.80 (2H, m), 5.67 – 5.61 (4H, m), 3.29 – 3.22 (2H, m). **^{13}C NMR** (75 MHz, CDCl$_3$) δ = 141.1 (CH), 124.4 (CH), 121.3 (CH), 34.9 (CH). **HRMS** (EI, m/z) calculated for C$_{10}$H$_{10}$ 130.0783, found 130.0786.

Large Scale Synthesis of Bullvalene (1)

A solution of (2*Z*,4*Z*)-bicyclo[4.2.2]deca-2,4,7,9-tetraene **4a** (12.0 g, 92.2 mmol) was dissolved in dry acetone (120 mL). This solution was distributed between 10 NMR tubes (10 mm diameter, pyrex grade A glass). These were arrayed around a medium pressure mercury lamp in a bath of water and irradiated for 55 hours. The solutions were combined and the solvent removed in vacuo (100 mmbar/25 °C). The residue was recrystallised from diethyl ether (four crops) to give bullvalene **1** as a white crystalline solid (8.46 g, 71%). **M.p.** 92-93 °C. **IR** (ATR): $\tilde{v}/cm^{-1}$ = 3025, 2928, 1634, 1452, 1367, 1079, 841, 821, 735, 664, 640, 556. **^{1}H NMR** (300 MHz, CDCl$_3$, -55 °C) δ = 6.01 – 5.91 (3H, m), 5.86 (3H, dd, *J* = 11.1, 8.4 Hz), 2.41 – 2.23 (4H, m). **^{13}C NMR** (75 MHz, CDCl$_3$, -55 °C) δ = 128.0 (CH), 127.2 (CH), 30.0 (CH), 20.4 (CH). **HRMS** (EI, m/z) calculated for C$_{10}$H$_{10}$ 130.0783, found 130.0780.

Synthesis of (2*Z*,4*Z*)-7-methylbicyclo[4.2.2]deca-2,4,7,9-tetraene (4b)
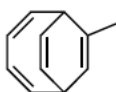
The reaction was done according to **procedure A**, at room temperature for 24h using cyclooctatetraene (340 µL, 3.00 mmol), propyne (3.50 mL, 1.27 mmol/mL in dichloromethane, 4.50 mmol, 1.50 eq) as the substituted acetylene, and 1,2-dichloroethane (4 mL) as the solvent. The silica pad was washed with dichloromethane, which was removed *in vacuo* (down to 90 mbar/40 °C due to the volatility of the product). The residue was purified by flash column chromatography using hexane as eluent (R$_f$ = 0.53). **4b** was obtained as a colorless oil (306 mg, 70%). **IR** (ATR): $\tilde{v}/cm^{-1}$ = 3032, 2909, 1445, 1375, 922, 854, 727, 669, 649. **^{1}H NMR** (300 MHz, CDCl$_3$) δ = 6.32 – 6.19 (2H, m), 5.82 – 5.62 (4H, m), 5.41 – 5.39 (1H, d, *J* = 5.6 Hz), 3.23 – 3.19 (1H, dd, *J* = 5.2 Hz, *J* = 8.6 Hz), 3.14 – 3.07 (1H, m), 1.79 (3H, d, *J* = 1.1 Hz). **^{13}C NMR** (75 MHz, CDCl$_3$) δ = 142.6 (CH), 142.1 (CH), 132.0 (CH), 124.8 (C), 121.3 (CH), 121.2 (CH), 118.0 (CH), 40.4 (CH), 35.2 (CH), 20.6 (CH$_3$). **HRMS** (EI, m/z) calculated for C$_{11}$H$_{12}$ 144.0939, found 144.0936.

Synthesis of (2*Z*,4*Z*)-7-hexylbicyclo[4.2.2]deca-2,4,7,9-tetraene (4c)
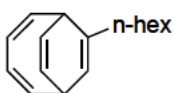
The reaction was done according to **procedure A**, at room temperature for 16 h using cyclooctatetraene (224 µL, 2.00 mmol), oct-1-yne (300 µL, 2.00 mmol, 1.00 eq) as the substituted acetylene and 1,2-dichloroethane (2 mL) as the

solvent. The silica pad was washed with dichloromethane, which was evaporated under vacuum. The residue was passed through a short silica column (Pasteur pipette), which was eluted with hexane. The desired product **4c** was obtained as a yellow oil (385 mg, 90%). **IR (ATR):** $\tilde{v}/cm^{-1}$ = 3010, 2923, 2853, 1673, 1456, 1393, 855, 723, 670, 646, 606. **^{1}H NMR** (300 MHz, CDCl$_3$) δ = 6.29 − 6.12 (2H, m), 5.79 − 5.61 (4H, m), 5.40 − 5.38 (1H, m), 3.25 − 3.20 (1H, dd, J = 8.7, 5.5 Hz), 3.17 − 3.10 (1H, m), 2.09 − 2.04 (2H, t, J = 7.10 Hz), 1.41 − 1.24 (8H, m), 0.89 − 0.84 (3H, m). **^{13}C NMR** (75 MHz, CDCl$_3$) δ = 142.1 (CH), 141.9 (CH), 136.7 (C), 124.4 (CH), 123.9 (CH), 121.5 (CH), 121.2 (CH), 116.9 (CH), 39.3 (C), 35.1 (C), 35.0 (C), 31.9 (C), 29.1 (C), 29.0 (1C), 22.75 (1C), 14.24 (1C). **HRMS** (EI, m/z) calculated for C$_{16}$H$_{22}$ 214.1722, found 214.1723.

Synthesis of ((2Z,4Z)-bicyclo[4.2.2]deca-2,4,7,9-tetraen-7-yl)methanol (4d)
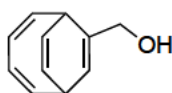
The reaction was done according to **procedure A**, at 55 °C for 18 h using cyclooctatetraene (0.90 mL, 8.0 mmol), prop-2-yn-1-ol (0.70 mL, 12.0 mmol, 1.5 eq) as the substituted acetylene and Trifluroethanol (4 mL) as the solvent. The silica pad was washed with dichloromethane and ethyl acetate, and then the solvent removed under vacuum. The desired product **4d** was purified by flash column chromatography using hexane/ethyl acetate (7:3) as eluent (R$_f$ = 0.55). **4d** was obtained as a colorless oil (1.1 g, 86%). **IR (ATR):** $\tilde{v}/cm^{-1}$ = 2249, 2124, 1052, 1023, 1005, 820, 757, 622. **^{1}H NMR** (300 MHz, CDCl$_3$) δ = 6.30 − 6.16 (2H, m), 5.83 − 5.61 (5H, m), 4.21 − 4.04 (2H, m), 3.44 (1H, dd, J = 8.8, 5.7 Hz), 3.24 − 3.17 (1H, m), 1.33 (1H, s). **^{13}C NMR** (75 MHz, CDCl$_3$) δ = 141.9 (CH), 141.4 (CH), 136.1 (C), 121.2 (CH), 121.0 (CH), 118.9 (CH), 64.8 (CH$_2$), 38.4 (CH), 34.87 (CH). **HRMS** (ESI, m/z) calculated for ([M+Na]$^+$) C$_{11}$H$_{12}$NaO 183.0786, found 183.0779.

Synthesis of (2Z,4Z)-7-benzylbicyclo[4.2.2]deca-2,4,7,9-tetraene (4e)
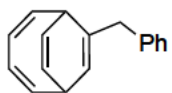
The reaction was done according to **procedure A**, at room temperature for 16 h using cyclooctatetraene (224 µL, 2.00 mmol), 3-phenyl-1-propyne (373 µL, 3.0 mmol, 1.50 eq) as the substituted acetylene and 1,2-dichloroethane (3 mL) as the solvent. The loaded frit was washed with dichloromethane, which was evaporated under vacuum. The desired product was purified by flash column chromatography using hexane as eluent (R$_f$ = 0.57). **4e** was obtained as a yellow oil (400 mg, 91%). **IR (ATR):** $\tilde{v}/cm^{-1}$ = 3010, 2919, 1600, 1493, 1429, 1392, 1358, 1032, 996, 928, 856, 819, 747, 726, 697, 677, 652, 588. **^{1}H NMR** (300 MHz, CDCl$_3$) δ = 7.22 − 7.10 (5H, m), 6.22 − 6.14 (1H, m), 6.02 − 5.95 (1H, m), 5.71 − 5.63 (2H, m), 5.56 − 5.54 (2H, m), 5.53 − 5.53 (2H, d, *J* = 6.1 Hz), 3.35 (2H, s), 3.35 − 3.05 (2H, m). **^{13}C NMR** (75 MHz, CDCl$_3$) δ = 142.1 (CH), 141.9 (CH), 139.9 (C), 1353 (CH), 129.2 (CH), 128.4 (C), 126.2 (CH), 124.8 (CH), 124.2 (CH), 121.3 (CH), 121.2 (CH), 119.3 (CH), 40.7 (CH), 38.4 (CH), 35.2 (CH). **HRMS** (EI, m/z) calculated for C$_{17}$H$_{16}$ 220.1252, found 220.1259.

Synthesis of ((2Z,4Z)-bicyclo[4.2.2]deca-2,4,7,9-tetraen-7-yl)trimethylsilane (4f)
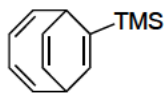
The reaction was done according to **procedure A**, at room temperature for 16 h using cyclooctatetraene (224 µL, 2.00 mmol), ethynyltrimethylsilane (416 µL, 3.00 mmol, 1.50 eq) as the substituted acetylene and 1,2-dichloroethane (2 mL) as the solvent. The silica pad was washed with dichloromethane, which was evaporated under vacuum to give the desired product as a yellow powder **4f** (404 mg, 100%). **M.p.** 30 °C. **IR** (ATR): $\tilde{v}$/cm^{-1} = 3010, 2901, 1244, 1055, 1034, 1034, 972, 945, 831, 747, 708, 689, 659, 645, 624. **^{1}H NMR** (300 MHz, CDCl$_3$) δ = 6.21 – 6.12 (2H, m), 5.90 – 5.88 (2H, d, J = 5.7 Hz), 5.79 – 5.65 (4H, m), 3.38 – 3.33 (1H, q, J = 5.6 Hz, 3.3 Hz), 3.27 – 3.21 (1H, m), 0.09 (9H, s). **^{13}C NMR** (75 MHz, CDCl$_3$) δ = 141.9 (CH) 140.4 (CH), 135.2 (CH), 129.0 (C), 124.5 (CH), 123.9 (CH), 122.5 (CH), 121.4 (CH), 36.8 (CH), 35.9 (CH), -1.0 (CH). **HRMS** (EI, m/z) calculated for C$_{13}$H$_{18}$Si 202.1178, found 202.1172.

Synthesis of ((2Z,4Z)-bicyclo[4.2.2]deca-2,4,7,9-tetraene-7,8-diyl)dimethanol (4g)
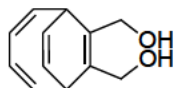
The reaction was done according to **procedure A**, for 16 h at 55 °C using cyclooctatetraene (224 µL, 2.00 mmol), but-2-yne-1,4-diol (344 mg, 4.00 mmol, 2.0 eq) as the substituted acetylene and Trifluroethanol (4 mL) as the solvent. The silica pad was washed with dichloromethane and ethyl acetate and the solvents were evaporated under vacuum. The crude product was purified by flash column chromatography using hexane/ethyl acetate as eluent (R$_f$ = 0.23). The desired product was recrystalized from hexane/dichloromethane (9:1) yielding **4g** as white crystals (300 mg, 80%). **M.p.** 90 – 91 °C. **IR** (ATR): $\tilde{v}$/cm^{-1} = 3258, 3005, 2923, 2873, 1389, 1194, 1255, 1151, 989, 724, 690, 661, 534. **^{1}H NMR** (300 MHz, CDCl$_3$) δ = 6.29 – 6.22 (2H, m), 5.76 – 5.70 (4H, m), 4.27 – 4.15 (4H, dd, J = 11.9, 9.38 Hz), 3.47 – 3.42 (2H, m), 1.97 (OH, s). **^{13}C NMR** (75 MHz, CDCl$_3$) δ = 141.77 (CH), 132.84 (C), 124.94 (CH), 121.19 (CH), 60.65 (CH$_2$), 38.14 (CH). **HRMS** (ESI, m/z) calculated for (MNa$^+$) C$_{12}$H$_{14}$NaO$_2$ 213.0886, found 213.0879.

Synthesis of (2Z,4Z)-7-methyl-8-pentylbicyclo[4.2.2]deca-2,4,7,9-tetraene (4h)
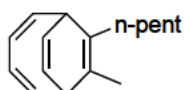
The reaction was done according to **procedure A**, at room temperature for 16 h using cyclooctatetraene (224 µL, 2.00 mmol), oct-2-yne (435 µL, 3.00 mmol, 1.50 eq) as the substituted acetylene and 1,2 dichloroethane (3 mL) as the solvent. The silica pad was washed with dichloromethane, which was evaporated under vacuum. The desired product **4h** was obtained as a yellow oil (373 mg, 87%). **IR** (ATR): $\tilde{v}$/cm^{-1} = 3008, 2953, 2922, 2856, 1455, 1390, 1376, 1054, 1032, 1013, 833, 786723, 658. **^{1}H NMR** (300 MHz, CDCl$_3$) δ = 6.23 – 6.13 (2H, m), 5.67 – 5.55 (4H, m), 3.07 – 2.98 (2H, m), 2.10 – 1.90 (2H, m), 1.66 (3H, s), 1.31 – 1.15 (6H, m), 0.83 – 0.78 (3H, t, J = 6.8

Hz,). ^{13}C NMR (75 MHz, CDCl$_3$) δ = 143.2 (CH), 142.5 (CH), 130.7 (C), 125.5 (C), 124.5 (CH), 124.0 (CH), 121.9 (CH), 121.2 (CH), 41.8 (CH), 39.9 (CH), 31.7 (CH$_2$), 31.6 (CH$_2$), 29.7 (CH$_2$), 22.8 (CH$_2$), 16.6 (CH$_3$), 14.2 (CH$_3$). **HRMS** (EI, m/z) calculated for C$_{16}$H$_{22}$ 214.1722, found 214.1723.

Synthesis of (2Z,4Z)-7-phenylbicyclo[4.2.2]deca-2,4,7,9-tetraene (4i)

The reaction was done according to **procedure A**, at room temperature for 16 h using cyclooctatetraene (224 µL, 2.00 mmol), phenylacetylene (329 µL, 3.00 mmol, 1.50 eq) as the substituted acetylene and 1,2-dichloroethane (3 mL) as the solvent. The loaded frit was washed with dichloromethane, which evaporated under vacuum. The crude target compound was passed through a short silica column (Pasteur pipette), and was eluted with hexane. The desired product **4i** was obtained as a yellow oil (260 mg, 63%). **IR** (ATR): ṽ/cm^{-1} = 2998, 1492, 1373, 1055, 959, 788, 761, 731, 690, 665, 639. ^{1}**H NMR** (300 MHz, CDCl$_3$) δ = 7.42 – 7.38 (2H, m), 7.34 – 7.27 (2H, m), 7.24 – 7.17 (1H, m), 6.42 – 6.26 (2H, m), 6.05 – 6.03 (1H, m), 5.88 – 5.79 (2H, m), 5.74 – 5.769 (1H, m), 3.83 – 3.80 (1H, m), 3.41 – 3.33 (1H, m). ^{13}**C NMR** (75 MHz, CDCl$_3$) δ = 141.93 (CH), 141.04 (CH), 139.88 (C), 135.19 (C), 128.42 (CH), 126.76 (CH), 126.50 (CH), 124.81 (CH), 124.72 (CH), 121.60 (CH), 120.50 (CH), 119.79 (CH), 38.34 (CH), 35.50 (CH). **HRMS** (EI, m/z) calculated for C$_{16}$H$_{14}$ 206.1096, found 206.1089.

Synthesis of methyl-bullvalene (5b)
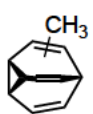
The reaction was done according to **procedure B**, using **4b** (170 mg, 1.18 mmol) in dry acetone (0.5 mL). After 20 h the solvent was evaporated and the crude target compound was purified by flash column chromatography using hexane as eluent (R$_f$ = 0.51). The desired product **5b** was obtained as a colorless oil (70 mg, 40%). **IR** (ATR): ṽ/cm^{-1} = 3022, 2960, 2925, 1638, 1440, 1366, 1310, 670, 670. ^{1}**H NMR** (500 MHz, CDCl$_3$, -60 °C) δ = 5.93 – 5.79 (4H, m), 5.71 (0.56H, d, 7.7 Hz, major), 5.58 (0.40H, d, 8.8 Hz, minor), 2.34 (0.4H, apparent q, 8.6 Hz, minor), 2.28 – 2.15 (3.6H, m), 1.83 (1.12H, s, minor), 1.81 (1.56, s, major). ^{13}**C NMR** (500 MHz, CDCl$_3$, -60 °C) δ = 138.42 (C, major), 135.25 (C minor), 127.99 (CH), 127.37 (CH), 127.17 (CH), 126.54 (CH), 119.97 (CH, major), 119.68 (CH, minor), 35.72 (CH major), 29.77 (CH, minor), 27.73 (CH$_3$, minor), 26.67 (CH$_3$, major), 23.71 (CH, minor), 20.25 (CH), 20.13 (CH), 19.94 (CH). **HRMS** (EI, m/z) calculated for C$_{11}$H$_{12}$ 144.0939, found 144.0936.

Synthesis of n-hexyl-bullvalane (5c)
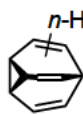
The reaction was done according to **procedure B**, using **4c** (165 mg, 0.78 mmol) dry acetone (0.5 mL). After 16 h the solvent was evaporated under vacuum. The crude product was purified by flash column chromatography using hexane/ethyl acetate (9:1) as eluent. The desired product **5c** was obtained as a colorless oil (150 mg, 81%). **IR** (ATR): $\tilde{v}/cm^{-1}$ = 3025, 2955, 2924, 2853, 1639, 1459, 1405, 1377, 1307, 1082, 985, 953, 908, 857, 831, 807, 732. **^{1}H NMR** (500 MHz, CDCl$_3$, -60 °C) δ = 5.98 – 5.90 (2H, m), 5.90 – 5.84 (2H, m), 5.72 (0.72H, d, 7.7 Hz), 5.58 (0.24H, d, 8.9 Hz), 2.39 (0.24H, apparent q, 8.1 Hz), 2.43 – 2.20 (3.7H, m), 2.11 – 2.00 (2H, m), 1.48 – 1.16 (8H, m), 0.88 – 0.84 (3H, m). **^{13}C NMR** (125 MHz, CDCl$_3$, -60 °C) δ = 143.03 (C, major), 139.31 (C, minor), 127.92 (CH, minor), 127.59 (CH, major), 126.92 (CH, major), 126.46 (CH, minor), 119.16 (CH, co-incident major and minor), 41.08 (CH$_2$, minor), 40.20 (CH$_2$, major), 34.39 (CH, major), 31.71 (CH$_2$), 31.69 (CH$_2$), 29.69 (CH, minor), 29.07 (CH$_2$), 29.03 (CH$_2$), 28.94 (CH$_2$), 28.16 (CH, minor), 22.89 (CH, minor), 22.63 (CH$_2$), 22.61 (CH$_2$), 20.09 (CH), 20.07 (CH), 19.64 (CH, major), 14.30 (CH$_3$), 14.28 (CH$_3$), trace isomer (discernable signals): 137.78, 130.58, 128.10, 127.13, 41.50, 31.87, 29.98, 29.92, 29.44, 27.61, 26.56. **HRMS** (EI, m/z) calculated for C$_{16}$H$_{22}$ 214.1722, found 214.1728.

Synthesis of methanol-bullvlane (5d)
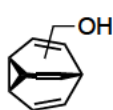
The reaction was done according to **procedure B**, using **4d** (30 mg, 0.19 mmol) in dry acetone (0.5 mL). After 20 h the solvent was evaporated under vacuum. The crude target compound was purified by flash chromatography using hexane/ethyl acetate (3:2) as eluent (R$_f$ = 0.24). The desired product **5d** was obtained as a yellow oil (19 mg, 63%). **IR** (ATR): $\tilde{v}/cm^{-1}$ = 2249, 2124, 1052, 1023, 1005, 820, 757, 622. **^{1}H NMR** (700 MHz, acetone-d6, -60 °C, isomers ratio a:b:c 57:25:18) δ = 5.83 – 5.62 (5H, m), 4.48 (0.14H, t, J = 5.9 Hz), 4.36 (0.2H, t, J = 5.9 Hz), 4.28 (0.46H, t, J = 5.9 Hz), 3.90 (0.41H, d J = 5.9 Hz, isomer b), 3.86 (0.94H, d J = 5.9 Hz, isomer a), 3.47 (0.3H, d J = 5.9 Hz, isomer c), 2.35 – 2.25 (1.14H, m), 2.23 – 2.17 (1.03H, m), 2.17 – 2.12 (0.98H, m), 2.10 – 2.06 (0.3H, m). **^{13}C NMR** (175 MHz, acetone-d6, -60 °C) δ = 141.4 (C, isomer a), 139.0 (C, isomer b), 131.6 (CH), 129.6 (CH, isomer c), 128.4 (CH), 127.9 (CH), 127.7 (CH), 127.5 (CH), 127.3 (CH), 127.2 (CH), 120.5 (CH, isomer b), 120.0 (CH, isomer a), 70.3 (CH$_2$, isomer c), 68.3 (CH$_2$, isomer c), 66.9 (CH$_2$, isomer a), 32.6 (CH, isomer a), 31.9 (C, isomer c), 30.9 (CH), 30.4 (CH), 25.3 (CH, isomer c), 21.3 (CH, isomer b), 20.7 (CH, isomer a), 20.2 (CH, isomer b), 19.3 (CH, isomer a). **HRMS** (ESI, m/z) calculated for (MNa$^+$) C$_{11}$H$_{12}$NaO 183.0786, found 183.0779.

Synthesis of benzyl-bullvalene (5e)
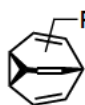
The reaction was done according to **procedure B**, using **4e** (188 mg, 0.85 mmol) in dry acetone (0.5 mL). After 16 h the solvent was evaporated under vacuum. The crude target compound was purified by flash column chromatography using hexane as eluent (R_f = 0.36). The desired product **5e** was obtained as a yellow oil (80 mg, 42%). **IR** (ATR): $\tilde{v}/cm^{-1}$ = 3023, 1638, 1599, 1492, 1451, 1153, 1029, 740, 696. **^{1}H NMR** (500 MHz, CDCl$_3$, -60 °C, isomer ratio major:minor 66:34) δ = 7.57 – 7.32 (5H, m), 6.17 – 6.03 (2H, m), 6.00 – 5.83 (2H, m), 3.66 (0.54H, s, major), 3.59 (1.06H, s, major), 2.67 – 2.58 (0.29H, m, minor), 2.52 – 2.25 (3.3H, m). **^{13}C NMR** (125 MHz, CDCl$_3$) δ = 140.85 (C, major), 139.67 (C, minor), 136.60 (C, coincident major and minor), 128.86 (CH), 128.54 (CH), 128.10 (CH), 128.03 (CH), 127.72 (CH), 126.80 (CH), 126.57 (CH), 125.95 (CH), 125.83 (CH), 122.36 (CH, minor), 121.84 (CH, major), 46.56 (CH$_2$, minor), 45.87 (CH$_2$, major), 33.83 (CH, major), 31.27 (CH), 29.77 (CH), 23.18 (CH, minor), 20.12 (CH), 20.10 (CH), 19.60 (CH). **HRMS** (EI, m/z) calculated for ([M-PhMe]$^+$) C$_{10}$H$_9$ 129.0704, found 129.0705.
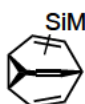
Synthesis of trimethylsilyl-bullvalane (5f)

The reaction was done according to **procedure B**, using **4f** (97 mg, 0.49 mmol) in dry acetone (0.5 mL). After 16 h the solvent was evaporated under vacuum. The crude target compound was purified by flash column chromatography using hexane as eluent (R_f = 0.59). The desired product **5f** was obtained as white crystals (68 mg, 70%). **M.p.** 60 °C **IR** (ATR): $\tilde{v}/cm^{-1}$ = 3023, 2953, 2918, 1604, 1401, 1373, 1245, 1043, 825, 739, 689, 619. **^{1}H NMR** (500 MHz, CDCl$_3$, -60 °C, major isomer) δ = 6.34 – 6.30 (1H, m), 5.97 – 5.91 (2H, m), 5.84 (2H, dd, J = 10.9, 8.4 Hz), 2.43 (1H, t, J = 8.4 Hz), 2.36 – 2.32 (3H, m), 0.05 (9H, s). **^{13}C NMR** (125 MHz, CDCl$_3$, -60 °C, major isomer) δ = 143.80 (C), 134.35 (CH), 128.55 (CH), 127.15 (CH), 31.96 (CH), 21.32 (CH), 20.03 (CH), -2.28 (CH$_3$). **HRMS** (EI, m/z) calculated for C$_{13}$H$_{18}$Si 202.1178, found 202.1173.

Synthesis of dimethanol-bullvalene (5g)
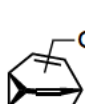
The reaction was done according to **procedure B**, using **4g** (400 mg 2.10 mmol) in in dry acetone (1 mL). After 26 h the solvent was evaporated under vacuum. The crude target compound was purified by flash chromatography using hexane/ethyl acetate (3:1) as eluent (R_f = 0.37). The desired product **5g** was obtained as a colorless oil (158 mg, 40%). **IR** (ATR): $\tilde{v}/cm^{-1}$ = 3022, 2922, 2862, 1436, 1406, 1052, 1007, 739, 728, 693, 669, 532. **^{1}H NMR** (700 MHz, tetrahydrofuran-d8, -80 °C) δ = 5.82 – 5.59 (4H, m), 4.78 (0.05H, t, J = 6.3 Hz), 4.69 – 4.60 (0.28H, m), 4.54 (0.09H, t, J = 6.4 Hz), 4.52 – 4.43 (1.32H, m), 4.41 (0.03H, t, J = 6.6 Hz), 4.12 – 4.07 (0.03H, m), 4.03 – 3.97 (0.05H, m), 3.90 – 3.76 (2.89H, m), 3.51 – 3.47 (0.09H, m), 3.47 – 3.37 (0.45H, m), 3.24 – 3.19 (0.04H, m),

2.44 – 2.33 (0.84H, m), 2.31 – 2.27 (0.09H, m), 2.25 – 2.22 (0.21H, m), 2.22 – 2.16 (0.31H, m), 2.16 – 2.11 (0.94H, m), 2.11 – 2.03 (0.55, m), 2.03 – 1.98 (0.24H, m). ^{13}**C NMR** (175 MHz, tetrahydrofuran-d8, -80 °C, isomers A:B:C:D:E:F 44:23:14:9:6:5) δ = 142.3 (C), 141.8 (C), 141.6 (C), 141.4 (C), 139.4 (C), 139.2 (C), 139.1 (C), 129.4 (CH$_2$), 129.4 (CH$_2$), 128.1 (CH$_2$), 128.0 (CH$_2$), 127.8 (CH$_2$), 127.8 (CH$_2$), 127.7 (CH$_2$), 127.6 (CH$_2$), 127.6 (CH$_2$), 127.5 (CH$_2$), 127.3 (CH$_2$), 127.2 (CH$_2$), 127.0 (CH$_2$), 127.0 (CH$_2$), 126.9 (CH$_2$), 122.2 (CH$_2$), 120.7 (CH$_2$), 120.2 (CH$_2$), 119.9 (CH$_2$), 119.7 (CH$_2$), 119.7 (CH$_2$), 70.2 (CH$_2$), 70.1 (CH$_2$), 70.0 (CH$_2$), 68.8 (CH$_2$), 68.7 (CH$_2$), 68.6 (CH$_2$), 67.6 (CH$_2$), 67.4 (CH$_2$), 34.5 (CH, isomer A), 33.0 (CH, isomers C and D), 32.3 (CH, isomer B), 31.9 (C, isomer C), 31.5 (C, isomer E), 30.9 (CH, isomer E), 30.4 (C, isomer D), 30.2 (CH, isomer F), 25.8 (CH, isomer E), 25.2 (CH, isomers C and D), 24.7 (CH, isomer E), 23.7 (CH, isomer C), 21.3 (CH, isomer B), 20.9 (CH, isomer F), 20.6 (CH, isomer A), 20.3 (CH, isomer B), 19.9 (CH, isomer F), 19.6 (CH, isomer A), 18.9 (CH, isomer B). **HRMS** (ESI, m/z) calculated for ([M+Na]$^+$) C$_{12}$H$_{14}$NaO$_2$ 213.0886, found 213.0879.

Synthesis of methyl-pentyl-bullvalene (5h)
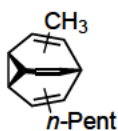
5h

The reaction was done according to **procedure B**, using **4h** (200 mg, 0.93 mmol) in in dry acetone (2 mL). After 16 h the solvent was evaporated under vacuum. The crude target compound was purified by flash column chromatography using hexane as eluent (R$_f$ = 0.54). The desired product **5h** was obtained as a colorless oil (66 mg, 35%). **IR** (ATR): $\tilde{v}$/cm^{-1} = 2952, 2925, 1180, 1011, 964, 941, 789, 723, 694, 664, 639. **^{1}H NMR** (700 MHz, acetone-d6, -60 °C) δ = 5.77 – 5.66 (2.0H, m), 5.57 – 5.47 (1.8H, m), 2.32 – 1.86 (6.6H, m), 1.76 – 1.70 (2.6H, m), 1.42 – 1.31 (6.4H, m), 0.88 – 0.79 (3.0H, m). **^{13}C NMR** (175 MHz, acetone-d6, -60 °C, isomers A:B:C:D, 42:30:17:11) δ = 142.0 (C), 140.7 (C), 138.7 (C), 138.0 (C), 137.4 (C), 136.5 (C), 134.3 (C), 133.7 (C),128.2 (CH), 127.7 (CH), 127.6 (CH), 127.4 (CH), 127.0 (CH), 126.8 (CH), 126.2 (CH), 120.8 (CH), 120.7 (CH), 120.6 (CH), 120.6 (CH), 120.1 (CH), 120.1 (CH), 119.8 (CH), 119.6 (CH), 41.7 (CH$_2$, isomer C), 41.4 (CH$_2$, isomer D), 41.2 (CH$_2$, isomer A), 40.8 (CH$_2$, isomer B), 40.7 (CH, isomer A), 36.5 (CH, isomer C), 35.0 (CH, isomer B), 31.9 (CH$_2$), 31.8 (CH$_2$), 31.7 (CH$_2$), 30.6 (CH, isomer D), 28.8 (CH$_2$), 28.8 (CH$_2$), 28.7 (CH$_2$), 27.4 (CH, isomer B), 27.3 (CH, isomer D), 26.7 (CH, isomer A), 26.5 (CH, isomer C), 23.8 (CH), 23.7 (CH), 23.1 (CH$_2$), 23.1 (CH$_2$), 22.9 (CH), 20.4 (CH), 20.3 (CH), 20.3 (CH), 20.3 (CH), 20.2 (CH), 20.2 (CH), 19.9 (CH), 19.9 (CH), 14.4 (CH$_3$), 14.4 (CH$_3$). **HRMS** (EI, m/z) calculated for C$_{16}$H$_{22}$ 214.1722, found 214.1725.

Synthesis of 1-phenyl-1,3a,4,6a-tetrahydro-1,4-ethenopentalene (6)
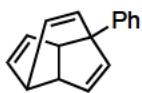
6

A solution (2Z,4Z)-7-phenylbicyclo[4.2.2]deca-2,4,7,9-tetraene **4i** (33 mg, 0.16 mmol) in dry acetone (0.5 mL) in an NMR tube was irradiated using a medium pressure mercury lamp for 4 hours. The solvent was removed *in vacuo*

and the residue purified with flash chromatography eluting with hexane to give the title compound **6** (21 mg, 64%) as a yellow gum. **IR** (ATR): $\tilde{v}/cm^{-1}$ = 3030, 2931, 791, 1617, 1391, 1361, 1325, 1233, 1208, 842, 780, 715, 680. **¹H NMR** (300 MHz, CDCl₃) δ = 7.35 – 7.28 (2H, m), 7.25 – 7.18 (1H, m), 7.10 – 7.06 (2H, m), 6.76 (1H, d, *J* = 5.7 Hz), 6.73 (1H, dd, *J* = 5.7, 2.9 Hz), 6.18 (1H, ddd, *J* = 9.3, 1.9, 1.0 Hz), 6.06 (1H, ddd, *J* = 9.3, 5.7, 1.3 Hz), 5.74 (1H, ddd, *J* = 5.7, 3.2, 0.5 Hz), 5.54 (1H, ddd, *J* = 5.7, 3.1, 0.5 Hz), 3.46-3.40 (1H, m), 3.18 (1H, ddd, *J* = 5.2, 3.1, 1.9 Hz), 2.66 – 2.60 (1H, m). **¹³C NMR** (75 MHz, CDCl₃) δ = 147.82 (CH), 146.14 (CH), 144.91 (C), 137.11 (CH), 132.37 (CH), 130.03 (CH), 128.49 (CH), 128.24 (CH), 126.27 (CH), 126.13 (CH), 69.43 (CH), 61.96 (CH), 54.40 (C), 41.75 (CH). **HRMS** (EI, m/z) calculated for $C_{16}H_{14}$ 206.1096, found 206.1095.

3   NMR Spectra

4a: ^{1}H NMR
(300 MHz, CDCl$_3$)

4a: ^{13}C NMR
(75 MHz, CDCl$_3$)
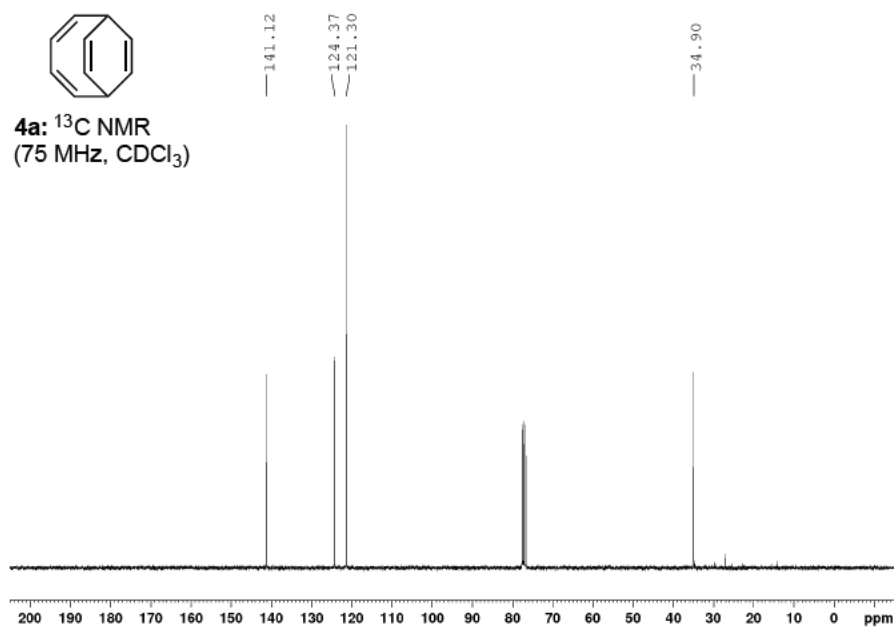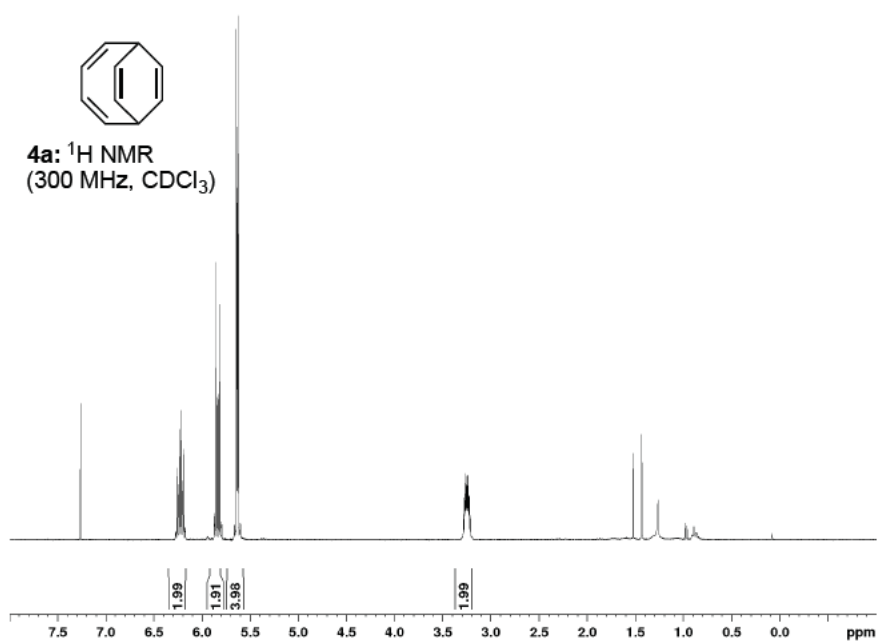
Figure 1: *upper:* ^{1}H NMR of (2*Z*,4*Z*)-bicyclo[4.2 2]deca-2,4,7,9-tetraene (**4a**). *lower:* ^{13}C NMR of (2*Z*,4*Z*)-bicyclo[4.2.2]deca-2,4,7,9-tetraene (**4a**).

4b: ^{1}H NMR
(300 MHz, CDCl$_3$)

4b: ^{13}C NMR
(75 MHz, CDCl$_3$)
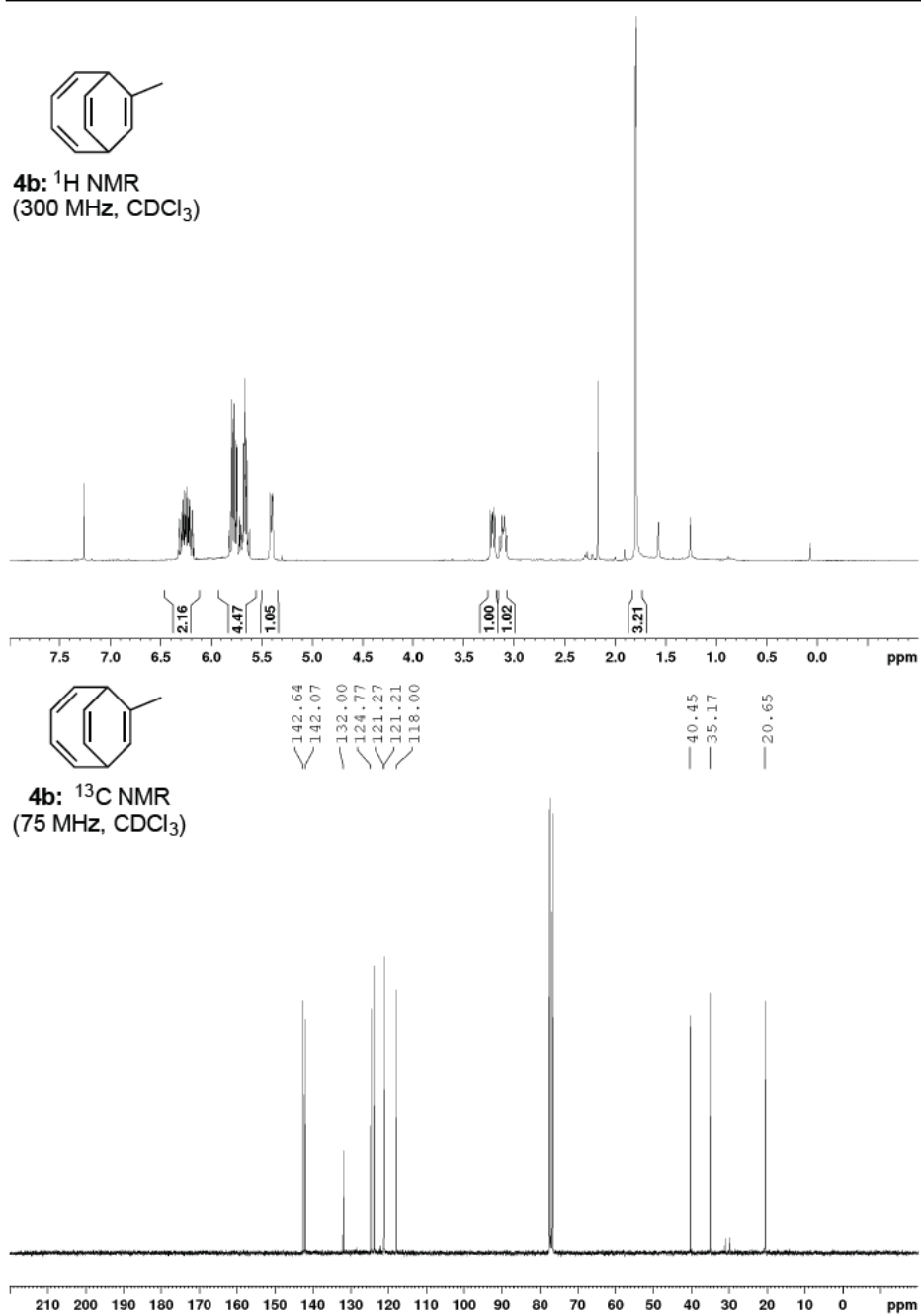
Figure 2: *upper:* ^{1}H NMR of (2Z,4Z)-7-methylbicyclo[4.2.2]deca-2,4,7,9-tetraene (**4b**). *lower:* ^{13}C NMR of (2Z,4Z)-7-methylbicyclo[4.2.2]deca-2,4,7,9-tetraene (**4b**).

4c: ¹H NMR
(300 MHz, CDCl₃)

4c: ¹³C NMR
(75 MHz, CDCl₃)
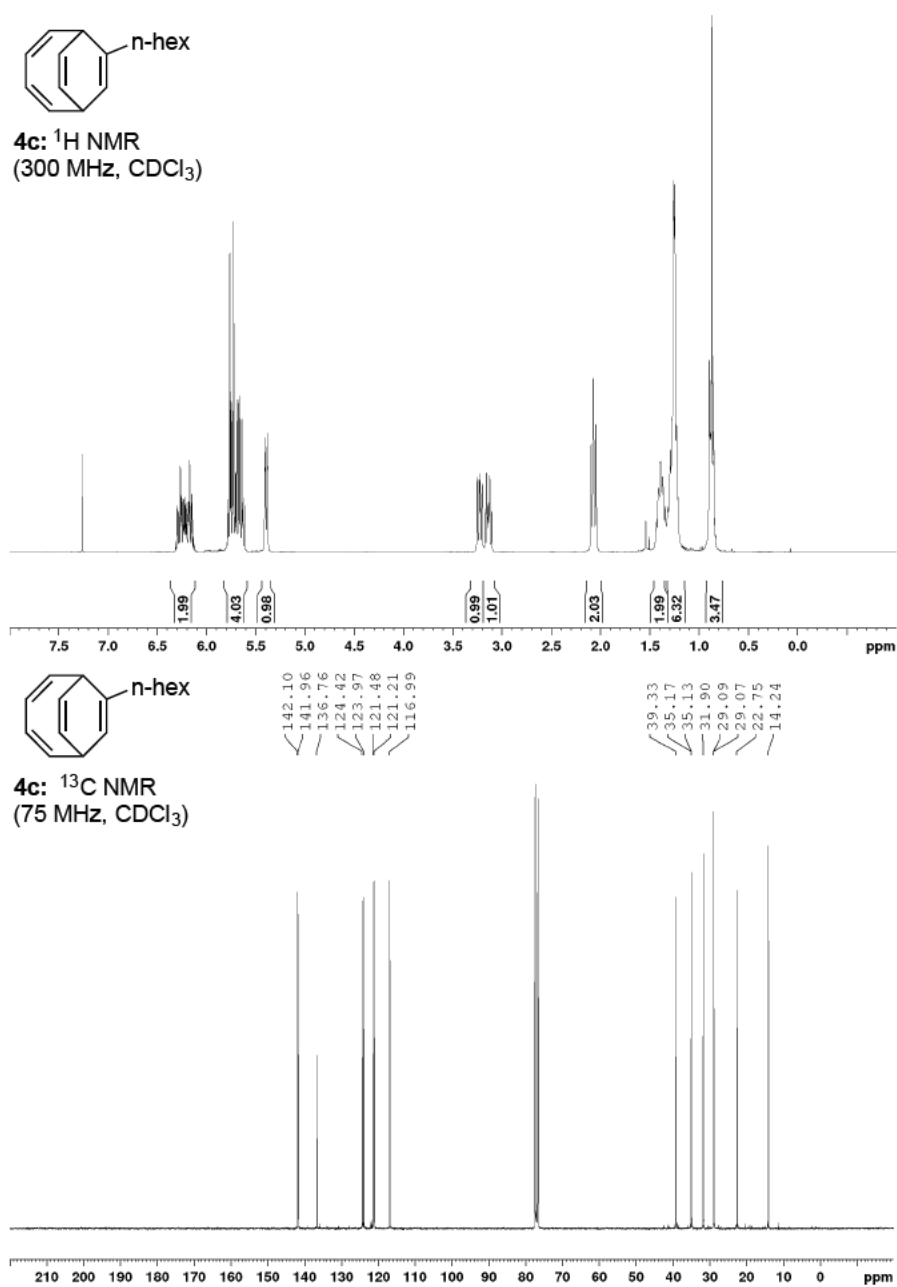
Figure 3: *upper:* ^{1}H NMR of (2*Z*,4*Z*)-7-hexylbicyclo[4.2.2]deca-2,4,7,9-tetraene (**4c**). *lower:* ^{13}C NMR of (2*Z*,4*Z*)-7-hexylbicyclo[4.2.2]deca-2,4,7,9-tetraene (**4c**).

4d: ^{1}H NMR
(300 MHz, CDCl$_3$)

4d: ^{13}C NMR
(75 MHz, CDCl$_3$)
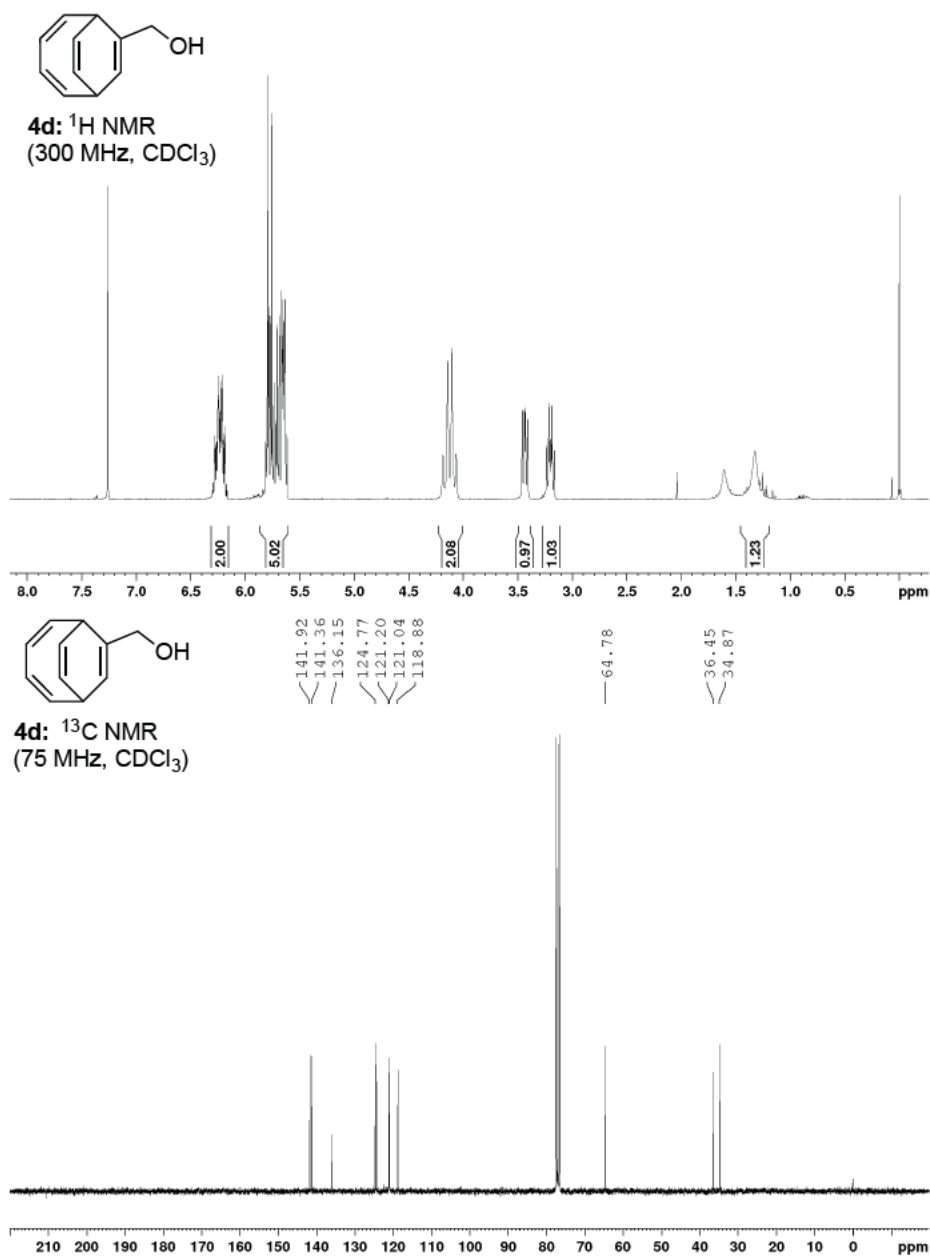
Figure 4: *upper:* ^{1}H NMR of ((2Z,4Z)-8-methylbicyclo[4.2.2]deca-2,4,7,9-tetraen-7-yl)methanol (**4d**). *lower:* ^{13}C NMR of ((2Z,4Z)-8-methylbicyclo[4.2.2]deca-2,4,7,9-tetraen-7-yl)methanol (**4d**).

4e: ^{1}H NMR
(300 MHz, CDCl$_3$)

4e: ^{13}C NMR
(75 MHz, CDCl$_3$)
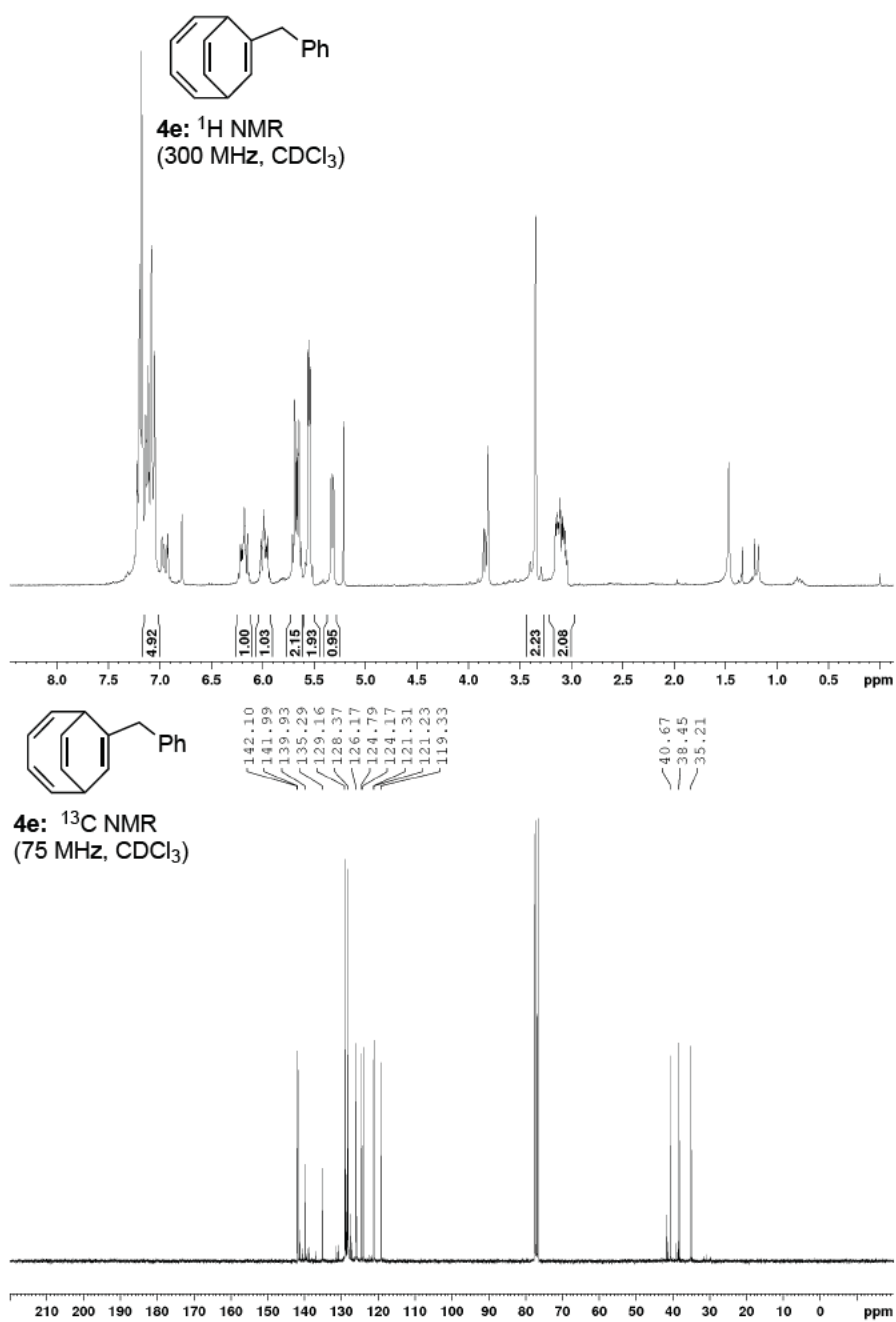
Figure 5: *upper:* ^{1}H NMR of (2Z,4Z)-7-benzylbicyclo[4.2.2]deca-2,4,7,9-tetraene (**4e**). *lower:* ^{13}C NMR of (2Z,4Z)-7-benzylbicyclo[4.2.2]deca-2,4,7,9-tetraene (**4e**).

4f: ^{1}H NMR
(300 MHz, CDCl$_3$)

4f: ^{13}C NMR
(75 MHz, CDCl$_3$)
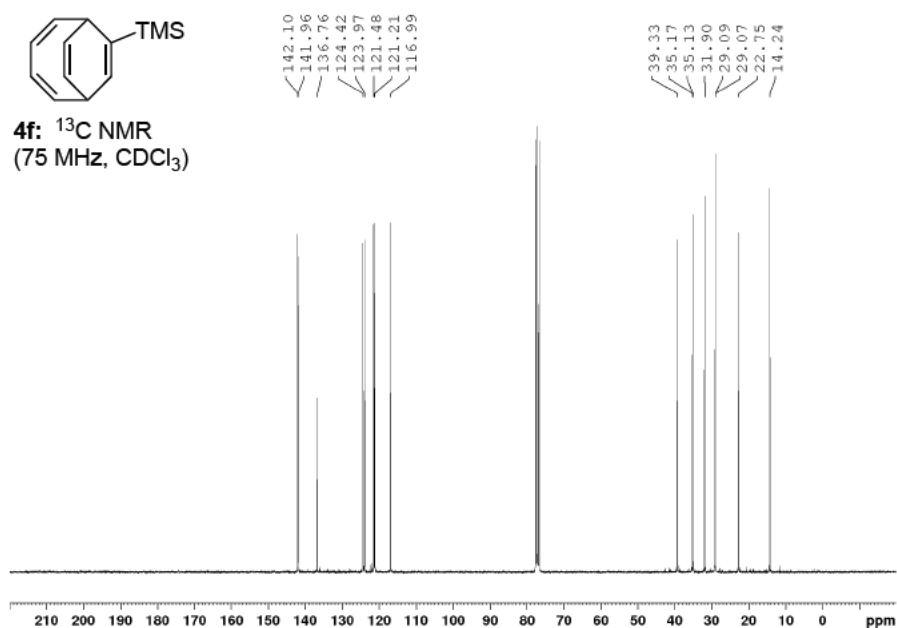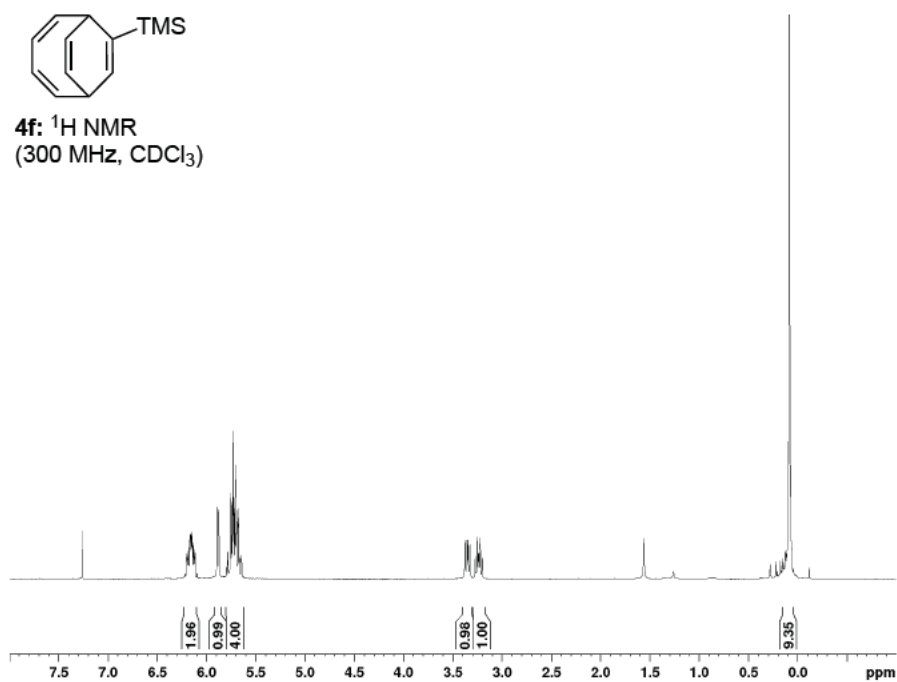
Figure 6: *upper:* ^{1}H NMR of ((2*Z*,4*Z*)-bicyclo[4.2.2]deca-2,4,7,9-tetraen-7-yl)trimethylsilane (**4f**). *lower:* ^{13}C NMR of ((2*Z*,4*Z*)-bicyclo[4.2.2]deca-2,4,7,9-tetraen-7-yl)trimethylsilane (**4f**).

4g: ^{1}H NMR
(300 MHz, CDCl$_3$)

Figure 7:.
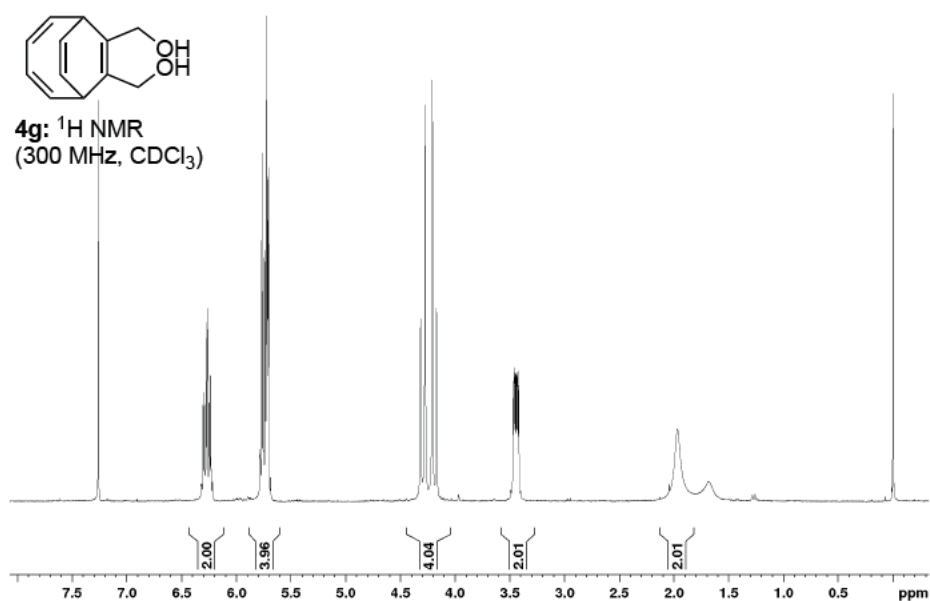
4g: ^{13}C NMR
(75 MHz, CDCl$_3$)
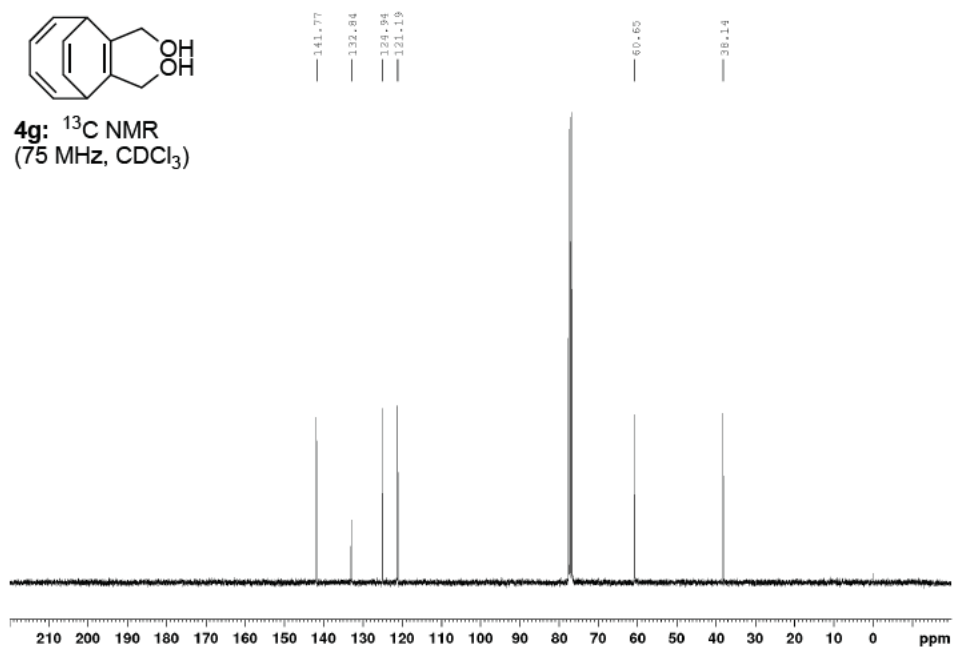
Figure 8: *upper:* ^{1}H NMR of (2Z,4Z)-bicyclo[4.2.2]deca-2,4,7,9-tetraene-7,8-diyl)dimethanol (**4g**). *lower:* ^{13}C NMR of (2Z,4Z)-bicyclo[4.2.2]deca-2,4,7,9-tetraene-7,8-diyl)dimethanol (**4g**).

4h: ^{1}H NMR
(300 MHz, CDCl$_3$)

4h: ^{13}C NMR
(75 MHz, CDCl$_3$)
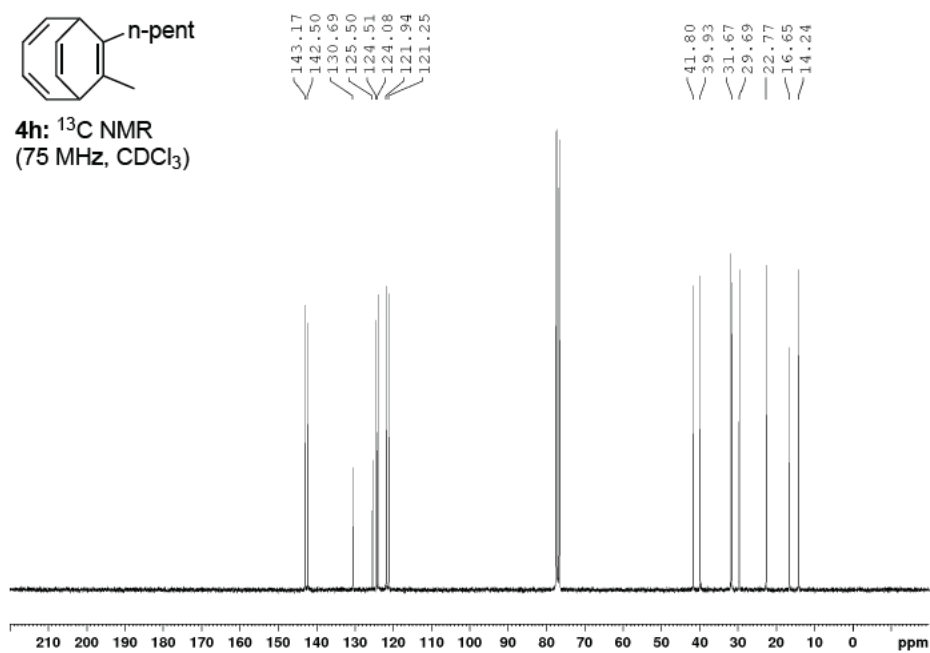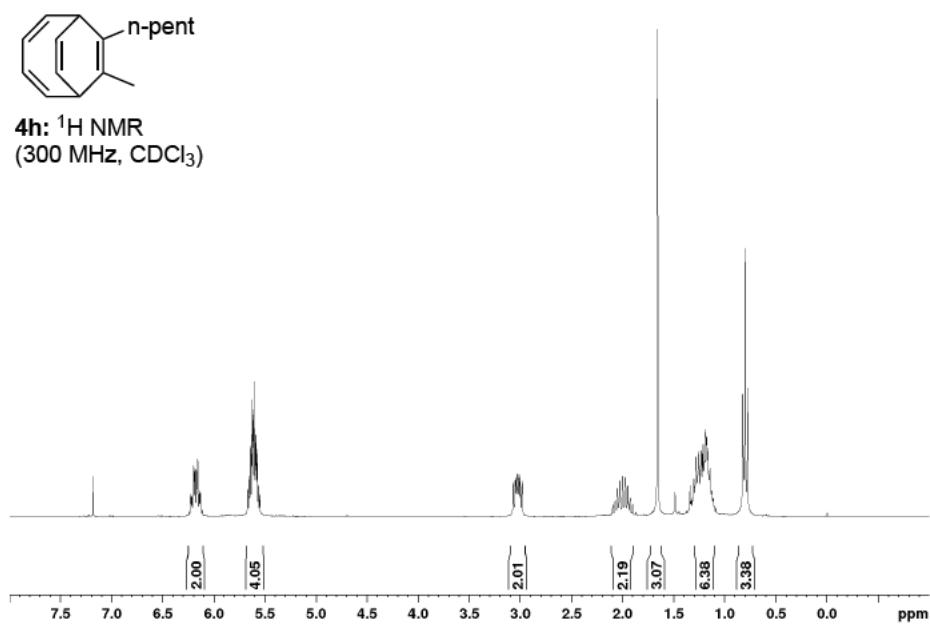
Figure 9: *upper:* ^{1}H NMR of (2Z,4Z)-7-methyl-8-pentylbicyclo[4.2.2]deca-2,4,7,9-tetraene (**4h**). *lower:* ^{13}C NMR of (2Z,4Z)-7-me hyl-8-pentylbicyclo[4.2.2]deca-2,4,7,9-tetraene (**4h**).

4i: ^{1}H NMR
(300 MHz, CDCl$_3$)

4i: ^{13}C NMR
(75 MHz, CDCl$_3$)
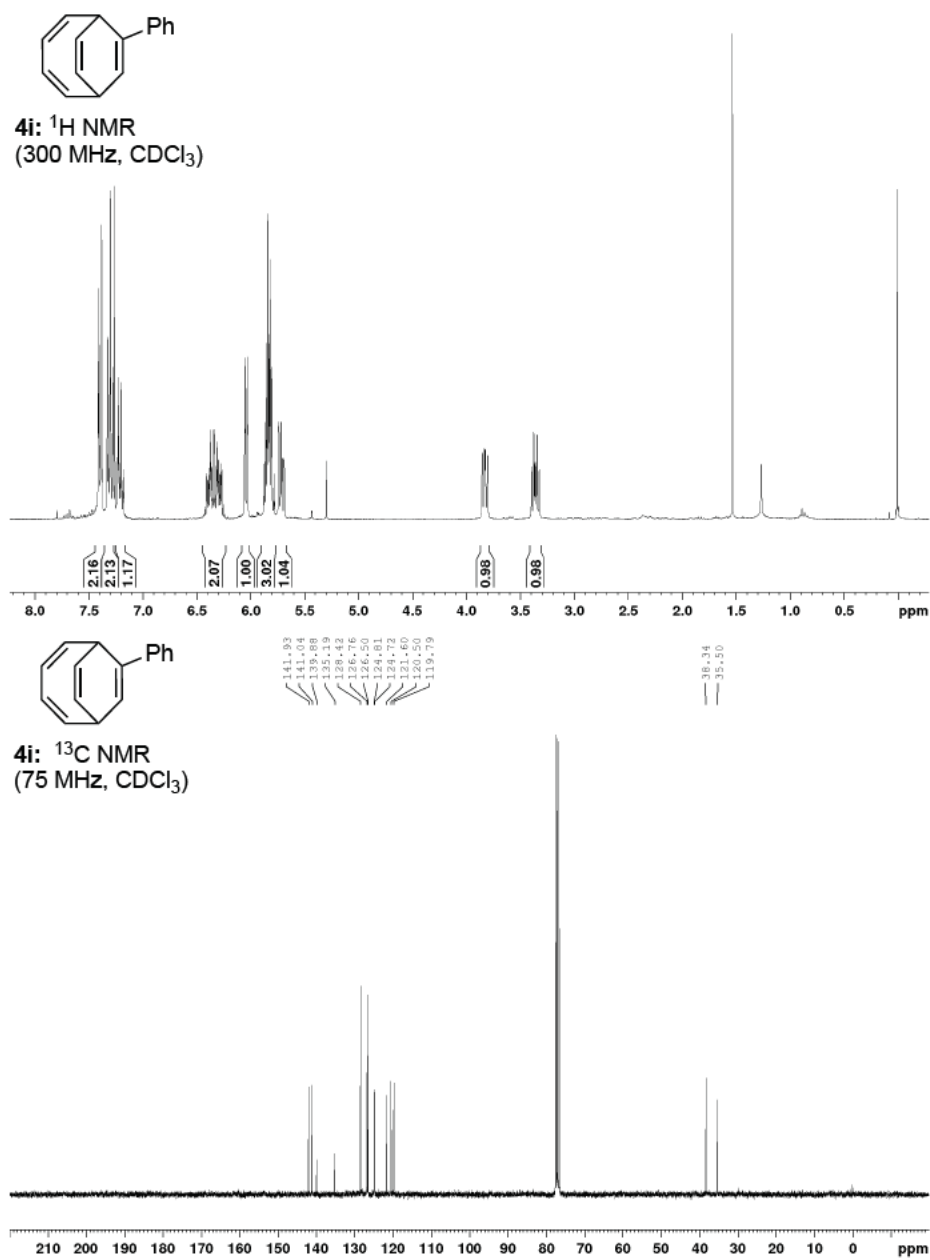
Figure 10: *upper:* ^{1}H NMR of (2Z,4Z)-7-phenylbicyclo[4.2.2]deca-2,4,7,9-tetraene (**4i**). *lower:* ^{13}C NMR of (2Z,4Z)-7-phenylbicyclo[4.2.2]deca-2,4,7,9-tetraene (**4i**).
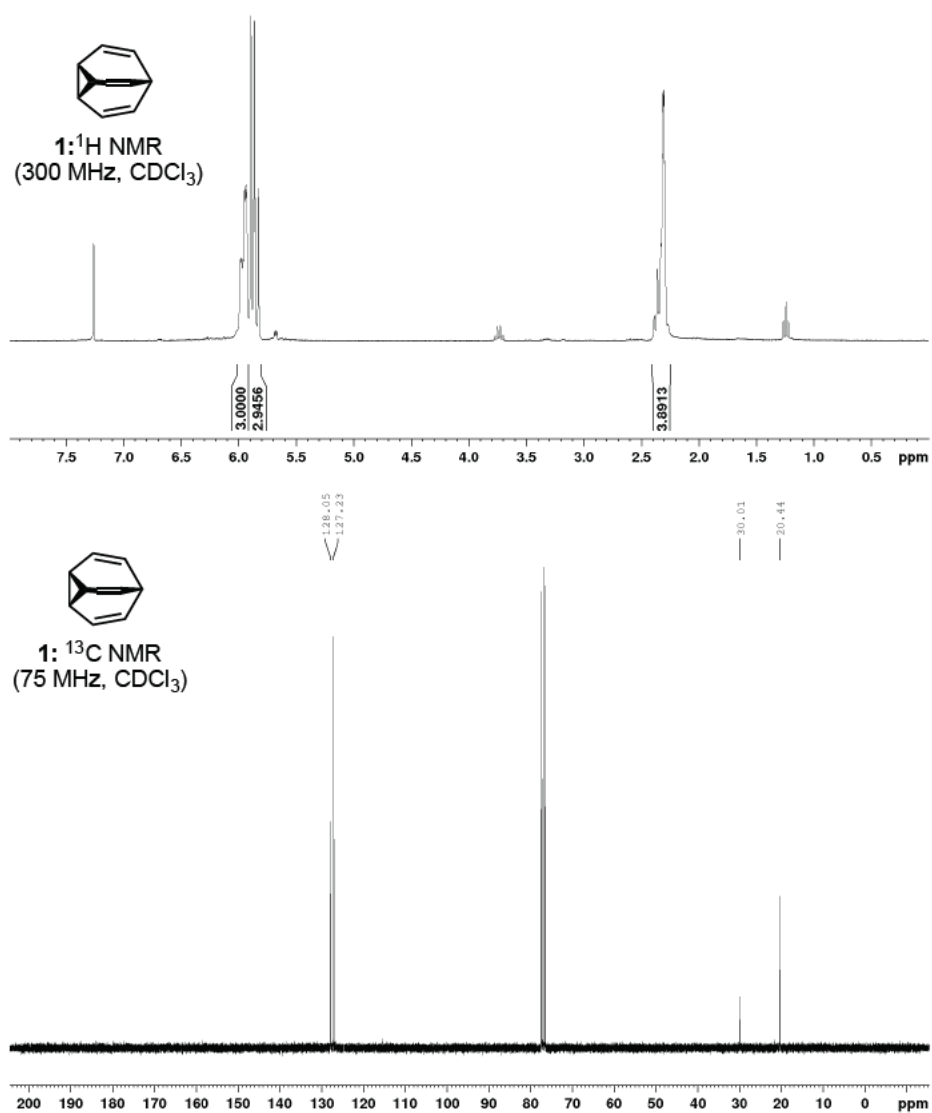
Figure 11: *upper:* ^{1}H NMR of bullvalene (**1**). *lower:* ^{13}C NMR of bullvalene (**1**).

5b: ^{1}H NMR
(500 MHz, CDCl$_3$)

5b: ^{13}C NMR
(125 MHz, CDCl$_3$)
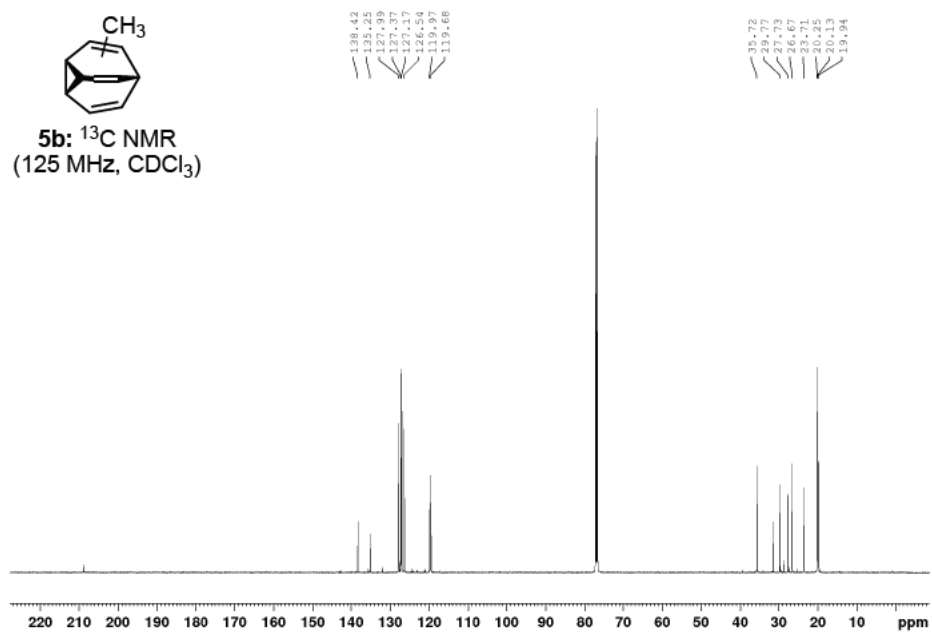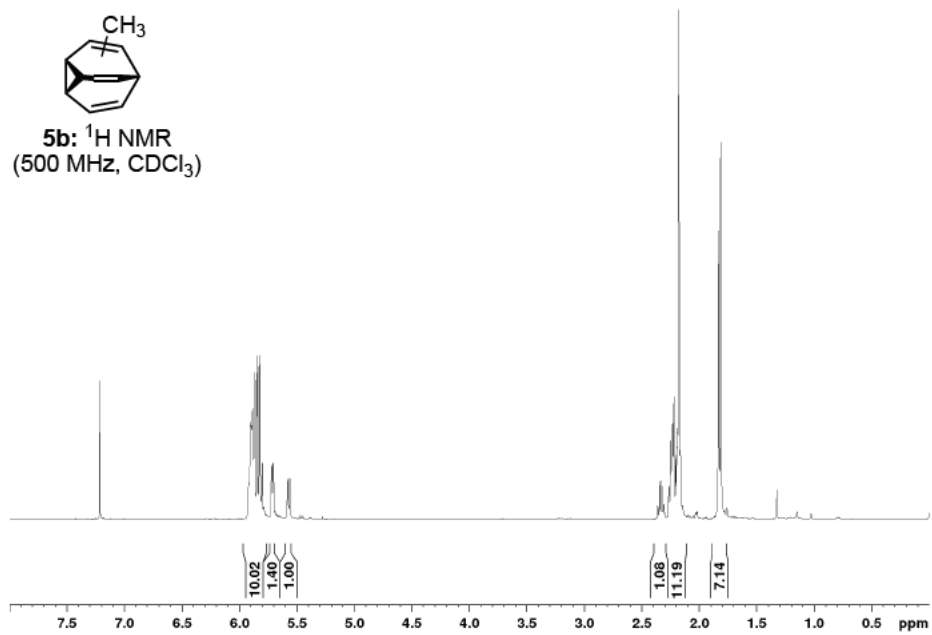
Figure 12: *upper:* ^{1}H NMR of methyl-bullvalene **(5b)**. *lower:* ^{13}C NMR of methyl-bullvalane **(5b)**.

5c: ¹H NMR
(500 MHz, CDCl₃)

n-Hex

5c: ¹³C NMR
(125 MHz, CDCl₃)
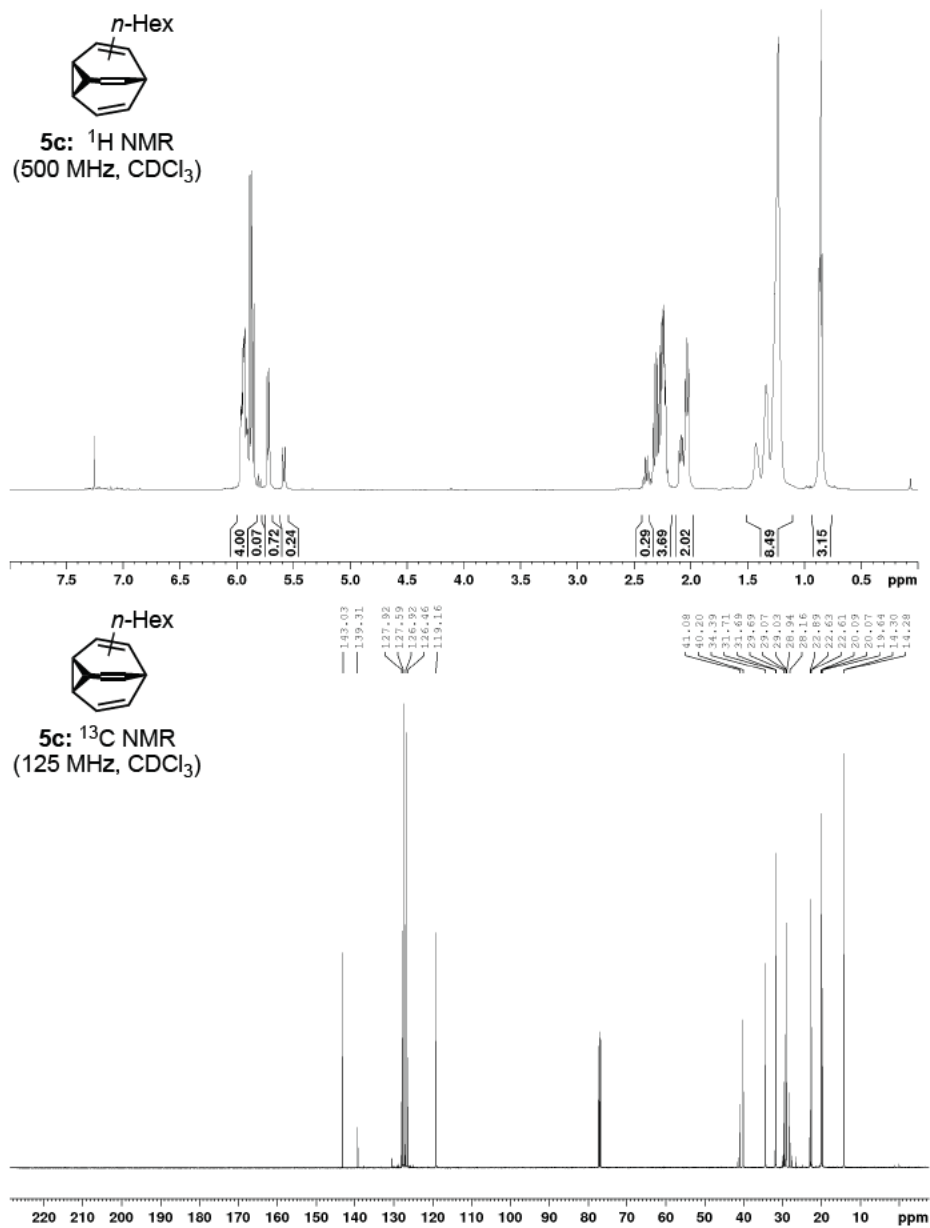
n-Hex

Figure 13: *upper:* ¹H NMR of n-hexyl-bullvalane (**5c**). *lower:* ¹³C NMR of n-hexyl-bullvalane (**5c**).

5d: ^{1}H NMR
(700 MHz, CDCl$_3$)

5d: ^{13}C NMR
(175 MHz, CDCl$_3$)

Figure 14: *upper:* ^{1}H NMR of methylenehydroxy-bullvalene (**5d**). *lower:* ^{13}C NMR of methylenehydroxy-bullvalene (**5d**).

5e: ¹H NMR
(500 MHz, CDCl₃)

5e: ¹³C NMR
(125 MHz, CDCl₃)
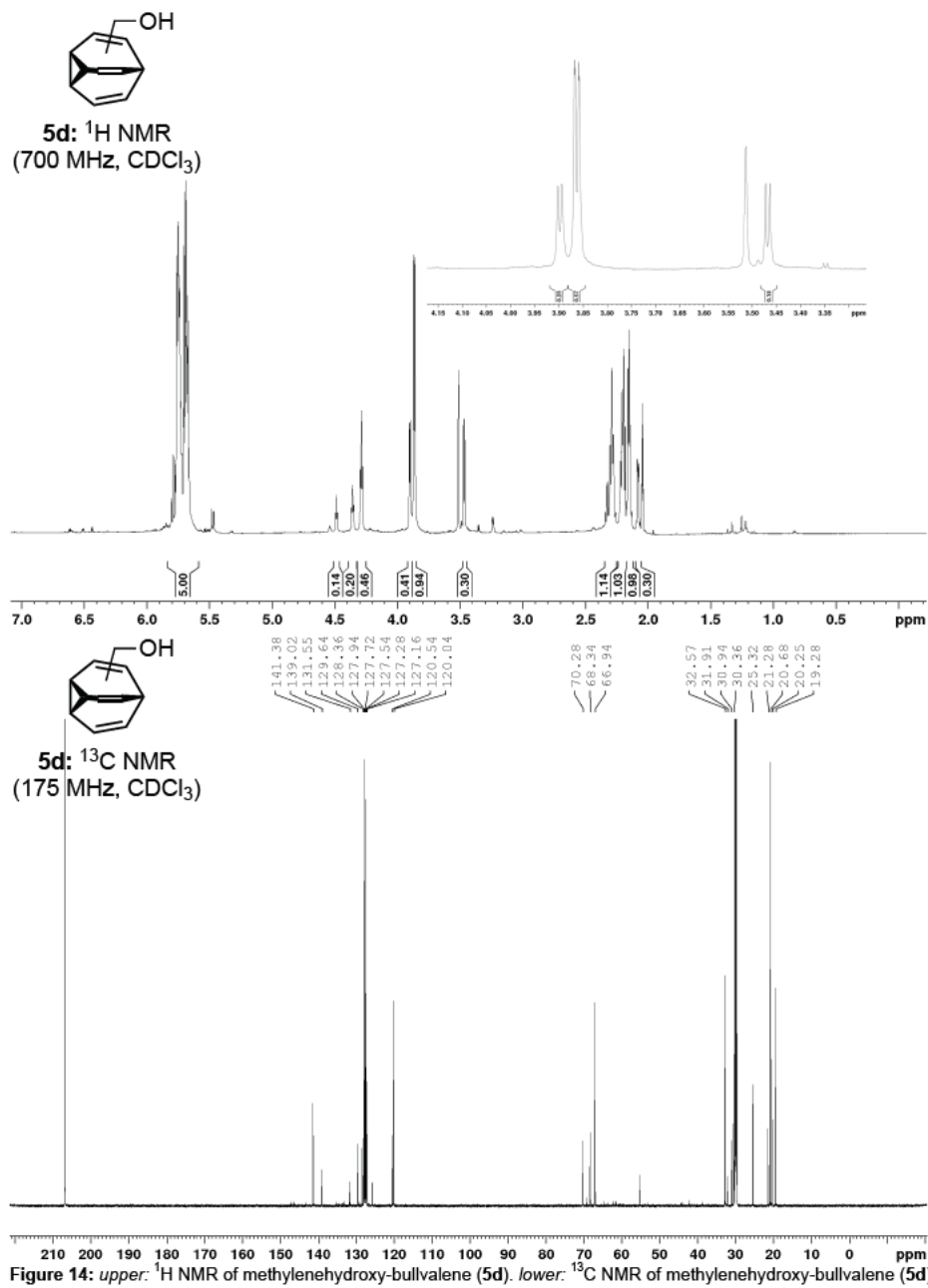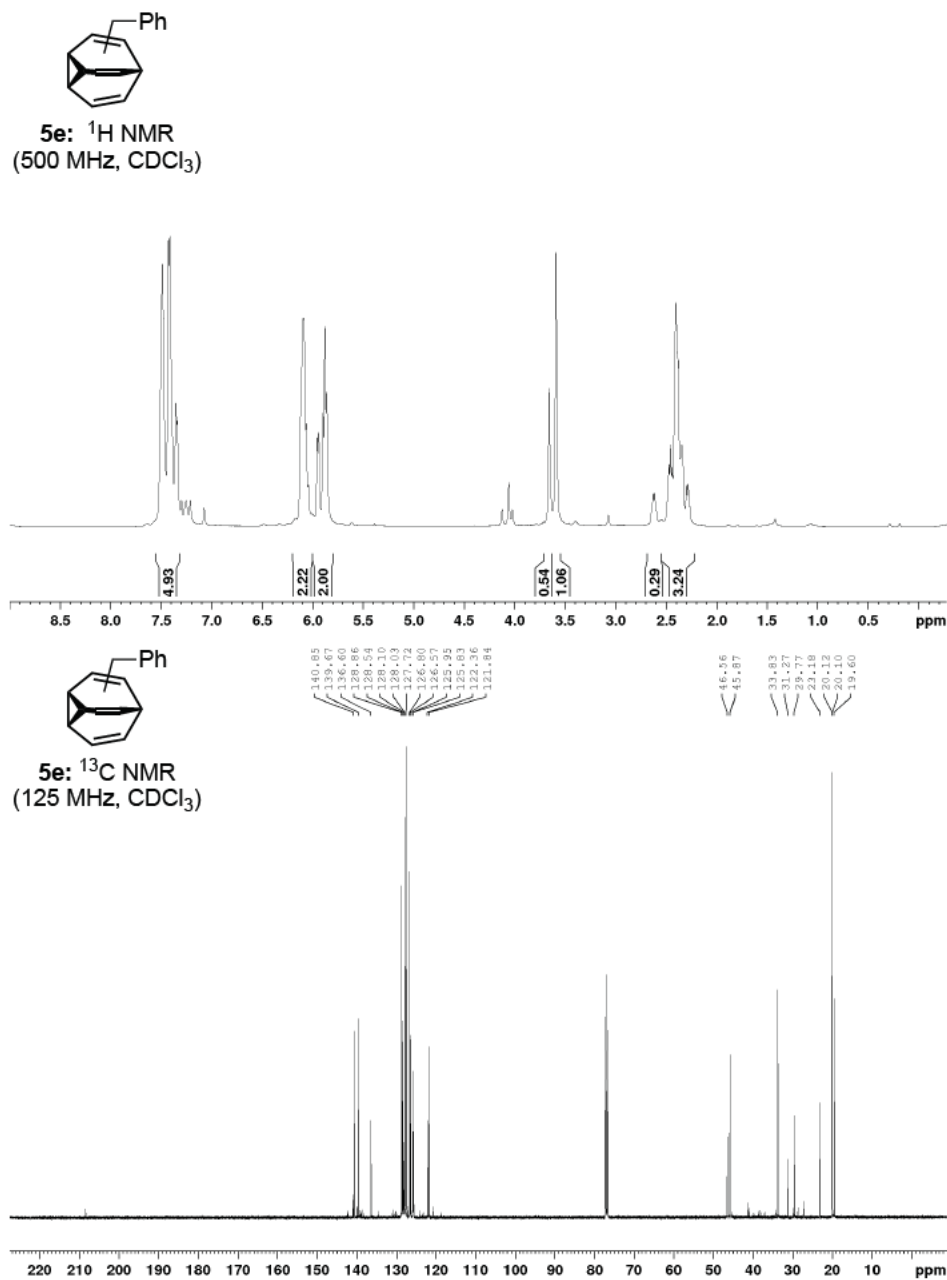
Figure 15: *upper:* ¹H NMR of benzyl-bullvalene (**5e**). *lower:* ¹³C NMR of benzyl-bullvalene (**5e**).

5f: ^{1}H NMR
(500 MHz, CDCl$_3$)

5f: ^{13}C NMR
(125 MHz, CDCl$_3$)
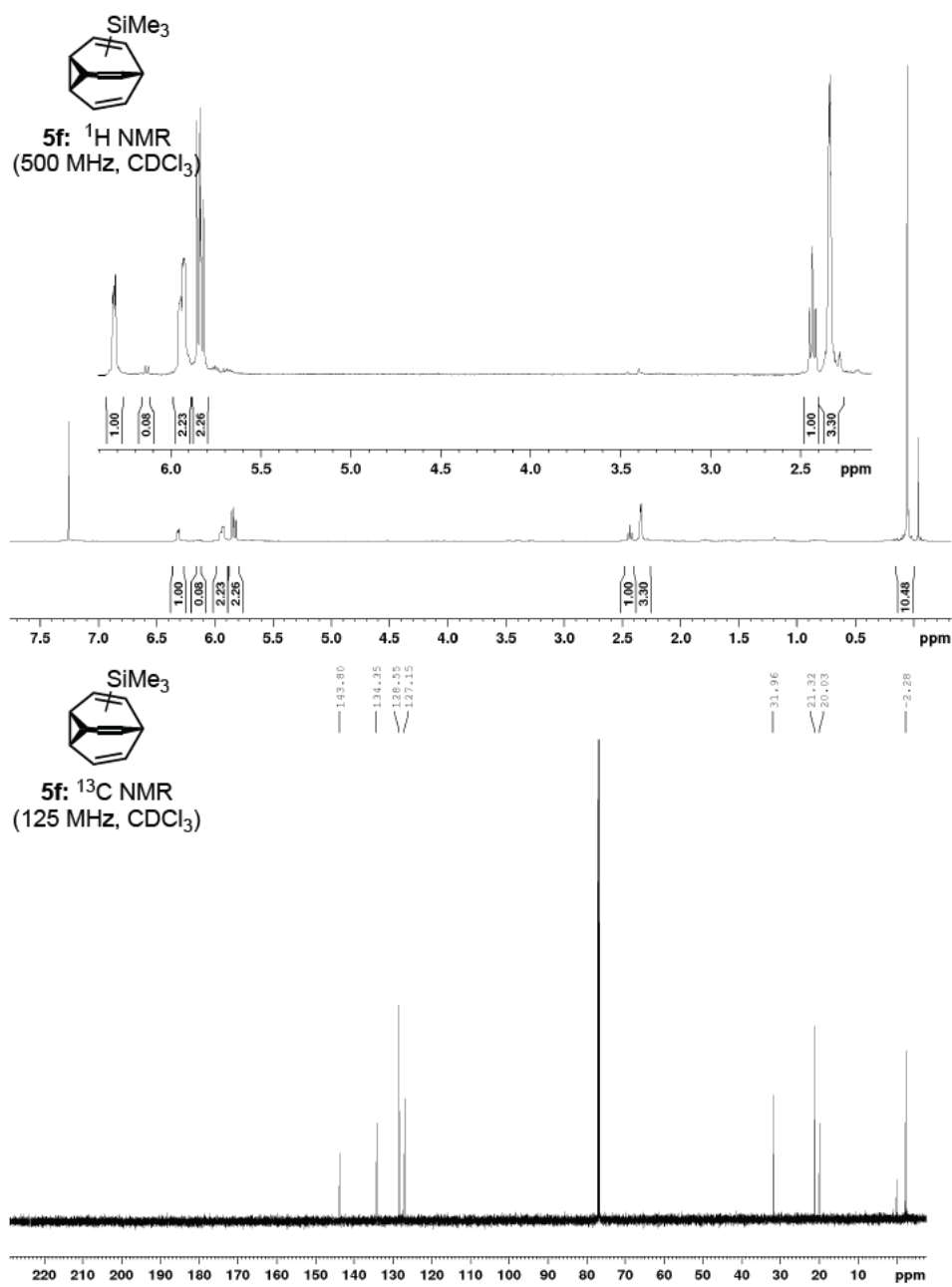
Figure 16: *upper:* ^{1}H NMR of trimethylsilyl-bullvalene (**5f**). *lower:* ^{13}C NMR of trimethylsilyl-bullvalene (**5f**).

5g: ^{1}H NMR
(700 MHz, THF-d_8)
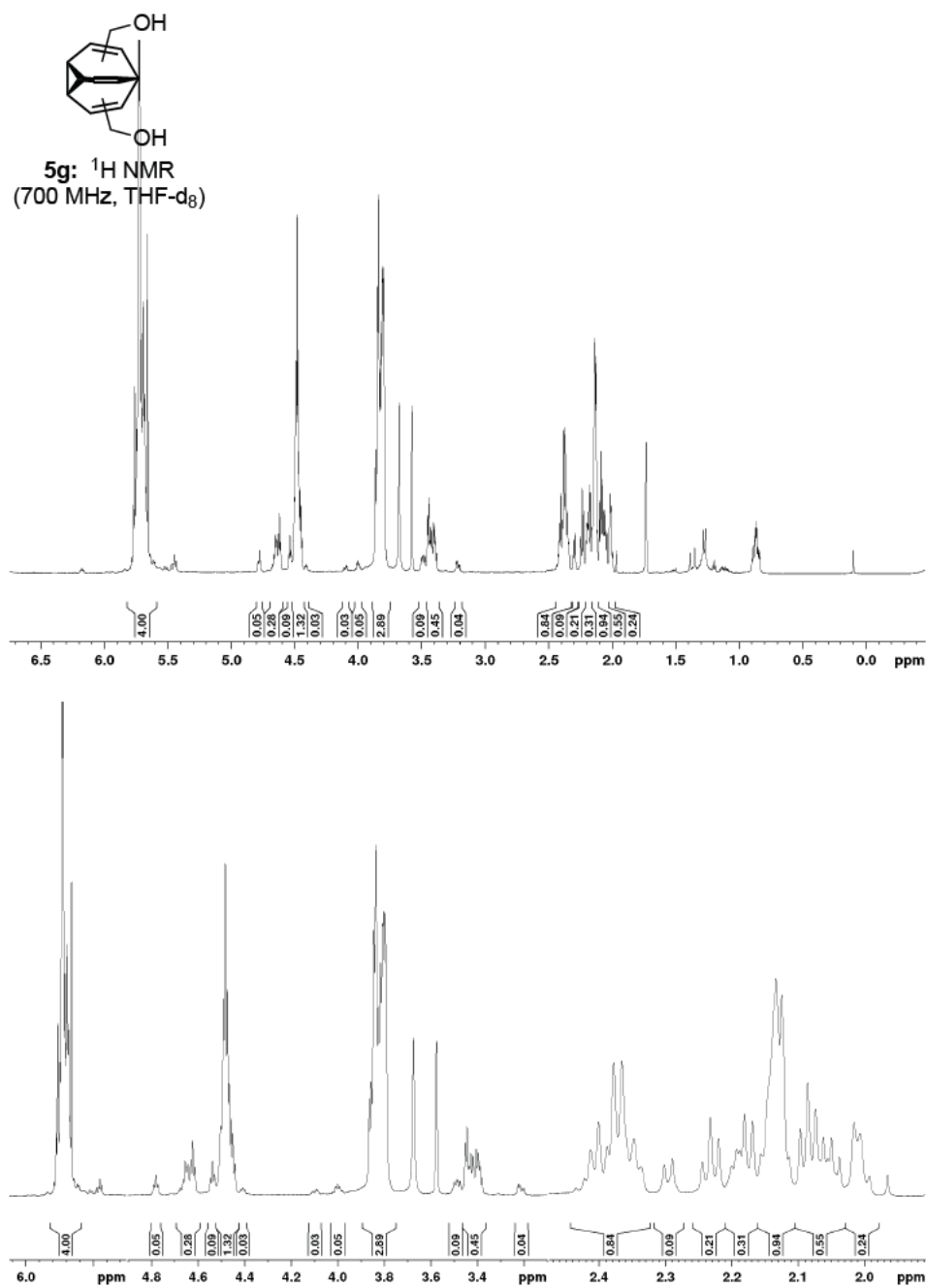
Figure 17. ^{1}H NMR of bis(methylenehydroxy)bullvalene (**5g**).

5g: ^{13}C NMR
(175 MHz, THF-d$_8$)
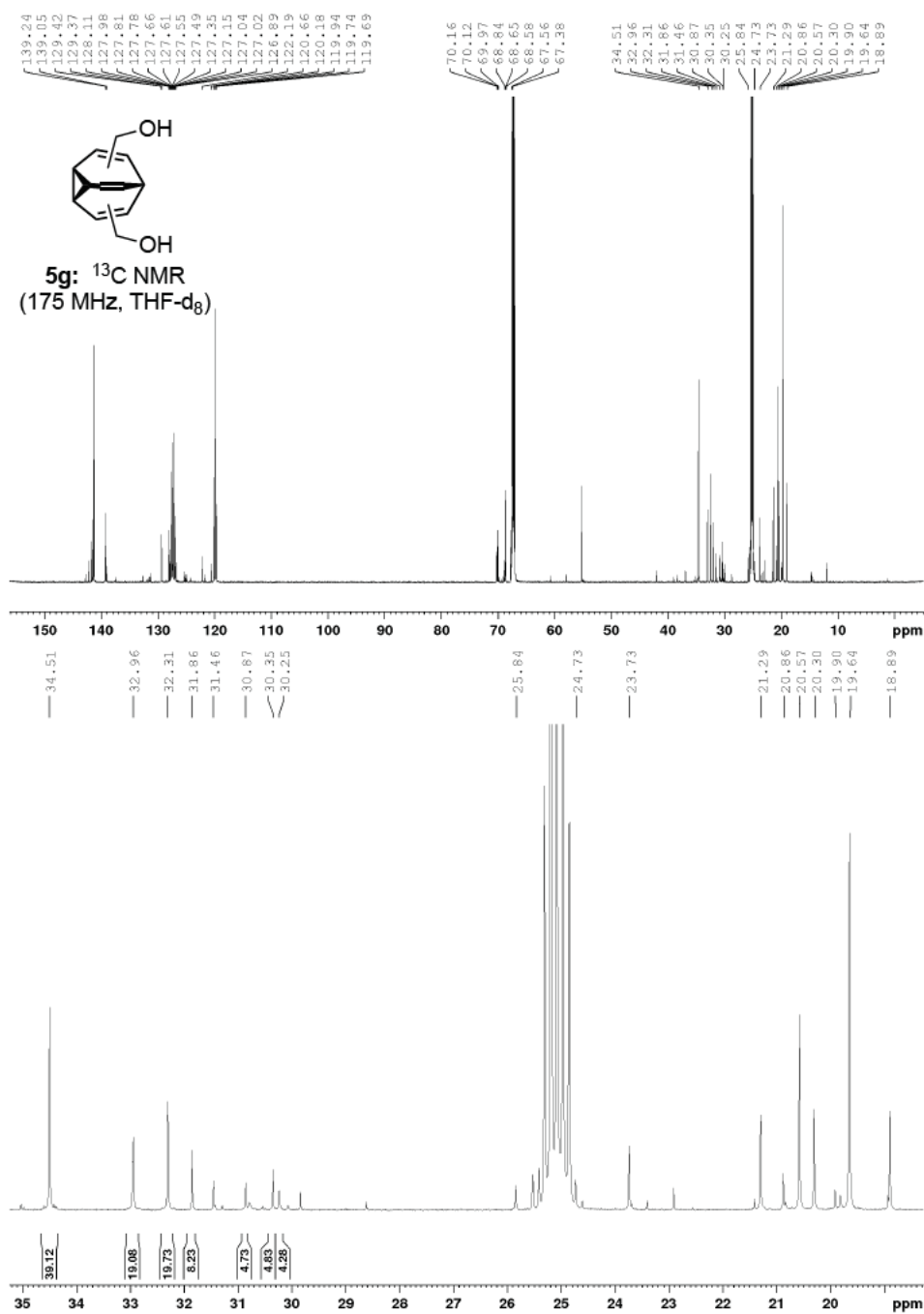
Figure 18. ^{13}C NMR of bis(methylenehydroxy)bullvalene (**5g**).

CH₃

n-Pentyl

5h: ¹H NMR
(700 MHz, acetone-d₆)
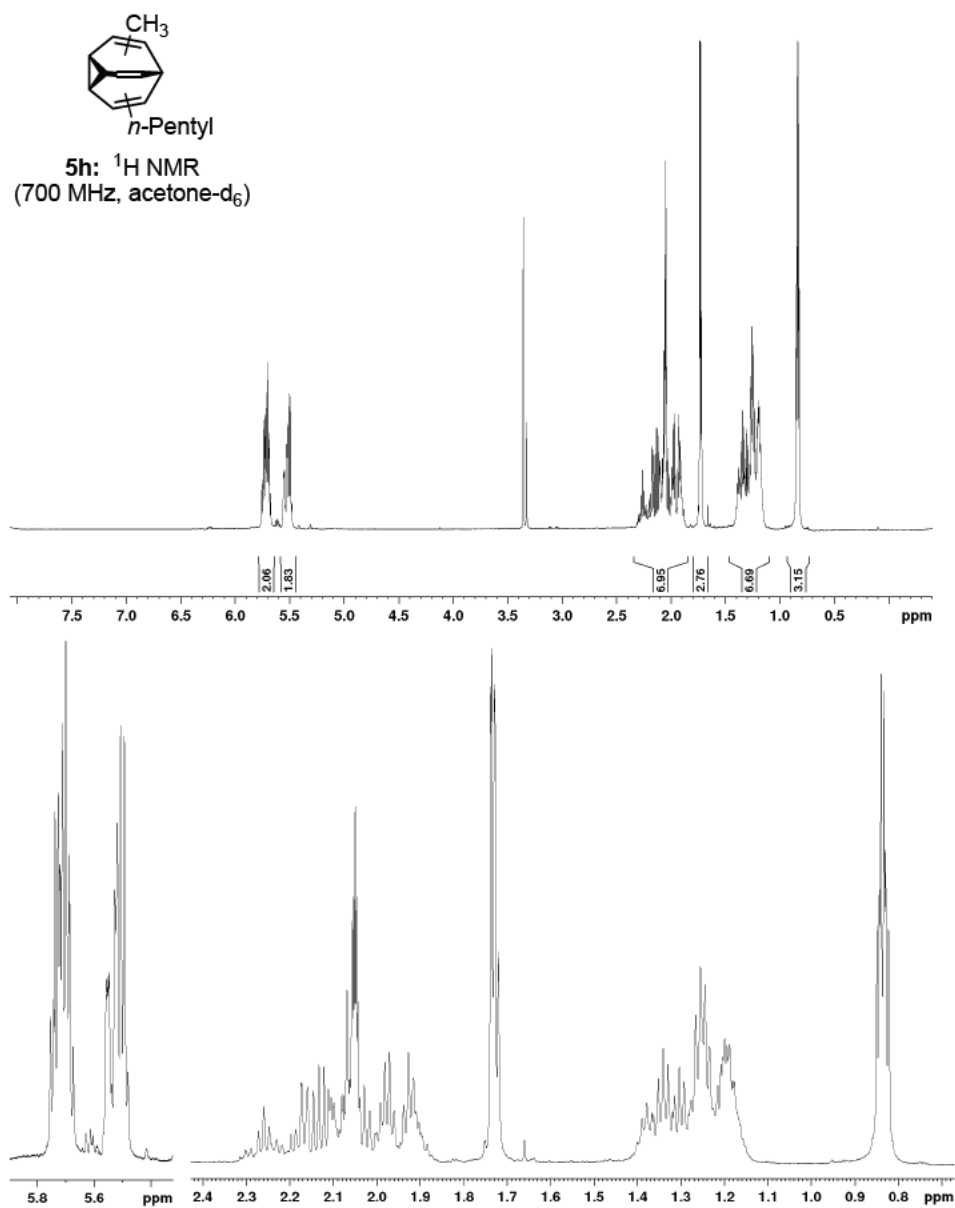
Figure 19. ¹H NMR of methyl(*n*-pentyl)bullvalene (**5h**).
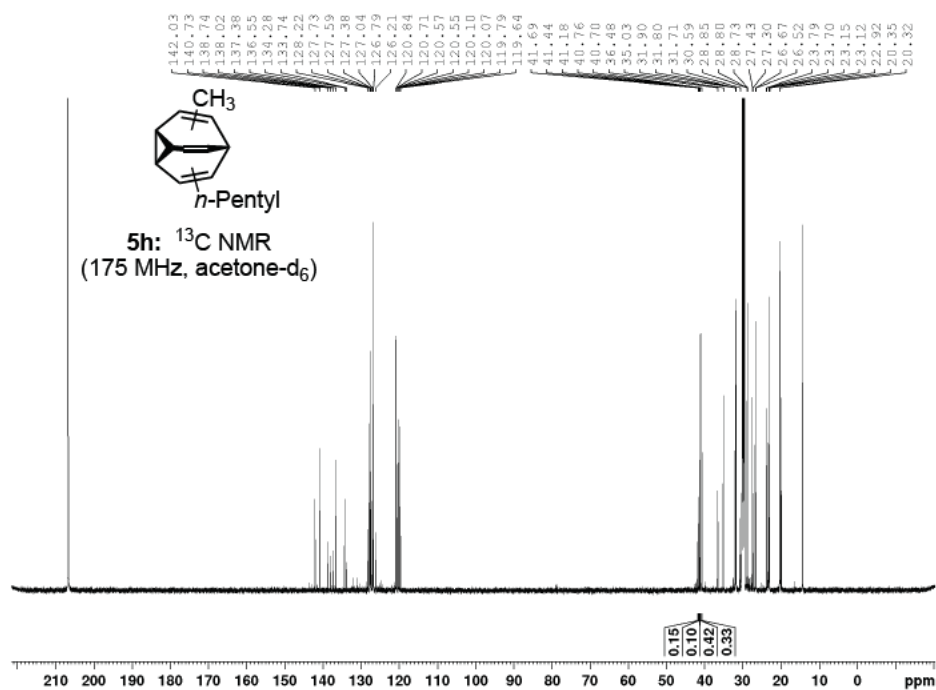
Figure 20: ^{13}C NMR of methyl(*n*-pentyl)bullvalene (**5h**).

142.03
140.73
138.74
138.02
137.38
136.55
134.28
133.74
128.22
127.73
127.59
127.38
127.04
126.79
126.21
120.84
120.71
120.57
120.55
120.10
120.07
119.79
119.64

5h: ^{13}C NMR
(175 MHz, acetone-d_6)

CH$_3$

n-Pentyl

41.69
41.44
41.18
40.76
40.70
36.48
35.03
31.90
31.80
31.71
30.59
28.85
28.80
28.73
27.43
27.30
26.67
26.52
23.79
23.70
23.15
23.12
22.92
20.35
20.32
20.31
20.25
20.23
20.20
19.93
19.86
14.42
14.40

0.15
0.10
0.42
0.33
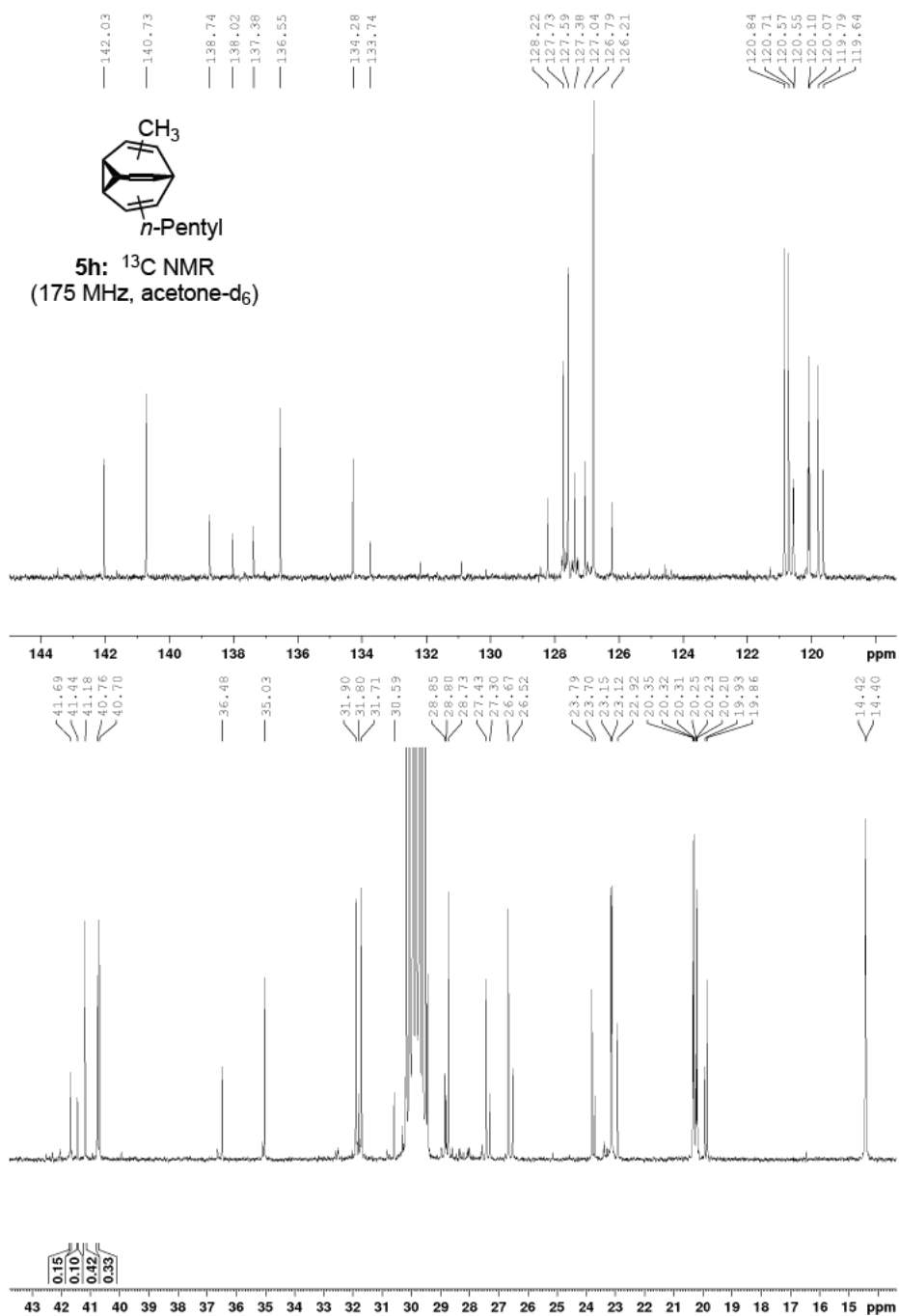
Figure 21: Expansions of he ^{13}C NMR of methyl(*n*-pentyl)bullvalene (**5h**).

Figure 22: *upper:* ^{1}H NMR of phenyl-lumibullvalene (**6**). *lower:* ^{13}C NMR of phenyl-lumibullvalene (**6**).
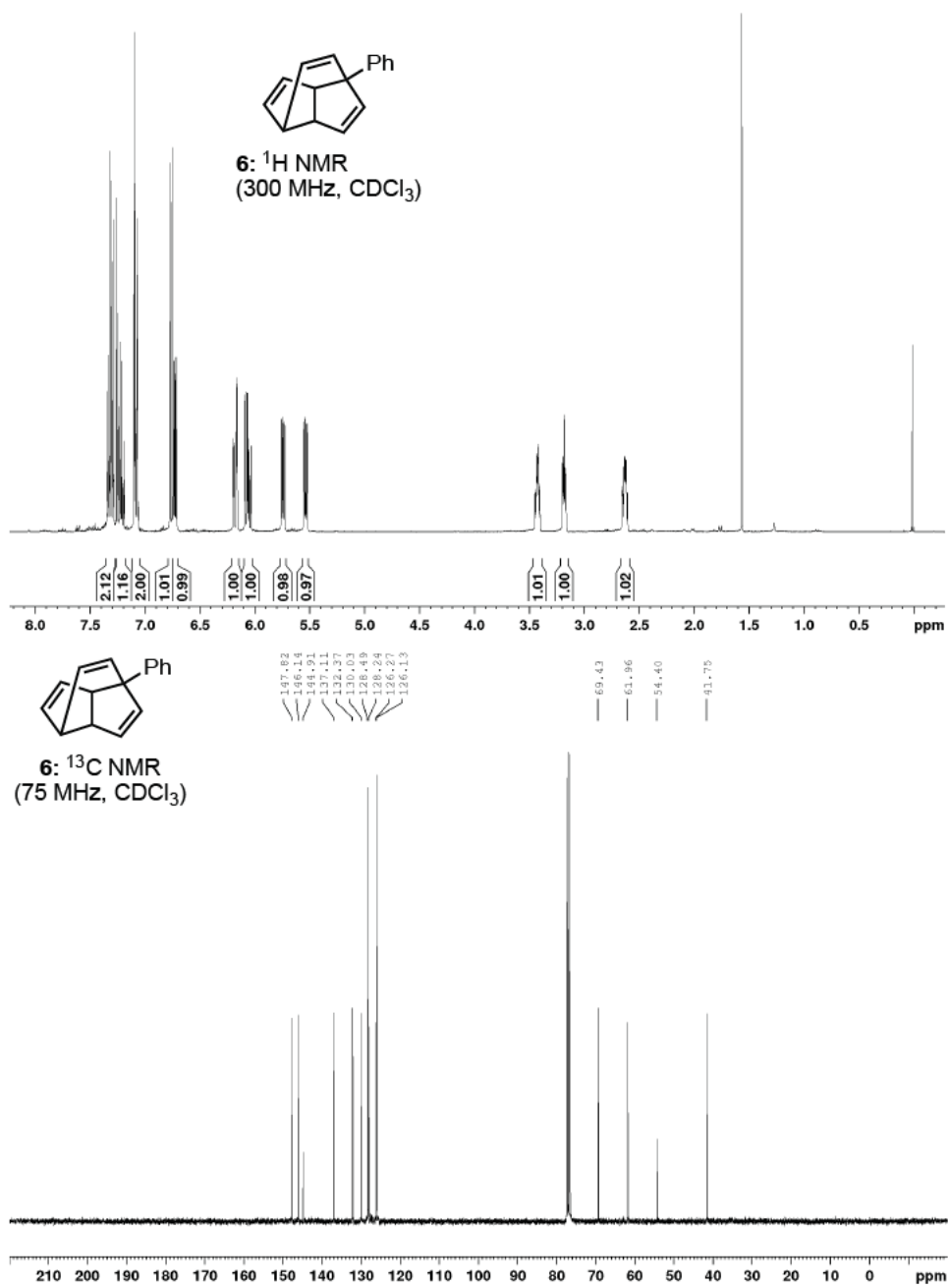
3.1   2D NMR Analysis

3.1.1   Methylenehydroxy-bullvalene 5d

The analysis of methylenehydroxy-bullvalene **5d** was routine. The elucidation of isomers could be concluded using HMBC correlations to the methylene protons.
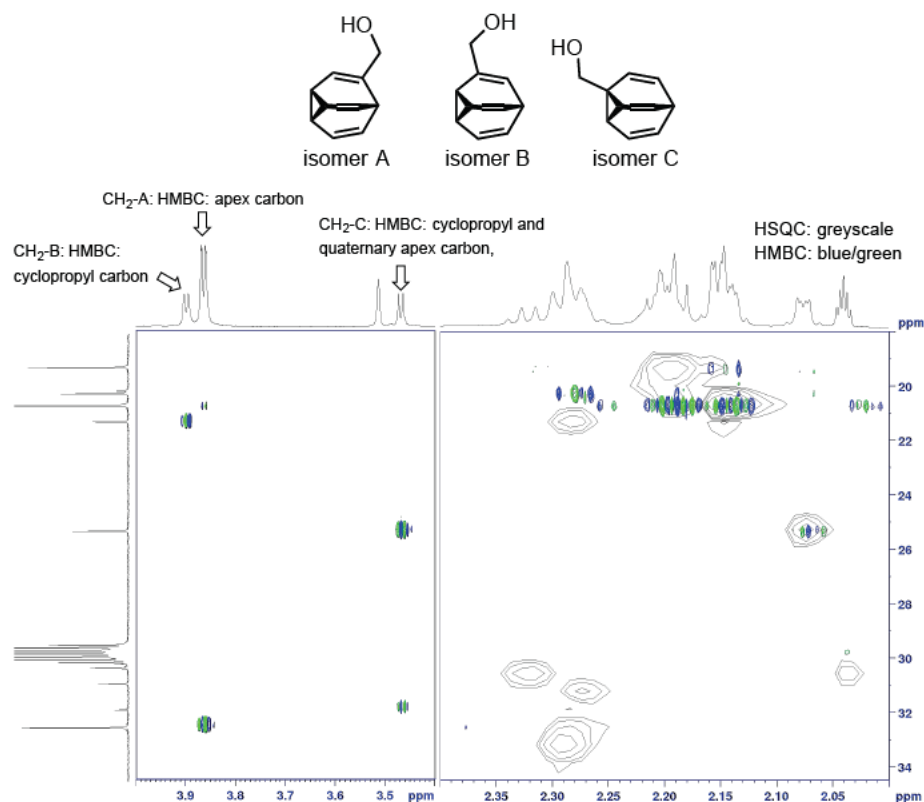
Figure 23. 700 MHz HSQC/HMBC analysis of methylenehydroxy-bullvalene **5c**.

3.1.2   Analysis of bis(methylenehydroxy)bullvalene 5g

For this ensemble the complexity and severe signal overlap made the analysis and structural elucidation challenging. In many cases signals can only be defined categorically. This is particularly true for the alkenic signals that are almost completely overlapping in the proton spectrum, and have very limited resolution in the carbon spectrum. This makes the whole region relatively fruitless for structural elucidation. The methylene signals are important, but also limited in their resolution and utility. In the proton spectrum they can be classed as either connected to an

alkene (3.7 – 3.9 ppm) or to a cyclopropane (3.35 – 3.55 ppm). The aliphatic methyne region of the spectrum (^{1}H; 1.95 – 2.45 ppm, ^{13}C; 18 – 35 ppm) represents the heart of the problem. While there is adequate resolution in the carbon spectrum, the proton spectrum is heavily overlapping. A set of high-resolution HSQC, H2BC, HMBC, and HSQC-TOCSY spectra were recorded. Non-uniform sampling was used to improve resolution in the carbon dimension. Effectively this permits for the isolation of all [1]J, [2]J, [3]J, and [4]J C–H correlations. In particular the HSQC-TOCSY spectrum correlates the apex methyne carbon environments to the cyclopropyl protons. This allows carbon signals to be grouped into their respective isomers with only minimal resolution and clarity in the proton dimension. A very high resolution HSQC experiment (F1 TD: 1024, F2 TD: 4096, no decoupling during acquisition, traditional-planes) allowed for the isolation of high quality proton signals resolved according to their attached carbons. 1D slices from the HSQC allow the proton spectra of individual isomers (in the aliphatic methyne region) to be fully reconstructed. Inspection of multiplicity and patterns of these signals allows for a robust confirmation of the assignments. Abstractions of this analysis are presented in the following Figures.
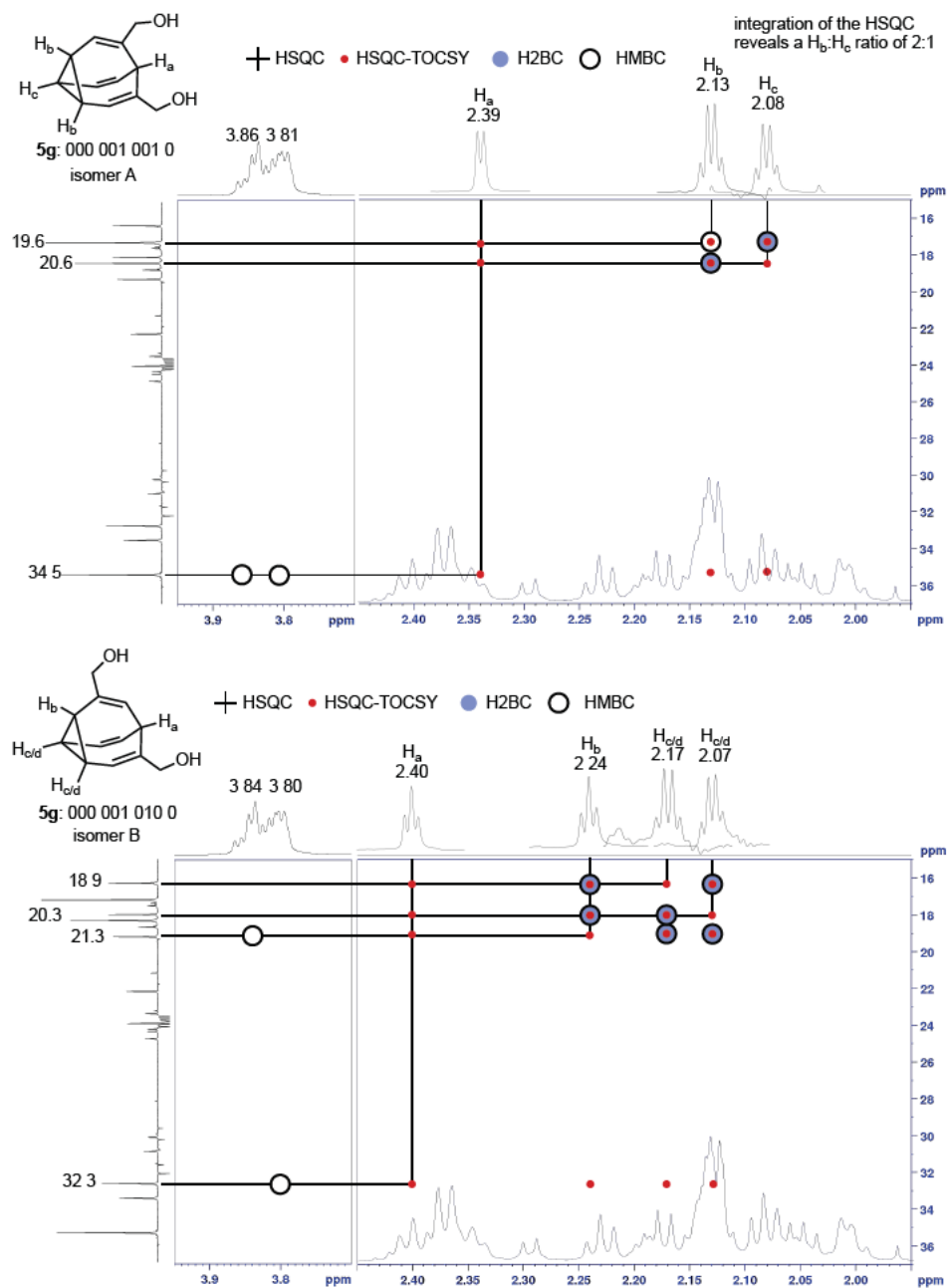
Figure 24. NMR analysis of **5g** isomers A and B.
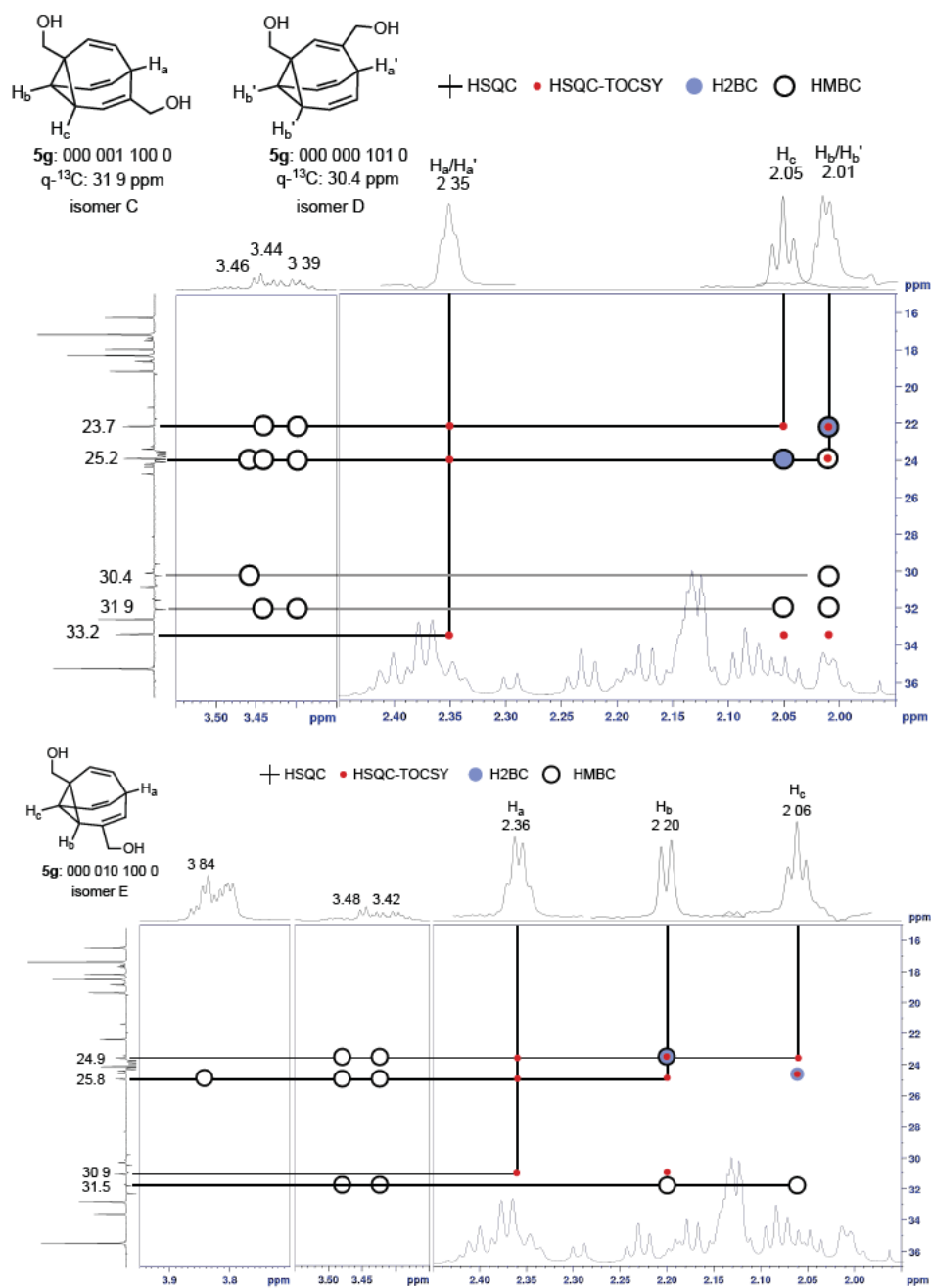
Figure 25. NMR analysis of **5g** isomers C, D and E.
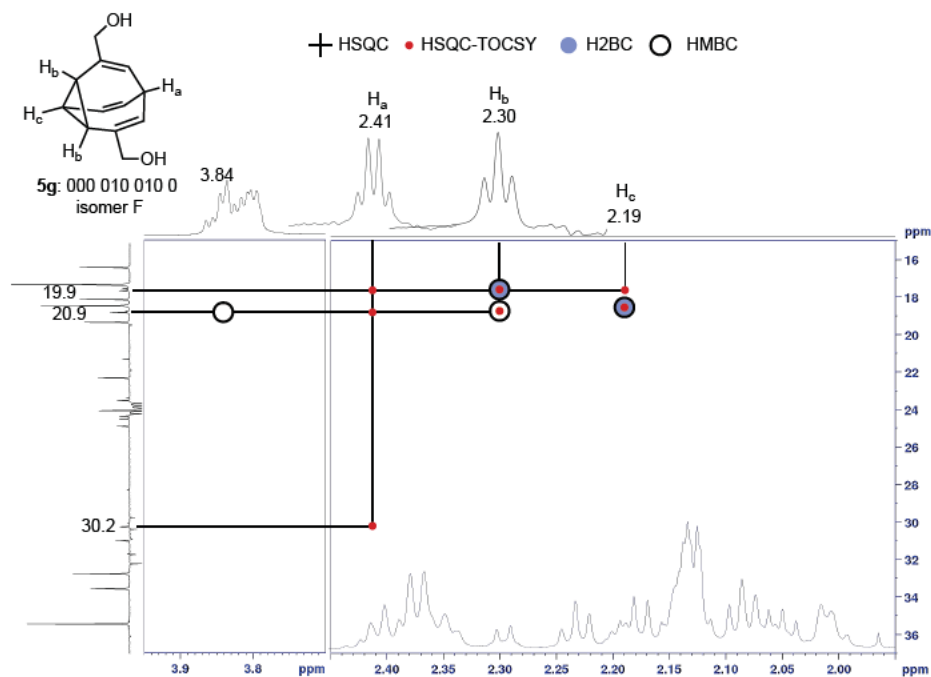
Figure 26. NMR analysis of **5g** isomer F.

3.1.3   Analysis of methyl(*n*-pentyl)bullvalene 5h

The analysis of this ensemble was simplified due to the limited range of populated isomers, and also the fact that both substituents are unique. Analysis of HMBC correlations of both the methyl and methylene environments with respect to the apex position carbon signals revealed the structures of the isomers present.
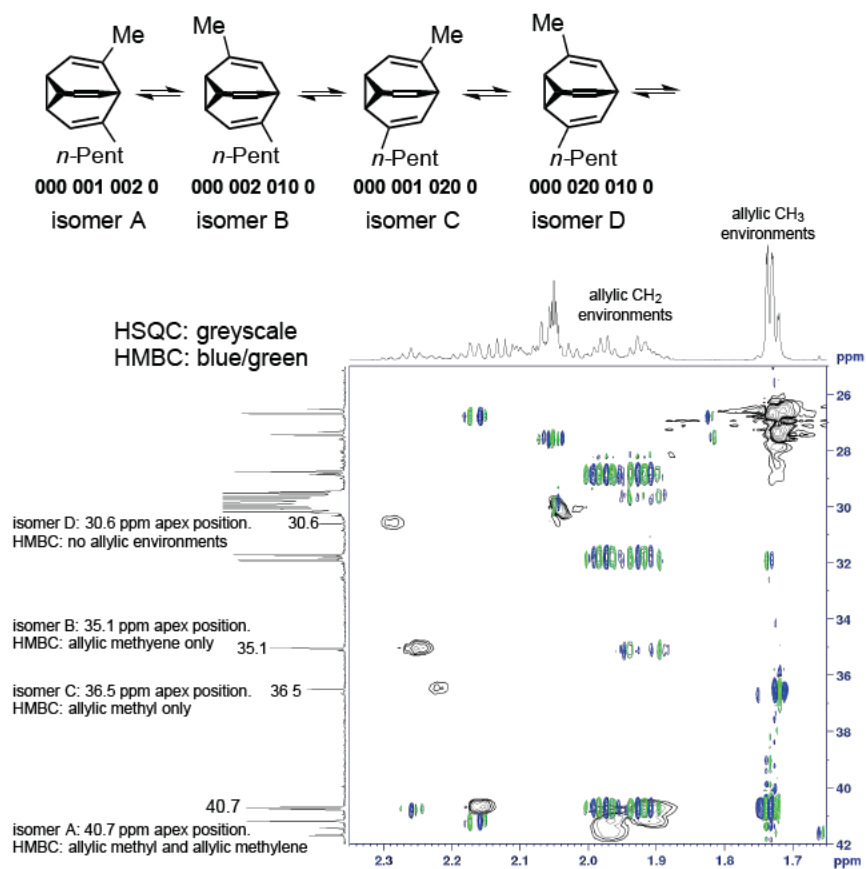
Figure 27. NMR analysis of methyl(*n*-pentyl)bullvalene **5h.**

4   Computational Section

4.1   Network Analysis Algorithm and Methodology
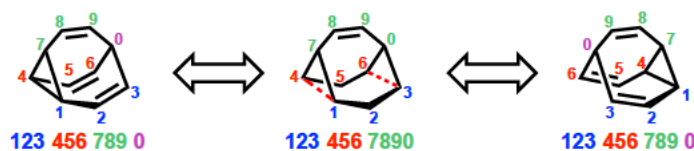
Figure 28. Numerical codes representing he positions on the bullvalene isomers and TS.

Symmetries of the substituted bullvalenes are reflected in their corresponding numerical codes (Figure 28). For the isomers with the C_{3v} symmetry, swapping two of the three initial 3-digit sequences represents reflection through one of the mirror planes and relates two enantiomers. Two such swaps produce a code equivalent to the initial one. Hence, each isomer can be represented by three different but completely equivalent codes. We always choose the code with the lowest number sequence. For transition states with the C_{2v} symmetry, the reflections through the two mirror planes are represented by either a swap of the two 3-digit sequences or a reversal of all three sequences (two 3-digit and one 4-digit).

Using these considerations, we produced a simple Fortran program CodeGen (provided as a separate SI file), that given the initial substitution string generates a list of codes of all possible isomers and transition states, identifies their chirality and connects them by Cope rearrangement paths. Subsequently, this list is sorted and possible duplicates (due to equivalent isomers) are removed. To illustrate the growing complexity of the rearrangement networks, Table 1 lists numbers of isomer/TS structures for different numbers of unique and equivalent substituents.

In the next step, generated lists of isomer and TS codes are transformed into corresponding starting geometries. This is achieved by connecting Z-matrices representing the preoptimized geometries of the unsubstituted bullvalene and the desired substituents. On the carbon represented by a certain position in the code, bond to a hydrogen atom is simply replaced by the bond to the connecting substituent atom.

Several possible orientations of the substituent as well as internal rotations within the substituent are considered. Hence, for each isomer/TS, a number of initial rotamer structures are generated. In this work, we used the interface to the program package ORCA 4.0[1] to quickly optimize the rotamers using the inexpensive semiempirical PM3 method[2] with the constraint of the bullvalene carbon cage and all bond lengths held fixed. Ten lowest energy rotamers were further reoptimized

[1] F. Neese, *WIREs Comput. Mol. Sci.* **2012**, *2*, 73
[2] J. J. P. Stewart, *J. Comp. Chem.* **1989**, *10*, 209

keeping the same constraints using DFT with the dispersion corrected functional PBE-D3BJ[3] and the 6-31G basis set.[4] Finally, only one rotamer with the lowest energy for each isomer/TS was kept and used as a starting geometry for the full optimization.

Table 1. Number of bullvalene isomers and TS depending on the nuber of unique/equivalent substituents. All degenrate enantiomers are included in the number of chiral structures, however, only the non-degenrate ones are being calculated.

number of substituents	number of isomers			number of TS		
	chiral	achiral	total	chiral	achiral	total
unique substituents						
0	0	1	1	0	1	1
1	0	4	4	2	3	5
2	18	12	30	38	7	45
3	216	24	240	348	12	360
4	1656	24	1680	2508	12	2520
5	10080	0	10080	15120	0	15120
6	50400	0	50400	75600	0	75600
7	201600	0	201600	302400	0	302400
8	604800	0	604800	907200	0	907200
9	1209600	0	1209600	1814400	0	1814400
10	1209600	0	1209600	1814400	0	1814400
equivalent substituents						
0	0	1	1	0	1	1
1	0	4	4	2	3	5
2	6	9	15	18	7	25
3	26	16	42	48	12	60
4	50	22	72	94	16	110
5	60	24	84	108	18	126
6	50	22	72	94	16	110
7	26	16	42	48	12	60
8	6	9	15	18	7	25
9	0	4	4	2	3	5
10	0	1	1	0	1	1

All isomer/TS geometries were then fully optimized using the hybrid dispersion corrected B3LYP-D3BJ[5] functional and the Def2-SVP basis set.[6] Finally, the single point energies were calculated with the same functional and the Def2-TZVPPd basis set,[7] with and without the use of the implicit continuous solvation model CPCM.[8]

The overall workflow is pictorially summarized in the flowchart on Figure 29.

[3] a) J. P. Perdew, K. Burke, and M. Ernzerhof, *Phys. Rev. Lett.* **1996**, *77*, 3865; *Phys. Rev. Lett.* **1997**, *78*, E1396, b) S. Grimme, S. Ehrlich, L. Goerigk, *J. Comp. Chem.* **2011**, *32*, 1456

[4] W. J. Hehre, R. Ditchfield, J. A. Pople, *J. Chem. Phys.* **1971**, *54*, 724; *J. Chem. Phys.* **1972**, *56*, 2257; M. M. Francl, W. J. Pietro, W. J. Hehre, J. S. Binkley, D. J. DeFrees, J. A. Pople, M. S. Gordon, *J. Chem. Phys.* **1982**, *77*, 3654

[5] A. D. Becke, *J. Chem. Phys.* **1993**, *98*, 5648; C. Lee, W. Yang, R. G. Parr, *Phys. Rev. B* **1998**, *37*, 785

[6] F. Weigend, R. Ahlrichs, *Phys. Chem. Chem. Phys.* **2005**, *7*, 3297

[7] D. Rappoport, F. Furche, *J. Chem. Phys.* **2010**, *133*, 134105

[8] V. Barone, M. Cossi, *J. Phys. Chem. A* **1998**, *102*, 1995; M. Cossi, N. Rega, G. Scalmani, V. Barone, *J. Comp. Chem.* **2003**, *24*, 669
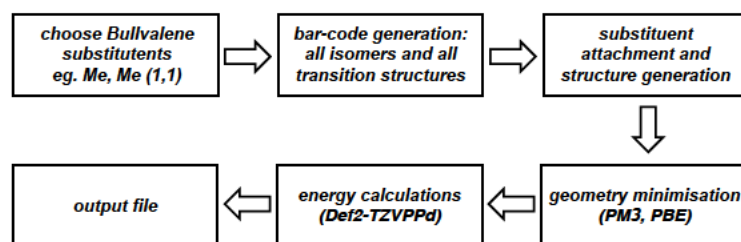
Figure 29. Simplified workflow

4.2 Isomer Stability Results

Table 2. Computational and experimental relative energies and ratios for monosubstituted bullvalenes at –60°C.

species	calculation						experiment	
	gas phase		CPCM acetone		CPCM chloroform			
	rel. energy	ratio	rel. energy	ratio	rel. energy	ratio	rel. energy	ratio
methyl-bullvalene, 5b							chloroform	
isomers 000 000 000 1	7.45	1%	7.35	1%	7.36	1%	> 8.4	0%
000 000 001 0	0.00	69%	0.00	68%	0.00	69%	0.0	58%
000 000 010 0	1.58	28%	1.54	29%	1.56	28%	0.6	42%
000 000 100 0	6.22	2%	6.27	2%	6.26	2%	> 8.4	0%
TS 000 000 0001	55.67		55.07		55.17			
000 000 0010	49.30		48.41		48.58			
000 001 0000 *	55.94		54.76		55.00			
000 010 0000	59.57		59.18		59.26			
n-hexyl-bullvalene, 5c							chloroform	
isomers 000 000 000 1	13.97	0%	11.17	0%	11.68	0%	> 8.7	0%
000 000 001 0	0.00	90%	0.00	71%	0.00	76%	0.0	68%
000 000 010 0	4.12	9%	1.90	24%	2.32	21%	1.8	25%
000 000 100 0	7.43	1%	5.00	4%	5.44	4%	4.0	7%
TS 000 000 0001	59.65		56.48		57.06			
000 000 0010	51.68		48.60		49.17			
000 001 0000 *	56.43		53.86		54.34			
000 010 0000	57.47		57.11		57.20			
methylenehydroxy-bullvalene, 5d							acetone	
isomers 000 000 000 1	8.77	1%	8.08	1%	7.94	1%	> 8.4	0%
000 000 001 0	1.96	24%	0.00	54%	0.12	47%	0.0	57%
000 000 010 0	0.00	73%	0.41	43%	0.00	50%	1.5	25%
000 000 100 0	6.50	2%	4.97	3%	4.94	3%	2.0	18%
TS 000 000 0001	54.99		54.07		53.98			
000 000 0010	47.91		47.73		47.43			
000 001 0000 *	55.20		54.05		54.04			
000 010 0000	60.42		59.87		59.69			
benzyl-bullvalene, 5e							chloroform	
isomers 000 000 000 1	17.67	0%	13.73	0%	14.53	0%	> 8.9	0%
000 000 001 0	0.00	78%	0.00	75%	0.00	75%	0.0	76%
000 000 010 0	2.23	22%	1.97	25%	2.01	24%	2.0	24%
000 000 100 0	9.68	0%	8.16	1%	8.47	1%	> 8.9	0%
TS 000 000 0001	63.47		59.40		60.22			
000 000 0010	49.89		49.03		49.17			
000 001 0000 *	57.90		55.97		56.34			
000 010 0000	60.33		58.44		58.84			
trimethylsilyl-bullvalene, 5f							chloroform	
isomers 000 000 000 1	23.86	0%	23.01	0%	23.17	0%	> 9.3	0%
000 000 001 0	0.00	94%	0.00	95%	0.00	95%	0.0	93%
000 000 010 0	5.12	5%	5.29	5%	5.26	5%	4.6	7%
000 000 100 0	9.29	1%	8.90	1%	8.96	1%	> 9.3	0%
TS 000 000 0001	71.44		70.19		70.42			
000 000 0010	52.75		51.97		52.12			
000 001 0000 *	51.80		51.29		51.38			
000 010 0000	59.86		59.81		59.83			

Table 3. Computational and experimental relative energies and ratios for bis(methylenehydroxy)bullvalene **5g**.

species	calculation										experiment			
	gas phase		CPCM acetone (−60°C)		CPCM chloroform (−60°C)		CPCM methanol (−60°C)		CPCM THF (−80°C)		methanol (−60°C)		THF (−80°C)	
	rel. energy	ratio	rel. energy	ratio	rel. energy	ratio	rel. energy	ratio	rel. energy	ratio	rel. energy	ratio	rel. energy	ratio
isomers														
000 000 001 1	12.99	0%	12.20	0%	12.46	0%	12.16	0%	12.36	0%	>7.7	0%	>7.2	0%
000 000 010 1	18.91	0%	14.10	0%	14.93	0%	14.00	0%	14.57	0%	>7.7	0%	>7.2	0%
000 000 011 0	23.77	0%	19.59	0%	20.46	0%	19.49	0%	20.10	0%	>7.7	0%	>7.2	0%
000 000 100 1	23.15	0%	16.35	0%	17.66	0%	16.20	0%	17.12	0%	>7.7	0%	>7.2	0%
000 000 101 0	11.17	0%	5.95	3%	6.93	2%	5.83	3%	6.52	2%	2.4	10%	2.6	9%
000 000 110 0	12.20	0%	9.77	0%	10.26	0%	9.72	0%	10.06	0%	>7.7	0%	>7.2	0%
000 001 001 0	0.00	98%	0.00	85%	0.00	90%	0.00	85%	0.00	91%	0.0	38%	0.0	44%
000 001 010 0 *	7.37	2%	3.83	10%	4.40	7%	3.76	10%	4.16	7%	0.7	25%	1.0	23%
000 001 100 0 *	13.98	0%	8.47	1%	9.44	0%	8.36	1%	9.03	0%	1.9	13%	1.8	14%
000 010 010 0	17.48	0%	9.80	0%	11.25	0%	9.63	0%	10.64	0%	3.0	7%	3.5	5%
000 010 100 0 *	13.33	0%	12.49	0%	12.66	0%	12.47	0%	12.59	0%	3.0	7%	3.3	6%
000 100 100 0	15.35	0%	11.69	0%	12.47	0%	11.59	0%	12.15	0%	>7.7	0%	>7.2	0%
TS														
000 000 0011	65.99		62.93		63.56		62.85		63.30					
000 000 0101	62.68		57.88		58.72		57.79		58.37					
000 000 0110	74.71		69.74		70.76		69.62		70.34					
000 000 1001	70.73		64.60		65.80		64.45		65.30					
000 001 0001 *	63.25		60.78		61.32		60.71		61.10					
000 001 0010 *	64.83		59.27		60.33		59.14		59.89					
000 001 0100 *	60.26		55.22		56.06		55.12		55.70					
000 001 1000 *	70.35		64.27		65.48		64.13		64.98					
000 010 0001 *	75.80		70.36		71.38		70.24		70.95					
000 010 0010 *	68.60		64.11		64.89		64.02		64.56					
000 011 0000 *	70.58		69.06		69.48		69.01		69.31					
000 101 0000 *	67.79		61.56		62.72		61.43		62.24					
001 001 0000	62.85		59.54		60.27		59.45		59.97					
001 010 0000 *	71.78		70.03		70.51		69.96		70.32					
001 100 0000 *	70.94		64.29		65.66		64.12		65.09					
010 010 0000	68.61		69.58		69.46		69.59		69.51					

Table 4. Computational and experimental relative energies and ratios for methyl(n-pentyl)bullvalene **5h** at –60°C.

species	calculation						experiment	
	gas phase		CPCM acetone		CPCM chloroform		acetone	
	rel. energy	ratio	rel. energy	ratio	rel. energy	ratio	rel. energy	ratio
isomers								
000 000 001 2	29.49	0%	27.32	0%	27.72	0%	> 7.9	0%
000 000 002 1	26.16	0%	24.79	0%	25.02	0%	> 7.9	0%
000 000 010 2	19.02	0%	17.09	0%	17.45	0%	> 7.9	0%
000 000 012 0	16.14	0%	15.91	0%	15.95	0%	> 7.9	0%
000 000 020 1	12.23	0%	12.85	0%	12.73	0%	> 7.9	0%
000 000 021 0	16.72	0%	16.63	0%	16.65	0%	> 7.9	0%
000 000 100 2	23.30	0%	21.59	0%	21.88	0%	> 7.9	0%
000 000 102 0	11.10	0%	9.81	0%	10.03	0%	> 7.9	0%
000 000 120 0	26.10	0%	24.89	0%	25.11	0%	> 7.9	0%
000 000 200 1	18.10	0%	16.45	0%	16.73	0%	> 7.9	0%
000 000 201 0	10.72	0%	9.18	0%	9.46	0%	> 7.9	0%
000 000 210 0	26.88	0%	24.83	0%	25.21	0%	> 7.9	0%
000 001 002 0 *	0.00	78%	0.00	79%	0.00	79%	0.0	42%
000 001 020 0 *	4.40	7%	4.63	6%	4.59	6%	1.6	17%
000 001 200 0 *	10.73	0%	9.23	0%	9.50	0%	> 7.9	0%
000 002 010 0 *	3.39	12%	3.51	11%	3.49	11%	0.6	30%
000 002 100 0 *	11.05	0%	9.72	0%	9.95	0%	> 7.9	0%
000 010 020 0 *	6.15	2%	6.05	3%	6.10	3%	2.4	11%
000 010 200 0 *	11.05	0%	10.33	0%	10.47	0%	> 7.9	0%
000 020 100 0 *	12.96	0%	11.71	0%	11.94	0%	> 7.9	0%
000 100 200 0 *	28.50	0%	26.71	0%	27.03	0%	> 7.9	0%
TS								
000 000 0012	80.65		78.19		78.64			
000 000 0021	75.84		73.87		74.22			
000 000 0102	62.25		59.83		60.28			
000 000 0120	62.41		61.55		61.69			
000 000 0201	57.75		57.15		57.25			
000 000 1002	67.80		65.69		66.05			
000 001 0002 *	79.54		76.69		77.23			
000 001 0020 *	57.56		56.57		56.78			
000 001 0200 *	60.18		57.59		58.08			
000 001 2000 *	68.86		66.13		66.64			
000 002 0001 *	84.37		81.68		82.18			
000 002 0010 *	57.67		55.91		56.26			
000 002 0100 *	57.65		55.89		56.23			
000 002 1000 *	64.60		62.94		63.24			
000 010 0002 *	72.56		70.59		70.95			
000 010 0020 *	64.16		62.36		62.70			
000 012 0000 *	77.31		74.67		75.17			
000 020 0001 *	65.66		65.44		65.48			
000 020 0010 *	59.20		58.87		58.95			
000 021 0000 *	76.43		75.68		75.84			
000 102 0000 *	64.40		62.43		62.83			
001 002 0000 *	67.55		66.17		66.43			
001 020 0000 *	64.22		63.76		63.87			
001 200 0000 *	65.70		63.85		64.20			
002 010 0000 *	69.67		68.54		68.77			
010 020 0000	68.29		68.22		68.25			

4.3 Network Analysis Diagrams

Graphics were constructed using the Gephi network visualisation software (gephi.org). Figure 30 shows the graph of bis(methylenehydroxy)bullvalene **5g**.
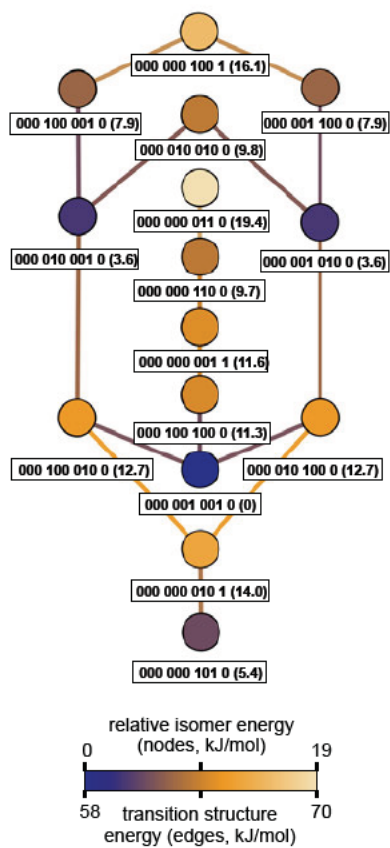
Figure 30. Reaction graph of **5g** (a mirror plane of symmetry bisects the graph vertically).

4.4   XYZ coordinates of the optimized structures

Isomers of methyl-bullvalene **5b**

Isomer 0000000001:

```
C   -0.010465  -0.005437   0.000000
C    1.463539   0.001854  -0.000000
C    2.256770   1.086306  -0.000000
C   -0.834831   1.034805  -0.766294
C   -0.208446   2.111580  -1.554239
C    0.917581   2.776007  -1.244840
C   -0.834831   1.034805   0.766294
C   -0.208446   2.111580   1.554238
C    0.917581   2.776007   1.244840
C    1.763202   2.529188  -0.000000
H   -0.451753  -1.005365   0.000000
H    1.937717  -0.984770  -0.000000
H    3.342160   0.938214  -0.000000
H   -1.750872   0.634010  -1.207691
H   -0.729024   2.380193  -2.478970
H    1.266857   3.556822  -1.929187
H   -1.750872   0.634010   1.207691
H   -0.729025   2.380193   2.478969
H    1.266857   3.556822   1.929187
C    2.965007   3.482015   0.000000
H    2.630161   4.531358   0.000000
H    3.590483   3.320653   0.892204
H    3.590483   3.320653  -0.892204
```

Isomer 0000000010:

```
C    0.018093  -0.016366  -0.016656
C    1.492336   0.012094  -0.037236
C    2.260811   1.114273  -0.024493
C   -0.838528   1.021529  -0.757012
C   -0.248940   2.121667  -1.542266
C    0.865301   2.804871  -1.230612
C   -0.806917   1.003065   0.773730
C   -0.195305   2.080475   1.576621
C    0.914268   2.785185   1.280677
C    1.708233   2.527858   0.001050
H   -0.408013  -1.022923  -0.024549
H    1.984187  -0.965619  -0.061042
H    3.348950   0.997328  -0.039594
H   -1.753981   0.607899  -1.187886
H   -0.787168   2.391943  -2.456420
H    1.196556   3.604966  -1.899992
H   -1.708594   0.580580   1.224722
H   -0.716703   2.316256   2.510674
H    2.559234   3.222943  -0.009642
C    1.436622   3.863058   2.187838
H    0.810034   3.985743   3.084337
H    2.467318   3.637858   2.516334
H    1.480575   4.834343   1.662837
```

Isomer 0000000100:

```
C    0.000147   0.008400   0.010920
C    1.475263  -0.001500  -0.004687
C    2.269456   1.082199  -0.012742
C   -0.825979   1.051240  -0.757200
C   -0.203026   2.116922  -1.565013
C    0.927295   2.776332  -1.260517
C   -0.814672   1.055879   0.773177
C   -0.202731   2.138324   1.584323
C    0.929159   2.785039   1.244925
C    1.741597   2.506079  -0.007525
H   -0.449336  -0.987964   0.018133
H    1.941085  -0.992078  -0.013470
H    3.354907   0.942085  -0.027597
H   -1.746791   0.649879  -1.188308
H   -0.725289   2.373438  -2.492245
H    1.290446   3.547883  -1.946733
H   -1.731650   0.653222   1.212870
H    1.298154   3.570025   1.913245
H    2.602689   3.188055  -0.007934
C   -0.947840   2.480314   2.849220
H   -0.449818   3.286319   3.408088
H   -1.980503   2.803256   2.626194
H   -1.028427   1.600440   3.512359
```

Isomer 0000001000:

```
C    0.001504   0.006855   0.006442
C    1.476598   0.004739   0.004971
C    2.272433   1.087295  -0.003828
C   -0.824740   1.050583  -0.760973
C   -0.203712   2.127141  -1.555485
C    0.927329   2.786300  -1.252938
C   -0.850433   1.027857   0.774093
C   -0.202987   2.112172   1.551543
C    0.922647   2.776143   1.242428
C    1.747195   2.512394  -0.004116
H   -0.438823  -0.993995  -0.007631
H    1.945231  -0.984684   0.005292
H    3.357700   0.945720  -0.008389
H   -1.733861   0.642119  -1.210881
H   -0.729321   2.393323  -2.478234
H    1.283711   3.565274  -1.934161
H   -0.719443   2.384845   2.478473
H    1.273702   3.556326   1.925303
H    2.606768   3.196266   0.000323
C   -2.120354   0.490421   1.410856
H   -2.569463  -0.310742   0.804268
H   -1.911823   0.078528   2.412412
H   -2.871165   1.290546   1.521858
```

Transition states of methyl-bullvalene **5b**

Transition state 0000000001:
```
C  -0.011607  -0.004017  -0.008274
C   1.382947   0.000390   0.007693
C   2.231119   1.102889   0.012860
C  -0.706871   1.401363  -1.398652
C   0.375558   2.036628  -2.006800
C   1.525366   2.529546  -1.398550
C  -0.901478   1.205355   0.079833
C  -0.504357   2.317310   1.005163
C   0.692667   2.907497   1.003106
C   1.837182   2.559485   0.079034
H  -0.516627  -0.961854  -0.156731
H   1.865097  -0.973254  -0.127994
H   3.299938   0.916427  -0.128062
H  -1.461643   0.948260  -2.046386
H   0.377963   2.032607  -3.101715
H   2.337863   2.860970  -2.051999
H  -1.934045   0.897738   0.285215
H  -1.259159   2.654013   1.723013
H   0.881213   3.711979   1.721998
C   3.039747   3.455531   0.383570
H   3.888918   3.220966  -0.277043
H   2.775963   4.515217   0.239028
H   3.368309   3.316774   1.425779
```

Transition state 0000010000:
```
C  -0.002015  -0.020954   0.034135
C   1.384375  -0.008940   0.001743
C   2.222903   1.108880  -0.032225
C  -0.706767   1.433891  -1.395342
C   0.380606   2.044914  -2.000843
C   1.561014   2.523445  -1.408586
C  -0.889534   1.196496   0.079957
C  -0.513522   2.312987   1.014410
C   0.678712   2.914341   1.009000
C   1.801500   2.549687   0.081831
H  -0.508498  -0.981952  -0.088936
H   1.874817  -0.978301  -0.135679
H   3.289893   0.937559  -0.194039
H  -1.469269   1.001263  -2.048746
H   0.368714   2.056702  -3.096241
H  -1.923857   0.887905   0.277036
H  -1.275593   2.643534   1.727550
H   0.870983   3.725367   1.718821
H   2.674870   3.176795   0.300941
C   2.651454   3.101707  -2.273711
H   3.653010   2.793006  -1.934878
H   2.544424   2.800714  -3.326837
H   2.629904   4.207289  -2.231597
```

Transition state 0000000010:
```
C   0.030729  -0.025723   0.001652
C   1.420386   0.005651  -0.025611
C   2.238651   1.135286  -0.032070
C  -0.726769   1.398004  -1.386969
C   0.338337   2.039371  -2.009144
C   1.490236   2.542026  -1.404029
C  -0.874548   1.173427   0.094156
C  -0.500742   2.286991   1.031932
C   0.678862   2.920728   1.038157
C   1.783706   2.564835   0.070640
H  -0.461122  -0.992704  -0.133102
H   1.924572  -0.954268  -0.177555
H   3.309597   0.985711  -0.191281
H  -1.491961   0.944663  -2.022657
H   0.328108   2.046193  -3.103942
H   2.292475   2.897474  -2.055735
H  -1.897550   0.844001   0.314465
H  -1.262839   2.589798   1.758097
H   2.650349   3.210792   0.260250
C   0.989298   4.029095   2.004920
H   0.143100   4.234819   2.677367
H   1.869432   3.777693   2.623905
H   1.239025   4.962231   1.468359
```

Transition state 0000100000:
```
C  -0.005839   0.002102   0.000427
C   1.387310  -0.002417  -0.004019
C   2.232228   1.105162  -0.000254
C  -0.701700   1.430637  -1.395623
C   0.381848   2.035915  -2.038010
C   1.522087   2.527180  -1.396622
C  -0.886486   1.219879   0.084192
C  -0.502203   2.322429   1.028966
C   0.695088   2.912553   1.028468
C   1.802919   2.545386   0.083034
H  -0.519293  -0.952470  -0.140894
H   1.867183  -0.976226  -0.146013
H   3.301982   0.930888  -0.141942
H  -1.469436   0.978492  -2.029994
H   2.347752   2.860638  -2.031757
H  -1.921121   0.912986   0.280742
H  -1.259489   2.644145   1.751050
H   0.901688   3.709360   1.750139
H   2.676732   3.178941   0.278846
C   0.404770   1.988459  -3.555428
H  -0.610956   2.033663  -3.977083
H   0.979939   2.826539  -3.977784
H   0.871370   1.052074  -3.910947
```

Isomers of *n*-hexyl-bullvalene **5c**

Isomer 0000000001:
```
C  -0.076949  -0.019270   0.062653
C   1.396671  -0.035876   0.041592
C   2.207870   1.033763  -0.005667
C  -0.903979   1.013176  -0.700417
C  -0.295360   2.076246  -1.519950
C   0.848938   2.730006  -1.260157
C  -0.860677   1.052229   0.833486
C  -0.189051   2.136135   1.571896
C   0.938686   2.774279   1.213004
C   1.743903   2.485119  -0.050599
H  -0.533745  -1.011557   0.099557
H   1.855766  -1.028348   0.092347
H   3.287834   0.858857   0.018246
H  -1.839385   0.618455  -1.105237
H  -0.859545   2.361151  -2.413754
H   1.154922   3.521345  -1.951270
H  -1.768963   0.679671   1.313889
H  -0.674357   2.437497   2.505646
H   1.320439   3.564676   1.868546
C   2.961702   3.433161  -0.087968
C   3.895116   3.290724  -1.290600
C   2.585942   4.471019  -0.043028
H   3.541563   3.278519   0.839541
C   5.075531   4.262871  -1.244252
C   4.280484   2.258219  -1.350967
H   3.333376   3.450139  -2.227206
C   6.021168   4.137894  -2.439156
H   4.693874   5.299369  -1.187026
H   5.644754   4.102961  -0.309539
C   7.203342   5.108151  -2.394939
H   6.402061   3.100947  -2.496734
H   5.451845   4.298534  -3.373883
C   8.142083   4.976220  -3.593605
H   6.819898   6.143272  -2.335957
H   7.770199   4.945457  -1.459951
H   8.982206   5.686648  -3.533487
H   8.567601   3.960364  -3.657016
H   7.609339   5.168265  -4.540357
```

Isomer 0000000010:
```
C  -0.586583   0.345957  -0.104392
C   0.384536  -0.425767   0.693185
C   1.594968   0.001258   1.089868
C  -0.160802   1.300659  -1.229482
C   1.251271   1.511920  -1.597968
C   2.292189   1.547344  -0.748051
C  -0.761548   1.856719   0.066206
C   0.021828   2.652596   1.030920
C   1.315256   2.481260   1.367841
C   2.160960   1.368373   0.752503
H  -1.517169  -0.188483  -0.311972
H   0.066460  -1.432679   0.981698
H   2.221043  -0.670585   1.685219
H  -0.848769   1.312872  -2.078721
H   1.446850   1.651834  -2.665854
H   3.296071   1.711474  -1.151219
H  -1.796086   2.192900  -0.041039
H  -0.523275   3.475070   1.506455
H   3.167237   1.431773   1.188561
C   2.012189   3.406770   2.331710
C   3.043894   4.326360   1.650766
H   1.265330   4.025961   2.857214
H   2.525607   2.804635   3.103437
C   2.411424   5.357921   0.714996
H   3.629203   4.848226   2.429038
H   3.769639   3.707209   1.095177
C   3.419201   6.274667   0.009946
H   1.787491   4.836981  -0.030166
H   1.713242   5.981784   1.301803
C   4.359075   5.580707  -0.986598
H   2.863360   7.065753  -0.525535
H   4.026803   6.795144   0.772697
C   3.641650   4.927601  -2.169217
H   5.078963   6.327697  -1.364722
H   4.968707   4.823674  -0.461774
H   2.967431   4.119903  -1.845054
H   3.032971   5.665716  -2.719364
H   4.360634   4.492076  -2.882157
```

Isomer 0000000100:
```
C  -0.086550   0.032335  -0.089431
C   1.385258  -0.049833  -0.033139
C   2.230494   0.992599   0.035077
C  -0.821044   1.143362  -0.854440
C  -0.109823   2.203910  -1.592966
C   1.034979   2.795193  -1.212660
C  -0.884169   1.092812   0.673728
C  -0.258592   2.111274   1.553173
C   0.916174   2.715060   1.287977
C   1.773942   2.440688   0.065357
H  -0.583360  -0.939930  -0.141936
H   1.802957  -1.061497  -0.052466
H   3.307110   0.798190   0.069434
H  -1.739583   0.805292  -1.341033
H  -0.574881   2.518807  -2.532588
H   1.466988   3.571754  -1.851670
H  -1.841833   0.724200   1.051667
H   1.291162   3.453474   2.004602
H   2.666434   3.077716   0.130422
C  -1.012771   2.415215   2.827203
C  -0.965633   1.268035   3.847850
H  -0.598829   3.327171   3.288483
H  -2.069728   2.637991   2.587179
C  -1.744725   1.563549   5.129673
H  -1.357882   0.343309   3.387580
H   0.090480   1.056231   4.091976
C  -1.692296   0.430365   6.154988
H  -1.353706   2.490533   5.589001
H  -2.799541   1.778476   4.875262
C  -2.467302   0.724778   7.440987
H  -2.085522  -0.496213   5.696047
H  -0.637050   0.214069   6.406260
C  -2.409169  -0.413665   8.458848
H  -2.072311   1.650965   7.897129
H  -3.520987   0.942149   7.186961
H  -2.975092  -0.172320   9.372965
H  -2.830155  -1.343970   8.041262
H  -1.369147  -0.629277   8.756999
```

Isomer 0000001000:
```
C  -0.003617   0.030742  -0.262393
C   1.470888   0.015711  -0.293598
C   2.277445   1.079500  -0.143789
C  -0.836205   1.187623  -0.831806
C  -0.221560   2.374403  -1.455634
C   0.924841   2.966507  -1.079766
C  -0.827700   0.916572   0.681209
C  -0.161323   1.870306   1.599879
C   0.963630   2.568923   1.375457
C   1.767652   2.490370   0.090745
H  -0.455890  -0.951088  -0.428098
H   1.928252  -0.965304  -0.458024
H   3.360978   0.932169  -0.189426
H  -1.758806   0.862658  -1.320234
H  -0.766069   2.791441  -2.308933
H   1.273605   3.843288  -1.634332
H  -0.669225   2.020095   2.558561
H   1.320675   3.249512   2.154898
H   2.634724   3.158086   0.185333
C  -2.077340   0.261889   1.257293
C  -1.791001  -0.691508   2.419821
H  -2.777171   1.051909   1.586506
H  -2.599283  -0.292085   0.458205
C  -3.046923  -1.353360   2.987626
H  -1.083413  -1.469359   2.080559
H  -1.268914  -0.147351   3.226503
C  -2.766679  -2.303914   4.152041
H  -3.755728  -0.570817   3.317124
H  -3.566104  -1.905576   2.181935
C  -4.020700  -2.970450   4.721267
H  -2.055557  -3.084784   3.823151
H  -2.249551  -1.750522   4.958210
C  -3.729767  -3.915858   5.886162
H  -4.730415  -2.187911   5.046705
H  -4.534836  -3.523521   3.913927
H  -4.650769  -4.379899   6.274108
H  -3.049593  -4.728682   5.580005
H  -3.247122  -3.381818   6.722141
```

Transition states of *n*-hexyl-bullvalene **5c**

Transition state 0000000001:

```
C  -0.031060  -0.015590  -0.035035
C   1.363262  -0.001463   0.034161
C   2.198524   1.107414   0.068221
C  -0.681496   1.362480  -1.453591
C   0.414411   2.015420  -2.022896
C   1.533645   2.527936  -1.377569
C  -0.935185   1.183311   0.018648
C  -0.588635   2.321594   0.930974
C   0.602554   2.922428   0.968789
C   1.793964   2.561761   0.111497
H  -0.522752  -0.977683  -0.199365
H   1.857152  -0.971246  -0.085910
H   3.272558   0.929368  -0.040177
H  -1.404379   0.896581  -2.127927
H   0.455805   2.008901  -3.117016
H   2.362736   2.870972  -2.003742
H  -1.971357   0.866388   0.188300
H  -1.386107   2.687222   1.585749
H   0.735296   3.765925   1.653503
C   2.992220   3.464259   0.452325
C   3.535951   3.293572   1.871109
H   3.802327   3.258647  -0.269264
H   2.693613   4.514657   0.286992
C   4.741287   4.187952   2.164720
H   2.741047   3.504183   2.607657
H   3.814707   2.237255   2.032046
C   5.294128   4.025540   3.581005
H   5.542825   3.974463   1.433018
H   4.461625   5.245386   2.000426
C   6.501374   4.916849   3.879154
H   4.492509   4.240040   4.312449
H   5.571859   2.967468   3.745096
C   7.045680   4.746735   5.296989
H   7.300459   4.700898   3.146458
H   6.221054   5.973234   3.713437
H   7.913449   5.400198   5.481552
H   6.277838   4.990201   6.050759
H   7.365811   3.706834   5.479070
```

Transition state 0000000010:

```
C   0.553140  -0.135117  -0.167245
C   1.843237   0.361507  -0.308346
C   2.249499   1.692615  -0.209639
C  -0.795070   1.112931  -1.249523
C  -0.079549   2.140417  -1.853218
C   0.924524   2.921565  -1.279458
C  -0.665859   0.674201   0.185276
C  -0.546705   1.730495   1.247748
C   0.356170   2.719521   1.249578
C   1.382609   2.866946   0.151230
H   0.381167  -1.187603  -0.407737
H   2.602964  -0.349225  -0.649511
H   3.281554   1.929291  -0.480701
H  -1.454572   0.511123  -1.880434
H  -0.236774   2.273896  -2.928493
H   1.479472   3.598031  -1.934554
H  -1.493087  -0.000785   0.437744
H  -1.266208   1.677915   2.072265
H   2.018949   3.734875   0.364676
C   0.380488   3.772058   2.327830
C  -0.075026   5.154151   1.833939
H  -0.262507   3.456552   3.166612
H   1.406735   3.858056   2.733656
C  -0.004579   6.236959   2.910973
H   0.537420   5.462506   0.967392
H  -1.108560   5.070197   1.454101
C  -0.472478   7.611048   2.430388
H  -0.613028   5.926924   3.780927
H   1.033623   6.313679   3.284760
C  -0.404816   8.697426   3.505684
H   0.136345   7.920592   1.560140
H  -1.510133   7.532661   2.055514
C  -0.875118  10.066366   3.015509
H  -1.013065   8.385036   4.374227
H   0.632936   8.773259   3.878962
H  -0.814954  10.826690   3.810740
H  -0.261885  10.419156   2.169017
H  -1.921661  10.027853   2.668696
```

Transition state 0000010000:

```
C  -0.503610   0.120880  -0.407547
C   0.810112  -0.313858  -0.540884
C   1.972233   0.410077  -0.276729
C  -0.649158   2.082021  -1.236409
C   0.595621   2.482415  -1.706191
C   1.848555   2.348635  -1.094035
C  -0.939976   1.468652   0.106426
C  -0.237237   2.042833   1.304486
C   1.087335   2.192354   1.385825
C   2.046189   1.799002   0.299537
H  -1.297203  -0.525754  -0.790914
H   0.949781  -1.290243  -1.016464
H   2.927699  -0.038018  -0.560819
H  -1.493231   2.142350  -1.928610
H   0.615832   2.845468  -2.740204
H  -2.022656   1.461458   0.283412
H  -0.864239   2.358675   2.144520
H   1.521527   2.626376   2.292309
H   3.070595   2.004575   0.630054
C   3.079981   2.814167  -1.838974
C   3.311524   4.332435  -1.707383
H   3.968115   2.280033  -1.460762
H   2.995984   2.561125  -2.908934
C   3.474616   4.829874  -0.270468
H   4.206942   4.605248  -2.295062
H   2.462628   4.861254  -2.176471
C   3.733734   6.333489  -0.173106
H   2.566749   4.584215   0.307808
H   4.304570   4.284318   0.217112
C   3.880448   6.838746   1.263642
H   4.645341   6.589138  -0.745376
H   2.907393   6.877278  -0.667994
C   4.133296   8.342965   1.355996
H   2.968366   6.579595   1.831751
H   4.705652   6.292875   1.756878
H   4.233822   8.675904   2.401554
H   5.058289   8.625418   0.825210
H   3.306558   8.914678   0.901438
```

Transition state 0000100000:

```
C  -0.151026   0.112416   0.139467
C   1.235763   0.015967   0.105016
C   2.152213   1.065916   0.035721
C  -0.785146   1.545294  -1.320536
C   0.323985   2.043733  -2.004070
C   1.515433   2.463156  -1.400083
C  -0.946404   1.390468   0.169453
C  -0.473984   2.503877   1.061799
C   0.759217   3.012898   1.017246
C   1.823035   2.534146   0.072089
H  -0.728720  -0.812125   0.061427
H   1.647665  -0.992624   0.000279
H   3.203454   0.814349  -0.125560
H  -1.604818   1.141725  -1.922379
H   2.349891   2.706545  -2.063013
H  -1.994953   1.161925   0.396665
H  -1.195348   2.905330   1.780688
H   1.031063   3.824262   1.699919
H   2.741108   3.114368   0.225130
C   0.287777   1.979836  -3.527007
C   0.363431   0.553507  -4.094329
H  -0.635811   2.462055  -3.889860
H   1.122532   2.576541  -3.931286
C   1.634167  -0.197048  -3.693975
H  -0.522460  -0.011241  -3.757559
H   0.291432   0.601340  -5.196744
C   1.777019  -1.585286  -4.330511
H   2.512832   0.412304  -3.973330
H   1.670616  -0.277710  -2.595982
C   0.646244  -2.575129  -4.015878
H   1.855388  -1.474478  -5.427524
H   2.735625  -2.026323  -4.001233
C   0.438439  -2.832752  -2.522745
H  -0.298740  -2.214583  -4.459415
H   0.866235  -3.529734  -4.525294
H  -0.329348  -3.604641  -2.351977
H   1.371443  -3.178899  -2.045275
H   0.118451  -1.921584  -1.994401
```

Isomers of methylenehydroxy-bullvalene **5d**

Isomer 0000000001:
```
C  -0.011012   0.020849  -0.012907
C   1.463022  -0.000772  -0.016223
C   2.276042   1.068726  -0.004245
C  -0.818046   1.088064  -0.755473
C  -0.180884   2.170354  -1.529005
C   0.956461   2.811329  -1.214577
C  -0.813455   1.065573   0.776830
C  -0.156801   2.108194   1.584335
C   0.981448   2.754069   1.277900
C   1.801574   2.513352   0.015871
H  -0.471019  -0.970478  -0.023793
H   1.918266  -0.996079  -0.028460
H   3.359184   0.901050  -0.004229
H  -1.744650   0.711480  -1.196139
H  -0.707813   2.469111  -2.440763
H   1.307638   3.622260  -1.858755
H  -1.733691   0.674424   1.217907
H  -0.652219   2.353283   2.529174
H   1.365706   3.485755   1.999830
C   3.033061   3.437303   0.022101
O   2.711910   4.803009  -0.089116
H   3.626854   3.224338   0.935266
H   3.667467   3.196053  -0.846109
H   2.051407   5.016802   0.583868
```

Isomer 0000000100:
```
C  -0.044771   0.009782  -0.046261
C   1.430040  -0.025258  -0.028333
C   2.245689   1.042125   0.005413
C  -0.834970   1.082368  -0.812075
C  -0.172786   2.155144  -1.578236
C   0.961661   2.788314  -1.234020
C  -0.861673   1.052867   0.716920
C  -0.247557   2.112054   1.550780
C   0.909176   2.740667   1.266196
C   1.746720   2.476380   0.028510
H  -0.510957  -0.978529  -0.071030
H   1.878582  -1.023637  -0.051125
H   3.328242   0.881086   0.008702
H  -1.750406   0.705664  -1.275404
H  -0.667930   2.443619  -2.510896
H   1.352254   3.569056  -1.894047
H  -1.782641   0.653376   1.147874
H   1.270047   3.503671   1.964720
H   2.619899   3.141866   0.061391
C  -1.021009   2.455146   2.801849
O  -1.282406   1.318803   3.607267
H  -0.487233   3.248775   3.361119
H  -2.013237   2.858585   2.532718
H  -0.434312   0.884775   3.774977
```

Isomer 0000000010:
```
C   0.052743  -0.054771  -0.080748
C   1.524280  -0.002150  -0.165299
C   2.280314   1.107560  -0.117108
C  -0.849223   1.015801  -0.711852
C  -0.309227   2.172096  -1.451216
C   0.811678   2.850385  -1.151463
C  -0.749324   0.895864   0.812348
C  -0.114379   1.927498   1.653503
C   0.964441   2.667264   1.338651
C   1.711941   2.508074   0.022053
H  -0.360414  -1.065091  -0.136876
H   2.026037  -0.968950  -0.273612
H   3.367865   1.007917  -0.188297
H  -1.777917   0.617034  -1.128048
H  -0.891968   2.490092  -2.321685
H   1.104041   3.692834  -1.786024
H  -1.623780   0.429835   1.273789
H  -0.567234   2.091153   2.635598
H   2.553091   3.217226   0.022384
C   1.515153   3.708746   2.285156
O   0.725575   3.965872   3.418822
H   2.499806   3.372535   2.659482
H   1.716260   4.636059   1.704748
H  -0.136182   4.276066   3.107400
```

Isomer 0000001000:
```
C   0.000246  -0.012443  -0.133707
C   1.474931  -0.021370  -0.148700
C   2.275608   1.055520  -0.085558
C  -0.830459   1.081613  -0.814647
C  -0.216254   2.215821  -1.530640
C   0.921844   2.846114  -1.193363
C  -0.830401   0.953797   0.716895
C  -0.180047   1.983927   1.560442
C   0.945601   2.664543   1.289305
C   1.757898   2.478934   0.020730
H  -0.446109  -1.008227  -0.193795
H   1.937638  -1.010716  -0.220874
H   3.360102   0.910768  -0.108843
H  -1.747004   0.710523  -1.281443
H  -0.753040   2.554807  -2.422369
H   1.271087   3.674142  -1.817997
H  -0.701358   2.218222   2.497067
H   1.293994   3.410598   2.010472
H   2.620769   3.157181   0.062429
C  -2.067773   0.337224   1.348707
O  -1.762669  -0.548365   2.404831
H  -2.745372   1.151772   1.680695
H  -2.617556  -0.255688   0.601279
H  -1.171583  -0.091344   3.018258
```

Transition states of methylenehydroxy-bullvalene **5d**

Transition state 0000000001:
```
C   0.013532  -0.029833  -0.081744
C   1.404294  -0.034765  -0.171936
C   2.260375   1.063649  -0.176262
C  -0.767752   1.455178  -1.348842
C   0.273290   2.112893  -2.001207
C   1.468414   2.565133  -1.449855
C  -0.856907   1.180691   0.126915
C  -0.383636   2.233819   1.085953
C   0.816242   2.814803   1.031592
C   1.873907   2.516574  -0.002621
H  -0.509226  -0.976683  -0.239257
H   1.865663  -1.001885  -0.397141
H   3.309589   0.881169  -0.432689
H  -1.570666   1.039911  -1.963327
H   0.198453   2.165499  -3.092108
H   2.238689   2.921177  -2.141210
H  -1.875286   0.867561   0.387244
H  -1.076477   2.521682   1.883049
H   1.093674   3.545856   1.796259
C   3.112078   3.383236   0.263344
O   3.616847   3.216193   1.565760
H   3.878173   3.161283  -0.508395
H   2.840652   4.446267   0.160270
H   3.709708   2.266394   1.726732
```

Transition state 0000010000:
```
C  -0.009872   0.000508  -0.094962
C   1.381878  -0.012376  -0.136089
C   2.239256   1.084645  -0.104686
C  -0.717637   1.508409  -1.399559
C   0.354644   2.158254  -2.002769
C   1.541371   2.599080  -1.411728
C  -0.878379   1.220063   0.067886
C  -0.456458   2.277481   1.048384
C   0.744744   2.860465   1.043486
C   1.836339   2.526077   0.066911
H  -0.534264  -0.941921  -0.272345
H   1.849052  -0.982685  -0.334461
H   3.304334   0.904427  -0.274056
H  -1.496798   1.108016  -2.053686
H   0.329985   2.228421  -3.094323
H  -1.910830   0.913430   0.275649
H  -1.193367   2.578725   1.799670
H   0.969356   3.627816   1.791177
H   2.723487   3.131150   0.294675
C   2.630936   3.182172  -2.286621
O   2.662778   2.679512  -3.601366
H   2.470723   4.272781  -2.383979
H   3.608167   3.061673  -1.775882
H   2.705879   1.714565  -3.536549
```

Transition state 0000000010:
```
C   0.031274  -0.009585  -0.002479
C   1.421642   0.040901  -0.022360
C   2.227041   1.178958  -0.004715
C  -0.740198   1.424298  -1.367155
C   0.318357   2.094621  -1.971927
C   1.460356   2.603137  -1.354213
C  -0.895939   1.171429   0.108662
C  -0.539678   2.273814   1.064038
C   0.639626   2.907502   1.088844
C   1.753436   2.599590   0.120364
H  -0.446203  -0.980790  -0.156051
H   1.936516  -0.910907  -0.188256
H   3.300278   1.044974  -0.162467
H  -1.494828   0.970083  -2.014439
H   0.310977   2.121071  -3.066440
H   2.258519   2.984167  -1.996453
H  -1.914556   0.822188   0.317791
H  -1.305207   2.560923   1.793926
H   2.594915   3.271114   0.325351
C   0.931036   3.995375   2.088743
O   1.354769   5.197250   1.467832
H   0.048705   4.150529   2.740986
H   1.768482   3.690956   2.741537
H   0.681805   5.437335   0.815664
```

Transition state 0000100000:
```
C  -0.012773   0.014656  -0.014840
C   1.377803   0.007984  -0.007662
C   2.228888   1.114826  -0.011312
C  -0.687276   1.434420  -1.445171
C   0.414230   2.022595  -2.062997
C   1.552779   2.512575  -1.415667
C  -0.892965   1.236565   0.032635
C  -0.518171   2.348291   0.971769
C   0.681522   2.933850   0.987545
C   1.806477   2.556551   0.067207
H  -0.526042  -0.940980  -0.149447
H   1.857574  -0.968349  -0.130934
H   3.299210   0.934626  -0.139175
H  -1.436244   0.989180  -2.104287
H   2.385927   2.839421  -2.045279
H  -1.930630   0.933462   0.219192
H  -1.285336   2.680259   1.678639
H   0.877982   3.735653   1.706440
H   2.679527   3.188112   0.271593
C   0.473637   1.936815  -3.585799
O  -0.787956   1.994192  -4.214203
H   1.158512   2.720016  -3.968550
H   0.908696   0.964805  -3.879754
H  -1.229631   2.797602  -3.905030
```

Isomers of benzyl-bullvalene **5e**

Isomer 0000000001:
```
C   0.039118  -0.079882  -0.106477
C   1.503490  -0.009373   0.036977
C   2.247054   1.106525   0.118299
C  -0.747006   0.933961  -0.944478
C  -0.087696   2.040088  -1.660986
C   0.973036   2.750964  -1.242160
C  -0.895664   0.921945   0.579749
C  -0.388702   2.015501   1.427417
C   0.731801   2.731303   1.232292
C   1.702992   2.531810   0.076277
H  -0.357755  -1.097138  -0.153209
H   2.018803  -0.974185   0.079829
H   3.332206   0.999425   0.223534
H  -1.598955   0.502193  -1.475778
H  -0.523778   2.294834  -2.632101
H   1.337484   3.552008  -1.888786
H  -1.833498   0.483240   0.929786
H  -1.003990   2.255224   2.300383
H   0.963809   3.520885   1.950181
C   2.919568   3.495466   0.203008
C   2.623757   4.975959   0.180079
H   3.437681   3.242434   1.142196
H   3.614260   3.251392  -0.616960
C   2.364461   5.683499   1.365821
C   2.068066   7.048478   1.344832
C   2.034704   7.741141   0.131592
C   2.315257   7.059186  -1.055442
C   2.610988   5.694219  -1.027322
H   2.411055   5.160055   2.324438
H   1.869958   7.574856   2.282193
H   1.804421   8.809351   0.112650
H   2.311778   7.593852  -2.008902
H   2.852432   5.178818  -1.960711
```

Isomer 0000000010:
```
C   0.160334  -0.085126   0.045954
C   1.497224   0.294351  -0.448613
C   1.985829   1.543685  -0.520682
C  -1.087603   0.770878  -0.208587
C  -1.043928   2.038848  -0.962211
C  -0.050023   2.942466  -0.930192
C  -0.519263   0.643872   1.208749
C   0.104679   1.776194   1.920444
C   0.879250   2.740609   1.387127
C   1.210723   2.778849  -0.101944
H  -0.032966  -1.160749   0.024746
H   2.131765  -0.533901  -0.779755
H   2.998679   1.691204  -0.908344
H  -1.995099   0.185002  -0.375829
H  -1.915072   2.244376  -1.592412
H  -0.143740   3.855245  -1.525801
H  -1.102295  -0.013850   1.858574
H  -0.097959   1.820348   2.996179
H   1.844001   3.657927  -0.280360
C   1.441349   3.859123   2.228614
C   0.990486   5.234012   1.765930
H   1.148859   3.705780   3.281880
H   2.544981   3.824185   2.200229
C   1.911806   6.271751   1.570524
C   1.490725   7.537405   1.149652
C   0.135699   7.781579   0.914006
C  -0.792768   6.751607   1.100473
C  -0.367845   5.489564   1.519460
H   2.974740   6.085280   1.750461
H   2.225406   8.333403   1.002021
H  -0.196329   8.768693   0.582284
H  -1.854694   6.932294   0.913454
H  -1.092400   4.681426   1.645984
```

Isomer 0000000100:
```
C   0.769763   0.107575   0.379830
C   2.141751   0.638613   0.281505
C   2.478473   1.917799   0.040478
C  -0.380340   0.624196  -0.498573
C  -0.192514   1.680542  -1.511393
C   0.609725   2.751216  -1.392055
C  -0.380512   0.903129   1.003000
C  -0.200803   2.253078   1.588779
C   0.609220   3.200653   1.079165
C   1.460651   3.026762  -0.165425
H   0.722050  -0.964838   0.584546
H   2.942457  -0.095238   0.417483
H   3.538712   2.184420  -0.012665
H  -1.084952  -0.155894  -0.798016
H  -0.765571   1.556536  -2.435791
H   0.666092   3.465019  -2.219783
H  -1.077937   0.278313   1.566889
H   0.681391   4.158404   1.605136
H   2.007212   3.964524  -0.333668
C  -0.963595   2.492745   2.872234
C  -0.557468   1.546292   3.989465
H  -0.805495   3.535720   3.195950
H  -2.047480   2.382419   2.691699
C  -1.516795   0.977891   4.838917
C  -1.139372   0.124115   5.879977
C   0.209369  -0.179216   6.082642
C   1.174728   0.375880   5.236088
C   0.794162   1.228932   4.198162
H  -2.574971   1.207956   4.682401
H  -1.902915  -0.308730   6.531833
H   0.507266  -0.849132   6.893312
H   2.231921   0.138848   5.382965
H   1.549251   1.648815   3.528717
```

Isomer 0000001000:
```
C   0.035420  -0.015409   0.224011
C   1.442177  -0.003318  -0.219985
C   2.151958   1.078833  -0.581204
C  -1.020297   0.928767  -0.361559
C  -0.716358   1.923986  -1.406581
C   0.422995   2.626752  -1.522788
C  -0.586376   1.079751   1.104155
C   0.228245   2.237548   1.544781
C   1.181584   2.873478   0.844847
C   1.593469   2.491310  -0.564841
H  -0.345936  -1.015738   0.446113
H   1.931235  -0.981932  -0.257770
H   3.191582   0.947345  -0.896976
H  -2.006614   0.469269  -0.466606
H  -1.507305   2.087417  -2.145562
H   0.522712   3.338555  -2.348154
H   0.010637   2.594329   2.556539
H   1.703727   3.712596   1.315206
H   2.385675   3.178495  -0.891269
C  -1.598326   0.606467   2.135617
C  -2.674941   1.611853   2.503749
H  -2.088339  -0.310465   1.763149
H  -1.062429   0.302888   3.052432
C  -3.439809   1.404997   3.663494
C  -4.462909   2.284731   4.020356
C  -4.738918   3.399094   3.221262
C  -3.981117   3.620445   2.069459
C  -2.958076   2.735567   1.712790
H  -3.227062   0.537869   4.296412
H  -5.044593   2.102912   4.927999
H  -5.536854   4.092468   3.498944
H  -4.182754   4.491805   1.440751
H  -2.369856   2.931406   0.815257
```

Transition states of benzyl-bullvalene **5e**

Transition state 0000000001:

```
C   0.184936  -0.163921  -0.594823
C   1.538858  -0.010657  -0.904322
C   2.335172   1.107694  -0.699596
C  -0.869738   1.521737  -1.180286
C  -0.003098   2.458624  -1.750465
C   1.247809   2.851152  -1.293277
C  -0.675656   0.825632   0.138725
C  -0.078860   1.604421   1.271692
C   1.063625   2.290413   1.199536
C   1.939153   2.401280  -0.026697
H  -0.320861  -1.062083  -0.957786
H   1.985196  -0.813612  -1.499948
H   3.322127   1.108833  -1.169667
H  -1.753494   1.230626  -1.753399
H  -0.289267   2.831303  -2.739396
H   1.848900   3.485113  -1.952430
H  -1.611078   0.350090   0.457319
H  -0.634036   1.603292   2.215073
H   1.408032   2.820432   2.091273
C   3.162636   3.304052   0.264428
C   3.980262   2.909818   1.472229
H   3.801098   3.313691  -0.634906
H   2.791853   4.332821   0.397328
C   3.955880   3.697162   2.633698
C   4.686227   3.336125   3.769611
C   5.458917   2.172683   3.763229
C   5.497634   1.380005   2.611843
C   4.768061   1.746481   1.479077
H   3.354821   4.611068   2.645952
H   4.651117   3.967294   4.661455
H   6.031578   1.886016   4.648904
H   6.103235   0.470067   2.594439
H   4.812016   1.117984   0.587841
```

Transition state 0000000010:

```
C   0.291934  -0.104585   0.088225
C   1.542190   0.246424  -0.408808
C   2.054782   1.533179  -0.567870
C  -1.185944   1.149908  -0.792771
C  -0.569272   2.042438  -1.663850
C   0.594248   2.777660  -1.438299
C  -0.746299   0.848348   0.615511
C  -0.307342   1.996144   1.480022
C   0.641697   2.881155   1.150753
C   1.385676   2.816018  -0.161069
H  -0.007368  -1.153955   0.023404
H   2.142560  -0.566842  -0.829267
H   3.003691   1.640248  -1.099511
H  -2.018091   0.553951  -1.176703
H  -0.975471   2.085452  -2.679632
H   1.015123   3.337121  -2.277309
H  -1.532246   0.284862   1.133427
H  -0.821068   2.111309   2.440718
H   2.106821   3.641009  -0.206346
C   1.002906   4.035098   2.052063
C   0.776103   5.390092   1.402346
H   0.415572   3.965766   2.984100
H   2.065396   3.959070   2.344991
C   1.710362   6.425235   1.546976
C   1.492031   7.676965   0.963577
C   0.333179   7.909521   0.218315
C  -0.602217   6.881706   0.060691
C  -0.381271   5.633208   0.646000
H   2.622067   6.247702   2.125227
H   2.232696   8.471366   1.088286
H   0.161587   8.885778  -0.242303
H  -1.508437   7.052124  -0.526646
H  -1.106468   4.827591   0.507499
```

Transition state 0000010000:

```
C   0.147616   0.010245   0.241583
C   1.510874   0.242167   0.289448
C   2.171169   1.460180   0.080060
C  -0.633765   1.046749  -1.507415
C   0.408521   1.699952  -2.141049
C   1.449770   2.455248  -1.568566
C  -0.910729   1.049818  -0.026148
C  -0.804458   2.370966   0.686466
C   0.279200   3.150611   0.645090
C   1.532332   2.808694  -0.104052
H  -0.196393  -1.026695   0.286327
H   2.153004  -0.640086   0.380142
H   3.262132   1.441346   0.022138
H  -1.264547   0.392730  -2.115710
H   0.499976   1.521803  -3.218168
H  -1.900996   0.615571   0.160512
H  -1.679674   2.701971   1.254768
H   0.272880   4.106549   1.178082
H   2.275032   3.602805   0.038392
C   2.509568   3.065023  -2.459638
C   2.391421   4.577630  -2.567643
H   3.517763   2.820449  -2.088564
H   2.440384   2.615907  -3.465687
C   1.135310   5.193851  -2.681077
C   1.028842   6.581605  -2.795939
C   2.177688   7.379347  -2.794908
C   3.432992   6.777580  -2.675278
C   3.535415   5.388016  -2.559639
H   0.233942   4.575932  -2.668766
H   0.042033   7.044051  -2.883087
H   2.093955   8.465652  -2.881803
H   4.337294   7.391873  -2.666315
H   4.521114   4.923172  -2.461384
```

Transition state 0000100000:

```
C   0.438199  -0.064807  -0.047489
C   1.791528   0.229825  -0.017596
C   2.380243   1.500602   0.026084
C  -0.512289   1.261155  -1.463503
C   0.456236   2.078200  -2.032166
C   1.465295   2.753866  -1.325978
C  -0.683846   0.940434  -0.000908
C  -0.583279   2.065194   0.992006
C   0.458129   2.897239   1.064005
C   1.656139   2.812416   0.165219
H   0.147190  -1.103067  -0.226879
H   2.475763  -0.611060  -0.168342
H   3.465743   1.563191  -0.083793
H  -1.139106   0.681684  -2.147768
H   2.231162   3.265408  -1.914476
H  -1.636194   0.415103   0.142781
H  -1.419567   2.192054   1.686893
H   0.460105   3.692743   1.815844
H   2.368251   3.607819   0.415463
C   0.551960   2.071904  -3.555978
C   1.022598   0.737146  -4.099880
H  -0.427421   2.316646  -3.996252
H   1.242618   2.868895  -3.878010
C   2.229476   0.173451  -3.653430
C   2.661360  -1.062923  -4.134393
C   1.891965  -1.763853  -5.070417
C   0.688579  -1.215683  -5.518706
C   0.259411   0.024954  -5.034281
H   2.823473   0.707940  -2.908843
H   3.603333  -1.486103  -3.774970
H   2.229751  -2.733219  -5.445829
H   0.077981  -1.754899  -6.247921
H  -0.685696   0.447803  -5.387644
```

Isomers of trimethylsilyl-bullvalene **5f**

Isomer 0000000001:
```
C  -0.010488  -0.010992   0.004649
C   1.463403  -0.002029   0.002094
C   2.256780   1.083661  -0.001714
C  -0.838474   1.025393  -0.762466
C  -0.217358   2.101658  -1.555084
C   0.908287   2.771382  -1.251015
C  -0.835860   1.028868   0.769883
C  -0.212050   2.108726   1.555478
C   0.912545   2.777051   1.244530
C   1.753352   2.524595  -0.004108
H  -0.449773  -1.011859   0.007663
H   1.938367  -0.988735   0.003486
H   3.338911   0.910666  -0.003208
H  -1.754396   0.621183  -1.201127
H  -0.741722   2.365731  -2.479479
H   1.233014   3.546647  -1.954189
H  -1.750278   0.626653   1.213487
H  -0.733269   2.377004   2.480439
H   1.239635   3.555499   1.943072
Si  3.253812   3.720100  -0.009288
C   2.629200   5.501642  -0.012400
H   3.476492   6.207610  -0.015035
H   2.013539   5.712789  -0.901506
H   2.015852   5.716663   0.877375
C   4.298018   3.414756   1.533568
H   5.167095   4.093490   1.551922
H   3.718318   3.586882   2.454698
H   4.678661   2.381249   1.566663
C   4.293279   3.407618  -1.553906
H   5.162439   4.086075  -1.577872
H   4.673632   2.373899  -1.583523
H   3.710896   3.575771  -2.474074
```

Isomer 0000000010:
```
C  -0.372638   0.166539  -0.071772
C   0.962640  -0.186476   0.446441
C   1.983572   0.665412   0.638232
C  -0.590431   1.229737  -1.150688
C   0.517139   1.989103  -1.761322
C   1.626629   2.408314  -1.130368
C  -1.062633   1.489421   0.285735
C  -0.437088   2.501700   1.157411
C   0.871058   2.838284   1.225372
C   1.912009   2.150056   0.336666
H  -1.060053  -0.680179  -0.144442
H   1.109062  -1.242243   0.695826
H   2.925273   0.276787   1.038682
H  -1.402773   0.993356  -1.842761
H   0.399074   2.225799  -2.823545
H   2.373219   2.973119  -1.697638
H  -2.144238   1.400768   0.416651
H  -1.143096   3.022480   1.813445
H   2.900160   2.577835   0.558911
Si  1.491551   4.162701   2.406430
C   2.326142   5.529045   1.399710
H   3.144596   5.127546   0.779506
H   1.602685   6.015185   0.724892
H   2.755281   6.303174   2.057968
C   0.069889   4.888781   3.412058
H  -0.430248   4.116929   4.019639
H   0.445494   5.665056   4.099293
H  -0.687601   5.355487   2.761338
C   2.767470   3.389355   3.568657
H   2.309174   2.595699   4.181195
H   3.601487   2.938352   3.005864
H   3.194661   4.144809   4.249484
```

Isomer 0000000100:
```
C  -0.506094   0.317220  -0.346811
C   0.849278  -0.253167  -0.231019
C   1.971911   0.430006   0.047971
C  -0.771698   1.701481  -0.954304
C   0.308723   2.564692  -1.467476
C   1.539249   2.685810  -0.942054
C  -0.999127   1.463326   0.541776
C  -0.174641   2.089502   1.606337
C   1.156623   2.297070   1.497350
C   2.002522   1.928802   0.290184
H  -1.277838  -0.420183  -0.582405
H   0.922354  -1.333462  -0.392534
H   2.920752  -0.112493   0.105159
H  -1.695126   1.754744  -1.536800
H   0.062365   3.149605  -2.359471
H   2.254119   3.362865  -1.420007
H  -2.059906   1.370340   0.793657
H   1.689299   2.766298   2.331078
H   3.040614   2.220219   0.500572
Si -1.098163   2.599073   3.171203
C  -1.891533   1.064036   3.938947
H  -2.571602   0.565377   3.228854
H  -1.121600   0.332554   4.234747
H  -2.477535   1.326096   4.835940
C   0.078223   3.394685   4.412644
H   0.552016   4.299355   3.998042
H  -0.473594   3.690956   5.320239
H   0.877026   2.699507   4.718305
C  -2.456947   3.828779   2.705561
H  -3.046751   4.122012   3.590330
H  -2.024187   4.742000   2.264967
H  -3.153314   3.398367   1.967209
```

Isomer 0000001000:
```
C   0.169477  -0.007730   0.262919
C   1.628305   0.174867   0.387231
C   2.306038   1.321668   0.212091
C  -0.674865   0.746878  -0.757446
C  -0.103123   1.722784  -1.704988
C   0.918009   2.562605  -1.465658
C  -0.859322   1.038833   0.750034
C  -0.399555   2.329541   1.322258
C   0.677617   3.049218   0.963647
C   1.642001   2.641883  -0.134015
H  -0.146055  -1.043955   0.411076
H   2.192148  -0.727190   0.646091
H   3.393863   1.315870   0.332627
H  -1.475033   0.143911  -1.195061
H  -0.572181   1.744324  -2.694005
H   1.245658   3.236388  -2.263525
H  -1.016089   2.737848   2.131399
H   0.878237   3.988070   1.489777
H   2.422521   3.410999  -0.210838
Si -2.435902   0.372868   1.561016
C  -2.951892  -1.275935   0.796402
H  -2.187960  -2.058056   0.935074
H  -3.875875  -1.629698   1.283774
H  -3.162353  -1.189958  -0.281943
C  -2.104383   0.123026   3.402233
H  -3.001180  -0.254799   3.921113
H  -1.290744  -0.605233   3.554952
H  -1.805079   1.064761   3.889961
C  -3.818336   1.632370   1.306829
H  -4.756849   1.295425   1.777881
H  -3.556664   2.611287   1.740001
H  -4.012353   1.784131   0.232117
```

Transition states of trimethylsilyl-bullvalene 5f

Transition state 0000000001:
```
C  -0.029322  -0.001650  -0.020884
C   1.368040  -0.006722  -0.011649
C   2.225191   1.087165   0.000290
C  -0.725225   1.405664  -1.381938
C   0.352199   2.047510  -1.998364
C   1.508212   2.537330  -1.402297
C  -0.913178   1.208476   0.096311
C  -0.501457   2.310683   1.025087
C   0.699149   2.895855   1.015954
C   1.832868   2.547379   0.076383
H  -0.540259  -0.955388  -0.175090
H   1.840848  -0.983770  -0.157390
H   3.287326   0.873664  -0.151905
H  -1.486646   0.958325  -2.025819
H   0.339402   2.052155  -3.093452
H   2.301903   2.866426  -2.079478
H  -1.945108   0.903307   0.308398
H  -1.248388   2.645210   1.752590
H   0.873927   3.691816   1.748785
Si  3.335638   3.670675   0.471355
C   4.788056   3.280942  -0.672288
H   5.637326   3.939290  -0.423429
H   5.135909   2.240909  -0.565722
H   4.540750   3.449832  -1.732658
C   2.816672   5.466502   0.219777
H   3.660096   6.150358   0.412053
H   2.475947   5.630409  -0.815237
H   1.991902   5.751951   0.891984
C   3.854112   3.358726   2.257833
H   4.734429   3.966903   2.524526
H   3.047242   3.605407   2.966170
H   4.116369   2.298321   2.406159
```

Transition state 0000010000:
```
C  -0.142123   0.017565  -0.056734
C   1.233626  -0.081114  -0.167443
C   2.163792   0.966579  -0.146694
C  -0.804020   1.661839  -1.318308
C   0.307995   2.213622  -1.929308
C   1.567622   2.528266  -1.371888
C  -0.922747   1.291626   0.137649
C  -0.413117   2.292417   1.138560
C   0.823921   2.794887   1.118234
C   1.870959   2.415133   0.113099
H  -0.733238  -0.886137  -0.229493
H   1.633916  -1.071231  -0.408518
H   3.207197   0.720071  -0.350405
H  -1.641339   1.370441  -1.958851
H   0.227850   2.321184  -3.015951
H  -1.966996   1.045717   0.368151
H  -1.114643   2.627565   1.909268
H   1.112218   3.534406   1.872413
H   2.804492   2.941730   0.351982
Si  2.928501   3.246818  -2.462812
C   2.513624   3.012831  -4.288310
H   2.379203   1.947152  -4.535817
H   1.591933   3.547294  -4.570184
H   3.330674   3.405837  -4.916047
C   3.064864   5.092975  -2.073085
H   3.860490   5.570192  -2.669901
H   2.116216   5.610487  -2.290576
H   3.299218   5.258096  -1.008301
C   4.597032   2.435521  -2.098745
H   5.392990   2.930429  -2.680375
H   4.872457   2.513074  -1.034064
H   4.590936   1.368199  -2.372711
```

Transition state 0000000010:
```
C  -0.502173   0.237714  -0.185326
C   0.746580  -0.139061   0.294233
C   1.834061   0.692156   0.564518
C  -0.246419   1.627641  -1.782167
C   1.111456   1.843747  -1.984088
C   2.086237   2.062668  -1.010228
C  -0.954722   1.648553  -0.453697
C  -0.582415   2.717175   0.536636
C   0.662388   2.982080   0.966561
C   1.853727   2.192803   0.469701
H  -1.199839  -0.553111  -0.473180
H   0.937563  -1.215537   0.353669
H   2.787603   0.216292   0.808185
H  -0.852102   1.336896  -2.644506
H   1.475839   1.709878  -3.007859
H   3.130533   2.079774  -1.333021
H  -2.039892   1.662882  -0.615003
H  -1.418452   3.311651   0.921343
H   2.773481   2.564583   0.940439
Si  1.005282   4.350314   2.215366
C   2.192190   5.598736   1.435792
H   1.736904   6.072049   0.550469
H   2.456487   6.394740   2.152188
H   3.129167   5.115978   1.112515
C  -0.595300   5.214642   2.713456
H  -0.385298   6.013396   3.444087
H  -1.091736   5.677109   1.844782
H  -1.305557   4.512375   3.179582
C   1.823663   3.587509   3.739647
H   2.085640   4.363252   4.478775
H   1.148656   2.864625   4.226375
H   2.750734   3.053204   3.474031
```

Transition state 0000100000:
```
C  -0.076247   0.045621   0.025516
C   1.313217  -0.017459   0.005637
C   2.208665   1.052400  -0.003248
C  -0.715485   1.507501  -1.376594
C   0.395865   2.054172  -2.027526
C   1.566508   2.487061  -1.387591
C  -0.903101   1.302004   0.105451
C  -0.464405   2.390347   1.043925
C   0.757760   2.926976   1.037551
C   1.848317   2.510981   0.092969
H  -0.630830  -0.887055  -0.106265
H   1.749749  -1.011381  -0.137070
H   3.267981   0.828955  -0.152644
H  -1.518886   1.091309  -1.993160
H   2.413314   2.784180  -2.011486
H  -1.948960   1.040804   0.309208
H  -1.203644   2.749088   1.767274
H   1.000314   3.716804   1.755694
H   2.751480   3.102763   0.285973
Si  0.403796   1.924924  -3.918182
C   1.815894   2.945632  -4.647002
H   2.801918   2.554262  -4.347484
H   1.771489   2.919776  -5.748599
H   1.756999   4.000302  -4.331695
C   0.631011   0.109530  -4.391808
H  -0.183387  -0.507294  -3.978145
H   0.643129  -0.028526  -5.486080
H   1.580005  -0.277984  -3.985799
C  -1.238202   2.555551  -4.607404
H  -1.260642   2.469495  -5.706819
H  -2.092979   1.983128  -4.211543
H  -1.394180   3.614726  -4.344382
```

Isomers of bis(methylenehydroxy)-bullvalene **5g**

Isomer 0000000011:
```
C   0.059144  -0.049242  -0.057035
C   1.528462   0.013721  -0.127114
C   2.277781   1.126562  -0.079730
C  -0.844152   1.013512  -0.675146
C  -0.321519   2.185016  -1.402016
C   0.793381   2.871535  -1.106569
C  -0.735178   0.902957   0.849454
C  -0.078762   1.929374   1.671786
C   1.006197   2.682649   1.378860
C   1.750828   2.550719   0.031829
H  -0.350504  -1.061578  -0.099148
H   2.039366  -0.950840  -0.207696
H   3.367263   1.014267  -0.119943
H  -1.779910   0.616628  -1.077013
H  -0.926274   2.521270  -2.250267
H   1.051042   3.753962  -1.698623
H  -1.602036   0.442013   1.329342
H  -0.538500   2.081539   2.655073
C   1.454216   3.687789   2.408587
O   1.204000   5.040541   2.002954
H   0.949010   3.480926   3.368776
H   2.537495   3.638180   2.592540
H   0.278753   5.088380   1.719584
C   2.982714   3.485708  -0.105823
O   2.694866   4.842665  -0.270791
H   3.670510   3.295620   0.744503
H   3.519083   3.162596  -1.013789
H   2.207317   5.146198   0.519635
```

Isomer 0000000110:
```
C  -0.109223   0.035192  -0.049144
C   1.353037  -0.027988   0.110593
C   2.178224   1.029609   0.198614
C  -0.810287   1.105722  -0.893914
C  -0.073959   2.157185  -1.618782
C   1.029241   2.780148  -1.176164
C  -0.966313   1.117635   0.625516
C  -0.411668   2.157910   1.521265
C   0.787967   2.769289   1.341606
C   1.695704   2.467383   0.149348
H  -0.595357  -0.942794  -0.085257
H   1.781564  -1.033813   0.161461
H   3.253469   0.855892   0.310365
H  -1.693827   0.736783  -1.420841
H  -0.483109   2.440101  -2.593672
H   1.489844   3.550587  -1.802150
H  -1.934148   0.739516   0.963060
H   2.576526   3.118387   0.235474
C  -1.238010   2.431090   2.773508
O  -0.780452   1.724255   3.904050
H  -1.274991   3.523172   2.961119
H  -2.277833   2.113171   2.597569
H   0.123403   2.048848   4.071920
C   1.354252   3.669418   2.418581
O   1.735372   2.942371   3.597485
H   2.221319   4.232491   2.029168
H   0.618148   4.408871   2.765676
H   2.285212   2.197761   3.312285
```

Isomer 0000000101:
```
C  -0.037916   0.016832   0.015608
C   1.435565  -0.012665   0.007051
C   2.252223   1.053829   0.000441
C  -0.840762   1.070246  -0.769679
C  -0.178387   2.110734  -1.574449
C   0.962574   2.750216  -1.264145
C  -0.841320   1.079442   0.758839
C  -0.216470   2.165785   1.547373
C   0.933415   2.788096   1.229038
C   1.778306   2.498227  -0.001531
H  -0.502337  -0.972469   0.021678
H   1.886400  -1.010037  -0.002644
H   3.334962   0.884705  -0.017753
H  -1.761534   0.682719  -1.212702
H  -0.668750   2.357802  -2.521327
H   1.355186   3.479386  -1.984003
H  -1.756445   0.693693   1.214045
H   1.287049   3.598691   1.874201
C  -0.978465   2.555645   2.791898
O  -1.229582   1.449879   3.642227
H  -0.441187   3.371095   3.314394
H  -1.974537   2.945562   2.517041
H  -0.376861   1.034382   3.831904
C   3.010493   3.421610   0.005346
O   2.689923   4.786072   0.131502
H   3.642431   3.170326   0.872437
H   3.606340   3.218594  -0.908514
H   2.039973   5.011084  -0.548125
```

Isomer 0000001001:
```
C  -0.012793   0.038805   0.000440
C   1.459759   0.004126  -0.070917
C   2.281229   1.066126  -0.066288
C  -0.843602   1.134815  -0.674311
C  -0.234214   2.238291  -1.438051
C   0.924058   2.857415  -1.157510
C  -0.784752   1.040219   0.862042
C  -0.078802   2.070282   1.655239
C   1.048218   2.718233   1.320281
C   1.819883   2.511872   0.023614
H  -0.479708  -0.949460  -0.038678
H   1.903225  -0.993976  -0.140564
H   3.361370   0.891386  -0.128718
H  -1.783566   0.766945  -1.097371
H  -0.799989   2.571803  -2.313857
H   1.252974   3.686973  -1.789515
H  -0.556928   2.314586   2.608546
H   1.454274   3.438985   2.041440
C  -2.039210   0.506312   1.533686
O  -2.956429   1.527420   1.854469
H  -2.495667  -0.273283   0.889796
H  -1.772391   0.022032   2.488093
H  -3.107209   2.048773   1.053549
C   3.057979   3.427197   0.009230
O   2.743892   4.797673  -0.046513
H   3.686515   3.181013   0.890017
H   3.654300   3.209369  -0.891517
H   2.132330   5.001077   0.674175
```

Isomer 0000001010:
```
C   0.019100  -0.031022   0.013883
C   1.491403  -0.091820   0.099086
C   2.323037   0.962360   0.120787
C  -0.720347   1.021397  -0.823242
C  -0.017508   2.061871  -1.596619
C   1.116700   2.685387  -1.233885
C  -0.818291   1.036386   0.715280
C  -0.196008   2.128407   1.496428
C   0.975650   2.745413   1.255709
C   1.856256   2.403129   0.060827
H  -0.461068  -1.013594  -0.006194
H   1.920090  -1.097924   0.141782
H   3.400863   0.782042   0.179914
H  -1.616975   0.631437  -1.315130
H  -0.478723   2.331747  -2.552095
H   1.540866   3.442044  -1.901351
H  -0.793445   2.470240   2.348507
H   2.731253   3.063887   0.097271
C  -2.144800   0.562942   1.287346
O  -3.080180   1.609138   1.423844
H  -2.538789  -0.264713   0.662639
H  -1.987883   0.157392   2.300914
H  -3.139727   2.061314   0.570662
C   1.465962   3.860730   2.139500
O   1.737952   5.043048   1.404379
H   0.742507   4.036765   2.960160
H   2.426547   3.579003   2.606025
H   0.933473   5.267169   0.915991
```

Isomer 0000010010:
```
C  -0.157478   0.027004   0.013341
C   1.308689  -0.127267  -0.001282
C   2.201070   0.875689  -0.012649
C  -0.868798   1.147962  -0.748508
C  -0.155014   2.167806  -1.540138
C   1.035117   2.729035  -1.252664
C  -0.858249   1.147909   0.787513
C  -0.132387   2.169948   1.561538
C   1.054420   2.725585   1.248186
C   1.826077   2.343182  -0.007584
H  -0.705377  -0.918658   0.020354
H   1.678646  -1.157251  -0.007546
H   3.267460   0.630770  -0.028353
H  -1.827084   0.847013  -1.179310
H  -0.673855   2.505212  -2.443887
H  -1.808103   0.846274   1.235904
H  -0.635285   2.515657   2.471763
H   2.759375   2.924151  -0.009782
C   1.629897   3.813320  -2.115552
O   1.663661   5.076285  -1.476431
H   2.648601   3.503469  -2.435825
H   1.028081   3.935920  -3.029980
H   2.139933   4.995718  -0.632552
C   1.649672   3.823262   2.084907
O   1.807865   5.030848   1.341114
H   1.038328   3.990983   2.991529
H   2.666502   3.551965   2.416416
H   0.941726   5.265058   0.973374
```

Isomer 0000001100:
```
C  -0.013881   0.004371  -0.163794
C   1.458966  -0.014079  -0.115581
C   2.262290   1.058521  -0.024374
C  -0.805399   1.109682  -0.872371
C  -0.161420   2.241470  -1.563301
C   0.966295   2.863022  -1.182877
C  -0.894464   0.954782   0.656922
C  -0.277030   1.981798   1.555679
C   0.870199   2.645625   1.295290
C   1.737501   2.479627   0.065586
H  -0.457073  -0.990140  -0.255168
H   1.917770  -1.006278  -0.171680
H   3.346791   0.913417  -0.009350
H  -1.699450   0.746302  -1.385654
H  -0.661874   2.580614  -2.475850
H   1.352341   3.687739  -1.789527
H   1.211323   3.375385   2.038060
H   2.595096   3.158701   0.163541
C  -2.191412   0.288022   1.127965
O  -2.017317  -0.660764   2.143997
H  -2.926833   1.071834   1.404406
H  -2.628396  -0.247282   0.270104
H  -1.655585  -0.189197   2.917765
C  -0.942805   2.266480   2.883608
O  -0.820740   1.172353   3.800387
H  -0.504956   3.180658   3.320961
H  -2.023518   2.439370   2.780046
H   0.117634   0.934143   3.837559
```

Isomer 0000010100:
```
C   0.065849   0.025602   0.060607
C   1.536522   0.063038  -0.049571
C   2.292023   1.171140  -0.134931
C  -0.837353   1.023138  -0.682391
C  -0.292494   2.081444  -1.550718
C   0.827184   2.800396  -1.337909
C  -0.738873   1.063716   0.842634
C  -0.116264   2.191168   1.574437
C   0.976684   2.861275   1.162131
C   1.723003   2.577419  -0.124984
H  -0.349646  -0.983788   0.116808
H   2.034141  -0.911866  -0.067961
H   3.378410   1.068095  -0.219883
H  -1.766155   0.582200  -1.052971
H  -0.870200   2.290209  -2.458274
H  -1.600536   0.641266   1.364728
H   1.353900   3.674369   1.792094
H   2.563482   3.277758  -0.207511
C   1.286579   3.848276  -2.314899
O   2.615227   3.620524  -2.756350
H   0.572371   3.915337  -3.159889
H   1.306595   4.838727  -1.826521
H   2.650645   2.717595  -3.102134
C  -0.801169   2.554646   2.870292
O  -0.934769   1.445866   3.742465
H  -0.266430   3.399315   3.347825
H  -1.832280   2.895210   2.668886
H  -0.053102   1.066014   3.861465
```

Isomer 0000011000:
```
C   0.078977  -0.007804  -0.143408
C   1.552042   0.044702  -0.099680
C   2.301671   1.156190  -0.012153
C  -0.763144   1.051156  -0.865912
C  -0.159472   2.198963  -1.565213
C   0.931835   2.893660  -1.188347
C  -0.826501   0.928057   0.663577
C  -0.256984   1.987808   1.528388
C   0.848735   2.713952   1.297982
C   1.722086   2.555382   0.070426
H  -0.323804  -1.021008  -0.218155
H   2.058822  -0.924306  -0.147177
H   3.391772   1.061041   0.008803
H  -1.641908   0.642911  -1.372514
H  -0.662191   2.500764  -2.491132
H  -0.826157   2.202969   2.441342
H   1.136266   3.476648   2.028479
H   2.558658   3.262476   0.132692
C   1.457442   4.037519  -2.012445
O   2.821656   3.862787  -2.357893
H   0.816538   4.184751  -2.904649
H   1.421199   4.973860  -1.427768
H   2.899576   3.000356  -2.789478
C  -2.065874   0.264719   1.242049
O  -1.773869  -0.605502   2.314108
H  -2.789154   1.052805   1.539525
H  -2.557735  -0.351404   0.473278
H  -1.237135  -0.121875   2.956420
```

Isomer 0000101000:
```
C   0.018008  -0.010571   0.050689
C   1.490951  -0.116156   0.052338
C   2.347878   0.913289  -0.024441
C  -0.723317   1.046994  -0.741642
C  -0.134130   2.152491  -1.521103
C   1.046816   2.737723  -1.246150
C  -0.754769   1.088982   0.798664
C  -0.031597   2.147737   1.536676
C   1.141301   2.715580   1.202872
C   1.917480   2.367304  -0.058571
H  -0.493690  -0.977019   0.056870
H   1.894485  -1.131903   0.109042
H   3.422611   0.707289  -0.024008
H  -1.661671   0.681845  -1.169520
H   1.347863   3.610866  -1.835609
H  -0.531265   2.490340   2.448266
H   1.559834   3.483394   1.861149
H   2.822081   2.989178  -0.091570
C  -1.110770   2.777075  -2.485195
O  -2.238232   3.283646  -1.766520
H  -0.619991   3.569636  -3.080149
H  -1.520747   2.033432  -3.188202
H  -1.896252   3.917331  -1.118395
C  -2.135783   0.778794   1.348231
O  -3.004938   1.871880   1.153606
H  -2.520479  -0.148650   0.875381
H  -2.093195   0.595640   2.435057
H  -2.946575   2.133189   0.219150
```

Isomer 0000100100:
```
C  -0.125482   0.083284   0.010913
C   1.340572  -0.077955   0.013478
C   2.239711   0.919744   0.016828
C  -0.840035   1.202331  -0.748900
C  -0.119764   2.214392  -1.556044
C   1.070087   2.751908  -1.226426
C  -0.836506   1.204476   0.778256
C  -0.122465   2.217099   1.591453
C   1.071359   2.747526   1.266723
C   1.857435   2.388604   0.018851
H  -0.674639  -0.861676   0.014099
H   1.703375  -1.110560   0.014547
H   3.305728   0.672527   0.020135
H  -1.799766   0.914640  -1.184611
H   1.502286   3.504935  -1.894375
H  -1.787207   0.880491   1.215447
H   1.504448   3.499190   1.934887
H   2.782078   2.981115   0.019566
C  -0.847552   2.654007  -2.803528
O  -2.150188   3.135298  -2.519559
H  -0.235781   3.400592  -3.347114
H  -0.992332   1.795034  -3.482197
H  -2.059411   3.832673  -1.854902
C  -0.856705   2.666555   2.833752
O  -2.042471   3.388771   2.544051
H  -1.075323   1.784194   3.473037
H  -0.217304   3.342677   3.420834
H  -2.625723   2.817227   2.027579
```

Isomer 0001001000:
```
C   0.003661  -0.021376   0.007390
C   1.474512   0.004859  -0.115110
C   2.250941   1.100425  -0.110906
C  -0.922713   1.016448  -0.652256
C  -0.348701   2.156527  -1.409121
C   0.792018   2.821508  -1.164124
C  -0.794380   0.932431   0.892616
C  -0.142587   2.030514   1.646719
C   0.953379   2.723613   1.302751
C   1.708445   2.513530   0.004513
H  -0.413332  -1.033053  -0.008636
H   1.955393  -0.973555  -0.213062
H   3.334448   0.979619  -0.206500
H  -0.924151   2.460496  -2.292730
H   1.082124   3.630583  -1.841692
H  -0.650819   2.292646   2.579654
H   1.310018   3.510404   1.974751
H   2.555156   3.212395  -0.023973
C  -2.224142   0.524433  -1.263303
O  -3.322994   1.383953  -0.962903
H  -2.099055   0.428573  -2.358462
H  -2.506629  -0.465003  -0.884164
H  -3.089735   2.280187  -1.245058
C  -1.960285   0.321636   1.672001
O  -3.025245   1.215404   1.850063
H  -2.283583  -0.625326   1.198374
H  -1.589615   0.051621   2.675556
H  -3.357129   1.421117   0.956254
```

Transition states of bis(methylenehydroxy)-bullvalene **5g**

Transition state 0000000011:
```
C  -0.031324   0.017910   0.042758
C   1.359891  -0.003418   0.057520
C   2.229656   1.082458   0.020703
C  -0.695390   1.407480  -1.400199
C   0.398792   1.997831  -2.026572
C   1.560248   2.482264  -1.433111
C  -0.879704   1.257222   0.082591
C  -0.440889   2.376535   0.974609
C   0.763563   2.970102   0.982187
C   1.891859   2.555899   0.035069
H  -0.562784  -0.930363  -0.067769
H   1.826286  -0.989081  -0.040080
H   3.291414   0.856642  -0.112715
H  -1.466191   0.954034  -2.028245
H   0.398907   1.968736  -3.120948
H   2.366235   2.805653  -2.096233
H  -1.920476   0.995355   0.308819
H  -1.186364   2.726472   1.698000
C   0.965701   4.105571   1.957022
O   1.033251   5.381737   1.309041
H   0.145282   4.098788   2.696070
H   1.907978   4.013024   2.515613
H   0.260496   5.451539   0.728925
C   3.196027   3.371768   0.215439
O   3.138999   4.679437  -0.273658
H   3.509426   3.320393   1.278058
H   3.981370   2.856302  -0.360749
H   2.463698   5.161589   0.240457
```

Transition state 0000000110:
```
C   0.087199   0.065597   0.143841
C   1.474621   0.101148   0.074721
C   2.279665   1.231999  -0.061978
C  -0.724340   1.345881  -1.358669
C   0.315632   1.934885  -2.065219
C   1.468702   2.505000  -1.529014
C  -0.833833   1.256526   0.137650
C  -0.477280   2.448988   0.993407
C   0.721474   3.063208   0.914914
C   1.791914   2.656234  -0.070572
H  -0.399851  -0.912652   0.129130
H   1.982696  -0.866167   0.007982
H   3.348265   1.084710  -0.237964
H  -1.499572   0.824790  -1.926196
H   0.281839   1.841300  -3.155287
H   2.254288   2.815705  -2.222340
H  -1.843600   0.924780   0.406258
H   2.647961   3.334323   0.036193
C  -1.494856   2.840839   2.054425
O  -1.227545   2.258511   3.311563
H  -1.557256   3.945510   2.122034
H  -2.493714   2.492518   1.747012
H  -0.366921   2.623025   3.587825
C   1.113401   4.107185   1.941582
O   1.290825   3.546553   3.250602
H   2.034814   4.629522   1.627099
H   0.333480   4.872684   2.061822
H   1.904974   2.802417   3.167796
```

Transition state 0000000101:
```
C  -0.073965   0.052960  -0.048692
C   1.318352   0.023102   0.032168
C   2.188253   1.107810   0.069861
C  -0.671521   1.460597  -1.482940
C   0.449851   2.070646  -2.045001
C   1.575043   2.546349  -1.381528
C  -0.942275   1.279898  -0.017599
C  -0.582641   2.393292   0.929708
C   0.637461   2.939146   0.985295
C   1.804237   2.571008   0.104701
H  -0.593091  -0.894906  -0.211708
H   1.783291  -0.962106  -0.077644
H   3.257762   0.900728  -0.045040
H  -1.401740   1.015143  -2.163351
H   0.504575   2.060848  -3.138231
H   2.427272   2.858603  -1.993331
H  -1.984321   0.986886   0.153011
H   0.837718   3.708867   1.737716
C  -1.687088   2.843888   1.849853
O  -2.255498   1.766496   2.575271
H  -1.314104   3.646590   2.515972
H  -2.517650   3.270047   1.259417
H  -1.535027   1.324056   3.045279
C   3.013415   3.442975   0.470668
O   3.355330   3.344898   1.831996
H   3.863667   3.173325  -0.189330
H   2.770617   4.500419   0.278718
H   3.431609   2.404927   2.049329
```

Transition state 0000001001:
```
C   0.012355  -0.035916  -0.302456
C   1.403835  -0.023937  -0.372786
C   2.253786   1.077282  -0.295213
C  -0.765925   1.543403  -1.469617
C   0.280414   2.249341  -2.057132
C   1.471882   2.655169  -1.462235
C  -0.891922   1.145810  -0.026579
C  -0.410724   2.121869   1.015547
C   0.783289   2.714848   1.019472
C   1.857250   2.511106  -0.017564
H  -0.494900  -0.970125  -0.566395
H   1.874042  -0.968812  -0.664600
H   3.305959   0.917615  -0.554303
H  -1.552146   1.166439  -2.131235
H   0.218414   2.381331  -3.141979
H   2.250743   3.055703  -2.118682
H  -1.102009   2.309674   1.841926
H   1.047037   3.377035   1.848915
C  -2.316077   0.683721   0.309413
O  -2.414622   0.133954   1.600052
H  -2.994831   1.551202   0.279861
H  -2.656000  -0.028791  -0.470825
H  -1.715751  -0.528717   1.694466
C   3.084411   3.365375   0.327645
O   3.574368   3.108033   1.620461
H   3.862088   3.207427  -0.448431
H   2.803933   4.430575   0.299307
H   3.679818   2.150510   1.712657
```

Transition state 0000010001:
```
C    0.018010   -0.046689    0.026084
C    1.402741   -0.032607   -0.000551
C    2.236452    1.089558   -0.016853
C   -0.693777    1.415728   -1.383255
C    0.393891    2.042245   -1.968681
C    1.589859    2.509255   -1.384322
C   -0.875509    1.161435    0.090397
C   -0.505969    2.295940    1.001220
C    0.680687    2.905460    0.991706
C    1.853872    2.535251    0.120762
H   -0.483913   -1.007760   -0.116035
H    1.896320   -0.997710   -0.153610
H    3.304706    0.912964   -0.175924
H   -1.451802    0.994239   -2.048934
H    0.380067    2.066394   -3.064689
H   -1.907049    0.844997    0.288750
H   -1.286910    2.666076    1.673145
H    0.840449    3.777554    1.632012
C    2.619055    3.093618   -2.318993
O    2.615546    4.529922   -2.286412
H    3.643034    2.801035   -2.053990
H    2.434895    2.739850   -3.348791
H    1.713401    4.817918   -2.490488
C    3.068888    3.377488    0.570657
O    2.862355    4.756889    0.477396
H    3.246174    3.136404    1.632409
H    3.975599    3.053331    0.023750
H    2.804226    4.957593   -0.476003
```

Transition state 0000010100:
```
C    0.079814    0.007364    0.201566
C    1.460932    0.066182    0.122444
C    2.250082    1.213835   -0.019819
C   -0.737633    1.331898   -1.317326
C    0.309803    1.932564   -1.993354
C    1.491056    2.481353   -1.461394
C   -0.856938    1.184502    0.175725
C   -0.519698    2.390291    1.019380
C    0.659822    3.019637    0.940799
C    1.772796    2.636698    0.014393
H   -0.391034   -0.979016    0.169793
H    1.986728   -0.890649    0.040966
H    3.318333    1.075223   -0.203349
H   -1.507959    0.835800   -1.913958
H    0.268843    1.880777   -3.087415
H   -1.863755    0.844283    0.444566
H    0.836842    3.887285    1.586651
H    2.614722    3.325828    0.143900
C    2.532321    3.063708   -2.387096
O    2.696844    4.460588   -2.199169
H    3.524704    2.626645   -2.193055
H    2.270841    2.817667   -3.435119
H    1.825956    4.870258   -2.297146
C   -1.597433    2.844315    1.967837
O   -2.044948    1.798159    2.813139
H   -1.245282    3.724137    2.542232
H   -2.488807    3.163061    1.398533
H   -1.266906    1.434262    3.258222
```

Transition state 0000010010:
```
C   -0.179031    0.054842   -0.132985
C    1.187544   -0.027051   -0.307742
C    2.104810    1.037026   -0.307911
C   -0.900485    1.746153   -1.338841
C    0.184785    2.324457   -1.964818
C    1.454555    2.615589   -1.423095
C   -0.956352    1.324121    0.108541
C   -0.422719    2.305024    1.116303
C    0.814132    2.818315    1.090430
C    1.819700    2.470848    0.028546
H   -0.771739   -0.850222   -0.292596
H    1.590244   -1.007419   -0.582594
H    3.145705    0.821880   -0.554493
H   -1.757962    1.468944   -1.958222
H    0.089360    2.484582   -3.044882
H   -1.990421    1.067874    0.371572
H   -1.108759    2.625272    1.908765
H    2.758304    3.005856    0.212867
C    2.504826    3.255562   -2.310265
O    3.800576    2.703011   -2.192336
H    2.150317    3.248903   -3.359682
H    2.616263    4.312868   -2.007619
H    3.746514    1.783535   -2.487645
C    1.270417    3.841917    2.095740
O    1.699817    5.039264    1.467390
H    0.468978    4.024539    2.838798
H    2.150083    3.467921    2.648437
H    0.969504    5.350243    0.914456
```

Transition state 0000011000:
```
C   -0.010649   -0.001458   -0.062056
C    1.375789   -0.034332   -0.160945
C    2.253349    1.048631   -0.147430
C   -0.742003    1.562821   -1.309640
C    0.320512    2.209677   -1.929891
C    1.542262    2.602725   -1.373894
C   -0.870516    1.213846    0.156052
C   -0.379022    2.252431    1.133511
C    0.831415    2.812583    1.104906
C    1.888110    2.488802    0.090769
H   -0.552573   -0.933314   -0.251719
H    1.817627   -1.006518   -0.402662
H    3.305322    0.854159   -0.373189
H   -1.534674    1.173849   -1.958476
H    0.260102    2.309292   -3.017845
H   -1.101495    2.573360    1.889146
H    1.085755    3.565500    1.857612
H    2.793792    3.071060    0.304101
C    2.609711    3.186636   -2.275186
O    2.575348    2.724936   -3.604455
H    2.471232    4.282936   -2.332096
H    3.603463    3.028420   -1.808841
H    2.612866    1.758120   -3.573106
C   -2.313904    0.823588    0.501821
O   -3.177028    1.933440    0.545569
H   -2.661630    0.057541   -0.221998
H   -2.335747    0.363248    1.502765
H   -3.056875    2.434498   -0.273629
```

Transition state 0000100001:
```
C  -0.046864   0.058799   0.050010
C   1.347002   0.015339   0.119942
C   2.228432   1.091113   0.115187
C  -0.634060   1.424914  -1.415387
C   0.489566   1.985357  -2.030585
C   1.616757   2.479520  -1.379801
C  -0.893866   1.302222   0.060327
C  -0.496606   2.427988   0.967920
C   0.718694   2.977516   0.988905
C   1.864536   2.561063   0.100818
H  -0.580054  -0.886607  -0.077336
H   1.799993  -0.978183   0.039587
H   3.294198   0.866096  -0.000845
H  -1.384722   0.965494  -2.065702
H   2.462616   2.749450  -2.019081
H  -1.944388   1.036950   0.229776
H  -1.260340   2.797180   1.659696
H   0.940170   3.767745   1.711773
C   0.580506   1.846497  -3.548814
O   1.390205   2.820923  -4.167452
H   1.041437   0.874059  -3.798368
H  -0.442347   1.831582  -3.975496
H   1.049213   3.689450  -3.911320
C   3.093244   3.428974   0.407930
O   3.457674   3.388577   1.766229
H   3.927095   3.117405  -0.254223
H   2.862189   4.480174   0.171521
H   3.523252   2.459127   2.027566
```

Transition state 0000110000:
```
C  -0.011722   0.008178   0.000277
C   1.389017  -0.000724   0.045484
C   2.230077   1.098951   0.082713
C  -0.647065   1.403329  -1.368674
C   0.438119   2.037940  -2.002857
C   1.579120   2.558131  -1.375140
C  -0.894552   1.222609   0.100983
C  -0.527617   2.329083   1.042642
C   0.668150   2.920372   1.044577
C   1.795582   2.538737   0.128009
H  -0.524393  -0.944642  -0.153958
H   1.868365  -0.977314  -0.079480
H   3.300212   0.929112  -0.054118
H  -1.396679   0.945927  -2.020297
H  -1.933916   0.915128   0.266701
H  -1.296841   2.659200   1.747590
H   0.864050   3.730305   1.754368
H   2.663734   3.166355   0.361188
C   0.459429   1.876773  -3.512708
O   1.350027   0.832561  -3.925721
H  -0.561496   1.672993  -3.881516
H   0.812534   2.783138  -4.023768
H   1.157511   0.060592  -3.372743
C   2.766265   3.037458  -2.200174
O   3.573665   2.018933  -2.745358
H   2.387170   3.720969  -2.988686
H   3.423486   3.646257  -1.560047
H   2.985800   1.462175  -3.290320
```

Transition state 0000100010:
```
C  -0.054307   0.009559   0.006148
C   1.334074   0.012144   0.046160
C   2.175669   1.127632   0.067291
C  -0.702281   1.442428  -1.439851
C   0.411744   2.035611  -2.026073
C   1.532317   2.524747  -1.344999
C  -0.937896   1.229599   0.031509
C  -0.592739   2.335423   0.986468
C   0.596439   2.948002   1.036855
C   1.745568   2.565182   0.141537
H  -0.560432  -0.947562  -0.143897
H   1.825189  -0.959660  -0.067667
H   3.250408   0.956657  -0.032853
H  -1.435129   1.000520  -2.119005
H   2.380855   2.857924  -1.950221
H  -1.978949   0.923261   0.192401
H  -1.380151   2.656863   1.677724
H   2.610204   3.191640   0.387979
C   0.510529   1.963333  -3.547613
O  -0.735259   2.003948  -4.207452
H   1.191458   2.760890  -3.906939
H   0.969852   1.001320  -3.837336
H  -1.194704   2.802501  -3.911955
C   0.875575   4.059728   2.013738
O   2.023579   3.804662   2.804939
H   1.097647   4.993657   1.467197
H  -0.024540   4.249716   2.631534
H   1.897938   2.943041   3.226466
```

Transition state 0001010000:
```
C   0.031170  -0.028410   0.000725
C   1.413996   0.020091  -0.044424
C   2.218980   1.163919  -0.090719
C  -0.770328   1.396053  -1.434524
C   0.300144   2.040818  -2.037228
C   1.484483   2.528292  -1.458576
C  -0.893568   1.160188   0.053114
C  -0.543124   2.298788   0.971240
C   0.634050   2.929415   0.956522
C   1.757877   2.588854   0.024475
H  -0.449399  -1.005099  -0.105540
H   1.930638  -0.935647  -0.180959
H   3.288226   1.023417  -0.266827
H   0.258142   2.075261  -3.131145
H  -1.911298   0.816555   0.282035
H  -1.311898   2.617395   1.682440
H   0.807705   3.753517   1.655805
H   2.607048   3.257564   0.203896
C  -1.895110   0.853481  -2.291651
O  -1.545161   0.578823  -3.626898
H  -2.334565  -0.033407  -1.790734
H  -2.705567   1.605526  -2.339928
H  -0.797640  -0.035840  -3.607522
C   2.540437   3.150597  -2.341945
O   2.722192   4.530840  -2.068671
H   3.525266   2.688666  -2.168354
H   2.281477   2.971787  -3.403912
H   1.858778   4.958786  -2.153998
```

Transition state 0010010000:
```
C  -0.026007   0.011421  -0.068498
C   1.369989  -0.004002  -0.045961
C   2.245247   1.075572   0.015459
C  -0.737457   1.450931  -1.393438
C   0.341449   2.096426  -1.999125
C   1.524332   2.553818  -1.420072
C  -0.912790   1.214860   0.081838
C  -0.507962   2.308842   1.025878
C   0.692698   2.892079   1.012337
C   1.803310   2.518120   0.070881
H  -0.538578  -0.936424  -0.251974
H   1.844854  -0.975873  -0.215985
H  -1.511964   1.037316  -2.043864
H   0.296524   2.142582  -3.095528
H  -1.942168   0.899088   0.289778
H  -1.257384   2.640446   1.751379
H   0.904961   3.691275   1.729729
H   2.673719   3.151102   0.286112
C   3.737742   0.794341  -0.080447
O   4.117406  -0.021612  -1.156304
H   4.289528   1.755703  -0.075947
H   4.039469   0.264707   0.842180
H   3.931256   0.505263  -1.957312
C   2.637676   2.952469  -2.359421
O   3.231255   1.854384  -3.068273
H   2.246887   3.686297  -3.090490
H   3.463628   3.436642  -1.820263
H   2.508457   1.349606  -3.468853
```

Transition state 0011000000:
```
C   0.006174  -0.009575  -0.128880
C   1.397219   0.006356  -0.130923
C   2.247050   1.112170  -0.060773
C  -0.771947   1.490936  -1.409965
C   0.307202   2.176592  -1.971551
C   1.468915   2.612628  -1.342701
C  -0.905337   1.173239   0.060198
C  -0.522101   2.217567   1.068892
C   0.672188   2.812995   1.106448
C   1.777285   2.534746   0.128510
H  -0.488162  -0.964020  -0.330547
H   1.895768  -0.946327  -0.333778
H   0.278154   2.268922  -3.061481
H   2.266225   3.012040  -1.975757
H  -1.924915   0.824017   0.268709
H  -1.276765   2.485325   1.815142
H   0.873859   3.558467   1.882147
H   2.636981   3.176904   0.359871
C   3.741102   0.908835  -0.197402
O   4.116101  -0.197845  -0.983384
H   4.202907   1.848688  -0.562879
H   4.173709   0.726805   0.804721
H   3.683666  -0.096197  -1.843396
C  -1.890170   1.004613  -2.307455
O  -1.500877   0.712029  -3.628747
H  -2.391623   0.140888  -1.825128
H  -2.658654   1.796723  -2.388153
H  -0.774017   0.074872  -3.577241
```

Transition state 0010100000:
```
C  -0.193275   0.128241  -0.062356
C   1.208500   0.014839  -0.084910
C   2.148144   1.033236  -0.091196
C  -0.795036   1.515583  -1.330875
C   0.295649   2.114612  -1.996647
C   1.440019   2.599487  -1.388614
C  -0.993443   1.380793   0.153021
C  -0.479158   2.415472   1.105340
C   0.766725   2.893967   1.085553
C   1.801616   2.501845   0.069954
H  -0.772614  -0.787958  -0.201380
H   1.598117  -0.981681  -0.317464
H  -1.591397   1.094388  -1.950151
H   2.257904   2.903357  -2.049735
H  -2.038141   1.136937   0.377205
H  -1.176320   2.764837   1.873019
H   1.067163   3.629818   1.837841
H   2.720500   3.072252   0.255180
C   3.551072   0.687053  -0.558123
O   3.568057  -0.065537  -1.750475
H   4.141332   1.621694  -0.649957
H   4.061463   0.070259   0.203593
H   2.975357   0.366807  -2.391659
C   0.424142   1.828724  -3.480109
O   1.235564   0.670847  -3.693865
H  -0.570417   1.700460  -3.947094
H   0.933090   2.651775  -4.003495
H   0.847077  -0.051014  -3.177812
```

Transition state 0100100000:
```
C   0.063199   0.000508  -0.022496
C   1.459447   0.018984   0.015383
C   2.253344   1.165408   0.110540
C  -0.601211   1.404694  -1.421201
C   0.510294   2.023066  -2.000389
C   1.595952   2.557772  -1.302490
C  -0.860467   1.189120   0.046895
C  -0.561020   2.299331   1.010867
C   0.614677   2.927402   1.073037
C   1.782813   2.593890   0.192343
H  -0.417993  -0.958178  -0.235211
H   3.335064   1.034240   0.009841
H  -1.316905   0.927508  -2.097619
H   2.455159   2.888368  -1.892702
H  -1.891612   0.844558   0.190222
H  -1.366548   2.596954   1.689293
H   0.757437   3.731176   1.801917
H   2.629536   3.244995   0.440594
C   2.169992  -1.253586  -0.410778
O   2.222061  -1.371895  -1.825191
H   3.186413  -1.283032   0.028324
H   1.632035  -2.142829  -0.047429
H   2.590397  -0.549017  -2.185767
C   0.701325   1.798638  -3.490108
O   1.441702   0.614440  -3.748129
H  -0.283541   1.770053  -3.996112
H   1.274963   2.623819  -3.939814
H   1.021247  -0.117939  -3.268855
```

Isomers of methyl(n-pentyl)-bullvalene **5h**

Isomer 0000000012:

```
C  -1.221115   0.495997   0.095935
C   0.099069  -0.150633   0.026852
C   1.287825   0.471485  -0.013678
C  -1.542889   1.815031  -0.598781
C  -0.563066   2.563321  -1.402449
C   0.754701   2.656976  -1.164559
C  -1.424644   1.767173   0.929838
C  -0.324515   2.420528   1.660234
C   0.974085   2.551701   1.307345
C   1.511408   1.979852  -0.026959
H  -2.062392  -0.200892   0.131553
H   0.091688  -1.244918   0.056443
H   2.186331  -0.152939  -0.002646
H  -2.570438   1.881712  -0.965368
H  -0.975026   3.126691  -2.245836
H   1.343016   3.303641  -1.822590
H  -2.383407   1.808826   1.453110
H  -0.621703   2.854571   2.620854
C   1.917465   3.272683   2.235878
H   1.387350   3.618111   3.135617
H   2.749522   2.627084   2.562658
H   2.375669   4.153536   1.756243
C   3.023820   2.251720  -0.209768
C   3.633519   1.718932  -1.509050
H   3.200272   3.338658  -0.160076
H   3.570616   1.811113   0.639941
C   5.130780   2.010867  -1.622353
H   3.470906   0.630415  -1.586590
H   3.113805   2.154850  -2.379216
C   5.761322   1.490324  -2.915465
H   5.299137   3.101734  -1.547945
H   5.657803   1.568653  -0.755995
C   7.257333   1.783140  -3.022304
H   5.589915   0.400773  -2.988049
H   5.233203   1.933978  -3.779206
H   7.681946   1.396888  -3.962834
H   7.455053   2.867938  -2.987359
H   7.814679   1.321211  -2.189783
```

Isomer 0000000102:

```
C  -0.055150  -0.008149  -0.020464
C   1.417830  -0.030398  -0.030554
C   2.228546   1.039800  -0.001407
C  -0.851250   1.062297  -0.786687
C  -0.187932   2.135030  -1.547771
C   0.945840   2.771937  -1.207495
C  -0.867854   1.029927   0.744445
C  -0.265835   2.102056   1.572938
C   0.881175   2.739574   1.272103
C   1.758696   2.488263   0.051711
H  -0.515719  -0.999143  -0.043914
H   1.873299  -1.023722  -0.094471
H   3.308168   0.868288  -0.052148
H  -1.767572   0.687152  -1.249588
H  -0.681775   2.423092  -2.481186
H   1.327878   3.551141  -1.876168
H  -1.798552   0.632109   1.158897
H   1.205647   3.537165   1.948084
C  -1.057046   2.468610   2.802881
H  -0.570607   3.273612   3.373322
H  -2.075129   2.803260   2.534431
H  -1.177274   1.597539   3.471553
C   2.975662   3.439107   0.076011
C   3.923764   3.296153   1.267003
H   3.544866   3.286787  -0.858468
H   2.597112   4.476138   0.037341
C   5.100950   4.271462   1.210275
H   3.372539   3.451118   2.210477
H   4.312408   2.264404   1.319636
C   6.061080   4.145293   2.394667
H   5.660679   4.116682   0.268736
H   4.716359   5.307524   1.161138
C   7.233616   5.123341   2.332554
H   5.498746   4.298844   3.333851
H   6.443576   3.109257   2.441431
H   7.906120   5.008783   3.197843
H   7.834202   4.968837   1.420126
H   6.880856   6.168558   2.319834
```

Isomer 0000000021:

```
C  -0.116186   0.018949  -0.044767
C   1.336299  -0.023391   0.192273
C   2.162521   1.032426   0.281564
C  -0.773563   1.049495  -0.967499
C   0.000723   2.076320  -1.682424
C   1.082645   2.719753  -1.217142
C  -0.992130   1.133054   0.542411
C  -0.434158   2.211371   1.376838
C   0.757678   2.837809   1.269073
C   1.751444   2.494019   0.136751
H  -0.596183  -0.962765  -0.066314
H   1.763632  -1.022868   0.321588
H   3.222956   0.843000   0.481044
H  -1.630652   0.661558  -1.523808
H  -0.365550   2.338429  -2.680115
H   1.544782   3.475966  -1.860657
H  -1.979795   0.795084   0.866648
H  -1.075912   2.510059   2.213309
C   1.151817   3.823870   2.345814
C   1.995048   3.190219   3.466318
H   1.699294   4.680215   1.921121
H   0.236781   4.243154   2.796866
C   2.462878   4.196050   4.517422
H   1.396833   2.395182   3.945207
H   2.870806   2.676672   3.033126
C   3.273955   3.566368   5.651711
H   3.068690   4.981679   4.027744
H   1.584485   4.717918   4.941617
C   3.742604   4.577525   6.697337
H   2.665765   2.782624   6.139044
H   4.148317   3.042969   5.223310
H   4.323236   4.094499   7.499643
H   4.381764   5.353668   6.243292
H   2.886702   5.091020   7.167213
C   3.021136   3.361059   0.164435
H   2.785276   4.426033   0.023223
H   3.580643   3.251017   1.103674
H   3.684998   3.053971  -0.658851
```

Isomer 0000000120:

```
C   0.428110   0.099619  -0.139099
C   1.599994   0.565749  -0.901047
C   1.864911   1.844716  -1.214247
C  -0.966737   0.730752  -0.292911
C  -1.237505   1.844615  -1.218623
C  -0.403530   2.866790  -1.465029
C  -0.181182   0.916472   1.001577
C   0.368271   2.211972   1.491967
C   0.885928   3.174883   0.691311
C   0.966116   3.003982  -0.828673
H   0.404648  -0.980652   0.026046
H   2.299240  -0.211780  -1.224553
H   2.771661   2.074434  -1.782955
H  -1.783293   0.008294  -0.214685
H  -2.203916   1.815987  -1.731838
H  -0.711099   3.642177  -2.173574
H  -0.555020   0.288645   1.814960
H   1.421184   3.918217  -1.232092
C   0.319890   2.308641   2.999738
H   0.939859   1.514420   3.453145
H   0.674309   3.267228   3.394486
H  -0.709827   2.151343   3.366125
C   1.504730   4.460310   1.191632
C   3.042952   4.460954   1.093834
H   1.113213   5.297109   0.585195
H   1.213656   4.674953   2.228984
C   3.715441   3.396817   1.960999
H   3.346128   4.311451   0.041493
H   3.418312   5.461215   1.375277
C   5.239144   3.374729   1.831552
H   3.439813   3.559068   3.019965
H   3.312533   2.404925   1.691481
C   5.902006   2.304903   2.698532
H   5.507433   3.210707   0.771701
H   5.645233   4.369184   2.093311
H   6.997848   2.305841   2.582563
H   5.679126   2.463637   3.767345
H   5.537967   1.297776   2.433771
```

Isomer 0000000201:
```
C  -0.045527   0.005638  -0.003383
C   1.426102  -0.009960   0.056351
C   2.233171   1.065091   0.080225
C  -0.821326   1.062406  -0.802661
C  -0.146976   2.116600  -1.581107
C   0.975117   2.764652  -1.230045
C  -0.881027   1.066557   0.721996
C  -0.274533   2.120730   1.567633
C   0.871497   2.763255   1.270569
C   1.754306   2.512870   0.054256
H  -0.502728  -0.986963  -0.018376
H   1.886002  -1.002910   0.080108
H   3.315888   0.904021   0.123255
H  -1.727932   0.674563  -1.274136
H  -0.620865   2.375714  -2.533163
H   1.373626   3.526948  -1.908194
H  -1.823125   0.678459   1.117495
H   1.233233   3.515795   1.980128
C  -0.988526   2.389228   2.873759
C  -0.987629   1.169616   3.819484
H  -0.515789   3.251261   3.369744
H  -2.036856   2.679381   2.676337
C   0.393888   0.551264   4.059174
H  -1.436098   1.471793   4.783031
H  -1.655020   0.391795   3.410002
C   1.402715   1.478052   4.740908
H   0.274417  -0.359948   4.672923
H   0.814122   0.217254   3.094211
C   2.767252   0.820253   4.942522
H   1.530952   2.391818   4.137406
H   0.996267   1.809233   5.714622
H   3.479884   1.499683   5.437502
H   2.687096  -0.089362   5.561838
H   3.204478   0.522272   3.974616
C   2.966021   3.452220   0.108485
H   2.642734   4.504985   0.093527
H   3.547995   3.284579   1.028480
H   3.629837   3.283445  -0.754170
```

Isomer 0000000210:
```
C  -0.161154   0.059628  -0.170511
C   1.306880  -0.052567  -0.123644
C   2.163333   0.976505  -0.013234
C  -0.880503   1.211726  -0.894277
C  -0.157544   2.282146  -1.602670
C   0.990651   2.844050  -1.193712
C  -0.920916   1.119275   0.628011
C  -0.282357   2.088712   1.561682
C   0.909126   2.692628   1.334662
C   1.724876   2.427208   0.065726
H  -0.680217  -0.899368  -0.246524
H   1.710076  -1.068515  -0.183037
H   3.237847   0.769643   0.012660
H  -1.811486   0.907094  -1.379279
H  -0.615502   2.634218  -2.532478
H   1.438590   3.636400  -1.801476
H  -1.882921   0.756156   0.999056
H   2.633516   3.040559   0.132780
C  -1.077003   2.261582   2.841828
C  -0.973962   1.043325   3.779436
H  -0.764165   3.161870   3.388449
H  -2.138944   2.418173   2.581645
C   0.445150   0.762497   4.274125
H  -1.643688   1.200412   4.644166
H  -1.357288   0.146051   3.260341
C   0.545655  -0.465391   5.180458
H   1.112317   0.630048   3.404311
H   0.827011   1.648413   4.815429
C   1.969209  -0.744520   5.661257
H  -0.121917  -0.334588   6.052040
H   0.159172  -1.346990   4.636753
H   2.015071  -1.635752   6.307740
H   2.649908  -0.912845   4.809647
H   2.369388   0.106981   6.237473
C   1.588881   3.636286   2.292494
H   1.009402   3.855773   3.196711
H   2.558947   3.216777   2.615071
H   1.814760   4.595132   1.792695
```

Isomer 0000001002:
```
C  -0.057004  -0.007458  -0.032728
C   1.416182  -0.019326  -0.035512
C   2.226306   1.051409  -0.004406
C  -0.859256   1.067451  -0.786063
C  -0.204882   2.156946  -1.530574
C   0.930051   2.793632  -1.193701
C  -0.904524   0.997884   0.748411
C  -0.261801   2.065408   1.549066
C   0.874482   2.725841   1.276140
C   1.755775   2.499547   0.054941
H  -0.506616  -1.002994  -0.082352
H   1.876299  -1.010758  -0.097476
H   3.306225   0.880805  -0.050280
H  -1.765892   0.686367  -1.264007
H  -0.708089   2.459784  -2.454392
H   1.300398   3.585764  -1.853582
H  -0.806009   2.348517   2.456752
H   1.184201   3.512703   1.970874
C  -2.188548   0.459998   1.355134
H  -2.931024   1.266086   1.477900
H  -2.639425  -0.319566   0.722234
H  -1.997240   0.019677   2.347964
C   2.967496   3.455360   0.084599
C   3.916956   3.308912   1.274099
H   3.536293   3.311729  -0.851505
C   2.584555   4.491071   0.052768
C   5.092487   4.286383   1.220088
H   3.366425   3.459344   2.218896
H   4.307315   2.277615   1.322170
C   6.054271   4.157254   2.402791
H   5.651262   4.135829   0.277317
C   7.225956   5.136397   2.341812
H   5.493214   4.307527   3.343256
H   6.437654   3.121387   2.445777
H   7.899735   5.019851   3.205821
H   7.825370   4.984917   1.428111
H   6.872396   6.181373   2.332575
```

Isomer 0000001020:
```
C   0.268659   0.057978   0.083619
C   1.670882   0.350416  -0.265344
C   2.176584   1.558866  -0.563494
C  -0.918481   0.790254  -0.564824
C  -0.743091   1.840753  -1.583945
C   0.242842   2.752239  -1.617133
C  -0.608006   0.997916   0.922080
C  -0.074504   2.291879   1.413208
C   0.783069   3.130254   0.800549
C   1.350836   2.831029  -0.583807
H   0.074299  -1.000864   0.275633
H   2.344355  -0.512596  -0.276197
H   3.241131   1.642283  -0.804027
H  -1.784159   0.145598  -0.740348
H  -1.497346   1.860381  -2.377172
H   0.259367   3.482285  -2.432353
H  -0.432589   2.581988   2.407997
H   2.013588   3.661213  -0.863875
C  -1.557284   0.324576   1.898570
H  -1.931954  -0.632585   1.504749
H  -1.051798   0.120529   2.857232
H  -2.428057   0.969306   2.104022
C   1.258264   4.393194   1.470675
C   2.736938   4.340243   1.885577
H   1.112331   5.248801   0.783876
H   0.639658   4.597657   2.361026
C   3.239431   5.640278   2.513527
H   2.875641   3.503386   2.592684
H   3.361470   4.095992   1.007265
C   4.707523   5.588370   2.941160
H   3.096489   6.471539   1.797676
H   2.612459   5.890089   3.389964
C   5.204265   6.891527   3.566022
H   4.846518   4.756850   3.655909
H   5.331001   5.336040   2.063881
H   6.263218   6.823181   3.862739
H   5.108837   7.734177   2.860382
H   4.621301   7.149975   4.466249
```

Isomer 0000001200:
```
C   0.254737  -0.078166  -0.033774
C   1.708750   0.163378  -0.006411
C   2.306205   1.364736   0.018574
C  -0.729404   0.815451  -0.802660
C  -0.294847   2.001983  -1.561477
C   0.704915   2.833296  -1.223575
C  -0.792117   0.743720   0.735262
C  -0.386645   1.926523   1.563661
C   0.637548   2.751503   1.261167
C   1.529887   2.666553   0.039506
H  -0.001268  -1.140111  -0.077125
H   2.334888  -0.734579  -0.017471
H   3.399255   1.418016   0.028932
H  -1.538036   0.261939  -1.287661
H  -0.846990   2.197048  -2.486426
H   0.936280   3.679704  -1.877787
H   0.828672   3.586052   1.944635
H   2.249817   3.494613   0.090773
C  -1.934489  -0.108692   1.272256
H  -2.164945  -0.924395   0.570953
H  -1.671130  -0.570134   2.237216
H  -2.857637   0.473130   1.412404
C  -1.234226   2.272751   2.773692
C  -2.479000   3.103084   2.419101
H  -1.543601   1.367086   3.319072
H  -0.619456   2.854462   3.479852
C  -3.368558   3.408231   3.623870
H  -2.145855   4.044930   1.948850
H  -3.072888   2.583156   1.647135
C  -4.589613   4.265448   3.284633
H  -3.704757   2.458292   4.080709
H  -2.768934   3.917216   4.401809
C  -5.476387   4.564503   4.492785
H  -4.250103   5.213432   2.828926
H  -5.184131   3.755025   2.504875
H  -6.345571   5.183080   4.217086
H  -5.858774   3.634645   4.946937
H  -4.916226   5.105064   5.274476
```

Isomer 0000002010:
```
C   0.018511   0.009822  -0.240698
C   1.492248   0.026701  -0.244208
C   2.269478   1.114760  -0.117875
C  -0.829746   1.124551  -0.873923
C  -0.229292   2.296819  -1.535748
C   0.893413   2.931143  -1.158309
C  -0.833917   0.922335   0.647465
C  -0.205904   1.928840   1.537807
C   0.907584   2.655549   1.325203
C   1.724955   2.521522   0.043321
H  -0.410808  -0.987496  -0.371266
H   1.976039  -0.948566  -0.359928
H   3.356862   0.991810  -0.134699
H  -1.736366   0.758106  -1.362955
H  -0.763543   2.665876  -2.417159
H   1.234271   3.792619  -1.741050
H  -0.741027   2.101446   2.478343
H   2.579087   3.209038   0.115485
C  -2.078246   0.267934   1.236568
H  -1.788426  -0.627306   2.443658
H  -2.797601   1.057416   1.521923
H  -2.578276  -0.331547   0.456504
C  -3.038208  -1.286323   3.027641
H  -1.063113  -1.406241   2.146806
H  -1.285263  -0.037979   3.230281
C  -2.753659  -2.181425   4.235407
H  -3.764088  -0.503241   3.317006
H  -3.540320  -1.882271   2.242253
C  -4.006937  -2.835882   4.815262
H  -2.027718  -2.962320   3.943775
H  -2.251150  -1.583480   5.017543
H  -3.769823  -3.472188   5.682998
H  -4.736000  -2.077167   5.146713
H  -4.510343  -3.468730   4.064809
C   1.402830   3.656229   2.331354
H   0.757422   3.699400   3.221882
H   2.428345   3.409907   2.660789
H   1.450255   4.668536   1.891059
```

Isomer 0000002001:
```
C  -0.005565   0.000964  -0.251421
C   1.467381   0.005322  -0.276700
C   2.264973   1.079342  -0.157753
C  -0.845565   1.131833  -0.859318
C  -0.233416   2.301702  -1.512968
C   0.906090   2.915859  -1.152886
C  -0.839796   0.908520   0.660586
C  -0.180696   1.896133   1.545255
C   0.938495   2.597657   1.303899
C   1.773691   2.509449   0.032982
H  -0.446244  -0.990569  -0.387598
H   1.937436  -0.974400  -0.409627
H   3.349686   0.932173  -0.197382
H  -1.763483   0.786017  -1.342093
H  -0.774734   2.688862  -2.382145
H   1.244202   3.776885  -1.739654
H  -0.690745   2.074256   2.497874
H   1.280978   3.304029   2.068075
C  -2.084986   0.263110   1.255729
C  -1.792713  -0.648236   2.450169
H  -2.792090   1.057740   1.557016
H  -2.600296  -0.321792   0.474559
C  -3.043725  -1.299858   3.039817
H  -1.078889  -1.431699   2.137841
H  -1.275362  -0.072842   3.238039
C  -2.757065  -2.209469   4.236185
H  -3.758631  -0.512138   3.343481
H  -3.559244  -1.882928   2.253474
C  -4.011540  -2.857194   4.820972
H  -2.041558  -2.994561   3.930407
H  -2.241697  -1.624142   5.019477
H  -3.772908  -3.503918   5.680523
H  -4.730172  -2.094634   5.166057
H  -4.527679  -3.478040   4.069155
C   2.976055   3.455492   0.139939
H   2.642593   4.496073   0.278696
H   3.612765   3.181224   0.995859
H   3.589585   3.410073  -0.773721
```

Isomer 0000002100:
```
C  -0.135690   0.112689   0.051424
C   1.297510   0.015070  -0.277268
C   2.151616   1.044426  -0.407411
C  -1.011216   1.272495  -0.437243
C  -0.509295   2.371186  -1.282678
C   0.706644   2.930867  -1.197477
C  -0.734148   1.118160   1.062665
C   0.188311   2.046360   1.797624
C   1.256660   2.655191   1.241070
C   1.743645   2.490053  -0.184518
H  -0.647451  -0.853272   0.055388
H   1.674182  -1.000018  -0.439003
H   3.195342   0.840044  -0.665932
H  -2.023305   0.957981  -0.705011
H  -1.207392   2.739431  -2.041354
H   0.972578   3.739822  -1.884899
H   1.875693   3.280945   1.892312
H   2.633958   3.121186  -0.309536
C  -1.957162   0.611333   1.828157
C  -3.096963   1.630134   1.940949
H  -2.347551  -0.283317   1.314193
H  -1.663398   0.265056   2.832065
C  -4.276553   1.126496   2.772674
H  -2.723202   2.573827   2.372422
H  -3.447219   1.891506   0.926975
C  -5.435413   2.121499   2.860576
H  -4.644941   0.173268   2.348597
H  -3.926970   0.882615   3.793548
C  -6.608396   1.615505   3.699180
H  -5.062507   3.073889   3.279770
H  -5.784536   2.360807   1.839495
H  -7.425729   2.353100   3.742984
H  -7.023051   0.681855   3.282734
H  -6.295269   1.402022   4.735230
C  -0.036457   2.225927   3.282960
H   0.700970   2.926574   3.699683
H  -1.039358   2.609974   3.524778
H   0.073803   1.268284   3.820638
```

Isomer 0000010020:
```
C  -0.760849   0.495163   0.068766
C   0.478010  -0.276686   0.270645
C   1.723985   0.224906   0.271027
C  -0.836397   1.682119  -0.899010
C   0.314056   2.134814  -1.703965
C   1.607809   2.161312  -1.327915
C  -0.931254   1.919370   0.609473
C   0.121665   2.623191   1.365159
C   1.451319   2.560886   1.157739
C   2.049357   1.690381   0.055941
H  -1.673261  -0.105606   0.105927
H   0.347975  -1.351228   0.434221
H   2.564404  -0.456789   0.434727
H  -1.793970   1.760619  -1.420335
H   0.067934   2.484613  -2.712358
H  -1.943477   2.135776   0.960895
H  -0.237837   3.272981   2.170367
H   3.141833   1.794313   0.106275
C   2.688734   2.652589  -2.249170
H   2.287004   2.953311  -3.228643
H   3.215322   3.520677  -1.815012
H   3.453219   1.872520  -2.414721
C   2.413575   3.373582   1.987403
C   3.188669   4.433650   1.184029
H   1.859178   3.868805   2.802488
H   3.143051   2.695295   2.468264
C   2.295060   5.443418   0.464645
H   3.873066   4.964942   1.869097
H   3.841327   3.935633   0.444654
C   3.074534   6.486877  -0.337207
H   1.604416   4.905766  -0.207973
H   1.650416   5.953464   1.205021
C   2.173491   7.478913  -1.071530
H   3.758874   7.033599   0.337281
H   3.724805   5.969402  -1.066692
H   2.758722   8.216109  -1.644502
H   1.504696   6.959051  -1.778094
H   1.534822   8.035321  -0.364790
```

Isomer 0000012000:
```
C   0.008353  -0.044817  -0.242020
C   1.482065  -0.043971  -0.263788
C   2.272237   1.037907  -0.167975
C  -0.825357   1.078791  -0.868189
C  -0.220672   2.241193  -1.547131
C   0.916787   2.880652  -1.211603
C  -0.833195   0.878217   0.653361
C  -0.184048   1.882359   1.527868
C   0.930612   2.585306   1.270032
C   1.744663   2.450688  -0.002162
H  -0.433363  -1.037935  -0.362985
H   1.953966  -1.025522  -0.375439
H   3.357883   0.903655  -0.201957
H  -1.740499   0.724135  -1.350175
H  -0.770333   2.602922  -2.422934
H  -0.697159   2.073005   2.476486
H   1.275629   3.308980   2.015296
H   2.606937   3.127707   0.073216
C   1.432339   4.053751  -1.995991
H   0.778263   4.299666  -2.846361
H   1.517470   4.950874  -1.356498
H   2.445481   3.851843  -2.388128
C  -2.080014   0.237964   1.250514
C  -1.792375  -0.656340   2.458891
H  -2.790707   1.034905   1.537261
H  -2.589951  -0.358579   0.474596
C  -3.044951  -1.301585   3.052161
H  -1.075996  -1.442980   2.160685
H  -1.279318  -0.069304   3.241039
C  -2.761987  -2.195326   4.261309
H  -3.761876  -0.510805   3.342901
H  -3.556880  -1.895365   2.271498
C  -4.018033  -2.836287   4.850168
H  -2.044892  -2.983822   3.968269
H  -2.249711  -1.599510   5.038713
H  -3.781959  -3.471923   5.718671
H  -4.738233  -2.069822   5.183162
H  -4.531374  -3.466909   4.104590
```

Isomer 0000010200:
```
C   0.120583  -0.069853   0.044114
C   1.591248   0.031261   0.009603
C   2.295838   1.173619  -0.021370
C  -0.786385   0.899286  -0.724080
C  -0.261368   2.011012  -1.539823
C   0.818603   2.772191  -1.272219
C  -0.766976   0.914671   0.807150
C  -0.250142   2.064553   1.586538
C   0.827780   2.788753   1.229428
C   1.659854   2.550053  -0.015971
H  -0.252172  -1.097182   0.066171
H   2.132831  -0.920005   0.001677
H   3.388566   1.120190  -0.052322
H  -1.675488   0.426443  -1.149355
H  -0.823339   2.222134  -2.455968
H  -1.642310   0.440895   1.259513
H   1.111734   3.636295   1.861893
H   2.469008   3.293376  -0.022225
C   1.253707   3.883988  -2.184223
H   0.594321   3.980583  -3.060238
H   1.260992   4.851387  -1.650483
H   2.284567   3.717901  -2.545549
C  -1.077867   2.451465   2.790840
C  -2.473770   2.983796   2.416119
H  -1.196241   1.577876   3.457832
H  -0.537902   3.220454   3.367731
C  -2.439616   4.205951   1.498544
H  -3.058126   2.182855   1.928075
H  -3.020824   3.229657   3.343969
C  -3.826142   4.745026   1.143829
H  -1.845371   5.006623   1.978435
H  -1.897385   3.950770   0.571291
C  -3.780721   5.955773   0.212294
H  -4.417418   3.938080   0.673016
H  -4.366520   5.009869   2.071336
H  -4.790930   6.321899  -0.032212
H  -3.224728   6.790802   0.671374
H  -3.275073   5.707886  -0.736284
```

Isomer 0000020100:
```
C   0.554398  -0.095731   0.470412
C   1.920799   0.437525   0.620580
C   2.316225   1.676906   0.288792
C  -0.339206   0.279347  -0.715848
C   0.082175   1.205783  -1.783995
C   0.842544   2.309130  -1.645190
C  -0.700321   0.754189   0.694712
C  -0.665522   2.180501   1.102137
C   0.257931   3.062394   0.671784
C   1.388644   2.731226  -0.283898
H   0.443769  -1.133041   0.796905
H   2.660209  -0.257338   1.031242
H   3.363936   1.954886   0.440200
H  -0.962187  -0.544920  -1.072830
H  -0.291672   0.964500  -2.784887
H  -1.525419   0.195400   1.145544
H   0.192830   4.096617   1.025961
H   1.977826   3.646660  -0.429300
C   1.134774   3.219761  -2.809756
C   0.475915   4.605962  -2.678311
H   2.228137   3.356216  -2.902991
H   0.793829   2.741590  -3.743798
C  -1.050079   4.561905  -2.606951
H   0.864662   5.116047  -1.778042
H   0.790336   5.230710  -3.533371
C  -1.694525   5.940653  -2.455858
H  -1.444536   4.068053  -3.515113
H  -1.355093   3.922176  -1.760864
C  -3.219544   5.887328  -2.372161
H  -1.291601   6.428322  -1.549064
H  -1.390803   6.584254  -3.301980
H  -3.658055   6.891781  -2.257498
H  -3.653112   5.435186  -3.280281
H  -3.548737   5.277926  -1.513535
C  -1.762965   2.599140   2.046628
H  -1.689155   3.665341   2.307219
H  -2.758020   2.421761   1.600802
H  -1.726922   2.012632   2.982008
```

Isomer 0000021000:
```
C  -0.242375  -0.013594   0.000635
C   1.160950  -0.112882  -0.440234
C   1.988463   0.916881  -0.684978
C  -1.175315   1.107200  -0.481341
C  -0.741825   2.158226  -1.421426
C   0.468502   2.746348  -1.486469
C  -0.756431   1.043124   0.991782
C   0.164589   2.063155   1.546226
C   1.186300   2.661453   0.913571
C   1.588396   2.370545  -0.518871
H  -0.737963  -0.981934   0.112563
H   1.539009  -1.129947  -0.585629
H   3.009552   0.707444  -1.019007
H  -2.203932   0.775036  -0.647545
H  -1.499952   2.473245  -2.147027
H  -0.032226   2.347859   2.585663
H   1.776481   3.403301   1.460855
H   2.462268   2.992633  -0.756379
C   0.791820   3.775966  -2.536641
C   1.790940   3.274290  -3.591063
H  -0.135980   4.096682  -3.040236
H   1.212168   4.676867  -2.049815
C   2.164588   4.333928  -4.627631
H   2.708849   2.914339  -3.091989
H   1.359371   2.391617  -4.095183
C   3.149696   3.836165  -5.687220
H   1.246546   4.698856  -5.125262
H   2.594966   5.213583  -4.113000
C   3.518873   4.900160  -6.720228
H   4.065245   3.471115  -5.186695
H   2.717090   2.956612  -6.197841
H   4.228746   4.512465  -7.468471
H   2.626143   5.257902  -7.260661
H   3.985206   5.777281  -6.240362
C  -1.818049   0.574838   1.971433
H  -2.444210   1.419909   2.303371
H  -2.481842  -0.178159   1.519686
H  -1.355156   0.123325   2.864913
```

Isomer 0000102000:
```
C  -0.116201   0.044801  -0.025516
C   1.325228  -0.145975  -0.269521
C   2.254061   0.824064  -0.309131
C  -0.883528   1.270835  -0.520905
C  -0.277555   2.374210  -1.305399
C   0.974449   2.831346  -1.115607
C  -0.684565   1.061921   0.983750
C   0.241037   1.921495   1.757398
C   1.387553   2.473445   1.327574
C   1.937145   2.290552  -0.074254
H  -0.696095  -0.881336  -0.070781
H   1.642783  -1.180278  -0.436214
H   3.296463   0.552401  -0.502900
H  -1.900162   1.031303  -0.842856
H   1.330023   3.653661  -1.745122
H  -0.048499   2.097783   2.798138
H   1.976105   3.072627   2.029679
H   2.873392   2.859669  -0.152563
C  -1.179922   2.973447  -2.353767
C  -0.682036   3.787164  -2.901521
H  -1.499341   2.210178  -3.085595
H  -2.100795   3.377573  -1.897004
C  -1.924381   0.617750   1.754577
C  -2.799287   1.767718   2.272718
H  -2.531742  -0.033896   1.103165
H  -1.608788  -0.009897   2.607197
C  -3.272032   2.749596   1.199211
H  -3.676822   1.334627   2.785701
H  -2.252113   2.330186   3.049679
C  -4.197570   3.842263   1.736889
H  -2.396043   3.223872   0.724990
H  -3.791231   2.197222   0.393506
C  -4.644999   4.831499   0.661334
H  -5.083323   3.375427   2.205485
H  -3.680223   4.385986   2.548430
H  -5.305149   5.612081   1.072435
H  -3.778653   5.334965   0.199734
H  -5.195864   4.320076  -0.146365
```

Isomer 0000100200:
```
C   0.090656  -0.013284  -0.006492
C   1.564403   0.049345  -0.036605
C   2.295678   1.174534  -0.025805
C  -0.804192   0.992799  -0.738121
C  -0.279297   2.126796  -1.537025
C   0.828388   2.823536  -1.214091
C  -0.770746   0.962553   0.793851
C  -0.231448   2.078909   1.606481
C   0.866178   2.784448   1.273550
C   1.683523   2.561411   0.014308
H  -0.306181  -1.031781  -0.016093
H   2.080058  -0.915621  -0.070074
H   3.387284   1.099122  -0.051064
H  -1.706382   0.544364  -1.163900
H   1.132243   3.647503  -1.868421
H  -1.653511   0.492568   1.235311
H   1.166000   3.612544   1.924305
H   2.503127   3.292636   0.013068
C  -1.090032   2.470711  -2.760473
C  -0.651599   3.314674  -3.313180
H  -1.161435   1.608711  -3.447424
H  -2.124978   2.741717  -2.484309
C  -1.068716   2.464982   2.804518
C  -2.457577   3.004002   2.410891
H  -1.200422   1.592061   3.470063
H  -0.530684   3.230671   3.387414
C  -2.406835   4.191812   1.449788
H  -3.051887   2.194816   1.949287
H  -3.003216   3.287812   3.328619
C  -3.786147   4.722661   1.057132
H  -1.813095   5.007079   1.904744
H  -1.854880   3.900229   0.539305
C  -3.722715   5.881690   0.062937
H  -4.380218   3.896788   0.623836
H  -4.332136   5.039509   1.964767
H  -4.727507   6.243551  -0.208680
H  -3.161621   6.734777   0.480552
H  -3.212385   5.578228  -0.866941
```

Isomer 0000201000:
```
C   0.099787  -0.018161   0.038639
C   1.571545   0.069445   0.063862
C   2.293988   1.201463   0.043772
C  -0.779985   0.956605  -0.752009
C  -0.243079   2.065094  -1.578277
C   0.847829   2.786003  -1.255761
C  -0.829900   0.957543   0.779966
C  -0.263282   2.090384   1.550030
C   0.822400   2.817759   1.240569
C   1.670660   2.584813   0.004181
H  -0.277807  -1.044425   0.032700
H   2.100641  -0.888348   0.098007
H   3.386234   1.134540   0.064090
H  -1.652857   0.472954  -1.200314
H   1.161439   3.585311  -1.935521
H  -0.804819   2.340976   2.468769
H   1.120433   3.626885   1.914975
H   2.481731   3.325576   0.000765
C  -1.039723   2.383459  -2.822584
C  -2.396413   3.036552  -2.517948
H  -0.452710   3.053220  -3.472709
H  -1.210503   1.455681  -3.400923
C  -3.221741   3.338630  -3.768699
H  -2.980469   2.383231  -1.844851
H  -2.219773   3.968256  -1.951679
C  -4.568288   4.001234  -3.470788
H  -2.636423   3.989325  -4.445179
H  -3.392113   2.400858  -4.330418
C  -5.387988   4.301822  -4.725046
H  -5.150457   3.349129  -2.794109
H  -4.394069   4.936452  -2.908028
H  -6.350252   4.778521  -4.478206
H  -4.843747   4.980031  -5.403898
H  -5.607141   3.379426  -5.289175
C  -2.074222   0.350963   1.404924
H  -2.456333  -0.491697   0.808708
H  -1.861272  -0.023133   2.420218
H  -2.878359   1.102063   1.480938
```

Isomer 0001002000:
```
C  -0.016704  -0.012519  -0.307014
C   1.458084  -0.046696  -0.339813
C   2.280097   1.000139  -0.164920
C  -0.872447   1.131096  -0.868696
C  -0.223817   2.346419  -1.424463
C   0.932380   2.916301  -1.048432
C  -0.837986   0.852230   0.660529
C  -0.162710   1.806473   1.576167
C   0.977861   2.485736   1.376555
C   1.787966   2.411144   0.097226
H  -0.473179  -0.992464  -0.476274
H   1.901143  -1.030957  -0.523674
H   3.361640   0.839299  -0.211915
H  -0.767881   2.812378  -2.253337
H   1.270162   3.812255  -1.578936
H  -0.681045   1.967064   2.527579
H   1.329695   3.160918   2.162993
H   2.661265   3.069876   0.197632
C  -2.109246   0.738559  -1.664991
H  -2.504913  -0.246118  -1.386065
H  -2.916131   1.479310  -1.535687
H  -1.860396   0.695908  -2.737814
C  -2.028882   0.166592   1.325299
C  -1.617639  -0.792478   2.446790
H  -2.706595   0.940962   1.729071
H  -2.618795  -0.394452   0.587607
C  -2.804147  -1.472284   3.130261
H  -0.941467  -1.560316   2.029587
H  -1.020852  -0.251750   3.201976
C  -2.399247  -2.444442   4.240194
H  -3.477608  -0.700738   3.548487
H  -3.403934  -2.012613   2.373590
C  -3.589437  -3.119235   4.920923
H  -1.726872  -3.213910   3.818731
H  -1.798472  -1.902833   4.993483
H  -3.265768  -3.812733   5.713615
H  -4.260081  -2.374521   5.382106
H  -4.188842  -3.696452   4.196595
```

Transition states of methyl(n-pentyl)-bullvalene **5h**

Transition state 0000000012:
```
C  -0.045126  -0.015143   0.042701
C   1.345133  -0.005880   0.144508
C   2.172888   1.105071   0.173782
C  -0.648031   1.321963  -1.423182
C   0.458599   1.964442  -1.986145
C   1.565640   2.497477  -1.335893
C  -0.925116   1.195471   0.051197
C  -0.594437   2.384588   0.899131
C   0.577442   3.035781   0.950941
C   1.805916   2.571458   0.159526
H  -0.545206  -0.974751  -0.109675
H   1.844468  -0.976234   0.056685
H   3.245996   0.913497   0.090856
H  -1.360826   0.842107  -2.098428
H   0.520390   1.933840  -3.078951
H   2.401361   2.823766  -1.962165
H  -1.968627   0.901964   0.218322
H  -1.438653   2.813226   1.449706
C   0.633487   4.354912   1.684784
H  -0.327038   4.556362   2.180747
H   1.424355   4.399607   2.448102
H   0.823667   5.185571   0.983478
C   3.070849   3.399265   0.472076
C   3.716161   3.114145   1.832568
H   3.816757   3.186702  -0.313026
H   2.842831   4.471765   0.376255
C   4.815455   4.114371   2.191064
H   2.953177   3.109645   2.628446
H   4.138106   2.094964   1.833583
C   5.511367   3.812959   3.519620
H   5.568413   4.138788   1.380818
H   4.384701   5.132804   2.227567
C   6.601374   4.822589   3.876964
H   4.754495   3.782559   4.324674
H   5.944682   2.796969   3.478495
H   7.083229   4.579037   4.837440
H   7.389220   4.848743   3.105170
H   6.188944   5.842475   3.959408
```

Transition state 0000000102:
```
C  -0.013050  -0.006147  -0.017934
C   1.384187   0.001159   0.033952
C   2.218455   1.107090   0.069009
C  -0.682556   1.374003  -1.405966
C   0.400169   2.036838  -1.994035
C   1.524692   2.549236  -1.364261
C  -0.914361   1.190767   0.067466
C  -0.573717   2.327164   0.996887
C   0.629629   2.913120   1.002446
C   1.805397   2.558724   0.121253
H  -0.510139  -0.965238  -0.182948
H   1.872045  -0.969883  -0.099562
H   3.291764   0.931628  -0.051261
H  -1.416747   0.910379  -2.069410
H   0.418539   2.038839  -3.088771
H   2.341659   2.904913  -1.999498
H  -1.947178   0.866014   0.245618
H   0.782371   3.752003   1.689547
C  -1.685515   2.782741   1.901182
H  -1.374246   3.621721   2.541312
H  -2.565173   3.103757   1.314510
H  -2.026800   1.958736   2.553497
C   3.006030   3.462767   0.453884
C   3.572007   3.282470   1.862728
H   3.806269   3.266175  -0.281231
H   2.701239   4.513378   0.302222
C   4.779041   4.178038   2.144948
H   2.787850   3.484645   2.612881
H   3.856484   2.225786   2.010974
C   5.354865   4.006754   3.552011
H   5.570541   3.973140   1.399659
H   4.494187   5.236243   1.993558
C   6.561443   4.903076   3.827687
H   4.562046   4.212259   4.294332
H   5.636339   2.948247   3.700745
H   6.952903   4.757230   4.847285
H   7.382988   4.694422   3.121553
H   6.299223   5.969248   3.719954
```

Transition state 0000000021:
```
C  -0.172633   0.049514  -0.085345
C   1.197223  -0.001229   0.160479
C   2.086331   1.065675   0.263711
C  -0.570661   1.423074  -1.630870
C   0.622944   1.986175  -2.069551
C   1.673096   2.457196  -1.288346
C  -0.993893   1.304330  -0.196414
C  -0.687282   2.425901   0.749142
C   0.512019   2.981847   0.976288
C   1.768861   2.543826   0.219151
H  -0.694821  -0.891681  -0.275549
H   1.650703  -0.997777   0.146683
H   3.152023   0.822110   0.306046
H  -1.233022   0.971372  -2.373651
H   0.813323   1.940386  -3.146804
H   2.592372   2.729658  -1.814642
H  -2.061770   1.059752  -0.139847
H  -1.535442   2.790082   1.339703
C   0.626945   4.003414   2.088255
H   1.062451   3.387847   3.429460
H   1.319364   4.816207   1.819157
H  -0.357163   4.479765   2.230933
C   1.253313   4.422871   4.537560
H   0.303551   2.645814   3.733749
H   1.996244   2.814216   3.297659
C   1.647483   3.814509   5.884907
H   2.024134   5.153332   4.227218
H   0.321125   5.006304   4.658079
C   1.840026   4.854655   6.987817
H   0.875384   3.085738   6.192019
H   2.577236   3.229908   5.759363
H   2.123343   4.386533   7.944218
H   2.630928   5.576401   6.721976
H   0.914691   5.430421   7.158970
C   3.010743   3.366727   0.588706
H   3.883546   2.992467   0.032335
H   2.876873   4.425519   0.322733
H   3.246469   3.298692   1.659465
```

Transition state 0000000120:
```
C   0.710886   0.129200  -0.039982
C   1.813814   0.486841  -0.809402
C   2.122342   1.759851  -1.281347
C  -1.036643   1.035955  -0.842796
C  -0.696922   1.784162  -1.964270
C   0.376635   2.661387  -2.078260
C  -0.337191   1.071689   0.486219
C   0.097540   2.390816   1.092132
C   0.859813   3.276092   0.421436
C   1.348495   3.015424  -0.988483
H   0.538094  -0.934651   0.142581
H   2.440021  -0.333541  -1.174713
H   2.955623   1.858367  -1.982089
H  -1.832455   0.293525  -0.944754
H  -1.260707   1.578484  -2.879884
H   0.591161   3.081387  -3.064384
H  -0.953011   0.539901   1.222103
H   1.939951   3.879395  -1.314972
C  -0.368416   2.563736   2.515037
H   0.037129   1.753961   3.148353
H  -0.071802   3.516558   2.968369
H  -1.468784   2.485569   2.574339
C   1.386589   4.566359   1.008322
C   2.891117   4.501084   1.336684
H   1.218201   5.380693   0.280621
H   0.834318   4.849813   1.915335
C   3.244244   3.460036   2.399078
H   3.462130   4.282169   0.416078
H   3.227598   5.499618   1.668839
C   4.741894   3.372756   2.696730
H   2.698147   3.690085   3.333267
H   2.879771   2.470736   2.071435
C   5.085585   2.325051   3.754917
H   5.281741   3.143232   1.759758
H   5.110790   4.363326   3.020886
H   6.169733   2.278071   3.946572
H   4.586362   2.547810   4.713254
H   4.757138   1.320234   3.439777
```

Transition state 0000000201:
```
C   -0.428120   0.561908  -0.408166
C    0.858838   0.054437  -0.602968
C    2.063108   0.694157  -0.351171
C   -0.552364   2.509781  -1.123769
C    0.683632   2.909660  -1.641314
C    1.940067   2.711205  -1.085646
C   -0.783841   1.877896   0.219935
C    0.004951   2.383670   1.399644
C    1.341644   2.450429   1.390718
C    2.251241   2.067286   0.246172
H   -1.267943  -0.023601  -0.790420
H    0.920325  -0.904552  -1.127636
H    2.977999   0.205884  -0.700252
H   -1.432483   2.621448  -1.761962
H    0.665442   3.314056  -2.658639
H    2.809541   2.960718  -1.701429
H   -1.854315   1.892952   0.457909
H    1.839715   2.851602   2.280612
C   -0.804157   2.888211   2.568375
C   -1.642620   4.135325   2.230240
H   -1.482459   2.088598   2.919682
H   -0.126043   3.120930   3.406423
C   -0.811668   5.326450   1.753756
H   -2.389504   3.883485   1.455463
H   -2.226260   4.421590   3.123370
C   -1.648779   6.563808   1.426319
H   -0.063237   5.582444   2.527530
H   -0.229931   5.032451   0.862809
C   -0.811268   7.745946   0.939772
H   -2.396942   6.299096   0.656513
H   -2.229647   6.861960   2.318593
H   -1.437877   8.621565   0.705280
H   -0.077309   8.055057   1.703212
H   -0.246484   7.483954   0.029213
C    3.708442   2.302481   0.652597
H    4.397761   2.041745  -0.165679
H    3.868796   3.360982   0.911605
H    3.966787   1.686563   1.528436
```

Transition state 0000010002:
```
C    0.017283  -0.046842   0.037394
C    1.402819  -0.009512  -0.001150
C    2.221594   1.119806  -0.035583
C   -0.713127   1.391832  -1.381861
C    0.358965   2.039353  -1.979304
C    1.549289   2.539981  -1.417726
C   -0.891888   1.149447   0.092467
C   -0.534377   2.305076   0.977804
C    0.644654   2.928931   0.952251
C    1.828081   2.570977   0.084036
H   -0.472422  -1.015257  -0.094846
H    1.908515  -0.968445  -0.155694
H    3.286538   0.955643  -0.223168
H   -1.465755   0.952610  -2.042152
H    0.329360   2.059704  -3.074022
H   -1.919340   0.824444   0.298691
H   -1.320728   2.689227   1.635589
H    0.773561   3.808381   1.590952
C    2.592712   3.088248  -2.363985
H    2.289373   2.925860  -3.408438
H    2.738397   4.173082  -2.218524
H    3.578667   2.616749  -2.234053
C    3.031504   3.438586   0.500666
C    3.501884   3.185562   1.934642
H    3.879291   3.253879  -0.175217
H    2.763319   4.502808   0.376227
C    4.722389   4.021528   2.321397
H    2.683265   3.388242   2.646138
H    3.736631   2.112839   2.053226
C    5.205182   3.776531   3.752371
H    5.549433   3.812337   1.616909
H    4.487541   5.095157   2.194429
C    6.426407   4.612602   4.132864
H    4.377436   3.987164   4.453929
H    5.436184   2.702808   3.876642
H    6.749707   4.413996   5.167306
H    7.280500   4.396543   3.468808
H    6.212248   5.691759   4.051296
```

Transition state 0000001002:
```
C    0.244658  -0.450791  -0.281009
C    1.501866  -0.043319   0.166066
C    1.942207   1.248488   0.435626
C   -0.418651   0.836098  -1.798310
C    0.547087   1.812538  -2.039168
C    1.274189   2.542076  -1.105862
C   -0.979348   0.412863  -0.464634
C   -1.183907   1.490319   0.569970
C   -0.277746   2.396115   0.941095
C    1.123249   2.517214   0.395056
H    0.132757  -1.493798  -0.591260
H    2.274093  -0.819511   0.177553
H    3.010799   1.388088   0.624367
H   -0.770703   0.254240  -2.655062
H    0.867900   1.916222  -3.080932
H    2.108533   3.143810  -1.478144
H   -2.160301   1.499592   1.066078
H   -0.552261   3.103720   1.729718
C   -2.253285  -0.419310  -0.618229
H   -2.120191  -1.219499  -1.362925
H   -2.525076  -0.886816   0.341450
H   -3.090478   0.217392  -0.945620
C    1.862971   3.692453   1.055377
C    1.268890   5.068566   0.753355
H    1.882627   3.521216   2.146275
H    2.915964   3.675245   0.723370
C    2.047315   6.215052   1.400017
H    1.232949   5.219490  -0.340010
H    0.218630   5.107998   1.091358
C    1.461992   7.597624   1.105627
H    2.086147   6.060669   2.494749
H    3.098715   6.183757   1.057329
C    2.245895   8.738940   1.752237
H    1.421979   7.747370   0.011224
H    0.411974   7.626254   1.449748
H    1.800978   9.720302   1.522025
H    2.271927   8.633305   2.850061
H    3.291028   8.755034   1.399366
```

Transition state 0000010020:
```
C   -0.693952   0.478147  -0.370436
C    0.473901  -0.236416  -0.178190
C    1.737340   0.283510   0.127726
C   -0.208781   2.197791  -1.620526
C    1.144138   2.178333  -1.912124
C    2.225097   1.907560  -1.050525
C   -0.824668   1.974471  -0.262961
C   -0.173103   2.682603   0.892283
C    1.124422   2.590070   1.209514
C    2.077150   1.713240   0.438133
H   -1.570667  -0.059201  -0.742110
H    0.438228  -1.307365  -0.403377
H    2.583772  -0.407233   0.118415
H   -0.904361   2.291497  -2.459176
H    1.405881   2.279085  -2.971150
H   -1.887114   2.247168  -0.296508
H   -0.806379   3.361601   1.473633
H    3.067168   1.755883   0.909012
C    3.630131   1.886187  -1.595153
H    4.146569   2.834567  -1.356178
H    4.231412   1.077428  -1.150902
H    3.646478   1.757271  -2.687992
C    1.741243   3.431305   2.298739
C    2.752289   4.460656   1.758384
H    0.942831   3.955264   2.850419
H    2.256022   2.776802   3.026533
C    2.142476   5.453689   0.766446
H    3.190605   5.011215   2.610050
H    3.594398   3.928269   1.283641
C    3.133984   6.481639   0.208796
H    1.685858   4.898111  -0.071324
H    1.309777   5.983035   1.264053
C    4.212972   5.882733  -0.696379
H    2.571825   7.241810  -0.361269
H    3.611985   7.024548   1.045195
H    4.869341   6.664285  -1.111727
H    4.856201   5.169927  -0.155232
H    3.759032   5.341381  -1.543678
```

Transition state 0000010200:

```
C   0.346293   0.250242   0.635672
C   1.704612   0.294243   0.351420
C   2.436921   1.391816  -0.103082
C  -0.694833   1.272388  -0.947341
C   0.219626   1.742230  -1.879273
C   1.438206   2.396080  -1.649853
C  -0.606193   1.412404   0.547028
C  -0.178523   2.745325   1.116699
C   0.951203   3.348235   0.725175
C   1.921759   2.795895  -0.277318
H  -0.101352  -0.724961   0.844912
H   2.235541  -0.663250   0.370888
H   3.472281   1.220921  -0.408271
H  -1.521825   0.661878  -1.319877
H   0.016782   1.473198  -2.921696
H  -1.567667   1.125460   0.991781
H   1.208870   4.315695   1.170217
H   2.766880   3.488794  -0.378191
C   2.319889   2.774442  -2.811620
H   3.383455   2.579260  -2.601508
H   2.051246   2.227420  -3.728024
H   2.233133   3.857201  -3.023083
C  -1.075238   3.341116   2.170479
C  -1.056040   2.557117   3.492131
H  -0.777246   4.385541   2.363266
H  -2.114552   3.375202   1.791008
C  -2.005471   3.123501   4.547990
H  -1.312275   1.499188   3.302283
H  -0.023080   2.548617   3.882604
C  -1.979916   2.356423   5.871581
H  -1.753550   4.184144   4.735637
H  -3.036935   3.127960   4.148001
C  -2.931471   2.927366   6.922305
H  -2.230382   1.296866   5.680346
H  -0.947969   2.352994   6.267364
H  -2.890775   2.354681   7.862767
H  -2.681992   3.975680   7.158574
H  -3.975465   2.910928   6.566052
```

Transition state 0000020001:

```
C   0.013977  -0.042770   0.050403
C   1.391414   0.003856  -0.075420
C   2.207748   1.139111  -0.126500
C  -0.805047   1.469336  -1.272087
C   0.233454   2.125004  -1.912495
C   1.463996   2.592801  -1.407154
C  -0.890369   1.152124   0.195105
C  -0.473170   2.254369   1.122079
C   0.700019   2.884681   1.047786
C   1.819814   2.582563   0.078350
H  -0.480495  -1.009125  -0.080048
H   1.891179  -0.947260  -0.287349
H   3.261132   0.983175  -0.375497
H  -1.601927   1.063039  -1.901241
H   0.124761   2.177143  -2.997285
H  -1.904899   0.818387   0.446940
H  -1.199225   2.575963   1.875782
H   0.891791   3.704501   1.748246
C   2.491982   3.178393  -2.362394
C   2.280140   2.953279  -3.859648
H   2.559788   4.267907  -2.176514
H   3.489126   2.789263  -2.104310
C   3.426431   3.514958  -4.702864
H   2.172368   1.872383  -4.059657
H   1.335832   3.422002  -4.186489
C   3.233234   3.320150  -6.207966
H   3.547030   4.593216  -4.487153
H   4.376529   3.040554  -4.393021
C   4.383735   3.879042  -7.044186
H   3.109035   2.242495  -6.419956
H   2.284697   3.796969  -6.515614
H   4.216103   3.724484  -8.122129
H   4.508444   4.962412  -6.877454
H   5.339502   3.394464  -6.782021
C   3.024031   3.447918   0.473558
H   3.269060   3.256362   1.529776
H   3.922789   3.232257  -0.117533
H   2.788861   4.518610   0.366686
```

Transition state 0000012000:

```
C  -0.005172   0.024360   0.078225
C   1.377796   0.012845   0.010150
C   2.244367   1.110823  -0.071555
C  -0.707209   1.495669  -1.352095
C   0.380162   2.075842  -1.979327
C   1.591238   2.517742  -1.415012
C  -0.897674   1.246036   0.124844
C  -0.433073   2.340866   1.057645
C   0.769492   2.918910   1.027035
C   1.860822   2.559804   0.066656
H  -0.525121  -0.933376  -0.021331
H   1.844221  -0.968602  -0.125230
H   3.301536   0.910924  -0.261297
H  -1.482305   1.070093  -1.996872
H   0.349153   2.078135  -3.074429
H  -1.142094   2.659921   1.828036
H   1.003382   3.691504   1.766549
H   2.749525   3.171360   0.266358
C   2.676655   3.059509  -2.310115
H   3.679764   2.760049  -1.968293
H   2.559588   2.720781  -3.350690
H   2.657962   4.165908  -2.308499
C  -2.353421   0.858873   0.439081
C  -3.376850   1.970345   0.204436
H  -2.624399  -0.014407  -0.180035
H  -2.402323   0.517645   1.488406
C  -4.813310   1.537562   0.501022
H  -3.128492   2.848976   0.825038
H  -3.306997   2.318630  -0.841132
C  -5.847168   2.641301   0.269433
H  -5.069125   0.661399  -0.124091
H  -4.882056   1.186688   1.547918
C  -7.280648   2.202637   0.565922
H  -5.589019   3.515159   0.895169
H  -5.774143   2.990817  -0.776653
H  -8.000816   3.017781   0.389917
H  -7.577195   1.351816  -0.070687
H  -7.390345   1.880860   1.615448
```

Transition state 0000020010:

```
C  -0.522146   0.201771  -0.357616
C   0.800796  -0.218512  -0.328134
C   1.926809   0.558546  -0.051411
C  -0.613752   2.060456  -1.421609
C   0.662115   2.423599  -1.827412
C   1.855505   2.381161  -1.093153
C  -1.005277   1.594923  -0.046204
C  -0.417682   2.309099   1.138249
C   0.891981   2.502712   1.338941
C   1.933437   2.003989   0.366196
H  -1.275038  -0.500246  -0.725708
H   0.994347  -1.240631  -0.669916
H   2.908839   0.101119  -0.195510
H  -1.397334   2.026834  -2.183420
H   0.773133   2.665362  -2.890711
H  -2.098964   1.590186   0.041600
H  -1.125816   2.690154   1.882064
H   2.926794   2.264840   0.750126
C   3.145901   2.776556  -1.778204
C   3.332385   4.305115  -1.849894
H   4.002090   2.334209  -1.241431
C   3.298653   5.009623  -0.493623
H   4.290652   4.521390  -2.356339
H   2.541307   4.729448  -2.493654
C   3.528037   6.519350  -0.577821
H   2.322285   4.823056  -0.013701
H   4.058470   4.562633   0.175276
C   3.463612   7.211521   0.783258
H   4.508197   6.715704  -1.049755
H   2.774448   6.961254  -1.254903
H   3.627317   8.297777   0.698003
H   2.480974   7.057826   1.260645
H   4.228501   6.811587   1.470514
C   1.420756   3.213411   2.554379
H   0.609168   3.549286   3.217093
H   2.089216   2.552784   3.135538
H   2.022351   4.094359   2.268861
```

Transition state 0000020100:
```
C  -0.152898   0.011293  -0.172521
C   1.226816  -0.115733  -0.227219
C   2.172453   0.903332  -0.092402
C  -0.705746   1.740977  -1.344694
C   0.438525   2.328133  -1.861933
C   1.658195   2.585003  -1.215946
C  -0.910806   1.288692   0.075337
C  -0.449353   2.207318   1.184450
C   0.807273   2.666848   1.241615
C   1.889067   2.339269   0.255358
H  -0.756803  -0.860413  -0.438380
H   1.613882  -1.095944  -0.524410
H   3.218337   0.657811  -0.292178
H  -1.508910   1.498604  -2.045865
H   0.428258   2.524063  -2.939557
H  -1.971701   1.052031   0.228977
H   1.084836   3.336865   2.062734
H   2.818598   2.832476   0.565632
C   2.796828   3.217271  -1.982404
C   2.932241   4.728759  -1.713055
H   3.747256   2.727301  -1.712489
H   2.657558   3.049772  -3.063955
C   1.720598   5.554088  -2.145607
H   3.116195   4.892018  -0.635288
H   3.834671   5.099034  -2.232143
C   1.876895   7.052412  -1.879877
H   1.533522   5.390672  -3.223923
H   0.819772   5.182705  -1.626460
C   0.660214   7.871629  -2.308913
H   2.067902   7.209438  -0.802368
H   2.778005   7.424846  -2.401080
H   0.797834   8.945319  -2.102805
H   0.466145   7.760999  -3.389279
H  -0.248394   7.542173  -1.777227
C  -1.487269   2.578882   2.205600
H  -1.082087   3.252572   2.975508
H  -2.349376   3.078373   1.727819
H  -1.885209   1.678999   2.708402
```

Transition state 0000100002:
```
C   0.319079  -0.503351  -0.841084
C   1.586891  -0.109170  -0.412743
C   1.965701   1.142941   0.056543
C  -0.492887   0.974749  -2.080078
C   0.407999   2.036194  -2.231549
C   1.126282   2.642655  -1.200410
C  -0.930368   0.329637  -0.792322
C  -1.175420   1.214483   0.391861
C  -0.292623   2.098295   0.860132
C   1.080288   2.344671   0.281913
H   0.222581  -1.483559  -1.314779
H   2.397632  -0.823546  -0.589245
H   3.035427   1.323306   0.198232
H  -0.880407   0.512700  -2.992420
H   1.896557   3.363203  -1.493338
H  -1.808069  -0.302523  -0.974114
H  -2.154029   1.133207   0.875641
H  -0.580946   2.719568   1.713729
C   0.774130   2.425800  -3.653401
C   1.150344   3.458670  -3.704787
H   1.563621   1.762747  -4.050846
H  -0.091566   2.350996  -4.329419
C   1.812239   3.431052   1.089743
C   2.117938   3.051523   2.538986
H   2.759029   3.672342   0.575453
C   1.204257   4.352641   1.061486
C   2.870129   4.143855   3.300406
H   1.180855   2.817781   3.073698
H   2.708434   2.118523   2.556641
C   3.182550   3.776118   4.752267
H   3.813845   4.376137   2.771897
H   2.279243   5.078867   3.279753
C   3.935703   4.870643   5.507243
H   2.237974   3.544834   5.277706
H   3.770852   2.840505   4.769307
H   4.145631   4.576832   6.548230
H   4.900772   5.097407   5.023199
H   3.354671   5.808022   5.535505
```

Transition state 0000021000:
```
C  -0.099867  -0.042543  -0.161422
C   1.277929  -0.144816  -0.246029
C   2.220155   0.884097  -0.127803
C  -0.695774   1.713968  -1.292620
C   0.435760   2.317757  -1.811975
C   1.676447   2.557966  -1.192388
C  -0.899540   1.210478   0.117231
C  -0.372109   2.111515   1.211255
C   0.870744   2.594175   1.275156
C   1.943497   2.307095   0.270853
H  -0.690277  -0.922761  -0.433663
H   1.671565  -1.114615  -0.567884
H   3.261419   0.649438  -0.360636
H  -1.505747   1.484781  -1.992030
H   0.404699   2.537238  -2.884634
H  -1.082593   2.385874   1.998418
H   1.142941   3.247866   2.110183
H   2.875260   2.802391   0.570102
C   2.794018   3.203599  -1.979604
C   2.915755   4.717147  -1.716150
H   3.754794   2.725889  -1.725319
H   2.638052   3.031502  -3.058105
C   1.690223   5.529256  -2.134632
H   3.112714   4.885321  -0.641400
H   3.807053   5.095514  -2.248444
C   1.836773   7.030103  -1.877434
H   1.489493   5.359682  -3.209513
H   0.800040   5.152408  -1.601322
C   0.606859   7.836471  -2.292834
H   2.041488   7.193557  -0.803405
H   2.727115   7.408176  -2.412872
H   0.737767   8.912199  -2.093182
H   0.398784   7.719466  -3.369908
H  -0.291235   7.501273  -1.747100
C  -2.370460   0.882382   0.385721
H  -2.782610   0.232193  -0.401679
H  -2.478604   0.362324   1.350735
H  -2.971511   1.804971   0.417143
```

Transition state 0000100020:
```
C  -0.355783   0.028544  -0.136099
C   0.982284  -0.017726   0.240899
C   1.826744   1.068112   0.471780
C  -0.594285   1.469515  -1.685324
C   0.642662   2.030814  -2.001834
C   1.572719   2.491655  -1.064003
C  -1.177073   1.278128  -0.310442
C  -1.036225   2.377471   0.702596
C   0.124431   2.943845   1.054426
C   1.432875   2.518228   0.433652
H  -0.843390  -0.911627  -0.407082
H   1.453526  -1.005977   0.243464
H   2.888519   0.863225   0.631404
H  -1.173397   1.035878  -2.505729
H   2.553368   2.793902  -1.442580
H  -2.236352   1.008056  -0.403399
H  -1.957402   2.721245   1.185797
H   2.243877   3.125644   0.854738
C   1.090233   1.973257  -3.451252
C   1.747665   2.818809  -3.705977
H   1.652953   1.043585  -3.651090
H   0.232419   1.997005  -4.140341
C   0.203656   4.008623   2.117536
C   0.873036   3.521155   3.412133
H   0.770096   4.875819   1.727140
C  -0.810468   4.375450   2.349094
C   1.004926   4.611411   4.475615
H   0.289154   2.674303   3.813961
H   1.874011   3.112265   3.184296
C   1.654520   4.127731   5.773700
H   1.592155   5.454237   4.064872
H   0.004452   5.026355   4.700313
C   1.783053   5.222115   6.832574
H   1.066148   3.284913   6.179966
H   2.653334   3.712588   5.545569
H   2.253701   4.843776   7.754225
H   2.395902   6.062747   6.465348
H   0.795404   5.630881   7.105471
```

Transition state 0000120000:
```
C   0.122417   0.381709   0.781510
C   1.500724   0.558451   0.693005
C   2.171735   1.591070   0.045389
C  -0.722086   0.737291  -1.129710
C   0.266696   1.038409  -2.073348
C   1.335355   1.934848  -1.881400
C  -0.920886   1.323294   0.240816
C  -0.730668   2.801068   0.418189
C   0.364190   3.447900   0.014901
C   1.536237   2.773783  -0.636482
H  -0.248316  -0.556233   1.202747
H   2.120521  -0.262086   1.069238
H   3.258474   1.516363  -0.043666
H  -1.403382  -0.080426  -1.379589
H  -1.908528   1.031428   0.618670
H  -1.545192   3.358242   0.891927
H   0.435932   4.530250   0.163596
H   2.304731   3.528895  -0.843140
C   0.242468   0.207994  -3.347124
H  -0.679340  -0.388111  -3.406495
H   0.286823   0.832189  -4.253327
H   1.094987  -0.491835  -3.392537
C   2.377984   2.148710  -2.955954
H   2.001890   3.303089  -3.901276
H   3.346045   2.387149  -2.483721
H   2.550528   1.236139  -3.546231
C   3.065063   3.575287  -4.967543
H   1.037722   3.074616  -4.389453
H   1.824233   4.210136  -3.298595
C   2.695384   4.673388  -5.972077
H   4.017530   3.840254  -4.470612
H   3.263945   2.637747  -5.517475
C   2.538762   6.065746  -5.357803
H   3.471376   4.710202  -6.756636
H   1.758812   4.390840  -6.487170
H   2.334585   6.823315  -6.131384
H   1.709227   6.105445  -4.633745
H   3.456663   6.370879  -4.826512
```

Transition state 0000200001:
```
C  -0.222077   0.071118   0.097389
C   1.163874  -0.045279   0.078131
C   2.101283   0.986004   0.022099
C  -0.826147   1.522699  -1.339252
C   0.291227   2.015430  -2.013980
C   1.489363   2.410292  -1.408650
C  -0.995172   1.360880   0.147676
C  -0.492753   2.453652   1.044290
C   0.748648   2.940318   1.002565
C   1.831431   2.470944   0.061298
H  -0.813731  -0.842169  -0.005412
H   1.561102  -1.059513  -0.032690
H   3.146048   0.707434  -0.143408
H  -1.647284   1.131987  -1.947359
H   2.326350   2.635488  -2.076330
H  -2.047772   1.151956   0.374995
H  -1.201541   2.864880   1.770140
H   1.025237   3.740158   1.697612
C   0.259387   1.949693  -3.537466
C   0.323340   0.519369  -4.096525
H  -0.657976   2.439342  -3.906025
H   1.101718   2.536143  -3.940841
C   1.578655  -0.247855  -3.683571
H  -0.566398  -0.042305  -3.759956
H   0.256423   0.560668  -5.199242
C   1.630564  -1.676945  -4.224894
H   2.475385   0.305692  -4.021580
H   1.639431  -0.272512  -2.583378
C   2.878069  -2.441202  -3.782932
H   0.727228  -2.220454  -3.891788
H   1.577919  -1.656345  -5.329083
H   2.890186  -3.469924  -4.177807
H   3.797158  -1.939207  -4.129999
H   2.934927  -2.503841  -2.682843
C   3.112931   3.271533   0.304876
H   3.921087   2.945389  -0.368083
H   2.934119   4.344307   0.130278
H   3.457104   3.138993   1.342834
```

Transition state 0000200010:
```
C  -0.898188   0.398248   0.166363
C   0.383459  -0.115813  -0.023702
C   1.561943   0.609345  -0.168960
C  -1.215720   2.003553  -1.165350
C  -0.091122   2.204602  -1.971557
C   1.223855   2.241036  -1.505444
C  -1.247114   1.852657   0.331937
C  -0.360152   2.719659   1.177397
C   0.961935   2.845661   1.010500
C   1.696131   2.105141  -0.083019
H  -1.739345  -0.298393   0.124011
H   0.453495  -1.195154  -0.193101
H   2.466199   0.062163  -0.447700
H  -2.175379   1.868037  -1.671343
H   2.018691   2.287454  -2.255678
H  -2.282479   1.942785   0.682869
H  -0.846526   3.278135   1.984368
H   2.760703   2.367852  -0.035935
C  -0.291748   2.223958  -3.482686
C   0.201712   0.951294  -4.189160
H  -1.362992   2.368913  -3.701036
H   0.228354   3.097855  -3.910746
C  -0.475681  -0.326721  -3.696535
H   0.047344   1.061021  -5.278337
H   1.293017   0.856125  -4.046374
C   0.026486  -1.594490  -4.388214
H  -0.320312  -0.419006  -2.609293
H  -1.569969  -0.240124  -3.837028
C  -0.639284  -2.866990  -3.865476
H  -0.135659  -1.510185  -5.478670
H   1.121297  -1.668292  -4.252783
H  -0.256324  -3.767936  -4.371444
H  -0.463106  -2.989847  -2.783248
H  -1.731566  -2.836973  -4.017754
C   1.804856   3.725870   1.889689
H   1.203596   4.230706   2.660569
H   2.593060   3.139427   2.395431
H   2.322417   4.499083   1.293666
```

Transition state 0000210000:
```
C  -0.458830   0.286069   0.216302
C   0.879328  -0.049213   0.030244
C   1.949439   0.828990  -0.119192
C  -0.938706   1.853189  -1.141750
C   0.158750   2.184845  -1.943887
C   1.474097   2.390320  -1.482215
C  -1.002846   1.684630   0.350911
C  -0.264170   2.665581   1.212297
C   1.024596   2.959363   1.034307
C   1.883776   2.330582  -0.023934
H  -1.199391  -0.516397   0.170406
H   1.095705  -1.109880  -0.134695
H   2.922278   0.408575  -0.385867
H  -1.864194   1.603131  -1.666735
H  -2.053453   1.638712   0.663147
H  -0.827662   3.157575   2.011433
H   1.506564   3.690423   1.691446
H   2.900166   2.731773   0.069940
C  -0.100503   2.163339  -3.448436
C   0.301674   0.851962  -4.148266
H  -1.175629   2.336158  -3.619586
H   0.414185   3.006217  -3.936698
C  -0.426075  -0.389475  -3.632671
H   0.118027   0.961273  -5.233098
H   1.388019   0.689957  -4.039922
C  -0.020927  -1.675111  -4.355212
H  -0.233219  -0.501353  -2.553530
H  -1.518884  -0.244290  -3.729564
C  -0.732283  -2.916130  -3.817133
H  -0.222477  -1.570287  -5.437271
H   1.072959  -1.808673  -4.265874
H  -0.419366  -3.830050  -4.347403
H  -0.518838  -3.061353  -2.744501
H  -1.826684  -2.826185  -3.923902
C   2.605916   2.734565  -2.422324
H   2.711274   3.834346  -2.492218
H   3.565504   2.351434  -2.043256
H   2.479336   2.349824  -3.441021
```

Transition state 0001020000:
```
C  -0.057508  -0.072833  -0.163184
C   1.328484  -0.183047  -0.186885
C   2.257919   0.841219  -0.034297
C  -0.674895   1.600430  -1.334257
C   0.468778   2.229248  -1.832358
C   1.679476   2.526937  -1.199163
C  -0.845574   1.182394   0.107228
C  -0.376254   2.120947   1.181847
C   0.864490   2.609457   1.253381
C   1.948191   2.283975   0.266938
H  -0.643303  -0.950311  -0.448534
H   1.729858  -1.158764  -0.480397
H   3.308734   0.610003  -0.225623
H   0.450996   2.435886  -2.908421
H  -1.896683   0.922917   0.287967
H  -1.112084   2.417705   1.936271
H   1.122678   3.298063   2.064587
H   2.870222   2.801915   0.559278
C  -1.838312   1.324820  -2.251801
H  -1.562164   1.436076  -3.311150
H  -2.238924   0.307858  -2.113221
H  -2.670310   2.023076  -2.040335
C   2.791867   3.182736  -1.984783
C   2.904475   4.695908  -1.714485
H   3.755772   2.709254  -1.733638
H   2.636154   3.015630  -3.064007
C   1.671155   5.498893  -2.127158
H   3.102162   4.861358  -0.639438
H   3.791848   5.083512  -2.246704
C   1.801974   6.999434  -1.860383
H   1.471514   5.333989  -3.203009
H   0.785597   5.108446  -1.595830
C   0.563604   7.795549  -2.270485
H   2.005138   7.158218  -0.785356
H   2.688145   7.390434  -2.393449
H   0.683043   8.871336  -2.063977
H   0.356578   7.683245  -3.348283
H  -0.330852   7.447391  -1.726824
```

Transition state 0010200000:
```
C  -0.133842   0.045763   0.085304
C   1.246765  -0.043145   0.030394
C   2.187817   1.000102  -0.044422
C  -0.805704   1.537234  -1.352796
C   0.308205   2.023003  -2.025159
C   1.515196   2.399114  -1.412963
C  -0.939527   1.316425   0.133522
C  -0.463533   2.400771   1.059635
C   0.771877   2.905273   1.026324
C   1.827954   2.463097   0.058258
H  -0.703634  -0.882829  -0.007643
H   1.655988  -1.052798  -0.084176
H  -1.634498   1.159545  -1.959463
H   2.351407   2.638735  -2.074255
H  -1.984365   1.075384   0.366295
H  -1.177958   2.777209   1.798798
H   1.051806   3.688873   1.737658
H   2.739070   3.053815   0.215340
C   3.652195   0.671369  -0.182801
H   4.168518   1.373073  -0.856262
H   4.158050   0.741186   0.798783
H   3.809845  -0.345385  -0.573886
C   0.283548   1.967196  -3.548429
C   0.438694   0.545154  -4.113134
H  -0.662427   2.399092  -3.915701
H   1.088014   2.607157  -3.948412
C   1.734597  -0.146622  -3.691563
H  -0.418217  -0.068717  -3.782901
H   0.378419   0.586657  -5.216339
C   1.890640  -1.561863  -4.248044
H   2.599215   0.468563  -4.006206
H   1.777599  -0.183799  -2.591600
C   3.173878  -2.247954  -3.780320
H   1.016508  -2.166527  -3.943929
H   1.865161  -1.531709  -5.352942
H   3.265176  -3.269057  -4.184428
H   4.066601  -1.682069  -4.096606
H   3.205199  -2.319436  -2.679558
```

Transition state 0010020000:
```
C  -0.018951  -0.000078   0.002690
C   1.353516  -0.001763  -0.032268
C   2.244150   1.103818  -0.060340
C  -0.703407   1.551053  -1.454048
C   0.425886   2.106627  -2.002824
C   1.633262   2.501040  -1.366061
C  -0.894103   1.229129   0.008115
C  -0.530973   2.317576   0.983466
C   0.674030   2.892822   1.032656
C   1.816351   2.535920   0.132824
H  -0.531256  -0.960175  -0.108359
H   1.830992  -0.981761  -0.141004
H  -1.482299   1.200315  -2.137185
H   0.439932   2.178818  -3.095418
H  -1.935901   0.928333   0.178657
H  -1.309196   2.647632   1.679365
H   0.858727   3.683038   1.767749
H   2.689699   3.148121   0.387851
C   3.723942   0.825083  -0.046637
H   3.951882  -0.183602  -0.423576
H   4.297901   1.546254  -0.648716
H   4.117450   0.900379   0.984484
C   2.696872   3.165755  -2.210481
C   2.788298   4.689624  -1.982956
H   3.691475   2.734186  -2.008780
H   2.492481   2.955001  -3.272364
C   1.471699   5.451845  -2.163837
H   3.168724   4.877455  -0.963836
H   3.552630   5.099095  -2.668013
C   0.911735   5.432809  -3.588117
H   0.714673   5.040693  -1.472344
H   1.625129   6.502264  -1.857086
C  -0.400544   6.204375  -3.721195
H   1.665373   5.851740  -4.280461
H   0.750079   4.390839  -3.911177
H  -0.782345   6.185271  -4.754723
H  -1.178103   5.772827  -3.068792
H  -0.275242   7.261235  -3.430310
```

Transition state 0012000000:
```
C   0.581715  -0.383158  -0.052808
C   1.893973   0.016442  -0.259962
C   2.436885   1.307097  -0.186906
C  -0.787468   0.955453  -1.047285
C  -0.006444   1.931022  -1.663865
C   1.104749   2.605828  -1.158149
C  -0.565099   0.492394   0.376115
C  -0.308922   1.522193   1.439340
C   0.680261   2.417495   1.383335
C   1.648713   2.523202   0.241887
H   0.326058  -1.418176  -0.294645
H   2.572077  -0.757720  -0.635777
H  -0.219218   2.106566  -2.724807
H   1.673191   3.229473  -1.852553
H  -1.407063  -0.137901   0.684879
H  -0.977276   1.517068   2.306520
H   0.802900   3.132080   2.203675
H   2.337825   3.357737   0.423855
C   3.888907   1.533960  -0.519602
H   4.034789   2.435152  -1.136484
H   4.478152   1.685811   0.404864
H   4.323976   0.681198  -1.062474
C  -1.911402   0.307353  -1.823612
C  -3.220669   1.119286  -1.765527
H  -1.621583   0.182865  -2.880259
H  -2.099508  -0.706523  -1.430632
C  -3.768191   1.349329  -0.356471
H  -3.049891   2.098034  -2.248498
H  -3.983808   0.602748  -2.376035
C  -5.086500   2.125354  -0.335407
H  -3.910943   0.374989   0.148474
H  -3.020148   1.897206   0.243234
C  -5.622413   2.365955   1.075388
H  -4.941864   3.094145  -0.847456
H  -5.840839   1.580238  -0.931993
H  -6.569437   2.929057   1.061699
H  -5.808143   1.412982   1.599408
H  -4.901185   2.939144   1.682216
```

Transition state 0020100000:

```
C  -0.274253   0.390938   0.579179
C   1.095334   0.181218   0.718662
C   2.145098   1.049684   0.405887
C  -0.676629   1.290310  -1.300332
C   0.521078   1.451800  -2.000974
C   1.701602   1.966616  -1.460623
C  -0.946383   1.659645   0.135961
C  -0.415294   2.957859   0.670268
C   0.869047   3.311771   0.592586
C   1.928929   2.472702  -0.060163
H  -0.931945  -0.467492   0.739971
H   1.380968  -0.838454   0.992512
H  -1.485886   0.755147  -1.805072
H   2.595701   1.923352  -2.088341
H  -2.024103   1.594765   0.330221
H  -1.130557   3.627633   1.158292
H   1.188828   4.268717   1.017507
H   2.883298   3.012588  -0.021832
C   3.585011   0.580523   0.497998
C   3.871340  -0.866242   0.073821
H   4.212145   1.254885  -0.109250
H   3.928981   0.725725   1.541133
C   3.500522  -1.170256  -1.377860
H   4.946348  -1.066610   0.229997
H   3.344044  -1.570170   0.741422
C   3.803710  -2.606676  -1.805200
H   2.428390  -0.963035  -1.528725
H   4.035055  -0.467920  -2.045030
C   3.406783  -2.896472  -3.252414
H   4.880601  -2.814295  -1.665754
H   3.274382  -3.303601  -1.129667
H   3.627999  -3.937648  -3.537315
H   2.327639  -2.728686  -3.409073
H   3.945516  -2.236409  -3.953231
C   0.598456   0.857293  -3.396244
H   1.332681   1.387894  -4.021418
H   0.904991  -0.203443  -3.355577
H  -0.373887   0.901991  -3.909948
```

Transition state 0100200000:

```
C  -0.246098   0.094013   0.165752
C   1.127617  -0.117521   0.089058
C   2.089369   0.900640   0.000973
C  -0.822935   1.568566  -1.307614
C   0.305448   1.980059  -2.010933
C   1.532025   2.321482  -1.421741
C  -0.960759   1.420493   0.185383
C  -0.419198   2.511682   1.064879
C   0.841665   2.943765   1.001094
C   1.855575   2.387449   0.046455
H  -0.892914  -0.786234   0.102920
H   3.124182   0.597032  -0.178784
H  -1.677217   1.215701  -1.893621
H   2.373846   2.506548  -2.093985
H  -2.016714   1.252132   0.430965
H  -1.108503   2.961609   1.786552
H   1.174619   3.743334   1.670426
H   2.814127   2.901886   0.185475
C   1.605398  -1.549229  -0.080644
H   1.023045  -2.244054   0.543717
H   1.500506  -1.880817  -1.128379
H   2.664629  -1.658191   0.197300
C   0.251774   1.879871  -3.530557
C   0.392512   0.442901  -4.061910
H  -0.703135   2.300389  -3.887211
H   1.045376   2.509422  -3.967494
C   1.746378  -0.202849  -3.768179
H  -0.407577  -0.179365  -3.622744
H   0.215625   0.444750  -5.153076
C   1.844621  -1.659435  -4.223082
H   2.546249   0.388187  -4.253586
H   1.948038  -0.146564  -2.686740
C   3.203722  -2.291593  -3.924427
H   1.047621  -2.244253  -3.727470
H   1.632867  -1.724438  -5.306144
H   3.247921  -3.342238  -4.253671
H   4.016846  -1.747068  -4.433619
H   3.421558  -2.270175  -2.843298
```

2. Experimental section for chapter 3

Network Analysis of Substituted Bullvalenes

Oussama Yahiaoui,[a] Lukáš F. Pašteka,*[b] Christopher J. Blake,[c] Christopher G. Newton[d] and Thomas Fallon[a]*

[a] *O. Yahiaoui, Dr. T. Fallon*
Department of Chemistry, The University of Adelaide
Adelaide, SA 5005 (Australia)
Institute of Natural and Mathematical Sciences, Massey University
1/5 University Ave, Albany, Auckland 0632, (New Zealand)
E-mail: thomas.fallon@adelaide.edu.au

[b] Dept. of Physical and Theoretical Chemistry, Faculty of Natural Sciences, Comenius University, Ilkovičova 6, Bratislava, Slovakia
E-mail: lukas f.pasteka@gmail.com

[c] Research School of Chemistry, Australian National University, Canberra, ACT 0200, Australia

[d] *Department of Chemistry, The University of Adelaide*
Adelaide, SA 5005 (Australia)

Supporting Information

Table of Contents

1. General Information

NMR analysis was conducted using a *Bruker Advance III-HD* 300, 500, 700, 500 *Agilent*, and 600 MHz Oxford spectrometer. Chemical shifts are referenced to the residual solvent resonance as the internal standard (CHCl$_3$: δ = 7.26 ppm for ^{1}H NMR and δ = 77.16 ppm for ^{13}C NMR). Data are reported as follows: chemical shift, multiplicity (br s = broad singlet, s = singlet, d = doublet, t = triplet, q = quartet, m = multiplet). The assignment of signals was assisted correlated spectroscopy (COSY), heteronuclear single quantum coherence (HSQC), heteronuclear multiple bond correlation (HMBC), total correlated spectroscopy (TOCSY), distortonless enhancement of polarization transfer (DEPT), and HSQC-TOCSY. For VT-NMR experiments, the sample temperature was calibrated using the methanol shift method.[1] High-resolution mass spectroscopy was recorded using an Agilent 6230 TOF LC/MS (ESI) for samples containing a hydroxy or an aldehyde. For the other samples the high-resolution mass spectrometry was recorded using a *Micromass/Waters Autospec Premier* spectrometer (EI). The samples were analysed in positive mode and most of them using magnet scan. The data were collected in centroid mode, scanned in 2 s with an inter-scan delay of 0.2 s. The mass spectrometer is run at 70 eV with trap current 200 uA. Source temperature was kept at 150 degrees. Samples were introduced by direct insertion probe and dry-ice was used to cool the probe. PFK was used as a reference via heated reference inlet. Infra-red spectra were recorded using a *PerkinElmer spectrum 100* FTIR spectrometer equipped with a zinc selenide crystal. Melting points were recorded using an Electrothermal IA9300 capillary melting point apparatus and are uncorrected.

Cyclooctatetraene was obtained as a generous gift from Dr Graham Gream (The University of Adelaide). The material was manufactured by BASF, most likely sometime in the 1970s. Samples were purified by vacuum distillation using a short vigrex column (20 mbar/ 60 C) and stored in a freezer under an atmosphere of argon. All other chemicals were purchased from commercial suppliers and used as received.

All reactions were performed in flame-dried glassware using conventional Schlenk techniques under static pressure of nitrogen. Liquids and solutions were transferred with syringes. 1,2-dichloroethane, 2,2,2-trifluoroethane, and acetone were dried over 4 Å molecular sieves.

---

[1] Amman, C. Meier P.; Merbach, A. E. *J. Magn. Reson.* **1982**, *46*, 319-321.

2. Experimental Procedures

General procedure A: Under argon atmosphere, a 20 mL oven-dried sealed tube was charged with CoBr$_2$(dppe) (10 mol%), zinc iodide (20 mol%), and zinc dust (30 mol%). The tube was flushed with argon and evacuated under high-vacuum three times. Afterwards, the solvent (either 1,2-dichlorethane or trifluoroethanol) was added and the reaction mixture stirred for 15 min at room temperature. **2** (1.00 mmol, 1.00 eq) and the substituted acetylene (1-2 eq) were added to the solution and the reaction stirred for 16 - 24 h at either room temperature or 55 °C. After the reaction was complete, the suspension was filtered through a short pad of silica gel eluting with either hexane or ethyl acetate. The solvent was evaporated under vacuum, and the desired product was purified by column chromatography.

General procedure B: A 20 mL pyrex sealed tube charged with 36 mM of **4a-g** in dry acetone. The solution was flushed with argon and was placed in a water bath 2.5 cm away from a 150W high-pressure mercury emission lamp (Osram SUPRATEC HTT 150-211). The tube was irradiated for 3 – 10h. After the reaction was complete, the solvent was evaporated and the desired product was purified by flash column chromatography on silica gel.
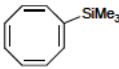
Synthesis of bromocyclooctatetraene
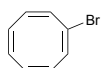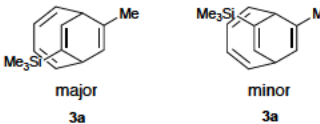
Prepared according to a reported procedure.[2] Under argon atmosphere an oven dried 250 mL two neck round bottom flask was equipped with a dropping funnel and a digital thermometer was charged with cyclooctatetraene (6.45 mL, 66.6 mmol, 1.00 eq) and dichloromethane (60 mL). The reaction mixture was cooled to -78 °C in a cooling bath of dry ice and acetone. Bromine (2.95 mL, 5.92 mmol, 0.10 eq) and dichloromethane (40 mL) were added to a dropping funnel. The solution of bromine was added slowly over one hour and the reaction stirred at -78 °C for another hour. Under argon atmosphere a solution of potassium *tert*-butoxide (9.00 g, 80.2 mmol, 1.20 eq) in tetrahydrofuran (40 mL) was prepared in an oven dried 100 mL round bottom flask. The potassium *tert*-butoxide solution was transferred into a dropping funnel, which was added slowly over one hour to the reaction solution. During the addition the temperature was maintained between -70 and -78 °C. The reaction was stirred for two hours at -78 °C and was quenched with an aqueous ammonium chloride solution and extracted with dichloromethane. The organic layer was washed with distilled water, aqueous sodium chloride solution, dried over MgSO$_4$ and the solvent was removed under vacuum. The product was obtained as a brown oil without any further purification (10.4 g, 85%). **IR** (ATR): v/cm^{-1} = 3006, 1623, 1372, 1214, 1048, 951, 916, 853, 806, 778, 727 **^{1}H NMR** (500 MHz, CDCl$_3$) = δ 6.22 (1H, s), 5.94 – 5.81 (5H, m), 5.66 – 5.61 (1H, m). **^{13}C NMR** (125 MHz, CDCl$_3$) δ 133.4 (CH), 132.9 (CH), 132.2 (CH), 131.0 (C), 121.5 (CH).

[2] Gasteiger, J.; Gream, G. E.; Huisgen, R.; Konz, W. E.; Schengg, U. *Chem. Ber.* **1971**, 104(8), 2412-2419

Synthesis of trimethylsilylcyclooctatetraene (2)

Under nitrogen atmosphere, an oven dried 250 mL round bottom flask was charged with bromocyclooctatetraene (4.00 g, 22.0 mmol, 1.00 eq) and anhydrous tetrahydrofuran (50 mL). The reaction mixture was cooled to -78 C in a cooling bath containing dry ice and acetone. N-butyllithium (22.0 mL, 2.00 M in cyclohexane, 26.2 mmol, 1.20 eq,) was added slowly over 20 min to the solution. The colour of the solution changed from brown to light dark brown. After 5 min, trimethylchlorosilane (3.33 mL, 26.22 mmol, 1.20 eq) was added and the reaction stirred for 2 hours at -78 C. The reaction was quenched with an aqueous ammonium chloride solution and extracted with dichloromethane. The organic layer was washed with distilled water, aqueous sodium chloride solution, dried over MgSO$_4$ and the solvent was removed under vacuum. The crude product was purified by column chromatography using hexane as eluent (R$_f$ = 0.59). The desired product was obtained as a yellow oil (3.00 g, 78%). **IR** (ATR): v/cm^{-1} = 2999, 2981, 2896, 2956, 1603, 1380, 1247, 1051, 952, 805, 708. **^{1}H NMR** (500 MHz, CDCl$_3$) δ = 6.12 – 5.91 (2H, m), 5.75 (5H, d, J = 12.7 Hz), 0.41 (9H, s). **^{13}C NMR** (125 MHz, CDCl$_3$) δ = 149.5 (C), 138.4 (CH), 134.8 (CH), 133.4 (CH), 132.0 (CH), 131.4 (CH), 131.4 (CH), 129.1 (CH), -1.7 (TMS). **HRMS** (EI, m/z) calculated for C$_{11}$H$_{16}$Si 176.1021 found 176.1022.

Synthesis of methyl-trimethylsilyl- bicyclo[4.2.2]deca-2,4,7,9-tetraene (3a)

The reaction was done according to **procedure A**, at room temperature for 16h using **2** (176 mg, 1.00 mmol, 1.00 eq), propyne (1.15 mL, of a 1.30 M solution in dichloromethane, 1.50 mmol, 1.50 eq) as the substituted acetylene, and 1,2-dichloroethane (4 mL) as the solvent. The silica pad was washed with hexane, which was removed in vacuo. The desired product was obtained without any further purification as a yellow oil (170 mg, 81%). **IR** (ATR): v/cm^{-1} = 3010, 2955, 1605, 1447, 1247, 1050, 834. **^{1}H NMR** (500 MHz, CDCl$_3$, isomer ratio 53:47) δ = 6.24 – 6.12 (4.1H, m), 5.93 (1H, d, J = 5.8 Hz, major), 5.90 (0.8H, d, J = 5.8 Hz), 5.72 – 5.62 (4.6H, m), 5.49 (1H, d, J = 6.2 Hz, major), 5.44 (1.4H, d, J = 6.1 Hz, minor), 3.30 (1H, d, J = 8.8 Hz, minor), 3.23 – 3.19 (2.2H, m, major), 3.12 – 3.08 (1.4H, dt, J = 8.9, 6.0 Hz, minor), 1.81 (2.4H, s, minor), 1.79 (4.5H, s, minor), 0.10 (7H, s, minor), 0.08 (9.1H, s, major). **^{13}C NMR** (125 MHz, CDCl$_3$) δ = 143.4 (CH, major), 142.8 (CH, minor), 141.8 (CH, minor), 141.2 (CH, major), 135.2 (C, minor), 134.9 (C, major), 132.8 (C, minor), 131.8 (C, major), 129.2 (CH, minor), 129.0 (CH, major), 125.0 (CH, major), 124.5 (CH, minor), 124.2 (CH, minor), 123.6 (CH, major), 119.0 (CH, major), 117.9 (CH, minor), 42.6 (CH, minor), 41.5 (CH, major), 37.4 (CH, major), 36.4 (CH, minor), 20.9 (CH$_3$, minor), 20.6 (CH$_3$, major), 1.0 (TMS, major) 1.0 (TMS, minor). **HRMS** (EI, m/z) calculated for C$_{14}$H$_{20}$Si 216.1334 found 216.1331.

Synthesis of hexyl-trimethylsilyl-bicyclo[4.2.2]deca-2,4,7,9-tetraene (3b)
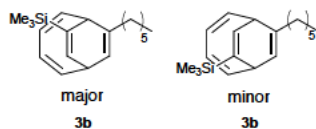
The reaction was done according to **procedure A,** at room temperature for 16h using **2** (176 mg, 1.00 mmol, 1.00 eq), oct-1-yne (221 µL, 1.50 mmol, 1.50 eq) as the substituted acetylene, and 1,2-dichloroethane (4 mL) as the solvent. The silica pad was washed with hexane, which was removed in vacuo. The desired product was obtained without any further purification as a yellow oil (246 mg, 86%). **IR** (ATR): v/cm^{-1} = 3010, 2924, 2854, 1601, 1456, 861, 679. **^{1}H NMR** (500 MHz, CDCl$_3$, ratio 59:41) δ = 6.22 – 6.17 (1.9H, m, major), 6.14 – 6.08 (1.8H, m, minor), 5.94 (0.6H, d, J = 5.8 H, minor), 5.90 (1H, d, J = 5.8 Hz, major), 5.68 – 5.60 (3.7H, m), 5.48 (0.8H, d, J = 6.3 Hz, minor), 5.43 (1H, d, J = 6.1 Hz, major), 3.32 (0.9H, d, J = 8.9 Hz, major), 3.25 (0.6H, dd, J = 8.8, 6.3 Hz, minor), 3.21 (0.9H, dd, J = 8.9, 5.9 Hz, minor), 3.13 (1.2H, dt, J = 8.9, 5.9 Hz, major), 2.08 (4.3H, dt, J = 15.1, 7.9 Hz), 1.42 – 1.39 (4.4H, m), 1.29 – 1.25 (12.9H, m), 0.88 (6.7H, t, J = 6.9 Hz), 0.11 (7H, s, major), 0.08 (5.5H, s, minor). **^{13}C NMR** (125 MHz, CDCl$_3$) δ 142.9 (CH, minor), 142.7 (CH, major), 141.2 (CH, major), 141.1 (CH, minor), 137.7 (C, major), 136.6 (C, minor), 135.6 (C, major), 134.7 (C, minor), 129.4 (C, minor), 129.2 (CH, major), 124.6 (CH, minor), 124.2 (CH, major), 124.1 (CH, major), 123.6 (CH, minor), 118 (CH, minor), 117.1 (CH, major), 41.4 (CH, major), 40.6 (CH, minor), 37.4 (CH, minor), 36.4 (CH, major), 36.2 (CH, major), 35.4 (CH$_2$, major), 35.3 (CH$_2$, minor), 32 (CH$_2$, major), 31.9 (CH$_2$, minor), 29.2 (CH$_2$), 29.1 (CH$_2$), 29.1 (CH$_2$), 22.8 (CH$_2$), 22.8 (CH$_2$), 14.2 (CH$_3$), -0.9 (TMS, minor), -1.0 (TMS, major). **HRMS** (ESI, m/z) calculated for C$_{19}$H$_{30}$Si 286.2117 found 286.2120.

Synthesis of benzyl-trimethylsilyl-bicyclo[4.2.2]deca-2,4,7,9-tetraene (3c)

The reaction was done according to **procedure A,** at room temperature for 16h using **2** (200 mg, 1.13 mmol, 1.00 eq), 3-phenyl-1-propyne (112 µL, 907 µmol, 0.80 eq) as the substituted acetylene, and 1,2-dichloroethane (4 mL) as the solvent. The silica pad was washed with hexane, which was removed in vacuo. The desired product was purified by column chromatography using hexane as eluent (R$_f$ = 0.37). The desired product was obtained as a yellow oil (250 mg, 83%). **IR** (ATR): v/cm^{-1} = 3010, 2953, 1604, 1494, 1245, 1046, 833. **^{1}H NMR** (500 MHz, CDCl$_3$, isomer ratio 55:45) δ = 7.30 – 7.27 (5H, m), 7.22 – 7.15 (6.6H, m), 6.23 – 6.18 (2.2H, m, minor), 6.04 – 5.98 (2.2H, m), 5.92 (0.8H, d, J = 5.7 Hz, minor), 5.89 (1H, d, J = 6.0 Hz, major), 5.72 – 5.63 (4.6H, m), 5.51 – 5.48 (2.2H, m), 3.54 – 3.41 (2H, m, minor), 3.54 – 3.44 (2.7H, m, major), 3.3 (0.8H, d, J = 9.18 Hz, minor), 3.25 (1H, dd, J = 8.7, 6.3 Hz, major), 3.22 (1.43H, m, major), 3.20 – 3.17 (0.7H, m, minor), 0.1 (8.63H, s, major), 0.02 (6.88H, s, minor). **^{13}C NMR** (125 MHz, CDCl$_3$) δ = 142.9 (CH, major), 142.6 (CH), 141.2 (CH, major), 141.1 (CH), 136.2 (C), 135.8 (C), 135.1 (C, major), 134.7 (C, major), 129.3 (CH), 129.1 (C, major), 129.1 (C), 128.3 (CH), 128. (CH), 126.1 (CH), 124.9 (CH, major), 124.5 (CH, minor), 124.4 (CH, minor), 123.8 (CH, major), 120.2 (CH, major), 119.5 (CH), 40.8 (CH$_2$), 40.5 (CH, minor), 39.2 (CH, major), 37.4 (CH, major), 36.5 (CH, minor), 0.9 (TMS, major), -1.2 (TMS, minor). **HRMS** (EI, m/z) calculated for C$_{20}$H$_{24}$Si 292.1647 found 292.1650.

Synthesis of methanol-trimethylsilyl-bicyclo[4.2.2]deca-2,4,7,9-tetraene (3d)
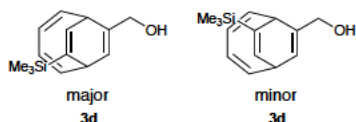
The reaction was done according to **procedure A,** at 55 C for 16h using **2** (300 mg, 1.70 mmol, 1.00 eq), prop-2-yn-1-ol (196 µL, 3.40 mmol, 2.00 eq) as the substituted acetylene, and trifluoroethanol (4 mL) as the solvent. The silica pad was washed with ethyl acetate, which was removed in vacuo. The desired product was purified by column chromatography using hexane/ethyl acetate (4:1) as eluents (R_f = 0.29). The desired product was obtained as a colourless oil (200 mg, 58%). **IR** (ATR): v/cm^{-1} = 3327, 3008, 2954, 1604, 1389, 1246, 1007, 833, 750, 689. **^{1}H NMR** (500MHz, CDCl$_3$, isomer ratio 60:40) δ = 6.20 – 6.12 (3.5H, m), 5.95 (1H, d, J = 5.7 Hz, major,), 5.89 (0.6H, d, J = 5.8 Hz, minor), 5.73 – 5.63 (6H, m), 4.17 – 4.07 (4.3H, m), 3.52 (0.7H, d, J = 8.9 Hz, minor), 3.41 (1.2H, dd, J = 8.9, 5.7 Hz, major), 3.30 (1.3H, dd, J = 8.9, 6.1 Hz, major), 3.18 (1H, dt, J = 8.9, 5.8 Hz, minor), 0.1 (4.8H, s, minor), 0.08 (9H, s, major). **^{13}C NMR** (125 MHz, CDCl$_3$) δ = 142.7 (CH, minor), 142.2 (CH, major), 141.1 (CH, major), 140.5 (CH, minor), 137.1 (C, minor), 136 (C, major), 135.1 (C, minor), 135 (C, major), 128.9 (CH, minor), 128.8 (CH, major), 124.9 (CH, major), 124.6 (CH, minor), 124.4 (CH, minor), 124.1 (CH, major), 119.9 (CH, major), 118.7 (CH, minor), 65.1 (CH2, minor), 64.8 (CH2, major), 38.5 (CH, minor), 37.5 (CH, major), 37 (CH, major), 36 (CH, minor), -1.0 (TMS). **HRMS** (EI, m/z) calculated for ([M+Na]$^+$) C$_{14}$H$_{20}$SiONa 255.1176 found 255.1173.
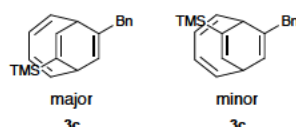
Synthesis of bis(trimethylsilyl)-bicyclo[4.2.2]deca-2,4,7,9-tetraene (3e)
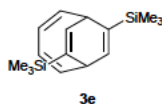
The reaction was done according to **procedure A**, at room temperature for 16 h using **2** (200 mg, 1.13 mmol, 1.00 eq), ethynyltrimethylsilane (314 µL, 2.00 mmol, 2.27 eq), as the substituted acetylene, and 1,2-dichloroethane (4 mL) as the solvent. The silica pad was washed with hexane, which was removed under vacuum. The desired product was obtained without any further purification as a yellow oil (300 mg, 96%). **IR** (ATR): v/cm^{-1} = 2953, 1594, 1387, 1245, 1083, 827. **^{1}H NMR** (500 MHz, CDCl$_3$) δ = 6.10 (2H, d, J = 9.0 Hz), 5.97 (2H, d, J = 5.96 Hz), 5.63 (2H, m), 3.34 (2H, d, J = 6.22 Hz), 0.09 (18H, s, TMS). **^{13}C NMR** (125 MHz, CDCl$_3$) δ = 141.2 (CH), 134.8 (C), 130.2 (CH), 124.1 (CH), 37.9 (CH), -1.0 (TMS). **HRMS** (ESI, m/z) calculated for C$_{16}$H$_{26}$Si$_2$ 274.1573 found 274.1580.

Synthesis ofdimethanol-trimethylsilyl-bicyclo[4.2.2]deca-2,4,7,9-tetraene (3f)
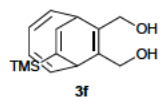
The reaction was done according to **procedure A**, at 55 C for three days using **2** (300 mg, 1.70 mmol, 1.00 eq), but-2-yne-1,4-diol (293 mg, 3.40 mmol, 2.00 eq) as the substituted acetylene, and trifluoroethanol (4 mL) as the solvent. The silica pad was washed with ethyl acetate, which was removed in vacuo. The desired product was purified by column chromatography using hexane/ethyl acetate (3:2) as eluents (R_f = 0.20). The desired product was obtained as a colourless powder (150 mg, 43%). **M.p** 40 C. **IR** (ATR): v/cm^{-1} = 3301, 2954, 2924, 2857, 1457, 1377, 1103, 723. 687. **^{1}H NMR** (500MHz, CDCl$_3$) δ = 6.20 (2H, d, J = 9.2 Hz), 5.95 (1H,

d, $J = 6.0$ Hz), 5.64 (2H, m), 4.35 – 4.16 (4H, m), 3.52 (1H, d, $J = 9.3$ Hz), 3.41 (1H, dd, $J = 8.9$, 5.6 Hz, m), 0.01 (9H, s). ^{13}C NMR (126MHz, CDCl$_3$) δ = 142.7 (CH), 141.1 (CH), 135.3 (C), 133.8 (C), 132.6 (C), 128.9 (CH), 125.1 (CH), 124.6 (CH), 61.1 (CH$_2$), 60.8 (CH$_2$), 40.6 (CH), 39.3 (CH), -1.0 (TMS). **HRMS** (ESI, m/z) calculated for ([M+Na]$^+$) C$_{15}$H$_{22}$SiO$_2$Na 285.1281 found. 285.1288.

Synthesis of methanol-*tert*-butyl(methoxy)dimethylsilane-trimethylsilyl-bicyclo[4.2.2]deca-2,4,7,9-tetraene (3g)
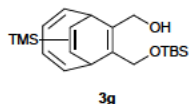
Under nitrogen atmosphere an oven dried round bottom flask was charged with **3f** (850 mg, 3.24 mmol. 1.00 eq) and tetrahydrofuran (24 mL). The solution was cooled to 0 °C an ice bath and NaH (388 mg, 60% dispersion in mineral oil, 9.27 mmol, 3.00 eq) was added in small portions. After completion of the addition, the reaction stirred for 30 min. *Tert*-butyldimethylsilyl chloride (488 mg, 3.24 mmol, 1.00 eq) in THF (24 mL) was added dropwise at 0 °C. The reaction mixture stirred for 16 h at room temperature and was quenched with water. The aqueous phase was extracted with dichloromethane. The combined organic layers were washed with a saturated sodium chloride solution, dried over Mg$_2$SO$_4$, and the solvent was evaporated under vacuo. The residue was purified by flash chromatography on silica gel eluting with 10% ethyl acetate in hexane to give the title compound as a colourless oil and as a 1:1 mixture of regioisomers (770 mg, 61%). **IR** (ATR): v/cm^{-1} = 3398, 3012, 2942, 2927, 2856, 1610, 1462, 1386, 1361, 1246, 1125, 1069, 1003, 881, 832, 774, 748, 689. ^{1}**H NMR** (600 MHz, CDCl$_3$) δ = 6.19 (1.9H, d, $J = 10.5$ Hz), 6.12 (2.3H, d, $J = 6.1$ Hz), 5.95 (2H, d, $J = 5.7$ Hz), 5.64 – 5.57 (4.2H, m), 4.35 – 4.24 (5.3H, m), 4.12 (2.4H, dd, $J = 12.2$, 6.6 Hz), 3.73 (1H, br, OH), 3.59 (1H, d, $J = 9.0$ Hz), 3.50 (1H, d, $J = 9.0$ Hz), 3.43 (1H, dd, $J = 9.1$, 5.9 Hz), 3.40 (1H, dd, $J = 9.0$, 5.8 Hz), 0.91 (30H, s), 0.09 (30H, TMS). ^{13}**C NMR** (150 MHz, CDCl$_3$) δ = (151 MHz, CDCl$_3$) δ = 142.8 (CH, major), 142.7 (CH, minor), 141.3 (CH, minor), 141.2 (CH, major), 135.2 (C, minor), 135 (C, major), 133.5 (C, major), 132.5 (C, minor) 132.2 (C, minor), 131.2 (C, major), 129.2 (CH, major), 129 (CH, minor), 124.9 (CH, major), 124.8 (CH), 124.4 (CH, minor), 124.4 (CH, major), 61.1 (CH$_2$), 60.7 (CH$_2$), 60.3 (CH$_2$), 60.1 (CH$_2$), 40.4 (CH, minor), 39.1 (CH, major), 38.9 (CH, major), 37.9 (CH, minor), 26.1 (CH$_3$, minor) , 26 (CH$_3$, major) , -1 (TMS, major), -1 (TMS, minor), -5.1 (CH$_3$, major), -5.2 (CH$_3$, minor). **HRMS** (ESI, m/z) calculated for ([M+Na]$^+$) C$_{21}$H$_{36}$Si$_2$O$_2$Na 399.2146 found 399.2159.

Synthesis of methyl-trimethylsilyl bullvalene (4a)
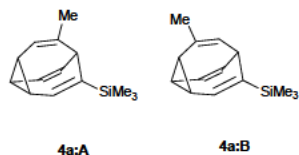
The reaction was done according to **procedure B**, using **3a** (163 mg, 0.75 mmol) in dry acetone (20 mL). After 8 h the solvent was evaporated under vacuum. The crude material was purified by flash chromatography using hexane as eluent (R$_f$ = 0.5). The desired product was obtained as a green oil (49 mg, 30%). **IR** (ATR): v/cm^{-1} = 3022, 2954, 1608, 1437, 1246, 1042. ^{1}**H NMR** (700 MHz, CDCl$_3$ – 60 °C, isomer **4a:A**, **4a:B** ratio 67:33) δ = 6.30 (1H, d, $J = 6.5$ Hz, **4a:A**), 6.26 (0.4H, dd, $J = 5.5$, 2.4 Hz, **4a:B**), 5.94 – 5.82 (4.9H, m), 5.75 (1.1H, d, $J = 7.5$ Hz, **4a:A**), 5.57 (0.6H, d, $J = 8.7$ Hz, **4a:B**), 2.45 (0.8H, t, $J = 8.7$ Hz, **4a:B**), 2.39

(1.3H, d, $J = 8.6$ Hz, **4a:A**), 2.33 – 2.05 (6H, m), 1.86 (2.6H, s, **4a:B**), 1.85 (3.9H, s, **4a:A**), 0.08 (10.3H, s, **4a:A**), 0.05 (6.4H, s, **4a:B**). **¹³C NMR** (175 MHz, CDCl₃) δ = 143.6 (C, **4a:B**), 142.7 (C, **4a:A**), 138.8 (CH, **4a:B**), 134.9 (C, **4a:B**), 134.7 (CH, **4a:A**), 133.7 (CH **4a:B**), 128.5 (CH, **4a:B**), 127.8 (CH, **4a:A**), 127.1 (CH, **4a:A**), 126.4 (CH, **4a:B**), 120.4 (CH, **4a:B**), 120.2 (CH, **4a:A**), 38 (CH, **4a:A**), 32.1 (CH, **4a:B**), 27.6 (CH₃, **4a:B**), 26.5 (CH₃, **4a:A**), 21.3 (CH, **4a:A**), 21.3 (CH, **4a:B**), 20.9 (CH, **4a:A**), 20.1 (CH, **4a:A**), 20.0 (CH, **4a:B**) -2.23 (TMS, **4a:B**), -2.28 (TMS, **4a:A**). **HRMS** (EI, m/z) calculated for ([M-TMS]) C₁₁H₁₀ 142.0783 found 142.0787.

Synthesis of hexyl-trimethylsilyl-bullvalene (4b)

The reaction was done according to **procedure B**, using **3b** (112 mg, 0.39 mmol) in dry acetone (20 mL). After 10 h the solvent was evaporated under vacuum. The crude material was purified by flash chromatography using hexane as eluent ($R_f = 0.55$). The desired product was obtained as a green oil (44 mg, 39%). **IR** (ATR): v/cm⁻¹ = 3023, 2925, 1608, 1042, 1457, 1246. **¹H NMR** (700 MHz, CDCl₃, – 60 C, isomer **4b:A**, **4b:B** ratio 76:24) δ = 6.30 (1H, d, $J = 6.8$ Hz, **4b:A**), 6.23 (0.4H, d, $J = 5.5$ Hz, **4b:B**), 5.90 – 5.80 (5.4H, m), 5.69 (1.6H, d, $J = 8.3$ Hz, **4b:A**), 5.51 (0.4H, d, $J = 8.7$ Hz, **4b:B**), 2.45 (0.5H, t, $J = 8.4$ Hz, **4b:B**), 2.36 (1.1H, d, $J = 8.5$ Hz, **4b:A**), 2.32 – 2.19 (6.5H, m), 2.08 – 2.02 (4.5H, m), 1.41 – 1.20 (25.6H, m), 0.89 – 0.83 (9.7H, m), 0.08 (10H, s, **4b:A**), 0.05 (6H, s, **4b:A**). **¹³C NMR** (176 MHz, CDCl₃, – 60 C, isomer **4b:A**, **4b:B** ratio 76:24) δ = 143.3 (C, **4b:B**), 143.2 (C, **4b:A**), 139.0 (C, **4b:A**), 138.9 (C, **4b:B**), 134.8 (CH, **4b:A**), 133.7 (CH, **4b:B**), 128.6 (CH, **4b:B**), 128.1 (CH, **4b:B**), 126.7 (CH, **4b:A**), 126.4 (CH, **4b:B**), 119.8 (CH, **4b:A**), 119.2 (CH, **4b:A**), 41.0 (CH₂), 39.8 (CH₂), 36.9 (CH, **4b:A**), 32.0 (CH, **4b:B**), 31.8 (CH₂), 31.7 (CH₂), 29.2 (CH₂), 29.1 (CH₂), 28.8 (CH₂), 28.7 (CH₂), 22.8 (CH₂), 22.4 (CH₂), 21.4 (CH, **4b:A**), 20.7 (CH, **4b:A**), 20.2 (CH, **4b:A**), 19.9 (CH, **4b:B**), 19.8 (CH, **4b:B**), 19.8 (CH, **4b:B**), 14.4 (CH₃), 14.3 (CH₃), -2.1 (TMS, **4b:A**), -2.2 (TMS, **4b:B**). **HRMS** (EI, m/z) calculated for C₁₉H₃₀Si 286.2117 found 286.2120.

Synthesis of benzyl-trimethylsilyl-bullvalene (4c)

The reaction was done according to procedure B, using **3c** (100 mg, 0.34 mmol) in dry acetone (20 mL). After 10 h the solvent was evaporated under vacuum. The crude material was purified by flash chromatography using hexane/EtOAc (99:1) as eluents ($R_f = 0.25$). The desired product was obtained as a colourless oil (43 mg, 43%). **IR** (ATR): v/cm⁻¹ = 3025, 2954, 1726, 1494, 1362, 1246, 1041, 831, 741, 697. **¹H NMR** (700 MHz, CDCl₃, – 60 C, isomer **4c:A**, **4c:B** ratio 70:30) δ = 7.33 – 7.31 (3.9H, m), 7.25 – 7.23 (4.5H, m), 7.14 (1.2H, d, $J = 6.0$ Hz), 6.32 (1H, d, $J = 7.0$ Hz, **4c:A**), 6.26 (0.4H, d, $J = 7.1$ Hz, **4c:B**), 5.89 – 5.83 (2.4H, m), 5.68 (1H, d, $J = 7.5$ Hz, **4c:A**), 5.67 (0.6H, d, $J = 8.9$ Hz, **4c:B**), 5.55 (1H, dd, $J = 11.0, 8.8$ Hz, **4c:A**), 3.45 (0.8H, s, **4c:B**), 3.37 (2.5H, dd, $J = 15.6, 23.0$ Hz, **4c:A**), 2.53 (0.4H, t, $J = 8.4$ Hz, **4c:B**), 2.32 – 2.31 (2.1H, m, **4c:A**), 2.29 – 2.26 (2H, m), 2.22 – 2.18 (1.6H, m, **4c:B**), 2.11 (0.6H, t, $J = 8.9$ Hz, **4c:B**), 0.07 (4.3H, s, **4c:B**), 0.04

(9.6H, s, **4c:A**). ^{13}**C NMR** (176 MHz, CDCl$_3$, – 60 C, isomer **4c:A**, **4c:B** ratio 70:30) δ = 143.3 (C, **4c:B**), 142.8 (C, **4c:A**), 141.4 (C, **4c:B**), 140.1 (C, **4c:A**), 139.8 (C, **4c:A**), 136.5 (C, **4c:B**), 134.9 (CH, **4c:A**), 134 (CH, **4c:B**), 129.2 (CH, **4c:A**), 128.7 (CH, **4c:B**), 128.6 (CH, **4c:B**), 128.5 (CH, **4c:B**), 128.4 (CH, **4c:A**), 126.7 (CH, **4c:A**), 126.7 (CH, **4c:B**), 126.2 (CH, **4c:B**), 123.1 (CH, **4c:B**), 122.2 (CH, **4c:A**), 46.7 (CH$_2$, **4c:B**) , 45.7 (CH$_2$, **4c:A**), 36.2 (CH, **4c:A**), 32.1 (CH, **4c:B**), 24.3 (CH, **4c:B**), 21.2 (CH, **4c:A**), 21.2 (CH, **4c:B**), 20.7 (CH, **4c:A**), 20.6 (CH, **4c:A**), 20 (CH, **4c:B**), -2.10 (TMS), -2.15 (TMS). **HRMS** (EI, m/z) calculated for C$_{19}$H$_{21}$Si 277.1413 found 277.1409.

Synthesis of methanol-trimethylsilyl-bullvalene (4d)
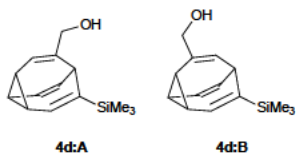
The reaction was done according to procedure B, using **3d** (70 mg, 0.30 mmol) in dry acetone (20 mL). After 10 h the solvent was evaporated under vacuum. The crude material was purified by flash chromatography using hexane/EtOAc (4:1) as eluents (R$_f$ = 0.20). The desired product was obtained as a colourless oil (40 mg, 57%). **IR** (ATR): v/cm^{-1} = 3320, 3023, 2952, 1641, 1607, 1403, 1246, 1151, 1041, 831, 689. ^{1}**H NMR** (700 MHz, CDCl$_3$, – 60 C, isomer **4d:A**, **4d:B** ratio 70:30) δ = 6.28 (1H, m, **4d:A**), 6.23 – 6.22 (0.7H, m, **4d:B**), 5.88 – 5.76 (7.3H, m), 4.03 – 3.96 (2.2H, s, **4d:A**), 3.91- 3.89 (0.9H, m, **4d:B**), 2.53 (1.2H, d, J = 8.5 Hz, **4d:A**), 2.50 (0.6H, d, J = 8.6 Hz, **4d:B**), 2.39 – 2.37 (0.75H, m), 2.29 (4H, m), 0.06 (9.7H, s, **4d:A**), 0.04 (5.1H, s, **4d:B**). ^{13}**C NMR** (176 MHz, CDCl$_3$) δ = 142.8 (C, **4d:B**), 142.7 (C, **4d:A**), 140.8 (C, **4d:A**), 137.6 (C, **4d:A**), 134.7 (CH, **4d:A**), 134.2 (CH, **4d:B**), 128.1 (CH, **4d:A**), 127.9 (CH, **4d:B**), 126.9 (CH, **4d:B**), 126.8 (CH, **4d:A**), 122.7 (CH, **4d:B**), 121.8 (CH, **4d:A**), 69.2 (CH$_2$, **4d:B**), 67.6 (CH$_2$, **4d:A**), 33.7 (CH, **4d:A**), 31.6 (CH, **4d:B**), 21.9 (CH, **4d:B**), 21.4 (CH, **4d:A**), 20.8 (CH, **4d:B**), 20.2 (CH, **4d:A**), 19.8 (CH, **4d:A**), 19.4 (CH, **4d:B**), -2.2 (TMS, **4d:B**), -2.2 (TMS, **4d:A**). **HRMS** (ESI, m/z) calculated for ([M+Na]$^+$) C$_{14}$H$_{20}$OSiNa 255.1176 found 255.1193.

Synthesis of bis-(trimethylsilylsilane) bullvalene (4e)
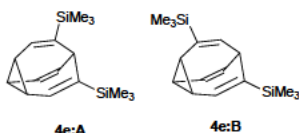
The reaction was done according to procedure B, using **3e** (152 mg, 0.55 mmol) in dry acetone (20 mL). After 8 h the solvent was evaporated under vacuum. The crude material was purified by flash chromatography using hexane as eluent (R$_f$ = 0.62). The desired product was obtained as a yellow oil (80 mg, 52%). **IR** (ATR): v/cm^{-1} = 3024, 2953, 1608, 1402, 1246, 1043. ^{1}**H NMR** (700 MHz, CDCl$_3$ – 60 C, isomer **4e:A**, **4e:B** ratio 68:32) δ = 6.30 (2.1H, s, **4e:A**), 6.22 (0.4H, s, **4e:B**), 6.05 (0.4H, d, J = 7.9 Hz, **4e:B**), 5.91 – 5.88 (2.6H, m), 5.82 – 5.80 (2.6H, m), 2.56 (1H, d, J = 8.1 Hz, **4e:A**), 2.39 (0.3H, m, **4e:B**), 2.36 (3.4H, s, **4e:A**), 2.30 – 2.24 (2.4H, m, **4e:B**), -0.09 (17.7H, s, TMS), -0.06 (7.9H, s, TMS). ^{13}**C NMR** (176 MHz, CDCl$_3$ – 60 C, isomer **4e:A**, **4e:B** ratio 68:32) δ = 143.7 (C, **4e:A**), 142.8 (C, **4e:B**), 141.5 (C, **4e:B**), 135.6 (CH, **4e:B**), 134.8 (CH, **4e:B**), 134.7 (CH, **4e:B**), 129 (CH, **4e:A**), 128.3 (CH, **4e:B**), 127.3 (CH, **4e:B**), 126.6 (CH, **4e:A**), 33.9 (CH, **4e:A**), 33.9 (CH, **4e:B**), 22.7 (CH, **4e:A**), 21.4 (CH, **4e:A**), 21.2 (CH, **4e:B**), 20.9 (CH, **4e:B**), 20.7

(CH, **4e:B**), -1.3 (TMS, **4e:A**), -2.1 (TMS, **4e:B**). **HRMS** (EI, m/z) calculated for [(M-TMS)] $C_{11}H_{11}$ 143.0861 found 143.0863.
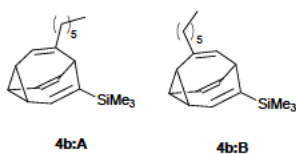
Synthesis of dimethanol-trimethylsilyl-bullvalene (4f)
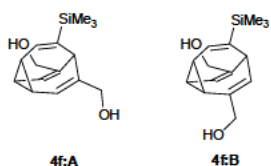
The reaction was done according to procedure B, using **3f** (300 mg, 1.14 mmol) in dry acetone (20 mL). After 10 h the solvent was evaporated under vacuum. The crude target compound was purified by flash chromatography using hexane/EtOAc (8:2) as eluents (R_f = 0.22). The desired product was obtained as a colourless oil (150 mg, 50%).

IR (ATR): v/cm^{-1} = 3301, 3010, 2952, 2925, 1610, 1439, 1386, 1246, 1123, 991, 879, 833, 748, 687. **^{1}H NMR** (700 MHz, CDCl$_3$, − 60 C, isomer **4f:A**, **4f:B** ratio 86:14) δ = 6.29 (1H, s, **4f:A**), 6.20 (0.4H, d, J = 8.3 Hz, **4f:B**) 5.89 − 5.75 (6.7H, m), 4.16 (3.6H, d, J = 11.5 Hz, **4f:A**), 4.05 − 3.81 (5.6H, m) 3.79 − 3.77 (2.5H, d, J = 11.9 Hz, **4f:A**), 2.78 (1H, s, **4f:A**), 2.64 (0.4H, d, J = 9.2 Hz, **4f:B**), 2.29 − 2.27 (4.7H, m) 0.08 (9.4H, s, **4f:A**), 0.04 − 0.01 (12.6H, m).**^{13}C NMR** (176 MHz, CDCl$_3$, − 60 C, isomer **4f:A**, **4f:B** ratio 86:14) δ = 142.1 (C, **4f:B**), 141.8 (C, **4f:A**), 140.5 (C, **4f:B**), 139.7 (C, **4f:A**), 136.9 (CH, **4f:B**), 135.3 (CH, **4f:A**), 134.6 (CH, **4f:B**), 123.7 (CH, **4f:A**), 123 (CH, **4f:B**), 122.7 (CH, **4f:B**), 69.9 (CH$_2$, **4f:B**), 68.7 (CH$_2$, **4f:A**), 68 (CH$_2$, **4f:B**), 35.5 (CH, **4f:A**), 33.4 (CH, **4f:B**), 20.3 (CH, **4f:A**) -2.35 (TMS). **HRMS** (EI, m/z) calculated for ([M+Na]$^+$) $C_{15}H_{22}O_2SiNa$ 285.1281 found 285.1281.

Synthesis of methanol *tert*-butyl(methoxy)dimethylsilane-trimethylsilyl-bullvalene (4g)
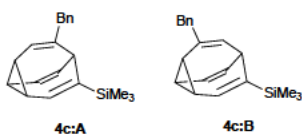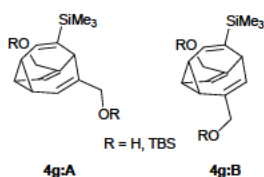

The reaction was done according to procedure B, using **3g** (200 mg, 531 µmol) in dry acetone (20 mL). After 10 h the solvent was evaporated under vacuum. The crude target compound was purified by flash chromatography using hexane/EtOAc (8:2) as eluents (R_f = 0.22). The desired product was obtained as a colourless oil (130 mg, 65%).

IR (ATR): v/cm^{-1} = 3377, 2953, 2927, 2856, 1609, 1462, 1361, 1247, 1144, 1063, 1005, 938, 832, 775, 750. **^{1}H NMR** (700 MHz, CDCl$_3$, − 60 C, isomer **4g:A**, **4g:B** ratio 77:23) δ = 6.28 (1H, d, J = 6.7 Hz, **4g:A**), 6.22 (1.1H, d, J = 8.0 Hz), 5.92 (1H, d, J = 6.0 Hz, **4g:A**), 5.90 (1.1H, d, J = 6.5 Hz, **4g:A**), 5.86 − 5.83 (3H, m), 4.24 (1H, d, J = 12.1 Hz, **4g:A**), 4.15 (1H, d, J = 12.1 Hz, **4g:A**), 4.08 − 4.05 (1.27H, m), 4.00 − 3.97 (1.6H, m), 3.93 − 3.88 (2H, m), 3.78 (1.1H, d, J = 12.0 Hz, **4g:A**), 3.06 (s, 1H), 2.66 (1.1H, s, **4g:A**), 2.62 (0.3H, d = 8.7 Hz, **4g:B**), 2.29 − 2.17 (8.3H, m), 0.89 − 0.85 (30H, m), 0.07 (15.6H, s). **^{13}C NMR** (176 MHz, CDCl$_3$, − 60 C, isomer **4g:A**, **4g:B** ratio 77:23) δ = 141.8 (C, **4g:B**), 141.4 (C, **4g:A**), 140.4 (C, **4g:B**), 140.2 (C, **4g:A**), 139.2 (C, **4g:A**), 136.9 (C, **4g:B**), 135.5 (CH, **4g:A**), 134.6 (CH, **4g:B**), 123.2 (CH, **4g:A**), 121.6 (CH, **4g:B**), 121.5 (CH, **4g:A**), 120.6 (CH, **4g:A**), 69.0 (CH$_2$, **4g:A**), 68.8 (CH$_2$, **4g:B**), 68.3 (CH$_2$, **4g:A**), 67.8 (CH$_2$, **4g:B**), 35.4 (CH, **4g:A**), 32.4 (CH, **4g:B**), 26.0 (CH$_3$), 20.2 (CH, **4g:A**), 18.7 (CH, **4g:A**), -2.30 (TMS, **4g:A**). **HRMS** (ESI, m/z) calculated for ([M+Na]$^+$) $C_{21}H_{36}Si_2O_2Na$ 399.2146 found 399.2142.

Synthesis of dimethanal-trimethylsilyl-bullvalene (4h)
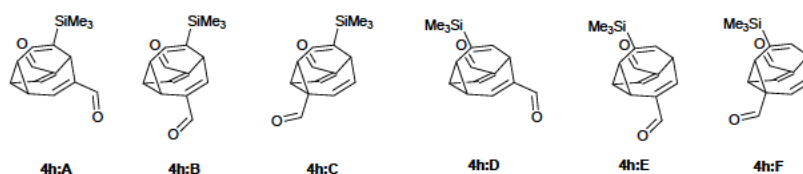
Under nitrogen atmosphere, a 50 mL round bottom flask was charged with oxalyl chloride (55 µL, 0.64 mmol, 2.40 eq) and anhydrous dichloromethane (2 mL). The solution was cooled down to -78 C in a bath of dry ice and acetone. A mixture of dimethyl sulfoxide (95 µL, 1.33 mmol, 5.00 eq) and dichloromethane (20 ml) was added slowly to the reaction mixture. After 5 min **4f** (70.0 mg, 0.26 mmol, 1.00 eq) in (2 mL) dichloromethane was added subsequently. Afterwards, the reaction stirred for another 10 min and triethylamine (0.37 ml, 2.67 mmol, 10.0 eq) was added. After 30 min the reaction was quenched with water and extracted with dichloromethane. The organic layer was washed with distilled water, aqueous sodium chloride solution, dried over $MgSO_4$ and the solvent was removed under vacuum. The crude product was purified through column chromatography with hexane/ethyl acetate (4/1) as eluents (R_f = 0.24). The desired product was obtained as a green oil (35 mg, 50%). **IR** (ATR): v/cm^{-1} = 3004, 2953, 2825, 2729, 1650, 1630, 1403, 1299, 1248, 1171, 1148, 1096, 1043, 961, 833. **^{1}H NMR** (700 MHz, CDCl$_3$, − 60 C, isomer **4h:A, 4h:B, 4h:C, 4h:D, 4h:E, 4h:F**, ratio 64:21:3.9:4.5:2.6: 3.2) = δ 9.24 (0.78H, s, **4h:C**), 9.05 (2.23H, s, **4h:A**), 9.04 (0.8H, s, **4h:B**), 6.90 (0.6H, d, J = 7.3 Hz, **4h:B**), 6.86 (2.4H, d, J = 5.4 Hz, **4h:A**), 6.80 (0.2H, d, J = 8.5 Hz, **4h:F**), 6.77 (0.67H, d, J = 8.8 Hz, **4h:B**), 6.33 − 6.30 (1.7H, m), 6.09 (0.3H, dd, J = 15.3, 10.1 Hz), 6.03 (0.1H, d, J = 8.6 Hz, **4h:E**), 5.97 (0.2H, d, J = 8.6 Hz, **4h:F**), 5.93 (0.2H, d, J = 5.7 Hz, **4h:C**), 5.77 − 5.68 (0.6H, m), 4.38 (1H, s, **4h:A**), 4.23 − 4.19 (0.2H, m, **4h:E**), 4.13 (0.1H, d, J = 9.3 Hz, **4h:C**), 4.03 (0.1H, dd, J = 9.3, 5.3 Hz, **4h:D**), 4.03 (0.1H, dd, J = 9.3, 5.8 Hz, **4h:D**), 3.82 (0.7H, d, J = 8.8 Hz, **4h:B**), 3.72 (0.2H, m, **4h:F**), 3.34 (0.82H, d, J = 8.5 Hz, **4h:B**), 2.90 − 2.86 (3.4H, m), 2.68 (1.7H, dd, J = 16.1, 8.1 Hz), 0.15 − 0.08 (3H, m), 0.04 (6.4H, s, **4h:B**), 0.03 (3.5H, s, **4h:D**), 0.02 (9.4H, s, isomer **a**). **^{13}C NMR** (176 MHz, CDCl$_3$, − 60 C, isomer **4h:A, 4h:B, 4h:C, 4h:D, 4h:E, 4h:F**, ratio 64:21:3.9:4.5:2.6: 3.2) δ = 191.3 (CH, **4h:F**), 191.1 (CH, **4h:B**), 191 (CH, **4h:E**), 190.7 (CH, **4h:A**), 188.4 (CH, **4h:C**), 188.1 (CH, **4h:D**), 152.1 (C, **4h:E**), 151.7 (CH, **4h:B**), 149.9 (C, **4h:F**). 149.5 (CH, **4h:A**), 148.3 (CH, two co-incident signals, **4h:B**, and **4h:E**), 144.4 (C, **4h:F**), 144.3 (C, **4h:A**), 142.8 (C, two co-incident signals, **4h:C** and **4h:D**), 142.5 (C, two co-incident signals, **4h:C** and **4h:D**), 141.4 (CH, **4h:B**), 140.9 (CH, **4h:C**), 139.6 (CH, **4h:D**), 139.7 (C, **4h:B**), 139.3 (C, **4h:A**), 139 (CH, **4h:E**), 137.1 (C, **4h:B**), 136.8 (CH, **4h:F**), 136.6 (CH, **4h:C**), 136.1 (CH, **4h:B**), 134.6 (CH, three co-incident signals, **4h:A**, **4h:C**, and **4h:D**), 134.0 (CH, **4h:E**), 131.1 (CH, **4h:F**), 127.3 (CH, two co-incident signals, **4h:C** and **4h:D**), 126.2 (CH, **4h:D**), 125.7 (CH, **4h:C**), 33.9 (CH, **4h:C**), 32.8 (CH, **4h:D**), 27.6 (CH, **4h:B**), 27.3 (CH, **4h:F**), 25.8 (CH, **4h:E**), 25.4 (CH, **4h:A**), 25.3 (CH, **4h:F**), 24.9 (CH, **4h:A**), 22.4 (CH), 22.8 (CH), 19.6 (CH), -2.5 (TMS), -2.72 (TMS). **HRMS** (ESI, m/z) calculated for ([M+Na]$^+$) C$_{15}$H$_{18}$SiO$_2$Na 281.0968 found 281.0970.

Synthesis of methanal- *tert*-butyl(methoxy)dimethylsilane-trimethylsilyl-bullvalene (4i)

4i:A   4i:B   4i:C   4i:D
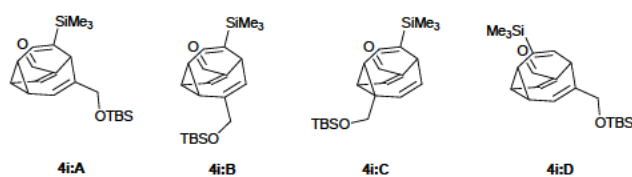
Under nitrogen atmosphere, a 50 mL round bottom flask was charged with oxalyl chloride (53.3 μL, 0.62 mmol, 1.30 eq) and anhydrous dichloromethane (2.5 mL). The solution was cooled down to -78 C in a bath of dry ice and acetone. A mixture of dimethyl sulfoxide (88 μL, 1.24 mmol, 2.6 eq) and dichloromethane (20 ml) was added slowly to the reaction mixture. After 5 min **4g** (180 mg, 0.47 mmol, 1.00 eq) in (2 mL) dichloromethane was added. Afterwards, the mixture stirred for another 10 min and triethylamine (0.30 mL, 2.39 mmol, 5.00 eq) was added. After 30 min, the reaction was quenched with water and the aqueous layer was extracted with dichloromethane. The organic phase was washed three times with distilled water, as saturated sodium chloride solution, and then dried over $MgSO_4$, and the solvent was evaporated under vacuum. The crude product was purified through column chromatography with hexane/ethyl acetate (9/1) as eluent (R_f = 0.21). The desired product was obtained as a green oil (72 mg, 40%). **IR** (ATR): v/cm^{-1} = 2895, 2928, 2856, 1678, 1632, 1471, 1462, 1361, 1312, 1248, 1160, 1143, 1005, 960, 921, 775, 753. **^{1}H NMR** (700 MHz, CDCl$_3$, − 60 C, isomer **4i:A**, **4i:B**, **4i:C**, **4i:D**, ratio 45:27:16:12) δ = 9.02 (0.2H, s, **4i:D**), 9.01 (0.3H, s, **4i:C**), 9.01 (0.6H, s, **4i:B**), 9.00 (1.1H, s, **4i:A**), 6.83 − 6.82 (2.4H, m), 6.26 (1H, d, J = 7.5 Hz, **4i:A**), 6.24 − 6.23 (0.9H, m), 6.00 − 5.98 (1.3H, m), 5.90 − 5.89 (0.9H, m), 5.84 − 5.81 (0.5H, m, **4i:D**), 5.80 − 5.76 (0.6H, m, **4i:D**), 5.69 − 5.66 (1H, m), 4.08 − 4.07 (1.5H, m), 4.05 − 4.00 (2.7H, m), 3.85 (0.6H, dd, J = 10.0, 4.9 Hz, **4i:C**), 3.64 (0.4H, d, J = 10.0 Hz, **4i:C**), 3.46 (0.6H, d, J = 8.9 Hz, **4i:B**), 3.44 (0.8H, d, J = 8.5 Hz, **4i:C**), 3.16 (1H, s, **4i:A**), 3.10 − 3.07 (0.4H, m, **4i:D**), 2.66 (1H, d, J = 8.2 Hz), 2.62 − 2.51 (5.5H, m), 0.85 − 0.84 (34.3H, m), 0.04 − 0.01 (48.5H, m). **^{13}C NMR** (175 MHz, CDCl$_3$, − 60 C, isomer **4i:A**, **4i:B**, **4i:C**, **4i:D**, ratio 45:27:16:12) δ = 191.7 (CH, **4i:D**), 191.7 (CH, **4i:B**), 191.6 (CH, **4i:C**), 191.2 (CH, **4i:A**), 152.1 (CH, **4i:D**), 151.5 (CH, **4i:A**), 151.4 (CH, **4i:C**), 151.2 (CH, **4i:B**), 144.3 (C, **4i:C**) 143.4 (C, **4i:B**), 142.6 (C, **4i:A**), 141.9 (C, **4i:D**), 139.7 (C, **4i:C**), 139.4 (C, **4i:A**), 139.3 (C, **4i:B**), 139 (C, **4i:D**), 138.6 (C, **4i:A**), 138.5 (C, **4i:D**), 137.7 (C, **4i:B**), 135.3 (CH, **4i:C**), 135.2 (CH, **4i:A**), 134.2 (CH, **4i:B**), 133.5 (CH, **4i:D**), 128.3 (CH, **4i:C**), 127.2 (CH, **4i:C**), 120.8 (CH, **4i:B**), 118.8 (CH, **4i:D**), 117.9 (CH, **4i:A**), 68.6 (CH$_2$, **4i:B**), 66.3 (CH$_2$, **4i:C**), 66.1 (CH$_2$, **4i:D**), 65.2 (CH$_2$, **4i:A**), 34.4 (C, **4i:C**), 28.6 (C, **4i:A**), 28.6 (CH, **4i:A**), 26.4 (CH, **4i:B**), 26.1 (CH, **4i:C**), 25.9 (CH$_3$), 25.8 (CH$_3$), 24.6 (CH), 23.9 (CH), 23.6 (CH), 22.9 (CH), 22.7 (CH), -2.5 (CH$_3$), -2.5 (CH$_3$), -5.1 (CH$_3$), -5.1 (CH$_3$), -5.3 (CH$_3$), -5.5 (CH$_3$), -5.59 (CH$_3$). **HRMS** (ESI, m/z) calculated for ([M+Na]$^+$) $C_{21}H_{34}Si_2O_2Na$ 397.1996 found 397.1990.

3. NMR spectra
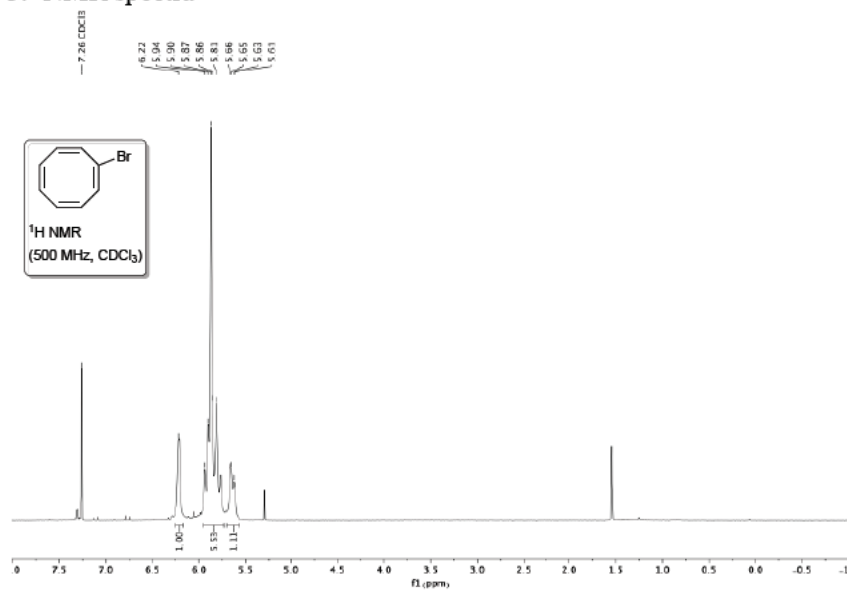
Figure 1: ^{1}H NMR of (1E,3Z,5Z,7Z)-1-bromocycloocta-1,3,5,7-tetraene
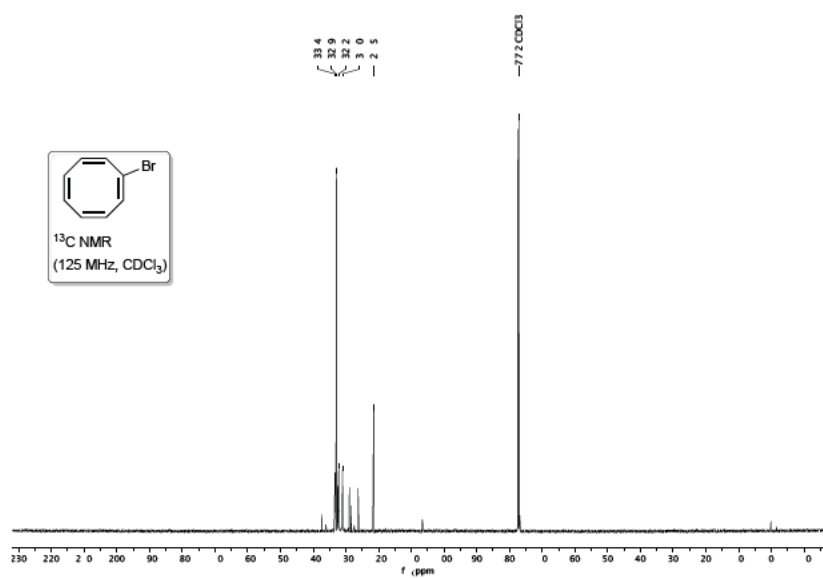
Figure 2: ^{13}C NMR of (1E,3Z,5Z,7Z)-1-bromocycloocta-1,3,5,7-tetraene

3. NMR spectra
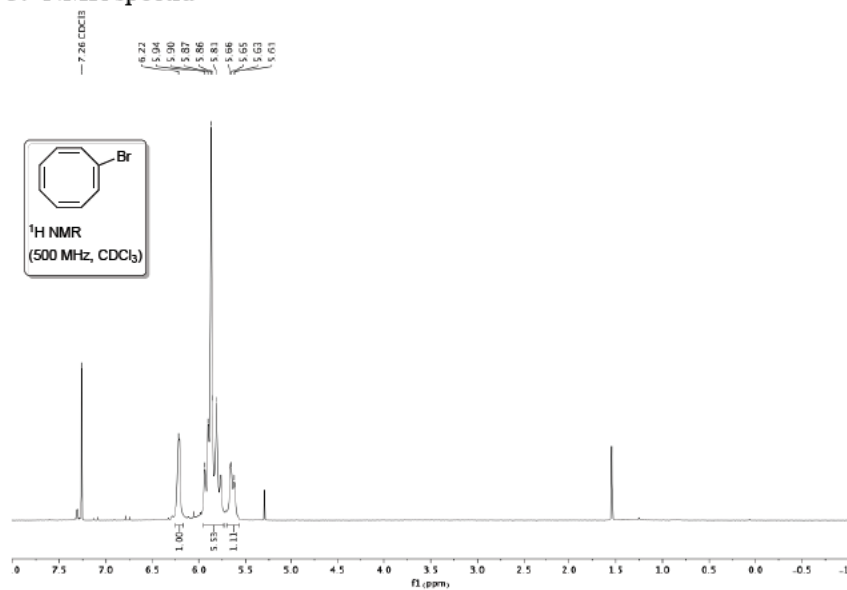
Figure 1: ^{1}H NMR of (1*E*,3*Z*,5*Z*,7*Z*)-1-bromocycloocta-1,3,5,7-tetraene
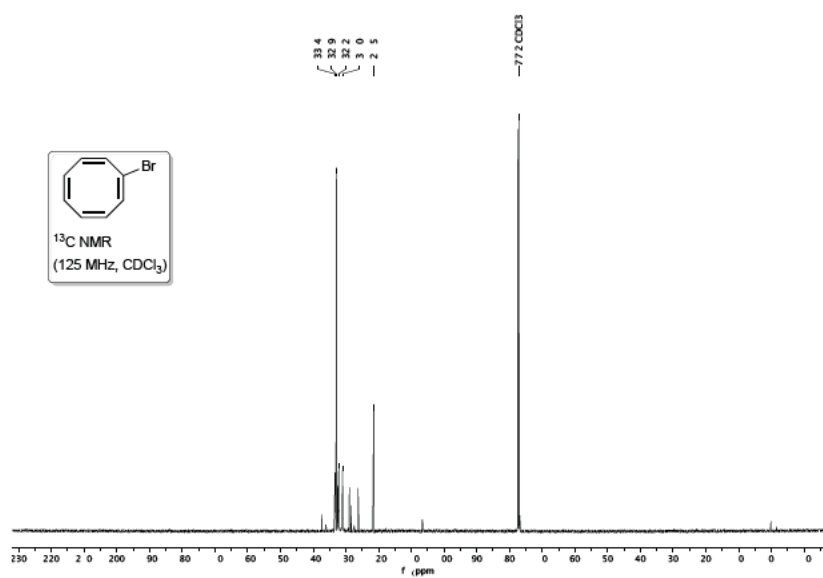
Figure 2: ^{13}C NMR of (1*E*,3*Z*,5*Z*,7*Z*)-1-bromocycloocta-1,3,5,7-tetraene
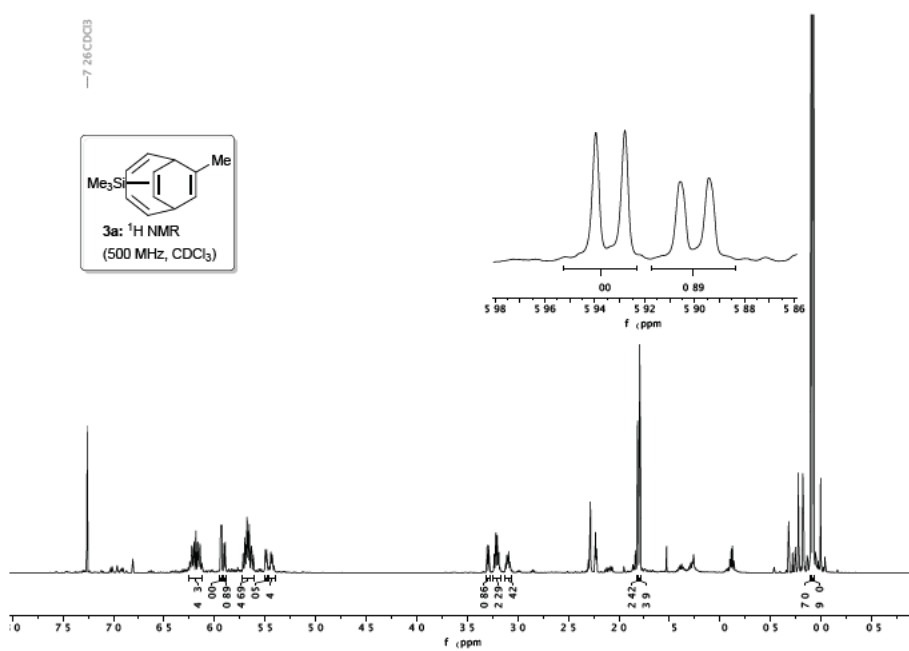
Figure 5: ^{1}H NMR of methyl-trimethylsilyl-bicyclo[4 2 2]deca-2,4,7,9-tetraene
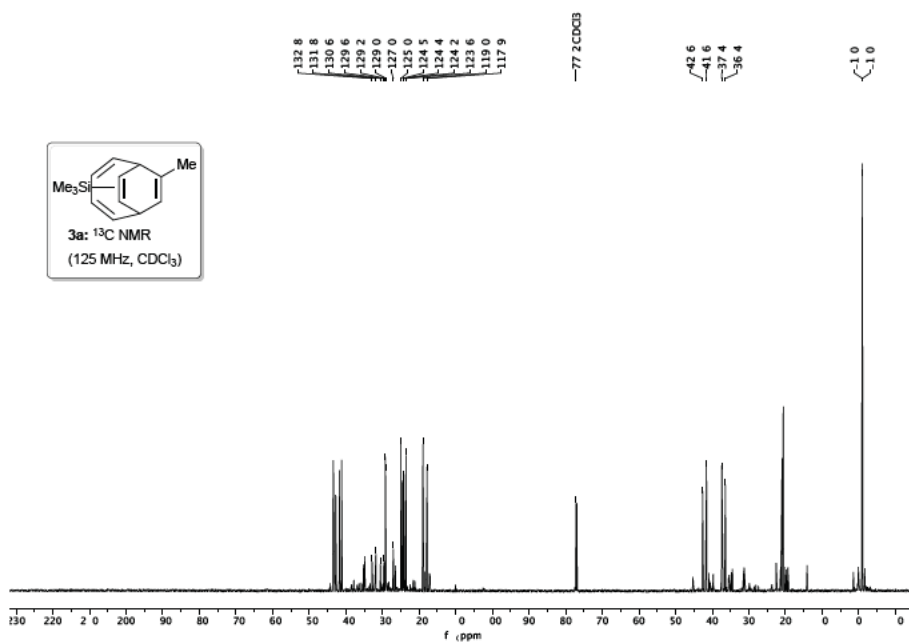
Figure 6: ^{13}C NMR of methyl-trimethylsilyl-bicyclo[4 2 2]deca-2,4,7,9-tetraene

S16
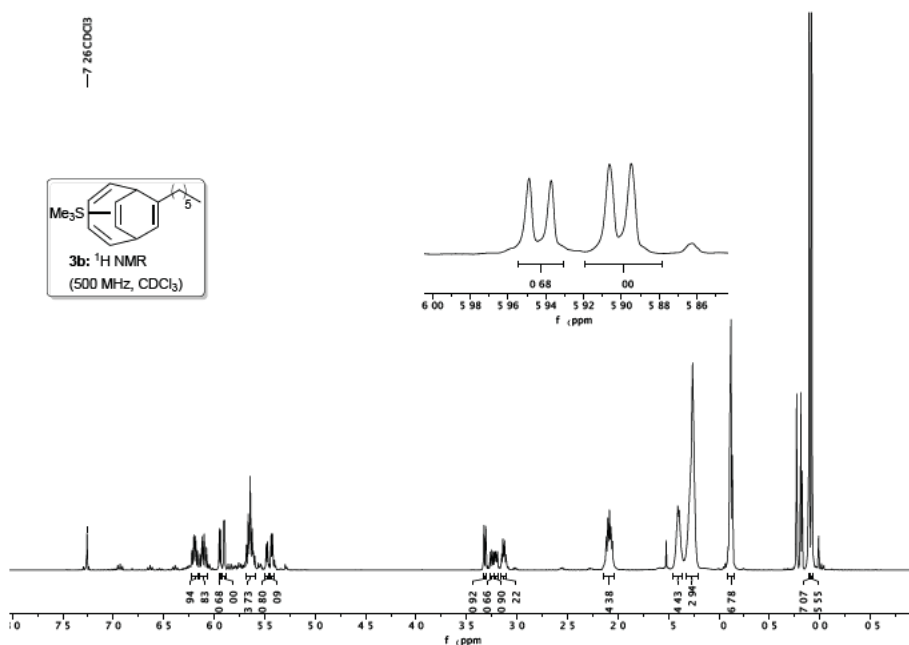
Figure 7: ^{1}H NMR of hexyl-trimethylsilyl-bicyclo[4 2 2]deca-2,4,7,9-tetraene
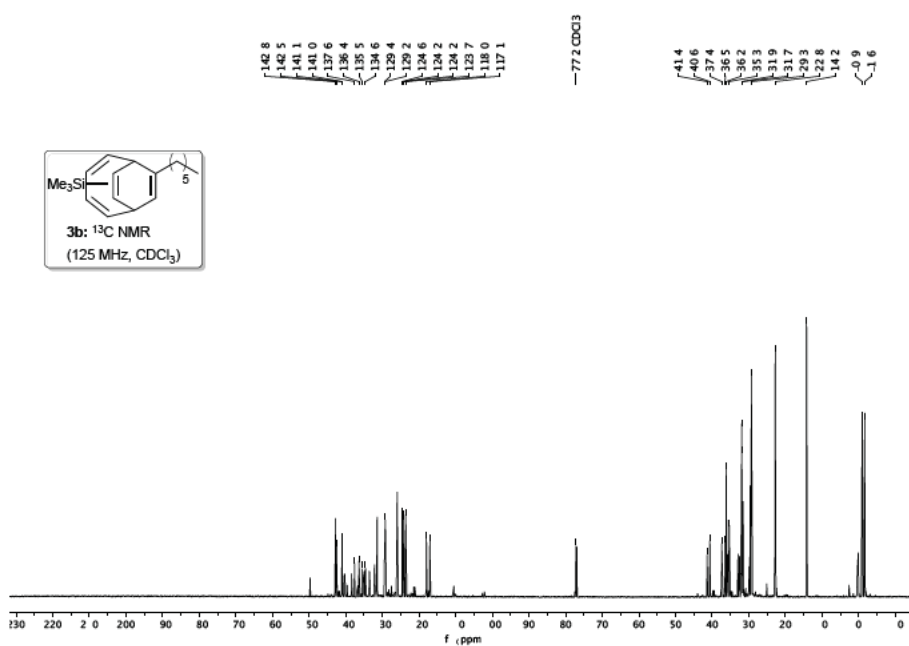
Figure 8: ^{13}C NMR of hexyl-trimethylsilyl-bicyclo[4 2 2]deca-2,4,7,9-tetraene
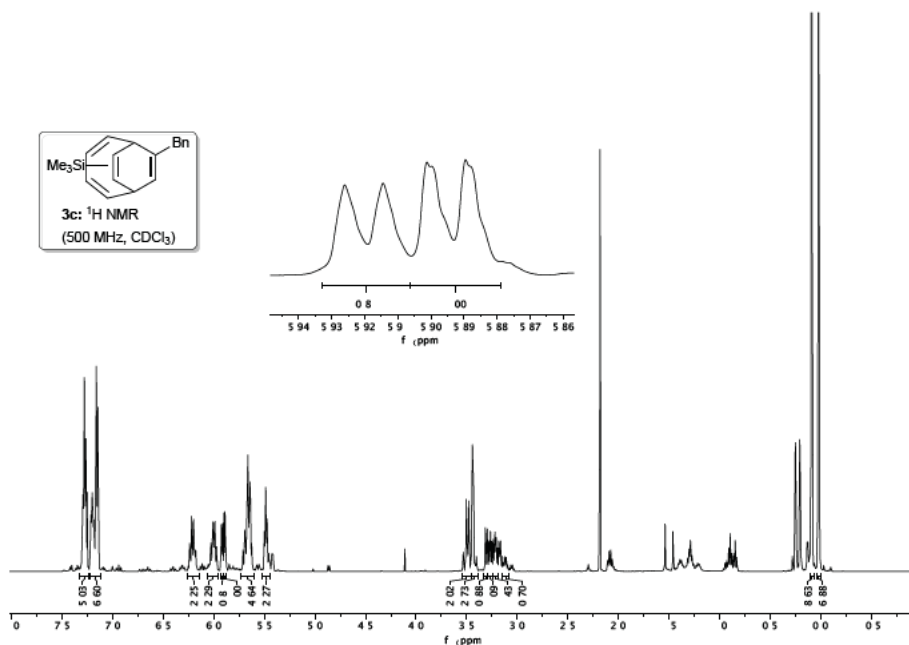
Figure 9: ^{1}H NMR of benzyl-trimethylsilyl-bicyclo[4 2 2]deca-2,4,7,9-tetraene
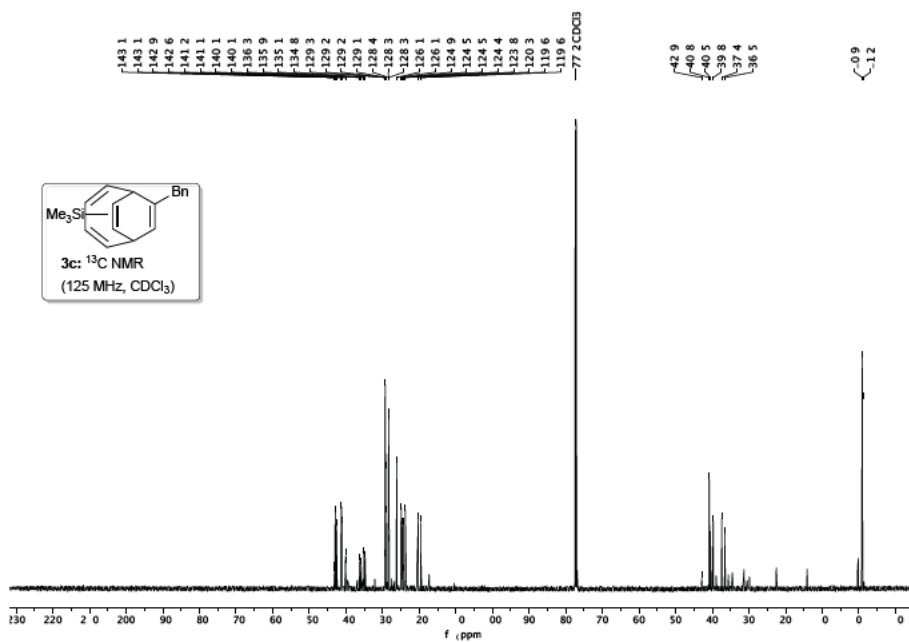
Figure 10: ^{13}C NMR of benzyl-trimethylsilyl-bicyclo[4 2 2]deca-2,4,7,9-tetraene
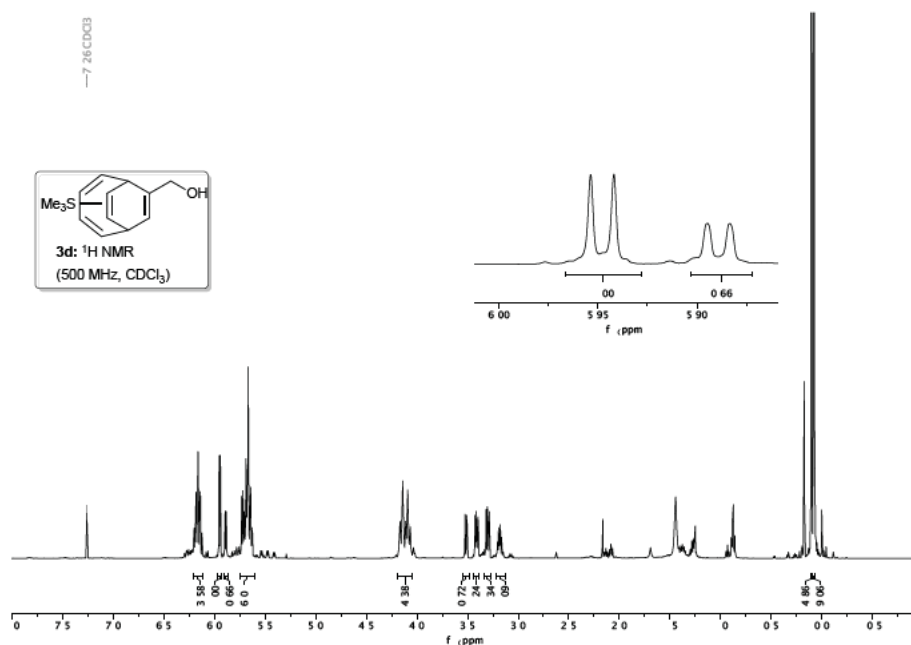
Figure 11: ^{1}H NMR of methanol-trimethylsilyl-bicyclo[4 2 2]deca-2,4,7,9-tetraene
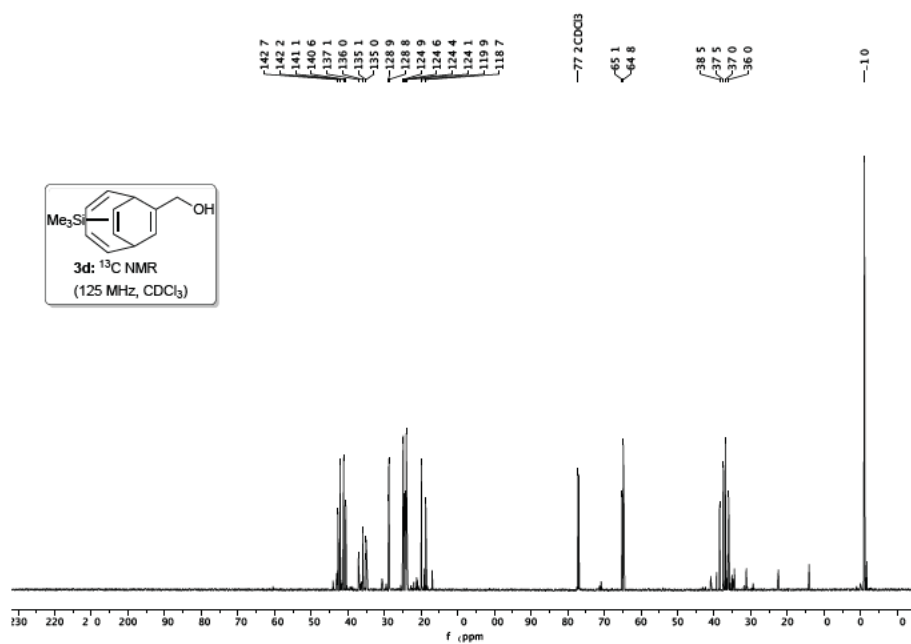
Figure 12: ^{13}C NMR of methanol-trimethylsilyl-bicyclo[4 2 2]deca-2,4,7,9-tetraene
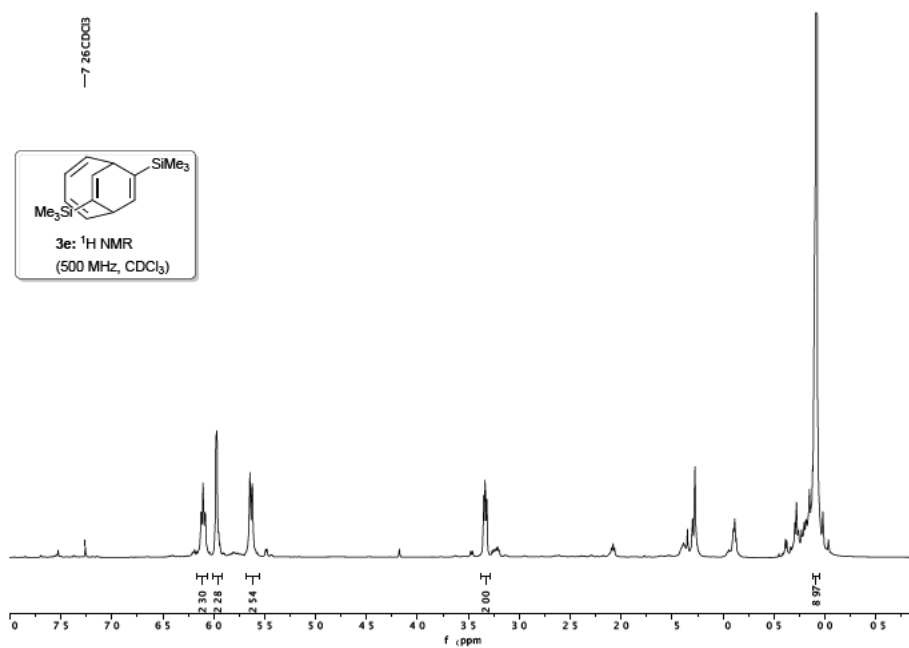
Figure 13: ^{1}H NMR of ditrimethylsilylbicyclo[4 2 2]deca-2,4,7,9-tetraene
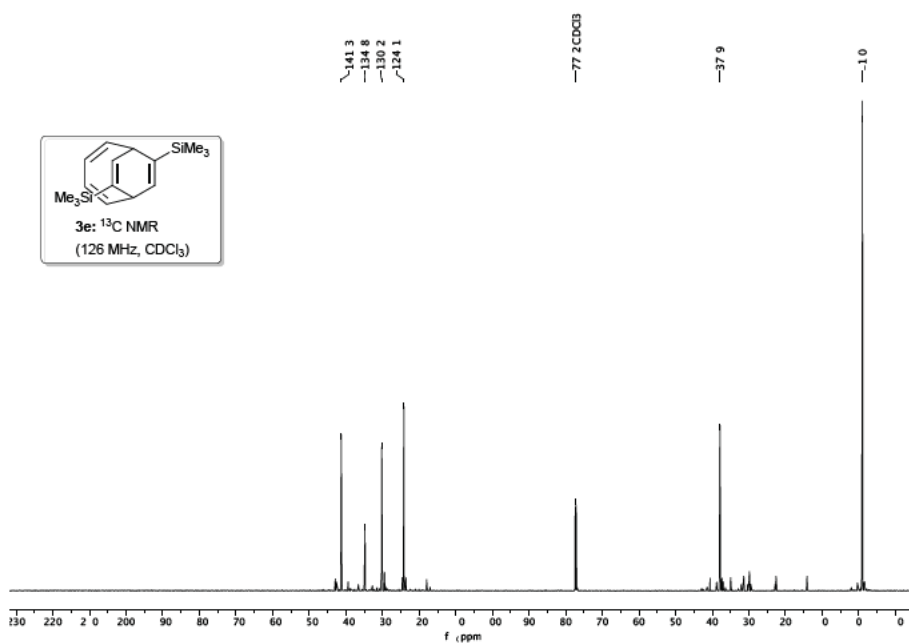
Figure 14: ^{13}C NMR of ditrimethylsilyl-bicyclo[4 2 2]deca-2,4,7,9-tetraene
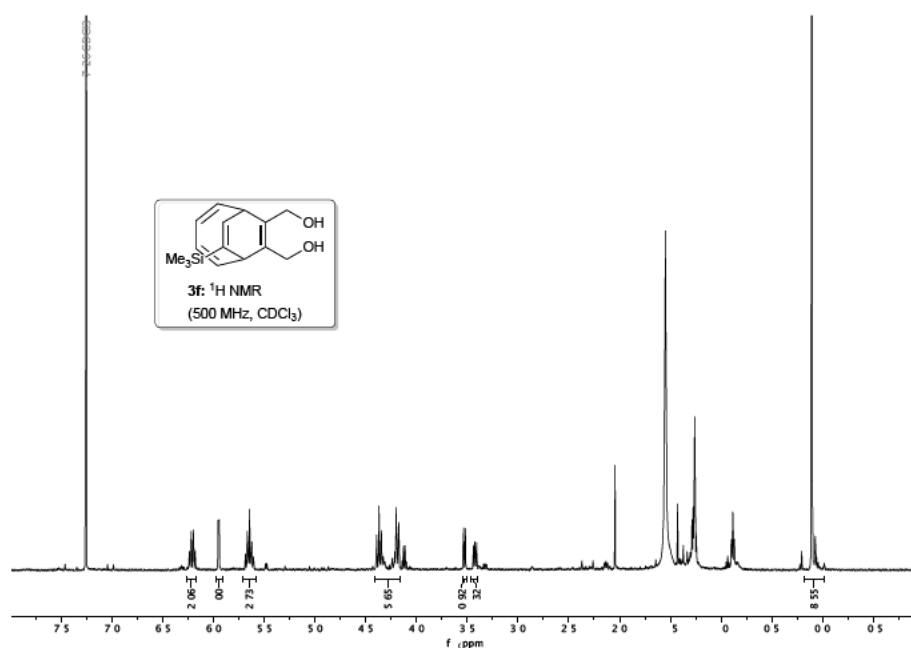
Figure 15: ¹H NMR of dimethanol-trimethylsilyl-bicyclo[4 2 2]deca-2,4,7,9-tetraene
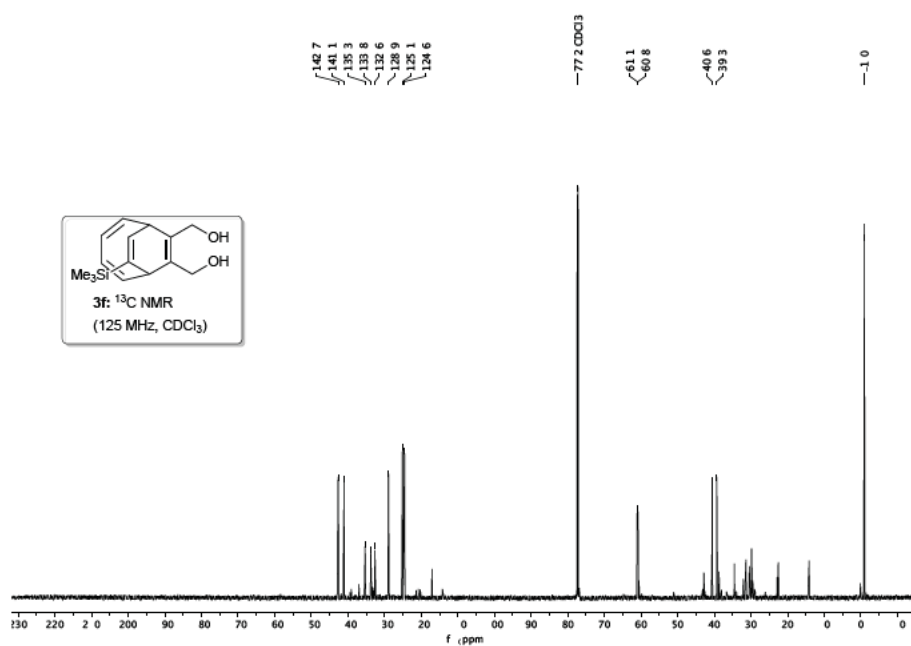
Figure 16: ¹³C NMR of dimethanol-trimethylsilyl-bicyclo[4 2 2]deca-2,4,7,9-tetraene
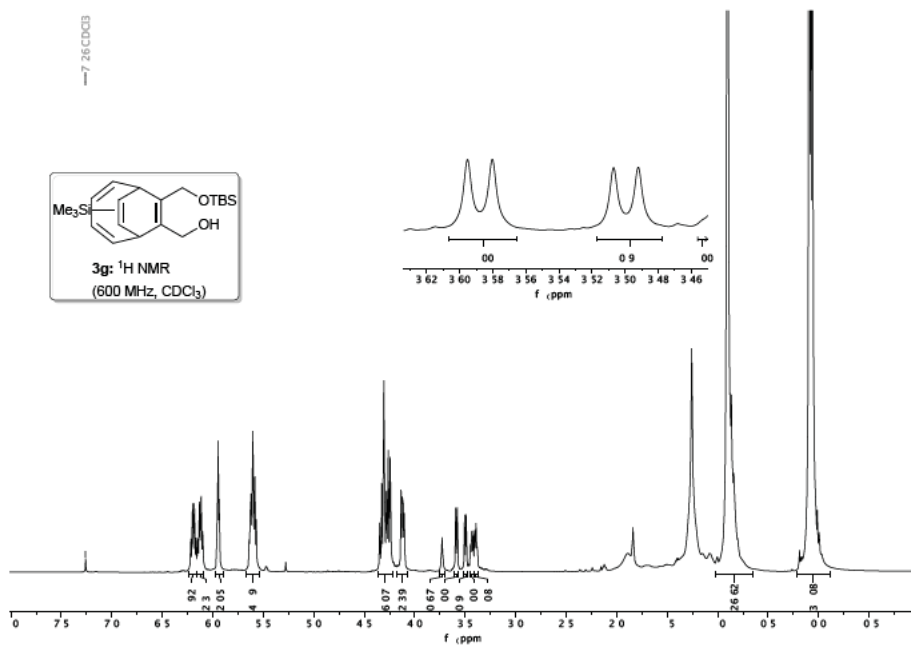
Figure 17: ¹H NMR of menthol-*tert*-butyldimethylsilyl(methoxy)methyl-trimethylsilyl)-trimethylsilyl-bicyclo[4 2 2]deca-2,4,7,9-tetraene
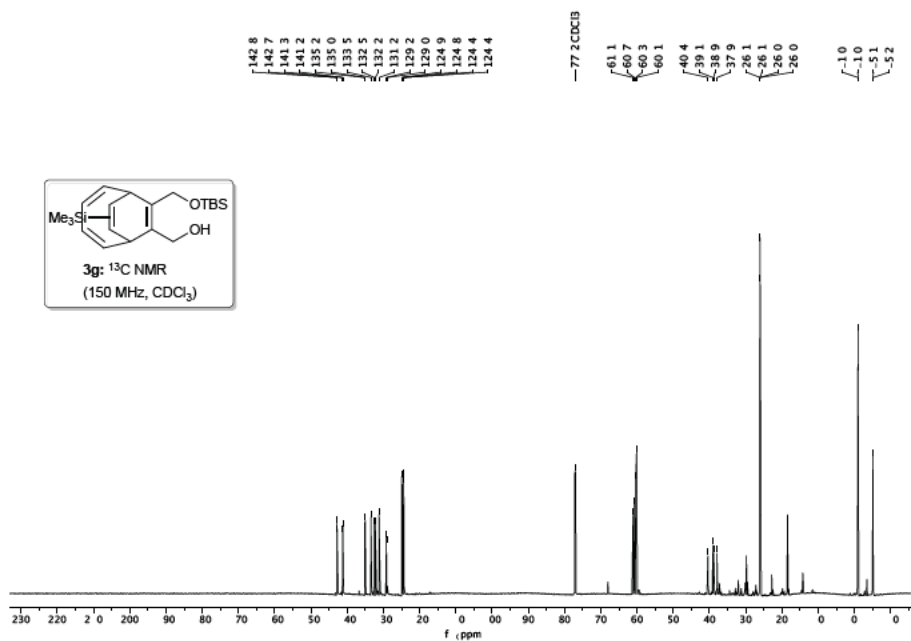
Figure 18: ¹³C NMR of menthol-*tert*-butyldimethylsilyl(methoxy)methyl-trimethylsilyl)-trimethylsilyl-bicyclo[4 2 2]deca-2,4,7,9-tetraene
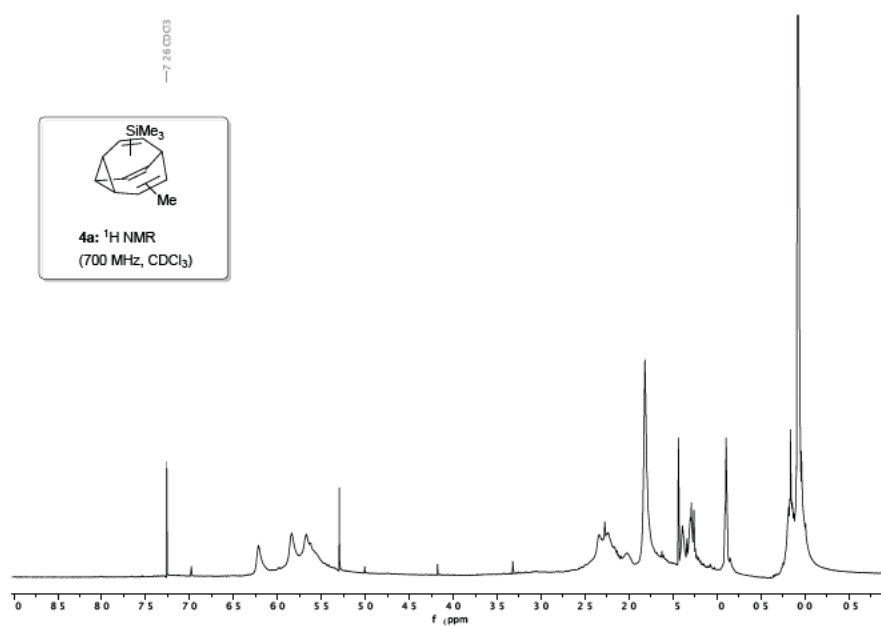
Figure 19: ^{1}H NMR of methyl-trimethylsilyl-bullvalene at room temperature
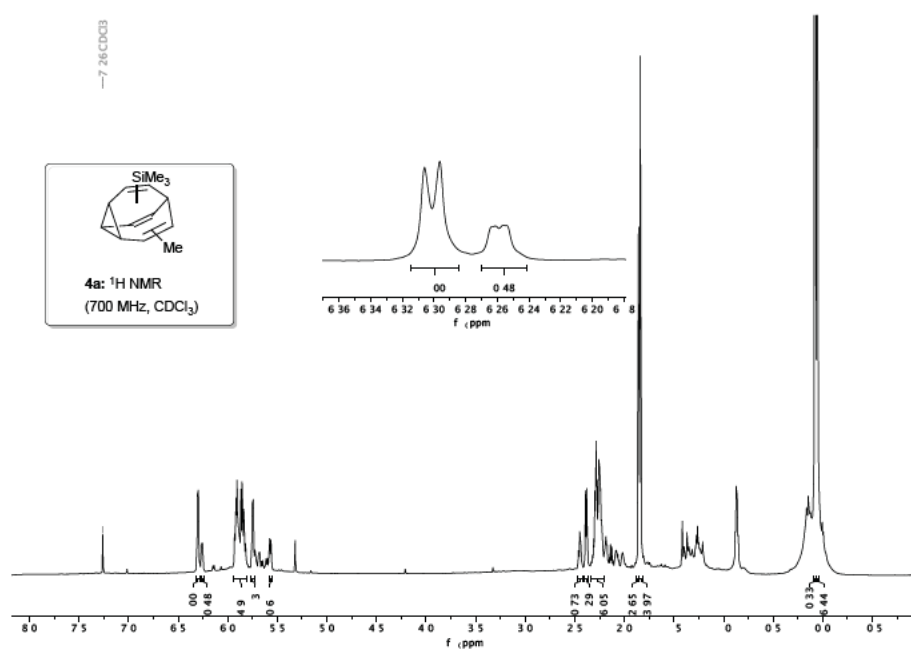
Figure 20: ^{1}H NMR of methyl-trimethylsilyl-bullvalene at -60 °C
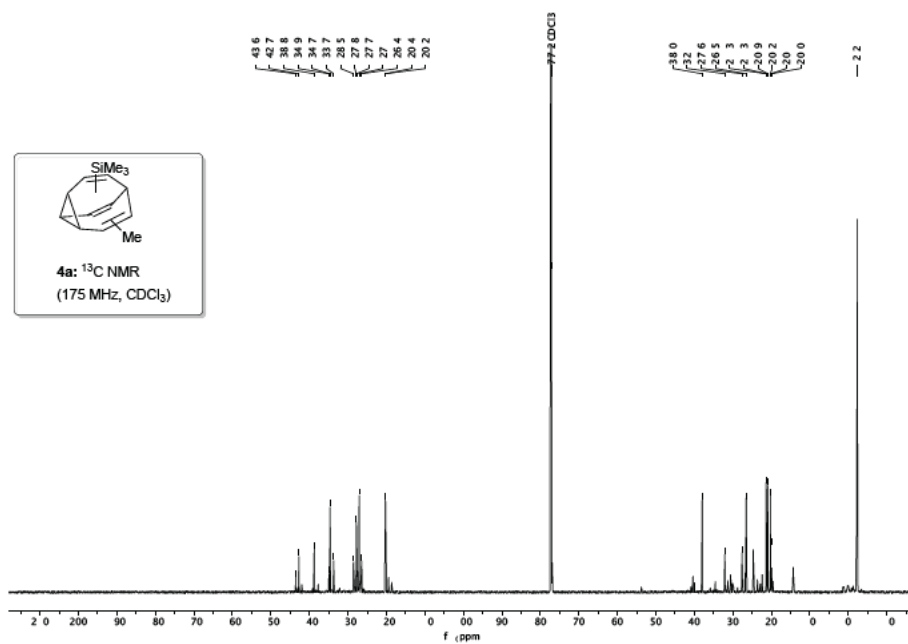
Figure 21: ^{13}C NMR of methyl-trimethylsilyl-bullvalene at -60 °C
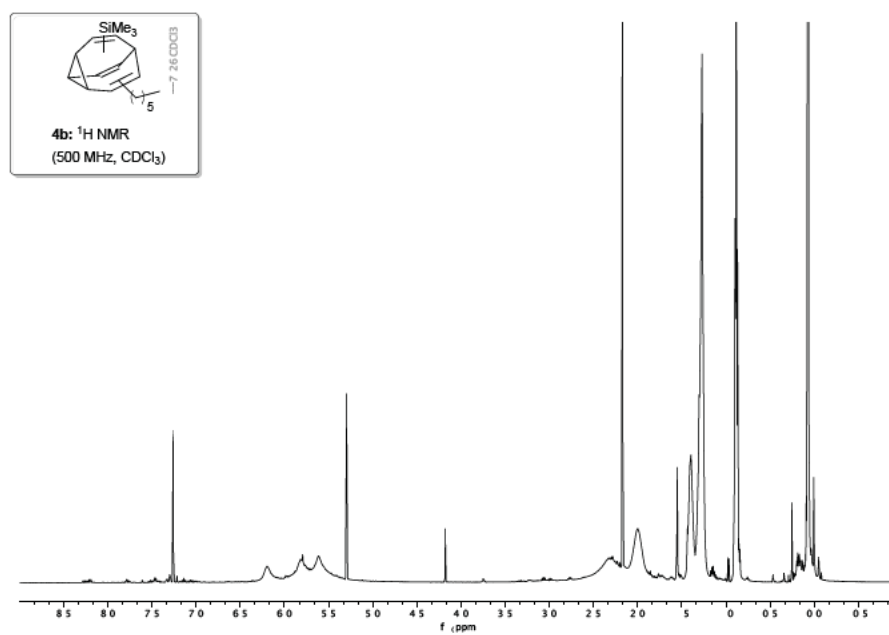
Figure 22: ^{1}H NMR of hexyl-trimethylsilyl-bullvalene at room temperature
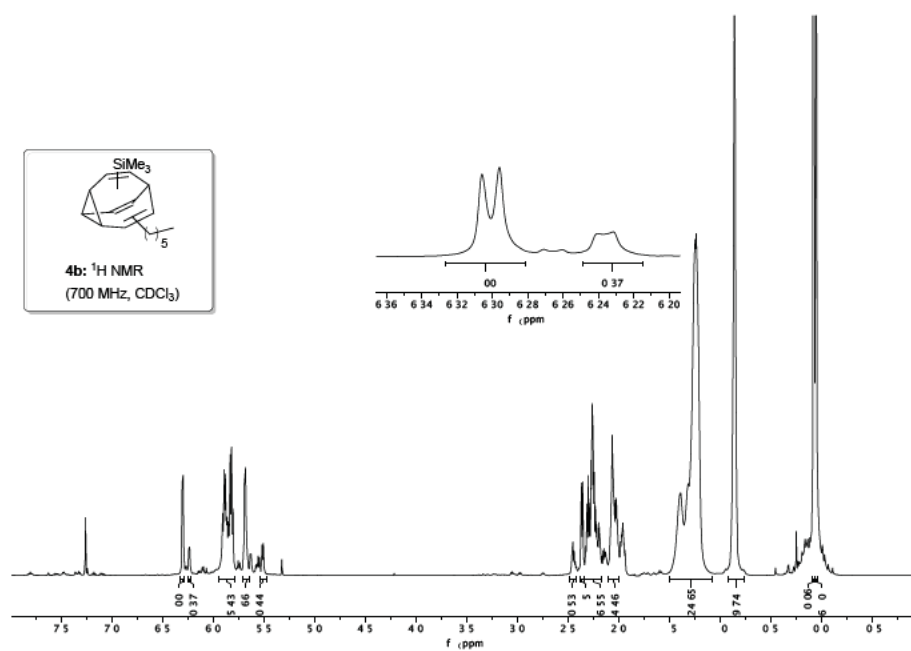
Figure 23: ^{1}H NMR of hexyl-trimethylsilyl-bullvalene at -60 °C
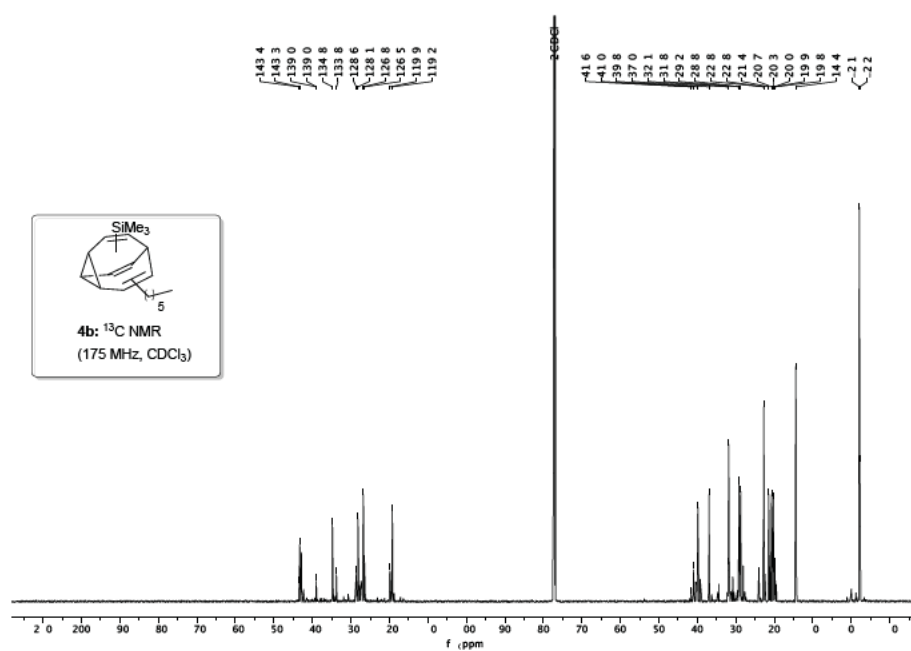
Figure 24: ^{13}C NMR of hexyl-trimethylsilyl-bullvalene at -60 °C
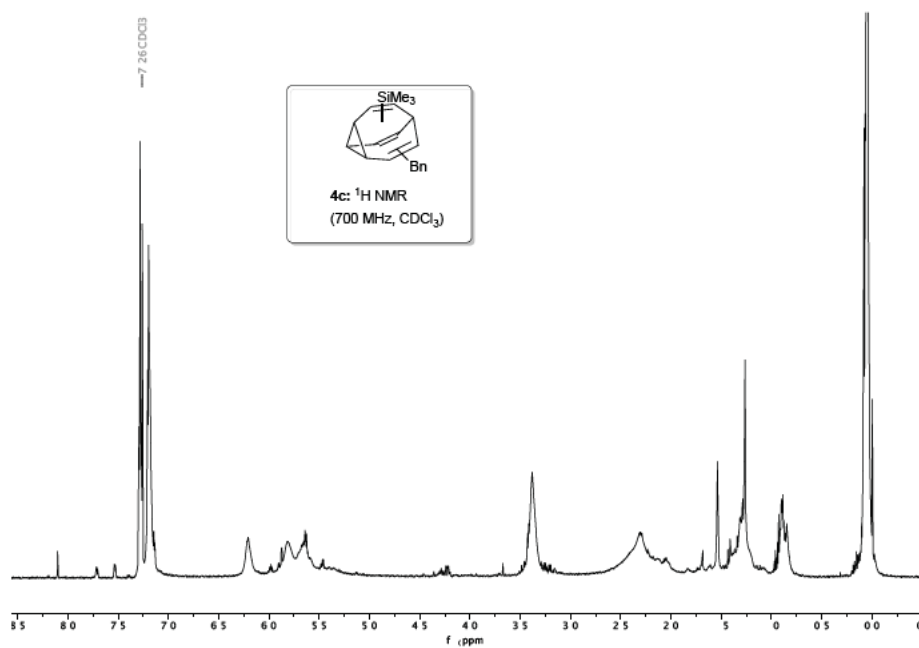
Figure 25: ^{1}H NMR of benzyl-trimethylsilyl-bullvalene at room temperature
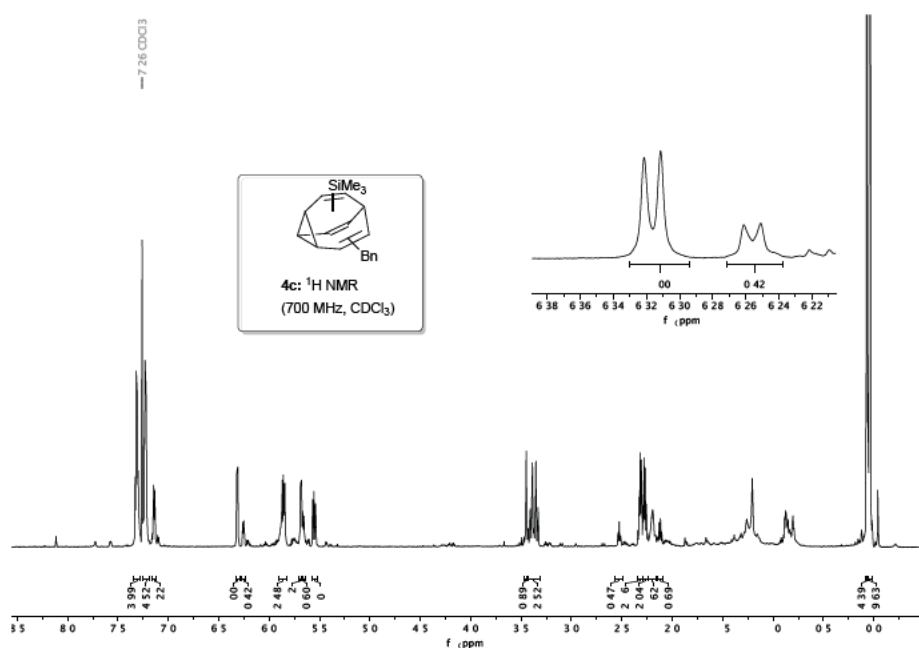
Figure 26: ^{1}H NMR of benzyl-trimethylsilyl-bullvalene at -60 °C
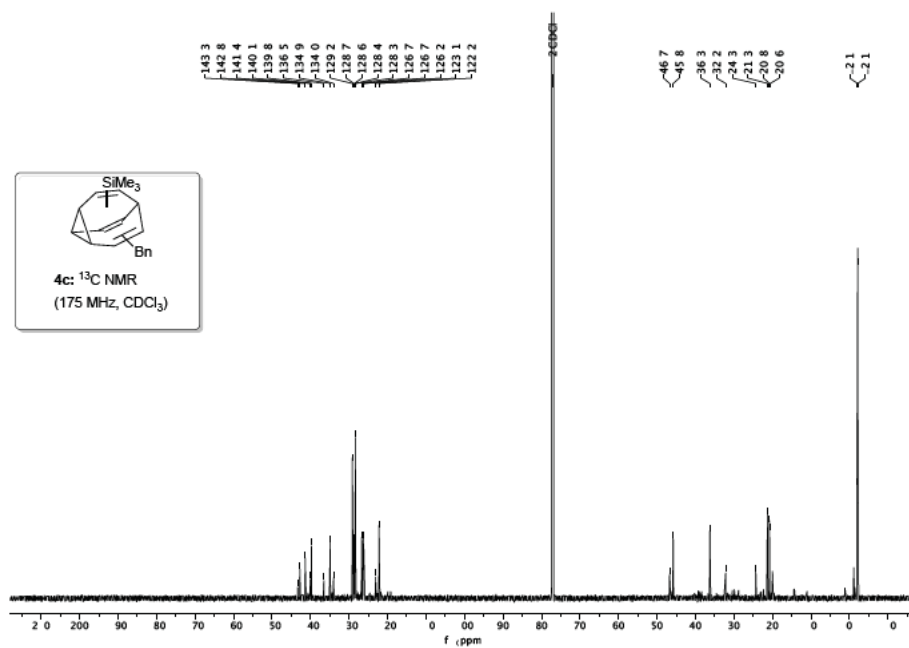
Figure 27: ^{13}C NMR benzyl-trimethylsilyl-bullvalene at -60 °C
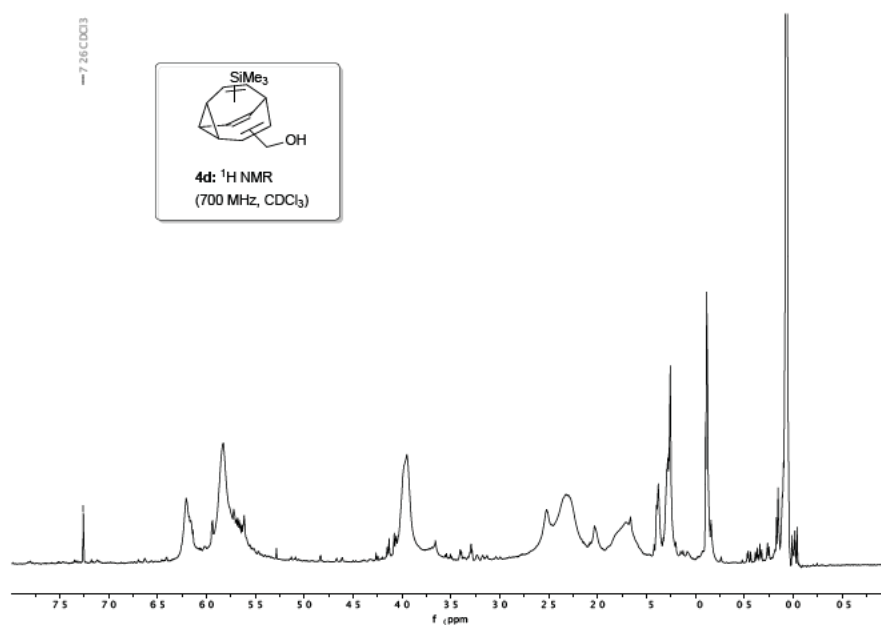
Figure 28: ^{1}H NMR of methanol-trimethylsilyl-bullvalene at room temperature
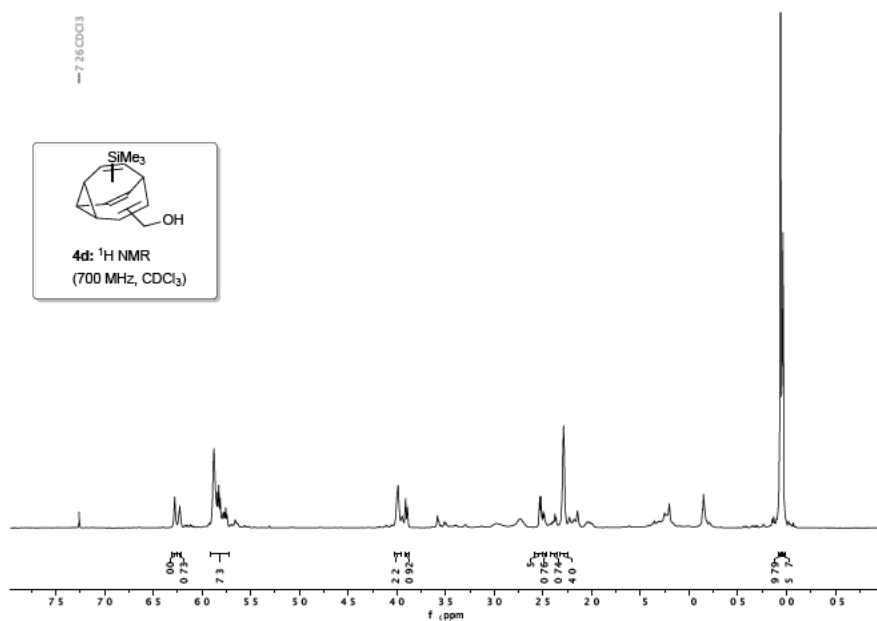
Figure 29: ¹H NMR of methanol-trimethylsilyl-bullvalene at -60 °C
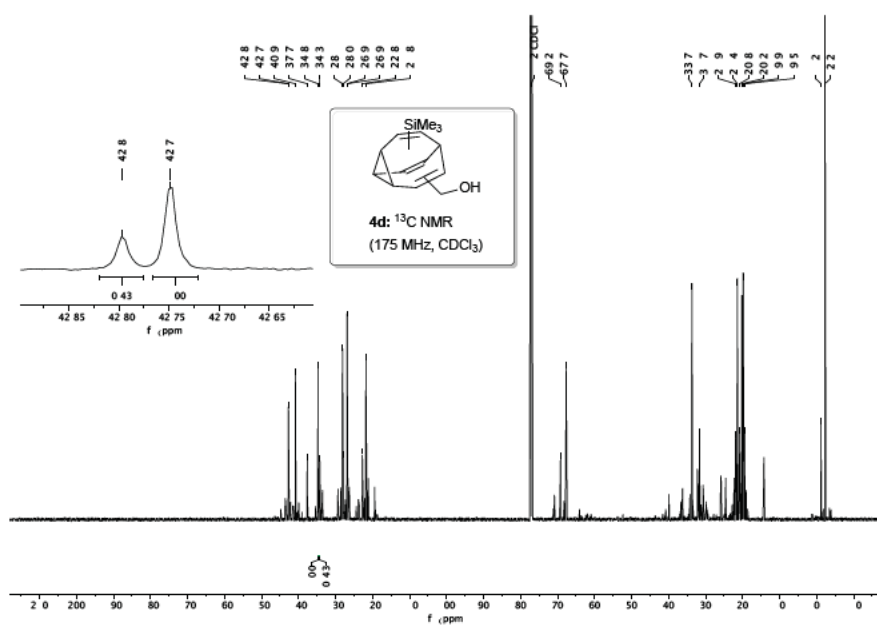
Figure 30: ¹³C NMR of methanol-trimethylsilyl-bullvalene at -60 °C
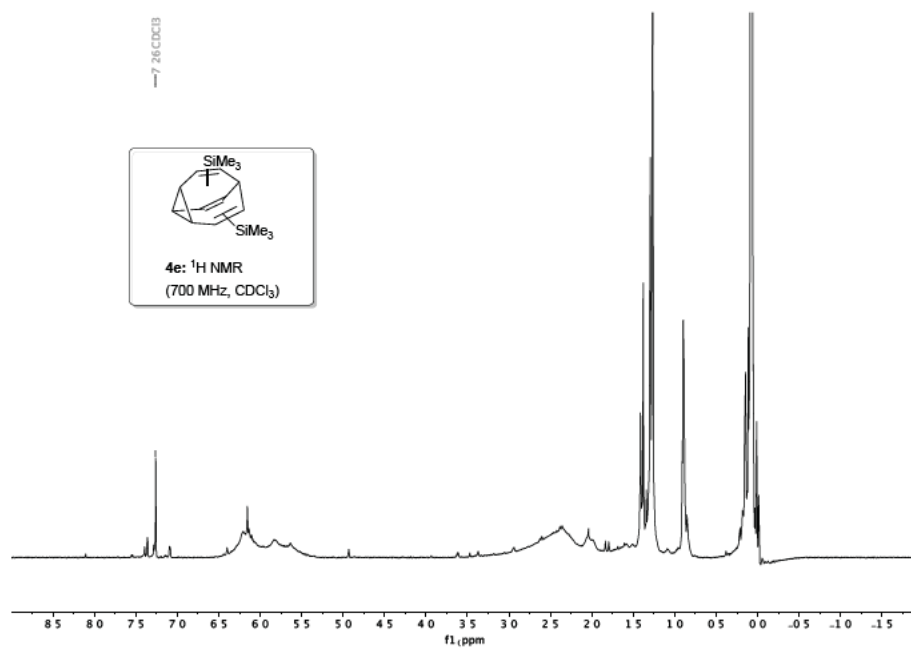
Figure 31: ^{1}H NMR of bis-(trimethylsilyl)-bullvalene at room temperature
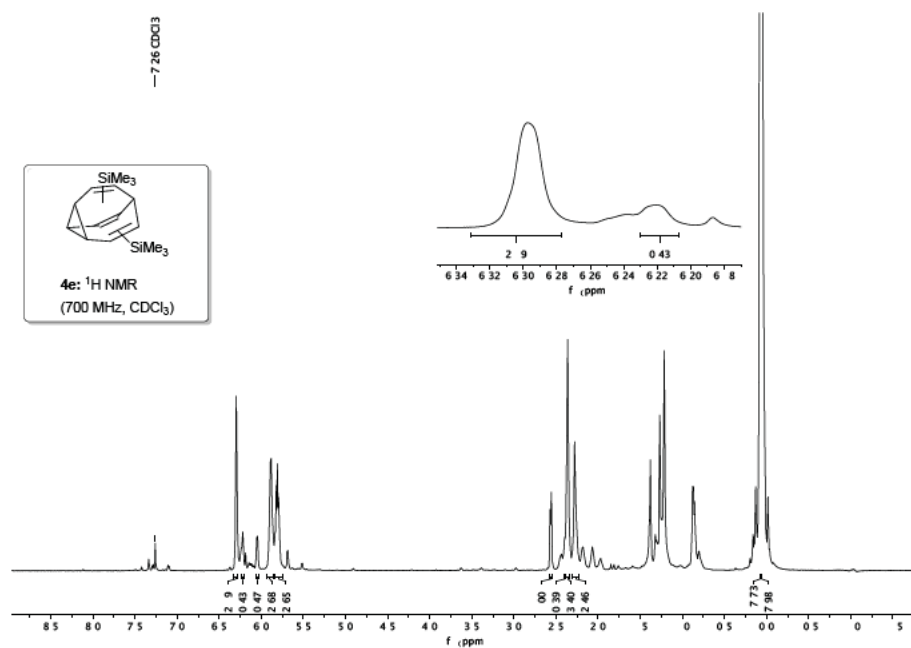
Figure 32: ^{1}H NMR of bis-(trimethylsilyl)-bullvalene at -60 °C
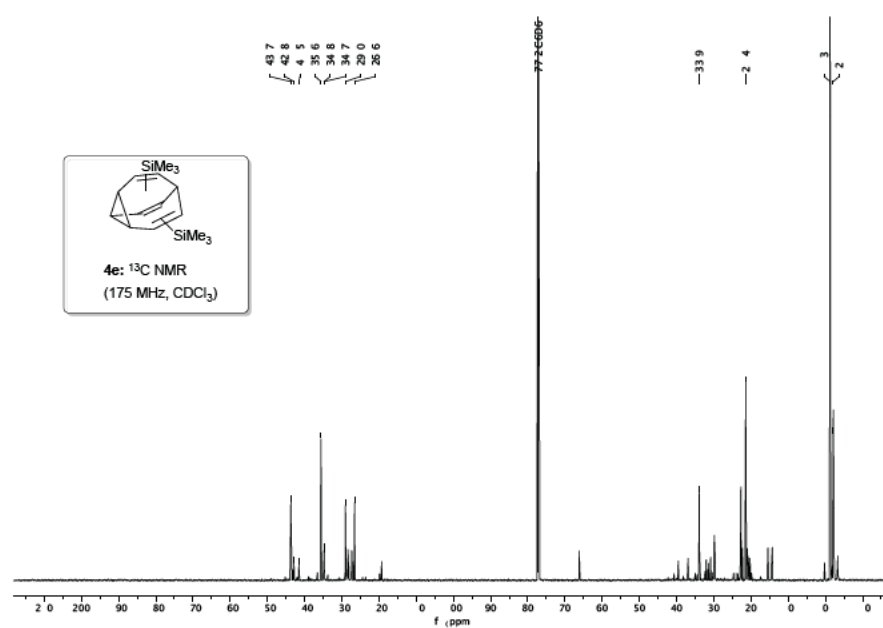
Figure 33: ^{13}C NMR of bis-(trimethylsilyl)-bullvalene at -60 °C
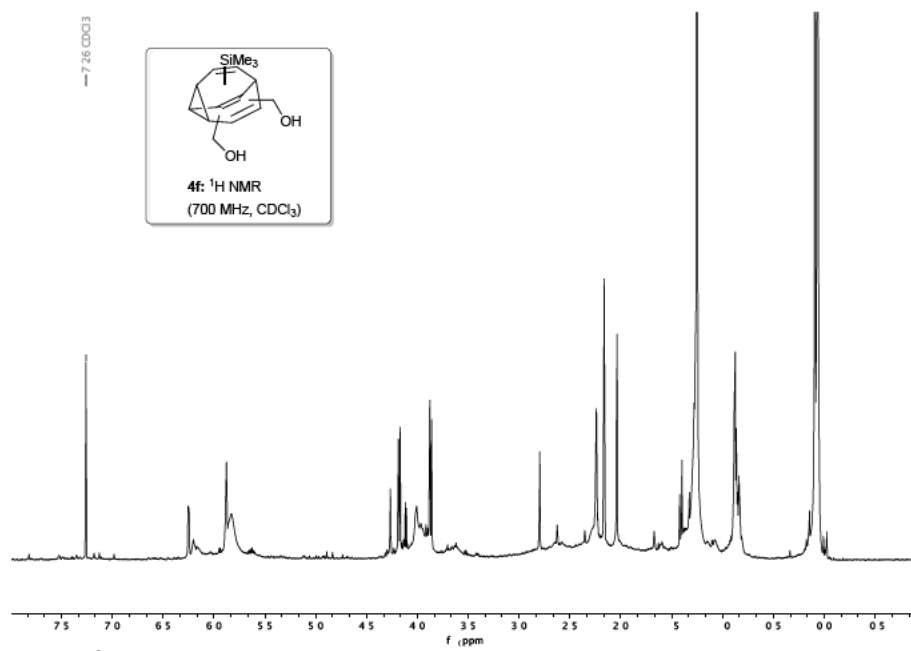
Figure 34: ^{1}H NMR of bis-(methylenehydroxy)-trimethylsilyl bullvalene at room temperature
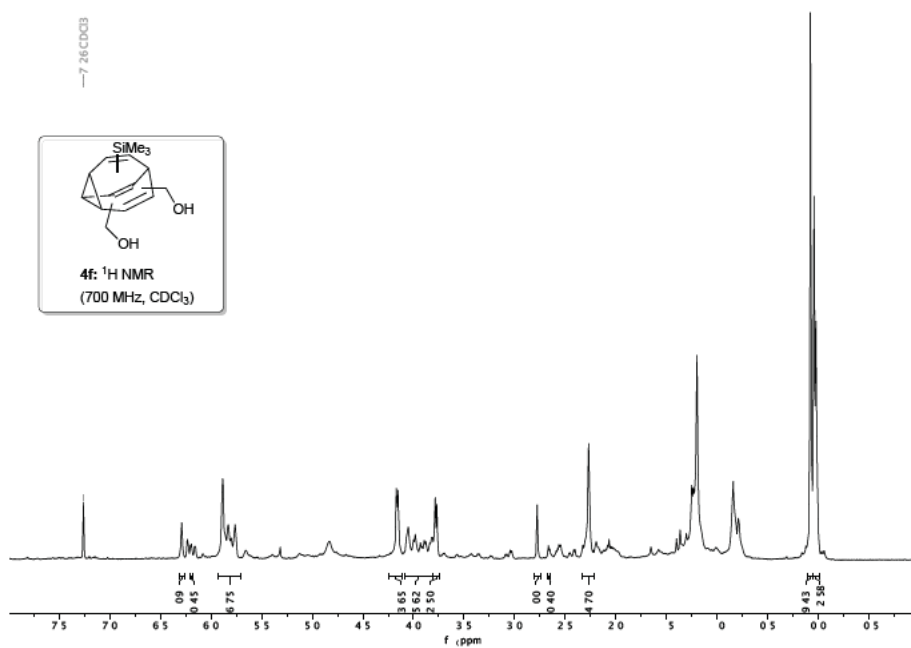
Figure 35: ^{1}H NMR of bis-(methylenehydroxy)-trimethylsilyl bullvalene at -60 °C
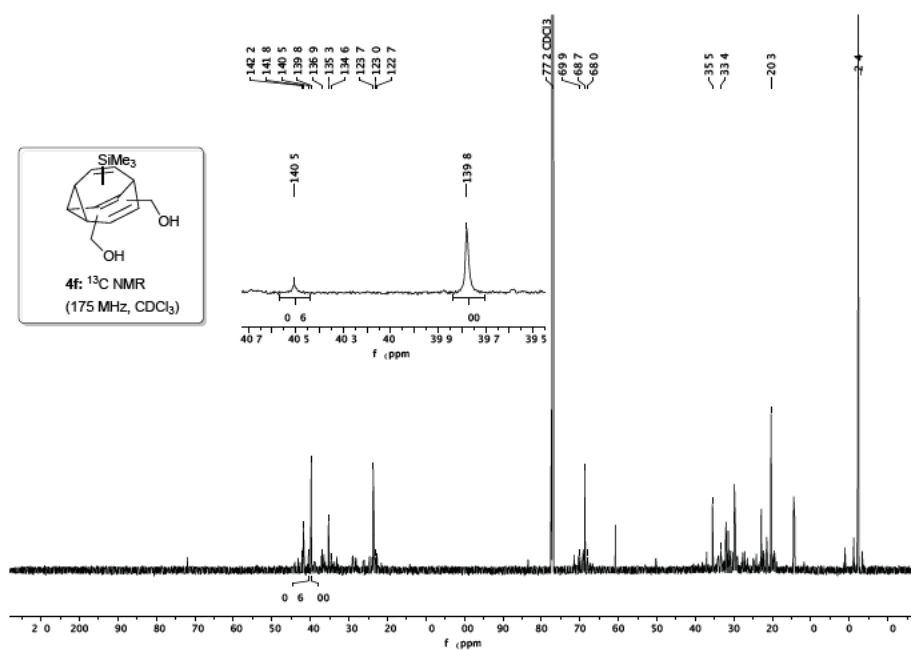
Figure 36: ^{13}C NMR of bis-(methylenehydroxy)-trimethylsilyl bullvalene at -60 °C
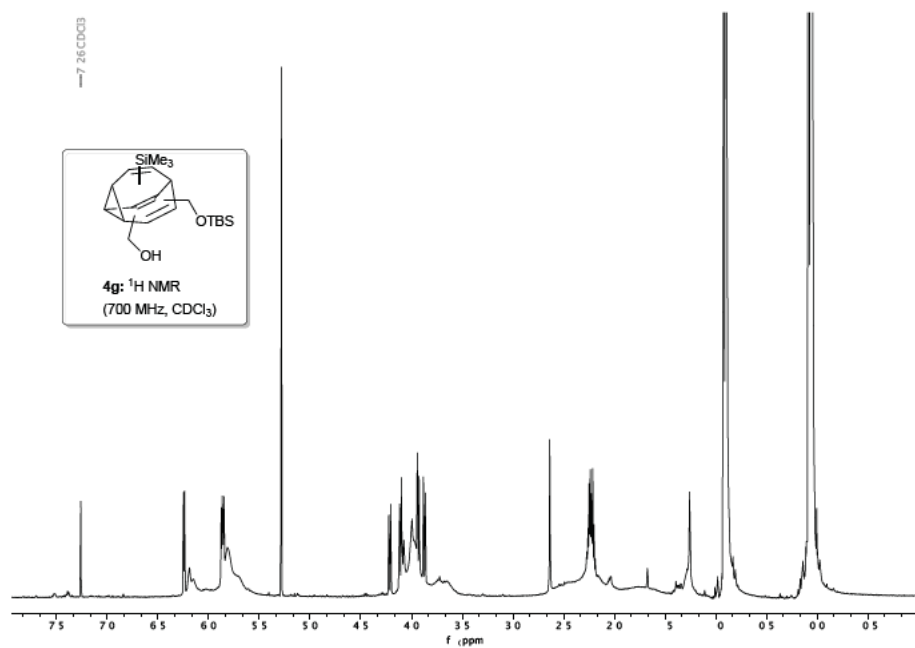
Figure 37: ^{1}H NMR of methylene-TBS-ether-trimethylsilyl bullvalene at room temperature
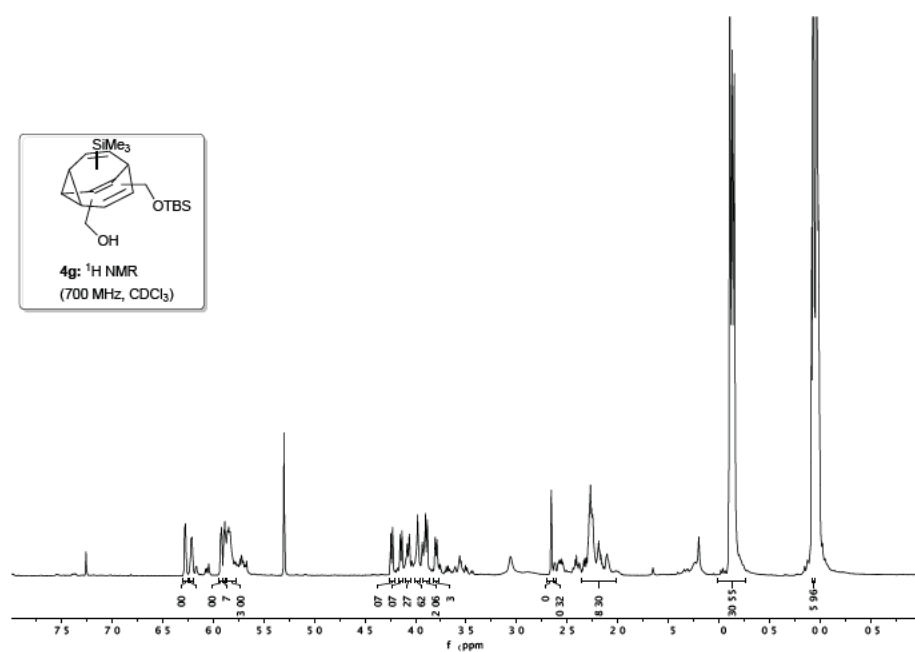
Figure 38: ^{1}H NMR of methylene-TBS-ether-trimethylsilyl bullvalene at -60 °C
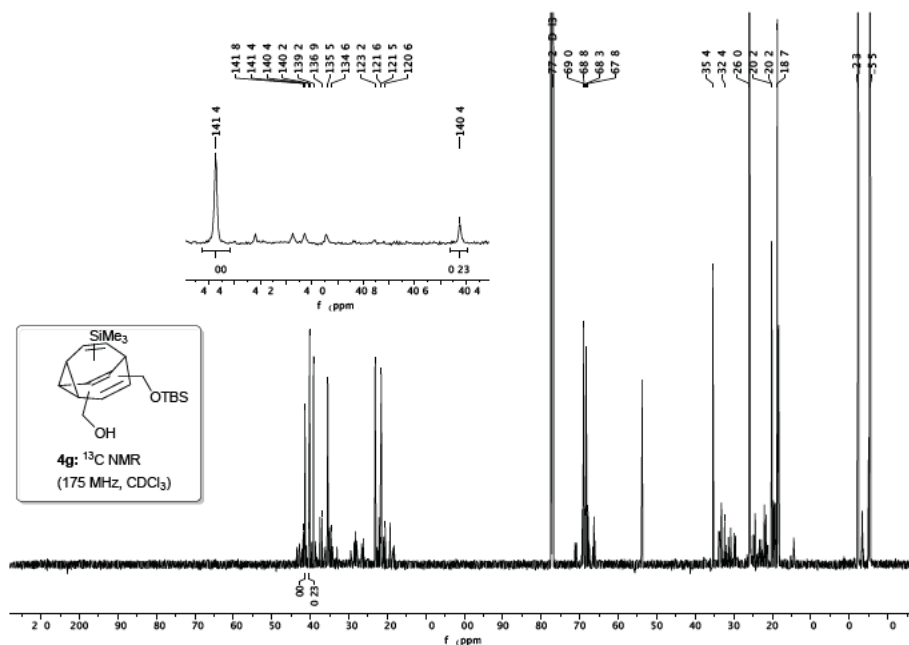
Figure 39: ^{13}C NMR of methylene-TBS-ether-trimethylsilyl bullvalene at -60 °C
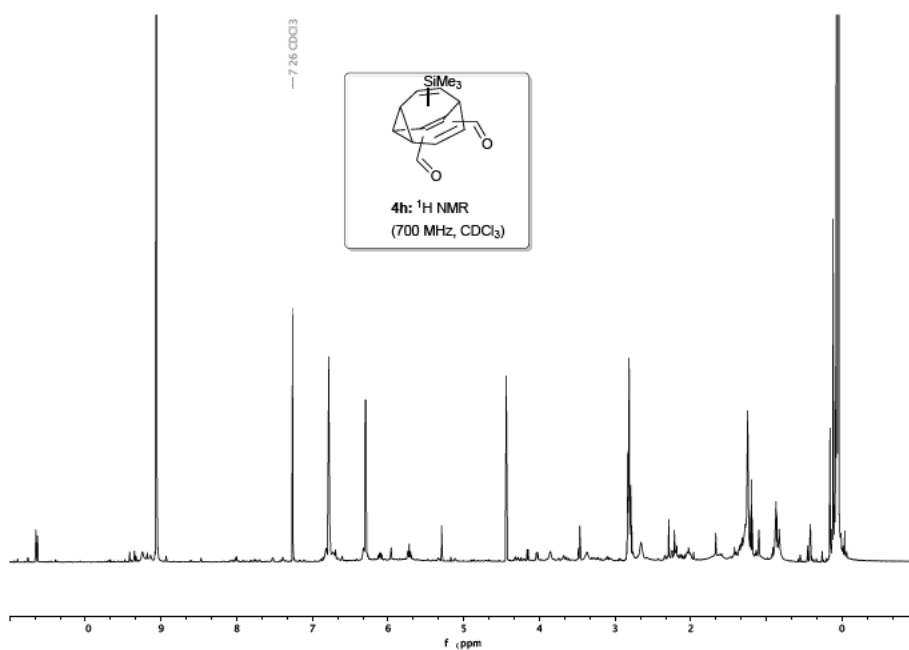
Figure 40: ^{1}H NMR of bis-(aldehyde)-trimethylsilyl bullvalene at room temperature
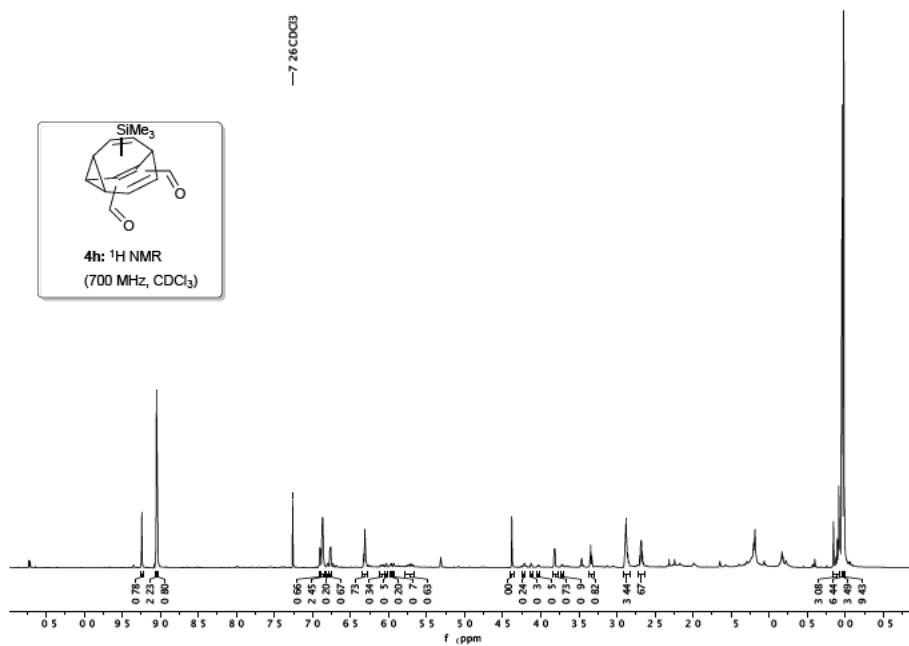
Figure 41: ¹H NMR of bis-(aldehyde)-trimethylsilyl bullvalene -60 °C
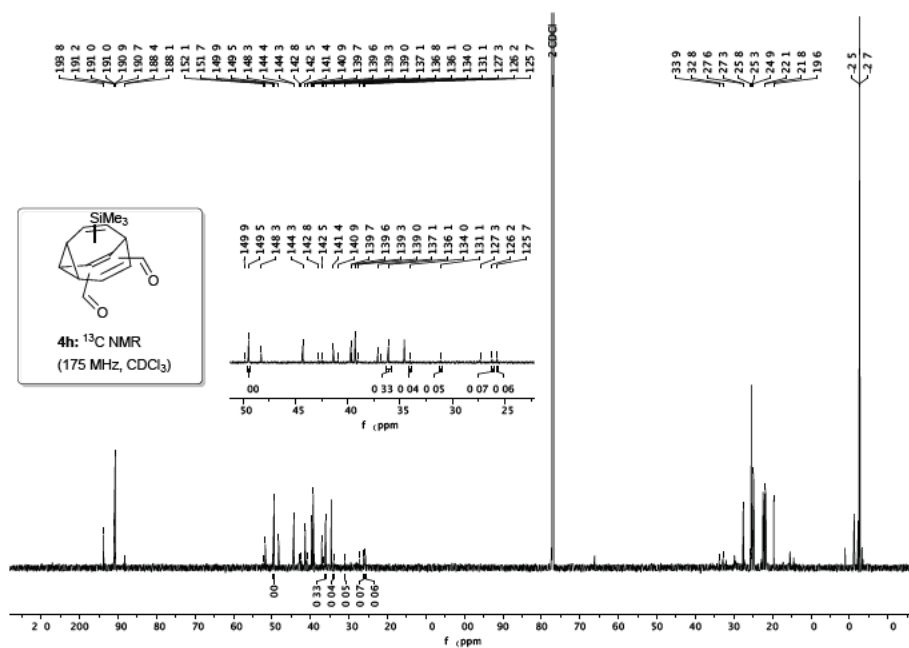
Figure 42: ¹³C NMR of bis-(aldehyde)-trimethylsilyl bullvalene -60 °C
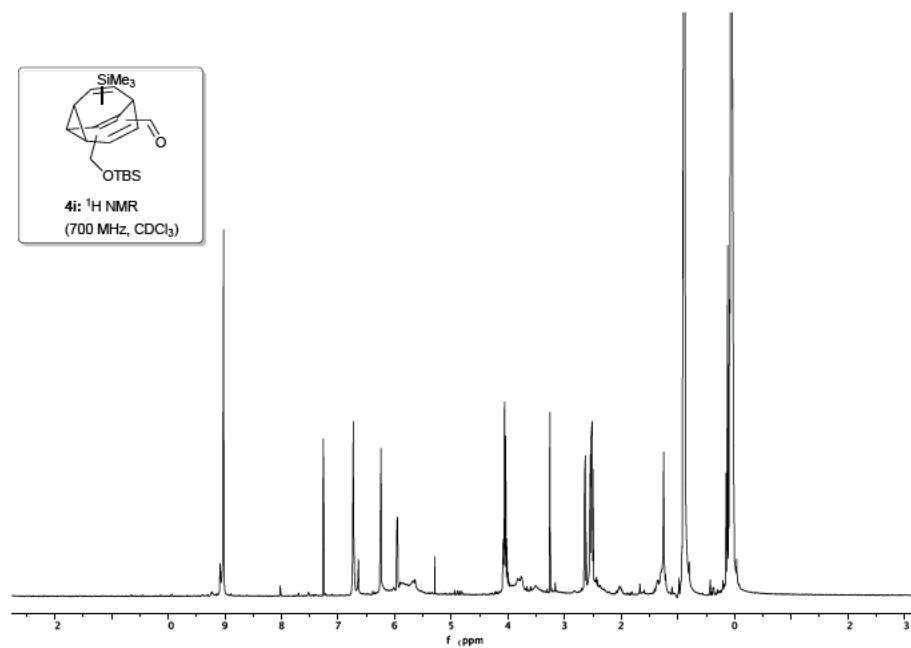
Figure 43: ¹H NMR of aldehyde-TBS-ether bullvalene at room temperature
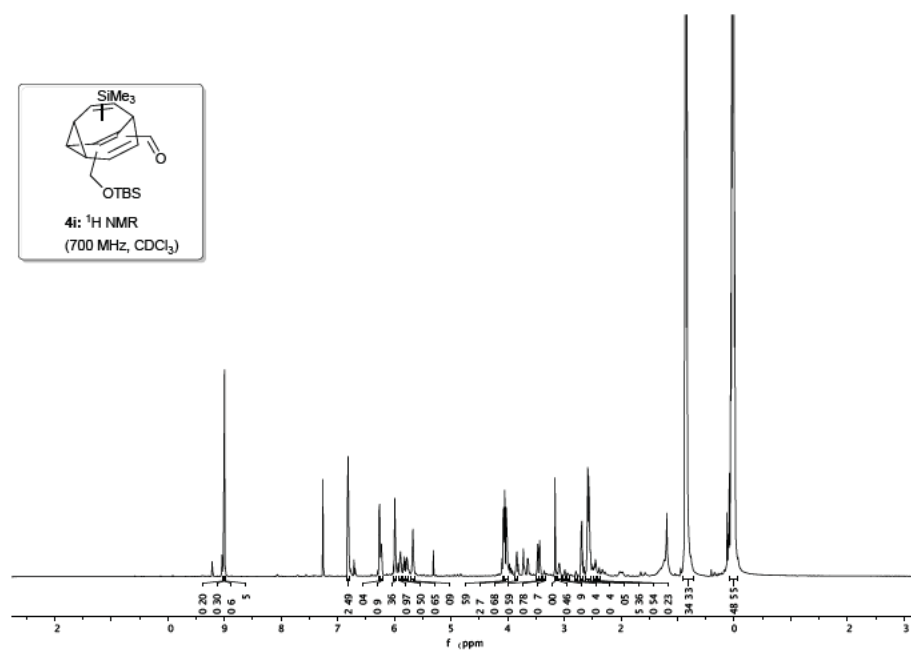
Figure 44: ¹H NMR of aldehyde-TBS-ether bullvalene -60 °C

Figure 45: ^{13}C NMR of aldehyde-TBS-ether bullvalene -60 °C

3.1. Structural Elucidation of Populated Isomers

Disubstituted bullvalenes:

The elucidation of the two most populated isomers for the disubstituted bullvalenes was routine and the analysis of methyl-trimethylsilyl-bullvalene **5a** is presented as an example to explain the method.

Isomer a: The bridgehead, or apex proton signal $\mathbf{H_a}$ is usually critical to structure elucidation. For **4a:A**, $\mathbf{H_a}$ is a doublet at 2.37 ppm which immediately identifies the structure (Figure 46).

Figure 46: ^{1}H NMR of methyl-trimethylsilyl-bullvalene showing **H$_a$** for isomer **a**, and **b** at -60 °C
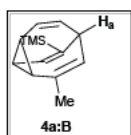
Isomer b: For **4a:B**, **H$_a$** is an apparent triplet at 2.45 ppm and the COSY spectrum shows two adjacent alkene proton signals indicating a single adjacent substituent (Figure 47). **H$_a$** is correlated to **H$_b$** which is a doublet indicating that the second substituent is in turn adjacent to **H$_b$**. The HMBC shows a correlation between the methyl proton signal at 1.86 ppm and one cyclopropyl proton at 27.4 ppm (Figure 48). This establishes the identity of the two substituents and confirms the structure of isomer **b**.
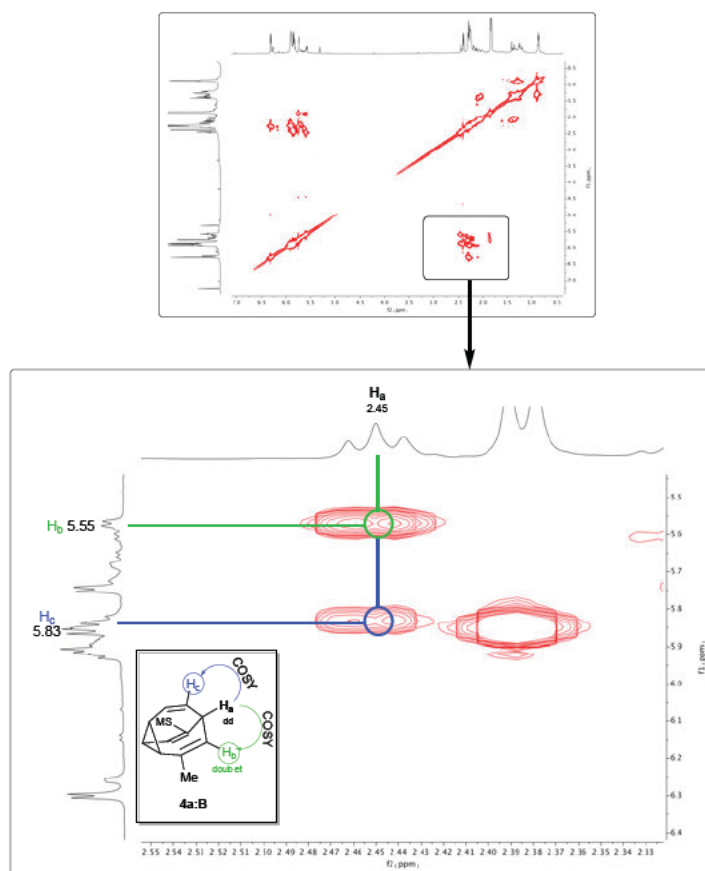
Figure 47: COSY spectrum indicating the correlation between **H$_a$** and alkenic protons (at -60 °C)
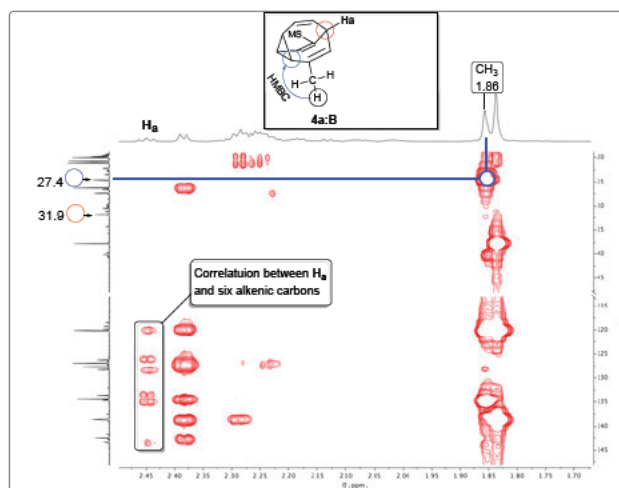
Figure 48: HMBC spectrum showing the coupling between the methyl proton a cyclopropyl ^{13}C signal (at -60 °C)

Analysis of 4f

4f:A: The room temperature ^{1}H NMR spectrum shows **4f:A** as a metastable isomer. The **H$_a$** signal is a singlet at 2.80 ppm immediately identifying the structure.
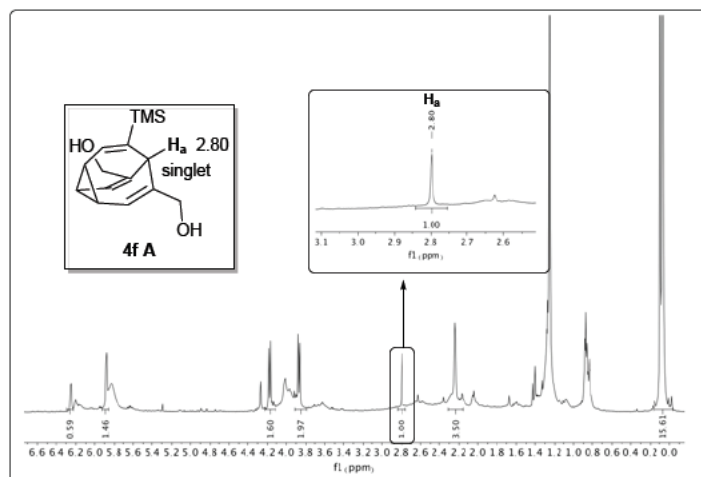
Figure 49: Room temperature ^{1}H NMR of **4f:A**

Low temperature NMR revealed isomer **4f:B** along with a range of minor isomers that could not be identified due to severe signal overlap.
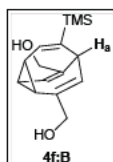
4f:B: The **H$_a$** signal at 2.58 ppm is a doublet indicating two adjacent substituents. The HMBC spectrum showed that **H$_a$** is correlated with six carbons indicating that the isomer does not have a mirror plane of symmetry, and therefore one of the substituents adjacent to **H$_a$** must be TMS (Figure 50). The DEPT spectrum showed that of the six alkenic signals three are quaternary. The HSQC-TOCSY shows only one correlation between **H$_a$** an alkene ^{13}C signal at 123 ppm (Figure 52). This establishes the position of the third substituent.
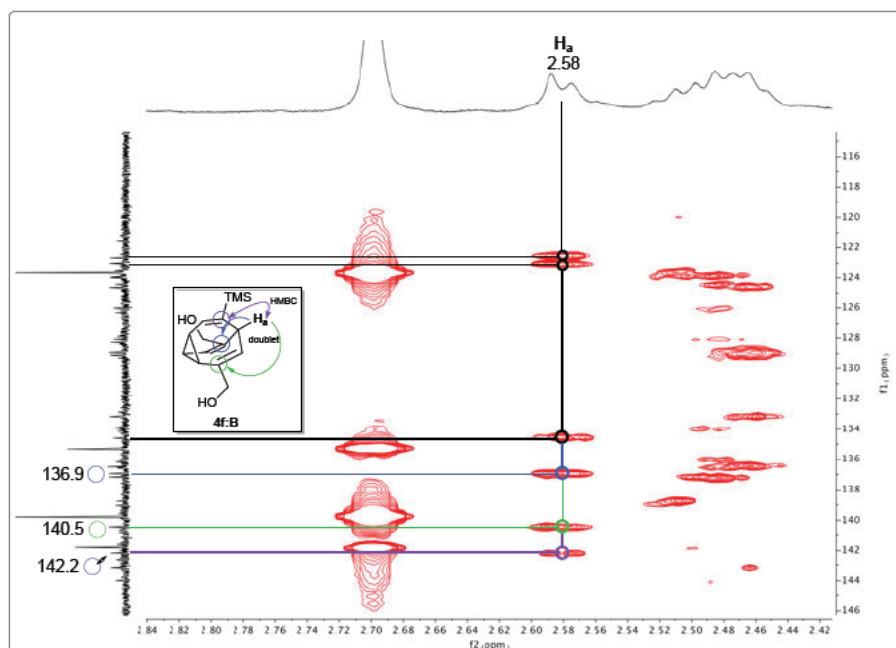
Figure 50: HMBC spectrum showing the correlation between **H$_a$** and the alkenic carbons (at -60 °C)
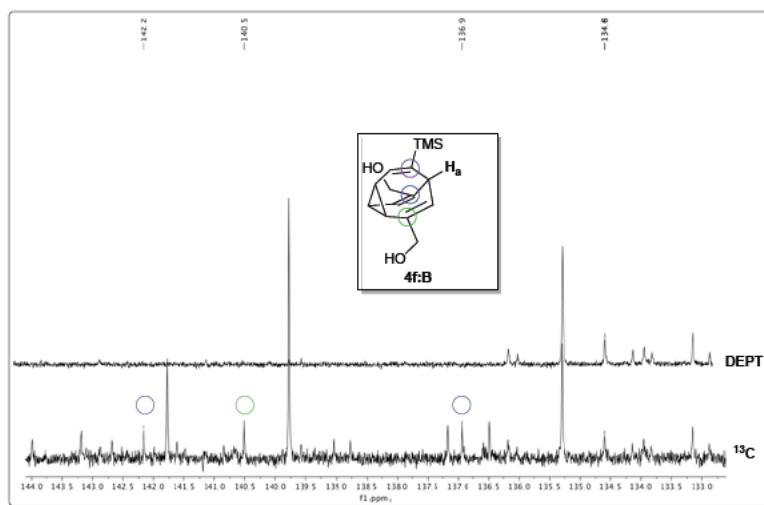
Figure 51: DEPT and ^{13}C NMR spectra to indicate the quaternary alkenic signals (at -60 °C)
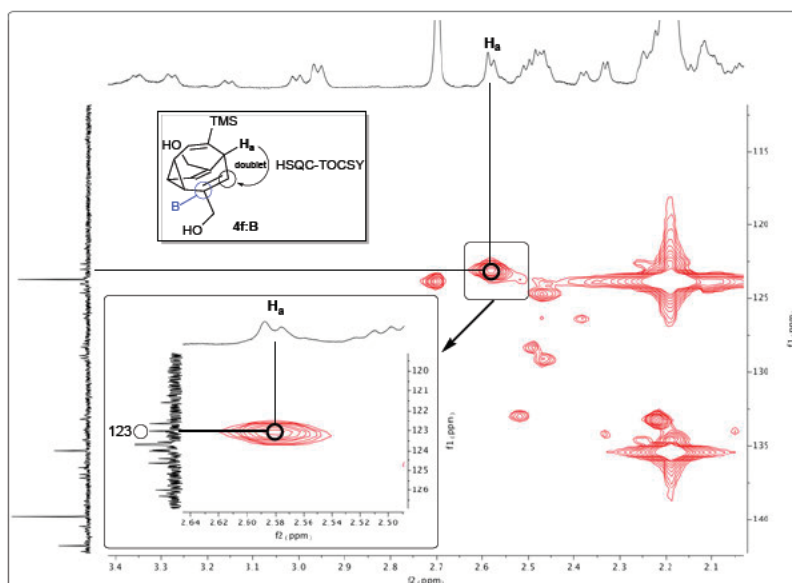
Figure 52: HSQC-TOCSY spectrum of **4f** indicating the correlation between **H$_a$** with only one alkenic proton (at -60 °C)

Analysis of 4g

4g:A: The **H$_a$** signal appears as a singlet at 3.26 ppm in the room temperature ^{1}H NMR spectrum, revealing the structure of **4g:A** (Figure 53).
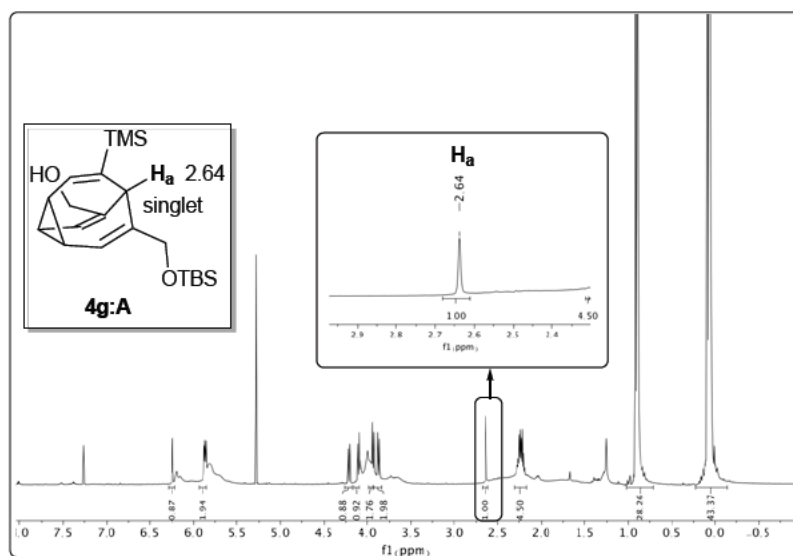
Figure 53: Room temperature ^{1}H NMR of **4g** showing the metastable **4g:A**
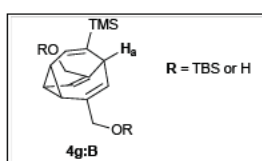
4g:B: For this bullvalene the CH_2OH and CH_2OTBS substituents could not spectroscopically distinguished. The isomer **4g:B** is generalised and assigned on the basis of analogy to **4f:B**. A range of other minor isomers could not be structurally elucidated due to severe signal overlap.

Analysis of 4h

4h:A: The **H_a** signal appears as a singlet at 4.44 ppm in the room temperature ^{1}H NMR spectrum, revealing the structure of **4h:A** (Figure 54).
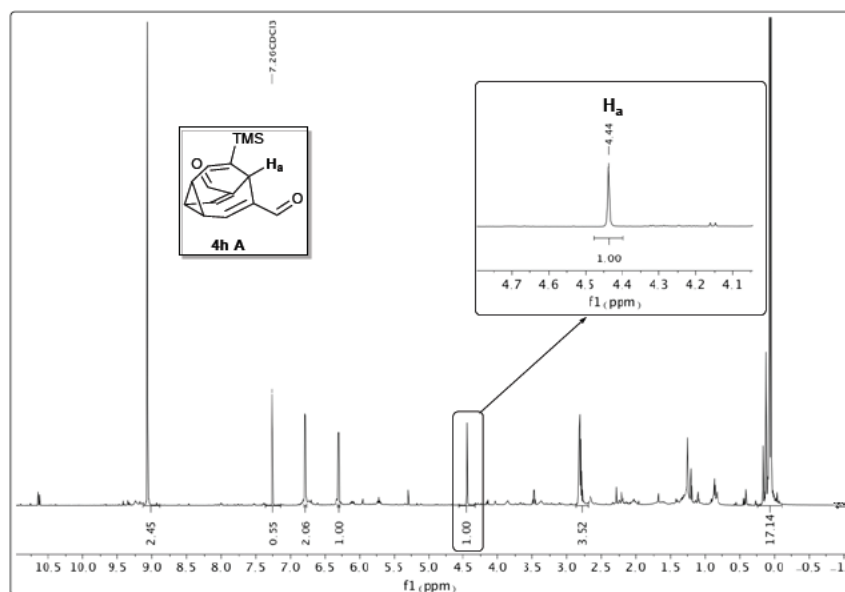
Figure 54: Room temperature proton NMR indicating the signal peaks for **4h:A**
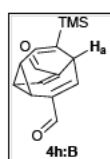
4h:B: The **H_b** signal at 3.81 ppm is a doublet in the ^{1}H NMR spectrum, indicating two adjacent substituents. The HMBC spectrum indicates that **4h:B** is unsymmetrical, because **H_a** is correlating with six alkenic ^{13}C signals and an aldehyde ^{13}C signal (Figure 55).
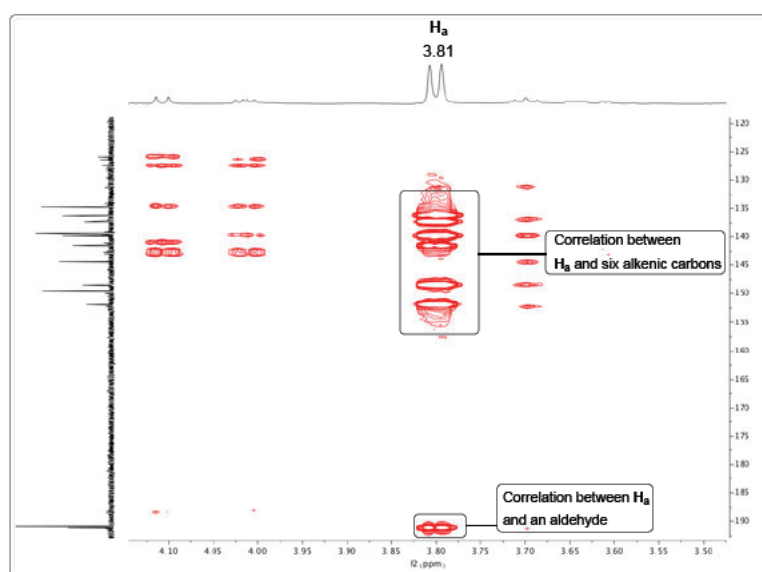
Figure 55: HMBC spectrum showing the correlation of **H$_a$** with six alkenic carbon and an aldehyde (at -60 °C)

The COSY spectrum shows a correlation between **H$_a$** and an alkenic proton signal **H$_b$** (Figure 56). Furthermore, **H$_b$** is a doublet signal and does not correlate with another akenic proton. This establishes the structure of **4h:B**.
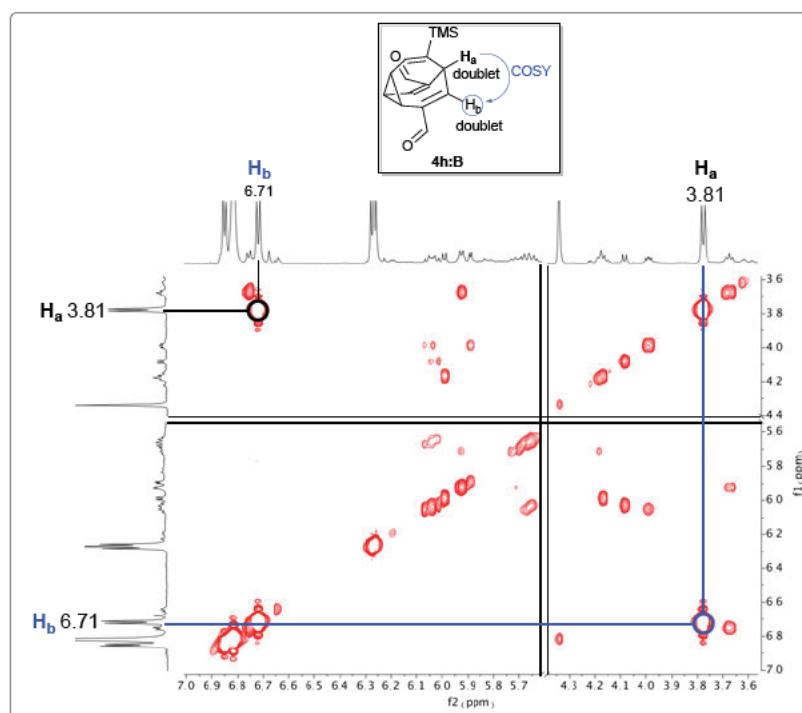
Figure 56: COSY spectrum showing the correlation between **H$_a$** and only one alkenic proton **H$_b$** (at -60 °C)
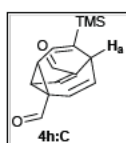
4h:C: The **H$_b$** signal at 4.12 ppm is a doublet in the ^{1}H NMR spectrum, indicating two adjacent substituents. The HMBC spectrum indicates that **4h:C** is unsymmetrical, because **H$_a$** is correlating with six alkenic ^{13}C signals, and establishes the TMS substituent as adjacent to **H$_a$** (Figure 57).
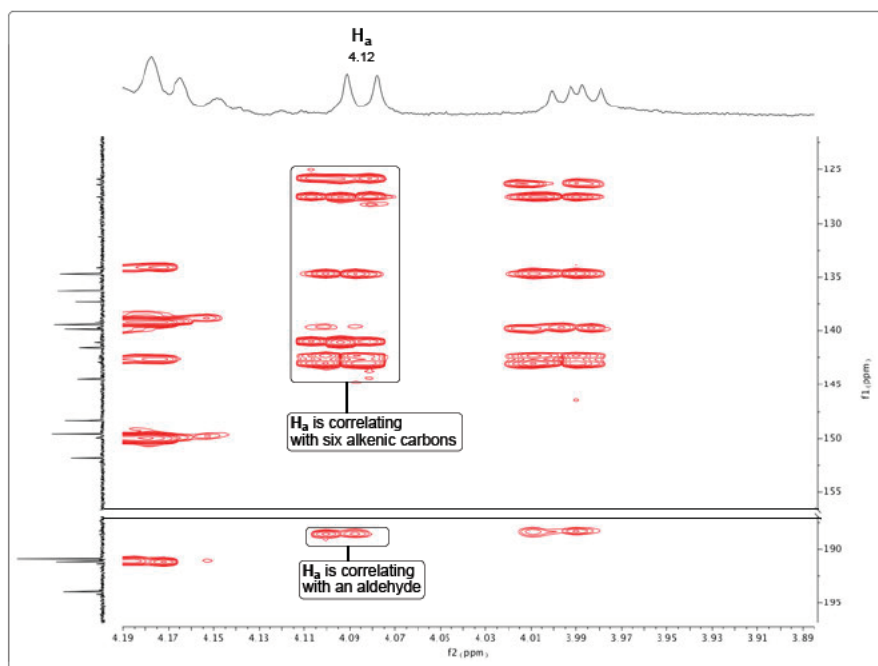
Figure 57: HMBC spectrum showing the correlation between H_a and six alkenic carbons and an aldehyde (at -60 °C)

The TOCSY spectrum indicates a correlation between H_a and two alkenic protons, indicating the position of the third substituent (Figure 58)
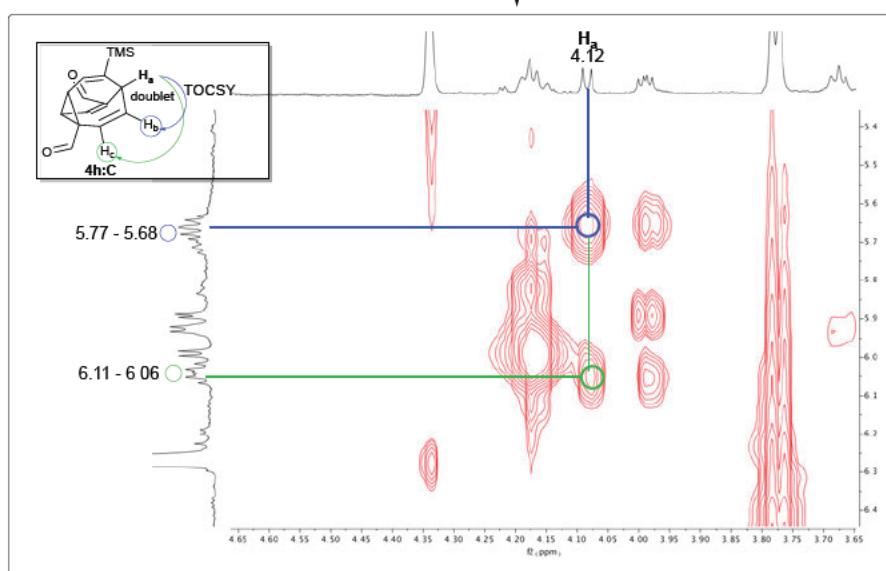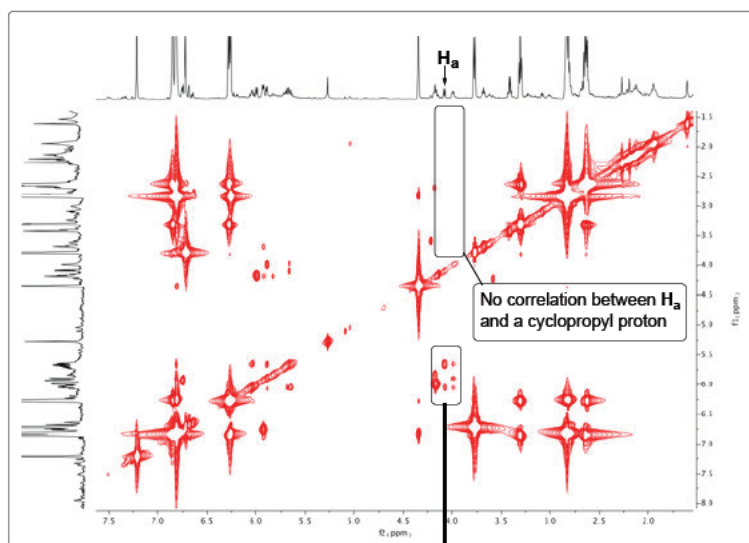
Figure 58: TOCSY spectrum indicating the correlation between **H$_a$** and two alkenic protons (at -60 °C)
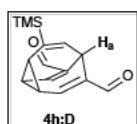
4h:D: The resolution of the **H$_a$** signal at 4.22 ppm in the proton NMR is not well defined, due to overlap with another signal. However, the HMBC spectrum shows clear correlations between **H$_a$** and four alkenic carbons, and an aldehyde carbon. This indicates that **4h:D** has an internal mirror plane of symmetry, and the adjacency of aldehyde substituents to **H$_a$** (Figure 59).
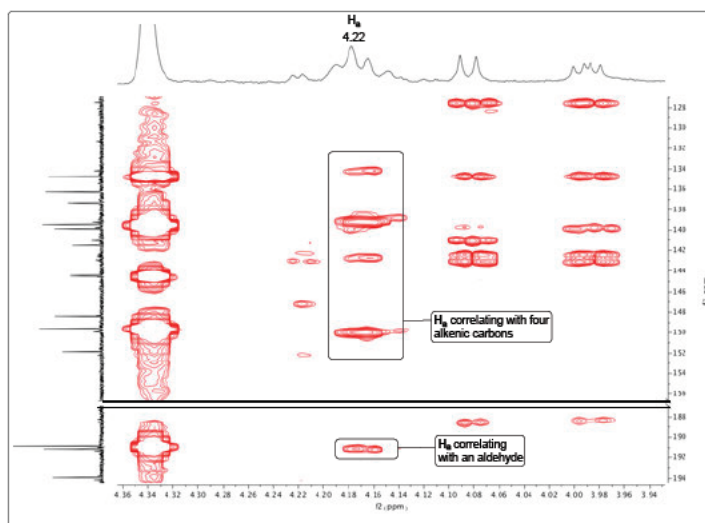
Figure 59: HMBC spectrum showing the correlation between **H$_a$** and four alkenic carbons (at -60 °C)

The COSY spectrum shows a correlation between **H$_a$** and only one alkenic signal, **H$_b$**. As **H$_b$** appears as a doublet, the structure of **4h:D** is confirmed (Figure 60).
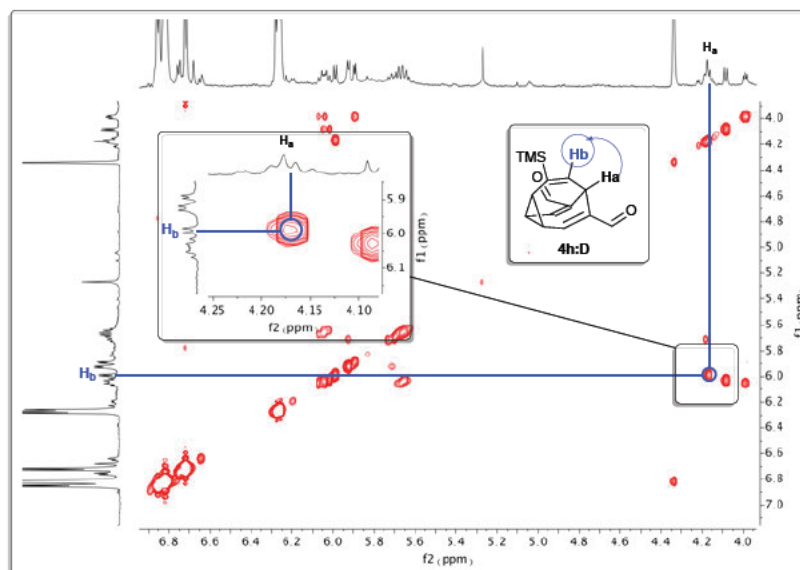
Figure 60: COSY spectrum indicating the correlation between **H$_a$** and **H$_b$** (at -60 °C)
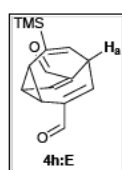
4h:E: The proton signal of H_a is an apparent triplet at 3.72 ppm, indicating one adjacent substituent. The HMBC spectrum **4h:E** reveals that H_a correlates with six alkenic carbons, as well as aldehyde carbon signal (Figure 61). This indicates that the structure does not have an internal mirror plane of symmetry. The correlation between H_a and an aldehyde carbon indicates the adjacency of an aldehyde to H_a. The COSY spectrum shows a correlation between H_a and two alkenic protons H_b and H_d, and both protons appear as doublet signals (Figure 62). So, the remaining two substituents must be attached to the alkenic carbons adjacent to carbon connected to H_b and H_d, respectively.
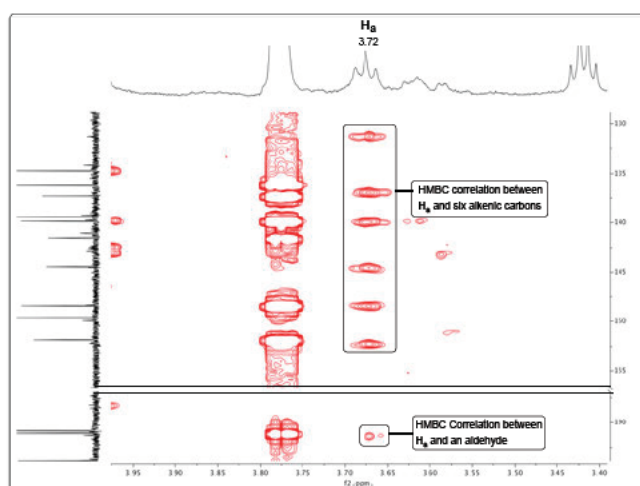
Figure 61: HMBC spectrum showing the correlation between H_a and, six alkenic carbons, and an aldehyde (at -60 °C)
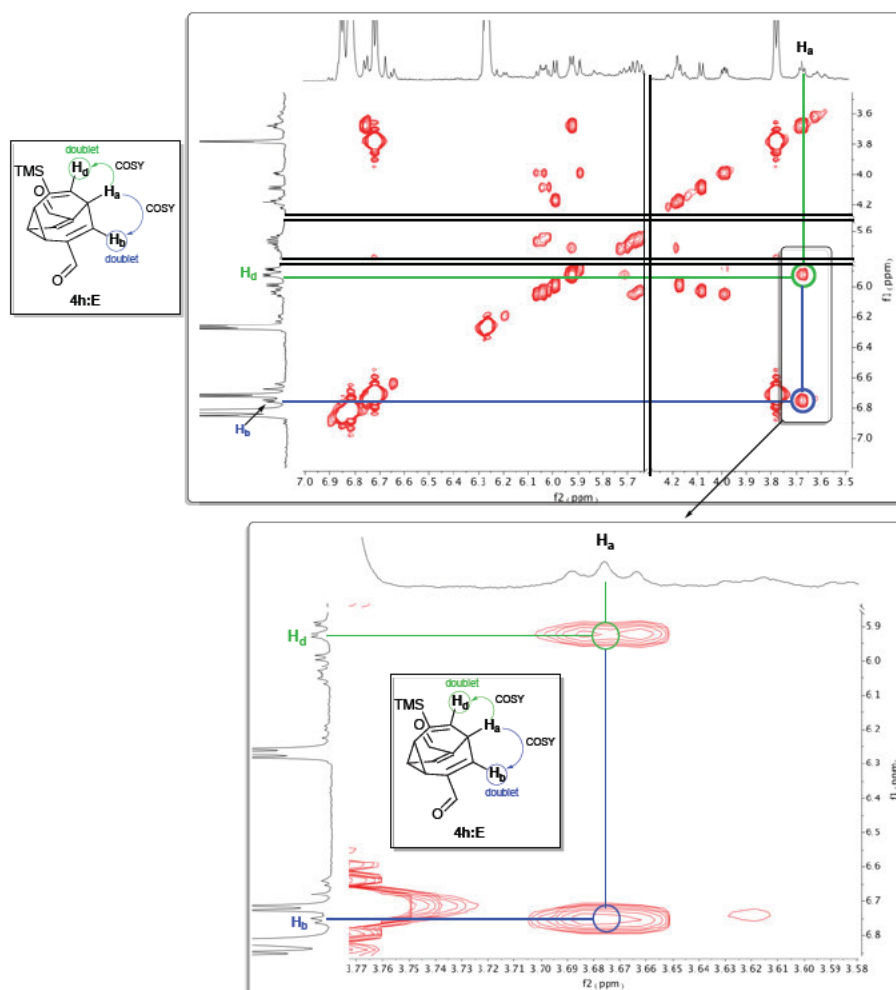
Figure 62: COSY spectrum showing the correlation between H_a and, H_b, and H_d (at -60 °C)
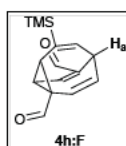
4h:F: The H_a signal appears as doublet of doublets at 4.03 ppm, indicating only one adjacent substituent. In The HMBC spectrum H_a correlates with six alkenic carbons and an aldehyde in the HMBC spectrum, which indicates a lack of a plane of symmetry and the position of an aldehyde substituent adjacent to H_a (Figure 63).
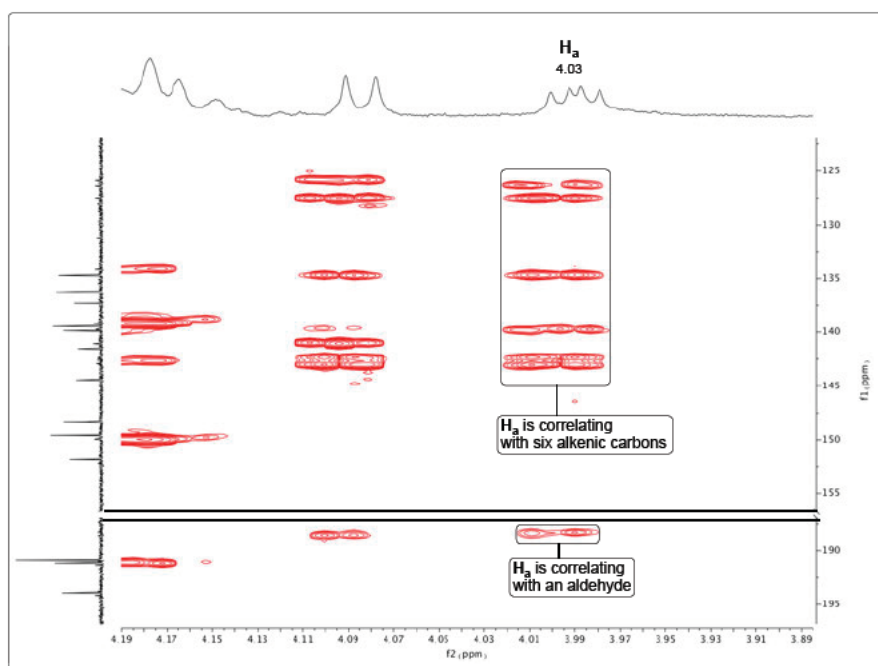
Figure 63: HMBC spectrum showing the correlation between **H$_a$** and six alkenic carbons and an aldehyde (at -60 °C)

The analysis of the TOCSY spectrum shows that **H$_a$** correlates with three alkenic proton signals at 5.77 − 5.68 (**H$_e$**), 5.94 − 5.93 (**H$_c$**), and 6.08 (**H$_b$**) ppm (Figure 64). This establishes the positions of the remaining substituents.
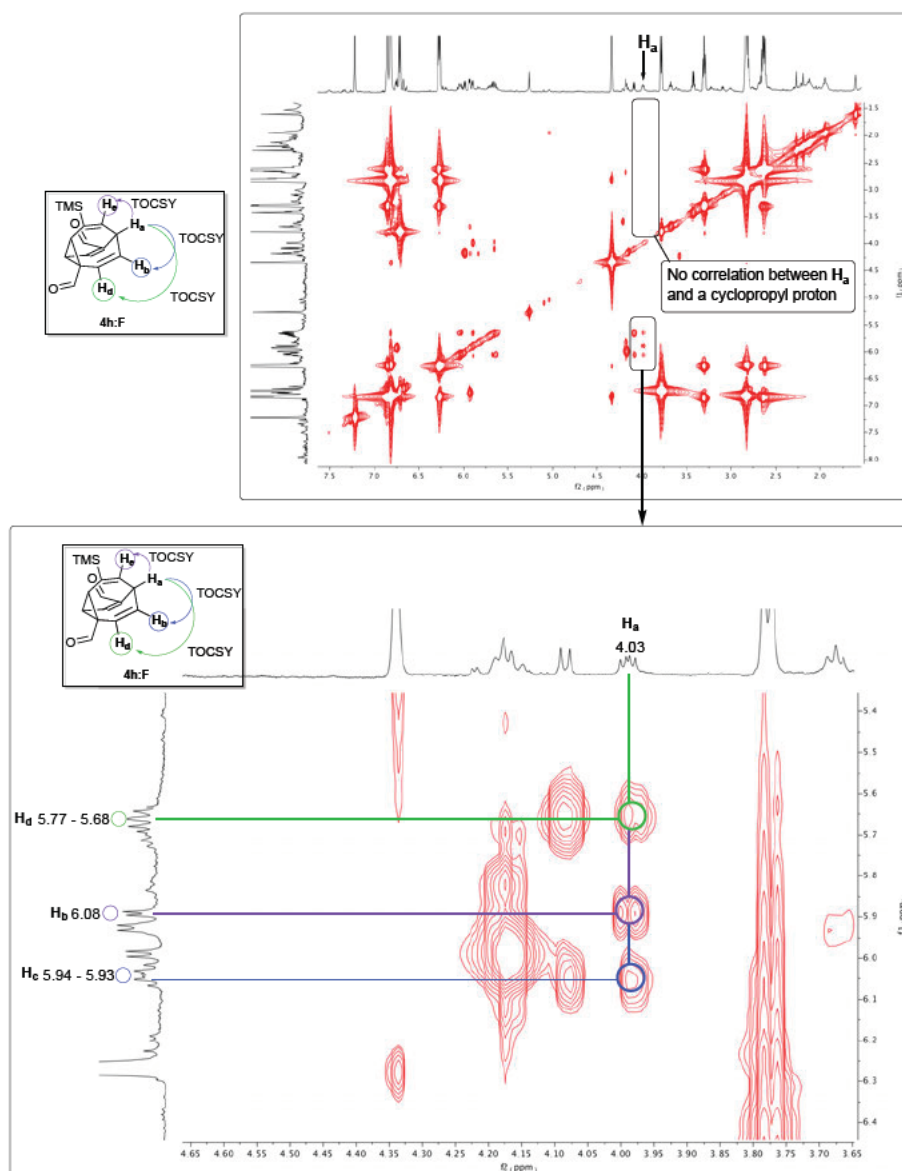
Figure 64: TOCSY spectrum indicating the correlation of the apex proton H_a to only two alkenic protons (at -60 °C)

The analysis of the COSY spectrum indicates a correlation between H_a and two alkenic protons H_e and H_b (Figure 65). While H_b correlates with an alkenic proton H_c, H_e shows no other correlations. These logical constraints are consistent only with the structure of isomer **d**.
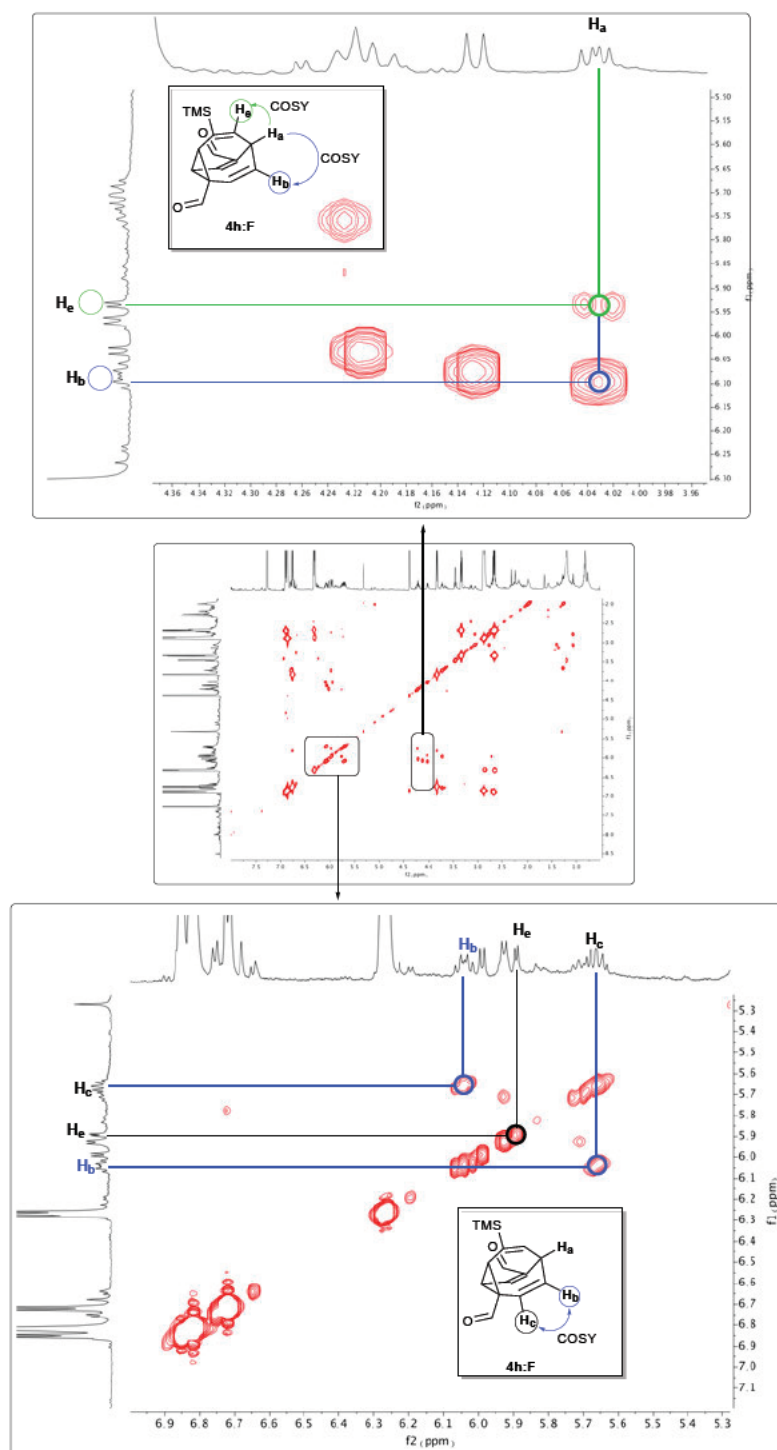
Figure 65: COSY spectrum showing the correlation between **H_a**, and, **H_b** and **H_e** (top), The correlation between **H_b** and **H_c** (bottom) (at -60 °C)

Analysis of 4i

4i:A: The structure of the meta-stable **4i:A** was revealed from the room temperature proton NMR spectrum. The apex proton is a singlet peak at 3.26 ppm (Figure 66).
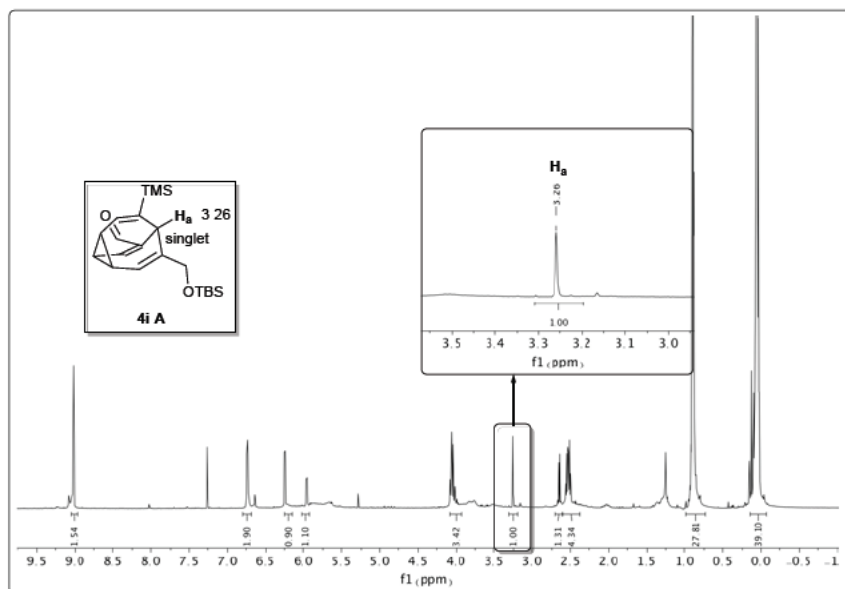
Figure 66: Room temperature ^{1}H NMR of **4g**
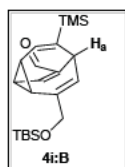
4i:B: This isomer was identified with a set of low temperature HSQC, HMBC, DEPT, COSY, TOCSY, and HSQC-TOCSY spectra. **H$_a$** appears as a doublet in the proton NMR at 3.47 ppm, indicating the adjacency of two substituents. The HMBC spectrum shows correlations between **H$_a$** the aldehyde carbon signal at 191.7 ppm (Figure 67), as well as six alkenic carbons (not shown). This indicates the adjacency of the aldehyde substituent to **H$_a$**. There is an absence of correlation between **H$_a$** and the methylene-OTBS carbon is (Figure 67), while this correlation is apparent in isomer **4:iA**. This indicates the non-adjacency of the methylene-OTBS substituent to **H$_a$**. HSQC-TOCSY experiment reveals a correlation between **H$_a$** and only *one* alkenic carbon signal at 120.9 ppm (Figure 68). This secures the position of the methylene-OTBS substituent, and the structure of isomer **b**.

- 129 -
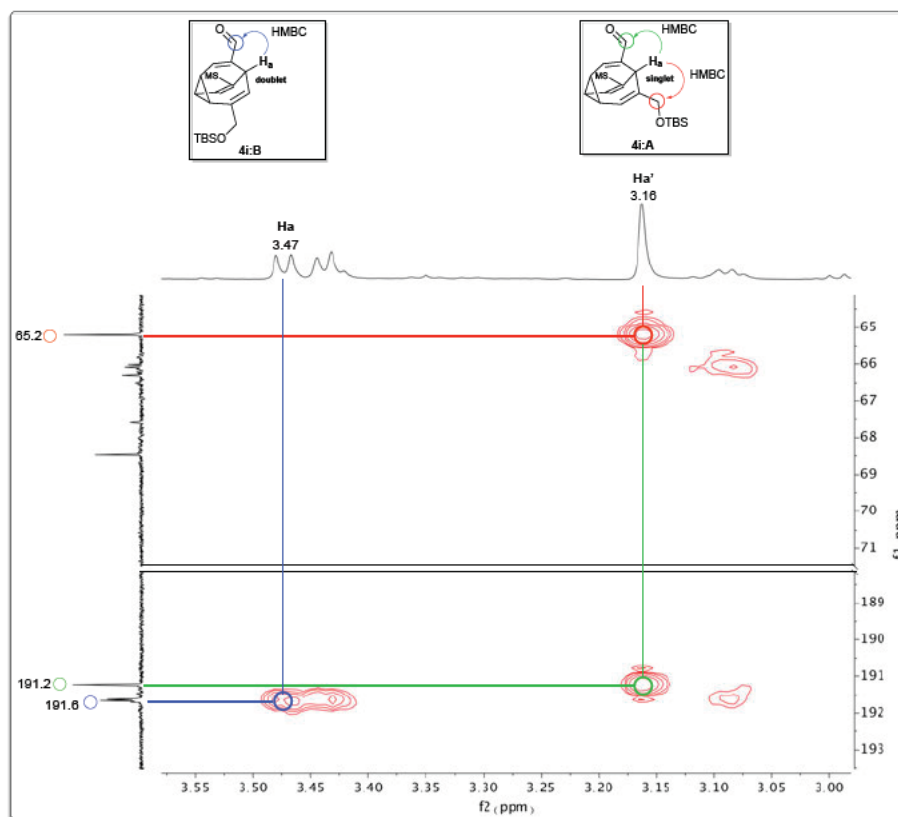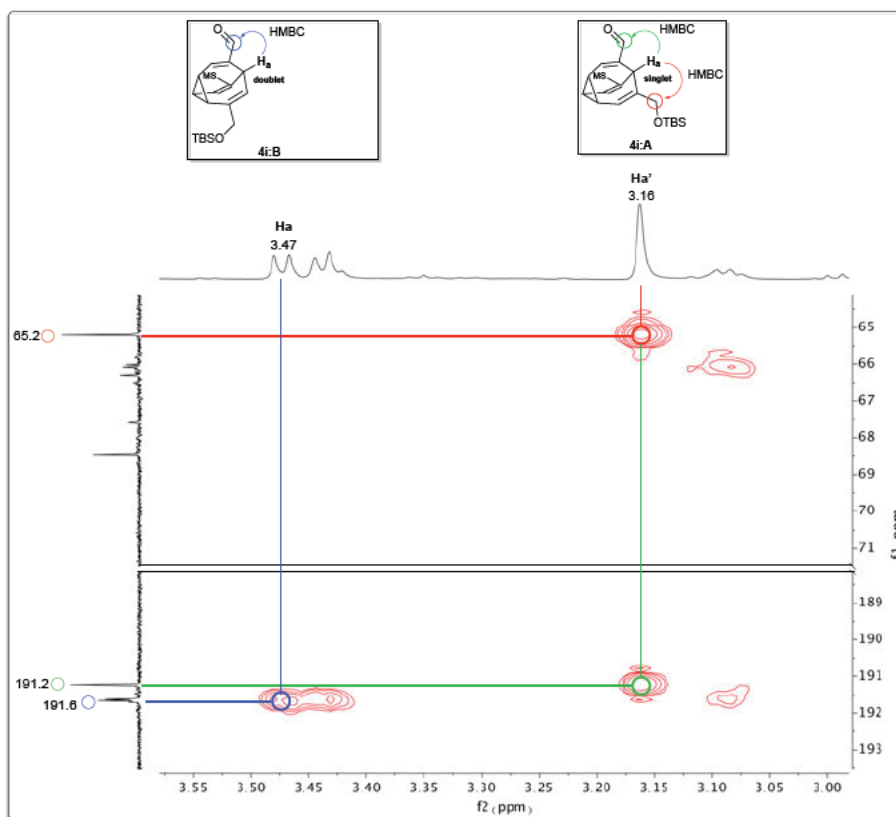
Figure 67: HMBC spectrum indicating the correlation between the apex proton (H_a and the aldehyde, and the CH_2 of CH_2OTBS for **4i:A** and **4i:B** (at -60 °C)
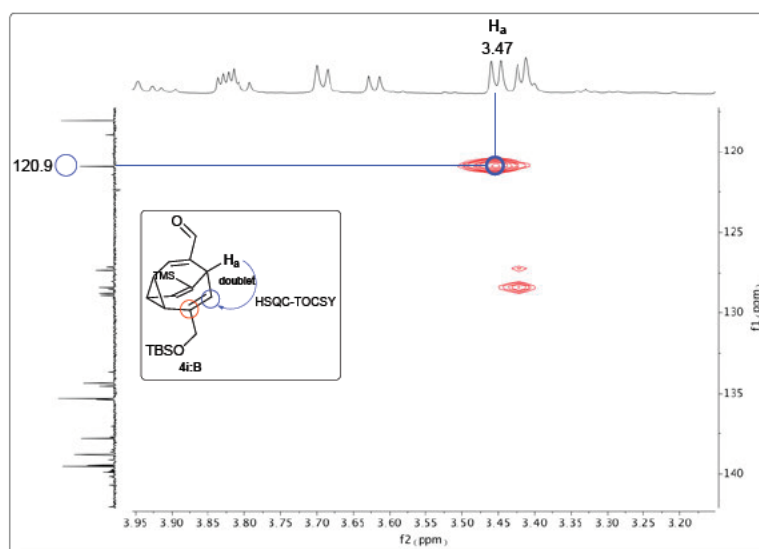
Figure 68: HSQC-TOCSY spectrum showing the correlation between H_a and one alkenic carbon (at -60 °C)
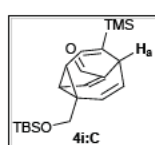
4i:C: The **H$_a$** proton signal appears as a doublet at 3.43 ppm, indicating two adjacent substituents. The HMBC spectrum shows a correlation between **H$_c$** and an aldehyde carbon signal, indicating the adjacency of the aldehyde group (Figure 69). However there is no correlation between **H$_a$** and a methylene carbon signal, indicating that the CH$_2$OTBS group is non-adjacent.
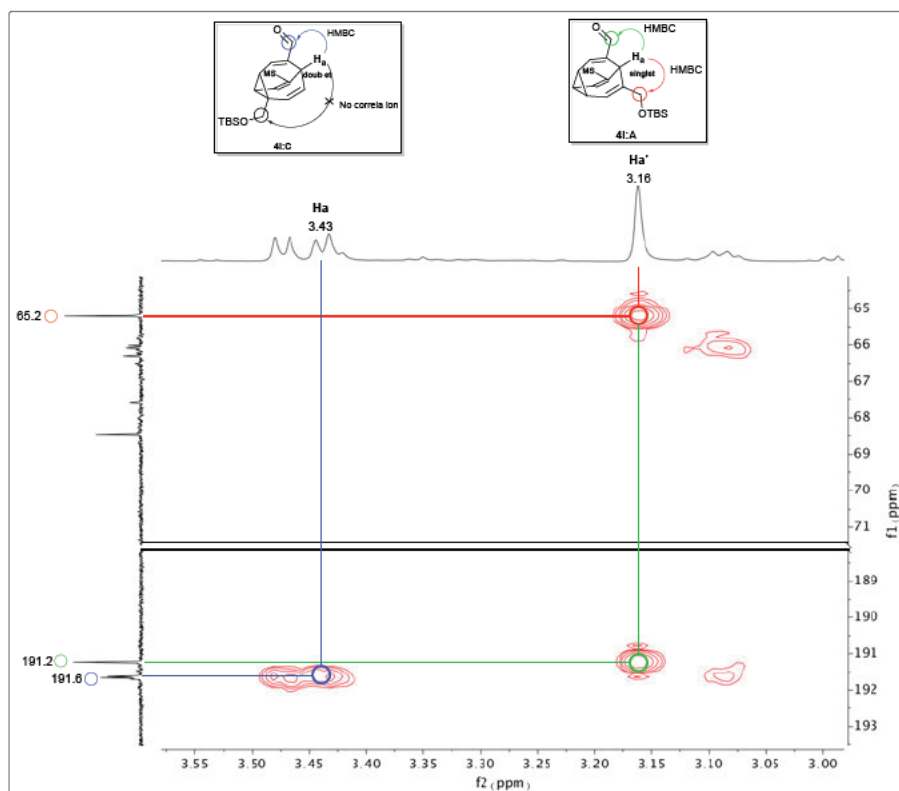
Figure 69: HMBC spectra of CH$_2$OTBS-TMS-CHO-bullvalene indicating correlation between the apex proton and the aldehyde, and the CH$_2$ of CH$_2$OTBS for isomer **a** and **c** (at -60 °C)

The HSQC-TOCSY spectrum indicates the correlation between **H$_a$** and two alkenic carbons at 127.3, and 128.5 ppm (Figure 70). However, there is no correlation between **H$_a$** and any of the cyclopropyl ^{13}C signals. Taken together, these logical constraints establish the position of the methylene-OTBS substituent.
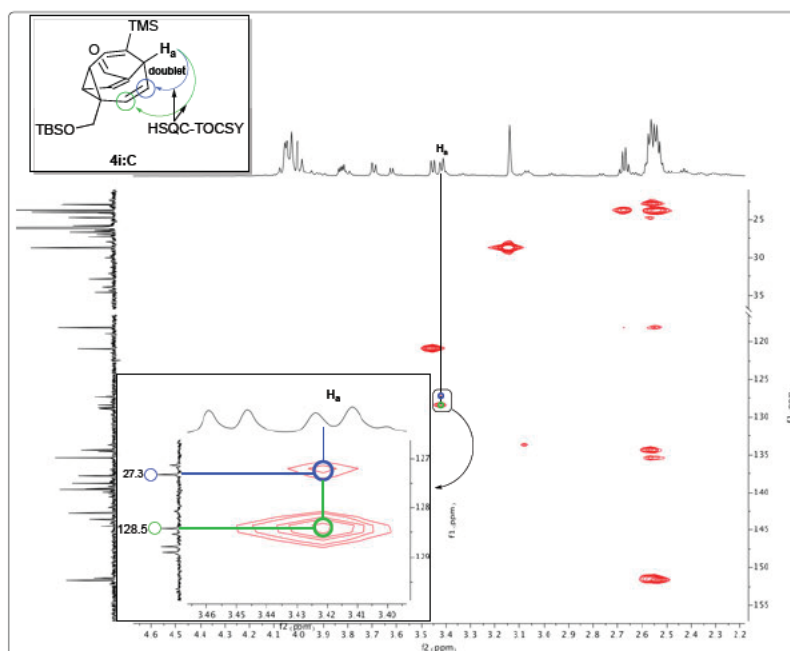
Figure 70: HSQC-TOCSY spectrum showing the correlation between **H**$_a$ and two alkenic carbons (at -60 °C)
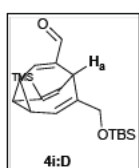
4i:D: HSQC-TOCSY spectrum shows that **H**$_a$ at 3.10 ppm correlates with only one alkenic carbon at 133.7 ppm, revealing the overall substitution pattern (Figure 71). The HMBC spectrum shows correlations with both methylene and aldehyde carbon signals, indicating their adjacency to **H**$_a$ (Figure 72).
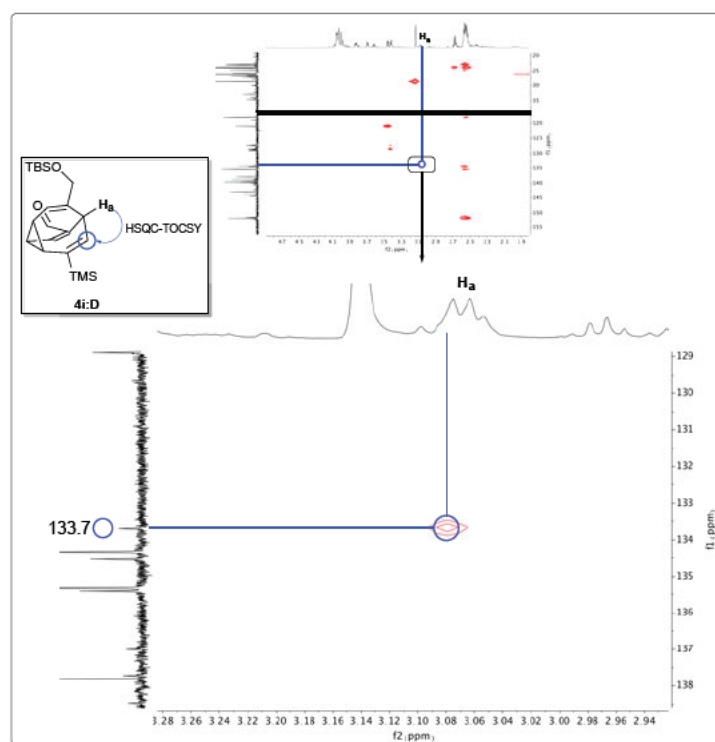
Figure 71: HSQC-TOCSY spectrum indicating the correlation between **H$_a$** and only one alkenic carbon (at -60 °C)
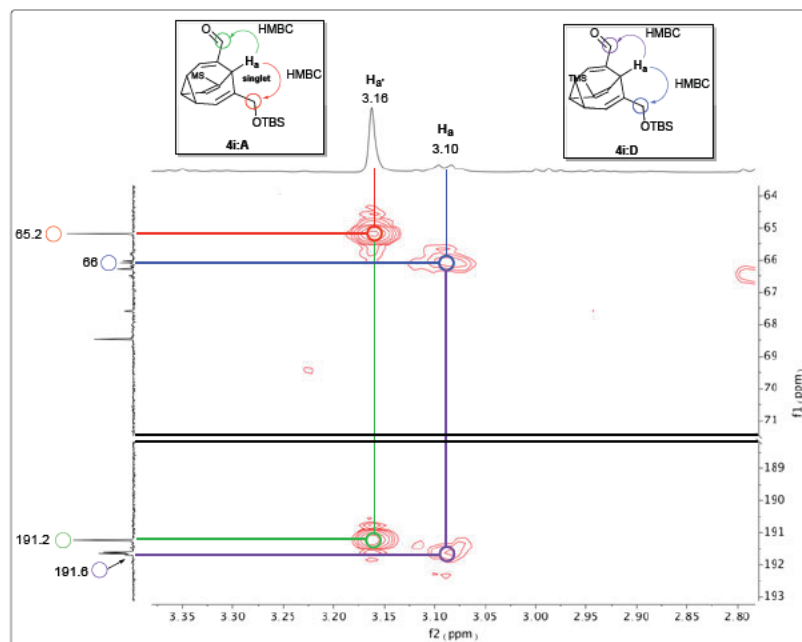
Figure 72: HMBC spectrum of **4i:A** and **4i:D** (at -60 °C)

4. Computational Section

4.1. Network Analysis Algorithm and Methodology
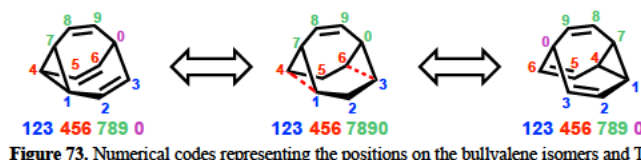
Figure 73. Numerical codes representing the positions on the bullvalene isomers and TS

Bullvalene isomer and TS codes were generated using our previously reported algorithm transformed into corresponding starting geometries.[3]

All *ab initio* calculations were performed using the program package ORCA 4.0.[4] The structures of the considered isomers and transition states (TSs) were optimized in a multi-step fashion. Initially, all internal rotations within the substituents were scanned and optimized using an inexpensive semiempirical PM3 method.[5] Selected lowest-energy rotamers were further reoptimized using DFT with the dispersion-corrected GGA functional PBE-D3BJ[6] and the 6-31G basis set.[7] Finally, a single rotamer with the lowest energy for each isomer/TS was kept and used as a starting geometry for the full optimization using the hybrid dispersion-corrected B3LYP-D3BJ[8] functional and the Def2-SVP basis set.[9] Subsequently, the single point energies were calculated with the same functional and the larger Def2-TZVPPd basis set,[10] with and without the use of the implicit continuous solvation model CPCM.[11]

Kinetic analysis of local kinetic features was performed using the *KinTek* software package (https://kintekcorp.com). Stochastic kinetic simulations of bullvalene networks **4d** and **4f** were performed using the Kinetiscope software package (http://hinsberg.net/kinetiscope).

[3] O. Yahiaoui, L. F. Pašteka, B. Judeel, T. Fallon, *Angew. Chem. Int. Ed.* **2018**, *57*, 2570–2574.
[4] F. Neese, *WIREs Comput Mol Sci* **2012**, *2*, 73
[5] J. J. P. Stewart, *J Comp Chem* **1989**, *10*, 209
[6] a) J. P. Perdew, K. Burke, and M. Ernzerhof, *Phys Rev Lett* **1996**, 77, 3865; *Phys Rev Lett* **1997**, 78, E1396, b) S. Gr mme, S. Ehr ch, L. Goer gk, *J Comp Chem* **2011**, *32*, 1456
[7] W. J. Hehre, R. D tchf e d, J. A. Pop e, *J Chem Phys* **1971**, *54*, 724; *J Chem Phys* **1972**, *56*, 2257; M. M. Franc , W. J. P etro, W. J. Hehre, J. S. B nk ey, D. J. DeFrees, J. A. Pop e, M. S. Gordon, *J Chem Phys* **1982**, 77, 3654
[8] A. D. Becke, *J Chem Phys* **1993**, *98*, 5648; C. Lee, W. Yang, R. G. Parr, *Phys Rev B* **1998**, *37*, 785
[9] F. We gend, R. Ah r chs, *Phys Chem Chem Phys* **2005**, *7*, 3297
[10] D. Rappoport, F. Furche, *J Chem Phys* **2010**, *133*, 134105
[11] V. Barone, M. Coss , *J Phys Chem A* **1998**, *102*, 1995; M. Coss , N. Rega, G. Sca man , V. Barone, *J Comp Chem* **2003**, *24*, 669

Table 1. Computational and experimental relative energies and ratios for bullvalene **4a**

isomer	gas phase			chloroform			Experimental (chloroform)	
	E_{rel} (kJ/mol)	pop. -60°C	pop. 25°C	E_{rel} (kJ/mol)	pop. -60°C	pop. 25°C		pop. -60°C
000 000 001 2	25.74	0.0%	0.0%	25.68	0.0%	0.0%		0.0%
000 000 002 1	42.21	0.0%	0.0%	41.20	0.0%	0.0%		0.0%
000 000 010 2	13.55	0.0%	0.1%	13.34	0.0%	0.1%		0.0%
000 000 012 0	23.38	0.0%	0.0%	23.20	0.0%	0.0%		0.0%
000 000 020 1	26.70	0.0%	0.0%	25.69	0.0%	0.0%		0.0%
000 000 021 0	21.35	0.0%	0.0%	20.97	0.0%	0.0%		0.0%
000 000 100 2	17.85	0.0%	0.0%	17.23	0.0%	0.0%		0.0%
000 000 102 0	10.35	0.1%	0.5%	9.82	0.2%	0.6%		0.0%
000 000 120 0	30.54	0.0%	0.0%	29.87	0.0%	0.0%		0.0%
000 000 200 1	31.41	0.0%	0.0%	30.53	0.0%	0.0%		0.0%
000 000 201 0	7.47	0.6%	1.6%	7.21	0.7%	1.7%		0.0%
000 000 210 0	28.61	0.0%	0.0%	28.77	0.0%	0.0%		0.0%
000 001 002 0 *	0.00	78.8%	64.6%	0.00	76.8%	62.8%		66.0%
000 001 020 0 *	2.83	16.0%	20.7%	2.59	17.8%	22.1%		34.0%
000 001 200 0 *	7.55	1.1%	3.1%	7.75	1.0%	2.8%		0.0%
000 002 010 0 *	6.45	2.1%	4.8%	6.34	2.1%	4.9%		0.0%
000 002 100 0 *	10.56	0.2%	0.9%	10.03	0.3%	1.1%		0.0%
000 010 020 0 *	7.84	0.9%	2.7%	7.78	0.9%	2.7%		0.0%
000 010 200 0 *	12.14	0.1%	0.5%	12.09	0.1%	0.5%		0.0%
000 020 100 0 *	11.82	0.1%	0.6%	11.21	0.1%	0.7%		0.0%
000 100 200 0 *	32.41	0.0%	0.0%	31.86	0.0%	0.0%		0.0%

Table 2. Computational and experimental relative energies and ratios for bullvalene **4b**

isomer	gas phase			chloroform			Experimental (chloroform)	
	E_{rel} (kJ/mol)	pop. -60°C	pop. 25°C	E_{rel} (kJ/mo)	pop. -60°C	pop. 25°C		pop. -60°C
000 000 001 2	35.20	0.0%	0.0%	33.86	0.0%	0.0%		0.0%
000 000 002 1	49.45	0.0%	0.0%	47.30	0.0%	0.0%		0.0%
000 000 010 2	23.36	0.0%	0.0%	21.70	0.0%	0.0%		0.0%
000 000 012 0	23.93	0.0%	0.0%	22.16	0.0%	0.0%		0.0%
000 000 020 1	24.46	0.0%	0.0%	23.63	0.0%	0.0%		0.0%
000 000 021 0	22.37	0.0%	0.0%	20.52	0.0%	0.0%		0.0%
000 000 100 2	27.29	0.0%	0.0%	24.50	0.0%	0.0%		0.0%
000 000 102 0	8.33	0.3%	0.9%	7.72	0.3%	1.0%		0.0%
000 000 120 0	36.97	0.0%	0.0%	35.12	0.0%	0.0%		0.0%
000 000 200 1	35.49	0.0%	0.0%	32.59	0.0%	0.0%		0.0%
000 000 201 0	10.54	0.1%	0.4%	11.01	0.1%	0.3%		0.0%
000 000 210 0	42.82	0.0%	0.0%	41.86	0.0%	0.0%		0.0%
000 001 002 0 *	1.66	24.3%	25.7%	0.73	34.7%	32.8%		76.0%
000 001 020 0 *	0.00	62.2%	50.3%	0.00	52.3%	44.0%		24.0%
000 001 200 0 *	8.51	0.5%	1.6%	8.57	0.4%	1.4%		0.0%
000 002 010 0 *	3.89	6.9%	10.5%	3.76	6.3%	9.6%		0.0%
000 002 100 0 *	11.71	0.1%	0.4%	11.61	0.1%	0.4%		0.0%
000 010 020 0 *	4.47	5.0%	8.3%	4.07	5.3%	8.5%		0.0%
000 010 200 0 *	13.60	0.0%	0.2%	13.84	0.0%	0.2%		0.0%
000 020 100 0 *	8.36	0.6%	1.7%	7.91	0.6%	1.8%		0.0%
000 100 200 0 *	33.68	0.0%	0.0%	32.00	0.0%	0.0%		0.0%

Table 3. Computational and experimental relative energies and ratios for bullvalene **4c**

isomer	gas phase			chloroform			Experimental (chloroform)	
	E_{rel} (kJ/mol)	pop. -60°C	pop. 25°C	E_{rel} (kJ/mol)	pop. -60°C	pop. 25°C		pop. -60°C
000 000 001 2	40.41	0.0%	0.0%	36.49	0.0%	0.0%		0.0%
000 000 002 1	46.24	0.0%	0.0%	45.96	0.0%	0.0%		0.0%
000 000 010 2	23.61	0.0%	0.0%	20.21	0.0%	0.0%		0.0%
000 000 012 0	21.80	0.0%	0.0%	20.79	0.0%	0.0%		0.0%
000 000 020 1	28.97	0.0%	0.0%	27.10	0.0%	0.0%		0.0%
000 000 021 0	19.49	0.0%	0.0%	18.46	0.0%	0.0%		0.0%
000 000 100 2	30.42	0.0%	0.0%	26.05	0.0%	0.0%		0.0%
000 000 102 0	12.12	0.0%	0.3%	10.81	0.1%	0.4%		0.0%
000 000 120 0	34.10	0.0%	0.0%	32.91	0.0%	0.0%		0.0%
000 000 200 1	37.03	0.0%	0.0%	34.18	0.0%	0.0%		0.0%
000 000 201 0	11.87	0.1%	0.3%	8.52	0.3%	1.1%		0.0%
000 000 210 0	38.29	0.0%	0.0%	37.27	0.0%	0.0%		0.0%
000 001 002 0 *	0.00	87.3%	72.4%	0.00	81.4%	65.4%		75.0%
000 001 020 0 *	4.75	6.0%	10.7%	3.70	10.1%	14.7%		25.0%
000 001 200 0 *	13.07	0.1%	0.4%	10.98	0.2%	0.8%		0.0%
000 002 010 0 *	6.38	2.4%	5.5%	6.01	2.8%	5.8%		0.0%
000 002 100 0 *	13.16	0.1%	0.4%	11.76	0.1%	0.6%		0.0%
000 010 020 0 *	6.98	1.7%	4.3%	6.37	2.2%	5.0%		0.0%
000 010 200 0 *	13.93	0.0%	0.3%	12.20	0.1%	0.5%		0.0%
000 020 100 0 *	6.40	2.4%	5.5%	6.01	2.7%	5.8%		0.0%
000 100 200 0 *	36.81	0.0%	0.0%	34.85	0.0%	0.0%		0.0%

Table 4. Computational and experimental relative energies and ratios for bullvalene **4d**

isomer	gas phase			chloroform			Experimental (chloroform)	
	E_{rel} (kJ/mol)	pop. -60°C	pop. 25°C	E_{rel} (kJ/mol)	pop. -60°C	pop. 25°C		pop. -60°C
000 000 001 2	30.65	0.0%	0.0%	28.20	0.0%	0.0%		0.0%
000 000 002 1	46.06	0.0%	0.0%	47.05	0.0%	0.0%		0.0%
000 000 010 2	17.78	0.0%	0.0%	15.08	0.0%	0.1%		0.0%
000 000 012 0	23.31	0.0%	0.0%	22.33	0.0%	0.0%		0.0%
000 000 020 1	28.04	0.0%	0.0%	25.14	0.0%	0.0%		0.0%
000 000 021 0	22.22	0.0%	0.0%	21.04	0.0%	0.0%		0.0%
000 000 100 2	22.30	0.0%	0.0%	19.05	0.0%	0.0%		0.0%
000 000 102 0	10.20	0.1%	0.6%	7.97	0.4%	1.1%		0.0%
000 000 120 0	30.45	0.0%	0.0%	31.36	0.0%	0.0%		0.0%
000 000 200 1	34.69	0.0%	0.0%	30.30	0.0%	0.0%		0.0%
000 000 201 0	8.05	0.5%	1.4%	4.48	2.7%	4.3%		0.0%
000 000 210 0	31.62	0.0%	0.0%	30.87	0.0%	0.0%		0.0%
000 001 002 0 *	0.00	88.0%	74.1%	0.00	67.1%	52.8%		76.0%
000 001 020 0 *	4.33	7.7%	12.9%	2.25	18.8%	21.3%		24.0%
000 001 200 0 *	8.36	0.8%	2.5%	4.70	4.7%	7.9%		0.0%
000 002 010 0 *	6.48	2.3%	5.4%	4.59	5.0%	8.3%		0.0%
000 002 100 0 *	15.59	0.0%	0.1%	11.41	0.1%	0.5%		0.0%
000 010 020 0 *	9.43	0.4%	1.7%	8.03	0.7%	2.1%		0.0%
000 010 200 0 *	11.67	0.1%	0.7%	9.59	0.3%	1.1%		0.0%
000 020 100 0 *	12.55	0.1%	0.5%	11.66	0.1%	0.5%		0.0%
000 100 200 0 *	32.74	0.0%	0.0%	31.45	0.0%	0.0%		0.0%

Table 5. Computational and experimental relative energies and ratios for bullvalene **4e**

isomer	gas phase			chloroform			Experimental (chloroform)	
	E_{rel} (kJ/mol)	pop. -60°C	pop. 25°C	E_{rel} (kJ/mol)	pop. -60°C	pop. 25°C		pop. -60°C
000 000 001 1	0.0%	0.0%	0.0%	60.07	0.0%	0.0%		0.0%
000 000 010 1	0.0%	0.0%	0.0%	24.21	0.0%	0.0%		0.0%
000 000 011 0	0.0%	0.0%	0.0%	45.24	0.0%	0.0%		0.0%
000 000 100 1	0.0%	0.0%	0.0%	28.79	0.0%	0.0%		0.0%
000 000 101 0	2.8%	3.4%	5.2%	4.59	7.2%	6.2%		0.0%
000 000 110 0	0.0%	0.0%	0.0%	52.88	0.0%	0.0%		0.0%
000 001 001 0	59.0%	72.5%	46.1%	0.00	48.0%	39.4%		70.0%
000 001 010 0 *	34.0%	20.9%	37.9%	1.59	39.1%	41.4%		30.0%
000 001 100 0 *	2.4%	1.5%	5.7%	5.76	3.7%	7.7%		0.0%
000 010 010 0	1.0%	1.2%	2.5%	6.78	1.1%	2.6%		0.0%
000 010 100 0 *	0.8%	0.5%	2.7%	8.23	0.9%	2.9%		0.0%
000 100 100 0	0.0%	0.0%	0.0%	49.90	0.0%	0.0%		0.0%

Table 6. Computational and experimental relative energies and ratios for bullvalene **4f**

isomer	gas phase			chloroform			experimental (chloroform)
	E_{rel} (kJ/mol)	pop. -60°C	pop. 25°C	E_{rel} (kJ/mol)	pop. -60°C	pop. 25°C	pop. -60°C
000 000 012 2	43.38	0.0%	0.0%	43.31	0.0%	0.0%	0.0%
000 000 021 2	77.35	0.0%	0.0%	73.63	0.0%	0.0%	0.0%
000 000 022 1	68.51	0.0%	0.0%	66.76	0.0%	0.0%	0.0%
000 000 102 2	24.67	0.0%	0.0%	22.87	0.0%	0.0%	0.0%
000 000 120 2	47.73	0.0%	0.0%	45.80	0.0%	0.0%	0.0%
000 000 122 0	55.01	0.0%	0.0%	54.14	0.0%	0.0%	0.0%
000 000 201 2	43.36	0.0%	0.0%	37.55	0.0%	0.0%	0.0%
000 000 202 1	59.00	0.0%	0.0%	56.24	0.0%	0.0%	0.0%
000 000 210 2	48.52	0.0%	0.0%	45.38	0.0%	0.0%	0.0%
000 000 212 0	82.72	0.0%	0.0%	78.69	0.0%	0.0%	0.0%
000 000 220 1	38.83	0.0%	0.0%	35.23	0.0%	0.0%	0.0%
000 000 221 0	38.66	0.0%	0.0%	37.65	0.0%	0.0%	0.0%
000 001 002 2 *	36.00	0.0%	0.0%	34.51	0.0%	0.0%	0.0%
000 001 020 2 *	39.35	0.0%	0.0%	34.79	0.0%	0.0%	0.0%
000 001 022 0 *	21.77	0.0%	0.0%	19.87	0.0%	0.1%	0.0%
000 001 200 2 *	43.35	0.0%	0.0%	37.61	0.0%	0.0%	0.0%
000 001 202 0 *	12.71	0.2%	1.0%	9.17	1.0%	3.4%	0.0%
000 001 220 0 *	15.02	0.0%	0.4%	12.09	0.2%	1.0%	0.0%
000 002 002 1	73.13	0.0%	0.0%	74.39	0.0%	0.0%	0.0%
000 002 010 2 *	20.71	0.0%	0.0%	19.08	0.0%	0.1%	0.0%
000 002 012 0 *	22.65	0.0%	0.0%	24.46	0.0%	0.0%	0.0%
000 002 020 1 *	54.65	0.0%	0.0%	53.52	0.0%	0.0%	0.0%
000 002 021 0 *	23.57	0.0%	0.0%	22.82	0.0%	0.0%	0.0%
000 002 100 2 *	24.80	0.0%	0.0%	22.81	0.0%	0.0%	0.0%
000 002 102 0 *	11.79	0.3%	1.4%	10.61	0.5%	1.9%	0.0%
000 002 120 0 *	39.78	0.0%	0.0%	45.28	0.0%	0.0%	0.0%
000 002 200 1 *	58.94	0.0%	0.0%	56.31	0.0%	0.0%	0.0%
000 002 201 0 *	12.55	0.2%	1.0%	8.74	1.3%	4.0%	0.0%
000 002 210 0 *	37.38	0.0%	0.0%	34.74	0.0%	0.0%	0.0%
000 010 020 2 *	26.32	0.0%	0.0%	21.63	0.0%	0.0%	0.0%
000 010 022 0 *	31.62	0.0%	0.0%	28.43	0.0%	0.0%	0.0%
000 010 200 2 *	28.91	0.0%	0.0%	24.22	0.0%	0.0%	0.0%
000 010 202 0 *	17.43	0.0%	0.1%	13.55	0.1%	0.6%	0.0%
000 010 220 0 *	19.83	0.0%	0.1%	19.99	0.0%	0.0%	0.0%
000 012 020 0 *	32.12	0.0%	0.0%	28.83	0.0%	0.0%	0.0%
000 012 200 0 *	35.69	0.0%	0.0%	32.45	0.0%	0.0%	0.0%
000 020 020 1	37.17	0.0%	0.0%	31.95	0.0%	0.0%	0.0%
000 020 021 0 *	31.35	0.0%	0.0%	28.00	0.0%	0.0%	0.0%
000 020 100 2 *	29.65	0.0%	0.0%	26.83	0.0%	0.0%	0.0%
000 020 102 0 *	18.18	0.0%	0.1%	16.10	0.0%	0.2%	0.0%
000 020 120 0 *	40.12	0.0%	0.0%	39.43	0.0%	0.0%	0.0%
000 020 200 1 *	39.86	0.0%	0.0%	37.50	0.0%	0.0%	0.0%
000 020 201 0 *	15.37	0.0%	0.3%	14.01	0.1%	0.5%	0.0%
000 020 210 0 *	40.31	0.0%	0.0%	37.57	0.0%	0.0%	0.0%
000 021 200 0 *	32.57	0.0%	0.0%	32.35	0.0%	0.0%	0.0%
000 022 100 0 *	36.57	0.0%	0.0%	36.01	0.0%	0.0%	0.0%
000 100 200 2 *	51.75	0.0%	0.0%	46.06	0.0%	0.0%	0.0%
000 100 202 0 *	40.89	0.0%	0.0%	35.63	0.0%	0.0%	0.0%
000 100 220 0 *	44.37	0.0%	0.0%	41.71	0.0%	0.0%	0.0%
000 102 200 0 *	40.27	0.0%	0.0%	35.15	0.0%	0.0%	0.0%
000 120 200 0 *	75.27	0.0%	0.0%	69.41	0.0%	0.0%	0.0%
000 200 200 1	42.03	0.0%	0.0%	37.47	0.0%	0.0%	0.0%
000 200 201 0 *	17.61	0.0%	0.1%	13.86	0.1%	0.5%	0.0%
000 200 210 0 *	64.52	0.0%	0.0%	61.95	0.0%	0.0%	0.0%
001 002 002 0	0.00	96.9%	82.2%	0.00	90.1%	68.0%	71.0%
001 002 020 0 *	9.10	1.1%	4.2%	7.28	3.0%	7.2%	29.0%
001 002 200 0 *	12.99	0.1%	0.9%	9.30	0.9%	3.2%	0.0%
001 020 020 0	13.72	0.0%	0.3%	9.19	0.5%	1.7%	0.0%
001 020 200 0 *	16.62	0.0%	0.2%	14.65	0.0%	0.4%	0.0%
001 200 200 0	18.53	0.0%	0.0%	14.54	0.0%	0.2%	0.0%
002 002 010 0	8.08	1.0%	6.3%	6.97	1.8%	4.1%	0.0%
002 002 100 0	12.48	0.1%	0.5%	11.48	0.1%	0.7%	0.0%
002 010 020 0 *	15.29	0.0%	0.3%	11.39	0.3%	1.4%	0.0%
002 010 200 0 *	17.75	0.0%	0.1%	13.66	0.0%	0.5%	0.0%
002 020 100 0 *	18.52	0.0%	0.1%	15.78	0.0%	0.2%	0.0%
002 100 200 0 *	40.61	0.0%	0.0%	35.58	0.0%	0.0%	0.0%
010 020 020 0	18.61	0.0%	0.0%	14.72	0.0%	0.2%	0.0%
010 020 200 0 *	20.72	0.0%	0.0%	19.70	0.0%	0.1%	0.0%
010 200 200 0	22.09	0.0%	0.0%	18.14	0.0%	0.0%	0.0%
020 020 100 0	29.11	0.0%	0.0%	23.62	0.0%	0.0%	0.0%
020 100 200 0 *	39.62	0.0%	0.0%	38.17	0.0%	0.0%	0.0%
100 200 200 0	73.52	0.0%	0.0%	71.47	0.0%	0.0%	0.0%

Table 7. Computational analysis of bullvalene **4g** at B3LYP-D3BJ/Def2-TZVPPD in the gas phase and CPCM solvent(chloroform) Note that Isomers 001 002 030 0 and 001 003 020 0 are experimentally indistinguishable

isomer	gas phase			chloroform			Experimental (chloroform)
	E_{rel} (kJ/mol)	pop. -60°C	pop. 25°C	E_{rel} (kJ/mol)	pop. -60°C	pop. 25°C	pop. -60°C
000 000 012 3	50.61	0.0%	0.0%	47.91	0.0%	0.0%	0.0%
000 000 013 2	46.41	0.0%	0.0%	44.42	0.0%	0.0%	0.0%
000 000 021 3	75.03	0.0%	0.0%	71.84	0.0%	0.0%	0.0%
000 000 023 1	65.65	0.0%	0.0%	62.75	0.0%	0.0%	0.0%
000 000 031 2	77.19	0.0%	0.0%	73.30	0.0%	0.0%	0.0%
000 000 032 1	64.29	0.0%	0.0%	63.01	0.0%	0.0%	0.0%
000 000 102 3	33.40	0.0%	0.0%	26.89	0.0%	0.0%	0.0%
000 000 103 2	19.20	0.0%	0.0%	17.80	0.0%	0.0%	0.0%
000 000 120 3	47.11	0.0%	0.0%	46.63	0.0%	0.0%	0.0%
000 000 123 0	53.97	0.0%	0.0%	53.23	0.0%	0.0%	0.0%
000 000 130 2	46.75	0.0%	0.0%	44.52	0.0%	0.0%	0.0%
000 000 132 0	52.14	0.0%	0.0%	50.45	0.0%	0.0%	0.0%
000 000 201 3	40.30	0.0%	0.0%	35.30	0.0%	0.0%	0.0%
000 000 203 1	53.31	0.0%	0.0%	51.48	0.0%	0.0%	0.0%
000 000 210 3	41.56	0.0%	0.0%	38.78	0.0%	0.0%	0.0%
000 000 213 0	82.80	0.0%	0.0%	77.41	0.0%	0.0%	0.0%
000 000 230 1	35.39	0.0%	0.0%	32.03	0.0%	0.0%	0.0%
000 000 231 0	41.87	0.0%	0.0%	38.81	0.0%	0.0%	0.0%
000 000 301 2	37.03	0.0%	0.0%	31.73	0.0%	0.0%	0.0%
000 000 302 1	54.35	0.0%	0.0%	52.92	0.0%	0.0%	0.0%
000 000 310 2	47.02	0.0%	0.0%	44.70	0.0%	0.0%	0.0%
000 000 312 0	75.94	0.0%	0.0%	73.89	0.0%	0.0%	0.0%
000 000 320 1	48.70	0.0%	0.0%	43.54	0.0%	0.0%	0.0%
000 000 321 0	45.17	0.0%	0.0%	43.34	0.0%	0.0%	0.0%
000 001 002 3 *	39.76	0.0%	0.0%	34.63	0.0%	0.0%	0.0%
000 001 003 2 *	35.32	0.0%	0.0%	33.36	0.0%	0.0%	0.0%
000 001 020 3 *	37.17	0.0%	0.0%	35.54	0.0%	0.0%	0.0%
000 001 023 0 *	23.55	0.0%	0.0%	20.70	0.0%	0.0%	0.0%
000 001 030 2 *	30.41	0.0%	0.0%	26.17	0.0%	0.0%	0.0%
000 001 032 0 *	16.95	0.0%	0.1%	16.73	0.0%	0.0%	0.0%
000 001 200 3 *	41.65	0.0%	0.0%	33.99	0.0%	0.0%	0.0%
000 001 203 0 *	12.77	0.0%	0.3%	8.47	0.4%	1.1%	0.0%
000 001 230 0 *	8.45	0.5%	1.5%	6.18	1.4%	2.6%	0.0%
000 001 300 2 *	38.35	0.0%	0.0%	34.59	0.0%	0.0%	0.0%
000 001 302 0 *	7.68	0.8%	2.0%	6.76	1.0%	2.1%	0.0%
000 001 320 0 *	23.73	0.0%	0.0%	17.41	0.0%	0.0%	0.0%
000 002 003 1 *	69.57	0.0%	0.0%	69.08	0.0%	0.0%	0.0%
000 002 010 3 *	23.03	0.0%	0.0%	17.08	0.0%	0.0%	0.0%
000 002 013 0 *	21.42	0.0%	0.0%	19.32	0.0%	0.0%	0.0%
000 002 030 1 *	48.05	0.0%	0.0%	48.17	0.0%	0.0%	0.0%
000 002 031 0 *	16.70	0.0%	0.1%	17.88	0.0%	0.0%	0.0%
000 002 100 3 *	32.56	0.0%	0.0%	25.36	0.0%	0.0%	0.0%
000 002 103 0 *	12.86	0.0%	0.2%	9.74	0.2%	0.6%	0.0%
000 002 130 0 *	37.73	0.0%	0.0%	34.79	0.0%	0.0%	0.0%
000 002 300 1 *	54.39	0.0%	0.0%	53.61	0.0%	0.0%	0.0%
000 002 301 0 *	9.92	0.2%	0.8%	8.81	0.3%	0.9%	0.0%
000 002 310 0 *	35.58	0.0%	0.0%	32.89	0.0%	0.0%	0.0%
000 003 010 2 *	13.63	0.0%	0.2%	11.77	0.1%	0.3%	0.0%
000 003 012 0 *	20.86	0.0%	0.0%	22.73	0.0%	0.0%	0.0%
000 003 020 1 *	53.78	0.0%	0.0%	49.08	0.0%	0.0%	0.0%
000 003 021 0 *	19.12	0.0%	0.0%	18.36	0.0%	0.0%	0.0%
000 003 100 2 *	20.98	0.0%	0.0%	18.32	0.0%	0.0%	0.0%
000 003 102 0 *	9.20	0.3%	1.1%	8.72	0.3%	1.0%	0.0%
000 003 120 0 *	39.44	0.0%	0.0%	38.06	0.0%	0.0%	0.0%
000 003 200 1 *	57.67	0.0%	0.0%	51.12	0.0%	0.0%	0.0%
000 003 201 0 *	14.71	0.0%	0.1%	8.11	0.5%	1.2%	0.0%
000 003 210 0 *	31.59	0.0%	0.0%	29.12	0.0%	0.0%	0.0%
000 010 020 3 *	26.63	0.0%	0.0%	24.11	0.0%	0.0%	0.0%
000 010 023 0 *	24.84	0.0%	0.0%	20.73	0.0%	0.0%	0.0%
000 010 030 2 *	19.46	0.0%	0.0%	17.03	0.0%	0.0%	0.0%

isomer	gas phase			chloroform			Experimental (chloroform)
	E_el (kJ/mol)	pop. -60°C	pop. 25°C	E_el (kJ/mol)	pop. -60°C	pop. 25°C	pop. -60°C
000 010 032 0 *	24.10	0.0%	0.0%	20.88	0.0%	0.0%	0.0%
000 010 200 3 *	26.64	0.0%	0.0%	23.05	0.0%	0.0%	0.0%
000 010 203 0 *	9.82	0.2%	0.8%	7.12	0.8%	1.8%	0.0%
000 010 230 0 *	13.23	0.0%	0.2%	11.60	0.1%	0.3%	0.0%
000 010 300 2 *	27.18	0.0%	0.0%	23.97	0.0%	0.0%	0.0%
000 010 302 0 *	21.07	0.0%	0.0%	17.80	0.0%	0.0%	0.0%
000 010 320 0 *	25.46	0.0%	0.0%	20.77	0.0%	0.0%	0.0%
000 012 030 0 *	19.29	0.0%	0.0%	17.68	0.0%	0.0%	0.0%
000 012 300 0 *	31.30	0.0%	0.0%	28.46	0.0%	0.0%	0.0%
000 013 020 0 *	29.97	0.0%	0.0%	26.85	0.0%	0.0%	0.0%
000 013 200 0 *	35.81	0.0%	0.0%	32.49	0.0%	0.0%	0.0%
000 020 030 1 *	30.16	0.0%	0.0%	26.80	0.0%	0.0%	0.0%
000 020 031 0 *	24.46	0.0%	0.0%	22.94	0.0%	0.0%	0.0%
000 020 100 3 *	32.85	0.0%	0.0%	29.18	0.0%	0.0%	0.0%
000 020 103 0 *	15.59	0.0%	0.1%	13.11	0.0%	0.2%	0.0%
000 020 130 0 *	36.60	0.0%	0.0%	34.84	0.0%	0.0%	0.0%
000 020 300 1 *	34.02	0.0%	0.0%	32.51	0.0%	0.0%	0.0%
000 020 301 0 *	11.86	0.1%	0.4%	9.17	0.3%	0.8%	0.0%
000 020 310 0 *	33.46	0.0%	0.0%	33.97	0.0%	0.0%	0.0%
000 021 030 0 *	24.17	0.0%	0.0%	23.32	0.0%	0.0%	0.0%
000 021 300 0 *	29.55	0.0%	0.0%	30.55	0.0%	0.0%	0.0%
000 023 100 0 *	32.19	0.0%	0.0%	30.93	0.0%	0.0%	0.0%
000 030 100 2 *	22.98	0.0%	0.0%	19.12	0.0%	0.0%	0.0%
000 030 102 0 *	10.16	0.2%	0.7%	8.61	0.4%	1.0%	0.0%
000 030 120 0 *	32.50	0.0%	0.0%	32.89	0.0%	0.0%	0.0%
000 030 200 1 *	32.00	0.0%	0.0%	30.67	0.0%	0.0%	0.0%
000 030 201 0 *	5.42	2.7%	4.9%	5.39	2.2%	3.6%	0.0%
000 030 210 0 *	36.33	0.0%	0.0%	36.09	0.0%	0.0%	0.0%
000 031 200 0 *	24.29	0.0%	0.0%	24.39	0.0%	0.0%	0.0%
000 032 100 0 *	25.59	0.0%	0.0%	21.89	0.0%	0.0%	0.0%
000 100 200 3 *	50.98	0.0%	0.0%	46.49	0.0%	0.0%	0.0%
000 100 203 0 *	39.43	0.0%	0.0%	36.15	0.0%	0.0%	0.0%
000 100 230 0 *	42.44	0.0%	0.0%	40.95	0.0%	0.0%	0.0%
000 100 300 2 *	49.66	0.0%	0.0%	46.19	0.0%	0.0%	0.0%
000 100 302 0 *	38.06	0.0%	0.0%	35.65	0.0%	0.0%	0.0%
000 100 320 0 *	48.58	0.0%	0.0%	42.19	0.0%	0.0%	0.0%
000 102 300 0 *	38.14	0.0%	0.0%	35.43	0.0%	0.0%	0.0%
000 103 200 0 *	37.87	0.0%	0.0%	32.78	0.0%	0.0%	0.0%
000 120 300 0 *	69.01	0.0%	0.0%	65.85	0.0%	0.0%	0.0%
000 130 200 0 *	67.64	0.0%	0.0%	61.75	0.0%	0.0%	0.0%
000 200 300 1 *	42.23	0.0%	0.0%	38.03	0.0%	0.0%	0.0%
000 200 301 0 *	12.06	0.1%	0.3%	9.00	0.3%	0.9%	0.0%
000 200 310 0 *	61.82	0.0%	0.0%	58.44	0.0%	0.0%	0.0%
000 201 300 0 *	16.88	0.0%	0.1%	14.28	0.0%	0.1%	0.0%
000 210 300 0 *	35.23	0.0%	0.0%	35.34	0.0%	0.0%	0.0%
001 002 003 0 *	0.00	58.3%	43.9%	0.56	32.7%	25.5%	77.0%
001 002 030 0 *	1.38	26.8%	25.2%	0.00	44.9%	31.9%	11.5%
001 002 300 0 *	10.43	0.2%	0.7%	7.98	0.5%	1.3%	0.0%
001 003 020 0 *	3.49	8.1%	10.7%	3.02	8.2%	9.4%	11.5%
001 003 200 0 *	13.44	0.0%	0.2%	6.37	1.2%	2.5%	0.0%
001 020 030 0 *	9.17	0.3%	1.1%	6.43	1.2%	2.4%	0.0%
001 020 300 0 *	10.80	0.1%	0.6%	9.95	0.2%	0.6%	0.0%
001 030 200 0 *	10.25	0.2%	0.7%	9.34	0.2%	0.7%	0.0%
001 200 300 0 *	19.63	0.0%	0.0%	16.30	0.0%	0.0%	0.0%
002 003 010 0 *	11.22	0.1%	0.5%	10.66	0.1%	0.4%	0.0%
002 003 100 0 *	15.74	0.0%	0.1%	14.72	0.0%	0.1%	0.0%
002 010 030 0 *	12.59	0.1%	0.3%	9.59	0.2%	0.7%	0.0%
002 010 300 0 *	15.53	0.0%	0.1%	12.24	0.0%	0.2%	0.0%
002 030 100 0 *	14.72	0.0%	0.1%	12.63	0.0%	0.2%	0.0%
002 100 300 0 *	37.43	0.0%	0.0%	35.27	0.0%	0.0%	0.0%
003 010 020 0 *	9.06	0.4%	1.1%	5.83	1.7%	3.0%	0.0%
003 010 200 0 *	11.31	0.1%	0.5%	7.59	0.6%	1.5%	0.0%
003 020 100 0 *	15.52	0.0%	0.1%	13.08	0.0%	0.2%	0.0%
003 100 200 0 *	38.00	0.0%	0.0%	33.17	0.0%	0.0%	0.0%
010 020 030 0 *	14.46	0.0%	0.1%	11.81	0.1%	0.3%	0.0%
010 020 300 0 *	18.03	0.0%	0.0%	14.60	0.0%	0.1%	0.0%
010 030 200 0 *	14.52	0.0%	0.1%	13.97	0.0%	0.1%	0.0%
010 200 300 0 *	21.02	0.0%	0.0%	16.22	0.0%	0.1%	0.0%
020 030 100 0 *	15.17	0.0%	0.1%	13.01	0.0%	0.2%	0.0%
020 100 300 0 *	38.76	0.0%	0.0%	37.41	0.0%	0.0%	0.0%
030 100 200 0 *	33.95	0.0%	0.0%	34.26	0.0%	0.0%	0.0%
100 200 300 0 *	65.69	0.0%	0.0%	62.84	0.0%	0.0%	0.0%

Table 8. Computational analysis of bullvalene **4h** at B3LYP-D3BJ/Def2-TZVPPD in the gas phase and CPCM solvent(chloroform)

isomer	gas phase			chloroform			perimental (chlorofor
	E_{rel} (kJ/mol)	pop. -60°C	pop. 25°C	E_{rel} (kJ/mol)	pop. -60°C	pop. 25°C	pop. -60°C
000 000 012 2	70.85	0.0%	0.0%	70.52	0.0%	0.0%	0.0
000 000 021 2	93.69	0.0%	0.0%	100.54	0.0%	0.0%	0.0
000 000 022 1	83.11	0.0%	0.0%	87.12	0.0%	0.0%	0.0
000 000 102 2	64.91	0.0%	0.0%	66.87	0.0%	0.0%	0.0
000 000 120 2	80.20	0.0%	0.0%	82.43	0.0%	0.0%	0.0
000 000 122 0	68.93	0.0%	0.0%	72.56	0.0%	0.0%	0.0
000 000 201 2	57.46	0.0%	0.0%	64.27	0.0%	0.0%	0.0
000 000 202 1	60.57	0.0%	0.0%	62.71	0.0%	0.0%	0.0
000 000 210 2	68.45	0.0%	0.0%	73.52	0.0%	0.0%	0.0
000 000 212 0	71.84	0.0%	0.0%	78.75	0.0%	0.0%	0.0
000 000 220 1	70.55	0.0%	0.0%	73.62	0.0%	0.0%	0.0
000 000 221 0	59.93	0.0%	0.0%	61.72	0.0%	0.0%	0.0
000 001 002 2 *	72.64	0.0%	0.0%	75.66	0.0%	0.0%	0.0
000 001 020 2 *	46.46	0.0%	0.0%	51.88	0.0%	0.0%	0.0
000 001 022 0 *	40.31	0.0%	0.0%	47.19	0.0%	0.0%	0.0
000 001 200 2 *	58.45	0.0%	0.0%	65.02	0.0%	0.0%	0.0
000 001 202 0 *	19.26	0.0%	0.1%	20.95	0.0%	0.0%	0.0
000 001 220 0 *	48.18	0.0%	0.0%	50.07	0.0%	0.0%	0.0
000 002 002 1	81.44	0.0%	0.0%	79.77	0.0%	0.0%	0.0
000 002 010 2 *	61.45	0.0%	0.0%	62.56	0.0%	0.0%	0.0
000 002 012 0 *	30.67	0.0%	0.0%	29.27	0.0%	0.0%	0.0
000 002 020 1 *	49.93	0.0%	0.0%	49.61	0.0%	0.0%	0.0
000 002 021 0 *	31.51	0.0%	0.0%	31.95	0.0%	0.0%	0.0
000 002 100 2 *	65.91	0.0%	0.0%	66.86	0.0%	0.0%	0.0
000 002 102 0 *	12.51	0.2%	1.2%	10.17	0.6%	3.0%	0.0
000 002 120 0 *	37.66	0.0%	0.0%	36.48	0.0%	0.0%	0.0
000 002 200 1 *	63.67	0.0%	0.0%	65.46	0.0%	0.0%	0.0
000 002 201 0 *	20.74	0.0%	0.0%	22.58	0.0%	0.0%	0.0
000 002 210 0 *	27.90	0.0%	0.0%	31.81	0.0%	0.0%	0.0
000 010 020 2 *	57.90	0.0%	0.0%	59.91	0.0%	0.0%	0.0
000 010 022 0 *	48.21	0.0%	0.0%	53.68	0.0%	0.0%	0.0
000 010 200 2 *	50.46	0.0%	0.0%	54.85	0.0%	0.0%	0.0
000 010 202 0 *	11.94	0.2%	1.5%	12.47	0.2%	1.2%	0.0
000 010 220 0 *	51.15	0.0%	0.0%	53.53	0.0%	0.0%	0.0
000 012 020 0 *	37.41	0.0%	0.0%	36.39	0.0%	0.0%	0.0
000 012 200 0 *	31.66	0.0%	0.0%	35.47	0.0%	0.0%	0.0
000 020 020 1	52.36	0.0%	0.0%	52.22	0.0%	0.0%	0.0
000 020 021 0 *	39.12	0.0%	0.0%	40.23	0.0%	0.0%	0.0
000 020 100 2 *	62.00	0.0%	0.0%	63.57	0.0%	0.0%	0.0
000 020 102 0 *	32.39	0.0%	0.0%	30.93	0.0%	0.0%	0.0
000 020 120 0 *	57.74	0.0%	0.0%	57.37	0.0%	0.0%	0.0
000 020 200 1 *	48.81	0.0%	0.0%	51.00	0.0%	0.0%	0.0
000 020 201 0 *	25.46	0.0%	0.0%	27.19	0.0%	0.0%	0.0
000 020 210 0 *	47.39	0.0%	0.0%	50.23	0.0%	0.0%	0.0
000 021 200 0 *	37.11	0.0%	0.0%	38.52	0.0%	0.0%	0.0
000 022 100 0 *	51.02	0.0%	0.0%	58.19	0.0%	0.0%	0.0
000 100 200 2 *	75.03	0.0%	0.0%	82.65	0.0%	0.0%	0.0
000 100 202 0 *	52.91	0.0%	0.0%	50.14	0.0%	0.0%	0.0
000 100 220 0 *	75.81	0.0%	0.0%	80.66	0.0%	0.0%	0.0
000 102 200 0 *	48.20	0.0%	0.0%	53.77	0.0%	0.0%	0.0
000 120 200 0 *	74.10	0.0%	0.0%	74.53	0.0%	0.0%	0.0
000 200 200 1	69.66	0.0%	0.0%	74.09	0.0%	0.0%	0.0
000 200 201 0 *	45.12	0.0%	0.0%	49.88	0.0%	0.0%	0.0
000 200 210 0 *	67.29	0.0%	0.0%	73.09	0.0%	0.0%	0.0
001 002 002 0	0.00	99.0%	94.3%	0.00	97.3%	90.4%	64.0
001 002 020 0 *	23.81	0.0%	0.0%	21.71	0.0%	0.0%	21.0
001 002 200 0 *	21.90	0.0%	0.0%	23.80	0.0%	0.0%	4.0
001 020 020 0	30.93	0.0%	0.0%	29.56	0.0%	0.0%	0.0
001 020 200 0 *	26.59	0.0%	0.0%	28.33	0.0%	0.0%	0.0
001 200 200 0	46.57	0.0%	0.0%	51.32	0.0%	0.0%	0.0
002 002 010 0	9.20	0.6%	2.3%	7.00	1.9%	5.4%	5.0
002 002 100 0	13.00	0.1%	0.5%	34.94	0.0%	0.0%	0.0
002 010 020 0 *	30.24	0.0%	0.0%	27.59	0.0%	0.0%	2.0
002 010 200 0 *	25.84	0.0%	0.0%	27.69	0.0%	0.0%	0.0
002 020 100 0 *	33.56	0.0%	0.0%	30.88	0.0%	0.0%	0.0
002 100 200 0 *	34.04	0.0%	0.0%	40.03	0.0%	0.0%	0.0
010 020 020 0	36.46	0.0%	0.0%	35.12	0.0%	0.0%	0.0
010 020 200 0 *	29.53	0.0%	0.0%	31.70	0.0%	0.0%	0.0
010 200 200 0	47.68	0.0%	0.0%	53.34	0.0%	0.0%	0.0
020 020 100 0	39.42	0.0%	0.0%	38.20	0.0%	0.0%	0.0
020 100 200 0 *	52.91	0.0%	0.0%	58.52	0.0%	0.0%	0.0
100 200 200 0	94.48	0.0%	0.0%	98.08	0.0%	0.0%	0.0

Table 9. Computational analysis of bullvalene **4i** at B3LYP-D3BJ/Def2-TZVPPD in the gas phase and CPCM solvent(chloroform)

isomer	gas phase			chloroform			Experimental (chloroform)
	E_{rel} (kJ/mol)	pop. -60°C	pop. 25°C	E_{rel} (kJ/mol)	pop. -60°C	pop. 25°C	pop. -60°C
000 000 012 3	70.35	0.0%	0.0%	73.24	0.0%	0.0%	0.0%
000 000 013 2	76.64	0.0%	0.0%	79.45	0.0%	0.0%	0.0%
000 000 021 3	86.84	0.0%	0.0%	85.99	0.0%	0.0%	0.0%
000 000 023 1	81.54	0.0%	0.0%	80.28	0.0%	0.0%	0.0%
000 000 031 2	95.87	0.0%	0.0%	97.22	0.0%	0.0%	0.0%
000 000 032 1	80.40	0.0%	0.0%	83.41	0.0%	0.0%	0.0%
000 000 102 3	49.94	0.0%	0.0%	46.11	0.0%	0.0%	0.0%
000 000 103 2	62.53	0.0%	0.0%	63.07	0.0%	0.0%	0.0%
000 000 120 3	60.93	0.0%	0.0%	61.82	0.0%	0.0%	0.0%
000 000 123 0	69.78	0.0%	0.0%	70.17	0.0%	0.0%	0.0%
000 000 130 2	80.17	0.0%	0.0%	79.66	0.0%	0.0%	0.0%
000 000 132 0	63.26	0.0%	0.0%	61.07	0.0%	0.0%	0.0%
000 000 201 3	49.11	0.0%	0.0%	49.58	0.0%	0.0%	0.0%
000 000 203 1	65.73	0.0%	0.0%	65.65	0.0%	0.0%	0.0%
000 000 210 3	49.50	0.0%	0.0%	50.63	0.0%	0.0%	0.0%
000 000 213 0	70.52	0.0%	0.0%	71.72	0.0%	0.0%	0.0%
000 000 230 1	56.24	0.0%	0.0%	56.81	0.0%	0.0%	0.0%
000 000 231 0	64.05	0.0%	0.0%	63.18	0.0%	0.0%	0.0%
000 000 301 2	62.41	0.0%	0.0%	62.11	0.0%	0.0%	0.0%
000 000 302 1	68.16	0.0%	0.0%	67.00	0.0%	0.0%	0.0%
000 000 310 2	77.80	0.0%	0.0%	80.21	0.0%	0.0%	0.0%
000 000 312 0	94.50	0.0%	0.0%	96.76	0.0%	0.0%	0.0%
000 000 320 1	63.70	0.0%	0.0%	61.66	0.0%	0.0%	0.0%
000 000 321 0	69.47	0.0%	0.0%	72.50	0.0%	0.0%	0.0%
000 001 002 3 *	56.47	0.0%	0.0%	53.58	0.0%	0.0%	0.0%
000 001 003 2 *	66.84	0.0%	0.0%	70.13	0.0%	0.0%	0.0%
000 001 020 3 *	37.64	0.0%	0.0%	35.74	0.0%	0.0%	0.0%
000 001 023 0 *	31.86	0.0%	0.0%	29.74	0.0%	0.0%	0.0%
000 001 030 2 *	53.78	0.0%	0.0%	56.38	0.0%	0.0%	0.0%
000 001 032 0 *	20.52	0.0%	0.0%	19.82	0.0%	0.0%	0.0%
000 001 200 3 *	50.55	0.0%	0.0%	50.99	0.0%	0.0%	0.0%
000 001 203 0 *	21.84	0.0%	0.0%	20.34	0.0%	0.0%	0.0%
000 001 230 0 *	29.73	0.0%	0.0%	30.74	0.0%	0.0%	0.0%
000 001 300 2 *	62.60	0.0%	0.0%	64.39	0.0%	0.0%	0.0%
000 001 302 0 *	6.01	2.1%	4.5%	5.02	2.8%	5.0%	0.0%
000 001 320 0 *	39.41	0.0%	0.0%	37.45	0.0%	0.0%	0.0%
000 002 003 1 *	76.48	0.0%	0.0%	77.09	0.0%	0.0%	0.0%
000 002 010 3 *	41.84	0.0%	0.0%	38.15	0.0%	0.0%	0.0%
000 002 013 0 *	27.79	0.0%	0.0%	27.58	0.0%	0.0%	0.0%
000 002 030 1 *	60.19	0.0%	0.0%	56.68	0.0%	0.0%	0.0%
000 002 031 0 *	18.83	0.0%	0.0%	18.59	0.0%	0.0%	0.0%
000 002 100 3 *	51.03	0.0%	0.0%	46.20	0.0%	0.0%	0.0%
000 002 103 0 *	10.30	0.2%	0.8%	7.89	0.6%	1.6%	0.0%
000 002 130 0 *	39.95	0.0%	0.0%	36.19	0.0%	0.0%	0.0%
000 002 300 1 *	67.24	0.0%	0.0%	63.54	0.0%	0.0%	0.0%
000 002 301 0 *	7.49	0.9%	2.5%	6.54	1.2%	2.7%	0.0%
000 002 310 0 *	34.66	0.0%	0.0%	33.63	0.0%	0.0%	0.0%
000 003 010 2 *	56.80	0.0%	0.0%	56.95	0.0%	0.0%	0.0%
000 003 012 0 *	31.40	0.0%	0.0%	29.41	0.0%	0.0%	0.0%
000 003 020 1 *	53.67	0.0%	0.0%	53.91	0.0%	0.0%	0.0%
000 003 021 0 *	30.02	0.0%	0.0%	30.36	0.0%	0.0%	0.0%
000 003 100 2 *	64.69	0.0%	0.0%	64.45	0.0%	0.0%	0.0%
000 003 102 0 *	23.22	0.0%	0.0%	22.70	0.0%	0.0%	0.0%
000 003 120 0 *	49.60	0.0%	0.0%	49.85	0.0%	0.0%	0.0%
000 003 200 1 *	65.00	0.0%	0.0%	66.23	0.0%	0.0%	0.0%
000 003 201 0 *	23.16	0.0%	0.0%	21.28	0.0%	0.0%	0.0%
000 003 210 0 *	37.91	0.0%	0.0%	39.12	0.0%	0.0%	0.0%
000 010 020 3 *	25.51	0.0%	0.0%	24.64	0.0%	0.0%	0.0%
000 010 023 0 *	32.19	0.0%	0.0%	30.22	0.0%	0.0%	0.0%
000 010 030 2 *	50.20	0.0%	0.0%	50.60	0.0%	0.0%	0.0%
000 010 032 0 *	29.08	0.0%	0.0%	26.47	0.0%	0.0%	0.0%
000 010 200 3 *	35.92	0.0%	0.0%	37.98	0.0%	0.0%	0.0%
000 010 203 0 *	23.25	0.0%	0.0%	23.09	0.0%	0.0%	0.0%
000 010 230 0 *	35.35	0.0%	0.0%	36.70	0.0%	0.0%	0.0%

Supporting Information for Organic Letters

isomer	gas phase			chloroform			Experimental (chloroform)
	E_rel (kJ/mol)	pop. -60°C	pop. 25°C	E_rel (kJ/mol)	pop. -60°C	pop. 25°C	pop. -60°C
000 010 302 0 *	16.40	0.0%	0.1%	14.38	0.0%	0.1%	0.0%
000 010 320 0 *	40.22	0.0%	0.0%	46.19	0.0%	0.0%	0.0%
000 012 030 0 *	27.45	0.0%	0.0%	25.24	0.0%	0.0%	0.0%
000 012 300 0 *	36.22	0.0%	0.0%	34.16	0.0%	0.0%	0.0%
000 013 020 0 *	32.59	0.0%	0.0%	31.73	0.0%	0.0%	0.0%
000 013 200 0 *	40.17	0.0%	0.0%	40.89	0.0%	0.0%	0.0%
000 020 030 1 *	39.68	0.0%	0.0%	35.96	0.0%	0.0%	0.0%
000 020 031 0 *	27.69	0.0%	0.0%	27.15	0.0%	0.0%	0.0%
000 020 100 3 *	32.34	0.0%	0.0%	30.05	0.0%	0.0%	0.0%
000 020 103 0 *	17.50	0.0%	0.0%	16.36	0.0%	0.1%	0.0%
000 020 130 0 *	42.29	0.0%	0.0%	40.71	0.0%	0.0%	0.0%
000 020 300 1 *	53.53	0.0%	0.0%	51.38	0.0%	0.0%	0.0%
000 020 301 0 *	18.10	0.0%	0.0%	16.96	0.0%	0.0%	0.0%
000 020 310 0 *	35.95	0.0%	0.0%	38.92	0.0%	0.0%	0.0%
000 021 030 0 *	32.39	0.0%	0.0%	31.43	0.0%	0.0%	0.0%
000 021 300 0 *	34.85	0.0%	0.0%	36.17	0.0%	0.0%	0.0%
000 023 100 0 *	37.03	0.0%	0.0%	36.90	0.0%	0.0%	0.0%
000 030 100 2 *	57.08	0.0%	0.0%	56.47	0.0%	0.0%	0.0%
000 030 102 0 *	9.91	0.2%	0.9%	7.38	0.7%	1.9%	0.0%
000 030 120 0 *	48.72	0.0%	0.0%	47.20	0.0%	0.0%	0.0%
000 030 200 1 *	46.38	0.0%	0.0%	44.03	0.0%	0.0%	0.0%
000 030 201 0 *	18.63	0.0%	0.0%	18.80	0.0%	0.0%	0.0%
000 030 210 0 *	43.61	0.0%	0.0%	43.55	0.0%	0.0%	0.0%
000 031 200 0 *	39.72	0.0%	0.0%	39.60	0.0%	0.0%	0.0%
000 032 100 0 *	30.98	0.0%	0.0%	29.18	0.0%	0.0%	0.0%
000 100 200 3 *	65.96	0.0%	0.0%	64.24	0.0%	0.0%	0.0%
000 100 203 0 *	54.32	0.0%	0.0%	52.91	0.0%	0.0%	0.0%
000 100 230 0 *	62.46	0.0%	0.0%	67.42	0.0%	0.0%	0.0%
000 100 300 2 *	80.80	0.0%	0.0%	81.94	0.0%	0.0%	0.0%
000 100 302 0 *	33.42	0.0%	0.0%	30.95	0.0%	0.0%	0.0%
000 100 320 0 *	73.33	0.0%	0.0%	78.05	0.0%	0.0%	0.0%
000 102 300 0 *	37.45	0.0%	0.0%	36.28	0.0%	0.0%	0.0%
000 103 200 0 *	51.61	0.0%	0.0%	49.28	0.0%	0.0%	0.0%
000 120 300 0 *	77.73	0.0%	0.0%	76.96	0.0%	0.0%	0.0%
000 130 200 0 *	81.99	0.0%	0.0%	79.70	0.0%	0.0%	0.0%
000 200 300 1 *	64.71	0.0%	0.0%	66.90	0.0%	0.0%	0.0%
000 200 301 0 *	38.34	0.0%	0.0%	40.24	0.0%	0.0%	0.0%
000 200 310 0 *	68.45	0.0%	0.0%	67.18	0.0%	0.0%	0.0%
000 201 300 0 *	40.18	0.0%	0.0%	40.97	0.0%	0.0%	0.0%
000 210 300 0 *	59.87	0.0%	0.0%	62.17	0.0%	0.0%	0.0%
001 002 003 0 *	1.26	30.6%	30.4%	0.00	47.4%	37.7%	45.0%
001 002 030 0 *	0.00	62.4%	50.6%	0.54	34.9%	30.3%	27.0%
001 002 300 0 *	9.38	0.3%	1.2%	7.84	0.6%	1.6%	16.0%
001 003 020 0 *	11.46	0.1%	0.5%	9.45	0.2%	0.8%	0.0%
001 003 200 0 *	23.01	0.0%	0.0%	21.03	0.0%	0.0%	0.0%
001 020 030 0 *	9.38	0.3%	1.2%	8.05	0.5%	1.5%	0.0%
001 020 300 0 *	21.40	0.0%	0.0%	20.26	0.0%	0.0%	0.0%
001 030 200 0 *	22.92	0.0%	0.0%	20.49	0.0%	0.0%	0.0%
001 200 300 0 *	41.73	0.0%	0.0%	44.04	0.0%	0.0%	0.0%
002 003 010 0 *	6.04	2.1%	4.4%	2.90	9.3%	11.7%	12.0%
002 003 100 0 *	26.22	0.0%	0.0%	24.25	0.0%	0.0%	0.0%
002 010 030 0 *	8.52	0.5%	1.6%	6.23	1.4%	3.1%	1.4%
002 010 300 0 *	13.61	0.0%	0.2%	11.98	0.1%	0.3%	0.0%
002 030 100 0 *	11.52	0.1%	0.5%	9.44	0.2%	0.8%	0.0%
002 100 300 0 *	37.60	0.0%	0.0%	35.95	0.0%	0.0%	0.0%
003 010 020 0 *	11.94	0.1%	0.4%	10.64	0.1%	0.5%	0.0%
003 010 200 0 *	20.87	0.0%	0.0%	21.46	0.0%	0.0%	0.0%
003 020 100 0 *	25.42	0.0%	0.0%	22.66	0.0%	0.0%	0.0%
003 100 200 0 *	53.94	0.0%	0.0%	51.28	0.0%	0.0%	0.0%
010 020 030 0 *	15.74	0.0%	0.1%	14.87	0.0%	0.1%	0.0%
010 020 300 0 *	23.91	0.0%	0.0%	20.95	0.0%	0.0%	0.0%
010 030 200 0 *	26.15	0.0%	0.0%	26.53	0.0%	0.0%	0.0%
010 200 300 0 *	43.19	0.0%	0.0%	46.59	0.0%	0.0%	0.0%
020 030 100 0 *	17.19	0.0%	0.1%	17.61	0.0%	0.0%	0.0%
020 100 300 0 *	33.75	0.0%	0.0%	34.15	0.0%	0.0%	0.0%
030 100 200 0 *	48.56	0.0%	0.0%	46.42	0.0%	0.0%	0.0%
100 200 300 0 *	83.45	0.0%	0.0%	84.36	0.0%	0.0%	0.0%

4.2. Kinetic Simulations

Local kinetic simulations were done using the software program *KinTec Explorer* (https://kintekcorp.com). This analysis considers only the first- and second-generation isomerisation pathways around the trisubstituted bullvalene isomer of interest. The second-generation reverse rate constants are set to zero to allow material to exit the simulation and reveal the half-life of the isomer in question.

Figure 74. Local kinetic simulation of bullvalene **4f:A** based on the energies from single point DFT calculations at B3LYP-D3BJ/Def2-TZVPPD/CPCM solvent(chloroform) at 25 C.

(000 010 002 3, AF)
rel E: 17.1 kJ/mol

$\Delta E^{\ddagger}$ = 61 0 kJ/mol
k = 128 s^{-1}

-$\Delta E^{\ddagger}$ = 60.1 kJ/mol
-k = 181 s^{-1}
(set to zero)

(000 020 003 1, AL)
rel E: 49.1 kJ/mol

$\Delta E^{\ddagger}$ = 66.1 kJ/mol
k = 16.3 s^{-1}

-$\Delta E^{\ddagger}$ = 54.4 kJ/mol
-k = 1811 s^{-1}
(set to zero)

Reactions	k+	k-
1	AM = AT	21.9	1.72e+07
2	AM = AQ	6.45	1.86e+07
3	AA = AQ	0	6820
4	AD = AT	0	2460
5	AM = AP	56.8	31600
6	AF = AP	0	128
7	AG = AT	0	1.01
8	AI = AP	0	564
9	AL = AQ	0	16.3

$t_{1/2}$ = 0.57s

$\Delta E^{\ddagger}$ = 63 0 kJ/mol
k = 56.8 s^{-1}

-$\Delta E^{\ddagger}$ = 47.3 kJ/mol
-k = 3.16 × 10^4 s^{-1}

(010 300 200 0, AP)
rel E: 16.2 kJ/mol

4g A
(001 002 003 0, AM)
rel E: 0.6 kJ/mol
$t_{1/2}$ = 0.57s

$\Delta E^{\ddagger}$ = 68.4 kJ/mol
k = 6.45 s^{-1}

-$\Delta E^{\ddagger}$ = 31.5 kJ/mol
-k = 1.86 × 10^7 s^{-1}

(020 100 300 0, AQ)
rel E: 37.4 kJ/mol

$\Delta E^{\ddagger}$ = 57.3 kJ/mol
k = 564 s^{-1}

-$\Delta E^{\ddagger}$ = 61.7 kJ/mol
-k = 93 s^{-1}
(set to zero)

$\Delta E^{\ddagger}$ = 51.1 kJ/mol
k = 6824 s^{-1}

-$\Delta E^{\ddagger}$ = 53.0 kJ/mol
-k = 3205 s^{-1}
(set to zero)

(000 003 010 2, AI)
rel E: 11.8 kJ/mol

-$\Delta E^{\ddagger}$ = 31.7 kJ/mol
-k = 1.72 × 10^7 s^{-1}

$\Delta E^{\ddagger}$ = 65.4 kJ/mol
k = 21.3 s^{-1}

(000 001 020 3, AA)
rel E: 35.5 kJ/mol

(000 002 030 1, AG)
rel E: 48.2 kJ/mol

$\Delta E^{\ddagger}$ = 72.9 kJ/mol
k = 1.01 s^{-1}

-$\Delta E^{\ddagger}$ = 59.0 kJ/mol
-k = 278 0 s^{-1}
(set to zero)

(030 200 100 0, AT)
rel E: 34.3 kJ/mol

$\Delta E^{\ddagger}$ = 53.6 kJ/mol
k = 2460 s^{-1}

-$\Delta E^{\ddagger}$ = 61.7 kJ/mol
-k = 93.7 s^{-1}
(set to zero)

(000 030 001 2 ,AD)
rel E: 26 2 kJ/mol

Figure 75. Local kinetic simulation of bullvalene **4g:A** based on the energies from single point DFT calculations at B3LYP-D3BJ/Def2-TZVPPD/CPCM solvent(chloroform) at 25 C.

	Reactions	k+	k-
1	AG = AJ	3.62	6.55e+10
2	AG = AI	3.62	6.55e+10
3	AA = AI	0	13700
4	AB = AJ	0	13700
5	AG = AH	50.6	1.13e+11
6	AC = AH	0	15000
7	AD = AH	0	15000
8	AE = AJ	0	854000
9	AF = AI	0	854000

(000 020 001 2 AB)
rel E 51 9 kJ/mol

$\Delta E^{\ddagger} = 49 4$ kJ/mol
k = 1 36 × 10^4 s^{-1}

$\Delta E^{\ddagger} = 56 0$ kJ/mol
k = 939 s^{-1}
(se o zero)

(000 001 020 2 AA)
rel E 51 9 kJ/mol

$\Delta E^{\ddagger} = 49 4$ kJ/mol
k = 1 36 × 10^4 s^{-1}

$\Delta E^{\ddagger} = 56 0$ kJ/mol
k = 939 s^{-1}
(se o zero)

$_{1/2}$ = 1 8h

(020 200 100 0 AJ)
rel E 58 5 kJ/mol

$\Delta E^{\ddagger} = 69 8$ kJ/mol
k = 3 52 s^{-1}

$\Delta E^{\ddagger} = 11 3$ kJ/mol
k = 6 55 × 10^{10} s^{-1}

SiMe$_3$

4h:A

(001 002 002 0 AG)
rel E 0 kJ/mol

$_{1/2}$ = 1 8 h

$\Delta E^{\ddagger} = 69 8$ kJ/mol
k = 3 52 s^{-1}

$\Delta E^{\ddagger} = 11 3$ kJ/mol
k = 6 55 × 10^{10} s^{-1}

(020 100 200 0 A)
rel E 58 5 kJ/mol

$\Delta E^{\ddagger} = 39 1$ kJ/mol
k = 8 54 × 10^5 s^{-1}

$\Delta E^{\ddagger} = 48 0$ kJ/mol
k = 2 35 × 10^4 s^{-1}
(se o zero)

$\Delta E^{\ddagger} = 39 1$ kJ/mol
k = 8 54 × 10^5 s^{-1}

$\Delta E^{\ddagger} = 48 0$ kJ/mol
k = 2 35 × 10^4 s^{-1}
(se o zero)

(000 002 020 1 AE)
rel E 49 6 kJ/mol

$\Delta E^{\ddagger} = 9 9$ kJ/mol
k = 1 13 × 10^{11} s^{-1}

$\Delta E^{\ddagger} = 63 3$ kJ/mol
k = 50 6 s^{-1}

(000 020 002 1 AF)
rel E 49 6 kJ/mol

$\Delta E^{\ddagger} = 49 2$ kJ/mol
k = 1 50 × 10^4 s^{-1}

$\Delta E^{\ddagger} = 39 9$ kJ/mol
k = 6 20 × 10^5 s^{-1}
(se o zero)

Me$_3$Si

(000 010 002 2 AD)
rel E 62 6 kJ/mol

(030 200 100 0 AH)
rel E 53 3 kJ/mol

$\Delta E^{\ddagger} = 49 2$ kJ/mol
k = 1 50 × 10^4 s^{-1}

$\Delta E^{\ddagger} = 39 9$ kJ/mol
k = 6 20 × 10^5 s^{-1}
(se o zero)

(000 002 010 2 AC)
rel E 62 6 kJ/mol

Figure 76. Local kinetic simulation of bullvalene **4h:A** based on the energies from single point DFT calculations at B3LYP-D3BJ/Def2-TZVPPD/CPCM solvent(chloroform) at 25 C.

Figure 77. Local kinetic simulation of bullvalene **4i:A** based on the energies from single point DFT calculations at B3LYP-D3BJ/Def2-TZVPPD/CPCM solvent(chloroform) at 25 °C.

Computational Analysis of tetrasubstituted buyllvalne 6

Table 10 Computational analysis of bullvalene **6** showing the 36 lowest energy isomers at B3LYP-D3BJ/Def2-TZVPPD in the gas phase and CPCM solvent(chloroform)

isomer	gas phase			chloroform		
	E_{rel} (kJ/mol)	pop. -60°C	pop. 25°C	E_{rel} (kJ/mol)	pop. -60°C	pop. 25°C
001 002 430 0 *	0.00	46.4%	28.8%	0.00	21.1%	15 3%
001 002 403 0 *	4.78	3.1%	4.2%	0.23	18.6%	14 0%
002 003 401 0 *	5.18	2.5%	3.6%	0.86	13.0%	10 8%
001 004 302 0 *	2.28	12.9%	11.5%	1.00	12.0%	10 2%
002 004 301 0 *	3.59	6.1%	6.8%	1.64	8.4%	7 9%
002 030 104 0 *	6.81	1.0%	1.9%	2.85	4.2%	4 9%
001 040 302 0 *	5.33	2.3%	3.4%	2.87	4.2%	4 8%
000 301 402 0 *	5.55	2.0%	3.1%	3.20	3.5%	4 2%
002 040 301 0 *	8.17	0.5%	1.1%	3.67	2.7%	3 5%
002 030 401 0 *	2.44	11.7%	10.8%	4.37	1.8%	2.6%
004 030 102 0 *	10.37	0.1%	0.4%	4.45	1.7%	2.6%
001 002 034 0 *	6.21	1.4%	2.4%	4.58	1.6%	2.4%
004 010 302 0 *	7.40	0.7%	1.5%	4.60	1.6%	2.4%
030 040 102 0 *	7.56	0.7%	1.4%	5.80	0.8%	1 5%
001 020 304 0 *	5.56	2.0%	3.1%	5.94	0.7%	1.4%
001 030 402 0 *	5.52	2.1%	3.1%	6.41	0.6%	1 2%
001 002 304 0 *	8.83	0.3%	0.8%	6.68	0.5%	1 0%
002 301 400 0 *	6.95	0.9%	1.7%	6.78	0.5%	1 0%
002 040 103 0 *	10.52	0.1%	0.4%	6.98	0.4%	0 9%
010 040 302 0 *	12.53	0.0%	0.2%	7.90	0.3%	0.6%
004 020 103 0 *	7.12	0.8%	1.6%	7.91	0.2%	0.6%
001 020 403 0 *	13.50	0.0%	0.1%	8.03	0.2%	0.6%
001 020 430 0 *	9.98	0.2%	0.5%	8.48	0.2%	0 5%
020 040 301 0 *	9.90	0.2%	0.5%	8.68	0.2%	0 5%
000 302 401 0 *	10.73	0.1%	0.4%	8.77	0.2%	0.4%
002 010 430 0 *	11.19	0.1%	0.3%	9.09	0.1%	0.4%
002 010 403 0 *	13.27	0.0%	0.1%	9.31	0.1%	0.4%
001 302 400 0 *	11.71	0.1%	0.3%	9.68	0.1%	0 3%
003 020 401 0 *	13.68	0.0%	0.1%	9.73	0.1%	0 3%
020 030 104 0 *	11.17	0.1%	0.3%	9.94	0.1%	0 3%
002 300 401 0 *	11.98	0.1%	0.2%	10.37	0.1%	0 2%
004 020 301 0 *	11.86	0.1%	0.2%	10.70	0.1%	0 2%
020 030 401 0 *	10.39	0.1%	0.4%	10.78	0.1%	0 2%
001 004 032 0 *	12.71	0.0%	0.2%	11.24	0.0%	0 2%
001 300 402 0 *	11.66	0.1%	0.3%	11.62	0.0%	0.1%
010 030 402 0 *	12.54	0.0%	0.2%	11.71	0.0%	0.1%
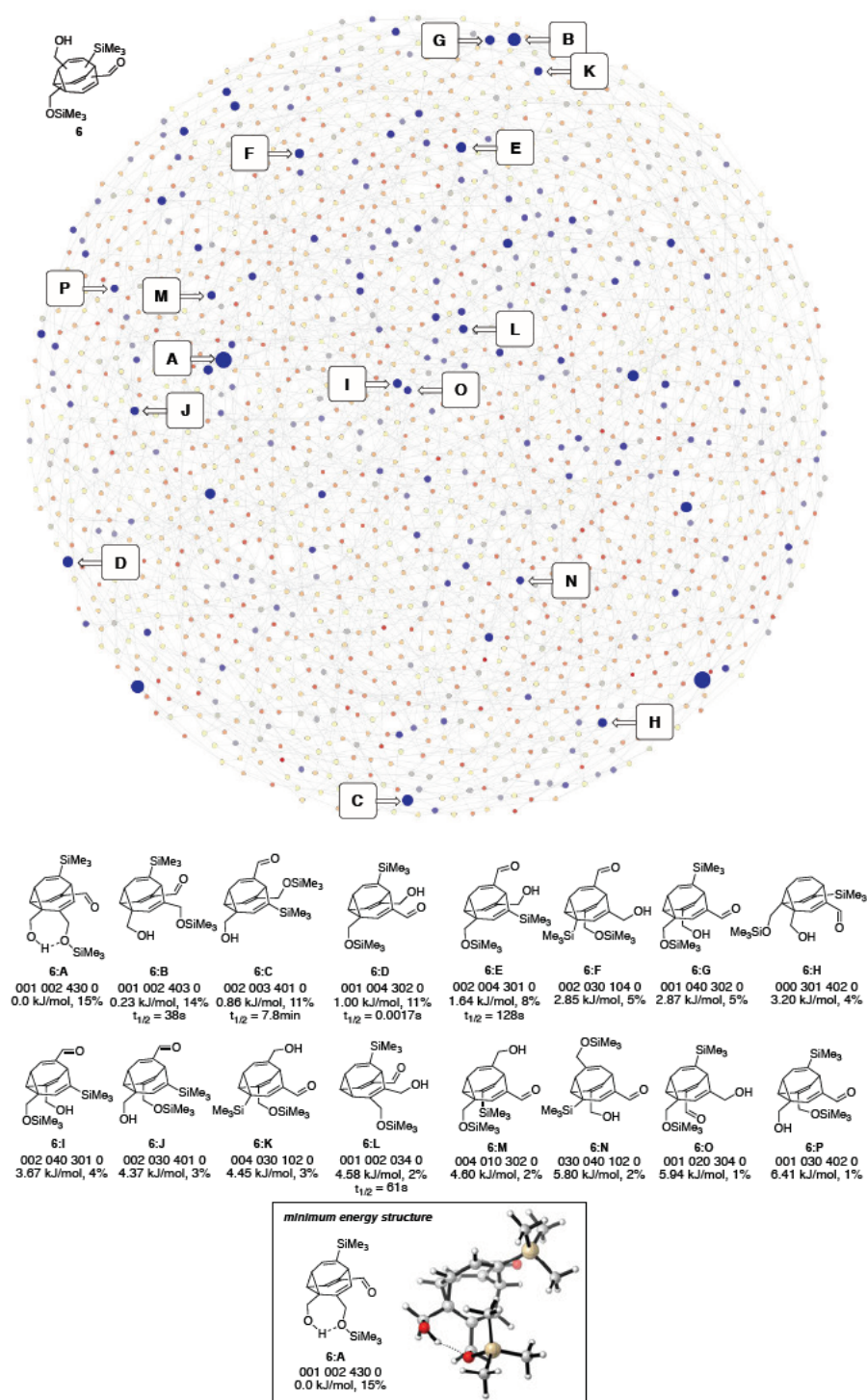
Figure 78 Network graph of tetrasubstituted bullvalene **6** highlighting the 16 lowest energy isomers **6A-L**

(001 020 040 3, AF)
rel E: 33.2 kJ/mol

$\Delta E^{\ddagger}$ = 50.0 kJ/mol
k = 10571 s^{-1}

-$\Delta E^{\ddagger}$ = 53.6 kJ/mol
-k = 2542 s^{-1}
(set to zero)

(001 400 030 2, AI)
rel E: 66.2 kJ/mol

$\Delta E^{\ddagger}$ = 72.1 kJ/mol
k = 1.44 s^{-1}

-$\Delta E^{\ddagger}$ = 55 9 kJ/mol
-k = 985 s^{-1}
(set to zero)

Reactions	k+	k-
1 AE = AP	132	9.12e+08
2 AE = AQ	13.1	3.25e+07
3 AE = AT	98.8	5.27e+10
4 AP = AC	0.447	0
5 AP = AE	9.12e+08	132
6 AP = AM	95500	0
7 AQ = AB	0.106	0
8 AQ = AE	3.25e+07	13.1
9 AQ = AF	10600	0
10 AT = AE	5.27e+10	98.8
11 AT = AI	1.44	0
12 AT = AL	286	0

$t_{1/2}$ = 38s

(020 100 304 0, AQ)
rel E: 36.7 kJ/mol

$\Delta E^{\ddagger}$ = 66.6 kJ/mol
k = 13.1 s^{-1}

-$\Delta E^{\ddagger}$ = 30.1 kJ/mol
-k = 3.25 × 10^7 s^{-1}

6 B
001 002 403 0
0.23 kJ/mol, 14%
$t_{1/2}$ = 32s

$\Delta E^{\ddagger}$ = 61.6 kJ/mol
k = 98.8 s^{-1}

-$\Delta E^{\ddagger}$ = 11.8 kJ/mol
-k = 5.27 × 10^{10} s^{-1}

(030 200 100 4, AT)
rel E: 50 0 kJ/mol

$\Delta E^{\ddagger}$ = 78 5 kJ/mol
k = 0.106 s^{-1}

-$\Delta E^{\ddagger}$ = 63.8 kJ/mol
-k = 41.5 s^{-1}
(set to zero)

$\Delta E^{\ddagger}$ = 59 0 kJ/mol
k = 286 s^{-1}

-$\Delta E^{\ddagger}$ = 50.4 kJ/mol
-k = 9206 s^{-1}
(set to zero)

(000 020 403 1, AB)
rel E: 51.5 kJ/mol

-$\Delta E^{\ddagger}$ = 21.9 kJ/mol
-k = 9.12 × 10^8 s^{-1}

$\Delta E^{\ddagger}$ = 60.9 kJ/mol
k = 132 s^{-1}

(002 030 400 1, AL)
rel E: 58 6 kJ/mol

(002 040 010 3, AM)
rel E: 44.4 kJ/mol

$\Delta E^{\ddagger}$ = 44.6 kJ/mol
k = 95490 s^{-1}

-$\Delta E^{\ddagger}$ = 39.4 kJ/mol
-k = 766243 s^{-1}
(set to zero)

(010 304 200 0, AP)
rel E: 39 3 kJ/mol

$\Delta E^{\ddagger}$ = 75.0 kJ/mol
k = 0.447 s^{-1}

-$\Delta E^{\ddagger}$ = 50.7 kJ/mol
-k = 8077 s^{-1}
(set to zero)

(000 403 010 2, AC)
rel E: 63 5 kJ/mol

Figure 79. Local kinetic simulation of bullvalene **6:B** based on the energies from single point DFT calculations at B3LYP-D3BJ/Def2-TZVPPD/CPCM solvent(chloroform) at 25 °C

(003 010 400 2, AK)
rel E: 62.3 kJ/mol

$\Delta E^{\ddagger}$ = 64.0 kJ/mol
k = 38 s^{-1}

-$\Delta E^{\ddagger}$ = 51.0 kJ/mol
-k = 7046 s^{-1}
(set to zero)

(000 030 401 2, AB)
rel E: 61.2 kJ/mol

$\Delta E^{\ddagger}$ = 81 6 kJ/mol
k = 0.0313 s^{-1}

-$\Delta E^{\ddagger}$ = 62.1 kJ/mol
-k = 80.1 s^{-1}
(set to zero)

$\Delta E^{\ddagger}$ = 69.3 kJ/mol
k = 4.4 s^{-1}

-$\Delta E^{\ddagger}$ = 20.8 kJ/mol
-k = 1.41 × 10^{9} s^{-1}

(010 300 200 4, AP)
rel E: 49.4 kJ/mol

6 C
002 003 401 0
0.86 kJ/mol, 11%
$t_{1/2}$ = 7.8 min

$\Delta E^{\ddagger}$ = 56.7 kJ/mol
k = 701 s^{-1}

-$\Delta E^{\ddagger}$ = 15.9 kJ/mol
-k = 1.02 × 10^{10} s^{-1}

(030 200 104 0, AT)
rel E: 41.7 kJ/mol

$\Delta E^{\ddagger}$ = 41.6 kJ/mol
k = 318732 s^{-1}

-$\Delta E^{\ddagger}$ = 43 8 kJ/mol
-k = 130981 s^{-1}
(set to zero)

$\Delta E^{\ddagger}$ = 54.4 kJ/mol
k = 1835 s^{-1}

-$\Delta E^{\ddagger}$ = 45.3 kJ/mol
-k = 69964 s^{-1}
(set to zero)

-$\Delta E^{\ddagger}$ = 28.0 kJ/mol
-k = 7.62 × 10^{7} s^{-1}

$\Delta E^{\ddagger}$ = 65.6 kJ/mol
k = 19.7 s^{-1}

(002 400 010 3, AI)
rel E: 47.2 kJ/mol

(002 030 040 1, AG)
rel E: 50.7 kJ/mol

(003 040 020 1, AM)
rel E: 55.8 kJ/mol

$\Delta E^{\ddagger}$ = 70.4 kJ/mol
k = 2.88 s^{-1}

-$\Delta E^{\ddagger}$ = 53.0 kJ/mol
-k = 3152 s^{-1}
(set to zero)

(020 104 300 0, AQ)
rel E: 38.4 kJ/mol

$\Delta E^{\ddagger}$ = 55.0 kJ/mol
k = 1432 s^{-1}

-$\Delta E^{\ddagger}$ = 56 5 kJ/mol
-k = 785 s^{-1}
(set to zero)

(000 401 020 3, AC)
rel E: 37 0 kJ/mol

Figure 80. Local kinetic simulation of bullvalene **6:C** based on the energies from single point DFT calculations at B3LYP-D3BJ/Def2-TZVPPD/CPCM solvent(chloroform) at 25 °C

(000 302 010 4, AC)
rel E: 48 3 kJ/mol

$\Delta E^{\ddagger}$ = 12.1 kJ/mol
k = 4.79 × 10^{10} s^{-1}

-$\Delta E^{\ddagger}$ = 9.6 kJ/mol
-k = 1 30 × 10^{11} s^{-1}
(set to zero)

(001 040 030 2, AH)
rel E: 56 6 kJ/mol

$\Delta E^{\ddagger}$ = 60.0 kJ/mol
k = 186 s^{-1}

-$\Delta E^{\ddagger}$ = 58.7 kJ/mol
-k = 315 s^{-1}
(set to zero)

1	AE = AO	563	4.05e+10
2	AE = AR	0.239	1.4e+07
3	AE = AS	36.2	1.17e+11
4	AO = AC	4.79e+10	0
5	AO = AE	4.05e+10	563
6	AO = AM	4.17	0
7	AR = AE	1.4e+07	0.239
8	AR = AI	484	0
9	AR = AL	0.0702	0
10	AS = AB	257	0
11	AS = AE	1.17e+11	36.2
12	AS = AH	186	0

$t_{1/2}$ = 0.0017s

010 203 400 0, AO)
rel E: 45.8 kJ/mol

$\Delta E^{\ddagger}$ = 57.3 kJ/mol
k = 563 s^{-1}

-$\Delta E^{\ddagger}$ = 12.5 kJ/mol
-k = 4 05 × 10^{10} s^{-1}

6 D
001 004 302 0
1.00 kJ/mol, 11%
$t_{1/2}$ = 0.0017s

$\Delta E^{\ddagger}$ = 64.1 kJ/mol
k = 36.2 s^{-1}

-$\Delta E^{\ddagger}$ = 9.8 kJ/mol
-k = 1.17 × 10^{11} s^{-1}

(040 100 203 0, AS)
rel E: 55.3 kJ/mol

$\Delta E^{\ddagger}$ = 69.4 kJ/mol
k = 4.17 s^{-1}

-$\Delta E^{\ddagger}$ = 60.4 kJ/mol
-k = 159 s^{-1}
(set to zero)

$\Delta E^{\ddagger}$ = 59.2 kJ/mol
k = 257 s^{-1}
-$\Delta E^{\ddagger}$ = 53.8 kJ/mol
-k = 2258 s^{-1}
(set to zero)

(004 030 010 2, AM)
rel E: 54 8 kJ/mol

-$\Delta E^{\ddagger}$ = 32 2 kJ/mol
-k = 1.40 × 10^{7} s^{-1}

$\Delta E^{\ddagger}$ = 76.5 kJ/mol
k = 0.239 s^{-1}

(000 040 302 1, AB)
rel E: 60.6 kJ/mol

(004 020 300 1, AL)
rel E: 54 0 kJ/mol

$\Delta E^{\ddagger}$ = 79.6 kJ/mol
k = 0 0702 s^{-1}

-$\Delta E^{\ddagger}$ = 70 9 kJ/mol
-k = 2 32 s^{-1}
(set to zero)

(020 400 100 3, AR)
rel E: 45.3 kJ/mol

$\Delta E^{\ddagger}$ = 57.7 kJ/mol
k = 484 s^{-1}

-$\Delta E^{\ddagger}$ = 68.0 kJ/mol
-k = 7.59 s^{-1}
(set to zero)

(001 300 020 4, AI)
rel E: 35.027 kJ/mol

6 D
001 004 302 0
1.00 kJ/mol, 11%
$t_{1/2}$ = 0.0017s

004 302 0100
$\Delta E^{\ddagger}$ = 57 3 kJ/mol
k = 563 s^{-1}

010 203 400 0, AO
rel E: 45.8 kJ/mol

rapid exit
through isomer
000 302 010 4, AC

A specific hydrogen bond in the transition structure t0043020100 contributes to the short half-life of bullvaene 6:D
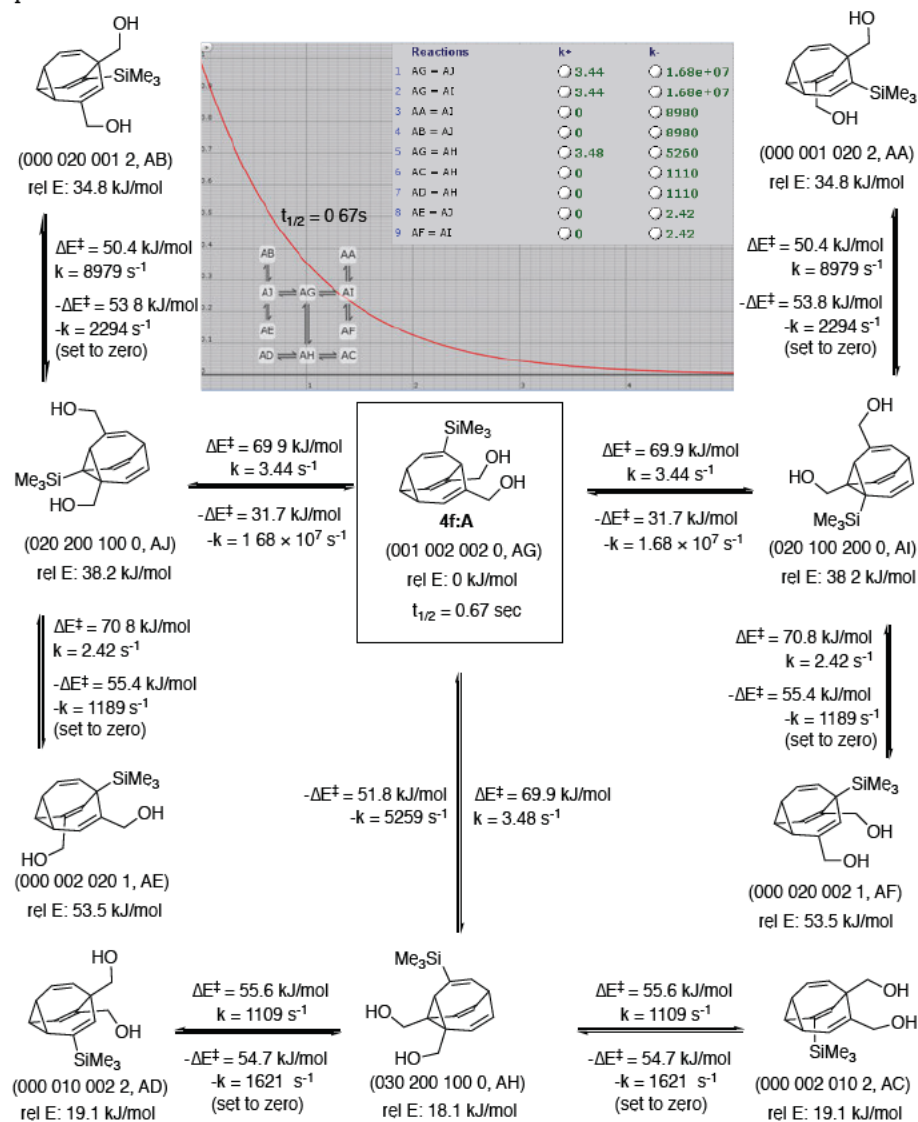
Figure 81. Local kinetic simulation of bullvalene **6:D** based on the energies from single point DFT calculations at B3LYP-D3BJ/Def2-TZVPPD/CPCM solvent(chloroform) at 25 °C
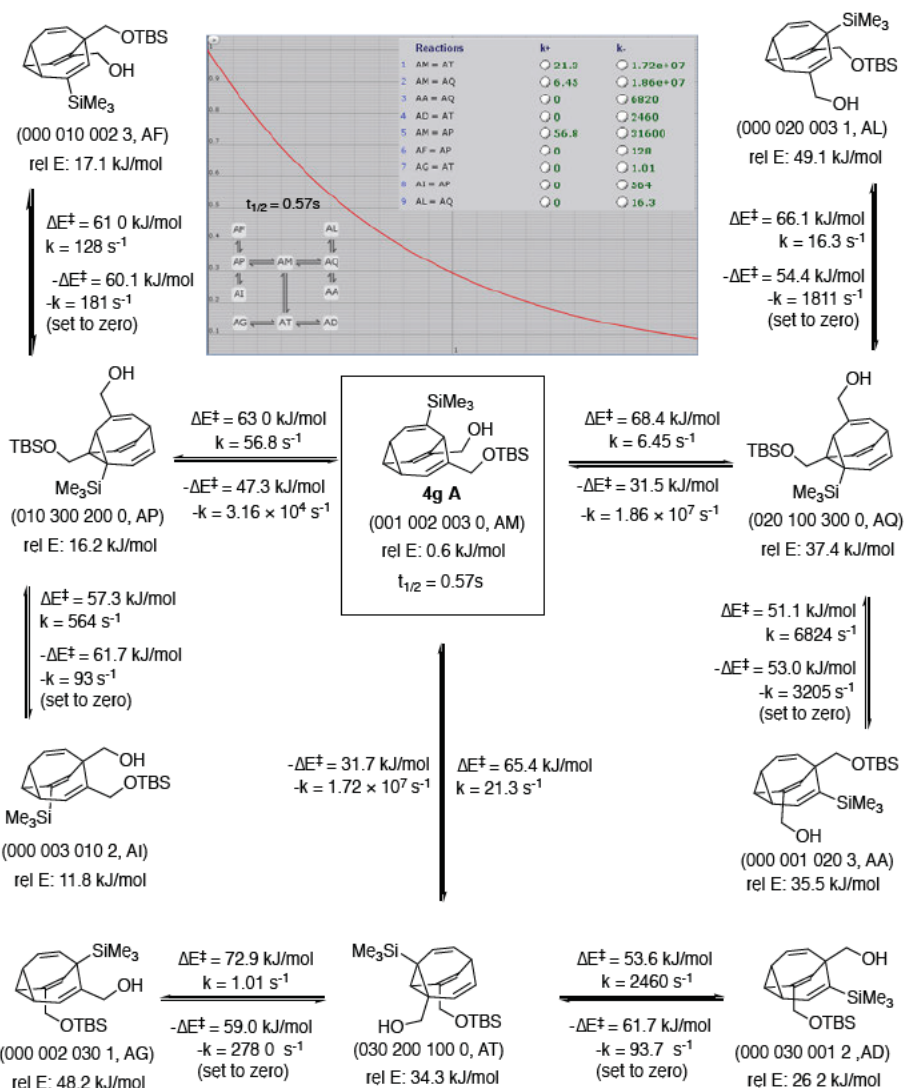
Figure 82. Local kinetic simulation of bullvalene **6:E** based on the energies from single point DFT calculations at B3LYP-D3BJ/Def2-TZVPPD/CPCM solvent(chloroform) at 25 °C
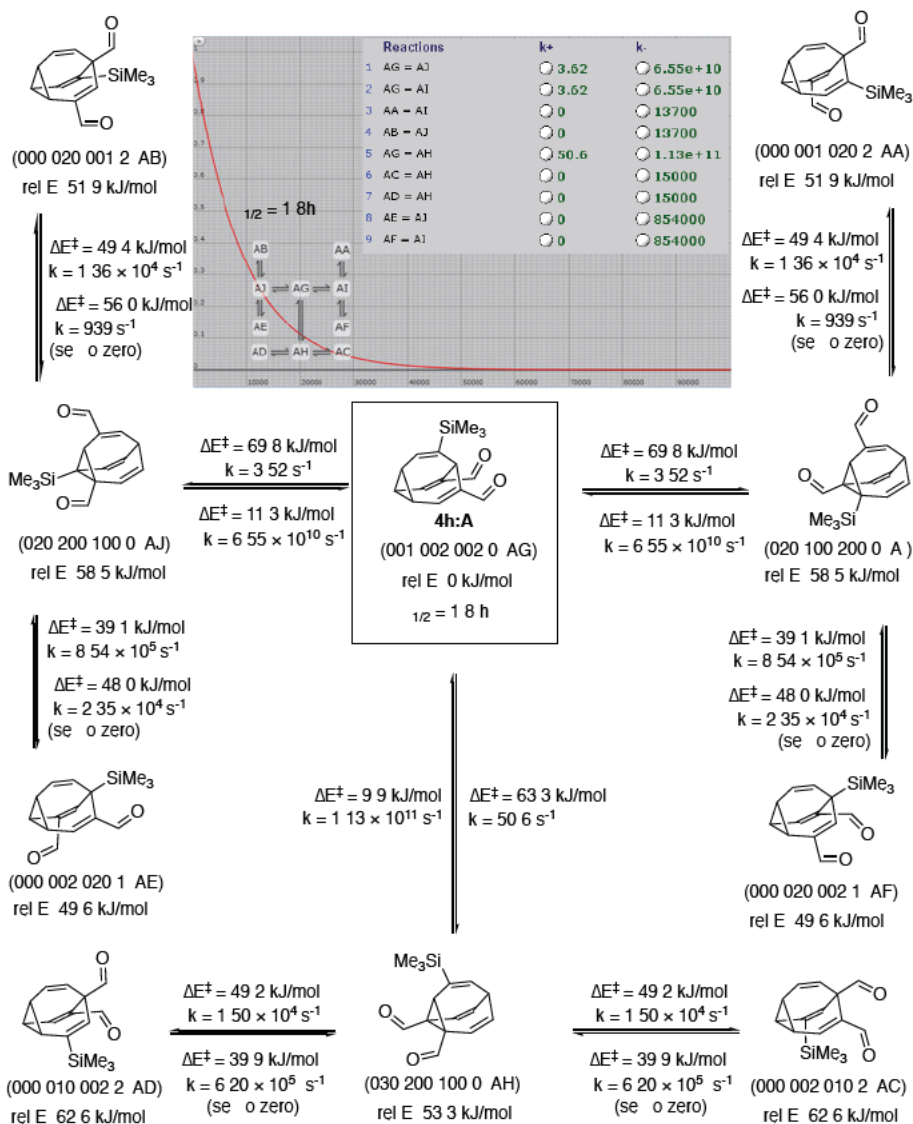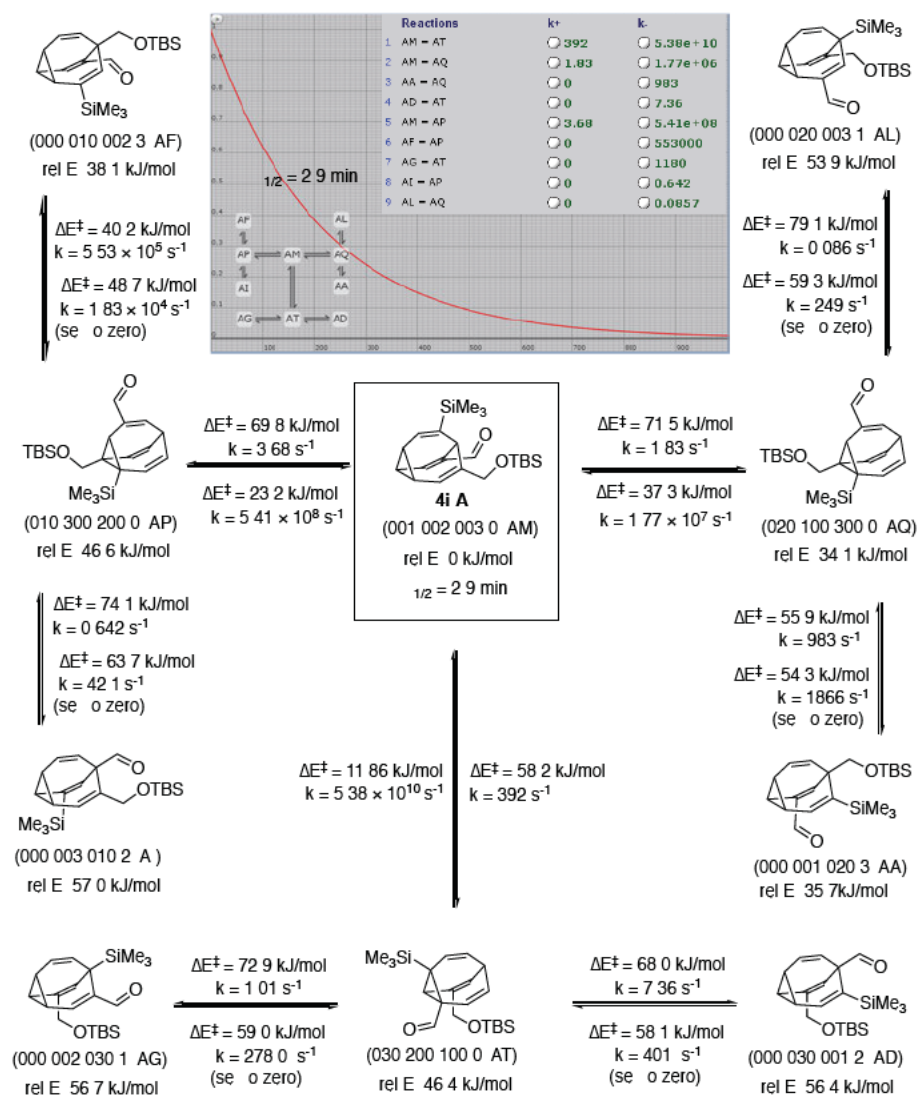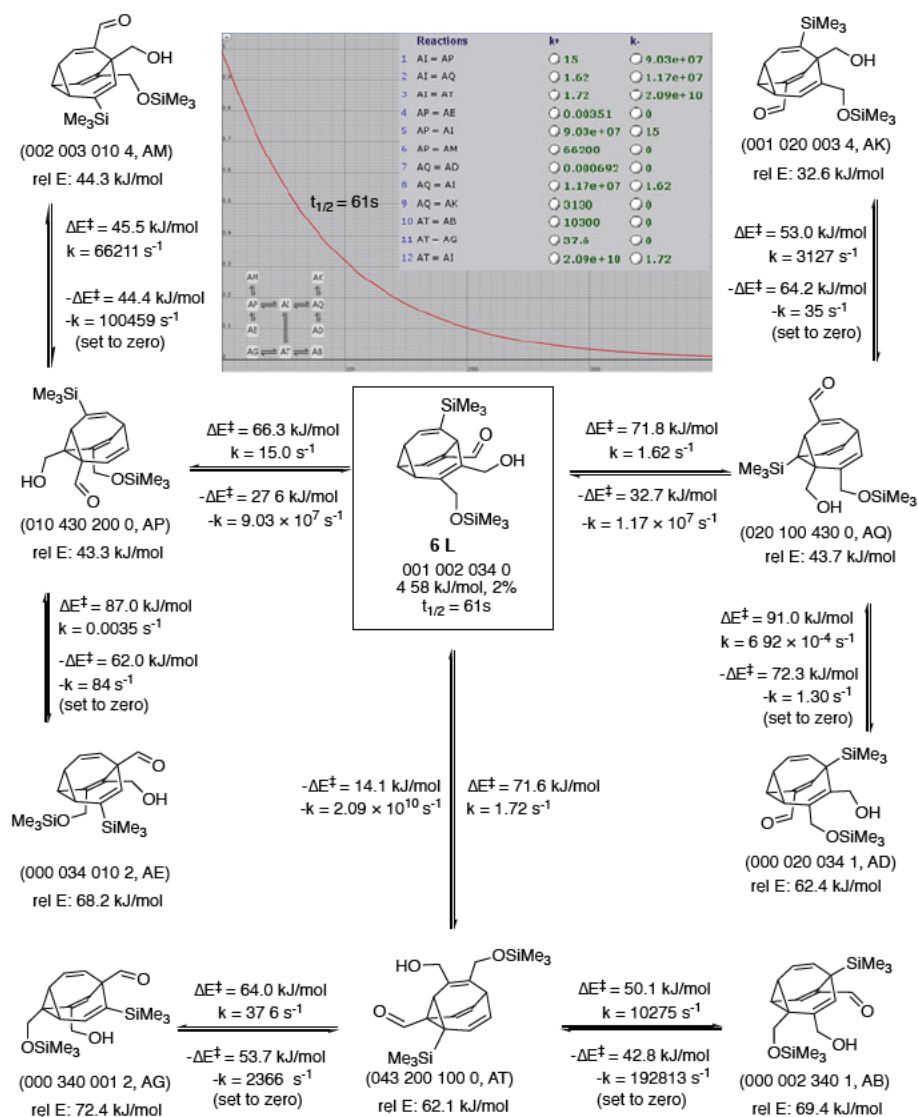
Figure 83. Local kinetic simulation of bullvalene **6:L** based on the energies from single point DFT calculations at B3LYP-D3BJ/Def2-TZVPPD/CPCM solvent(chloroform) at 25 °C

Stochastic simulations were performed using the software *Kinetiscope*
(http://hinsberg.net/kinetiscope/). The simulation box contained 100,000 particle. The following
mechanism parameters where used:

Table 11. Kinetic parameters for bullvalene **4d** based on the energies from single point DFT calculations at B3LYP-D3BJ/Def2-TZVPPD/CPCM solvent(chloroform) at 25 C.

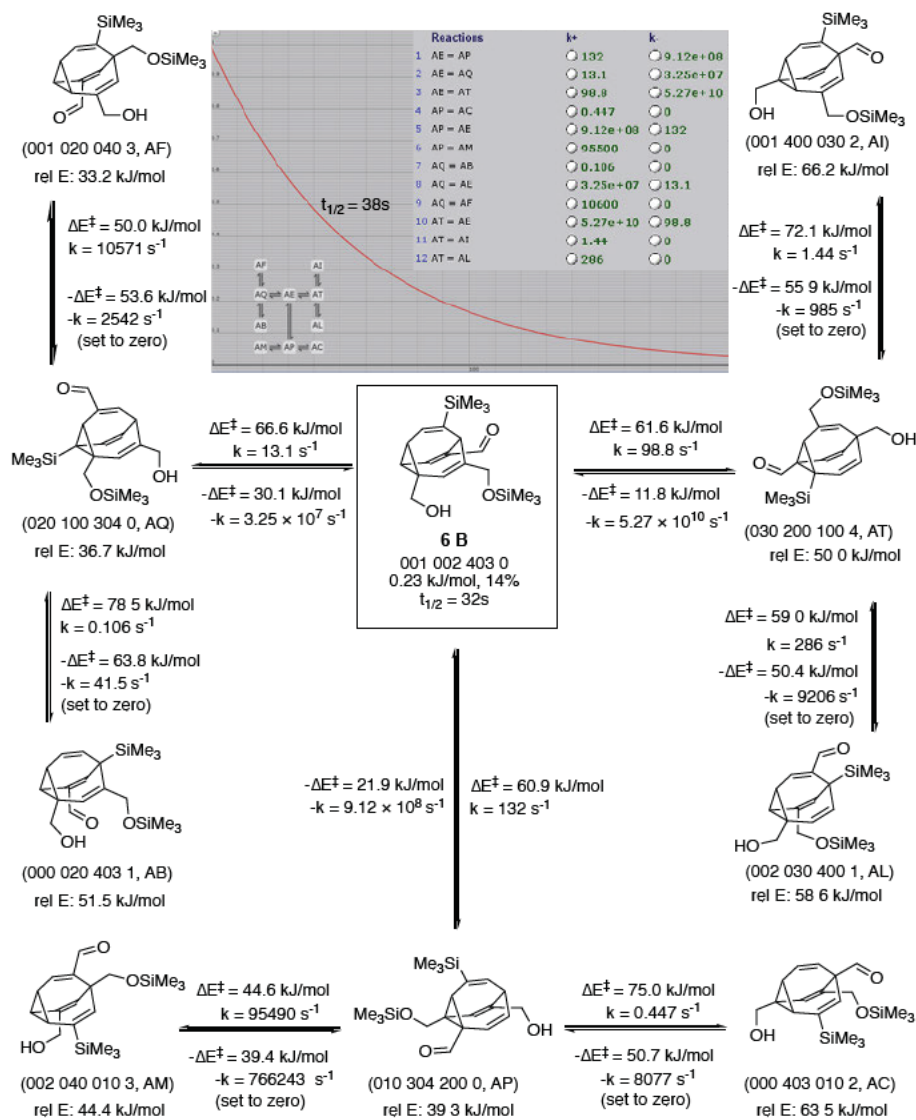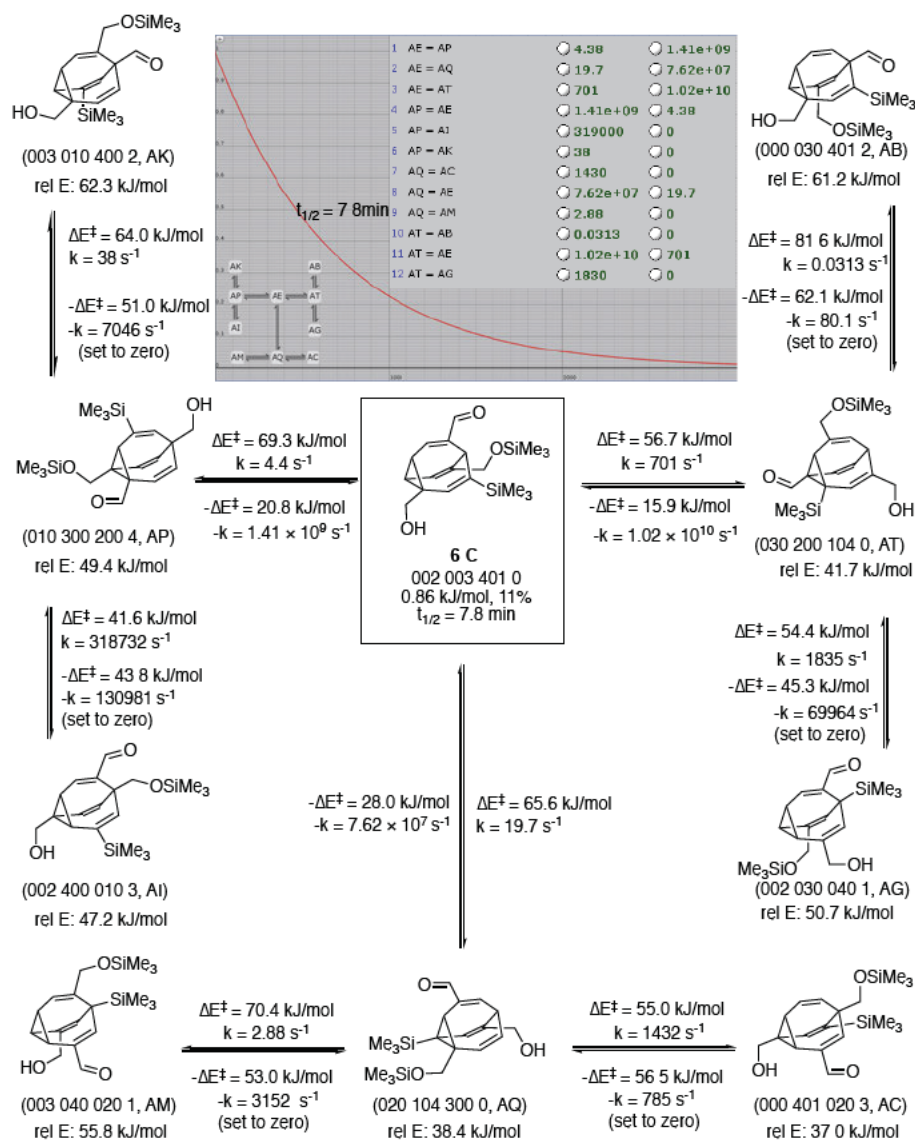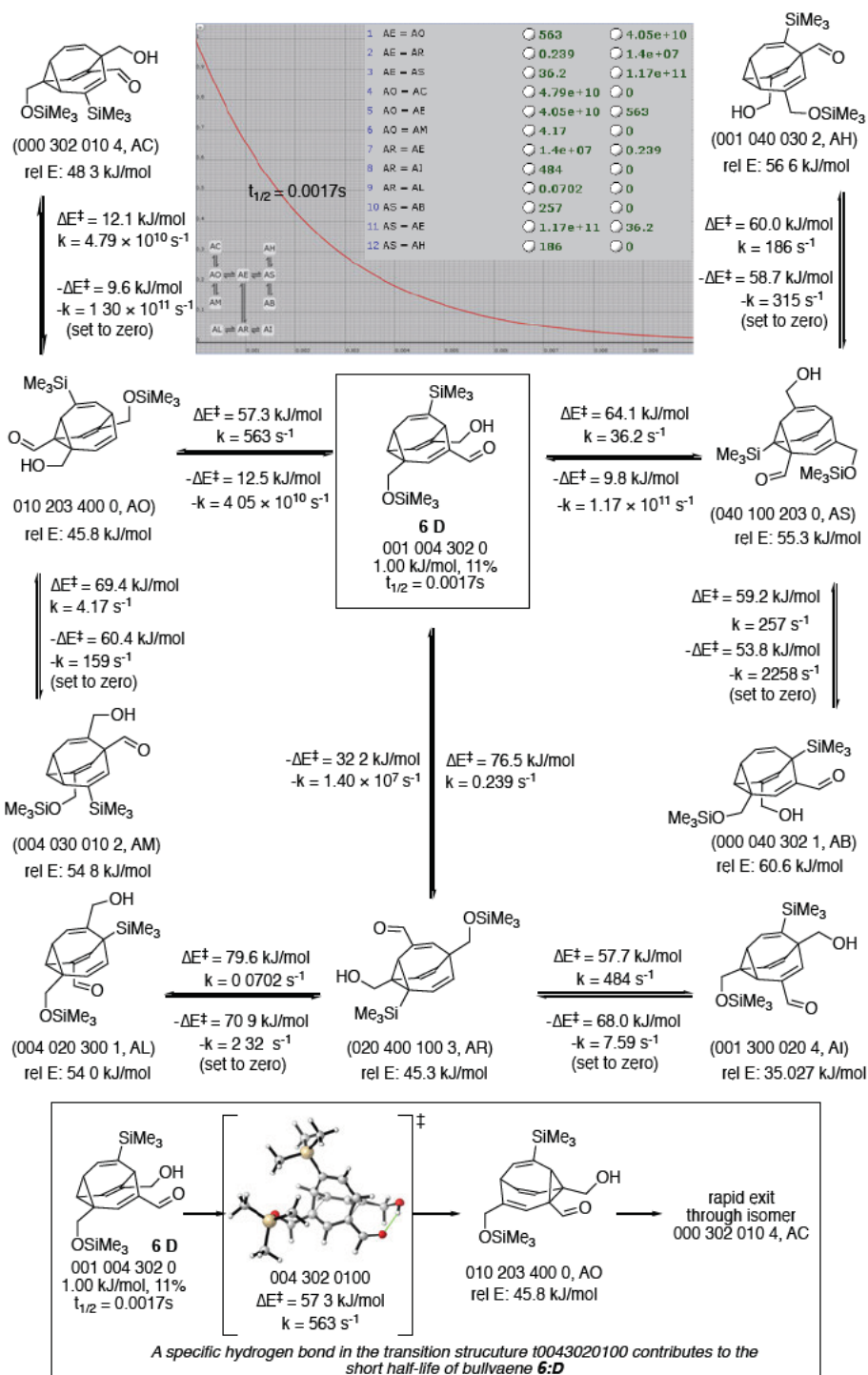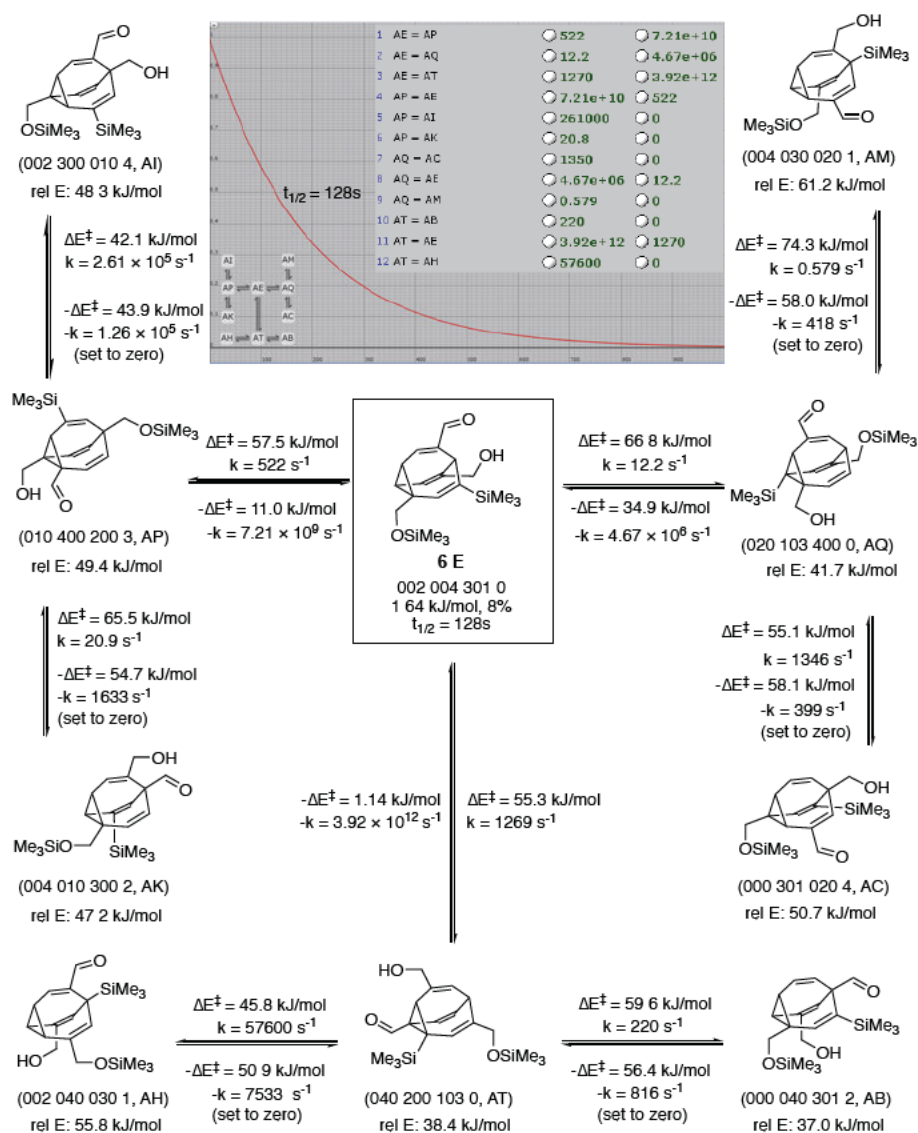| reaction step	Source isomer	Target isomer	k (298K)	-k (289K)
AA <=> AL	000 000 001 2	000 000 210 0	1101 712643	3240 817066
AB <=> AI	000 000 002 1	000 000 120 0	3623 011512	6 42287973
AC <=> AK	000 000 010 2	000 000 201 0	153106 2625	2121 116799
AD <=> AF	000 000 012 0	000 000 021 0	28530 65771	16972 59121
AE <=> AH	000 000 020 1	000 000 102 0	87517 13794	85 48391076
AG <=> AJ	000 000 100 2	000 000 200 1	502 5521956	47132 49186
AA <=> BD	000 000 001 2	000 200 100 0	89042 12867	330963 4302
AA <=> BC	000 000 001 2	000 100 200 0	89042 12867	330963 4302
AM <=> BA	000 001 002 0	000 020 100 0	4076 684344	451472 0628
AN <=> BB	000 002 001 0	000 100 020 0	4076 684344	451472 0628
AO <=> AU	000 001 020 0	000 002 100 0	8117 832402	327693 5297
AP <=> AV	000 020 002 0	000 100 002 0	8117 832402	327693 5297
AQ <=> AG	000 001 200 0	000 000 100 2	2536 812262	830762 8787
AR <=> AG	000 200 001 0	000 000 100 2	2536 812262	830762 8787
AB <=> BC	000 000 002 1	000 100 200 0	37603 46949	69 27485653
AB <=> BD	000 000 002 1	000 200 100 0	37603 46949	69 27485653
AN <=> AY	000 002 001 0	000 010 200 0	1144 59225	54971 94275
AM <=> AZ	000 001 002 0	000 200 010 0	1144 59225	54971 94275
AS <=> AQ	000 002 010 0	000 001 200 0	2038 442584	2133 567041
AT <=> AR	000 010 002 0	000 200 001 0	2038 442584	2133 567041
AU <=> AJ	000 002 100 0	000 000 200 1	18 77961214	38413 44417
AV <=> AJ	000 100 002 0	000 000 200 1	18 77961214	38413 44417
AC <=> AZ	000 000 010 2	000 200 010 0	7338 376037	799 5953507
AC <=> AY	000 000 010 2	000 010 200 0	7338 376037	799 5953507
AT <=> AX	000 010 002 0	000 020 010 0	1386 088683	5570 050325
AS <=> AW	000 002 010 0	000 010 020 0	1386 088683	5570 050325
AD <=> AL	000 000 012 0	000 000 210 0	3207 891503	101048 8864
AD <=> AL	000 000 012 0	000 000 210 0	3207 891503	101048 8864
AE <=> BB	000 000 020 1	000 100 020 0	441 1613401	1 913710528
AE <=> BA	000 000 020 1	000 020 100 0	441 1613401	1 913710528
AP <=> AW	000 020 001 0	000 010 020 0	8 132462361	83 94189846
AO <=> AX	000 001 020 0	000 020 010 0	8 132462361	83 94189846
AF <=> AI	000 000 021 0	000 000 120 0	1599 757492	103000 7281
AF <=> AI	000 000 021 0	000 000 120 0	1599 757492	103000 7281
AH <=> AK	000 000 102 0	000 000 201 0	5622 907166	1376 94393
AH <=> AK	000 000 102 0	000 000 201 0	5622 907166	1376 94393
AM <=> BD	000 001 002 0	000 200 100 0	27 02595143	8815739 048
AN <=> BC	000 002 001 0	000 100 200 0	27 02595143	8815739 048
AO <=> BA	000 001 020 0	000 020 100 0	62 41379736	2786 511664
AP <=> BB	000 020 001 0	000 100 020 0	62 41379736	2786 511664
AQ <=> AU	000 001 200 0	000 002 100 0	1567 037128	23529 38834
AR <=> AV	000 200 001 0	000 100 002 0	1567 037128	23529 38834
AS <=> AY	000 002 010 0	000 010 200 0	89 16660364	672 140939
AT <=> AZ	000 010 002 0	000 200 010 0	89 16660364	672 140939
AW <=> AX	000 010 020 0	000 020 010 0	206 1627418	206 1627418
AX <=> AW	000 020 010 0	000 010 020 0	206 1627418	206 1627418

Figure 84. Kinetic simulation of **4f** from an initial population of **4d:A** at 25 C.

Figure 85. Kinetic simulation of **4f** from an initial population of **4d:A** at 25 C.

Table 12. Kinetic parameters for bullvalene **4f** based on the energies from single point DFT calculations at B3LYP-D3BJ/Def2-TZVPPD/CPCM solvent(chloroform) at 25 C.
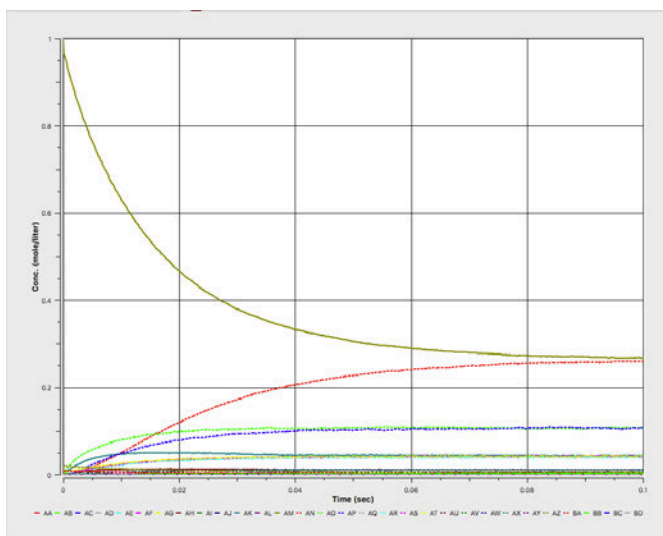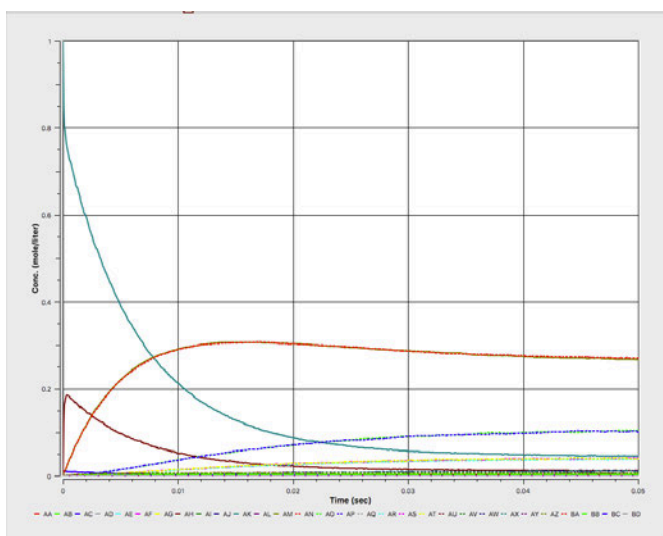
reaction step code	Source isomer	Target isomer	k (298K)	-k (289K)
AA <=> AL	000 000 012 2	000 000 221 0	13541 7002	1382 233818
AB <=> AJ	000 000 021 2	000 000 212 0	2196 39108	16978 75777
AC <=> AF	000 000 022 1	000 000 122 0	178 893936	1 09996249
AD <=> AK	000 000 102 2	000 000 220 1	69 2049898	10184 40667
AE <=> AH	000 000 120 2	000 000 202 1	33 046706	2235 294765
AG <=> AI	000 000 201 2	000 000 210 2	890 040666	20972 62955
AM <=> DF	000 001 002 2	000 220 100 0	4434 60687	80893 10148

AN <=> DE	000 002 001 2	000 100 220 0	4434 60687	80893 10148
AO <=> DD	000 001 020 2	000 202 100 0	217044 607	304644 1891
AP <=> DC	000 020 001 2	000 100 202 0	217044 607	304644 1891
AQ <=> CY	000 001 022 0	000 022 100 0	8437 8713	5694713 191
AR <=> CZ	000 022 001 0	000 100 022 0	8437 8713	5694713 191
AS <=> DB	000 001 200 2	000 200 100 2	36844 7619	1118487 199
AT <=> DA	000 200 001 2	000 100 200 2	36844 7619	1118487 199
AU <=> CK	000 001 202 0	000 020 100 2	3052 0303	3799800 553
AV <=> CL	000 202 001 0	000 100 020 2	3052 0303	3799800 553
AW <=> BH	000 001 220 0	000 002 100 2	1019 64183	77046 682
AX <=> BI	000 220 001 0	000 100 002 2	1019 64183	77046 682
AN <=> DO	000 002 001 2	000 210 200 0	2 91038431	187782 3709
AM <=> DN	000 001 002 2	000 200 210 0	2 91038431	187782 3709
AY <=> DI	000 002 002 1	000 120 200 0	12 9769681	1 736536263
AY <=> DJ	000 002 002 1	000 200 120 0	12 9769681	1 736536263
AZ <=> DM	000 002 010 2	000 201 200 0	49882 5557	6086 29336
BA <=> DL	000 010 002 2	000 200 201 0	49882 5557	6086 29336
BB <=> CW	000 002 012 0	000 021 200 0	130 7465	3161 233905
BC <=> CX	000 012 002 0	000 200 021 0	130 7465	3161 233905
BD <=> DG	000 002 020 1	000 102 200 0	1392503 04	839 2427035
BE <=> DH	000 020 002 1	000 200 102 0	1392503 04	839 2427035
BF <=> CF	000 002 021 0	000 012 200 0	2074 5486	101004 0324
BG <=> CG	000 021 002 0	000 200 012 0	2074 5486	101004 0324
BH <=> DK	000 002 100 2	000 200 200 1	112 245856	41733 79586
BI <=> DK	000 100 002 2	000 200 200 1	112 245856	41733 79586
BJ <=> CQ	000 002 102 0	000 020 200 1	2 76841928	143386 5027
BK <=> CR	000 102 002 0	000 200 020 1	2 76841928	143386 5027
BL <=> BN	000 002 120 0	000 002 200 1	23 8089268	2043 055241
BM <=> BO	000 120 002 0	000 200 002 1	23 8089268	2043 055241
BN <=> DA	000 002 200 1	000 100 200 2	16777 7936	268 5826488
BO <=> DB	000 200 002 1	000 200 100 2	16777 7936	268 5826488
BP <=> BX	000 002 201 0	000 010 200 2	442 35597	227926 1683
BQ <=> BY	000 201 002 0	000 200 010 2	442 35597	227926 1683
BR <=> AS	000 002 210 0	000 001 200 2	127 943132	406 8991557
BS <=> AT	000 210 002 0	000 200 001 2	127 943132	406 8991557
BA <=> CC	000 010 002 2	000 220 010 0	766 942432	1107 910987
AZ <=> CB	000 002 010 2	000 010 220 0	766 942432	1107 910987
BT <=> CA	000 010 020 2	000 202 010 0	16529 7632	634 4447782
BU <=> BZ	000 020 010 2	000 010 202 0	16529 7632	634 4447782
BV <=> BW	000 010 022 0	000 022 010 0	1538 83204	1538 83204
BW <=> BV	000 022 010 0	000 010 022 0	1538 83204	1538 83204
BX <=> BY	000 010 200 2	000 200 010 2	3082 48508	3082 485085
BY <=> BX	000 200 010 2	000 010 200 2	3082 48508	3082 485085
AA <=> DN	000 000 012 2	000 200 210 0	1139 29177	2110901 287
AA <=> DO	000 000 012 2	000 210 200 0	1139 29177	2110901 287
BC <=> CU	000 012 002 0	000 020 210 0	728 35504	144618 6914
BB <=> CV	000 002 012 0	000 210 020 0	728 35504	144618 6914
CD <=> BR	000 012 020 0	000 002 210 0	7645 87145	83117 21804
CE <=> BS	000 020 012 0	000 210 002 0	7645 87145	83117 21804
CF <=> AI	000 012 200 0	000 000 210 2	1862 08021	344219 731
CG <=> AI	000 200 012 0	000 000 210 2	1862 08021	344219 731
AP <=> CV	000 020 001 2	000 210 020 0	11 7295279	36 04401262
AO <=> CU	000 001 020 2	000 020 210 0	11 7295279	36 04401262
BE <=> CP	000 020 002 1	000 120 020 0	53 2738642	0 180661612
BD <=> CO	000 002 020 1	000 020 120 0	53 2738642	0 180661612
BU <=> CT	000 020 010 2	000 201 020 0	2049 91106	94 84274614
BT <=> CS	000 010 020 2	000 020 201 0	2049 91106	94 84274614
CE <=> CJ	000 020 012 0	000 021 020 0	418 728387	299 7726368
CD <=> CI	000 012 020 0	000 020 021 0	418 728387	299 7726368
CH <=> CN	000 020 020 1	000 102 020 0	1032 43832	1 716328589
CH <=> CM	000 020 020 1	000 020 102 0	1032 43832	1 716328589
CK <=> CR	000 020 100 2	000 200 020 1	9 89653789	735 7417288
CL <=> CQ	000 100 020 2	000 020 200 1	9 89653789	735 7417288
AB <=> DJ	000 000 021 2	000 200 120 0	981 126356	178 526068
AB <=> DI	000 000 021 2	000 120 200 0	981 126356	178 526068

BG <=> CO	000 021 002 0	000 020 120 0	170 724951	139043 6458
BF <=> CP	000 002 021 0	000 120 020 0	170 724951	139043 6458
CJ <=> BL	000 021 020 0	000 002 120 0	1604 60755	1712438 299
CI <=> BM	000 020 021 0	000 120 002 0	1604 60755	1712438 299
CW <=> AE	000 021 200 0	000 000 120 2	1105 45425	252003 4176
CX <=> AE	000 200 021 0	000 000 120 2	1105 45425	252003 4176
AC <=> DE	000 000 022 1	000 100 220 0	86136 39	3 502038929
AC <=> DF	000 000 022 1	000 220 100 0	86136 39	3 502038929
AR <=> CB	000 022 001 0	000 010 220 0	2966 28818	3112 113054
AQ <=> CC	000 001 022 0	000 220 010 0	2966 28818	3112 113054
BW <=> AW	000 022 010 0	000 001 220 0	66575 7949	91 25283423
BV <=> AX	000 010 022 0	000 220 001 0	66575 7949	91 25283423
CY <=> AK	000 022 100 0	000 000 220 1	1169 19945	854 7975828
CZ <=> AK	000 100 022 0	000 000 220 1	1169 19945	854 7975828
AD <=> DL	000 000 102 2	000 200 201 0	132544 5	3503 083571
AD <=> DM	000 000 102 2	000 201 200 0	132544 5	3503 083571
BK <=> CS	000 102 002 0	000 020 201 0	2937 21851	11613 35458
BJ <=> CT	000 002 102 0	000 201 020 0	2937 21851	11613 35458
CN <=> BP	000 102 020 0	000 002 201 0	29266 6224	1505 1084
CM <=> BQ	000 020 102 0	000 201 002 0	29266 6224	1505 1084
DG <=> AG	000 102 200 0	000 000 201 2	18081 4677	47714 37375
DH <=> AG	000 200 102 0	000 000 201 2	18081 4677	47714 37375
AF <=> AL	000 000 122 0	000 000 221 0	1242092 46	1600 403318
AF <=> AL	000 000 122 0	000 000 221 0	1242092 46	1600 403318
AH <=> DC	000 000 202 1	000 100 202 0	51976 9491	12 64400151
AH <=> DD	000 000 202 1	000 202 100 0	51976 9491	12 64400151
AV <=> BZ	000 202 001 0	000 010 202 0	47 0462237	275 7667761
AU <=> CA	000 001 202 0	000 202 010 0	47 0462237	275 7667761
AJ <=> AJ	000 000 212 0	000 000 212 0	162747 523	162747 5226
AJ <=> AJ	000 000 212 0	000 100 212 0	162747 523	162747 5226
AM <=> EP	000 001 002 2	100 200 200 0	764 65515	2303416776
AN <=> EP	000 002 001 2	100 200 200 0	764 65515	2303416776
DP <=> EO	001 002 002 0	020 200 100 0	3 43567604	16839115 88
DP <=> EN	001 002 002 0	020 100 200 0	3 43567604	16839115 88
DQ <=> EH	001 002 020 0	002 200 100 0	93 0454964	8513264 178
DR <=> EG	001 020 002 0	002 100 200 0	93 0454964	8513264 178
DS <=> DB	001 002 200 0	000 200 100 2	7 85279731	21868540 14
DT <=> DA	001 200 002 0	000 100 200 2	7 85279731	21868540 14
AO <=> EN	000 001 020 2	020 100 200 0	2293 88115	8978 992568
AP <=> EO	000 020 001 2	020 200 100 0	2293 88115	8978 992568
DR <=> EM	001 020 002 0	020 020 100 0	38 2689214	27987 74848
DQ <=> EM	001 002 020 0	020 020 100 0	38 2689214	27987 74848
DU <=> EE	001 020 020 0	002 020 100 0	149 06112	2129 265621
DU <=> EF	001 020 020 0	002 100 020 0	149 06112	2129 265621
DV <=> CK	001 020 200 0	000 020 100 2	160 29377	21818 82409
DW <=> CL	001 200 020 0	000 100 020 2	160 29377	21818 82409
AQ <=> DF	000 001 022 0	000 220 100 0	1758 1445	11832607 4
AR <=> DE	000 022 001 0	000 100 220 0	1758 1445	11832607 4
AS <=> EG	000 001 200 2	002 100 200 0	67812 4758	29976 77114
AT <=> EH	000 200 001 2	002 200 100 0	67812 4758	29976 77114
DT <=> EF	001 200 002 0	002 100 020 0	2023 11492	27701 16654
DS <=> EE	001 002 200 0	002 020 100 0	2023 11492	27701 16654
DW <=> DZ	001 200 020 0	002 002 100 0	14739 5482	4097 469637
DV <=> DZ	001 020 200 0	002 002 100 0	14739 5482	4097 469637
DX <=> BH	001 200 200 0	000 002 100 2	3855 97798	108483 8541
DX <=> BI	001 200 200 0	000 100 002 2	3855 97798	108483 8541
AU <=> DD	000 001 202 0	000 202 100 0	17 897485	776987 3376
AV <=> DC	000 202 001 0	000 100 202 0	17 897485	776987 3376
AW <=> CY	000 001 220 0	000 022 100 0	108 093156	1683381 776
AX <=> CZ	000 220 001 0	000 100 022 0	108 093156	1683381 776
AY <=> EP	000 002 002 1	100 200 200 0	18545 6438	5717 424063
DP <=> EL	001 002 002 0	010 200 200 0	3 48076004	5258 722369
DY <=> DX	002 002 010 0	001 200 200 0	438 994324	9308 904397
DZ <=> DK	002 002 100 0	000 200 200 1	2 09970349	75473 8672
AZ <=> EL	000 002 010 2	010 200 200 0	1620 81542	1109 477209

|				
BA <=> EL	000 010 002 2	010 200 200 0	1620 81542	1109 477209
DY <=> EK	002 002 010 0	010 200 020 0	46 5363085	7915 610819
DY <=> EJ	002 002 010 0	010 020 200 0	46 5363085	7915 610819
EA <=> EC	002 010 020 0	002 010 200 0	212 704978	531 9178053
EB <=> ED	002 020 010 0	002 200 010 0	212 704978	531 9178053
EC <=> BX	002 010 200 0	000 010 200 2	59 1970467	4185 559749
ED <=> BY	002 200 010 0	000 200 010 2	59 1970467	4185 559749
BB <=> DO	000 002 012 0	000 210 200 0	10 0551773	37537337 48
BC <=> DN	000 012 002 0	000 200 210 0	10 0551773	37537337 48
BD <=> EO	000 002 020 1	020 200 100 0	1189 47679	2 422008699
BE <=> EN	000 020 002 1	020 100 200 0	1189 47679	2 422008699
DQ <=> EJ	001 002 020 0	010 020 200 0	40 3110045	6056 885967
DR <=> EK	001 020 002 0	010 200 020 0	40 3110045	6056 885967
EB <=> DV	002 020 010 0	001 020 200 0	34 9621966	130 2776712
EA <=> DW	002 010 020 0	001 200 020 0	34 9621966	130 2776712
EE <=> CQ	002 020 100 0	000 020 200 1	0 349402	2244 244531
EF <=> CR	002 100 020 0	000 200 020 1	0 349402	2244 244531
BF <=> DI	000 002 021 0	000 120 200 0	0 42905515	62759316 68
BG <=> DJ	000 021 002 0	000 200 120 0	0 42905515	62759316 68
BJ <=> DM	000 002 102 0	000 201 200 0	1777 05047	6614 778138
BK <=> DL	000 102 002 0	000 200 201 0	1777 05047	6614 778138
BL <=> CW	000 002 120 0	000 021 200 0	286458 108	1553 936425
BM <=> CX	000 120 002 0	000 200 021 0	286458 108	1553 936425
BN <=> EH	000 002 200 1	002 200 100 0	22169 47	5 16795119
BO <=> EG	000 200 002 1	002 100 200 0	22169 47	5 16795119
DS <=> ED	001 002 200 0	002 200 010 0	727 121372	4240 997452
DT <=> EC	001 200 002 0	002 010 200 0	727 121372	4240 997452
BP <=> DG	000 002 201 0	000 102 200 0	14 4944852	616630 7148
BQ <=> DH	000 201 002 0	000 200 102 0	14 4944852	616630 7148
BR <=> CF	000 002 210 0	000 012 200 0	5585 35901	2217 770688
BS <=> CG	000 210 002 0	000 200 012 0	5585 35901	2217 770688
BT <=> EK	000 010 020 2	010 200 020 0	143 691304	65 94360453
BU <=> EJ	000 020 010 2	010 020 200 0	143 691304	65 94360453
EA <=> EI	002 010 020 0	010 020 020 0	127 237609	487 7442512
EB <=> EI	002 020 010 0	010 020 020 0	127 237609	487 7442512
BV <=> CC	000 010 022 0	000 220 010 0	7958 21733	264 0786472
BW <=> CB	000 022 010 0	000 010 220 0	7958 21733	264 0786472
BZ <=> CA	000 010 202 0	000 202 010 0	10 633714	10 633714
CA <=> BZ	000 202 010 0	000 010 202 0	10 633714	10 633714
CD <=> CU	000 012 020 0	000 020 210 0	2 89948015	98 68535131
CE <=> CV	000 020 012 0	000 210 020 0	2 89948015	98 68535131
CH <=> EM	000 020 021 0	020 020 100 0	173 489643	6 00688226
DU <=> EI	001 020 020 0	010 020 020 0	26 8465635	250 4076235
CI <=> CP	000 020 021 0	000 120 020 0	252 264048	25442 7693
CJ <=> CO	000 021 020 0	000 020 120 0	252 264048	25442 7693
CM <=> CT	000 020 102 0	000 201 020 0	295 985436	127 6851899
CN <=> CS	000 102 020 0	000 020 201 0	295 985436	127 6851899
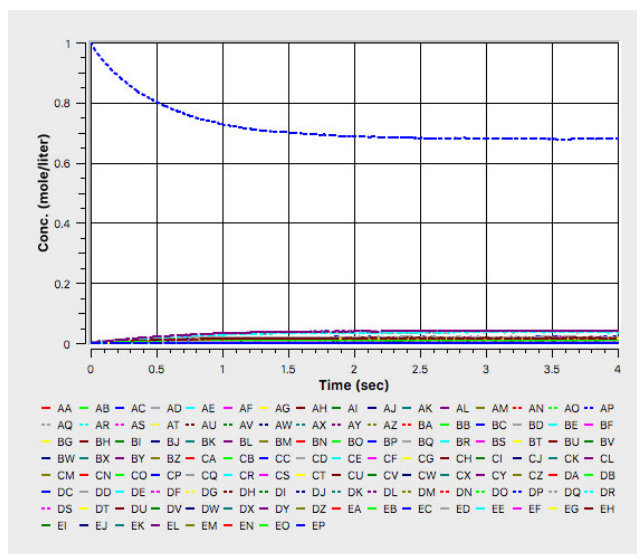
Figure 86. Kinetic simulation of **4f** from an initial population of **4f:A** at 25 °C
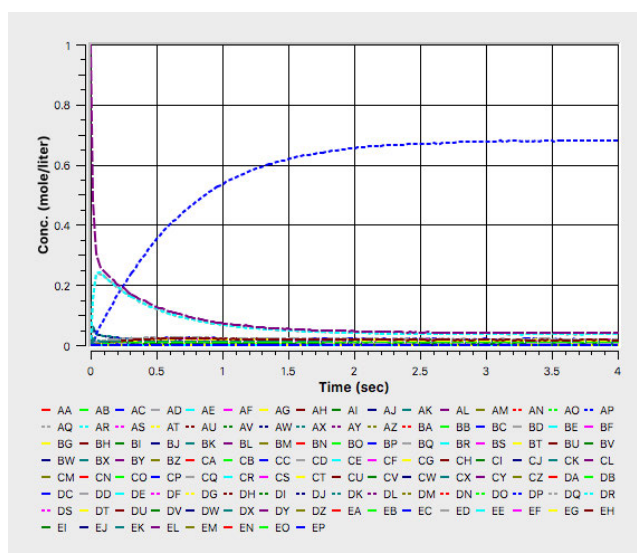

Figure 87. Kinetic simulation of **4f** from an initial population of **4f:D** at 25 °C

2.1. Experimental section for addition section of chapter 3

This project was not included in the publication and was abandoned, therefore most of the compounds are missing data such as IR, MS, ^1H– and ^{13}C–NMR.

General procedure A: Under argon atmosphere, a 20 mL oven–dried sealed tube was charged with CoBr$_2$(dppe) (10 mol%), zinc iodide (20 mol%), and zinc dust (30 mol%). The tube was flushed with argon and evacuated under high–vacuum three times. Afterwards, the solvent (either 1,2–dichlorethane or trifluoroethanol) was added and the reaction mixture stirred for 15 min at room temperature. **COT–Me** (1.00 mmol, 1.00 eq) and the substituted acetylene (1–2 eq) were added to the solution and the reaction stirred for 16 – 24 h at either room temperature or 55 °C. After the reaction was complete, the suspension was filtered through a short pad of silica gel eluting with either hexane or ethyl acetate. The solvent was evaporated under vacuum, and the desired product was purified by column chromatography.

General procedure B: A 20 mL pyrex sealed tube charged with 36 mM of **8a–e** in dry acetone. The solution was flushed with argon and was placed in a water bath 2.5 cm away from a 150W high–pressure mercury emission lamp (Osram SUPRATEC HTT 150–211). The tube was irradiated for 3 – 10h. After the reaction was complete, the solvent was evaporated and the desired product was purified by flash column chromatography on silica gel.

Synthesis of methyl–cyclooctatetraene (5)
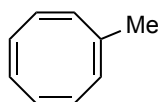
Under nitrogen atmosphere, an oven dried 250 mL round bottom flask was charged with bromocyclooctatetraene (8.00 g, 43.7 mmol, 1.00 eq) and anhydrous tetrahydrofuran (70 mL). The reaction mixture was cooled to –78 °C in a cooling bath containing dry ice and acetone. *N*–butyllithium (17.5 mL, 2.50 M in cyclohexane, 43.7 mmol, 1.00 eq) was added slowly over 20 min to the solution. The colour of the solution changed from brown to light dark brown. After 5 min, methyliodode (2.72 mL, 43.7 mmol, 1.00 eq) was added and the reaction stirred for 2 hours at –78 °C. The reaction was quenched with an aqueous ammonium chloride solution and extracted with dichloromethane. The organic layer was washed with distilled water, aqueous sodium chloride solution, dried over MgSO$_4$ and the solvent was removed under vacuum. The crude product was purified by column chromatography using hexane as eluent (R$_f$ = 0.55). The desired product was obtained

as a yellow oil (3.50 g, 68%). **¹H NMR** (600 MHz, CDCl₃) δ = 5.79 (3H, s), 5.75 (4H, s), 3.76 (3H, s).

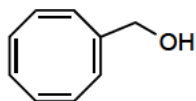## Synthesis of COT–CH₂OH (4)

Under nitrogen atmosphere, an oven dried 250 mL round bottom flask was charged with bromocyclooctatetraene (2.00 g, 10.9 mmol, 1.00 eq) and anhydrous tetrahydrofuran (20 mL). The reaction mixture was cooled to –78 °C in a cooling bath containing dry ice and acetone. *N*–butyllithium (4.4 mL, 2.5 M in cyclohexane, 11 mmol, 1.2 eq) was added slowly over 20 min to the solution. The colour of the solution changed from brown to light dark brown. After 5 min, methyl formate (670 µL, 10.9 mmol, 1.00 eq) was added and the reaction stirred for 2 hours at –78 °C. The reaction was quenched with an aqueous ammonium chloride solution and extracted with dichloromethane. The organic layer was washed with distilled water, aqueous sodium chloride solution, dried over MgSO₄ and the solvent was removed under vacuum. The aldehyde product (1.2 g) was used for the next reaction without any further purification. (data of the aldehyde reported in here[168].

The aldehyde (1.2 g, 9.1 mmol, 1.0 eq) was dissolved in a mixture of MeOH/THF (1:1) at 0 °C and NaBH₄ (312 mg, 10.9 mmol, 1.20 eq) was added slowly. After 2 hours, the reaction was quenched at 0 °C with distilled water and the organic layer was extracted with ethyl acetate. The organic layer was washed with distilled water, aqueous sodium chloride solution, dried over MgSO₄ and the solvent was removed under vacuum. The crude material was used without any further purification (900 mg, 62% over two steps). **¹H NMR** (500MHz, CDCl₃) δ = 5.92 – 5.79 (7H, m), 4.01 (2H, s). **¹³C NMR** (125MHz, CDCl₃) δ = 143.6 (C), 133.3 (CH), 132.1 (CH), 131.9 (CH), 131.8 (CH), 131.7 (CH), 131.6 (CH), 66.47 (CH₂). Further data are reported here.[169]
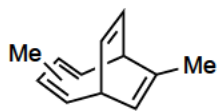
Synthesis of Me–TMS–BDT (7b)
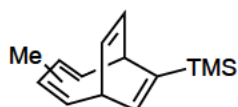
The reaction was done according to **procedure A,** at room temperature for 16h using COT–Me (118.2 mg, 1.00 mmol, 1.00 eq), TMS–acetylene (213 µL, 1.50 mmol, 1.50 eq) as the substituted acetylene, and 1,2–dichloroethane (4 mL) as the solvent. The silica pad was washed with hexane, which was
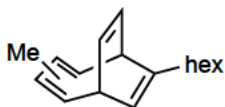
removed *in vacuo*. The desired product was obtained without any further purification as a yellow oil (122 mg, 56%). Data are reported in experimental section bove (compound **3a**)
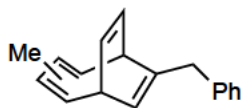
Synthesis of bis(Me)–BDT (8a)

The reaction was done according to **procedure A,** at room temperature for 16h using COT–Me (300 mg, 2.54 mmol, 1.00 eq), propyne (1.15 mL, 2.25 M, 5.08 mmol, 2.00 eq) as the substituted acetylene, and 1,2–dichloroethane (4 mL) as the solvent. The silica pad was washed with hexane, which was removed *in vacuo*. The desired product was obtained without any further purification as a yellow oil (300 mg, 75%). **IR** (ATR): v/cm^{-1} = 3009, 2911, 1447, 1375, 860. **H NMR** (600MHz, CDCl$_3$) δ = 6.37 – 6.22 (4H, m), 5.73 – 5.65 (4H, m), 5.48 – 5.47 (2H, d, J = 6.0 Hz), 5.45 – 5.44 (2H, d, J = 6.05 Hz), 3.21 – 3.19 (1H, d, J = 8.77 Hz), 3.09 –3.06 (2H, m), 2.99 – 2.96 (1H, q, J = 6.54, 8.44 Hz), 1.85 (6H, s), 1.81 (6H, s).^{13}**C NMR** (150MHz, CDCl$_3$) δ = 144.1, 143.7, 143.6, 143.0, 134.6, 132.2, 125.2 (CH), 124.4 (CH), 123.5 (CH), 118.2 (CH), 118.0 (CH), 46.6 (CH), 40.8 (CH), 35.5 (CH), 20.6 (CH$_3$), 20.3 (CH$_3$).

Synthesis of hexyl–BDT (8b)

The reaction was done according to **procedure A,** at room temperature for 16h using COT–Me (300 mg, 2.54 mmol, 1.00 eq), 1–octyne (562 µL, 3.80 mmol, 1.50 eq) as the substituted acetylene, and 1,2–dichloroethane (4 mL) as the solvent. The silica pad was washed with hexane, which was removed *in vacuo*. The desired product was obtained without any further purification as a yellow oil (139 mg, 40%). **IR** (ATR): v/cm^{-1} = 3009, 2924, 1457, 1376, 1376, 861. **^{1}H NMR** (600MHz, CDCl$_3$): δ = 7.68 – 6.60 (5H, m), 6.26 – 6.18 (3H, m), 6.15 – 6.09 (5H, m), 5.92 – 5.84 (4H, m), 3.69 (1H, ddd, J = 14.5, 8.6, 6.0 Hz), 3.63 (1H, d, J = 8.8 Hz), 3.60 – 3.57 (1H, m), 3.55 – 3.50 (2H, m), 3.43 (1H, ddd, J = = 20.8, 14.8, 6.3 Hz), 3.02 – 2.98 (3H, m), 2.58 – 2.51 (7H, m), 2.29 (3H, s), 2.24 (3H, s), 1.76 – 1.71 (28H, m), 1.35 – 1.33 (15H, m). **^{13}C NMR** (150MHz, CDCl$_3$) δ =1436, 143.5, 143.1, 142.9, 136.9, 132.3, 132.1, 124.8, 124.4, 124.0, 123.5, 118.4, 118.0, 117.2, 117.0, 117.0, 45.2, 40.8, 39.7, 36.1, 35.5, 35.1, 34.8, 31.9, 31.9, 31.9, 31.9, 29.6, 29.3, 29.2, 29.1, 29.1, 29.1, 22.7, 14.2.

Synthesis of benzyl–BDT (8c)

The reaction was done according to **procedure A,** at room temperature for 16h using COT–Me (300 mg, 2.54 mmol, 1.00 eq), 3–phenyl–1–propyne (253 μL, 2.00 mmol, 0.80 eq) as the substituted acetylene, and 1,2– dichloroethane (4 mL) as the solvent. The silica pad was washed with hexane, which was removed *in vacuo*. The desired product was obtained without any further purification as a yellow oil (350 mg, 59%). **IR** (ATR): v/cm^{-1} = 2908, 1601, 1493, 1073, 836. **^{1}H NMR** (600MHz, CDCl$_3$) δ = 7.29 – 7.25 (9H, m), 7.21 – 7.14 (10H, m), 6.34 – 6.25 (2H, m), 6.15 – 6.12 (1H, m), 6.08 – 6.04 (1.5H, m), 5.71 – 5.63 (5H, m), 5.45 – 5.40 (4H, m), 3.43 (2H, s), 3.18 (1H, d, *J* = 8.7 Hz), 3.11 – 3.05 (2H, m), 3.03 – 2.99 (1H, m), 1.79 (2H, s), 1.77 (2H, s). **^{13}C NMR** (150 MHz, CDCl$_3$) δ = 143.6, 143.6, 143.2, 142.9, 135.4, 135.4, 132.1, 132.0, 129.1, 128.5, 128.3, 128.3, 128.3, 124.6, 124.4, 123.7, 119.5, 119.4, 118.3, 118.3, 118.1, 118.1, 44.3, 44.3, 40.8, 40.6, 40.36, 38.8, 38.7, 38.4, 35.5, 20.5, 20.3.

Synthesis of menthol–BDT (8d)
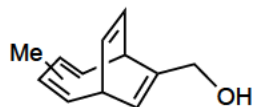
The reaction was done according to **procedure A,** at 55 °C for one days using COT–Me (300 mg, 2.54 mmol, 1.00 eq), propargyl alcohol (296 μL, 5.08 mmol. 2.00 eq) as the substituted acetylene, and TFE (4 mL) as the solvent. The silica pad was washed with ethyl acetate, and the solvent was removed under vacuum. The desired product was purified by flash column chromatography using hexane/ethyl acetate (1:4) as eluent (R$_f$ = 0.30). The product was obtained as colourless oil (200 mg, 45%). **^{1}H NMR** (600MHz, CDCl$_3$) δ = 6.30 – 3.18 (7H, m), 5.76 – 5.70 (2H, m), 5.71 – 5.65 (6H, m), 5.64 – 5.61 (4H, m), 5.47 – 5.46 (1H, m), 5.41 – 5.40 (1H, m), 4.16 – 4.09 (4H, m), 4.06 – 4.01 (4H, m), 3.41 – 3.39 (1H, m), 3.36 (1H, d, *J* = 8.8 Hz) 3.26 – 3.23 (1H, m), 3.19 – 3.16 (1H, m), 3.14 – 3.11 (1H, m), 3.04 – 3.01 (1H, m). 2.21 (3H, brs, OH), 1.83 (3H, s), 1.78 (3H, s). **^{13}C NMR** (150 MHz, CDCl$_3$) δ = 143.5, 142.9, 142.8, 142.3, 141.8, 141.3, 136.1, 136.1, 135.9, 131.9, 131.7, 125.0, 124.7, 124.6, 124.3, 124.2, 123.9, 121.1, 120.9, 118.7, 118.6, 118.5, 117.9, 117.9, 64.3, 64.2, 64.2, 64.0, 41.8, 40.3, 36.5, 36.2, 34.9, 34.7, 20.4, 20.2.

Synthesis of dimenthol–methyl–BDT (8e)
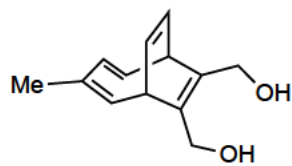
The reaction was done according to **procedure A,** at 55 °C for three days using COT–Me (118 mg, 1.00 mmol, 1.00 eq), buty–2–yne–1,4–diol (129 mg, 1.50 mmol. 1.50 eq) as the substituted acetylene, and TFE (4 mL) as the solvent. The silica pad was washed with ethyl acetate, and the solvent was removed under vacuum. The desired product was purified by flash column chromatography using hexane/ethyl acetate (2:3) as eluent (R_f = 0.29). The product was obtained as colourless oil (101 mg, 50%). IR (ATR): 3315, 3011, 2954, 2926. 2871, 1457, 1387, 1244, 991, 853, 683. ^{1}**H NMR** (600MHz, CDCl$_3$) δ = 6.31 – 6.28 (1H, t, J = 10.44 Hz), 6.26 – 6.22 (2H, m), 5.73 – 5.61 (2H, m), 5.48 – 5.47 (1H, d, J = 6.11 Hz), 4.20 (2H, s), 4.17 (2H, s), 3.40 – 3.39 (1H, d, J = 9.06 Hz), 3.30 – 3.27 (1H, dd, J = 6.23, 2.45 Hz), 1.83 (3H, s). ^{13}**C NMR** (150MHz, CDCl$_3$) δ = 142.9 (CH), 142.8 (CH), 136.9 (C), 133.2, (C), 132.7 (C), 125.4 (CH), 124.5 (CH) 117.0 (CH) , 60.2 (CH2), 59.9 (CH2), 38.47 (CH), 34.4 (CH), 20.2 (CH3).

Synthesis of dimethyl–bullvalene (9a)
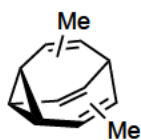
The reaction was done according to **procedure B**, using **8a** (120 mg, 758 μmol) in dry acetone (5 ml). After 5 h the solvent was evaporated under vacuum. The crude material was purified by flash chromatography using hexane as eluent (Rf = 0.24). The desired product was obtained as a yellow oil (67 mg, 70%). ^{1}**H NMR** (700MHz, CDCl$_3$, –60 ºC) δ = 5.93 – 5.85 (5H, m), 5.74–5.71 (2H, m), 5.65 – 5.61 (1H, m) 2.41 – 2.37 (0.5H, m), 2.33 – 2.31 (1H, m), 2.25 – 2.18 (6H, m), 1.87 – 1.85 (9H, m). ^{13}**C NMR** (175 MHz, CDCl$_3$, –60 ºC) δ = 138.4, 137.6, 137.6, 135.1, 135.1, 134.7, 128.1, 128.0, 127.4, 127.4, 127.3, 127.2, 127.0, 126.7, 126.6, 126.6, 125.9, 120.0, 119.9, 119.9, 119.4, 119.2, 41.9, 41.8, 35.8, 35.8, 30.6, 29.7, 27.7, 27.6, 27.4, 26.8, 26.7, 26.7, 23.7, 23.6, 22.4, 20.39, 20.3, 20.2, 20.1, 20.1, 20.0, 20.0, 19.9, 19.8, 19.3, 19.7.

Synthesis of methyl–hexyl–bullvalene (9b)

The reaction was done according to **procedure B**, using **8b** (95.0 mg, 516 μmol) in dry acetone (5 ml). After 8 h the solvent was evaporated under vacuum. The

crude material was purified by flash chromatography using hexane as eluent (Rf = 0.29). The desired product was obtained as a yellow oil (44 mg, 37%). **^{1}H NMR** (700MHz, CDCl$_3$, –60 ºC) δ = 5.94 – 5.85 (3.5H, m), 5.75 – 5.57 (3H, m), 2.34 – 2.14 (5H, m), 2.09 – 2.03 (4H, m), 1.87 (3H, brs), 1.59 – 1.51 (5H, m), 1.38 – 1.24 (23H, m), 0.89 – 0.86 (12H, m). **^{13}C NMR** (17 MHz, CDCl$_3$, –60 ºC) δ = ^{13}C NMR (176 MHz, CDCl$_3$) δ = 143.1, 142.1, 137.7, 137.7, 137.7, 134.8, 134.6, 134.4, 132.5, 132.1, 131.9, 131.7, 128.0, 128.0, 127.7, 127.7, 127.4, 127.3, 127.3, 127.3, 127.1, 127.0, 126.95 126.7, 126.6, 126.6, 126.4, 125.9, 125.7, 120.0, 119.9, 119.5, 119.4, 119.4, 119.4, 119.3, 118.6, 118.6, 41.1, 41.0, 40.8, 40.4, 40.4, 40.3, 34.7, 34.5, 32.0, 32.0, 31.9, 31.6, 30.8, 30.5, 29.9, 29.78, 29.7, 29.4, 29.4, 29.2, 29.1, 29.1, 29.1, 29.1, 29.0, 28.9, 28.6, 28.2, 28.2, 27.6, 27.6, 26.8, 26.6, 23.6, 23.6, 20.3, 20.3, 20.1, 20.01 20.0, 19.9, 19.9, 19.8, 19.8, 19.8, 19.7, 19.6, 14.4, 14.4, 14.4, 14.4, 14.4, 14.3, 14.3.

Synthesis methyl–benzyl–bullvalene (9c)

The reaction was done according to procedure B, using **8c** (60.0 mg, 344 µmol) in dry acetone (5 ml). After 2 h the solvent was evaporated under vacuum. The crude material was purified by flash chromatography using hexane as eluent (Rf = 0.29). The desired product was obtained as a yellow oil (20 mg, 33%). **^{1}H NMR** (700MHz, CDCl$_3$, –60 ºC) δ = 7.27 (3H, brs), 7.19 (4H, brs), 7.12 – 7.10 (1H, m), 5.86 – 5.82 (2H, m), 5.71 – 5.72 (1H, m), 5.69 – 55.61 (2H, m), 5.58 – 5.57 (1H, m), 5.36 – 5.35 (0.2H, m), 3.42 (1H, brs), 3.36 – 3.31 (2H, m), 2.37 – 2.35 (0.3H, m), 2.19 – 1.97 (7H, m), 1.84 – 1.82 (0.2H, m), 1.63 – 1.60 (1H, 1.49 – 1.46 (1H). **^{13}C NMR** (175 MHz, CDCl$_3$, –60 ºC) δ = 142.6, 142.3, 141.1, 140.9, 140.6, 140.4, 140.2, 140.1, 140.1, 139.9, 139.7, 139.6, 138.9, 138.7, 138.0, 136.5, 136.1, 129.2, 129.2, 129.1, 128.8, 128.8, 128.7, 128.6, 128.4, 128.3, 128.2, 128.1, 128.0, 127.9, 127.9, 127.6, 127.5, 127.1, 127.1, 127.0, 126.8, 126.8, 126.6, 126.4, 126.2, 126.2, 126.2, 126.1, 126.0, 125.9, 122.9, 122.2, 122.1, 121.7, 121.6, 121.5, 119.8, 119.7, 119.5, 119.1, 119.1, 46.7, 46.7, 46.3, 46.1, 41.1, 40.7, 40.0, 39.3, 38.4, 34.5, 34.2, 33.9, 31.3, 31.2, 30.4, 30.4, 29.9, 29.9, 23.2, 23.2, 22.9, 22.9, 22.5, 22.3, 22.2, 20.4, 20.4, 20.1, 20.7, 20.0, 19.9, 19.9, 19.9, 19.5, 19.6, 19.5, 14.4, 14.3, 14.3, 14.2.

Synthesis of methyl–menthol–bullvalene

The reaction was done according to **procedure B**, using **8d** (90.0 mg, 416 µmol) in dry acetone (5 ml). After 3 h the solvent was evaporated under vacuum. The crude material was purified by flash chromatography using hexane/EtAOc (4:1) as eluents (Rf = 0.29). The desired product was obtained as a yellow oil (55 mg, 61%). **^{1}H NMR** (700MHz, CDCl$_3$, –60 °C) δ = 5.92 – 5.79 (8H, m), 5.71 – 5.69 (0.5H, m), 5.61 (0.25H, d, *J* = 8.7 Hz), 5.58 (.13H, d, *J* = 7.5 Hz), 4.03 (1H, s), 3.97 (2H, s), 2.52 – 2.37 (3H, m), 2.29 – 2.14 (5H, m), 1.85 (2H, brs). **^{13}C NMR** (175 MHz, CDCl$_3$, –60 °C) δ = 140.7, 140.7, 139.9, 137.9, 137.9, 137.8, 137.7, 135.0, 129.2, 128.4, 128.3, 127.7, 127.7, 127.6, 127.5, 127.5, 127.2, 127.2, 127.2, 127.0, 126.8, 126.6, 126.5, 126.4, 126.4, 122.7, 122.6, 122.3, 122.2, 121.8, 121.5, 120.0, 119.9, 119.57, 119.4, 119.3, 118.6, 71.3, 69.5, 69.5, 69.5, 68.7, 68.2, 68.2, 37.7, 35.5, 31.9, 29.8, 29.4, 27.6, 27.6, 26.7, 26.6, 25.1, 23.8, 23.3, 22.8, 21.2, 21.0, 20.9, 20.5, 20.2, 20.2, 20.1, 19.9, 19.8, 19.6, 19.5, 19.2, 19.0, 18.8.

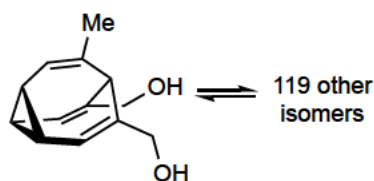## Synthesis of methyl–dimenthol–bullvalene (8e)

The reaction was done according to procedure B, using **8e** (90.0 mg, 440 µmol) in dry acetone (5 ml). After 3 h the solvent was evaporated under vacuum. The crude material was purified by flash chromatography using hexane/EtAOc (2:3) as eluents (Rf = 0.20). The desired product was obtained as a colourless oil (37 mg, 41%). **^{1}H NMR** (700MHz, CDCl$_3$) δ = 5.82 – 5.82 (3H, m), 5.63 – 5.56 (2H, m), 4.14 – 4.09 (2H, m), 4.00 (2H, brs), 3.90 – 3.87 (2H, m).

NMR spectra
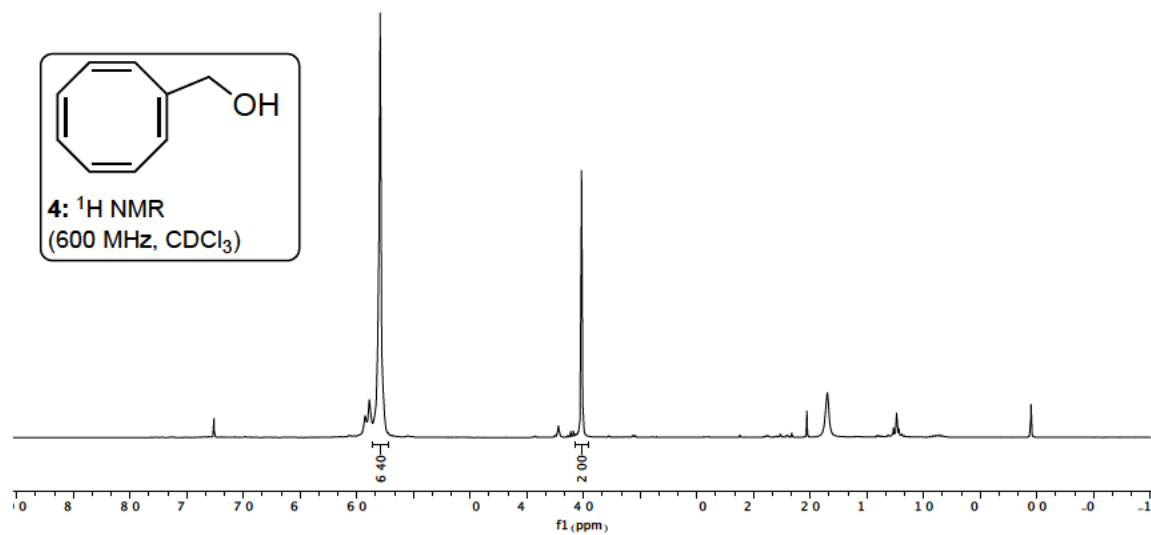
Figure 7.1: ^{1}H NMR of COT–CH$_2$OH.
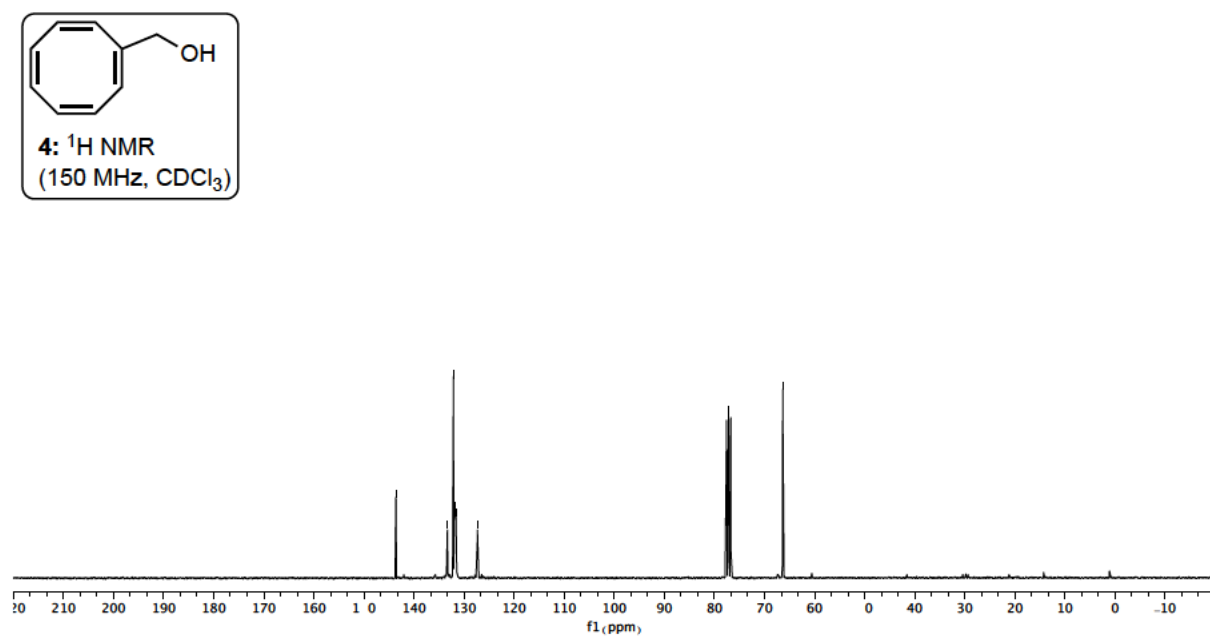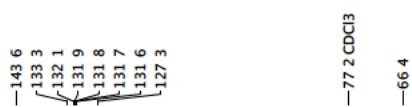
Figure 7.2: ^{13}C NMR of COT–CH$_2$OH.
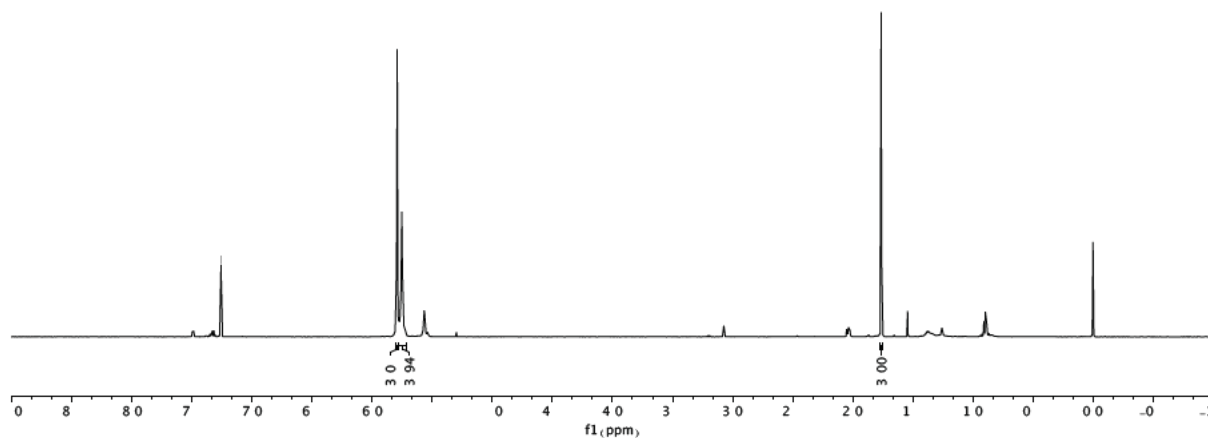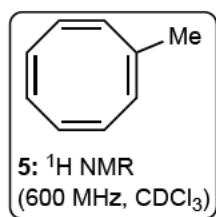
Figure 7.3: ^{1}H NMR of COT–Me.
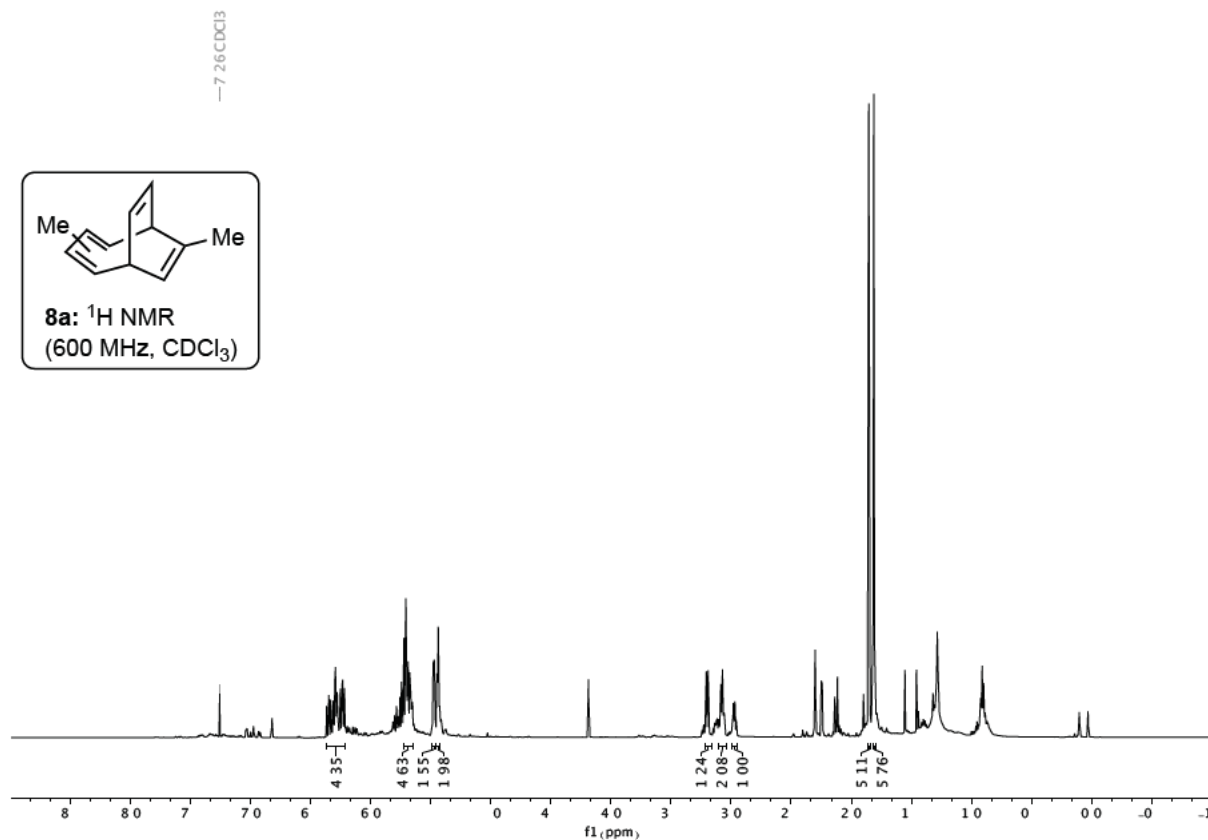
Figure 7.4: ¹H NMR of dimethyl–BDT.

Figure 7.5: ¹³C NMR of dimethyl–BDT.

—7 26 CDCl3

8b: ¹H NMR
(600 MHz, CDCl₃)

11 3 3 4 89 4 14   0 61 1 00 0 92 1 72 1 07 3 20 7 18 2 24 2 14 28 8 14 9

f1 (ppm)

Figure 7.6: ¹H NMR of hexyl–BDT.

143 6 143 5 143 1 142 9 136 9 132 3 132 1 124 8 124 4 124 0 123 6 118 4 118 0 117 2 117 0 117 0   —77 2 CDCl3   45 2 40 8 39 7 36 1 35 5 35 1 34 8 31 9 31 9 31 9 31 9 29 6 29 3 29 2 29 1 29 1 29 1 22 7 14 2

8b: ¹³C NMR
(150 MHz, CDCl₃)

f1 (ppm)

Figure 7.7: ¹³C NMR of dimethyl–BDT.
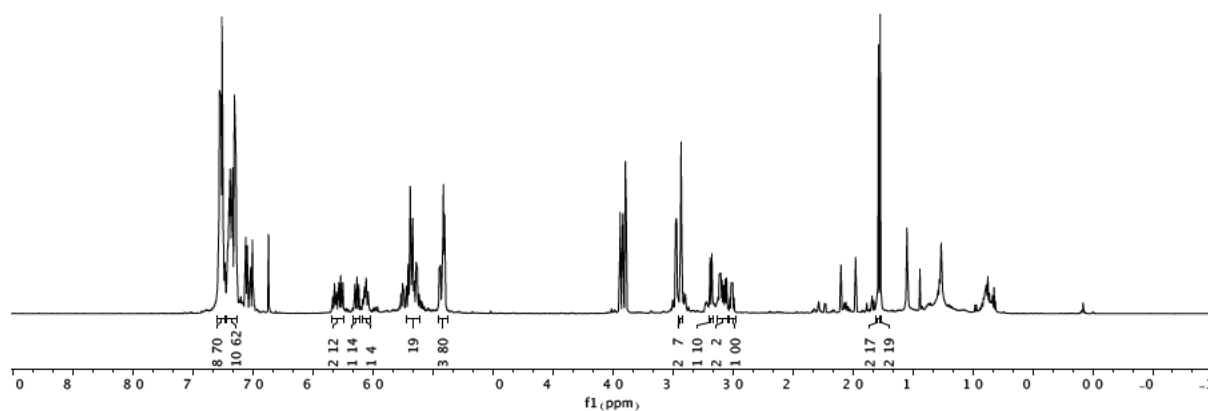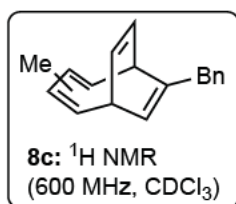
Figure 7.8: [^1]H NMR of benzyl–BDT.
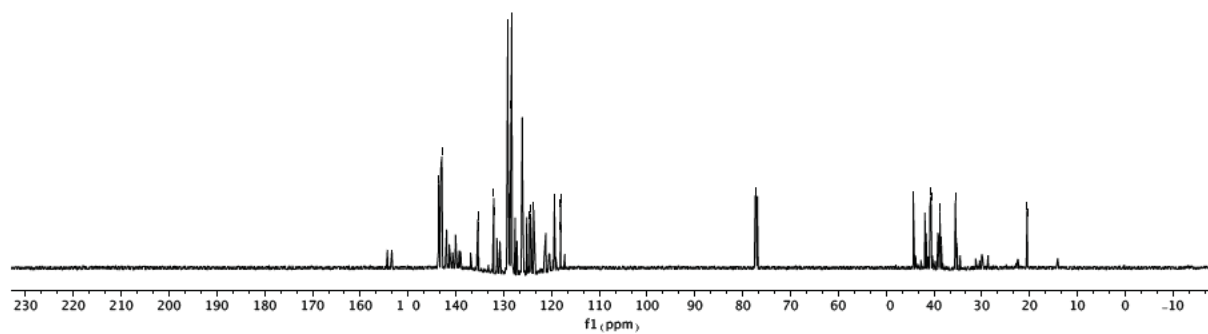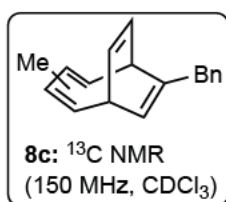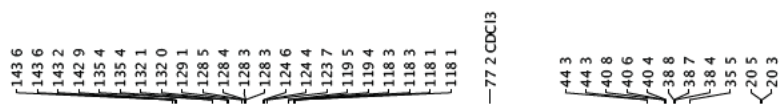
Figure 7.9: [^13]C NMR of benzyl–BDT.
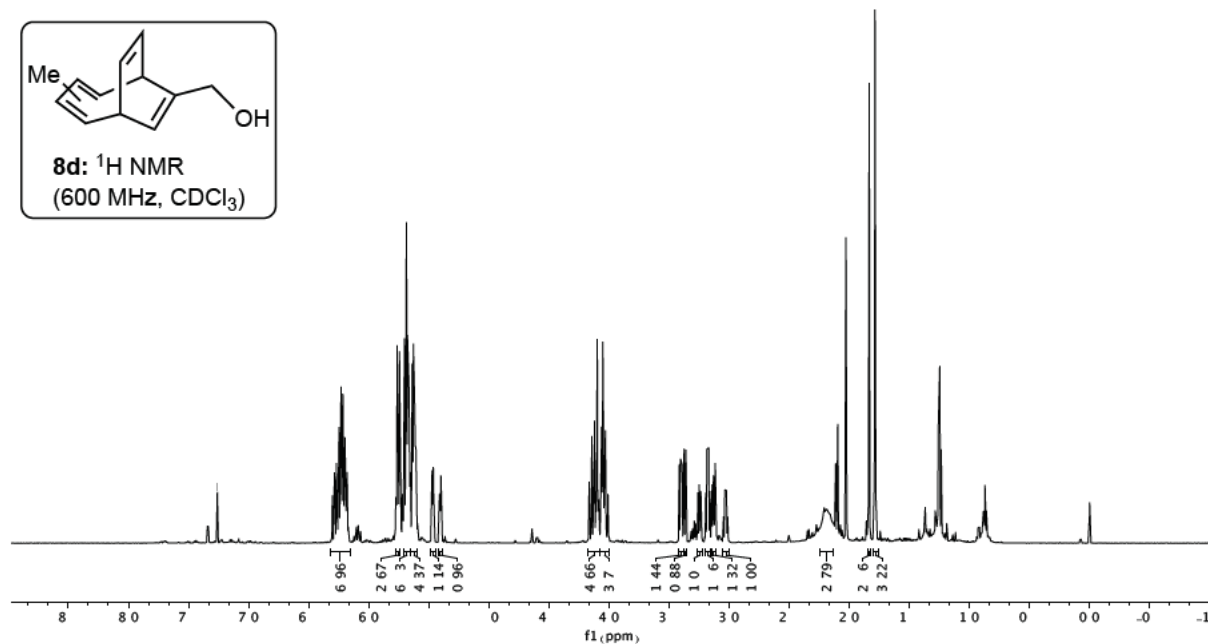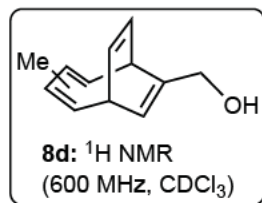
Figure 7.10: ^{1}H NMR of menthol–BDT.

Figure 7.11: ^{13}C NMR of menthol–BDT.

Figure 7.12: ^{1}H NMR of dimenthol–methyl–BDT.

Figure 7.13: ^{13}C NMR of dimenthol–methyl–BDT.

—7 26 CDCl3

9a: ^{1}H NMR
(700 MHz, CDCl$_3$)
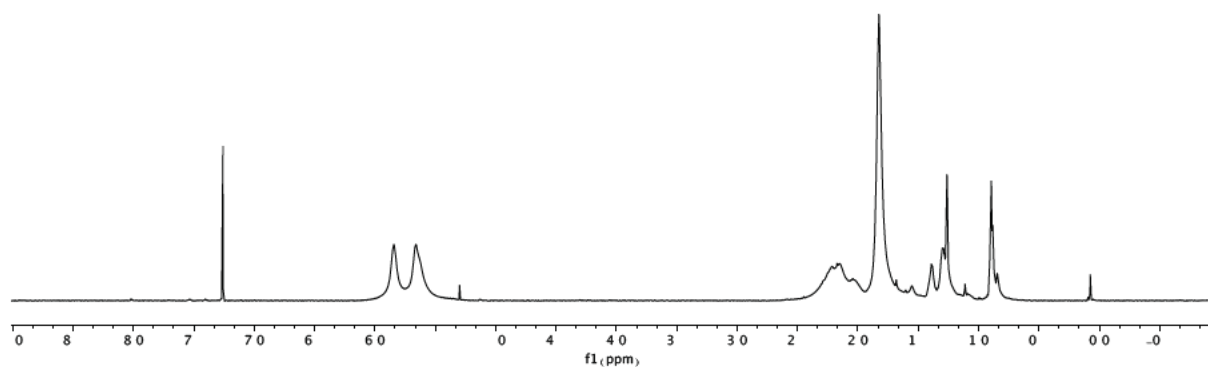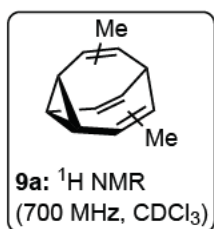
Figure 7.14: ^{1}H NMR of dimethyl–bullvalene at room temperature.

—7 26 CDCl3

9a: ^{1}H NMR
(700 MHz, CDCl$_3$)
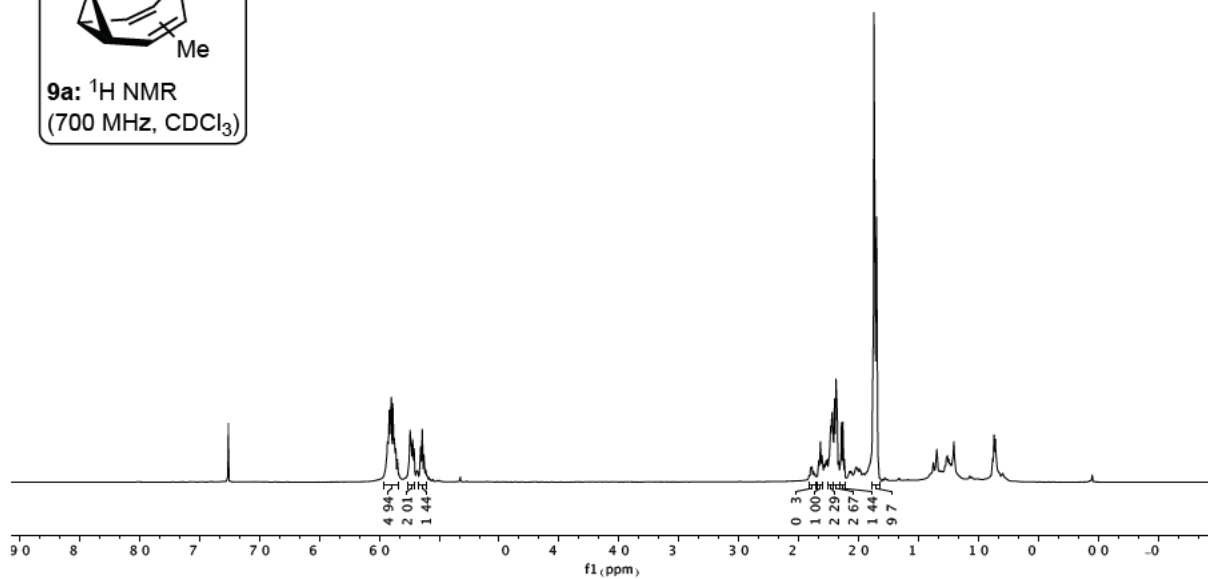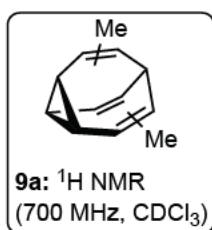
Figure 7.15: ^{1}H NMR of dimethyl–bullvalene at –60 °C.
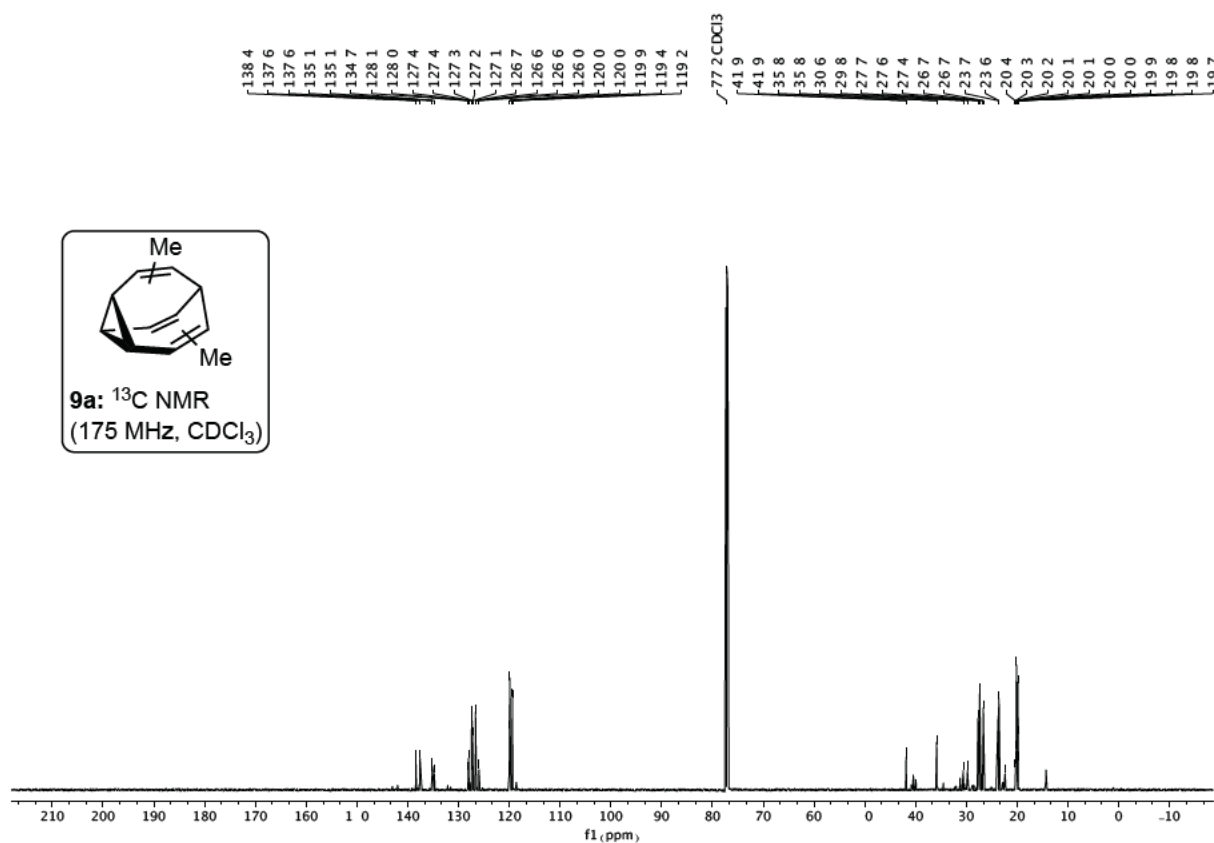
Figure 7.16: ^{13}C NMR of dimethyl–bullvalene at –60 °C.
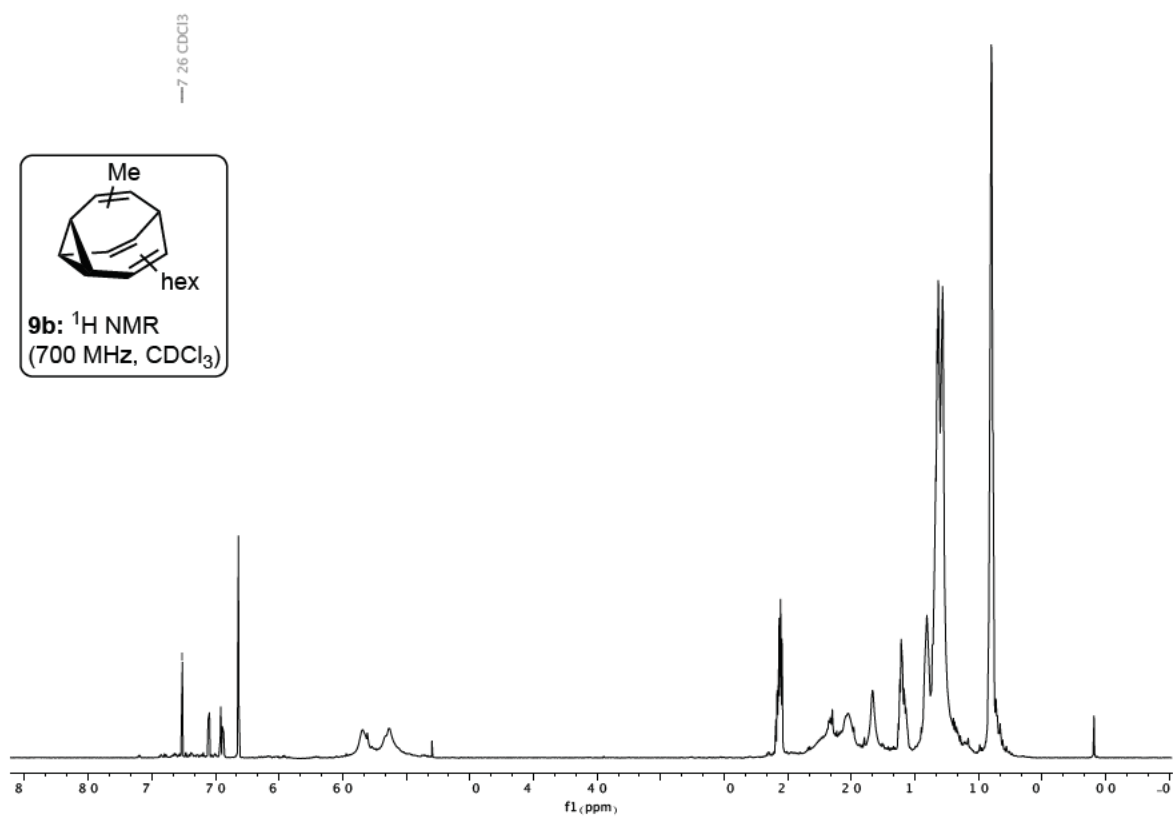
Figure 7.17: ^{1}H NMR of methyl–hexyl–bullvalene at room temperature.
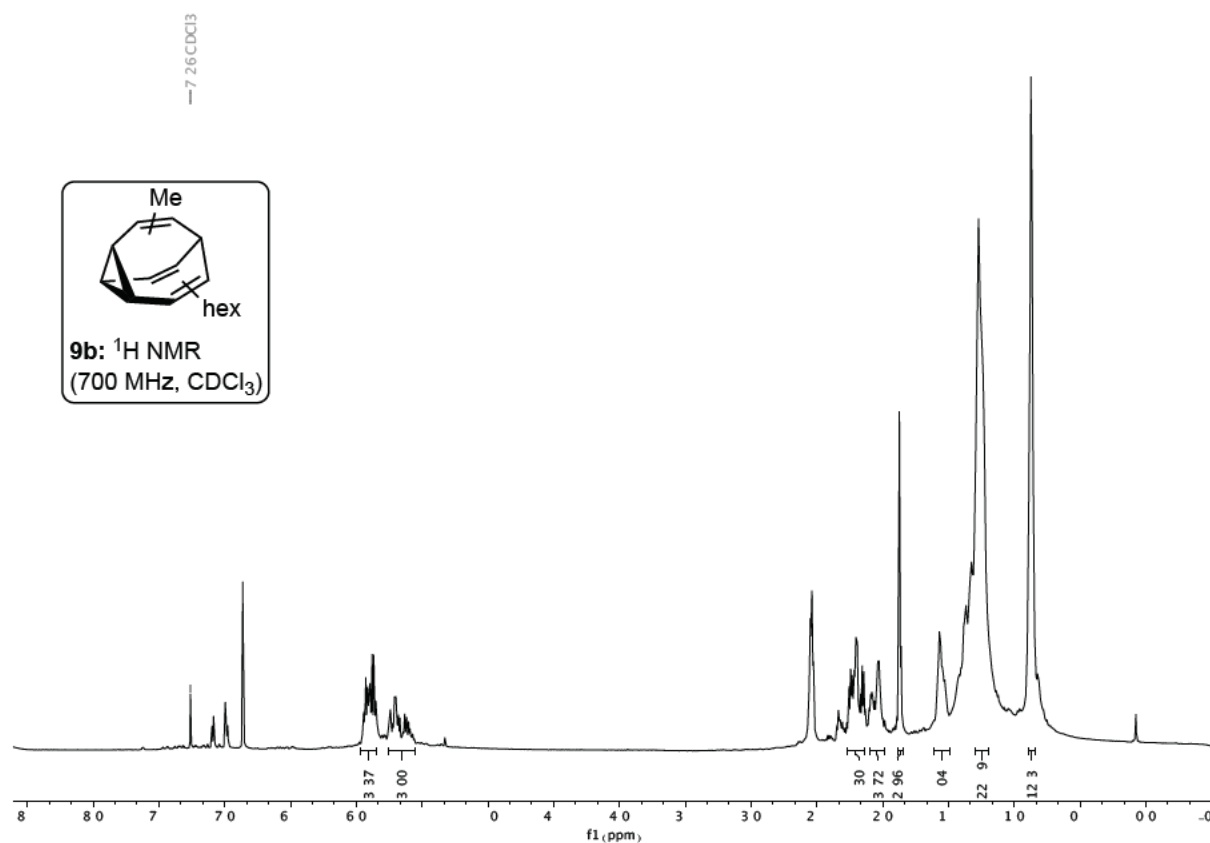
Figure 7.18: ^{1}H NMR of methyl–hexyl–bullvalene at room temperature.
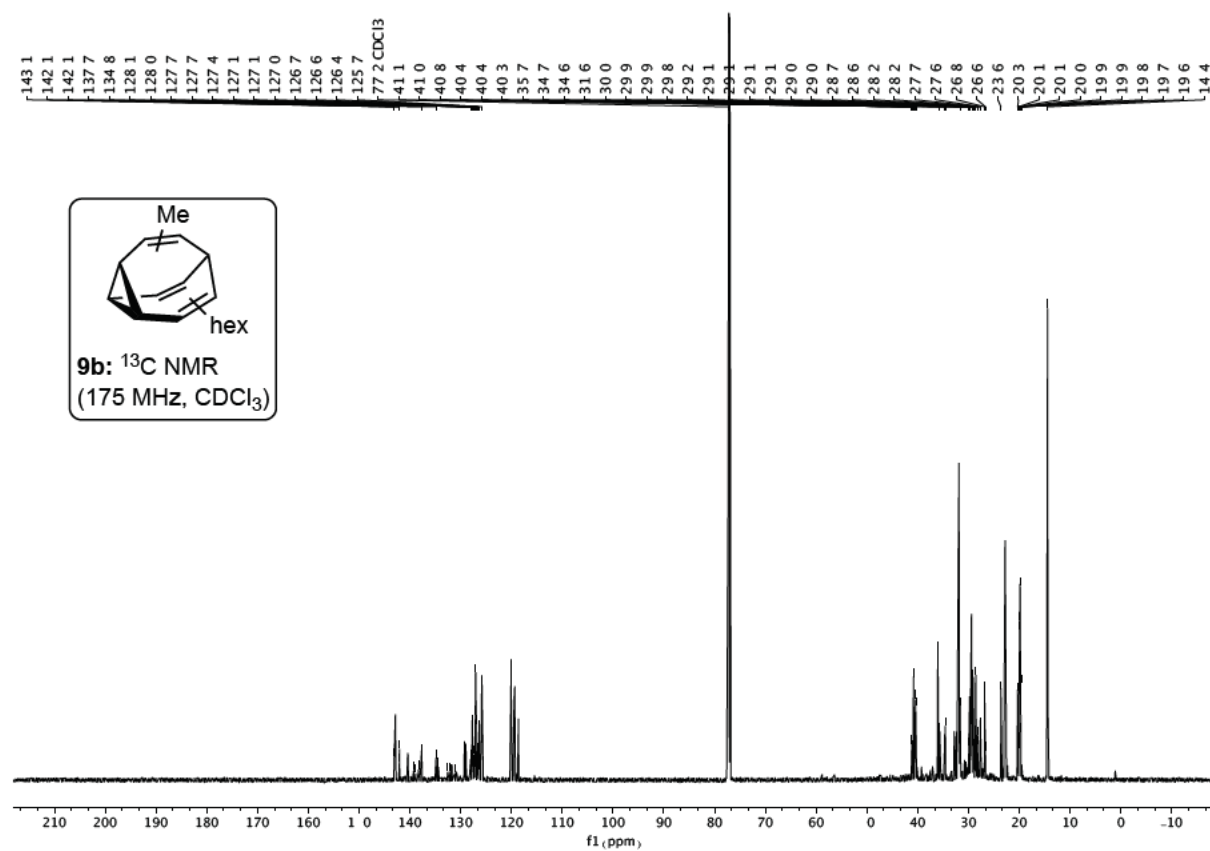
Figure 7.19: ^{13}C NMR methyl–hexyl–bullvalene at –60 °C.
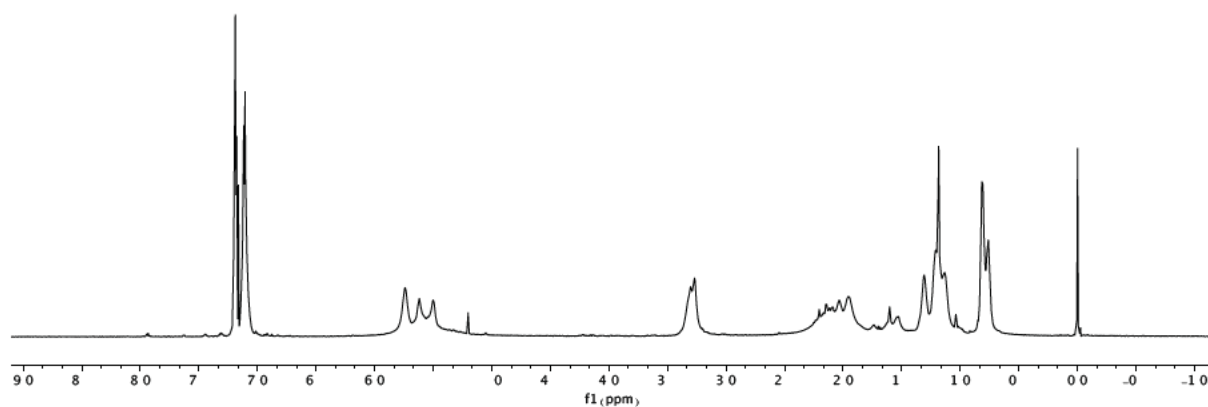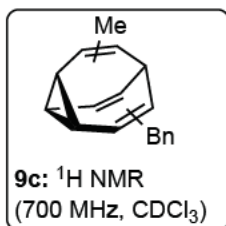
Figure 7.20: ^{1}H NMR of methyl–benzyl–bullvalene at room temperature.
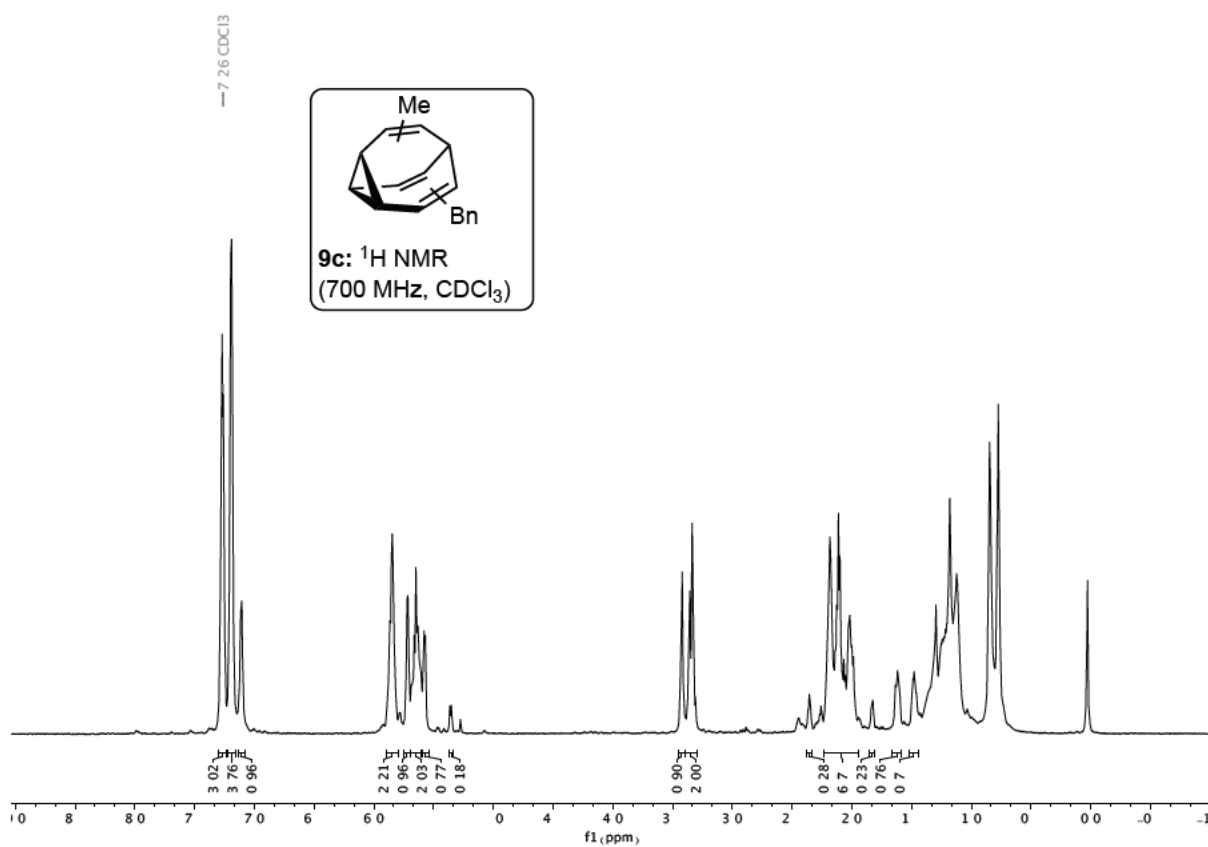
Figure 7.21: ^{1}H NMR of methyl–benzyl–bullvalene at –60 °C.

9c: ^{13}C NMR
(175 MHz, CDCl$_3$)
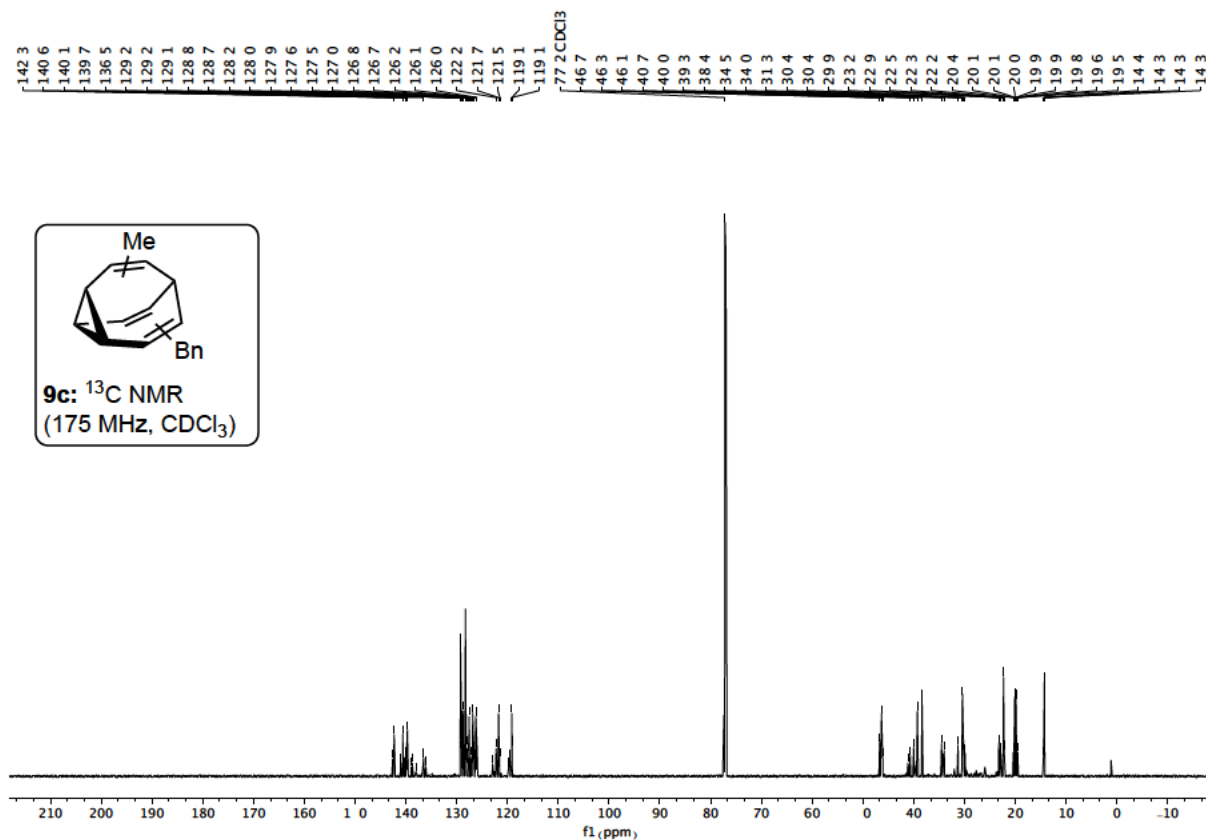
Figure 7.22: ^{13}C NMR methyl–benzyl–bullvalene at –60 ℃.

9d: ^{1}H NMR
(700 MHz, CDCl$_3$)
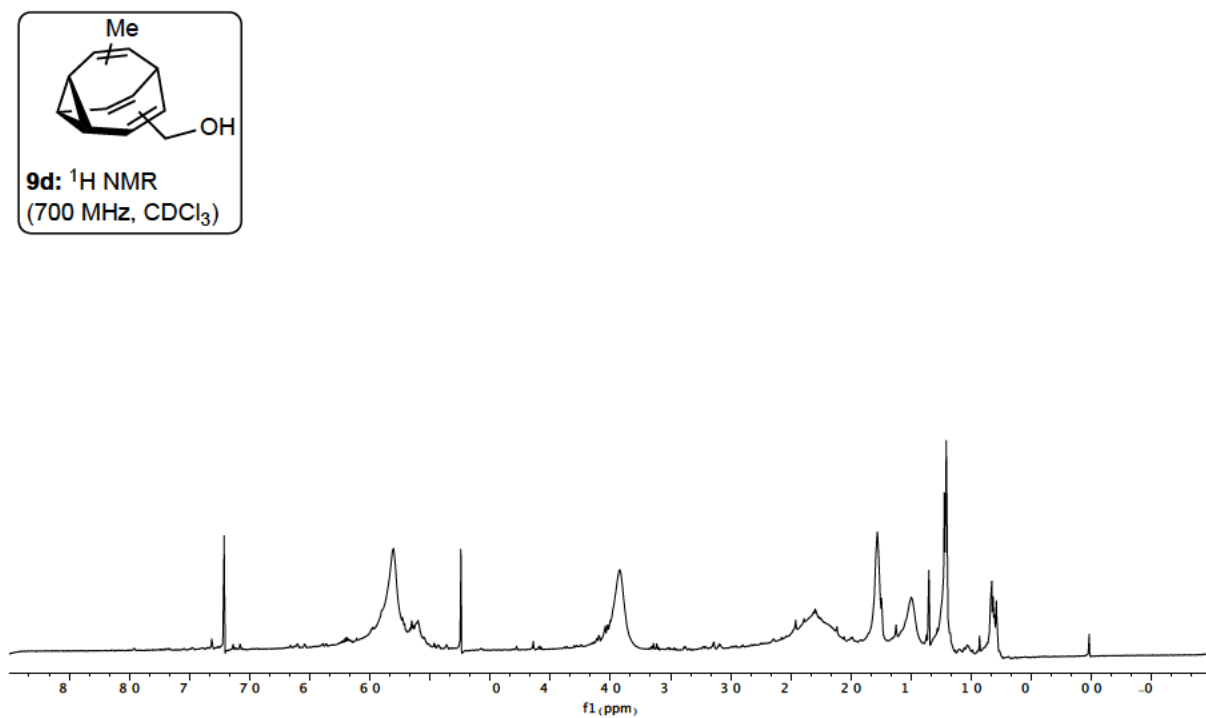
Figure 7.23: ^{1}H NMR of methyl–menthol–bullvalene at room temperature.
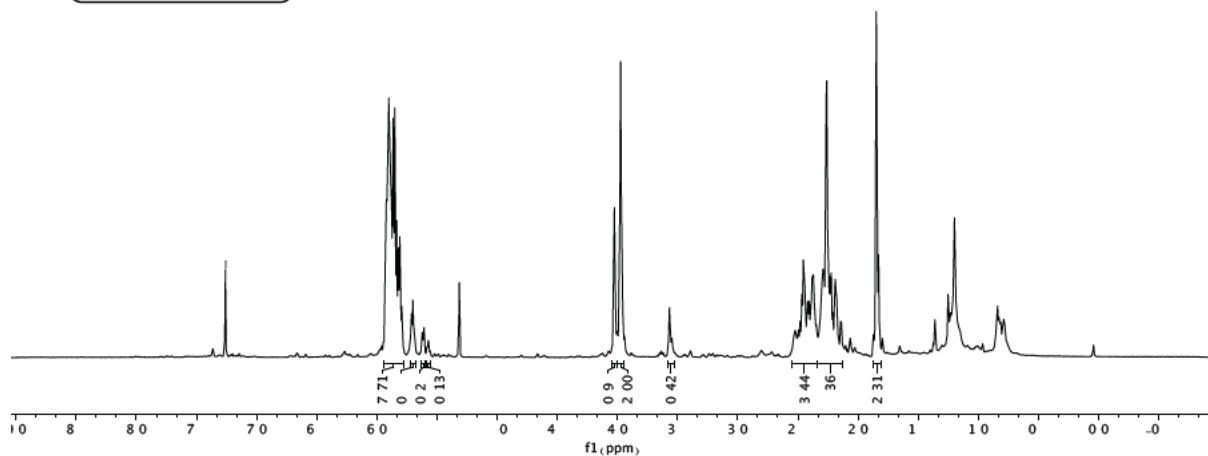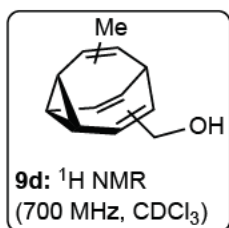
Figure 7.24: ^{1}H NMR of methyl–menthol–bullvalene at –60 °C.
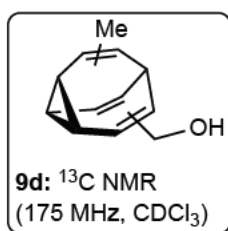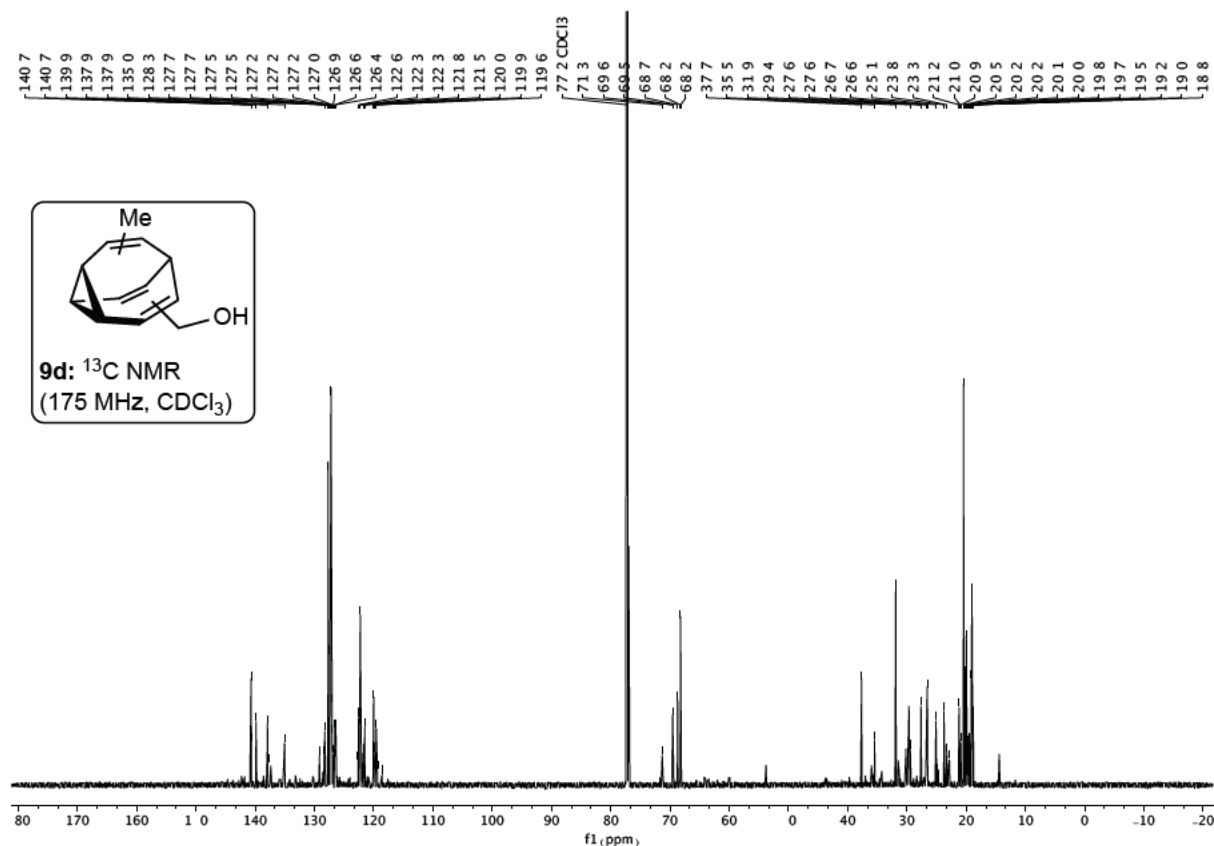
Figure 7.25: ^{13}C NMR methyl–menthol–bullvalene at –60 °C.
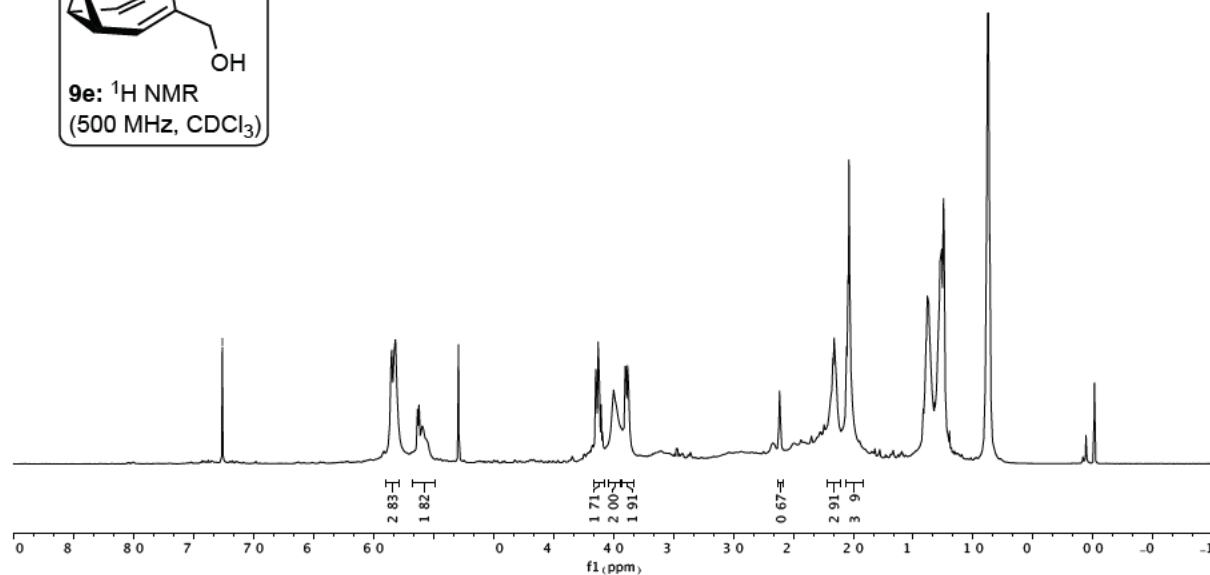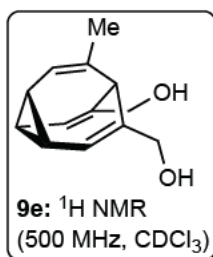
Figure 7.26: ^{1}H NMR of methyl–dimenthol–bullvalene at –60 °C.

3. Experimental section for chapter 4

NMR analysis was conducted using a *Bruker UltraShield Avance III–HD* 600 MHz, and an *Agilent* 500 MHz DD2 console. Chemical shifts are referenced to the residual solvent resonance as the internal standard (CDCl$_3$: δ = 7.26 ppm for ^{1}H NMR and δ = 77.16 ppm for ^{13}C NMR, TMS: δ = 0.00 ppm for ^{1}H NMR).[1] Data are reported as follows: chemical shift, multiplicity (ap. = apparent, brs = broad singlet, s = singlet, d = doublet, t = triplet, q = quartet, m = multiplet). The assignment of signals was assisted using correlated spectroscopy (COSY). High–resolution mass spectroscopy was recorded using an Agilent 6230 TOF LC/MS (ESI). Infra–red spectra were recorded using ATR on a *PerkinElmer spectrum 100* FTIR spectrometer equipped with a zinc selenide crystal.

Cyclooctatetraene was obtained as a generous gift from Dr Graham Gream (The University of Adelaide). The material was manufactured by BASF, most likely sometime in the 1970s. Samples were purified by vacuum distillation using a short vigreux column (20 mbar/ 60 °C) and stored in a freezer under an atmosphere of nitrogen. All other chemicals were purchased from commercial suppliers and used as received.

All reactions were performed in oven–dried glassware using conventional Schlenk techniques under positive pressure of nitrogen. Liquids and solutions were transferred with syringes. Dimethyl sulfoxide was dried following the rapid purification procedure outlined in Purification of Laboratory Chemicals (5th Edition, by Amarego and Chai), and stored over 4 Å molecular sieves under an atmosphere of nitrogen. Tetrahydrofuran and dichloromethane were purified by a Pure Solv™ Micro solvent purification system; tetrahydrofuran was then stored over 4 Å molecular sieves under an atmosphere of nitrogen.

Compounds TMS–alcohol–bullvalene 31[84] and diol–bullvalene **33**[27] were synthesized according to procedures developed in our laboratory.

Synthesis of 2–methylmalonic acid 46
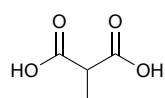
Synthesised starting from diethyl malonate according to the procedure by Lu, **2016**, using MeI in place of CD$_3$I.[109]

Synthesis of trimethylsilyl–aldehyde–bullvalene 32
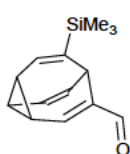
Under nitrogen atmosphere, an oven dried 10 mL round bottom flask was charged with oxalyl chloride (18 µL, 0.20 mmol, 1.20 eq) and anhydrous dichloromethane (2 mL). The solution was cooled down to –78 °C in a bath of dry ice and acetone. A mixture of anhydrous dimethyl sulfoxide (31 µL, 0.43 mmol, 2.50 eq) and dichloromethane (2 mL) was added slowly to the reaction mixture. After 5 min, **31** (40 mg, 0.17 mmol, 1.00 eq) in dichloromethane (2 mL) was added. The reaction was stirred for another 30 min, then triethylamine (120 µL, 0.86 mmol, 5.00 eq) was added. After 30 min, the reaction was quenched by addition of ammonium chloride salt, followed by addition of water, and warming up slowly to room temperature. The aqueous layer was extracted with dichloromethane. The organic phase was washed three times with distilled water, once with saturated aqueous sodium chloride, dried over $MgSO_4$, filtered, and the solvent was evaporated under vacuum. The crude product was purified through column chromatography with 3% NEt_3 and hexane/ethyl acetate (9/1) as eluent (R_f = 0.25) (5 mg, 12% yield). **IR** (ATR): v/cm^{-1} = 3029, 2954, 2812, 2721, 1674, 1632, 1401, 1307, 1247, 1157, 1042, 910, 870, 832, 754, 730, 690. **^{1}H NMR** (600 MHz, CDCl$_3$, – 60 °C) δ = 9.03 (1H, s), 6.89 – 6.84 (1H, m), 6.34 – 6.28 (1H, m), 5.99 – 5.92 (1H, m), 5.78 (1H, dd, J = 11.0, 8.7 Hz), 3.39 (1H, d, J = 8.7 Hz), 2.66 – 2.58 (3H, m), 0.03 (9H, s). **^{13}C NMR** (150 MHz, CDCl$_3$, – 60 °C) δ = 191.7 (CH) 151.6 (CH), 144.1 (C), 139.5 (C), 134.5 (CH), 128.4 (CH), 127.3 (CH), 26.9 (CH), 24.4 (CH), 23.5 (CH), 23.2 (CH), –2.5 (TMS). **HRMS** (ESI, m/z) calculated for ([M+2H]$^+$) $C_{14}H_{20}OSi^+$ 232.1278 found 232.1236.

Synthesis of methylhydroxy–TMS–bullvalene 30
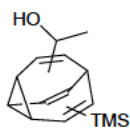
Under nitrogen atmosphere, an oven dried 5 mL round bottom flask was charged with trimethylsilyl–aldehyde–bullvalene **32** (13 mg, 56 µmol, 1.00 eq) and anhydrous tetrahydrofuran (1 mL). The solution was cooled to – 78 °C in a bath of dry ice and acetone. Methyllithium lithium bromide (75 µL, 1.50 M in diethyl ether, 110 µmol, 2.00 eq) was added slowly and the reaction stirred for 2 hours at – 78 °C. The reaction was quenched with saturated ammonium chloride and extracted with dichloromethane. The organic layer was washed with distilled water and saturated aqueous sodium chloride, dried over $MgSO_4$, and filtered. The solvent was evaporated under vacuum. The desired product was

obtained as a yellow oil without any further purification (10 mg, 77% yield). **IR** (ATR): v/cm⁻¹ = 3392, 3024, 2953, 2927, 1710, 1641, 1608, 1439, 1403, 1364, 1246, 1155, 1062, 1045, 886, 831, 747, 6789. **¹H NMR** (600 MHz, CDCl₃, – 60 °C) δ = 6.33 – 6.27 (2.5H, m), 6.27 – 6.17 (1.8H, m), 5.99 – 5.66 (18.8H, m), 4.23 – 4.10 (3.2H, m), 3.28 – 3.17 (1.1H, m), 2.75 (1H, d, J = 8.5 Hz), 2.55 – 2.43 (3.8H, m), 2.37 – 2.25 (9.2H, m), 1.82 (1.7H, brs), 1.55 (1.9H, brs), 1.35 – 1.15 (24.5H, m), 0.10 – –0.01 (45.0H, m). **¹³C NMR** (150 MHz, CDCl₃, – 60 °C) δ = 145.7, 145.3, 135.3, 135.1, 128.7, 128.2, 126.9, 126.7, 126.1, 121.4, 119.2, 73.4, 72.2, 33.0, 32.1, 31.5, 22.5, 21.9, 21.5, 21.4, 20.3, 20.2, 19.6, 19.5, 0.1, –1.6, –1.7, –2.1, –2.2, –2.2, –2.2. **HRMS** (ESI, m/z) calculated for ([M+K]⁺) $C_{15}H_{22}OSiK^+$ 285.1072 found 285.1072.

Synthesis of dialdehyde–bullvalene 34
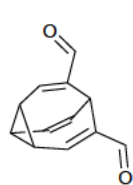
isomer a   isomer b

Under nitrogen atmosphere, an oven dried 10 mL round bottom flask was charged with oxalyl chloride (110 μL, 1.3 mmol, 2.40 eq) and anhydrous dichloromethane (5 mL). The solution was cooled down to –78 °C in a bath of dry ice and acetone. A mixture of anhydrous dimethyl sulfoxide (190 μL, 2.6 mmol, 5.00 eq) and dichloromethane (3 mL) was added slowly to the reaction mixture. After 5 min **33** (100 mg, 526 μmol, 1.00 eq) in dichloromethane (2 mL) was added. The reaction was stirred for another 2 h, then triethylamine (730 μL, 5.3 mmol, 10.0 eq) was added. After 2 h the reaction was quenched by addition of ammonium chloride salt, followed by addition of water, and warming up slowly to room temperature. The mixture was extracted with dichloromethane and the organic phase was washed three times with distilled water, three times with a saturated aqueous sodium chloride solution, dried over MgSO₄, filtered, and the solvent was evaporated under vacuum. The desired product was obtained as a yellow solid without any further purification (90 mg, 93% yield). **IR** (ATR): v/cm⁻¹ = 2924, 2831, 2734, 1665, 1629, 1403, 1349, 1307, 1194, 1165, 1145, 1009, 974, 927, 884, 852, 783, 762, 688, 665. **¹H NMR** (600 MHz, CDCl₃, – 60 °C, isomer **a** : **b** ratio 73 : 27) δ = 9.16 (0.3H, s), 8.96 (2.1H, s), 6.89 – 6.81 (2.3H, m), 6.73 (0.4H, d, J = 8.9 Hz), 5.96 – 5.87 (1.4H, m), 5.67 – 5.55 (1.5H, m), 4.08 (1H, d, J = 8.9 Hz, isomer **a**), 3.60 (0.4H, ap.t, J = 8.8 Hz, isomer **b**), 3.23 (0.4H, ap.t, J = 8.5 Hz), 2.88 – 2.76 (3.1H, m), 2.65 – 2.56 (0.8H, m). **¹³C NMR** (150 MHz, CDCl₃, – 60 °C) δ = 193.7 (CH, isomer **b**), 191.0 (CH, isomer **b**), 190.8 (CH, isomer **a**), 151.8 (CH, isomer **b**), 149.9 (CH, isomer **a**), 147.8 (CH, isomer **b**), 139.3 (C, isomer **b**), 138.4 (C, isomer **a**), 136.3 (C, isomer **b**), 128.8 (CH, isomer

b), 127.6 (CH, isomer **a**), 127.1 (CH, isomer **a**), 124.7 (CH, isomer **b**), 25.3 (CH, isomer **b**), 25.3 (CH, isomer **a**), 24.7 (CH, isomer **a**), 22.1 (CH, isomer **b**), 21.1 (CH, isomer **b**), 20.5 (CH, isomer **a**), 18.6 (CH, isomer **b**). **HRMS** (ESI, m/z) calculated for ([M+H]$^+$) $C_{12}H_{11}O_2^+$ 187.0754 found 187.0757.

Synthesis of bis(methylhydroxy)–bullvalene 35
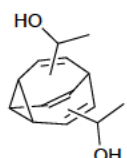
Under nitrogen atmosphere, an oven dried 5 mL round bottom flask was charged with dialdehyde–bullvalene **34** (50 mg, 270 μmol, 1.00 eq) and anhydrous tetrahydrofuran (2 mL). The solution was cooled to – 78 °C in a bath of dry ice and acetone. Methyllithium lithium bromide (470 μL, 1.50 M in diethyl ether, 710 μmol, 2.65 eq) was added slowly and the reaction stirred for 2 hours at –78 °C. The reaction was quenched with saturated ammonium chloride solution and extracted with dichloromethane. The organic layer was washed with distilled water, then saturated aqueous sodium chloride solution, dried with MgSO$_4$, and filtered. The solvent was evaporated under vacuum. The desired product was obtained as a yellow oil without any further purification (50 mg, 85% yield). **IR** (ATR): v/cm^{-1} = 3338, 3025, 2964, 2923, 2853, 1655, 1368, 1260, 1153, 1062, 1012, 881, 806, 765, 742, 701. **^{1}H NMR** (600 MHz, CDCl$_3$, – 60 °C) δ = 6.04 – 5.59 (19.8H, m), 4.29 – 4.18 (1.7H, m), 4.18 – 3.97 (6.0H, m), 2.81 (1H, ap.d, J = 8.9 Hz), 2.59 (1.7H, ap.d, J = 9.1 Hz), 2.32 – 2.02 (10.6H, m), 1.97 – 1.82 (1.1H, m), 1.34 – 1.05 (28.8H, m). **^{13}C NMR** (150 MHz, CDCl$_3$, – 60 °C) δ = 143.4, 143.3, 143.2, 127.8, 127.5, 127.2, 127.0, 122.3, 121.5, 74.4, 73.5, 70.5, 53.8, 33.7, 32.0, 26.9, 23.1, 23.0, 20.9, 20.2, 20.0, 19.9, 19.1, 18.9, 18.5. **HRMS** (ESI, m/z) calculated for ([M+NH$_4$]$^+$) $C_{14}H_{22}O_2N^+$ 236.1645 found 236.1647.

Synthesis of bis–(4–methoxyphenyl methanol)–bullvalene 36
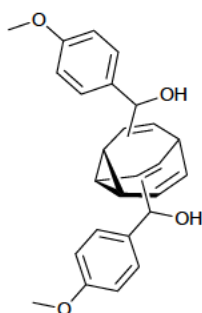
Under nitrogen atmosphere, an oven dried 5 mL round bottom flask was charged with 1–bromo–4–methoxybenzene (130 μL, 670 μmol, 2.50 eq) and anhydrous tetrahydrofuran (2 mL). The solution was cooled to – 78 °C in a bath of dry ice and acetone. *N*–butyllithium (270 μL, 2.50 M in cyclohexane, 670 μmol, 2.50 eq) was added slowly and the reaction stirred for 2 hours at – 78 °C. Dialdehyde–bullvalene **34** (50 mg, 270 μmol, 1.00 eq) was added and the reaction stirred for 1 h at – 78 °C and 3 h at room temperature. The reaction was

quenched with a saturated aqueous ammonium chloride solution and extracted with ethyl acetate. The organic layer was washed with water, then saturated aqueous sodium chloride solution, dried with $MgSO_4$, and filtered. The solvent was evaporated under vacuum and the desired was obtained after purification through column chromatography with hexane/ethyl acetate as eluents (9/1) (R_f = 0.25) (70 mg, 65% yield). **IR** (ATR): v/cm^{-1} = 3368, 3090, 3028, 2836, 1610, 1584, 1509, 1463, 1441, 1302, 1244, 1171, 1108, 1032, 907, 832, 727. **^{1}H NMR** (600 MHz, CDCl$_3$, – 60 °C) δ = 7.29 (3.0H, ap.d, J = 8.0 Hz), 7.24 – 7.07 (10.4H, m), 6.86 – 6.71 (14.4H, m), 6.06 (1.2H, brs), 5.89 (3.4H, brs), 5.82 – 5.67 (4.8H, m), 5.30 – 5.16 (3.4H, m), 5.00 – 4.78 (3.4H, m), 4.78 – 4.61 (3.6H, m), 3.81 – 3.69 (23.0H, m), 2.55 – 2.41 (2.0H, m), 2.27 (1H, ap.d, J = 9.1 Hz), 2.24 – 2.05 (8.7H, m). **^{13}C NMR** (150 MHz, CDCl$_3$, – 60 °C) δ = 158.2, 157.8, 157.6, 142.5, 142.3, 135.0, 132.8, 128.5, 128.3, 127.7, 126.9, 126.5, 123.9, 112.9, 112.8, 55.2, 55.2, 55.2, 55.2, 32.4, 31.8, 21.4, 19.6, 19.4, 19.1, 14.5, 14.1. **HRMS** (ESI, m/z) calculated for ([M+Na]$^+$) $C_{26}H_{26}O_4Na^+$ 425.1723 found 425.1710.

Synthesis of bis–(3,4–dimethoxyphenyl methanol)–bullvalene 37
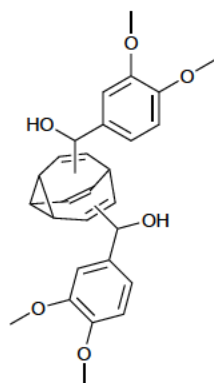
Under nitrogen atmosphere, an oven dried 5 mL round bottom flask was charged with dimethoxy 4–bromo–1,2–dimethoxybenzene (60 μL, 400 μmol, 2.50 eq) and anhydrous tetrahydrofuran (2 mL). The solution was cooled to – 78 °C in a bath of dry ice and acetone. N–butyllithium (160 μL, 2.50 M in cyclohexane, 400 μmol, 2.50 eq) was added slowly and the reaction stirred for 2 hours at – 78 °C. Dialdehyde–bullvalene **34** (30 mg, 160 μmol, 1.00 eq) was added and the reaction stirred for 1 h at – 78 °C and 3 h at room temperature. The reaction was quenched with saturated aqueous ammonium chloride solution and extracted with ethyl acetate. The organic layer was washed with water and a saturated aqueous sodium chloride solution. The solvent was evaporated under vacuum and the desired product was obtained after purification through column chromatography with hexane/ethyl acetate as eluents (8/2) (R_f = 0.23) (30 mg, 40% yield). **IR** (ATR): v/cm^{-1} = 3486, 2934, 2835, 1732, 1510, 1462, 1414, 1256, 1230, 1133, 1024, 864, 811, 745. **^{1}H NMR** (600 MHz, CDCl$_3$, – 60 °C) δ = 6.99 (1.0H, ap.d, J = 8.0 Hz), 6.91 – 6.64 (13.7H, m), 6.00 – 5.93 (1.3H, m), 5.88 (2.9H, brs), 5.81 – 5.74 (1.7H, m), 5.60 – 5.53 (1.2H, m), 5.29 (1.2H, ap.t, J = 9.9 Hz), 5.24 (0.9H, brs), 5.00 (1.7H, brs), 4.75 (1.0H, brs), 4.72 – 4.61 (1.8H, m), 3.92 – 3.69 (30.9H, m), 2.51 (1H, ap.d, J = 8.9 Hz), 2.24 – 2.18 (2.9H, m), 2.18 – 2.08 (3.7H, m). **^{13}C NMR**

(150 MHz, CDCl₃, – 60 °C) δ = 147.7, 147.6, 147.4, 147.4, 146.9, 146.7, 142.4, 142.0, 141.8, 135.5, 135.2, 132.9, 127.8, 127.1, 126.5, 124.3, 119.4, 117.5, 117.2, 109.6, 109.3, 108.4, 107.8, 55.8, 55.8, 55.7, 55.7, 55.6, 32.8, 28.1, 19.7, 19.5, 19.3. **HRMS** (ESI, m/z) calculated for ([M+Na]⁺) $C_{28}H_{30}O_6Na^+$ 485.1935 found 485.1923.

Synthesis of bis(TMS) dimethyl diester dibullvalene **32**
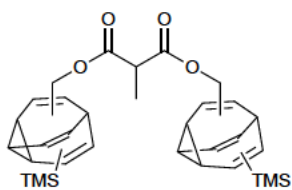
Under nitrogen atmosphere, an oven dried 5 mL round bottom flask was charged with 2–methylmalonic acid **46** (6 mg, 50 μmol, 0.50 eq), 4–dimethyl aminopyridine (3 mg, 20 μmol, 0.20 eq), N,N′– dicyclohexylcarbodiimide (22 mg, 110 μmol, 1.00 eq), and anhydrous dichloromethane (2 mL) with stirring for 30 min at 0 °C. **31** (25 mg, 110 μmol, 1.00 eq) was added and the reaction stirred at room temperature overnight. The suspension was passed through a pad of celite. The organic layer was washed three times with a 1M sodium hydroxide aqueous solution, and the solvent was evaporated under vacuum. The crude product was purified through column chromatography using hexane/ethyl acetate (5%) as eluents (R_f = 0.13). The desired product was obtained as yellow oil (20 mg, 34% yield). **IR** (ATR): v/cm^{-1} = 3026, 2953, 2925, 1735, 1608, 1459, 1377, 1342, 1246, 1175, 1081, 1042, 1005, 950, 833, 751, 690. **¹H NMR** (600 MHz, CDCl₃, – 60 °C) δ = 6.34 – 6.28 (1.0H, m), 6.26 (0.4H, m), 6.07 – 5.97 (1.3H, m), 5.97 – 5.75 (5.1H, m), 4.54 (0.5H, ap.t, J = 12.3 Hz), 4.45 (0.9H, ap.d, J = 12.0 Hz), 4.40 (0.3H, ap.d, J = 12.2 Hz), 4.35 (0.8H, ap.d, J = 12.0 Hz), 4.30 (0.2H, ap.d, J = 12.5 Hz), 3.07 (1H, brs), 2.47 (0.8H, ap.d, J = 8.6 Hz), 2.45 – 2.20 (8.1H, m), 1.96 (2.4H, brs), 1.72 (2.8H, brs), 1.63 – 1.54 (2.0H, m), 1.50 – 1.37 (2.3H, m), 1.33 – 0.99 (24.7H, m), 0.89 – 0.69 (7.0H, m), 0.10 – 0.01 (16.2H, m). **¹³C NMR** (150 MHz, CDCl₃, – 60 °C) δ = 177.7, 175.1, 172.9, 142.4, 135.7, 135.6, 135.0, 134.3, 132.8, 127.8, 127.5, 127.52, 127.2, 127.2, 127.0, 126.6, 126.1, 125.5, 70.0, 69.0, 56.0, 35.0, 34.2, 33.9, 33.8, 32.0, 31.7, 29.9, 29.6, 27.5, 27.4, 27.3, 26.1, 25.2, 25.1, 22.9, 22.1, 21.7, 20.7, 20.4, 20.4, 20.2, 20.1, 19.4, 19.3, 19.0, 14.5, 9.1, 9.1, 9.0, 0.1, –1.2, –1.9, –2.1, –2.2, –2.3, –2.3. **HRMS** (ESI, m/z) calculated for ([M+Na]⁺) $C_{32}H_{42}O_4Si_2Na^+$ 569.2514 found 569.2506.

NMR spectrum
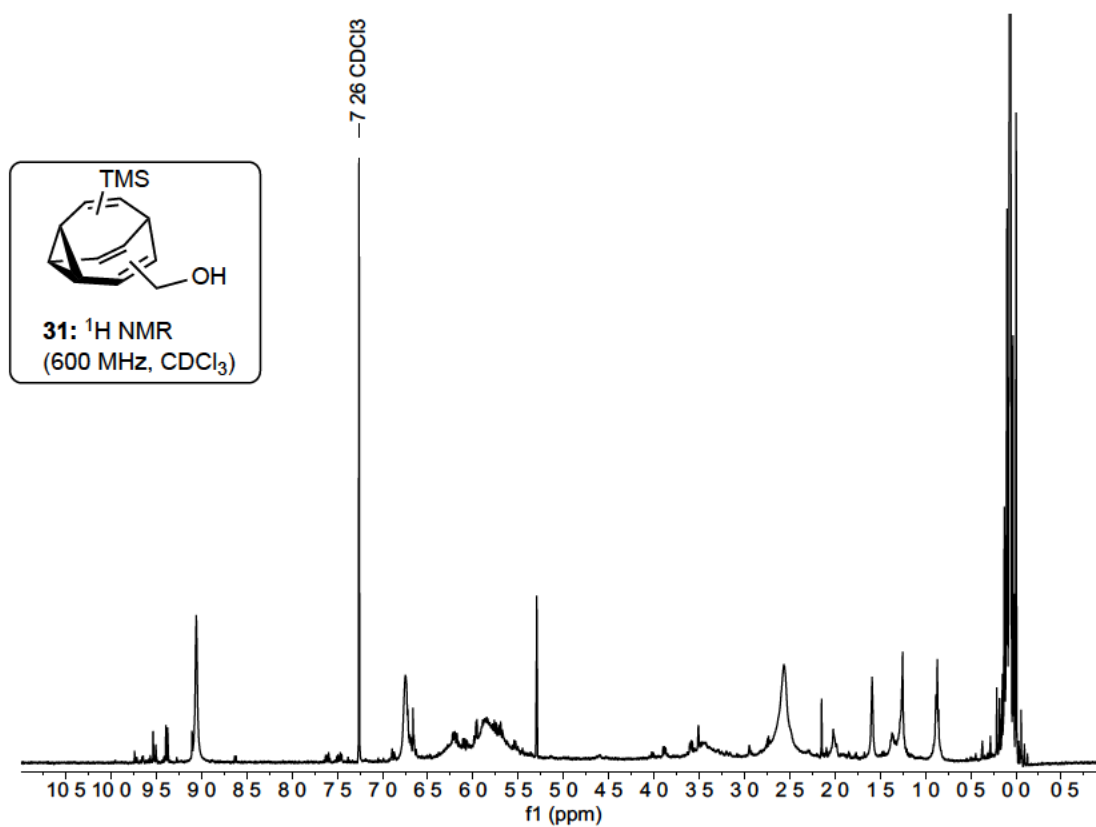
Figure S27: ¹H NMR of trimethylsilyl–aldehyde–bullvalene 32 at room temperature.
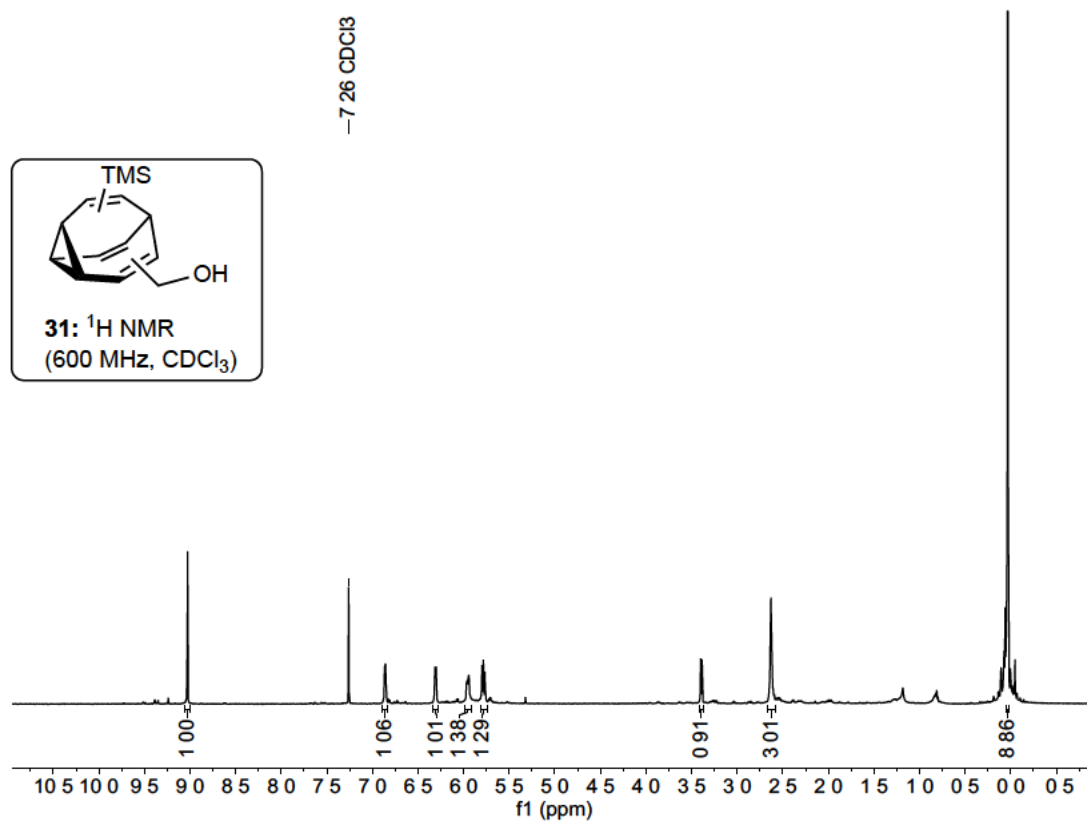
Figure S28: ¹H NMR of trimethylsilyl–aldehyde–bullvalene 32 at – 60 °C.
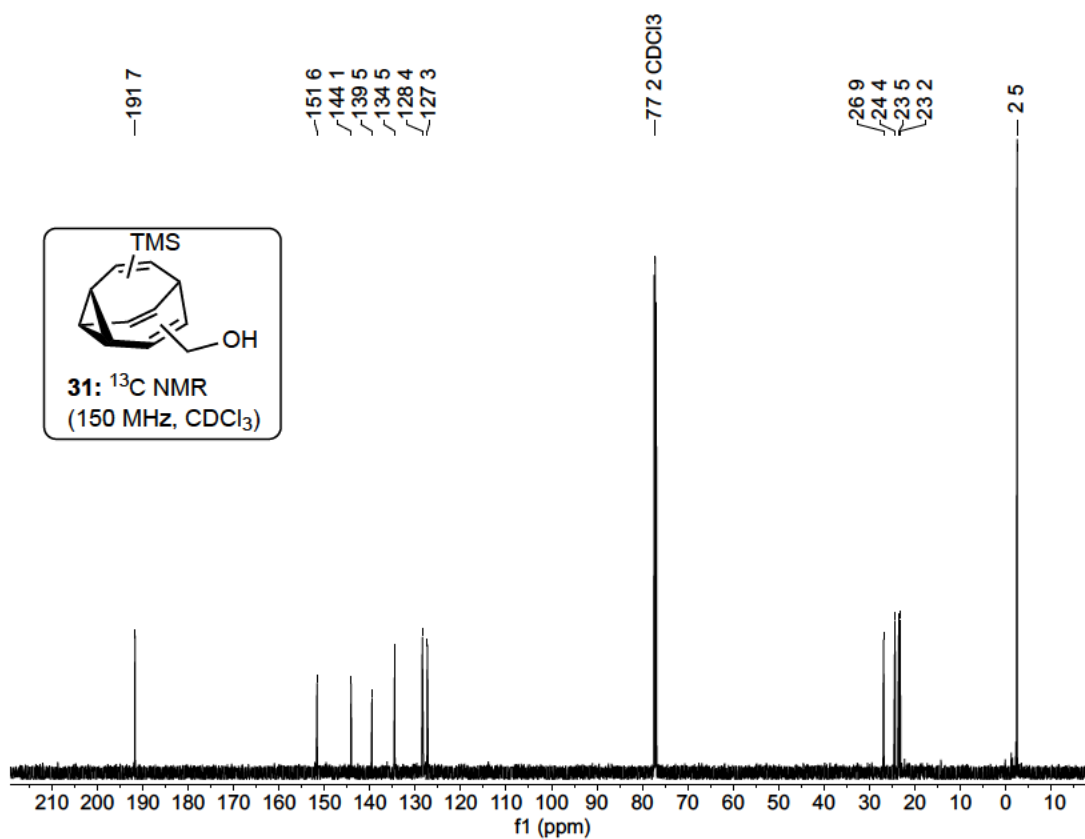
Figure S29: ^{13}C NMR of trimethylsilyl–aldehyde–bullvalene 32 at – 60 °C.
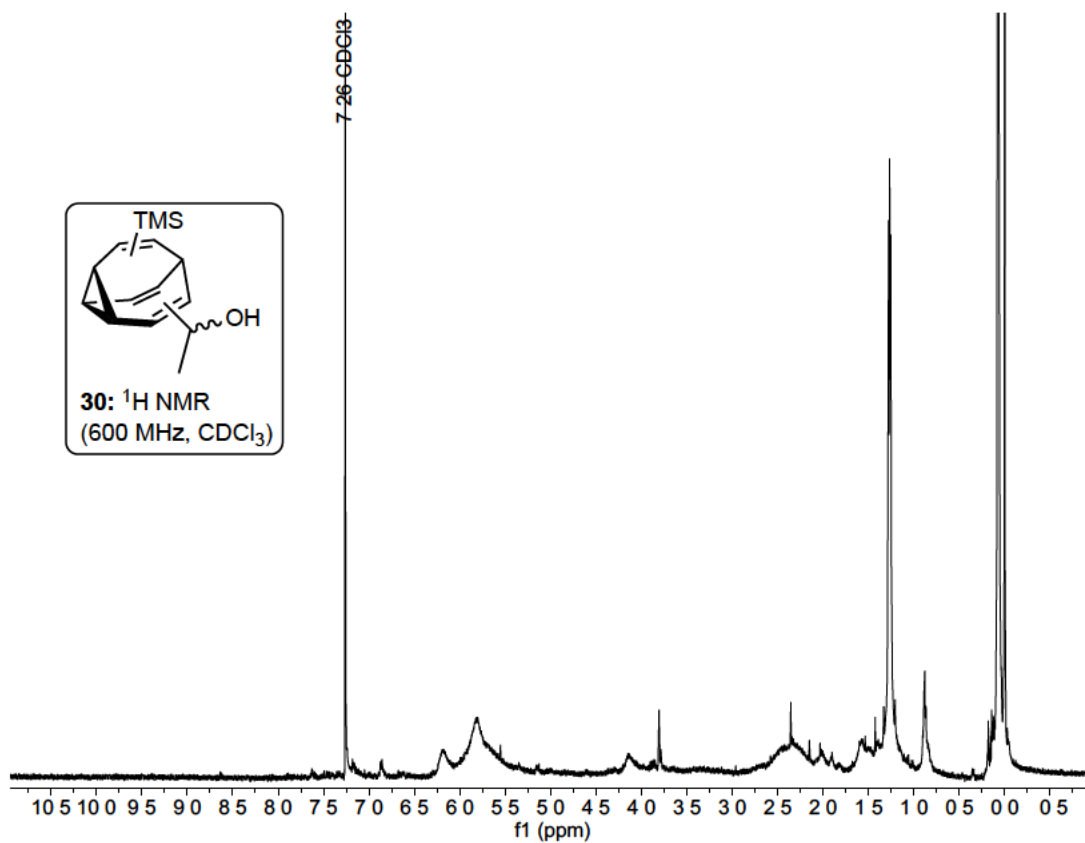
Figure S30: ^{1}H NMR methylhydroxy–TMS–bullvalene 30 at room temperature.
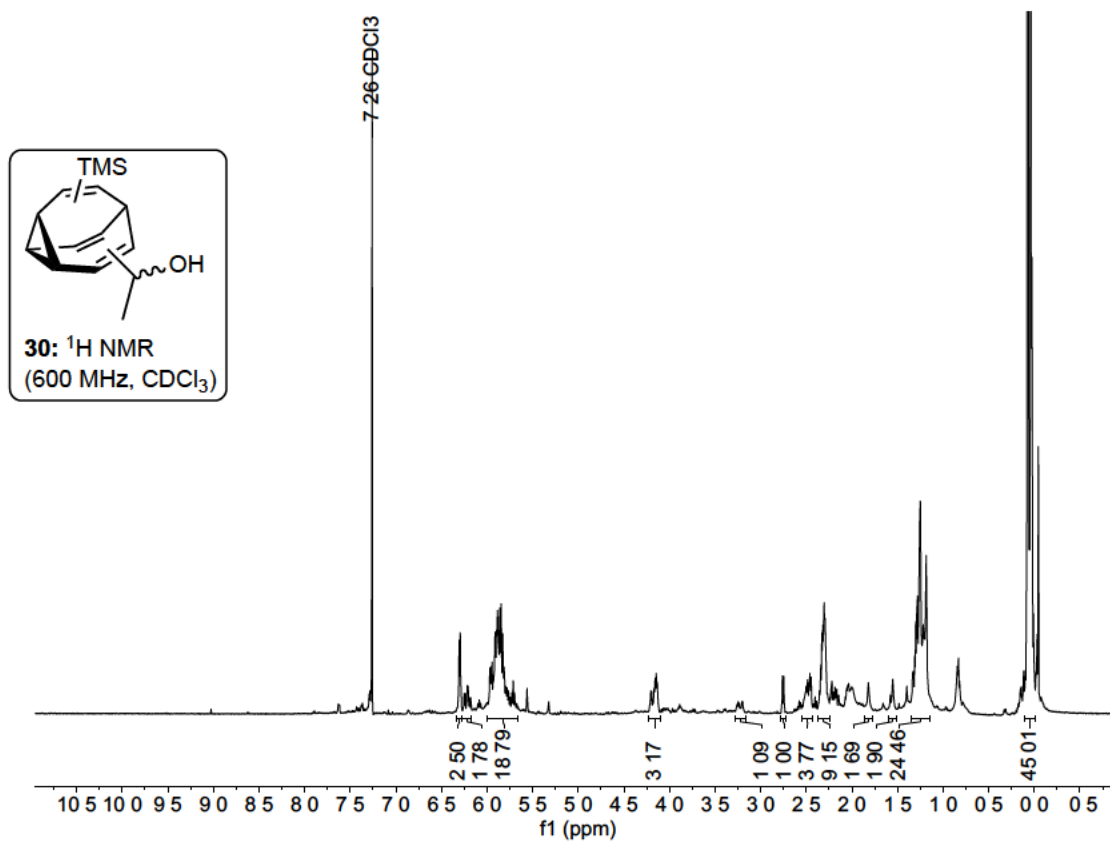
Figure S31: ^{1}H NMR of methylhydroxy–TMS–bullvalene 30 at – 60 °C.
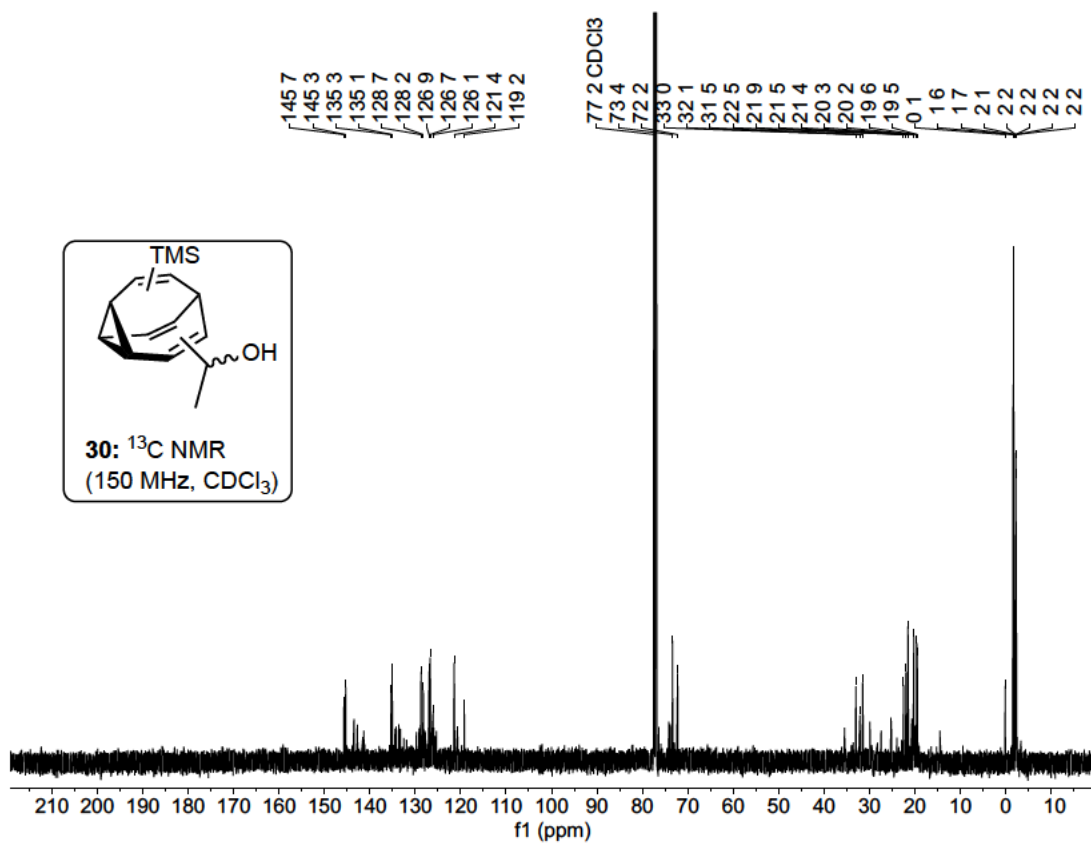
Figure S32: ^{13}C NMR of methylhydroxy–TMS–bullvalene 30 at – 60 °C.
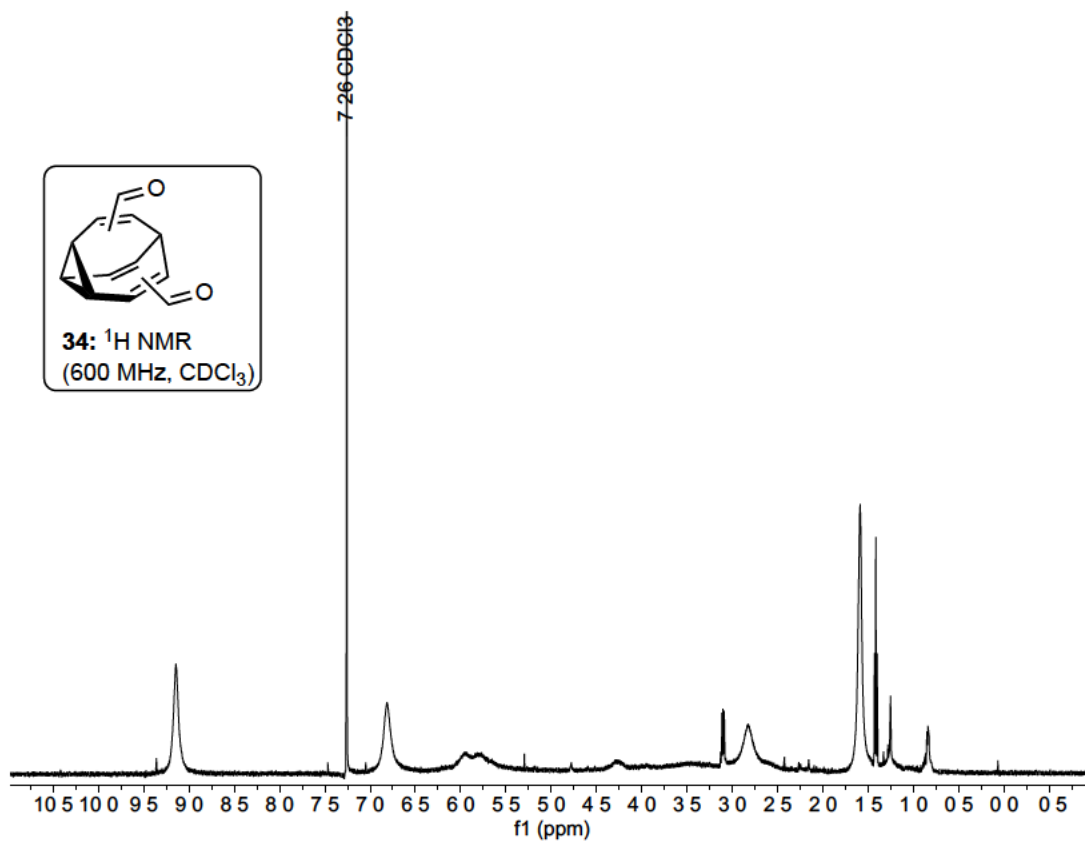
Figure S33: ^{1}H NMR of dialdehyde–bullvalene 34 at room temperature.
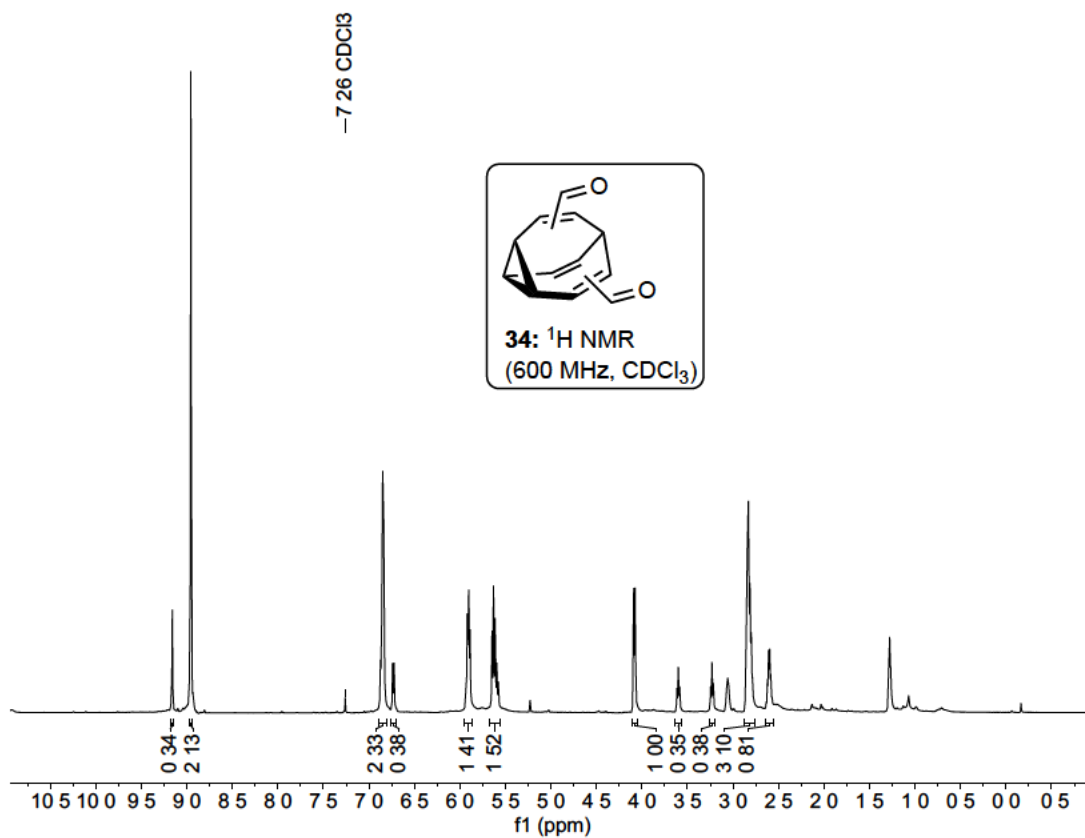
Figure S34: ^{1}H NMR of dialdehyde–bullvalene 34 at – 60 °C.
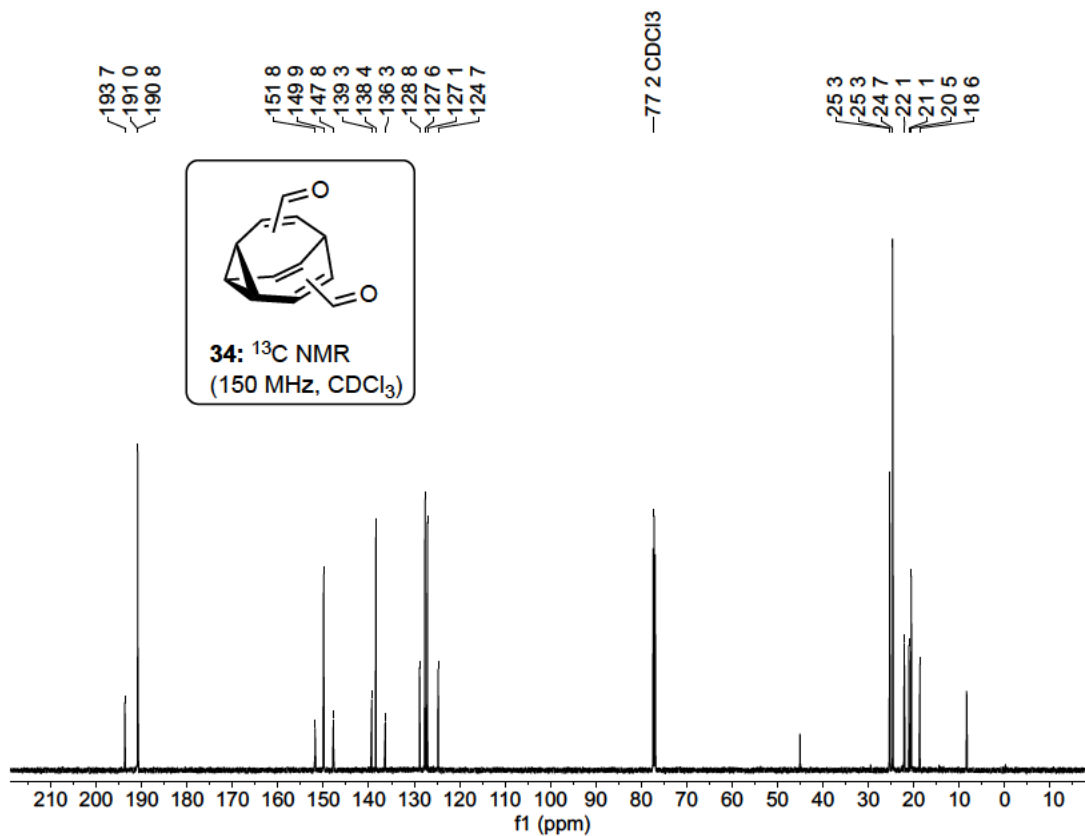
Figure S35: ^{13}C NMR of dialdehyde–bullvalene 34 at – 60 °C.
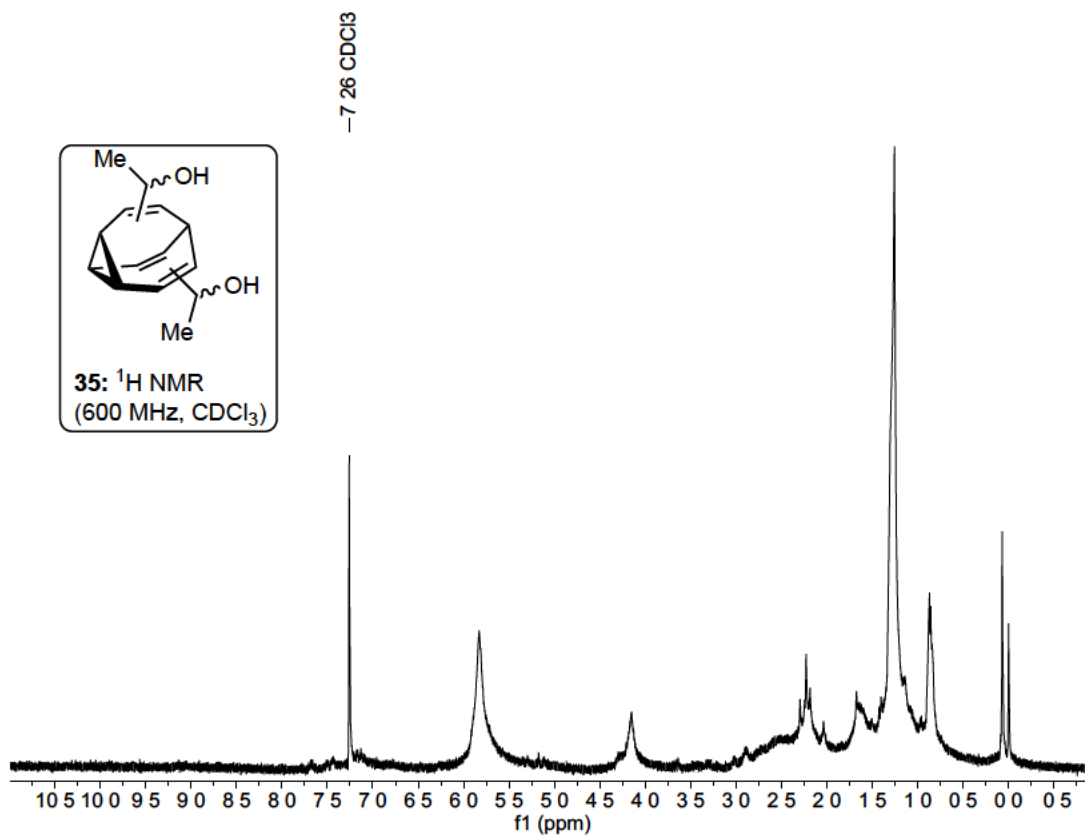
Figure S36: ^{1}H NMR bis(methylhydroxy) bullvalene 35 at room temperature.

−7 26 CDCl3

Me ∿ **OH**

∿ **OH**
Me

35: ¹H NMR
(600 MHz, CDCl₃)

19 81   1 70 6 04   1 00 1 67 10 61 1 09   28 84

105 100 95 90 85 80 75 70 65 60 55 50 45 40 35 30 25 20 15 10 05 00 05
f1 (ppm)
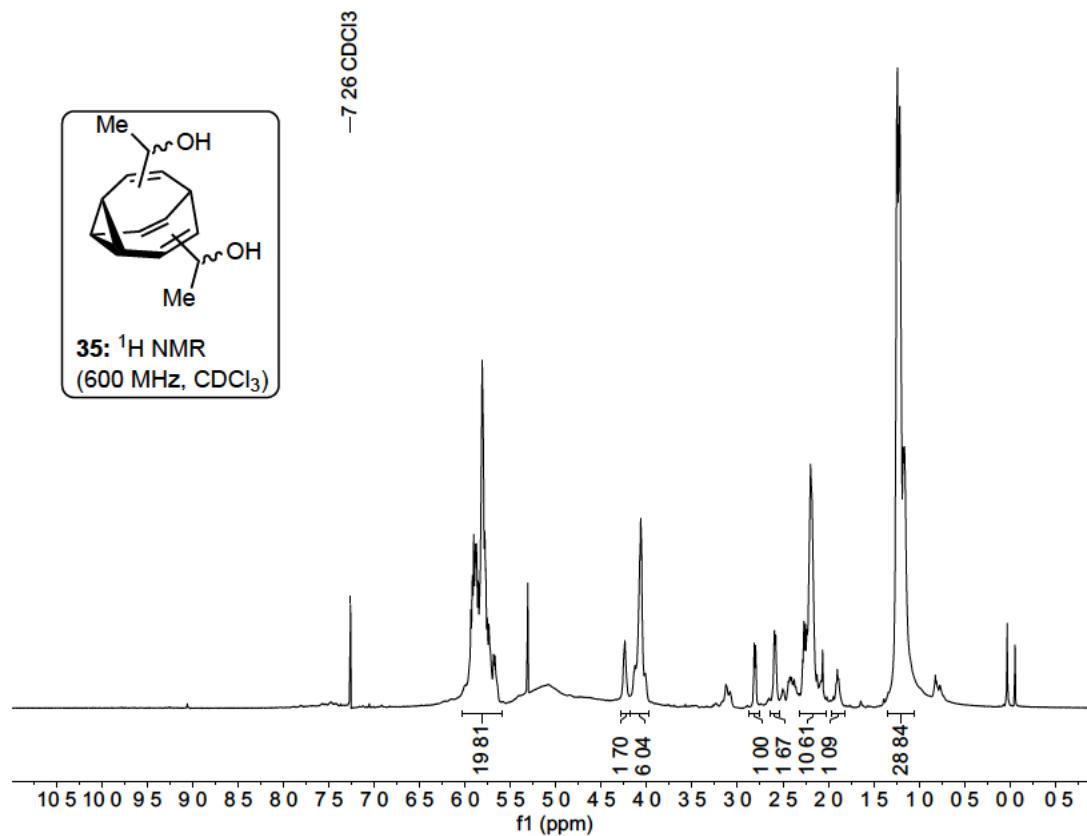
Figure S37: ¹H NMR of bis(methylhydroxy) bullvalene 35 at − 60 °C.

143 4
143 3
143 2
127 8
127 5
127 2
127 0
123 3
121 5

77 2 CDCl3
74 4
73 5
70 5

53 8
33 7
32 0
26 9
23 1
23 0
20 9
20 2
20 0
19 9
19 1
18 9
18 5

Me ∿ **OH**

∿ **OH**
Me

35: ¹³C NMR
(150 MHz, CDCl₃)

210 200 190 180 170 160 150 140 130 120 110 100 90 80 70 60 50 40 30 20 10 0 10
f1 (ppm)
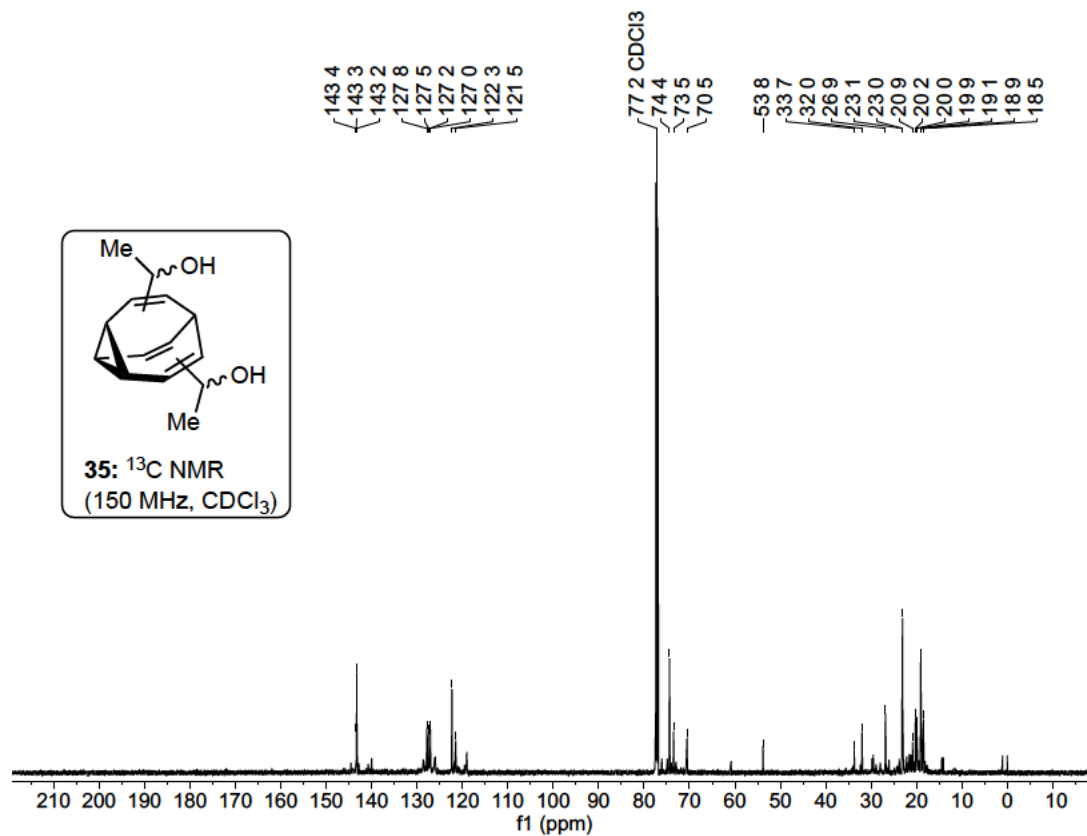
Figure S38: ¹³C NMR bis(methylhydroxy) bullvalene 35 − 60 °C.
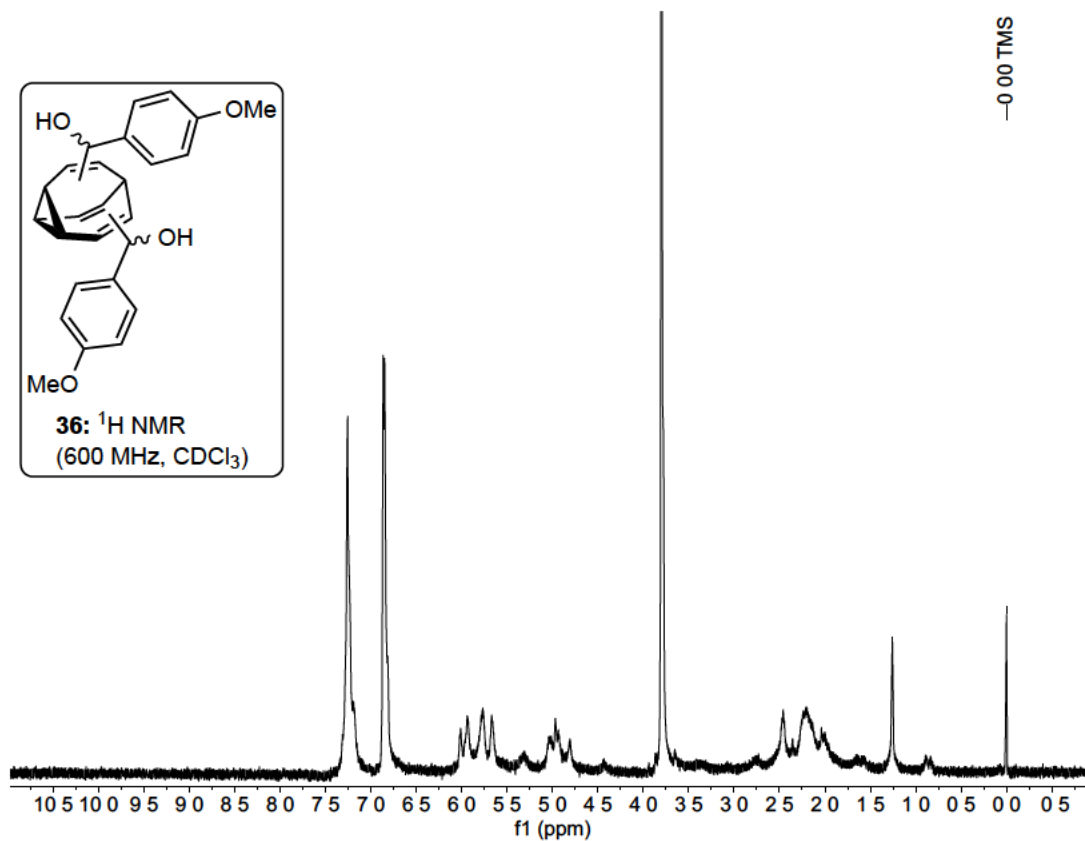
Figure S39: ¹H NMR of bis–(4–methoxyphenyl methanol)–bullvalene 36 at room temperature.
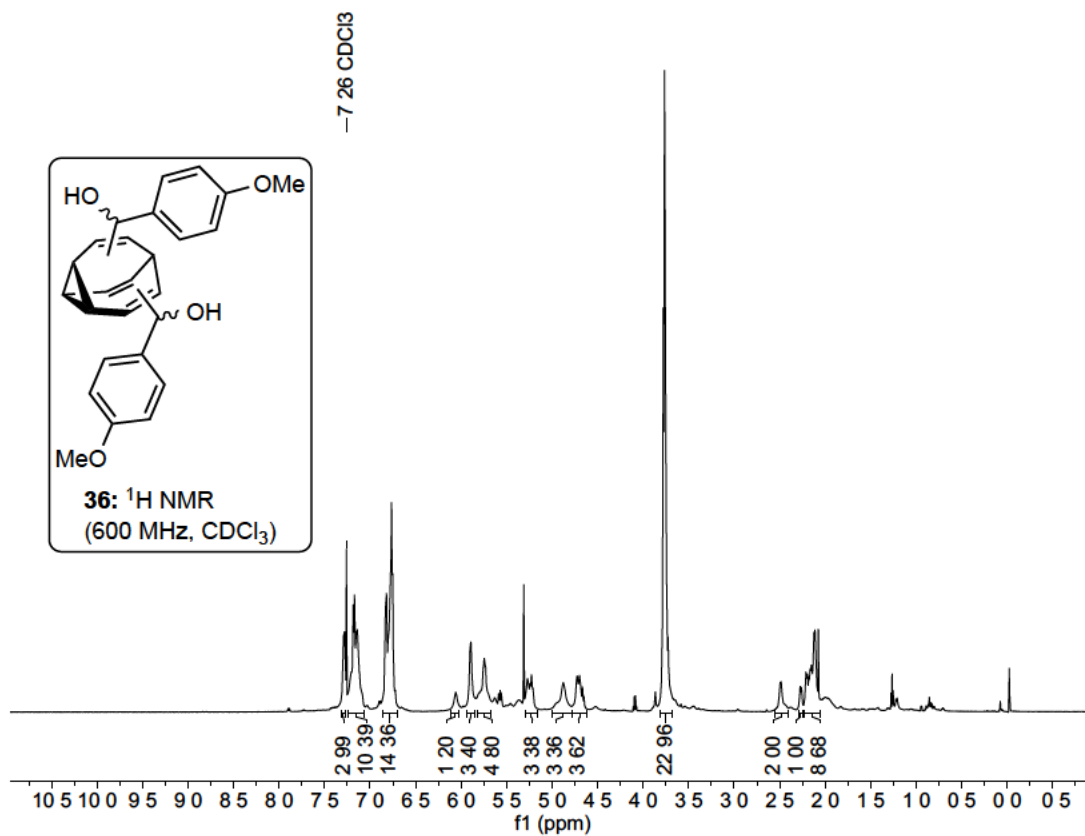
Figure S40: ¹H NMR of bis–(4–methoxyphenyl methanol)–bullvalene 36 at – 60 °C.
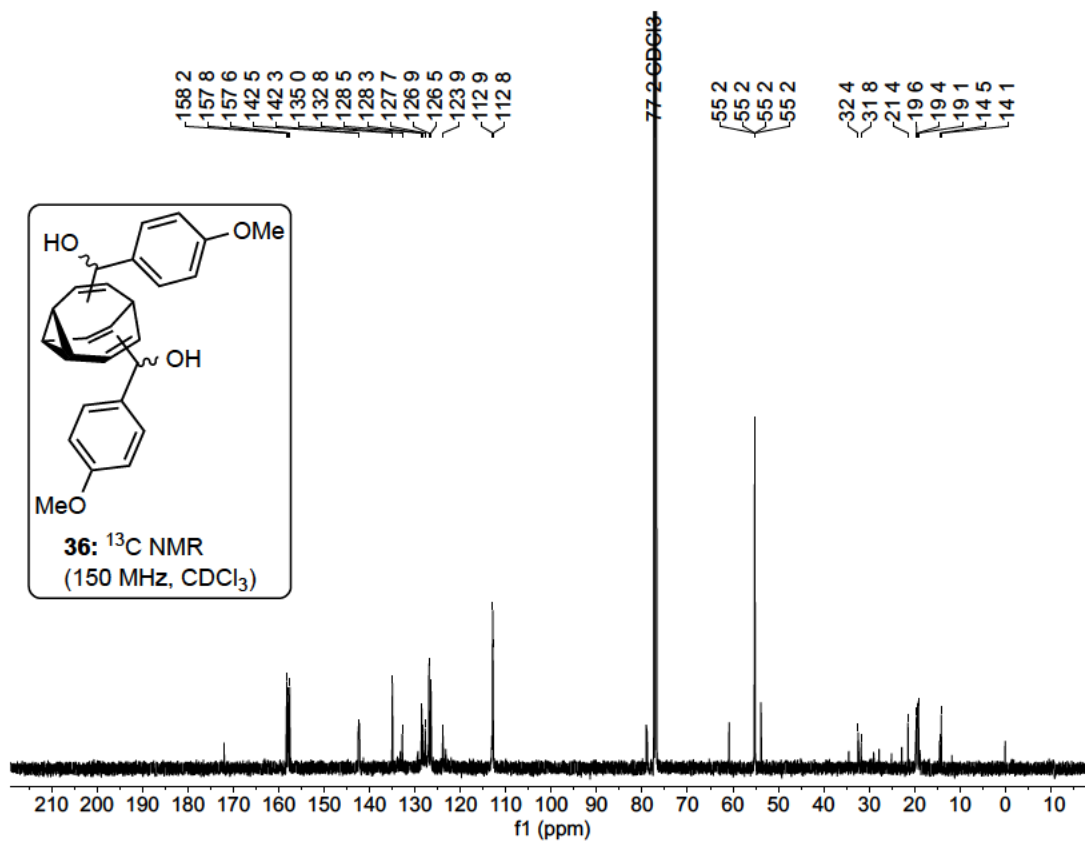
Figure S41: ^{13}C NMR of bis–(4–methoxyphenyl methanol)–bullvalene 36 at – 60 °C.
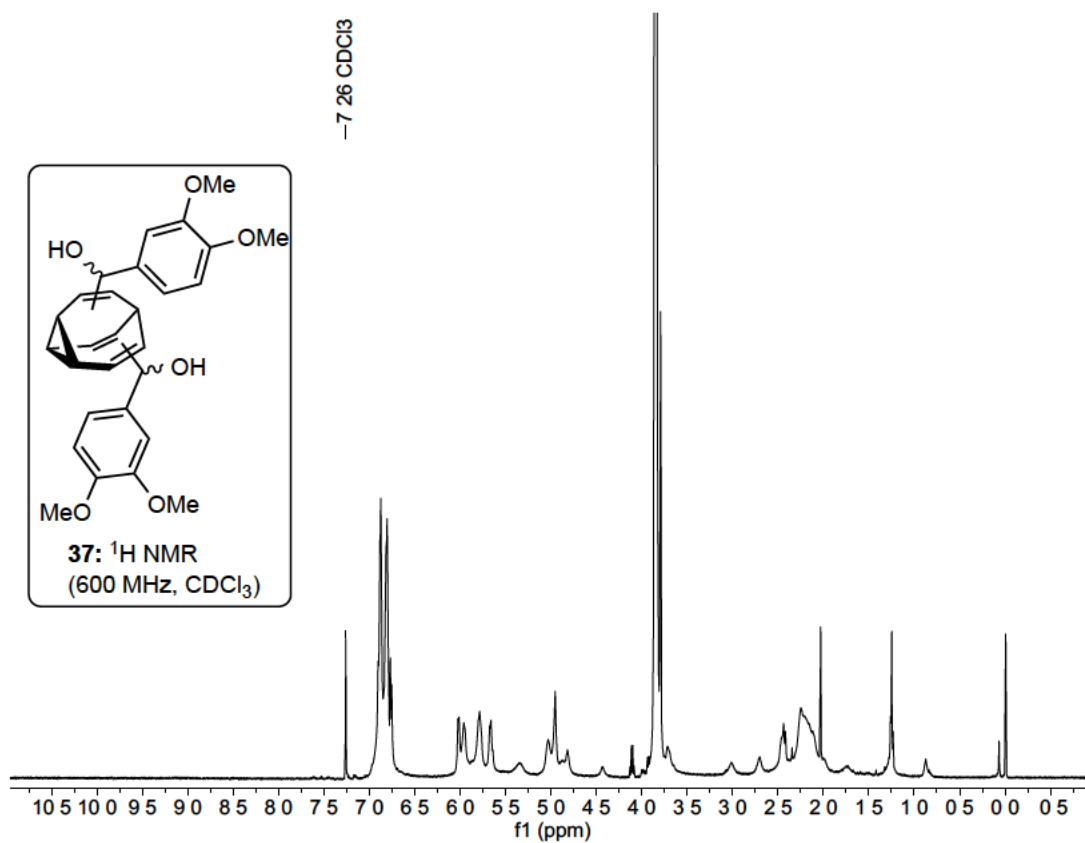
Figure S42: ^{1}H NMR of bis–(3,4–dimethoxyphenyl methanol)–bullvalene 37 at room temperature.
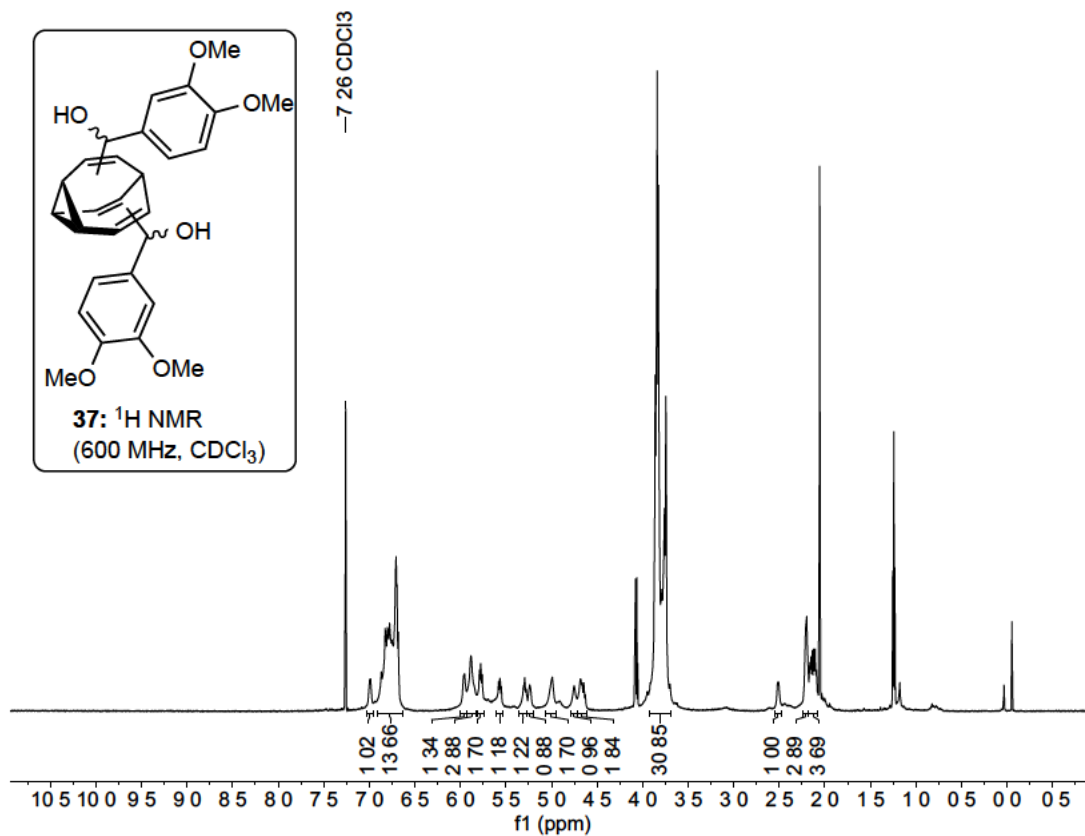
Figure S43: ^{1}H NMR of bis–(3,4–dimethoxyphenyl methanol)–bullvalene 37 at – 60 °C.
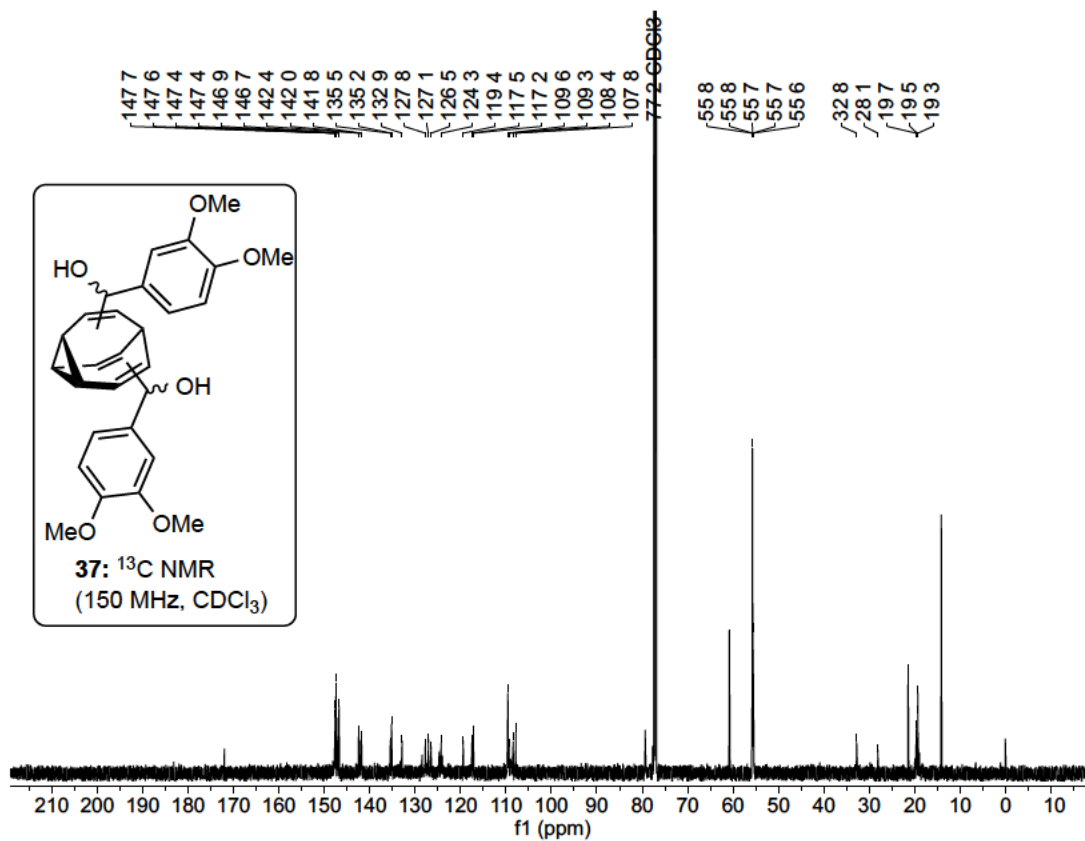
Figure S44: ^{13}C NMR of bis–(3,4–dimethoxyphenyl methanol)–bullvalene 37 at – 60 °C.
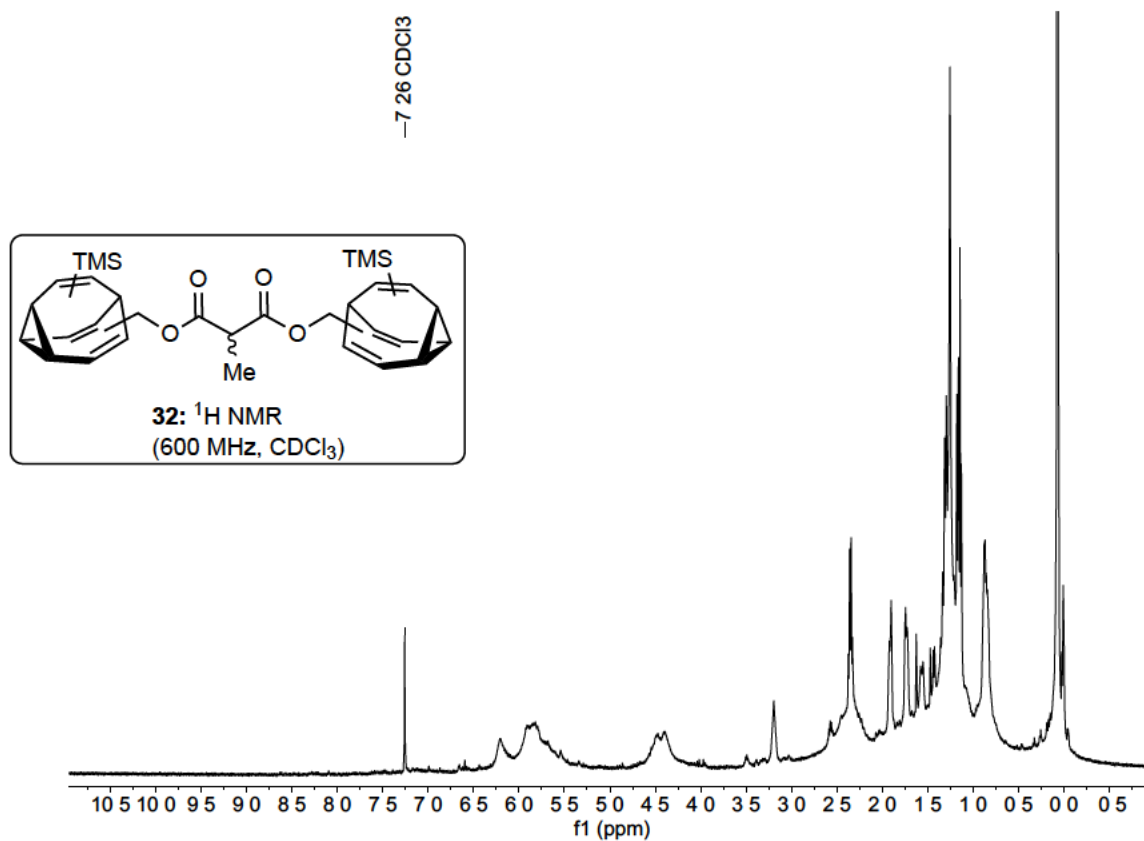
Figure S45: ^{1}H NMR of bis(TMS) methylmalonic diester dibullvalene 32 at room temperature.
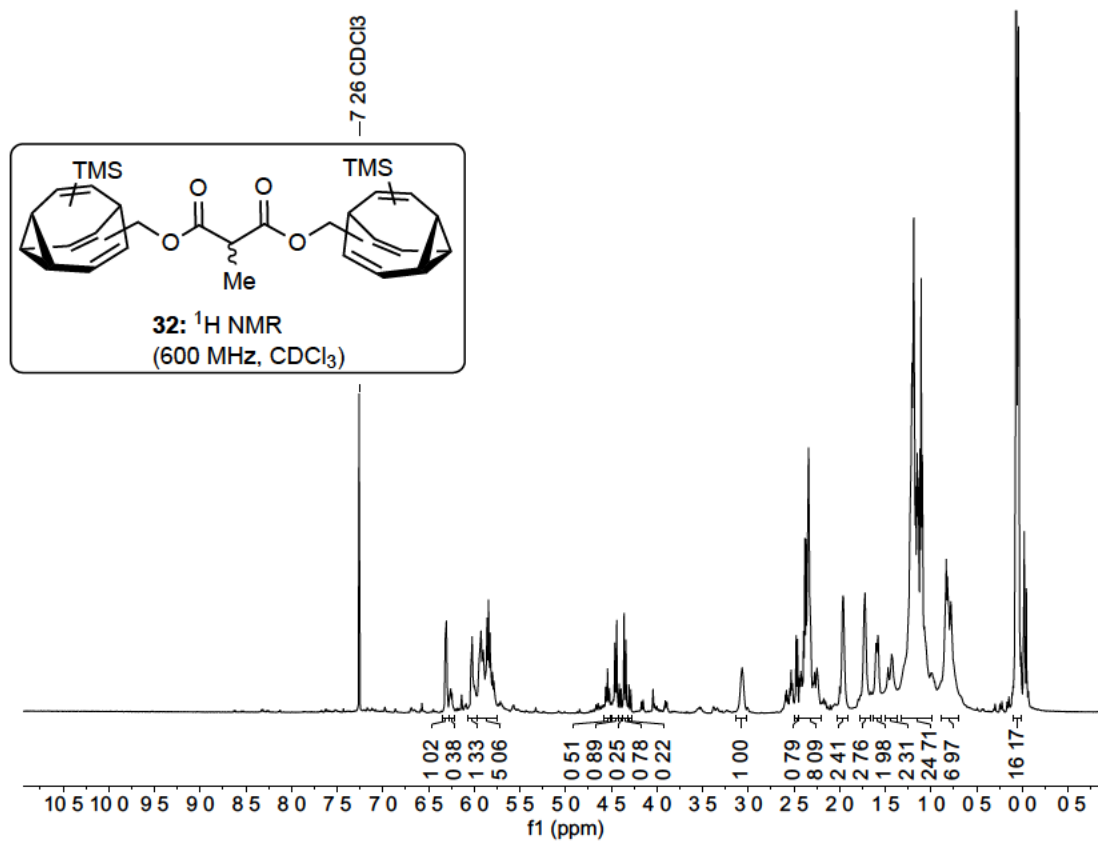
Figure S46: ^{1}H NMR of bis(TMS) methylmalonic diester dibullvalene 32 at − 60 °C.
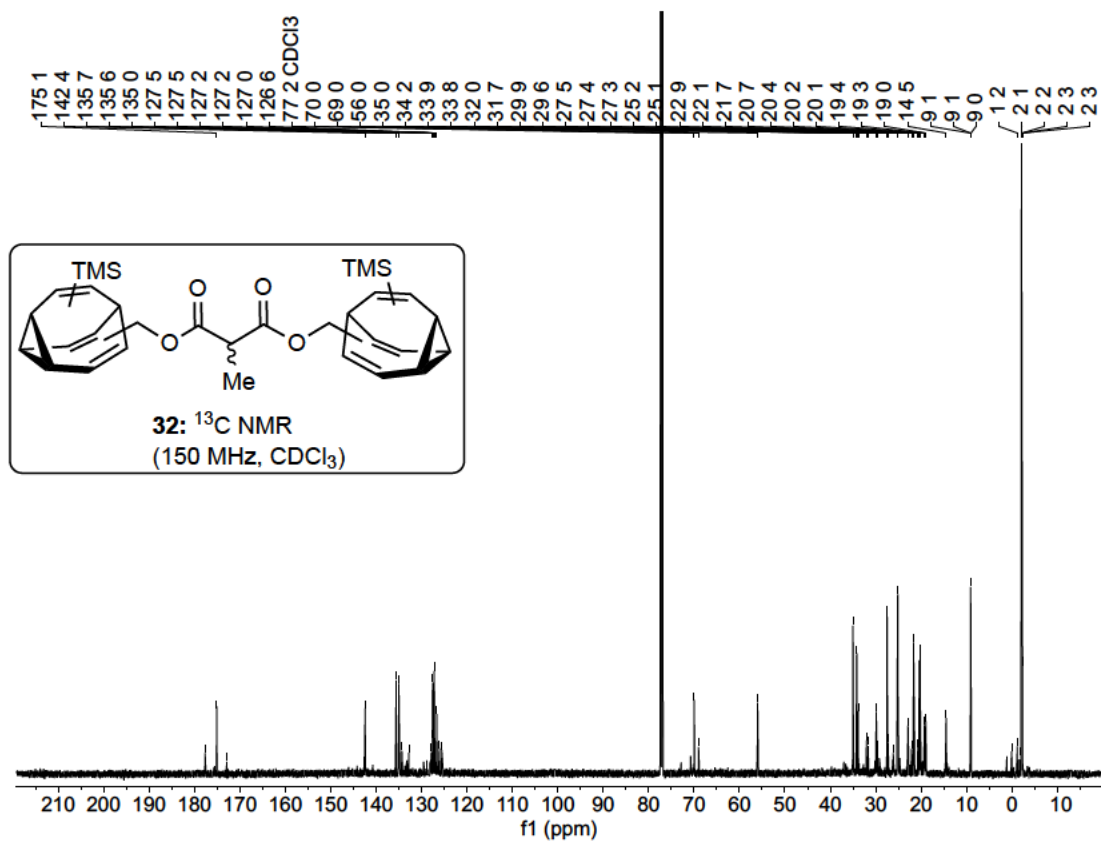
Figure S47: ¹³C NMR of bis(TMS) methylmalonic diester dibullvalene 32 at – 60 °C.
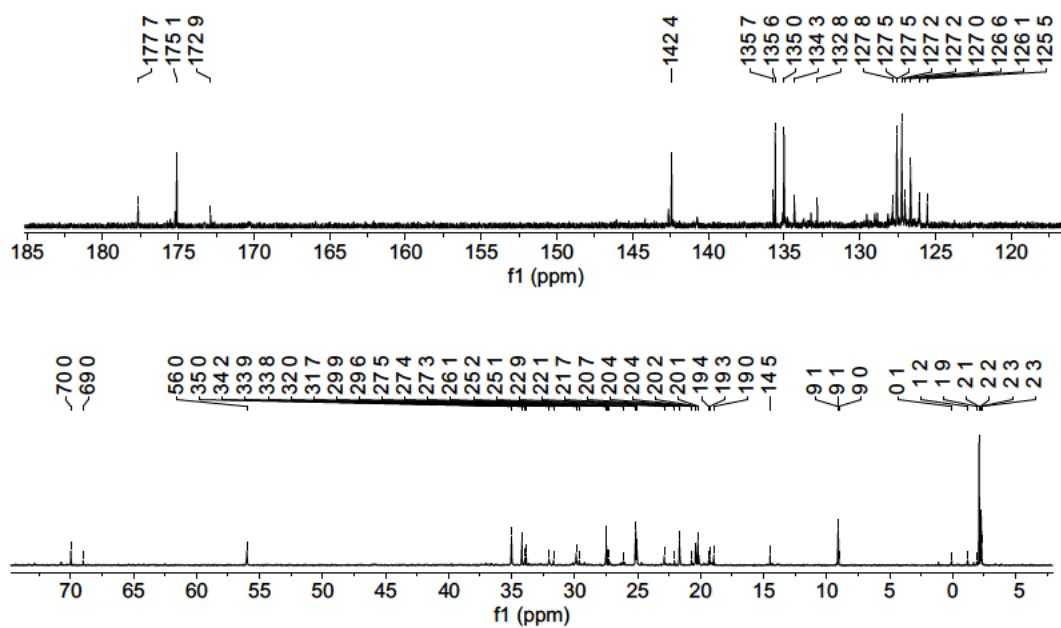
Figure S48: ¹³C NMR of bis(TMS) methylmalonic diester dibullvalene 32 at – 60 °C.

Table containing the configuration of the central stereocentre

Table 2: Configuration of the central stereocentre for isomer 1

helicity	isomer 1	chirality	isomer 1 – 30	helicity	ranking
P	000 200 100 0	**meso**	000 200 100 0	P	30
P	000 200 100 0	R	000 100 200 0	M	29
P	000 200 100 0	R	000 000 210 0	achiral	28
P	000 200 100 0	R	000 000 001 2	achiral	27
P	000 200 100 0	R	000 000 120 0	achiral	26
P	000 200 100 0	R	000 000 002 1	achiral	25
P	000 200 100 0	R	000 000 021 0	achiral	24
P	000 200 100 0	R	000 000 012 0	achiral	23
P	000 200 100 0	R	000 200 010 0	P	22
P	000 200 100 0	R	000 010 200 0	M	21
P	000 200 100 0	R	000 000 201 0	achiral	20
P	000 200 100 0	R	000 000 010 1	achiral	19
P	000 200 100 0	R	000 020 100 0	P	18
P	000 200 100 0	R	000 100 020 0	M	17
P	000 200 100 0	R	000 000 102 0	achiral	16
P	000 200 100 0	R	000 002 001 0	P	15
P	000 200 100 0	R	000 001 002 0	M	14
P	000 200 100 0	R	000 000 020 1	achiral	13
P	000 200 100 0	R	000 200 001 0	P	12
P	000 200 100 0	R	000 001 200 0	M	11
P	000 200 100 0	R	000 000 200 1	achiral	10
P	000 200 100 0	R	000 000 100 2	achiral	9
P	000 200 100 0	R	000 020 010 0	P	8
P	000 200 100 0	R	000 010 020 0	M	7
P	000 200 100 0	R	000 010 002 0	P	6
P	000 200 100 0	R	000 002 010 0	M	5
P	000 200 100 0	R	000 100 002 0	P	4
P	000 200 100 0	R	000 002 100 0	M	3
P	000 200 100 0	R	000 020 001 0	P	2
P	000 200 100 0	R	000 001 020 0	M	1

Table 3: Configuration of the central stereocentre for isomer 2

helicity	isomer 2	chirality	isomer 1 – 30	helicity	ranking
M	000 100 200 0	S	000 200 100 0	P	30
M	000 100 200 0	**meso**	000 100 200 0	M	29
M	000 100 200 0	R	000 000 210 0	achiral	28
M	000 100 200 0	R	000 000 001 2	achiral	27
M	000 100 200 0	R	000 000 120 0	achiral	26
M	000 100 200 0	R	000 000 002 1	achiral	25
M	000 100 200 0	R	000 000 021 0	achiral	24
M	000 100 200 0	R	000 000 012 0	achiral	23
M	000 100 200 0	R	000 200 010 0	P	22
M	000 100 200 0	R	000 010 200 0	M	21
M	000 100 200 0	R	000 000 201 0	achiral	20
M	000 100 200 0	R	000 000 010 1	achiral	19
M	000 100 200 0	R	000 020 100 0	P	18
M	000 100 200 0	R	000 100 020 0	M	17
M	000 100 200 0	R	000 000 102 0	achiral	16
M	000 100 200 0	R	000 002 001 0	P	15
M	000 100 200 0	R	000 001 002 0	M	14
M	000 100 200 0	R	000 000 020 1	achiral	13
M	000 100 200 0	R	000 200 001 0	P	12
M	000 100 200 0	R	000 001 200 0	M	11
M	000 100 200 0	R	000 000 200 1	achiral	10
M	000 100 200 0	R	000 000 100 2	achiral	9
M	000 100 200 0	R	000 020 010 0	P	8
M	000 100 200 0	R	000 010 020 0	M	7
M	000 100 200 0	R	000 010 002 0	P	6
M	000 100 200 0	R	000 002 010 0	M	5
M	000 100 200 0	R	000 100 002 0	P	4
M	000 100 200 0	R	000 002 100 0	M	3
M	000 100 200 0	R	000 020 001 0	P	2
M	000 100 200 0	R	000 001 020 0	M	1

Table 4: Configuration of the central stereocentre for isomer 3

helicity	isomer 3	chirality	isomer 1 – 30	helicity	ranking
achiral	000 000 210 0	S	000 200 100 0	P	30
achiral	000 000 210 0	S	000 100 200 0	M	29
achiral	000 000 210 0	**meso**	000 000 210 0	achiral	28
achiral	000 000 210 0	R	000 000 001 2	achiral	27
achiral	000 000 210 0	R	000 000 120 0	achiral	26
achiral	000 000 210 0	R	000 000 002 1	achiral	25
achiral	000 000 210 0	R	000 000 021 0	achiral	24
achiral	000 000 210 0	R	000 000 012 0	achiral	23
achiral	000 000 210 0	R	000 200 010 0	P	22
achiral	000 000 210 0	R	000 010 200 0	M	21
achiral	000 000 210 0	R	000 000 201 0	achiral	20
achiral	000 000 210 0	R	000 000 010 1	achiral	19
achiral	000 000 210 0	R	000 020 100 0	P	18
achiral	000 000 210 0	R	000 100 020 0	M	17
achiral	000 000 210 0	R	000 000 102 0	achiral	16
achiral	000 000 210 0	R	000 002 001 0	P	15
achiral	000 000 210 0	R	000 001 002 0	M	14
achiral	000 000 210 0	R	000 000 020 1	achiral	13
achiral	000 000 210 0	R	000 200 001 0	P	12
achiral	000 000 210 0	R	000 001 200 0	M	11
achiral	000 000 210 0	R	000 000 200 1	achiral	10
achiral	000 000 210 0	R	000 000 100 2	achiral	9
achiral	000 000 210 0	R	000 020 010 0	P	8
achiral	000 000 210 0	R	000 010 020 0	M	7
achiral	000 000 210 0	R	000 010 002 0	P	6
achiral	000 000 210 0	R	000 002 010 0	M	5
achiral	000 000 210 0	R	000 100 002 0	P	4
achiral	000 000 210 0	R	000 002 100 0	M	3
achiral	000 000 210 0	R	000 020 001 0	P	2
achiral	000 000 210 0	R	000 001 020 0	M	1

Table 5: Configuration of the central stereocentre for isomer 4

helicity	isomer 4	chirality	isomer 1 – 30	helicity	ranking

achiral	000 000 001 2	S	000 200 100 0	P	30
achiral	000 000 001 2	S	000 100 200 0	M	29
achiral	000 000 001 2	S	000 000 210 0	achiral	28
achiral	000 000 001 2	meso	000 000 001 2	achiral	27
achiral	000 000 001 2	R	000 000 120 0	achiral	26
achiral	000 000 001 2	R	000 000 002 1	achiral	25
achiral	000 000 001 2	R	000 000 021 0	achiral	24
achiral	000 000 001 2	R	000 000 012 0	achiral	23
achiral	000 000 001 2	R	000 200 010 0	P	22
achiral	000 000 001 2	R	000 010 200 0	M	21
achiral	000 000 001 2	R	000 000 201 0	achiral	20
achiral	000 000 001 2	R	000 000 010 1	achiral	19
achiral	000 000 001 2	R	000 020 100 0	P	18
achiral	000 000 001 2	R	000 100 020 0	M	17
achiral	000 000 001 2	R	000 000 102 0	achiral	16
achiral	000 000 001 2	R	000 002 001 0	P	15
achiral	000 000 001 2	R	000 001 002 0	M	14
achiral	000 000 001 2	R	000 000 020 1	achiral	13
achiral	000 000 001 2	R	000 200 001 0	P	12
achiral	000 000 001 2	R	000 001 200 0	M	11
achiral	000 000 001 2	R	000 000 200 1	achiral	10
achiral	000 000 001 2	R	000 000 100 2	achiral	9
achiral	000 000 001 2	R	000 020 010 0	P	8
achiral	000 000 001 2	R	000 010 020 0	M	7
achiral	000 000 001 2	R	000 010 002 0	P	6
achiral	000 000 001 2	R	000 002 010 0	M	5
achiral	000 000 001 2	R	000 100 002 0	P	4
achiral	000 000 001 2	R	000 002 100 0	M	3
achiral	000 000 001 2	R	000 020 001 0	P	2
achiral	000 000 001 2	R	000 001 020 0	M	1

Table 6: Configuration of the central stereocentre for isomer 5

helicity	isomer 5	chirality	isomer 1 – 30	helicity	ranking
achiral	000 000 120 0	S	000 200 100 0	P	30

achiral	000 000 120 0	S	000 100 200 0	M	29
achiral	000 000 120 0	S	000 000 210 0	achiral	28
achiral	000 000 120 0	S	000 000 001 2	achiral	27
achiral	000 000 120 0	meso	000 000 120 0	achiral	26
achiral	000 000 120 0	R	000 000 002 1	achiral	25
achiral	000 000 120 0	R	000 000 021 0	achiral	24
achiral	000 000 120 0	R	000 000 012 0	achiral	23
achiral	000 000 120 0	R	000 200 010 0	P	22
achiral	000 000 120 0	R	000 010 200 0	M	21
achiral	000 000 120 0	R	000 000 201 0	achiral	20
achiral	000 000 120 0	R	000 000 010 1	achiral	19
achiral	000 000 120 0	R	000 020 100 0	P	18
achiral	000 000 120 0	R	000 100 020 0	M	17
achiral	000 000 120 0	R	000 000 102 0	achiral	16
achiral	000 000 120 0	R	000 002 001 0	P	15
achiral	000 000 120 0	R	000 001 002 0	M	14
achiral	000 000 120 0	R	000 000 020 1	achiral	13
achiral	000 000 120 0	R	000 200 001 0	P	12
achiral	000 000 120 0	R	000 001 200 0	M	11
achiral	000 000 120 0	R	000 000 200 1	achiral	10
achiral	000 000 120 0	R	000 000 100 2	achiral	9
achiral	000 000 120 0	R	000 020 010 0	P	8
achiral	000 000 120 0	R	000 010 020 0	M	7
achiral	000 000 120 0	R	000 010 002 0	P	6
achiral	000 000 120 0	R	000 002 010 0	M	5
achiral	000 000 120 0	R	000 100 002 0	P	4
achiral	000 000 120 0	R	000 002 100 0	M	3
achiral	000 000 120 0	R	000 020 001 0	P	2
achiral	000 000 120 0	R	000 001 020 0	M	1

Table 7: Configuration of the central stereocentre for isomer 6

helicity	isomer 6	chirality	isomer 1 – 30	helicity	ranking
achiral	000 000 002 1	S	000 200 100 0	P	30
achiral	000 000 002 1	S	000 100 200 0	M	29

helicity		chirality		helicity	ranking
achiral	000 000 002 1	S	000 000 210 0	achiral	28
achiral	000 000 002 1	S	000 000 001 2	achiral	27
achiral	000 000 002 1	S	000 000 120 0	achiral	26
achiral	000 000 002 1	meso	000 000 002 1	achiral	25
achiral	000 000 002 1	R	000 000 021 0	achiral	24
achiral	000 000 002 1	R	000 000 012 0	achiral	23
achiral	000 000 002 1	R	000 200 010 0	P	22
achiral	000 000 002 1	R	000 010 200 0	M	21
achiral	000 000 002 1	R	000 000 201 0	achiral	20
achiral	000 000 002 1	R	000 000 010 1	achiral	19
achiral	000 000 002 1	R	000 020 100 0	P	18
achiral	000 000 002 1	R	000 100 020 0	M	17
achiral	000 000 002 1	R	000 000 102 0	achiral	16
achiral	000 000 002 1	R	000 002 001 0	P	15
achiral	000 000 002 1	R	000 001 002 0	M	14
achiral	000 000 002 1	R	000 000 020 1	achiral	13
achiral	000 000 002 1	R	000 200 001 0	P	12
achiral	000 000 002 1	R	000 001 200 0	M	11
achiral	000 000 002 1	R	000 000 200 1	achiral	10
achiral	000 000 002 1	R	000 000 100 2	achiral	9
achiral	000 000 002 1	R	000 020 010 0	P	8
achiral	000 000 002 1	R	000 010 020 0	M	7
achiral	000 000 002 1	R	000 010 002 0	P	6
achiral	000 000 002 1	R	000 002 010 0	M	5
achiral	000 000 002 1	R	000 100 002 0	P	4
achiral	000 000 002 1	R	000 002 100 0	M	3
achiral	000 000 002 1	R	000 020 001 0	P	2
achiral	000 000 002 1	R	000 001 020 0	M	1

Table 8: Configuration of the central stereocentre for isomer 7

helicity	isomer 7	chirality	isomer 1 – 30	helicity	ranking
achiral	000 000 021 0	S	000 200 100 0	P	30
achiral	000 000 021 0	S	000 100 200 0	M	29
achiral	000 000 021 0	S	000 000 210 0	achiral	28

achiral	000 000 021 0	S	000 000 001 2	achiral	27
achiral	000 000 021 0	S	000 000 120 0	achiral	26
achiral	000 000 021 0	S	000 000 002 1	achiral	25
achiral	000 000 021 0	meso	000 000 021 0	achiral	24
achiral	000 000 021 0	R	000 000 012 0	achiral	23
achiral	000 000 021 0	R	000 200 010 0	P	22
achiral	000 000 021 0	R	000 010 200 0	M	21
achiral	000 000 021 0	R	000 000 201 0	achiral	20
achiral	000 000 021 0	R	000 000 010 1	achiral	19
achiral	000 000 021 0	R	000 020 100 0	P	18
achiral	000 000 021 0	R	000 100 020 0	M	17
achiral	000 000 021 0	R	000 000 102 0	achiral	16
achiral	000 000 021 0	R	000 002 001 0	P	15
achiral	000 000 021 0	R	000 001 002 0	M	14
achiral	000 000 021 0	R	000 000 020 1	achiral	13
achiral	000 000 021 0	R	000 200 001 0	P	12
achiral	000 000 021 0	R	000 001 200 0	M	11
achiral	000 000 021 0	R	000 000 200 1	achiral	10
achiral	000 000 021 0	R	000 000 100 2	achiral	9
achiral	000 000 021 0	R	000 020 010 0	P	8
achiral	000 000 021 0	R	000 010 020 0	M	7
achiral	000 000 021 0	R	000 010 002 0	P	6
achiral	000 000 021 0	R	000 002 010 0	M	5
achiral	000 000 021 0	R	000 100 002 0	P	4
achiral	000 000 021 0	R	000 002 100 0	M	3
achiral	000 000 021 0	R	000 020 001 0	P	2
achiral	000 000 021 0	R	000 001 020 0	M	1

Table 9: Configuration of the central stereocentre for isomer 8

helicity	isomer 8	chirality	isomer 1 – 30	helicity	ranking
achiral	000 000 012 0	S	000 200 100 0	P	30
achiral	000 000 012 0	S	000 100 200 0	M	29
achiral	000 000 012 0	S	000 000 210 0	achiral	28
achiral	000 000 012 0	S	000 000 001 2	achiral	27

achiral	000 000 012 0	S	000 000 120 0	achiral	26
achiral	000 000 012 0	S	000 000 002 1	achiral	25
achiral	000 000 012 0	S	000 000 021 0	achiral	24
achiral	000 000 012 0	meso	000 000 012 0	achiral	23
achiral	000 000 012 0	R	000 200 010 0	P	22
achiral	000 000 012 0	R	000 010 200 0	M	21
achiral	000 000 012 0	R	000 000 201 0	achiral	20
achiral	000 000 012 0	R	000 000 010 1	achiral	19
achiral	000 000 012 0	R	000 020 100 0	P	18
achiral	000 000 012 0	R	000 100 020 0	M	17
achiral	000 000 012 0	R	000 000 102 0	achiral	16
achiral	000 000 012 0	R	000 002 001 0	P	15
achiral	000 000 012 0	R	000 001 002 0	M	14
achiral	000 000 012 0	R	000 000 020 1	achiral	13
achiral	000 000 012 0	R	000 200 001 0	P	12
achiral	000 000 012 0	R	000 001 200 0	M	11
achiral	000 000 012 0	R	000 000 200 1	achiral	10
achiral	000 000 012 0	R	000 000 100 2	achiral	9
achiral	000 000 012 0	R	000 020 010 0	P	8
achiral	000 000 012 0	R	000 010 020 0	M	7
achiral	000 000 012 0	R	000 010 002 0	P	6
achiral	000 000 012 0	R	000 002 010 0	M	5
achiral	000 000 012 0	R	000 100 002 0	P	4
achiral	000 000 012 0	R	000 002 100 0	M	3
achiral	000 000 012 0	R	000 020 001 0	P	2
achiral	000 000 012 0	R	000 001 020 0	M	1

Table 10: Configuration of the central stereocentre for isomer 9

helicity	isomer 9	chirality	isomer 1 – 30	helicity	ranking
P	000 200 010 0	S	000 200 100 0	P	30
P	000 200 010 0	S	000 100 200 0	M	29
P	000 200 010 0	S	000 000 210 0	achiral	28
P	000 200 010 0	S	000 000 001 2	achiral	27
P	000 200 010 0	S	000 000 120 0	achiral	26

P	000 200 010 0	S	000 000 002 1	achiral	25
P	000 200 010 0	S	000 000 021 0	achiral	24
P	000 200 010 0	S	000 000 012 0	achiral	23
P	000 200 010 0	meso	000 200 010 0	P	22
P	000 200 010 0	R	000 010 200 0	M	21
P	000 200 010 0	R	000 000 201 0	achiral	20
P	000 200 010 0	R	000 000 010 1	achiral	19
P	000 200 010 0	R	000 020 100 0	P	18
P	000 200 010 0	R	000 100 020 0	M	17
P	000 200 010 0	R	000 000 102 0	achiral	16
P	000 200 010 0	R	000 002 001 0	P	15
P	000 200 010 0	R	000 001 002 0	M	14
P	000 200 010 0	R	000 000 020 1	achiral	13
P	000 200 010 0	R	000 200 001 0	P	12
P	000 200 010 0	R	000 001 200 0	M	11
P	000 200 010 0	R	000 000 200 1	achiral	10
P	000 200 010 0	R	000 000 100 2	achiral	9
P	000 200 010 0	R	000 020 010 0	P	8
P	000 200 010 0	R	000 010 020 0	M	7
P	000 200 010 0	R	000 010 002 0	P	6
P	000 200 010 0	R	000 002 010 0	M	5
P	000 200 010 0	R	000 100 002 0	P	4
P	000 200 010 0	R	000 002 100 0	M	3
P	000 200 010 0	R	000 020 001 0	P	2
P	000 200 010 0	R	000 001 020 0	M	1

Table 11: Configuration of the central stereocentre for isomer 10

helicity	isomer 10	chirality	isomer 1 – 30	helicity	ranking
M	000 010 200 0	S	000 200 100 0	P	30
M	000 010 200 0	S	000 100 200 0	M	29
M	000 010 200 0	S	000 000 210 0	achiral	28
M	000 010 200 0	S	000 000 001 2	achiral	27
M	000 010 200 0	S	000 000 120 0	achiral	26

M	000 010 200 0	S	000 000 002 1	achiral	25
M	000 010 200 0	S	000 000 021 0	achiral	24
M	000 010 200 0	S	000 000 012 0	achiral	23
M	000 010 200 0	S	000 200 010 0	P	22
M	000 010 200 0	meso	000 010 200 0	M	21
M	000 010 200 0	R	000 000 201 0	achiral	20
M	000 010 200 0	R	000 000 010 1	achiral	19
M	000 010 200 0	R	000 020 100 0	P	18
M	000 010 200 0	R	000 100 020 0	M	17
M	000 010 200 0	R	000 000 102 0	achiral	16
M	000 010 200 0	R	000 002 001 0	P	15
M	000 010 200 0	R	000 001 002 0	M	14
M	000 010 200 0	R	000 000 020 1	achiral	13
M	000 010 200 0	R	000 200 001 0	P	12
M	000 010 200 0	R	000 001 200 0	M	11
M	000 010 200 0	R	000 000 200 1	achiral	10
M	000 010 200 0	R	000 000 100 2	achiral	9
M	000 010 200 0	R	000 020 010 0	P	8
M	000 010 200 0	R	000 010 020 0	M	7
M	000 010 200 0	R	000 010 002 0	P	6
M	000 010 200 0	R	000 002 010 0	M	5
M	000 010 200 0	R	000 100 002 0	P	4
M	000 010 200 0	R	000 002 100 0	M	3
M	000 010 200 0	R	000 020 001 0	P	2
M	000 010 200 0	R	000 001 020 0	M	1

Table 12: Configuration of the central stereocentre for isomer 11

helicity	isomer 11	chirality	isomer 1 – 30	helicity	ranking
achiral	000 000 201 0	S	000 200 100 0	P	30
achiral	000 000 201 0	S	000 100 200 0	M	29
achiral	000 000 201 0	S	000 000 210 0	achiral	28
achiral	000 000 201 0	S	000 000 001 2	achiral	27
achiral	000 000 201 0	S	000 000 120 0	achiral	26
achiral	000 000 201 0	S	000 000 002 1	achiral	25

achiral	000 000 201 0	S	000 000 021 0	achiral	24
achiral	000 000 201 0	S	000 000 012 0	achiral	23
achiral	000 000 201 0	S	000 200 010 0	P	22
achiral	000 000 201 0	S	000 010 200 0	M	21
achiral	000 000 201 0	meso	000 000 201 0	achiral	20
achiral	000 000 201 0	R	000 000 010 1	achiral	19
achiral	000 000 201 0	R	000 020 100 0	P	18
achiral	000 000 201 0	R	000 100 020 0	M	17
achiral	000 000 201 0	R	000 000 102 0	achiral	16
achiral	000 000 201 0	R	000 002 001 0	P	15
achiral	000 000 201 0	R	000 001 002 0	M	14
achiral	000 000 201 0	R	000 000 020 1	achiral	13
achiral	000 000 201 0	R	000 200 001 0	P	12
achiral	000 000 201 0	R	000 001 200 0	M	11
achiral	000 000 201 0	R	000 000 200 1	achiral	10
achiral	000 000 201 0	R	000 000 100 2	achiral	9
achiral	000 000 201 0	R	000 020 010 0	P	8
achiral	000 000 201 0	R	000 010 020 0	M	7
achiral	000 000 201 0	R	000 010 002 0	P	6
achiral	000 000 201 0	R	000 002 010 0	M	5
achiral	000 000 201 0	R	000 100 002 0	P	4
achiral	000 000 201 0	R	000 002 100 0	M	3
achiral	000 000 201 0	R	000 020 001 0	P	2
achiral	000 000 201 0	R	000 001 020 0	M	1

Table 13: Configuration of the central stereocentre for isomer 12

helicity	isomer 12	chirality	isomer 1 – 30	helicity	ranking
achiral	000 000 010 1	S	000 200 100 0	P	30
achiral	000 000 010 1	S	000 100 200 0	M	29
achiral	000 000 010 1	S	000 000 210 0	achiral	28
achiral	000 000 010 1	S	000 000 001 2	achiral	27
achiral	000 000 010 1	S	000 000 120 0	achiral	26
achiral	000 000 010 1	S	000 000 002 1	achiral	25
achiral	000 000 010 1	S	000 000 021 0	achiral	24

achiral	000 000 010 1	S	000 000 012 0	achiral	23
achiral	000 000 010 1	S	000 200 010 0	P	22
achiral	000 000 010 1	S	000 010 200 0	M	21
achiral	000 000 010 1	S	000 000 201 0	achiral	20
achiral	000 000 010 1	meso	000 000 010 1	achiral	19
achiral	000 000 010 1	R	000 020 100 0	P	18
achiral	000 000 010 1	R	000 100 020 0	M	17
achiral	000 000 010 1	R	000 000 102 0	achiral	16
achiral	000 000 010 1	R	000 002 001 0	P	15
achiral	000 000 010 1	R	000 001 002 0	M	14
achiral	000 000 010 1	R	000 000 020 1	achiral	13
achiral	000 000 010 1	R	000 200 001 0	P	12
achiral	000 000 010 1	R	000 001 200 0	M	11
achiral	000 000 010 1	R	000 000 200 1	achiral	10
achiral	000 000 010 1	R	000 000 100 2	achiral	9
achiral	000 000 010 1	R	000 020 010 0	P	8
achiral	000 000 010 1	R	000 010 020 0	M	7
achiral	000 000 010 1	R	000 010 002 0	P	6
achiral	000 000 010 1	R	000 002 010 0	M	5
achiral	000 000 010 1	R	000 100 002 0	P	4
achiral	000 000 010 1	R	000 002 100 0	M	3
achiral	000 000 010 1	R	000 020 001 0	P	2
achiral	000 000 010 1	R	000 001 020 0	M	1

Table 14: Configuration of the central stereocentre for isomer 13

helicity	isomer 13	chirality	isomer 1 – 30	helicity	ranking
P	000 020 100 0	S	000 200 100 0	P	30
P	000 020 100 0	S	000 100 200 0	M	29
P	000 020 100 0	S	000 000 210 0	achiral	28
P	000 020 100 0	S	000 000 001 2	achiral	27
P	000 020 100 0	S	000 000 120 0	achiral	26
P	000 020 100 0	S	000 000 002 1	achiral	25
P	000 020 100 0	S	000 000 021 0	achiral	24
P	000 020 100 0	S	000 000 012 0	achiral	23

P	000 020 100 0	S	000 200 010 0	P	22
P	000 020 100 0	S	000 010 200 0	M	21
P	000 020 100 0	S	000 000 201 0	achiral	20
P	000 020 100 0	S	000 000 010 1	achiral	19
P	000 020 100 0	meso	000 020 100 0	P	18
P	000 020 100 0	R	000 100 020 0	M	17
P	000 020 100 0	R	000 000 102 0	achiral	16
P	000 020 100 0	R	000 002 001 0	P	15
P	000 020 100 0	R	000 001 002 0	M	14
P	000 020 100 0	R	000 000 020 1	achiral	13
P	000 020 100 0	R	000 200 001 0	P	12
P	000 020 100 0	R	000 001 200 0	M	11
P	000 020 100 0	R	000 000 200 1	achiral	10
P	000 020 100 0	R	000 000 100 2	achiral	9
P	000 020 100 0	R	000 020 010 0	P	8
P	000 020 100 0	R	000 010 020 0	M	7
P	000 020 100 0	R	000 010 002 0	P	6
P	000 020 100 0	R	000 002 010 0	M	5
P	000 020 100 0	R	000 100 002 0	P	4
P	000 020 100 0	R	000 002 100 0	M	3
P	000 020 100 0	R	000 020 001 0	P	2
P	000 020 100 0	R	000 001 020 0	M	1

Table 15: Configuration of the central stereocentre for isomer 14

helicity	isomer 14	chirality	isomer 1 – 30	helicity	ranking
M	000 100 020 0	S	000 200 100 0	P	30
M	000 100 020 0	S	000 100 200 0	M	29
M	000 100 020 0	S	000 000 210 0	achiral	28
M	000 100 020 0	S	000 000 001 2	achiral	27
M	000 100 020 0	S	000 000 120 0	achiral	26
M	000 100 020 0	S	000 000 002 1	achiral	25
M	000 100 020 0	S	000 000 021 0	achiral	24
M	000 100 020 0	S	000 000 012 0	achiral	23

M	000 100 020 0	S	000 200 010 0	P	22
M	000 100 020 0	S	000 010 200 0	M	21
M	000 100 020 0	S	000 000 201 0	achiral	20
M	000 100 020 0	S	000 000 010 1	achiral	19
M	000 100 020 0	S	000 020 100 0	P	18
M	000 100 020 0	meso	000 100 020 0	M	17
M	000 100 020 0	R	000 000 102 0	achiral	16
M	000 100 020 0	R	000 002 001 0	P	15
M	000 100 020 0	R	000 001 002 0	M	14
M	000 100 020 0	R	000 000 020 1	achiral	13
M	000 100 020 0	R	000 200 001 0	P	12
M	000 100 020 0	R	000 001 200 0	M	11
M	000 100 020 0	R	000 000 200 1	achiral	10
M	000 100 020 0	R	000 000 100 2	achiral	9
M	000 100 020 0	R	000 020 010 0	P	8
M	000 100 020 0	R	000 010 020 0	M	7
M	000 100 020 0	R	000 010 002 0	P	6
M	000 100 020 0	R	000 002 010 0	M	5
M	000 100 020 0	R	000 100 002 0	P	4
M	000 100 020 0	R	000 002 100 0	M	3
M	000 100 020 0	R	000 020 001 0	P	2
M	000 100 020 0	R	000 001 020 0	M	1

Table 16: Configuration of the central stereocentre for isomer 15

helicity	isomer 15	chirality	isomer 1 – 30	helicity	ranking
achiral	000 000 102 0	S	000 200 100 0	P	30
achiral	000 000 102 0	S	000 100 200 0	M	29
achiral	000 000 102 0	S	000 000 210 0	achiral	28
achiral	000 000 102 0	S	000 000 001 2	achiral	27
achiral	000 000 102 0	S	000 000 120 0	achiral	26
achiral	000 000 102 0	S	000 000 002 1	achiral	25
achiral	000 000 102 0	S	000 000 021 0	achiral	24
achiral	000 000 102 0	S	000 000 012 0	achiral	23

achiral	000 000 102 0	S	000 200 010 0	P	22
achiral	000 000 102 0	S	000 010 200 0	M	21
achiral	000 000 102 0	S	000 000 201 0	achiral	20
achiral	000 000 102 0	S	000 000 010 1	achiral	19
achiral	000 000 102 0	S	000 020 100 0	P	18
achiral	000 000 102 0	S	000 100 020 0	M	17
achiral	000 000 102 0	meso	000 000 102 0	achiral	16
achiral	000 000 102 0	R	000 002 001 0	P	15
achiral	000 000 102 0	R	000 001 002 0	M	14
achiral	000 000 102 0	R	000 000 020 1	achiral	13
achiral	000 000 102 0	R	000 200 001 0	P	12
achiral	000 000 102 0	R	000 001 200 0	M	11
achiral	000 000 102 0	R	000 000 200 1	achiral	10
achiral	000 000 102 0	R	000 000 100 2	achiral	9
achiral	000 000 102 0	R	000 020 010 0	P	8
achiral	000 000 102 0	R	000 010 020 0	M	7
achiral	000 000 102 0	R	000 010 002 0	P	6
achiral	000 000 102 0	R	000 002 010 0	M	5
achiral	000 000 102 0	R	000 100 002 0	P	4
achiral	000 000 102 0	R	000 002 100 0	M	3
achiral	000 000 102 0	R	000 020 001 0	P	2
achiral	000 000 102 0	R	000 001 020 0	M	1

Table 17: Configuration of the central stereocentre for isomer 16

helicity	isomer 16	chirality	isomer 1 – 30	helicity	ranking
P	000 002 001 0	S	000 200 100 0	P	30
P	000 002 001 0	S	000 100 200 0	M	29
P	000 002 001 0	S	000 000 210 0	achiral	28
P	000 002 001 0	S	000 000 001 2	achiral	27
P	000 002 001 0	S	000 000 120 0	achiral	26
P	000 002 001 0	S	000 000 002 1	achiral	25
P	000 002 001 0	S	000 000 021 0	achiral	24
P	000 002 001 0	S	000 000 012 0	achiral	23
P	000 002 001 0	S	000 200 010 0	P	22

helicity	isomer	chirality	isomer 1 – 30	helicity	ranking
P	000 002 001 0	S	000 010 200 0	M	21
P	000 002 001 0	S	000 000 201 0	achiral	20
P	000 002 001 0	S	000 000 010 1	achiral	19
P	000 002 001 0	S	000 020 100 0	P	18
P	000 002 001 0	S	000 100 020 0	M	17
P	000 002 001 0	S	000 000 102 0	achiral	16
P	000 002 001 0	meso	000 002 001 0	P	15
P	000 002 001 0	R	000 001 002 0	M	14
P	000 002 001 0	R	000 000 020 1	achiral	13
P	000 002 001 0	R	000 200 001 0	P	12
P	000 002 001 0	R	000 001 200 0	M	11
P	000 002 001 0	R	000 000 200 1	achiral	10
P	000 002 001 0	R	000 000 100 2	achiral	9
P	000 002 001 0	R	000 020 010 0	P	8
P	000 002 001 0	R	000 010 020 0	M	7
P	000 002 001 0	R	000 010 002 0	P	6
P	000 002 001 0	R	000 002 010 0	M	5
P	000 002 001 0	R	000 100 002 0	P	4
P	000 002 001 0	R	000 002 100 0	M	3
P	000 002 001 0	R	000 020 001 0	P	2
P	000 002 001 0	R	000 001 020 0	M	1

Table 18: Configuration of the central stereocentre for isomer 17

helicity	isomer 17	chirality	isomer 1 – 30	helicity	ranking
M	000 001 002 0	S	000 200 100 0	P	30
M	000 001 002 0	S	000 100 200 0	M	29
M	000 001 002 0	S	000 000 210 0	achiral	28
M	000 001 002 0	S	000 000 001 2	achiral	27
M	000 001 002 0	S	000 000 120 0	achiral	26
M	000 001 002 0	S	000 000 002 1	achiral	25
M	000 001 002 0	S	000 000 021 0	achiral	24
M	000 001 002 0	S	000 000 012 0	achiral	23
M	000 001 002 0	S	000 200 010 0	P	22

M	000 001 002 0	S	000 010 200 0	M	21
M	000 001 002 0	S	000 000 201 0	achiral	20
M	000 001 002 0	S	000 000 010 1	achiral	19
M	000 001 002 0	S	000 020 100 0	P	18
M	000 001 002 0	S	000 100 020 0	M	17
M	000 001 002 0	S	000 000 102 0	achiral	16
M	000 001 002 0	S	000 002 001 0	P	15
M	000 001 002 0	meso	000 001 002 0	M	14
M	000 001 002 0	R	000 000 020 1	achiral	13
M	000 001 002 0	R	000 200 001 0	P	12
M	000 001 002 0	R	000 001 200 0	M	11
M	000 001 002 0	R	000 000 200 1	achiral	10
M	000 001 002 0	R	000 000 100 2	achiral	9
M	000 001 002 0	R	000 020 010 0	P	8
M	000 001 002 0	R	000 010 020 0	M	7
M	000 001 002 0	R	000 010 002 0	P	6
M	000 001 002 0	R	000 002 010 0	M	5
M	000 001 002 0	R	000 100 002 0	P	4
M	000 001 002 0	R	000 002 100 0	M	3
M	000 001 002 0	R	000 020 001 0	P	2
M	000 001 002 0	R	000 001 020 0	M	1

Table 19: Configuration of the central stereocentre for isomer 18

helicity	isomer 18	chirality	isomer 1 – 30	helicity	ranking
achiral	000 000 020 1	S	000 200 100 0	P	30
achiral	000 000 020 1	S	000 100 200 0	M	29
achiral	000 000 020 1	S	000 000 210 0	achiral	28
achiral	000 000 020 1	S	000 000 001 2	achiral	27
achiral	000 000 020 1	S	000 000 120 0	achiral	26
achiral	000 000 020 1	S	000 000 002 1	achiral	25
achiral	000 000 020 1	S	000 000 021 0	achiral	24
achiral	000 000 020 1	S	000 000 012 0	achiral	23
achiral	000 000 020 1	S	000 200 010 0	P	22

achiral	000 000 020 1	S	000 010 200 0	M	21
achiral	000 000 020 1	S	000 000 201 0	achiral	20
achiral	000 000 020 1	S	000 000 010 1	achiral	19
achiral	000 000 020 1	S	000 020 100 0	P	18
achiral	000 000 020 1	S	000 100 020 0	M	17
achiral	000 000 020 1	S	000 000 102 0	achiral	16
achiral	000 000 020 1	S	000 002 001 0	P	15
achiral	000 000 020 1	S	000 001 002 0	M	14
achiral	000 000 020 1	meso	000 000 020 1	achiral	13
achiral	000 000 020 1	R	000 200 001 0	P	12
achiral	000 000 020 1	R	000 001 200 0	M	11
achiral	000 000 020 1	R	000 000 200 1	achiral	10
achiral	000 000 020 1	R	000 000 100 2	achiral	9
achiral	000 000 020 1	R	000 020 010 0	P	8
achiral	000 000 020 1	R	000 010 020 0	M	7
achiral	000 000 020 1	R	000 010 002 0	P	6
achiral	000 000 020 1	R	000 002 010 0	M	5
achiral	000 000 020 1	R	000 100 002 0	P	4
achiral	000 000 020 1	R	000 002 100 0	M	3
achiral	000 000 020 1	R	000 020 001 0	P	2
achiral	000 000 020 1	R	000 001 020 0	M	1

Table 20: Configuration of the central stereocentre for isomer 19

helicity	isomer 19	chirality	isomer 1 – 30	helicity	ranking
P	000 200 001 0	S	000 200 100 0	P	30
P	000 200 001 0	S	000 100 200 0	M	29
P	000 200 001 0	S	000 000 210 0	achiral	28
P	000 200 001 0	S	000 000 001 2	achiral	27
P	000 200 001 0	S	000 000 120 0	achiral	26
P	000 200 001 0	S	000 000 002 1	achiral	25
P	000 200 001 0	S	000 000 021 0	achiral	24
P	000 200 001 0	S	000 000 012 0	achiral	23
P	000 200 001 0	S	000 200 010 0	P	22
P	000 200 001 0	S	000 010 200 0	M	21

P	000 200 001 0	S	000 000 201 0	achiral	20
P	000 200 001 0	S	000 000 010 1	achiral	19
P	000 200 001 0	S	000 020 100 0	P	18
P	000 200 001 0	S	000 100 020 0	M	17
P	000 200 001 0	S	000 000 102 0	achiral	16
P	000 200 001 0	S	000 002 001 0	P	15
P	000 200 001 0	S	000 001 002 0	M	14
P	000 200 001 0	S	000 000 020 1	achiral	13
P	000 200 001 0	meso	000 200 001 0	P	12
P	000 200 001 0	R	000 001 200 0	M	11
P	000 200 001 0	R	000 000 200 1	achiral	10
P	000 200 001 0	R	000 000 100 2	achiral	9
P	000 200 001 0	R	000 020 010 0	P	8
P	000 200 001 0	R	000 010 020 0	M	7
P	000 200 001 0	R	000 010 002 0	P	6
P	000 200 001 0	R	000 002 010 0	M	5
P	000 200 001 0	R	000 100 002 0	P	4
P	000 200 001 0	R	000 002 100 0	M	3
P	000 200 001 0	R	000 020 001 0	P	2
P	000 200 001 0	R	000 001 020 0	M	1

Table 21: Configuration of the central stereocentre for isomer 20

helicity	isomer 20	chirality	isomer 1 – 30	helicity	ranking
M	000 001 200 0	S	000 200 100 0	P	30
M	000 001 200 0	S	000 100 200 0	M	29
M	000 001 200 0	S	000 000 210 0	achiral	28
M	000 001 200 0	S	000 000 001 2	achiral	27
M	000 001 200 0	S	000 000 120 0	achiral	26
M	000 001 200 0	S	000 000 002 1	achiral	25
M	000 001 200 0	S	000 000 021 0	achiral	24
M	000 001 200 0	S	000 000 012 0	achiral	23
M	000 001 200 0	S	000 200 010 0	P	22
M	000 001 200 0	S	000 010 200 0	M	21
M	000 001 200 0	S	000 000 201 0	achiral	20

M	000 001 200 0	S	000 000 010 1	achiral	19
M	000 001 200 0	S	000 020 100 0	P	18
M	000 001 200 0	S	000 100 020 0	M	17
M	000 001 200 0	S	000 000 102 0	achiral	16
M	000 001 200 0	S	000 002 001 0	P	15
M	000 001 200 0	S	000 001 002 0	M	14
M	000 001 200 0	S	000 000 020 1	achiral	13
M	000 001 200 0	S	000 200 001 0	P	12
M	000 001 200 0	meso	000 001 200 0	M	11
M	000 001 200 0	R	000 000 200 1	achiral	10
M	000 001 200 0	R	000 000 100 2	achiral	9
M	000 001 200 0	R	000 020 010 0	P	8
M	000 001 200 0	R	000 010 020 0	M	7
M	000 001 200 0	R	000 010 002 0	P	6
M	000 001 200 0	R	000 002 010 0	M	5
M	000 001 200 0	R	000 100 002 0	P	4
M	000 001 200 0	R	000 002 100 0	M	3
M	000 001 200 0	R	000 020 001 0	P	2
M	000 001 200 0	R	000 001 020 0	M	1

Table 22: Configuration of the central stereocentre for isomer 21

helicity	isomer 21	chirality	isomer 1 – 30	helicity	ranking
achiral	000 000 200 1	S	000 200 100 0	P	30
achiral	000 000 200 1	S	000 100 200 0	M	29
achiral	000 000 200 1	S	000 000 210 0	achiral	28
achiral	000 000 200 1	S	000 000 001 2	achiral	27
achiral	000 000 200 1	S	000 000 120 0	achiral	26
achiral	000 000 200 1	S	000 000 002 1	achiral	25
achiral	000 000 200 1	S	000 000 021 0	achiral	24
achiral	000 000 200 1	S	000 000 012 0	achiral	23
achiral	000 000 200 1	S	000 200 010 0	P	22
achiral	000 000 200 1	S	000 010 200 0	M	21
achiral	000 000 200 1	S	000 000 201 0	achiral	20
achiral	000 000 200 1	S	000 000 010 1	achiral	19

achiral	000 000 200 1	S	000 020 100 0	P	18
achiral	000 000 200 1	S	000 100 020 0	M	17
achiral	000 000 200 1	S	000 000 102 0	achiral	16
achiral	000 000 200 1	S	000 002 001 0	P	15
achiral	000 000 200 1	S	000 001 002 0	M	14
achiral	000 000 200 1	S	000 000 020 1	achiral	13
achiral	000 000 200 1	S	000 200 001 0	P	12
achiral	000 000 200 1	S	000 001 200 0	M	11
achiral	000 000 200 1	meso	000 000 200 1	achiral	10
achiral	000 000 200 1	R	000 000 100 2	achiral	9
achiral	000 000 200 1	R	000 020 010 0	P	8
achiral	000 000 200 1	R	000 010 020 0	M	7
achiral	000 000 200 1	R	000 010 002 0	P	6
achiral	000 000 200 1	R	000 002 010 0	M	5
achiral	000 000 200 1	R	000 100 002 0	P	4
achiral	000 000 200 1	R	000 002 100 0	M	3
achiral	000 000 200 1	R	000 020 001 0	P	2
achiral	000 000 200 1	R	000 001 020 0	M	1

Table 23: Configuration of the central stereocentre for isomer 22

helicity	isomer 22	chirality	isomer 1 – 30	helicity	ranking
achiral	000 000 100 2	S	000 200 100 0	P	30
achiral	000 000 100 2	S	000 100 200 0	M	29
achiral	000 000 100 2	S	000 000 210 0	achiral	28
achiral	000 000 100 2	S	000 000 001 2	achiral	27
achiral	000 000 100 2	S	000 000 120 0	achiral	26
achiral	000 000 100 2	S	000 000 002 1	achiral	25
achiral	000 000 100 2	S	000 000 021 0	achiral	24
achiral	000 000 100 2	S	000 000 012 0	achiral	23
achiral	000 000 100 2	S	000 200 010 0	P	22
achiral	000 000 100 2	S	000 010 200 0	M	21
achiral	000 000 100 2	S	000 000 201 0	achiral	20
achiral	000 000 100 2	S	000 000 010 1	achiral	19
achiral	000 000 100 2	S	000 020 100 0	P	18

achiral	000 000 100 2	S	000 100 020 0	M	17
achiral	000 000 100 2	S	000 000 102 0	achiral	16
achiral	000 000 100 2	S	000 002 001 0	P	15
achiral	000 000 100 2	S	000 001 002 0	M	14
achiral	000 000 100 2	S	000 000 020 1	achiral	13
achiral	000 000 100 2	S	000 200 001 0	P	12
achiral	000 000 100 2	S	000 001 200 0	M	11
achiral	000 000 100 2	S	000 000 200 1	achiral	10
achiral	000 000 100 2	meso	000 000 100 2	achiral	9
achiral	000 000 100 2	R	000 020 010 0	P	8
achiral	000 000 100 2	R	000 010 020 0	M	7
achiral	000 000 100 2	R	000 010 002 0	P	6
achiral	000 000 100 2	R	000 002 010 0	M	5
achiral	000 000 100 2	R	000 100 002 0	P	4
achiral	000 000 100 2	R	000 002 100 0	M	3
achiral	000 000 100 2	R	000 020 001 0	P	2
achiral	000 000 100 2	R	000 001 020 0	M	1

Table 24: Configuration of the central stereocentre for isomer 23

helicity	isomer 23	chirality	isomer 1 – 30	helicity	ranking
P	000 020 010 0	S	000 200 100 0	P	30
P	000 020 010 0	S	000 100 200 0	M	29
P	000 020 010 0	S	000 000 210 0	achiral	28
P	000 020 010 0	S	000 000 001 2	achiral	27
P	000 020 010 0	S	000 000 120 0	achiral	26
P	000 020 010 0	S	000 000 002 1	achiral	25
P	000 020 010 0	S	000 000 021 0	achiral	24
P	000 020 010 0	S	000 000 012 0	achiral	23
P	000 020 010 0	S	000 200 010 0	P	22
P	000 020 010 0	S	000 010 200 0	M	21
P	000 020 010 0	S	000 000 201 0	achiral	20
P	000 020 010 0	S	000 000 010 1	achiral	19
P	000 020 010 0	S	000 020 100 0	P	18
P	000 020 010 0	S	000 100 020 0	M	17

P	000 020 010 0	S	000 000 102 0	achiral	16
P	000 020 010 0	S	000 002 001 0	P	15
P	000 020 010 0	S	000 001 002 0	M	14
P	000 020 010 0	S	000 000 020 1	achiral	13
P	000 020 010 0	S	000 200 001 0	P	12
P	000 020 010 0	S	000 001 200 0	M	11
P	000 020 010 0	S	000 000 200 1	achiral	10
P	000 020 010 0	S	000 000 100 2	achiral	9
P	000 020 010 0	meso	000 020 010 0	P	8
P	000 020 010 0	R	000 010 020 0	M	7
P	000 020 010 0	R	000 010 002 0	P	6
P	000 020 010 0	R	000 002 010 0	M	5
P	000 020 010 0	R	000 100 002 0	P	4
P	000 020 010 0	R	000 002 100 0	M	3
P	000 020 010 0	R	000 020 001 0	P	2
P	000 020 010 0	R	000 001 020 0	M	1

Table 25: Configuration of the central stereocentre for isomer 24

helicity	isomer 24	chirality	isomer 1 – 30	helicity	ranking
M	000 010 020 0	S	000 200 100 0	P	30
M	000 010 020 0	S	000 100 200 0	M	29
M	000 010 020 0	S	000 000 210 0	achiral	28
M	000 010 020 0	S	000 000 001 2	achiral	27
M	000 010 020 0	S	000 000 120 0	achiral	26
M	000 010 020 0	S	000 000 002 1	achiral	25
M	000 010 020 0	S	000 000 021 0	achiral	24
M	000 010 020 0	S	000 000 012 0	achiral	23
M	000 010 020 0	S	000 200 010 0	P	22
M	000 010 020 0	S	000 010 200 0	M	21
M	000 010 020 0	S	000 000 201 0	achiral	20
M	000 010 020 0	S	000 000 010 1	achiral	19
M	000 010 020 0	S	000 020 100 0	P	18
M	000 010 020 0	S	000 100 020 0	M	17
M	000 010 020 0	S	000 000 102 0	achiral	16

M	000 010 020 0	S	000 002 001 0	P	15
M	000 010 020 0	S	000 001 002 0	M	14
M	000 010 020 0	S	000 000 020 1	achiral	13
M	000 010 020 0	S	000 200 001 0	P	12
M	000 010 020 0	S	000 001 200 0	M	11
M	000 010 020 0	S	000 000 200 1	achiral	10
M	000 010 020 0	S	000 000 100 2	achiral	9
M	000 010 020 0	S	000 020 010 0	P	8
M	000 010 020 0	meso	000 010 020 0	M	7
M	000 010 020 0	R	000 010 002 0	P	6
M	000 010 020 0	R	000 002 010 0	M	5
M	000 010 020 0	R	000 100 002 0	P	4
M	000 010 020 0	R	000 002 100 0	M	3
M	000 010 020 0	R	000 020 001 0	P	2
M	000 010 020 0	R	000 001 020 0	M	1

Table 26: Configuration of the central stereocentre for isomer 25

helicity	isomer 25	chirality	isomer 1 – 30	helicity	ranking
P	000 010 002 0	S	000 200 100 0	P	30
P	000 010 002 0	S	000 100 200 0	M	29
P	000 010 002 0	S	000 000 210 0	achiral	28
P	000 010 002 0	S	000 000 001 2	achiral	27
P	000 010 002 0	S	000 000 120 0	achiral	26
P	000 010 002 0	S	000 000 002 1	achiral	25
P	000 010 002 0	S	000 000 021 0	achiral	24
P	000 010 002 0	S	000 000 012 0	achiral	23
P	000 010 002 0	S	000 200 010 0	P	22
P	000 010 002 0	S	000 010 200 0	M	21
P	000 010 002 0	S	000 000 201 0	achiral	20
P	000 010 002 0	S	000 000 010 1	achiral	19
P	000 010 002 0	S	000 020 100 0	P	18
P	000 010 002 0	S	000 100 020 0	M	17
P	000 010 002 0	S	000 000 102 0	achiral	16
P	000 010 002 0	S	000 002 001 0	P	15

P	000 010 002 0	S	000 001 002 0	M	14
P	000 010 002 0	S	000 000 020 1	achiral	13
P	000 010 002 0	S	000 200 001 0	P	12
P	000 010 002 0	S	000 001 200 0	M	11
P	000 010 002 0	S	000 000 200 1	achiral	10
P	000 010 002 0	S	000 000 100 2	achiral	9
P	000 010 002 0	S	000 020 010 0	P	8
P	000 010 002 0	S	000 010 020 0	M	7
P	000 010 002 0	meso	000 010 002 0	P	6
P	000 010 002 0	R	000 002 010 0	M	5
P	000 010 002 0	R	000 100 002 0	P	4
P	000 010 002 0	R	000 002 100 0	M	3
P	000 010 002 0	R	000 020 001 0	P	2
P	000 010 002 0	R	000 001 020 0	M	1

Table 27: Configuration of the central stereocentre for isomer 26

helicity	isomer 26	chirality	isomer 1 – 30	helicity	ranking
M	000 002 010 0	S	000 200 100 0	P	30
M	000 002 010 0	S	000 100 200 0	M	29
M	000 002 010 0	S	000 000 210 0	achiral	28
M	000 002 010 0	S	000 000 001 2	achiral	27
M	000 002 010 0	S	000 000 120 0	achiral	26
M	000 002 010 0	S	000 000 002 1	achiral	25
M	000 002 010 0	S	000 000 021 0	achiral	24
M	000 002 010 0	S	000 000 012 0	achiral	23
M	000 002 010 0	S	000 200 010 0	P	22
M	000 002 010 0	S	000 010 200 0	M	21
M	000 002 010 0	S	000 000 201 0	achiral	20
M	000 002 010 0	S	000 000 010 1	achiral	19
M	000 002 010 0	S	000 020 100 0	P	18
M	000 002 010 0	S	000 100 020 0	M	17
M	000 002 010 0	S	000 000 102 0	achiral	16
M	000 002 010 0	S	000 002 001 0	P	15

M	000 002 010 0	S	000 001 002 0	M	14
M	000 002 010 0	S	000 000 020 1	achiral	13
M	000 002 010 0	S	000 200 001 0	P	12
M	000 002 010 0	S	000 001 200 0	M	11
M	000 002 010 0	S	000 000 200 1	achiral	10
M	000 002 010 0	S	000 000 100 2	achiral	9
M	000 002 010 0	S	000 020 010 0	P	8
M	000 002 010 0	S	000 010 020 0	M	7
M	000 002 010 0	S	000 010 002 0	P	6
M	000 002 010 0	meso	000 002 010 0	M	5
M	000 002 010 0	R	000 100 002 0	P	4
M	000 002 010 0	R	000 002 100 0	M	3
M	000 002 010 0	R	000 020 001 0	P	2
M	000 002 010 0	R	000 001 020 0	M	1

Table 28: Configuration of the central stereocentre for isomer 27

helicity	isomer 27	chirality	isomer 1 – 30	helicity	ranking
P	000 100 002 0	S	000 200 100 0	P	30
P	000 100 002 0	S	000 100 200 0	M	29
P	000 100 002 0	S	000 000 210 0	achiral	28
P	000 100 002 0	S	000 000 001 2	achiral	27
P	000 100 002 0	S	000 000 120 0	achiral	26
P	000 100 002 0	S	000 000 002 1	achiral	25
P	000 100 002 0	S	000 000 021 0	achiral	24
P	000 100 002 0	S	000 000 012 0	achiral	23
P	000 100 002 0	S	000 200 010 0	P	22
P	000 100 002 0	S	000 010 200 0	M	21
P	000 100 002 0	S	000 000 201 0	achiral	20
P	000 100 002 0	S	000 000 010 1	achiral	19
P	000 100 002 0	S	000 020 100 0	P	18
P	000 100 002 0	S	000 100 020 0	M	17
P	000 100 002 0	S	000 000 102 0	achiral	16
P	000 100 002 0	S	000 002 001 0	P	15
P	000 100 002 0	S	000 001 002 0	M	14

P	000 100 002 0	S	000 000 020 1	achiral	13
P	000 100 002 0	S	000 200 001 0	P	12
P	000 100 002 0	S	000 001 200 0	M	11
P	000 100 002 0	S	000 000 200 1	achiral	10
P	000 100 002 0	S	000 000 100 2	achiral	9
P	000 100 002 0	S	000 020 010 0	P	8
P	000 100 002 0	S	000 010 020 0	M	7
P	000 100 002 0	S	000 010 002 0	P	6
P	000 100 002 0	S	000 002 010 0	M	5
P	000 100 002 0	meso	000 100 002 0	P	4
P	000 100 002 0	R	000 002 100 0	M	3
P	000 100 002 0	R	000 020 001 0	P	2
P	000 100 002 0	R	000 001 020 0	M	1

Table 29: Configuration of the central stereocentre for isomer 27

helicity	isomer 28	chirality	isomer 1 – 30	helicity	ranking
M	000 002 100 0	S	000 200 100 0	P	30
M	000 002 100 0	S	000 100 200 0	M	29
M	000 002 100 0	S	000 000 210 0	achiral	28
M	000 002 100 0	S	000 000 001 2	achiral	27
M	000 002 100 0	S	000 000 120 0	achiral	26
M	000 002 100 0	S	000 000 002 1	achiral	25
M	000 002 100 0	S	000 000 021 0	achiral	24
M	000 002 100 0	S	000 000 012 0	achiral	23
M	000 002 100 0	S	000 200 010 0	P	22
M	000 002 100 0	S	000 010 200 0	M	21
M	000 002 100 0	S	000 000 201 0	achiral	20
M	000 002 100 0	S	000 000 010 1	achiral	19
M	000 002 100 0	S	000 020 100 0	P	18
M	000 002 100 0	S	000 100 020 0	M	17
M	000 002 100 0	S	000 000 102 0	achiral	16
M	000 002 100 0	S	000 002 001 0	P	15
M	000 002 100 0	S	000 001 002 0	M	14
M	000 002 100 0	S	000 000 020 1	achiral	13

M	000 002 100 0	S	000 200 001 0	P	12
M	000 002 100 0	S	000 001 200 0	M	11
M	000 002 100 0	S	000 000 200 1	achiral	10
M	000 002 100 0	S	000 000 100 2	achiral	9
M	000 002 100 0	S	000 020 010 0	P	8
M	000 002 100 0	S	000 010 020 0	M	7
M	000 002 100 0	S	000 010 002 0	P	6
M	000 002 100 0	S	000 002 010 0	M	5
M	000 002 100 0	meso	000 100 002 0	P	4
M	000 002 100 0	R	000 002 100 0	M	3
M	000 002 100 0	R	000 020 001 0	P	2
M	000 002 100 0	R	000 001 020 0	M	1

Table 30: Configuration of the central stereocentre for isomer 28

helicity	isomer 28	chirality	isomer 1 – 30	helicity	ranking
M	000 002 100 0	S	000 200 100 0	P	30
M	000 002 100 0	S	000 100 200 0	M	29
M	000 002 100 0	S	000 000 210 0	achiral	28
M	000 002 100 0	S	000 000 001 2	achiral	27
M	000 002 100 0	S	000 000 120 0	achiral	26
M	000 002 100 0	S	000 000 002 1	achiral	25
M	000 002 100 0	S	000 000 021 0	achiral	24
M	000 002 100 0	S	000 000 012 0	achiral	23
M	000 002 100 0	S	000 200 010 0	P	22
M	000 002 100 0	S	000 010 200 0	M	21
M	000 002 100 0	S	000 000 201 0	achiral	20
M	000 002 100 0	S	000 000 010 1	achiral	19
M	000 002 100 0	S	000 020 100 0	P	18
M	000 002 100 0	S	000 100 020 0	M	17
M	000 002 100 0	S	000 000 102 0	achiral	16
M	000 002 100 0	S	000 002 001 0	P	15
M	000 002 100 0	S	000 001 002 0	M	14
M	000 002 100 0	S	000 000 020 1	achiral	13
M	000 002 100 0	S	000 200 001 0	P	12

M	000 002 100 0	S	000 001 200 0	M	11
M	000 002 100 0	S	000 000 200 1	achiral	10
M	000 002 100 0	S	000 000 100 2	achiral	9
M	000 002 100 0	S	000 020 010 0	P	8
M	000 002 100 0	S	000 010 020 0	M	7
M	000 002 100 0	S	000 010 002 0	P	6
M	000 002 100 0	S	000 002 010 0	M	5
M	000 002 100 0	S	000 100 002 0	P	4
M	000 002 100 0	meso	000 002 100 0	M	3
M	000 002 100 0	R	000 020 001 0	P	2
M	000 002 100 0	R	000 001 020 0	M	1

Table 31: Configuration of the central stereocentre for isomer 29

helicity	isomer 29	chirality	isomer 1 – 30	helicity	ranking
P	000 020 001 0	S	000 200 100 0	P	30
P	000 020 001 0	S	000 100 200 0	M	29
P	000 020 001 0	S	000 000 210 0	achiral	28
P	000 020 001 0	S	000 000 001 2	achiral	27
P	000 020 001 0	S	000 000 120 0	achiral	26
P	000 020 001 0	S	000 000 002 1	achiral	25
P	000 020 001 0	S	000 000 021 0	achiral	24
P	000 020 001 0	S	000 000 012 0	achiral	23
P	000 020 001 0	S	000 200 010 0	P	22
P	000 020 001 0	S	000 010 200 0	M	21
P	000 020 001 0	S	000 000 201 0	achiral	20
P	000 020 001 0	S	000 000 010 1	achiral	19
P	000 020 001 0	S	000 020 100 0	P	18
P	000 020 001 0	S	000 100 020 0	M	17
P	000 020 001 0	S	000 000 102 0	achiral	16
P	000 020 001 0	S	000 002 001 0	P	15
P	000 020 001 0	S	000 001 002 0	M	14
P	000 020 001 0	S	000 000 020 1	achiral	13
P	000 020 001 0	S	000 200 001 0	P	12

P	000 020 001 0	S	000 001 200 0	M	11
P	000 020 001 0	S	000 000 200 1	achiral	10
P	000 020 001 0	S	000 000 100 2	achiral	9
P	000 020 001 0	S	000 020 010 0	P	8
P	000 020 001 0	S	000 010 020 0	M	7
P	000 020 001 0	S	000 010 002 0	P	6
P	000 020 001 0	S	000 002 010 0	M	5
P	000 020 001 0	S	000 100 002 0	P	4
P	000 020 001 0	S	000 002 100 0	M	3
P	000 020 001 0	meso	000 020 001 0	P	2
P	000 020 001 0	R	000 001 020 0	M	1

Table 32: Configuration of the central stereocentre for isomer 30

helicity	isomer 30	chirality	isomer 1 – 30	helicity	ranking
achiral	000 001 020 0	S	000 200 100 0	P	30
achiral	000 001 020 0	S	000 100 200 0	M	29
achiral	000 001 020 0	S	000 000 210 0	achiral	28
achiral	000 001 020 0	S	000 000 001 2	achiral	27
achiral	000 001 020 0	S	000 000 120 0	achiral	26
achiral	000 001 020 0	S	000 000 002 1	achiral	25
achiral	000 001 020 0	S	000 000 021 0	achiral	24
achiral	000 001 020 0	S	000 000 012 0	achiral	23
achiral	000 001 020 0	S	000 200 010 0	P	22
achiral	000 001 020 0	S	000 010 200 0	M	21
achiral	000 001 020 0	S	000 000 201 0	achiral	20
achiral	000 001 020 0	S	000 000 010 1	achiral	19
achiral	000 001 020 0	S	000 020 100 0	P	18
achiral	000 001 020 0	S	000 100 020 0	M	17
achiral	000 001 020 0	S	000 000 102 0	achiral	16
achiral	000 001 020 0	S	000 002 001 0	P	15
achiral	000 001 020 0	S	000 001 002 0	M	14
achiral	000 001 020 0	S	000 000 020 1	achiral	13
achiral	000 001 020 0	S	000 200 001 0	P	12

achiral	000 001 020 0	S	000 001 200 0	M	11
achiral	000 001 020 0	S	000 000 200 1	achiral	10
achiral	000 001 020 0	S	000 000 100 2	achiral	9
achiral	000 001 020 0	S	000 020 010 0	P	8
achiral	000 001 020 0	S	000 010 020 0	M	7
achiral	000 001 020 0	S	000 010 002 0	P	6
achiral	000 001 020 0	S	000 002 010 0	M	5
achiral	000 001 020 0	S	000 100 002 0	P	4
achiral	000 001 020 0	S	000 002 100 0	M	3
achiral	000 001 020 0	S	000 020 001 0	P	2
achiral	000 001 020 0	meso	000 001 020 0	M	1

Experimental section for Chapter 6

WILEY-VCH

Supporting Information

Total Synthesis of Endiandric Acid J and Beilcyclone A from Cyclooctatetraene

Oussama Yahiaoui, Adrian Almass and Thomas Fallon

Department of Chemistry, The University of Adelaide, SA 5005 (Australia)

E-mail: thomas.fallon@adelaide.edu.au

Table of Contents

General Procedures

NMR analysis was conducted using either an Agilent 600 MHz DD2 console with an Oxford 600 MHz magnet and Agilent cryoprobe, a *Bruker Advance III-HD* 600 MHz, and an *Agilent* 500 MHz. Chemical shifts are referenced to the residual solvent resonance as the internal standard (CDCl$_3$: δ = 7.26 ppm for ^{1}H NMR and δ = 77.16 ppm for ^{13}C NMR). Data are reported as follows: chemical shift, multiplicity (brs = broad singlet, s = singlet, d = doublet, t = triplet, q = quartet, m = multiplet). The assignment of signals was assisted correlated spectroscopy (COSY), heteronuclear single quantum coherence (HSQC). High-resolution mass spectroscopy was recorded using an Agilent 6230 TOF LC/MS (ESI). Infra-red spectra were recorded using a *PerkinElmer spectrum 100* FTIR spectrometer equipped with a zinc selenide crystal. Cyclooctatetraene was obtained as a generous gift from Dr Graham Gream (The University of Adelaide). The material was manufactured by BASF, most likely sometime in the 1970s. Samples were purified by vacuum distillation using a short vigrex column (20 mbar/ 60 °C), and stored in a freezer under an atmosphere of argon. All other chemicals were purchased from commercial suppliers and used as received. All reactions were performed in flame-dried glassware using conventional Schlenk techniques under static pressure of nitrogen. Liquids and solutions were transferred with syringes.

Diethyl ether (Et$_2$O) and tetrahydrofuran (THF) were purified by a Pure Solv^{TM} Micro solvent purification system and stored over 4 Å molecular sieves under an atmosphere of nitrogen. 1,2-dichloroethane was dried through storage over 4 Å molecular sieves under an atmosphere of nitrogen. Toluene was dried following the rapid purification procedures outlined in Purification of Laboratory Chemicals (5th Edition, by Amarego and Chai), and stored over 4 Å molecular sieves under an atmosphere of nitrogen.

Experimental Procedures

Synthesis of Cyclooctatriene oxide (3)

COT-monoepoxide was synthesized according to the work of Pineschi and colleagues[1] starting from 5g of cyclooctatetraene. Product obtained as a yellow oil (71%).

Synthesis of (2Z,4Z,7Z)-6-decylcycloocta-2,4,7-trien-1-ol (4)
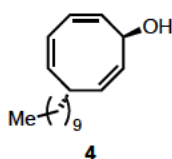
Under nitrogen atmosphere, an oven dried round bottom flask was charged with magnesium powder (989 mg, 40.7 mmol, 4.90 eq), anhydrous Et$_2$O (5 mL), and 1,2-dibromoethane (20 μL). Upon activation of the magnesium 1-bromodecane (5.63 mL, 27.1 mmol, 3.30 eq) was added dropwise. The mixture was stirred for 2 h before being added dropwise to a stirred suspension of CuCN (2.68 g, 29.9 mmol, 3.60 eq) in anhydrous tetrahydrofuran (20 ml) at –18 °C. This was allowed to stir for an hour at –18 °C before a solution of COT-monoepoxide (1.00 g, 8.32 mmol, 1.00 eq) in anhydrous tetrahydrofuran (2 mL) was added. The resulting mixture was allowed to stir for a further hour at –18 °C. The reaction was quenched with saturated aqueous NH$_4$Cl solution. The aqueous layers were extracted with Et$_2$O and the organic layer was washed with distilled water and saturated NaCl solution. The organic phase was dried over MgSO$_4$ and the solvent was removed in vacuo. The desired product was purified through column chromatography using buffered silica and hexane/Et$_2$O (9:1) as eluent. **4** was obtained as a yellow oil (2.1 g, 96%). **IR** (ATR): v/cm^{-1} = 3350, 3012, 2922, 2853, 1668, 1649, 1611, 1465, 1377, 1254, 1037, 771, 721, 669. **^{1}H NMR** (600 MHz, CDCl$_3$) δ: 6.13 – 6.11 (1H, m), 6.09 – 6.07 (1H, m), 5.58 – 5.55 (1H, m), 5.39 – 5.34 (2H, m), 5.18 (1H, dd, J = 10.2, 7.0 Hz), 4.87 (1H, brs), 2.79 – 2.75 (1H, m), 2.09 (1H, brs),1.55 – 1.51 (2H, m), 1.25 (18H, m), 0.87 (3H, t, J = 7.0 Hz). **^{13}C NMR** (150 MHz, CDCl$_3$) δ: 132.9, 132.8, 132.3, 130.9, 127.5, 126.4, 70.0, 37.4, 36.4, 32.1, 29.8, 29.7, 29.5, 27.4, 22.8, 14.3. **HRMS** (ESI, m/z) calculated for ([M]) C$_{18}$H$_{31}$O 262.2297 found 262.2265.

**Synthesis of (1Z,3Z,6Z)-5-decyl-8-(vinyloxy)cycloocta-1,3,6-triene (5)**
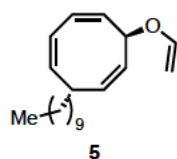
Under nitrogen atmosphere an oven dried round bottom flask was charged with AuClPPh$_3$ (47.1 mg, 95.3 μmol, 0.10 eq) AgOAc (15.9 mg, 95.3 μmol, 0.10 eq) and freshly distilled butyl vinyl ether (4 mL) The mixture was stirred at room temperature for 10 min before decyl alcohol **4** (250 mg, 952 μmol, 1.00 eq) and acetic acid (1.72 μL, 25.6 μmol, 0.03 eq) were added, and allowed to stir for 12 h. The reaction was diluted in diethyl ether and quenched with triethylamine (20 μL) before filtrated through a pad of Al$_2$O$_3$. The solvent was then removed at 28 °C in vacuo. Under nitrogen atmosphere another oven dried round bottom flask was

charged with AuClPPh$_3$ (23.6 mg, 47.6 μmol, 0.05 eq.) AgOAc (7.95 mg, 47.6 μmol, 0.05 eq) and freshly distilled butyl vinyl ether (4 mL). The mixture was stirred at room temperature for 10 min before the crude material and acetic acid (0.86 μL, 12.8 μmol, 0.01 eq) were added. After 12 h, the reaction was quenched with triethylamine (20 μL) before filtrated through a pad of Al$_2$O$_3$. The solvent was then removed at 28 °C in vacuo and the product was used as impurified intermediate for the next step. **^{1}H NMR** (600 MHz, CDCl$_3$) δ: 6.69 (1H, dd, J = 14.3, 6.8, Hz), 6.52 – 6.49 (2H, m), 5.94 – 5.91 (1H, m), 5.79 – 5.76 (1H, m), 5.71 – 5.68 (1H, m), 5.57 – 5.54 (1H, m), 5.33 (1H, brs), 4.53 (1H, dd, J = 14.3, 1.8 Hz), 4.37 (1H, dd, J = 6.8, 1.8 Hz), 3.14 (1H, brs), 1.92 – 1.85 (3H, m), 1.60 (27H, m), 1.22 (5H, t, J = 7.0 Hz). **^{13}C NMR** (150 MHz, CDCl$_3$) δ: 150.4, 132.8, 132.8, 129.7, 128.4, 127.5, 127.3, 88.9, 76.6, 37.6, 36.4, 32.1, 29.8, 29.7, 29.5, 27.4, 22.8, 14.3.

Synthesis of 2-((1S,6R)-8-decylbicyclo[4.2.0]octa-2,4-dien-7-yl)acetaldehyde (6a, 6b)
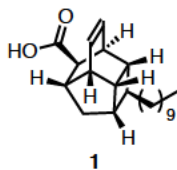

6a   **6b**
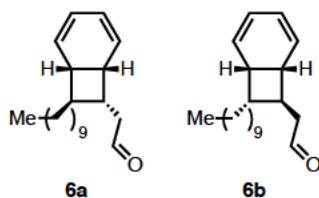
Under nitrogen atmosphere an oven dried round bottom flask was charged with **5** (270 mg) and anhydrous toluene (5 mL). The solution was heated at 60 °C overnight. Upon completion of the reaction the solvent was removed in vacuo. The crude material was purified by column chromatography using buffered silica and hexane/EtAOc (9:1)

as eluent (R$_f$ = 0.23), affording the aldehyde **6a** and **6b** as an inseparable ~2:1 mixture (**6a:6b** or **6b:6a**) as a yellow oil (134 mg, 48%, over two steps). **IR** (ATR): v/cm^{-1} = 3029, 2921, 2852, 2712, 1724, 1675, 1613, 1465, 1378, 1320, 1237, 1195, 998, 961, 814, 705, 663. **^{1}H NMR** (600 MHz, CDCl$_3$) δ: 9.77 (1H, s), 9.68 (0.5H, dd, J = 2.5 Hz), 5.89 - 5.85 (2H, m), 5.72 - 5.69 (1H, m,), 5.67 - 5.64 (1H, m), 5.61 – 5.57 (2H, m), 5.42 - 5.40 (1H, m), 3.24 - 3.23 (1H, m,), 3.18-3.14 (0.6H, m), 2.84 - 2.79 (2H m), 2.70 - 2.62 (2H, m), 2.60 - 2.55 (2H, m), 2.53 - 2.8 (1H, m), 2.32 – 2.27 (1H, m),1.59 – 1.42 (4H, m), 1.25 - 1.33 (33H, m), 0.88 (6H, t, J = 7.0 Hz). **^{13}C NMR** (150 MHz, CDCl$_3$) δ: 202.3, 201.7, 127.8, 126.5, 126.1, 125.6, 124.8, 124.3, 122.3, 121.4, 52.4, 51.5, 50.3, 45.8, 45.4, 44.5, 37.4, 36.9, 36.2, 35.1, 33.9, 32.1, 30.3, 29.9, 29.8, 29.8, 29.7, 29.5, 29.5, 28.3, 28, 22.8, 14.3. **HRMS** (ESI, m/z) calculated for ([M+Na]) C$_{20}$H$_{32}$O 311.2345 found 311.2319.

4

Synthesis of Endiandric acid J ester (9) in one pot starting from (6a,6b)
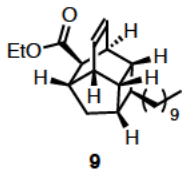
Under nitrogen atmosphere an oven dried round bottom flask was charged with **6a,6b** (16 mg, 91 μmol, 1.0 eq) (carbomethoxymethylene)triphenylphosphorane (79.1 mg, 227 μmol, 2.50 eq.) and anhydrous 1,2-dichloroethane (0.1 mL). The mixture was heated at 55 °C for 3 hrs. Anhydrous toluene (30 mL) was added and the reaction mixture was heated at 120 °C for 5 hrs. The solvent was removed in vacuo and the crude material was purified by column chromatography using hexane/Et$_2$O (1%) as eluents (R_f = 0.21). The desired product was obtained as a colorless oil (12 mg, 54%, over two steps). **IR (ATR):** v/cm^{-1} = 2956, 2923, 2853, 1736, 1611, 1532, 1465, 1367, 1305, 1205, 1179, 1042, 790, 691. **^{1}H NMR** (600 MHz, CDCl$_3$) δ: 6.21 - 6.15 (2H, m), 4.13 – 4.03 (2H, m), 3.02 – 2.99 (1H, m), 2.80 (1H, d, J = 3.8 Hz), 2.67 (1H, d, J = 5.5 Hz), 2.58 (1H, dd, J = 6.9 Hz), 2.36 – 2.33 (1H, m), 2.23 – 2.21 (1H, m), 1.91 – 1.87 (1H, m), 1.66 – 1.60 (2H, m), 1.53 – 1.43 (2H, m), 1.26 (21H, m), 0.88 (3H, t, J = 7.0 Hz). **^{13}C NMR** (150 MHz, CDCl$_3$) δ: 175, 131.9, 131.4, 60.3, 49.3, 42.1, 40.4, 40.3, 39.7, 39.6, 38.7, 38.5, 36.5, 35.3, 32.1, 29.9, 29.9, 29.8, 29.8, 29.5, 27.4, 22.8, 14.4, 14.2. **HRMS** (ESI, m/z) calculated for ([M+Na]) C$_{24}$H$_{38}$O$_2$ 381.2764 found 381.2707.

Synthesis of Endiandric acid J (1)
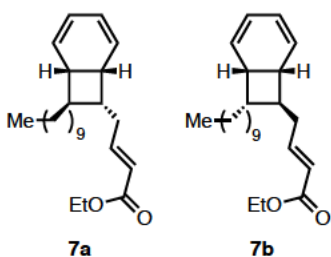
A 25 mL round bottom flask was charged with **9** (25 mg, 70 μmol, 1.0 eq), lithium hydroxide (5.00 mg, 0.21 mmol, 3.00 eq), and THF/water/methanol in a ratio of 1:1:1 (10 mL). The reaction mixture was heated at 50 °C overnight. After reaction the solution was acidified until pH = 1 and extracted with ethyl acetate three times. The organic layer was washed with distilled water and saturated NaCl solution and dried over MgSO$_4$. The solvent was evaporated in vacuo and the crude material was purified on column chromatography using hexane/EAOc (9:1) as eluent (R_f = 0.18). The product was obtained as a colorless oil (18 mg, 72 %). **IR (ATR):** v/cm^{-1} = 3047, 2966, 2922, 2852, 1753, 1464, 1366, 1296, 1204, 1176, 1095, 1042, 855, 808, 719, 690. **^{1}H NMR** (600 MHz, CDCl$_3$) δ: 6.25 – 6.20 (2H, m), 3.02 – 3.00 (1H, m), 2.87 (1H, d, J = 3.8 Hz), 2.65 – 2.71 (1H, m), 2.54 (1H, t, J = 5.2 Hz), 2.34 (1H, dt, J = 8.9, 5.5 Hz), 2.23 (1H, t, J = 6.4 Hz), 1.89 (1H, ddd, J = 12.9, 7.6, 5.4 Hz), 1.66 – 1.68, (2H, m), 1.54 (1H, d, J = 12.7 Hz), 1.43 – 1.51 (2H, m), 1.26 (16H, m), 0.88 (3H, t, J = 6.9 Hz). **^{13}C NMR** (150 MHz, CDCl$_3$) δ: 180.3, 132.1, 131.4, 49.1, 42.0, 40.4, 40.3, 39.8, 39.6, 38.7, 38.5, 36.5, 35.2, 32.1, 29.9, 29.9, 29.8, 29.8, 29.8, 29.5, 27.4, 22.9, 14.3. **HRMS** (ESI, m/z) calculated for ([M+K]$^+$) C$_{22}$H$_{34}$O$_2$ 367.2608 found 367.2645.

5

Synthesis of Beilcyclone A (2) in one pot starting from (6a,6b)
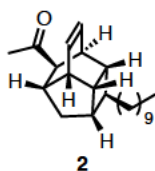
Under nitrogen atmosphere an oven dried round bottom flask was charged with **6a,6b** (16 mg, 91 µmol, 1.0 eq) acetylmethylene-triphenylphosphorane (86.7 mg, 272 µmol, 3.00 eq) and anhydrous 1,2-dichloroethane (0.1 mL). The mixture was heated at 40 °C for 24 h. anhydrous toluene (5 mL), and heated at 120 °C for 5 hrs. The solvent was removed in vacuo and the crude material was purified by column chromatography using hexane/Et$_2$O (1%) as eluents as eluent (Rf = 0.27). The desired product was obtained as a colourless oil (12 mg, 61%, over two steps). **IR** (ATR): v/cm^{-1} = 2954, 2922, 2852, 1714, 1459, 1363, 160, 1169, 1019, 966, 802, 702, 665. **^{1}H NMR** (600 MHz, CDCl$_3$) δ: 6.20 (1H, ddd, J = 8.0, 6.4, 1.0 Hz), 6.11 (1H, ddd, J = 8.0, 6.4, 1.0 Hz), 3.02 (1H, dt, J = 7.3, 4.1 Hz), 2.78 (1H, d, J = 3.6 Hz), 2.68 – 2.65 (2H, m), 2.35 (1H, dt, J = 9.8, 5.4 Hz), 2.23 (1H, dt, J = 6.3, 3.5 Hz), 2.12 (3H, s), 1.89 (1H, ddd, J = 12.7, 7.5, 5.2 Hz), 1.69 − 1.64 (2H, m), 1.53 − 1.45 (2H, m), 1.26 (16H, brs), 0.88 (3H, t, J = 6.9 Hz). **^{13}C NMR** (150 MHz, CDCl$_3$) δ: 209.3, 132.4, 130.5, 57.9, 42.4, 40.4, 40.4, 40.1, 39.8, 38.5, 37.0, 36.5, 35.6, 32.1, 29.9, 29.9, 29.8, 29.8, 29.5, 28.5, 27.5, 22.8, 14.3. **HRMS** (ESI, m/z) calculated for ([M+Na]) C$_{24}$H$_{38}$O$_2$ 351.2658 found 351.2687.

Synthesis of ethyl (*E*)-4-((1*S*,6*R*)-8-decylbicyclo[4.2.0]octa-2,4-dien-7-yl)but-2-enoate (7a,7b)

Under nitrogen atmosphere an oven dried round bottom flask was charged with **6a,6b** (60.0 mg, 208 µmol, 1.00 eq) (carbomethoxymethylene)triphenylphosphorane (181 mg, 519 µmol, 2.50 eq.) and anhydrous 1,2-dichloroethane (0.2 mL). The mixture was heated at 55 °C for 3 hrs. After reaction the solvent was removed in vacuo. The crude material was purified by column chromatography using hexane/Et$_2$O (9.5:0.5) as eluent (R$_f$ = 0.23) affording **7a** and **7b** as an inseparable ~1:1 mixture (**7a:7b** or **7b:7a**) as a colorless oil (50 mg, 67%). **IR** (ATR): v/cm^{-1} =3030, 2921, 2852, 1721, 1653, 1465, 1366, 1320, 1306, 1264, 1192, 1149, 1095, 1042, 979, 850, 718. **^{1}H NMR** (600 MHz, CDCl$_3$) δ: 6.94 – 6.84 (2H, m), 5.85 - 5.79 (4H, m), 5.65 - 5.63 (2H, m), 5.60 - 5.50 (4H, m), 4.19 – 4.15 (4H, m), 3.18 (1H, brs), 3.11 (0.8H, brs), 2.51 - 2.47 (4H, m), 2.42 - 2.25 (6H, m), 1.49 – 1.34 (4H, m), 1.25 (33H, m), 0.88 (7H, m). **^{13}CNMR** (150 MHz, CDCl$_3$) δ: 166.8, 166.7, 148.5, 147.5, 127.6, 126.8, 126.7, 125.9, 124.6, 124.1, 122.1, 122, 121.7, 121.3, 60.3, 52.5, 51.1, 50.7, 49.5, 38.6, 37.2, 36.7, 36.3, 34.5, 34.2, 33.7, 32.1, 30.5, 30, 29.8, 29.8, 29.8, 29.8, 29.7, 29.5, 28.3, 28.2, 22.8, 14.4, 14.2. **HRMS** (ESI, m/z) calculated for ([M+Na]) C$_{22}$H$_{34}$O$_2$ 311.2319 found 311.2345.

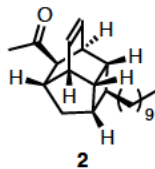**Synthesis of (E)-5-((1S,6R)-8-decylbicyclo[4.2.0]octa-2,4-dien-7-yl)pent-3-en-2-one (8a,8b)**
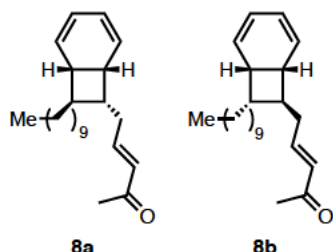
Under nitrogen atmosphere an oven dried round bottom flask was charged with **6a,6b** (10.0 mg, 34.7 μmol, 1.00 eq.), acetylmethylene-triphenylphosphorane (33.1 mg, 100 μmol, 3.00 eq) and anhydrous 1,2-dichloroethane (0.1 mL). The mixture was heated at 40 °C for 24 h. After reaction the solvent was removed in vacuo. The crude material was purified by column chromatography using hexane/Et$_2$O (9.5:0.5) as eluent (R$_f$ = 0.30) affording the desired compound as a colourless oil (6.2 mg, 57%). **IR** (ATR): v/cm^{-1} = 2921, 1721, 1653, 1465, 1192. **^{1}H NMR** (600 MHz, CDCl$_3$) δ: 6.81 - 6.67 (2H, m), 6.07 (2H, dd, J = 15.8 7.8 Hz), 5.89 – 5.84 (2H, m), 5.68 – 5.64 (2H, m), 5.62 – 5.56 (2H, m), 5.53 – 5.48 (2H, m), 3.19 (1H, brs), 3.13 (0.9H, brs), 2.57 – 2.49 (3H, m), 2.46 – 2.27 (5H, m) 2.23 (5H, s), 1.49 – 1.36 (4H, m), 1.26 (35H, m), 0.88 (7H, m). **^{13}CNMR** (150 MHz, CDCl$_3$): 198.7, 147.6, 146.7, 132.1, 131.7, 127.7, 126.9, 126.5, 125.8, 124.7, 124.2, 122.1, 121.3, 52.5, 51.3, 50.8, 49.5, 39.1, 37.2, 36.8, 36.4, 34.6, 34.2, 34.0, 32.1, 30.6, 30.0, 29.9, 29.8, 29.8, 29.5, 28.4, 28.2, 22.9, 14.3. **HRMS** (ESI, m/z) calculated for ([M+Na]) C$_{24}$H$_{38}$O$_2$ 329.2839 found 329.2838.

Synthesis of Endiandric ester J (9)
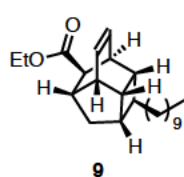
Under nitrogen atmosphere **7a,7b** (20 mg, 56 mmol) was dissolved in anhydrous toluene (20 mL), and heated at 120 °C for 5 hrs. The solvent was removed in vacuo and the crude material was purified by column chromatography using hexane/Et$_2$O (1%) as eluents (R$_f$ = 0.21). The desired product was obtained as a colorless oil (17 mg, 85%). **IR** (ATR): v/cm^{-1} = 2956, 2923, 2853, 1736, 1611, 1532, 1465, 1367, 1305, 1205, 1179, 1042, 790, 691. **^{1}H NMR** (600 MHz, CDCl$_3$) δ: 6.21 - 6.15 (2H, m), 4.13 – 4.03 (2H, m), 3.02 – 2.99 (1H, m), 2.80 (1H, d, J = 3.8 Hz), 2.67 (1H, d, J = 5.5 Hz), 2.58 (1H, dd, J = 6.9 Hz), 2.36 – 2.33 (1H, m), 2.23 – 2.21 (1H, m), 1.91 – 1.87 (1H, m), 1.66 – 1.60 (2H, m), 1.53 – 1.43 (2H, m), 1.26 (21H, m), 0.88 (3H, t, J = 7.0 Hz). **^{13}C NMR** (150 MHz, CDCl$_3$) δ: 175, 131.9, 131.4, 60.3, 49.3, 42.1, 40.4, 40.3, 39.7, 39.6, 38.7, 38.5, 36.5, 35.3, 32.1, 29.9, 29.9, 29.8, 29.8, 29.5, 27.4, 22.8, 14.4, 14.2. **HRMS** (ESI, m/z) calculated for ([M+Na]) C$_{24}$H$_{38}$O$_2$ 381.2764 found 381.2707.
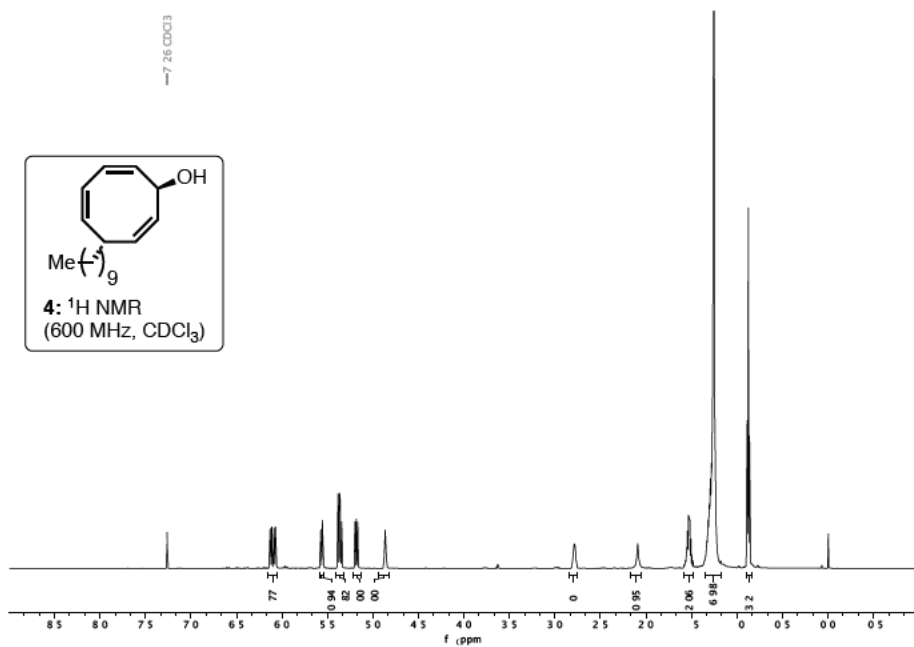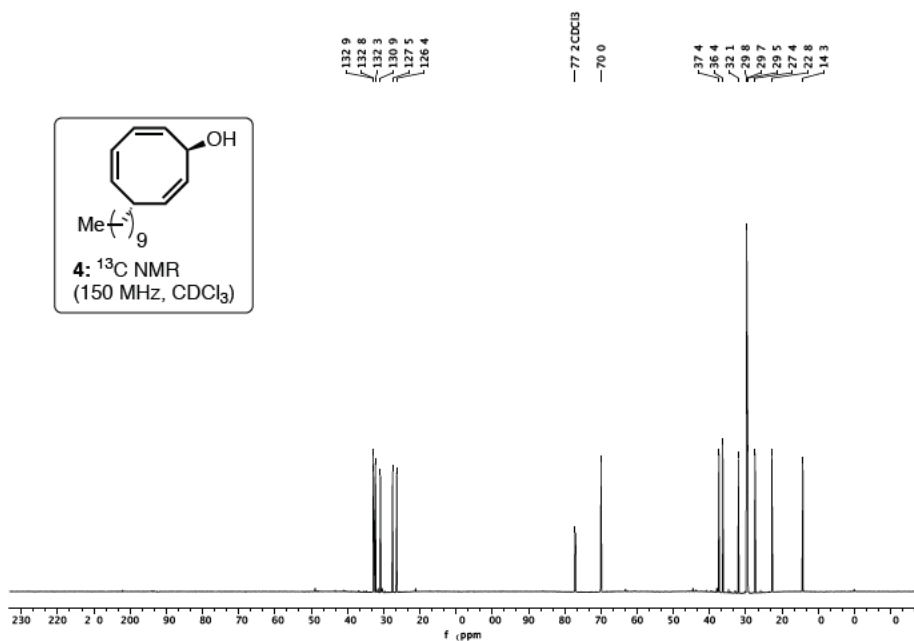
Synthesis of Beilcyclone A (2)

Under nitrogen atmosphere **8a,8b** (40.0 mg, 0.12 mmol) was dissolved in anhydrous toluene (30 mL), and heated at 120 °C for 5 hrs. The solvent was removed in vacuo and the crude material was purified by column chromatography using hexane/Et$_2$O (1%) as eluents as eluent (Rf = 0.27). The desired product was obtained as a colourless oil (25 mg, 62%). **IR** (ATR): v/cm^{-1} = 2954, 2922, 2852, 1714, 1459, 1363, 160, 1169, 1019, 966, 802, 702, 665. **^{1}H NMR** (600 MHz, CDCl$_3$) δ: 6.20 (1H, ddd, J = 8.0, 6.4, 1.0 Hz), 6.11 (1H, ddd, J = 8.0, 6.4, 1.0 Hz), 3.02 (1H, dt, J = 7.3, 4.1 Hz), 2.78 (1H, d, J = 3.6 Hz), 2.68 – 2.65 (2H, m), 2.35 (1H, dt, J = 9.8, 5.4 Hz), 2.23 (1H, dt, J = 6.3, 3.5 Hz), 2.12 (3H, s), 1.89 (1H, ddd, J = 12.7, 7.5, 5.2 Hz), 1.69 – 1.64 (2H, m), 1.53 − 1.45 (2H, m), 1.26 (16H, brs), 0.88 (3H, t, J = 6.9 Hz). **^{13}C NMR** (150 MHz, CDCl$_3$) δ: 209.3, 132.4, 130.5, 57.9, 42.4, 40.4, 40.4, 40.1, 39.8, 38.5, 37.0, 36.5, 35.6, 32.1, 29.9, 29.9, 29.8, 29.8, 29.5, 28.5, 27.5, 22.8, 14.3. **HRMS** (ESI, m/z) calculated for ([M+Na]) C$_{24}$H$_{38}$O$_2$ 351.2658 found 351.2687.

NMR spectra

Figure 1: ^{1}H NMR of **4**

Figure 2: ^{13}C NMR of **4**

9
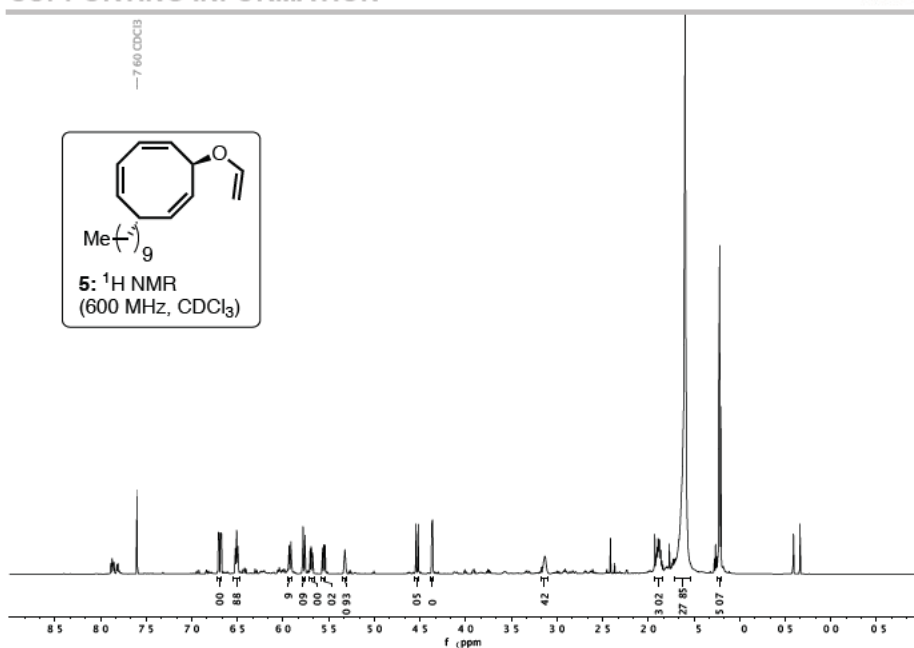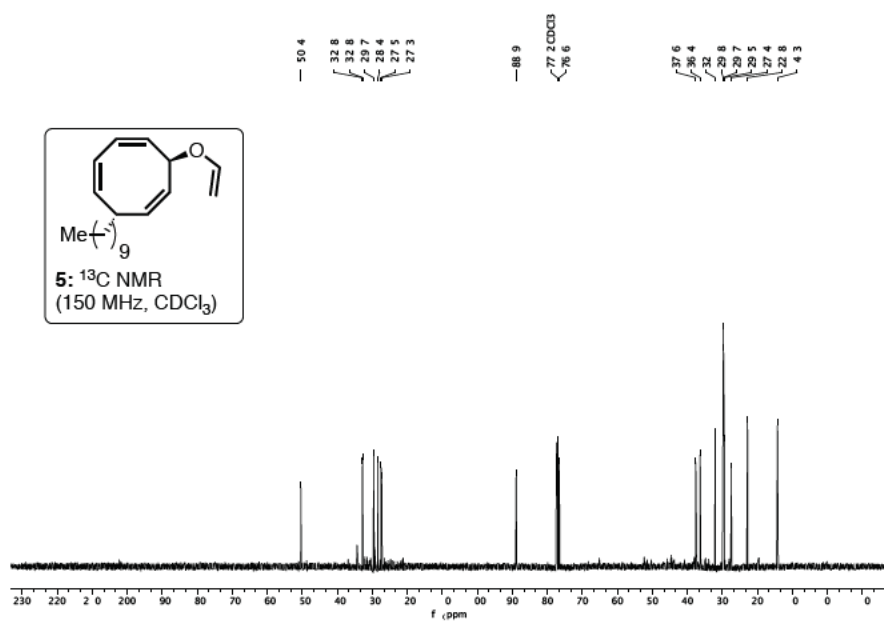
Figure 3: ^{1}H NMR of **5.**

Figure 4: ^{13}C NMR of **5**
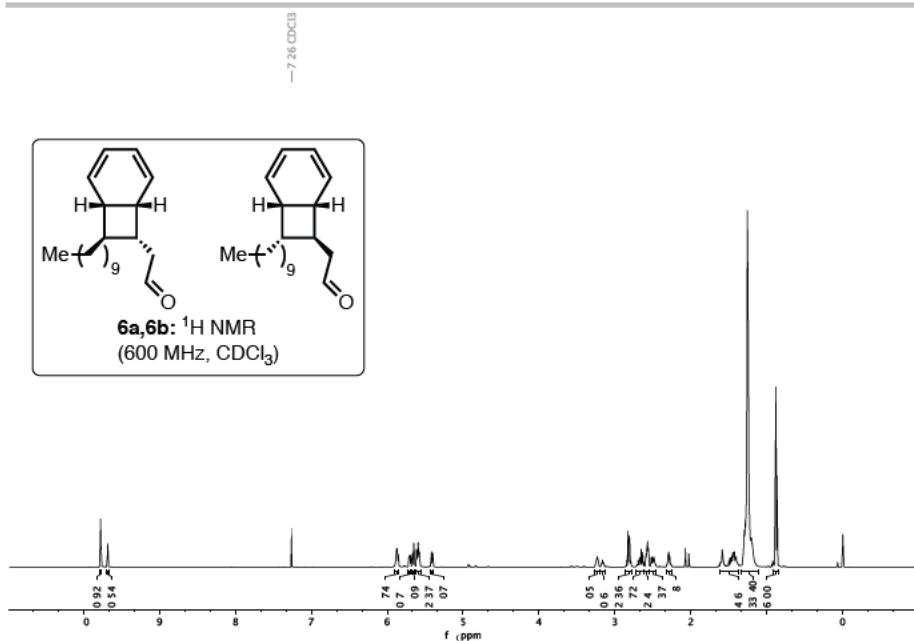
Figure 5: ^{1}H NMR of 6a,6b.
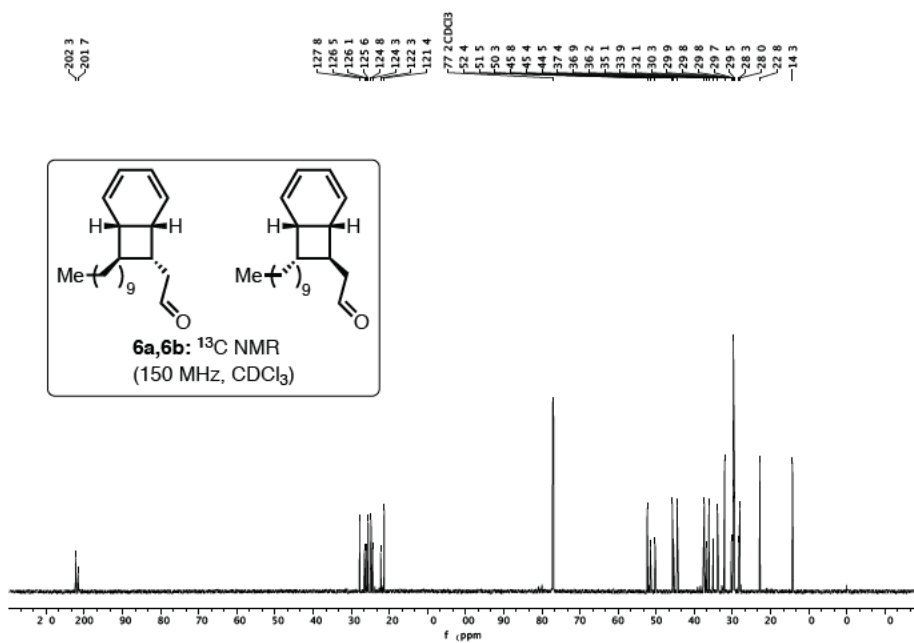
Figure 6: ^{13}C NMR of 6a,6b
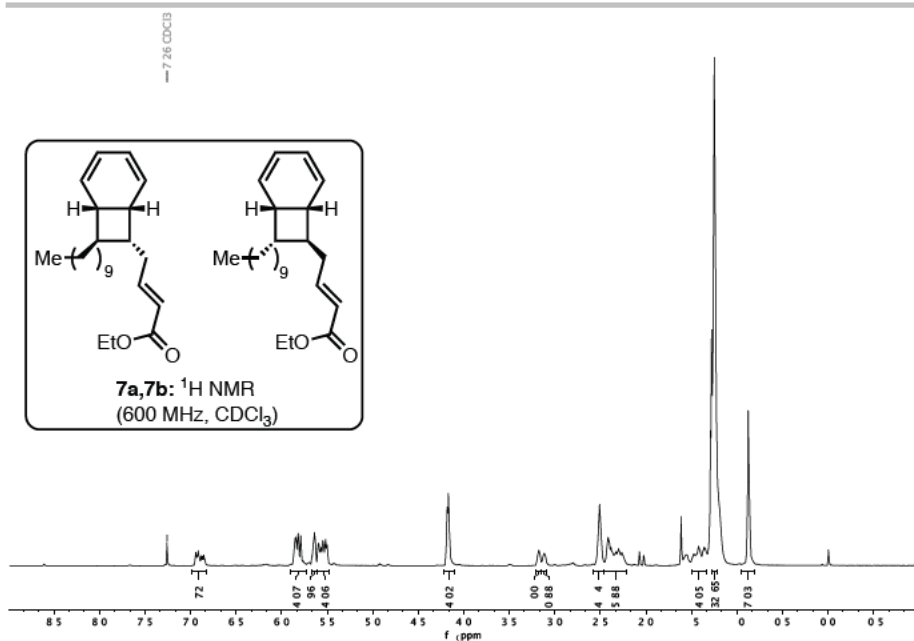
Figure 7: ¹H NMR of **7a,7b**.
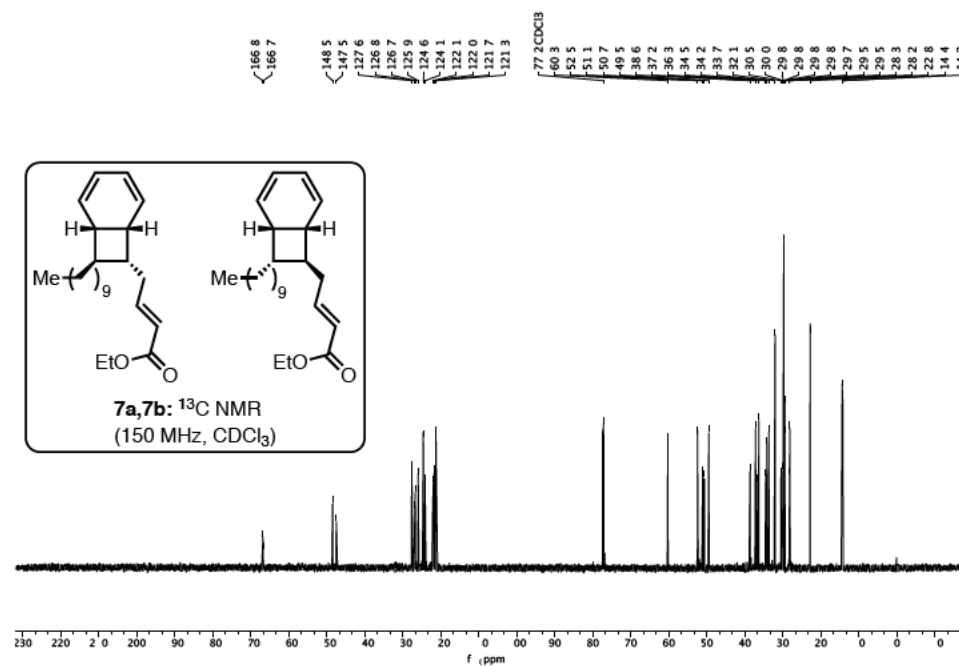
Figure 8: ¹³C NMR of **7a,7b**
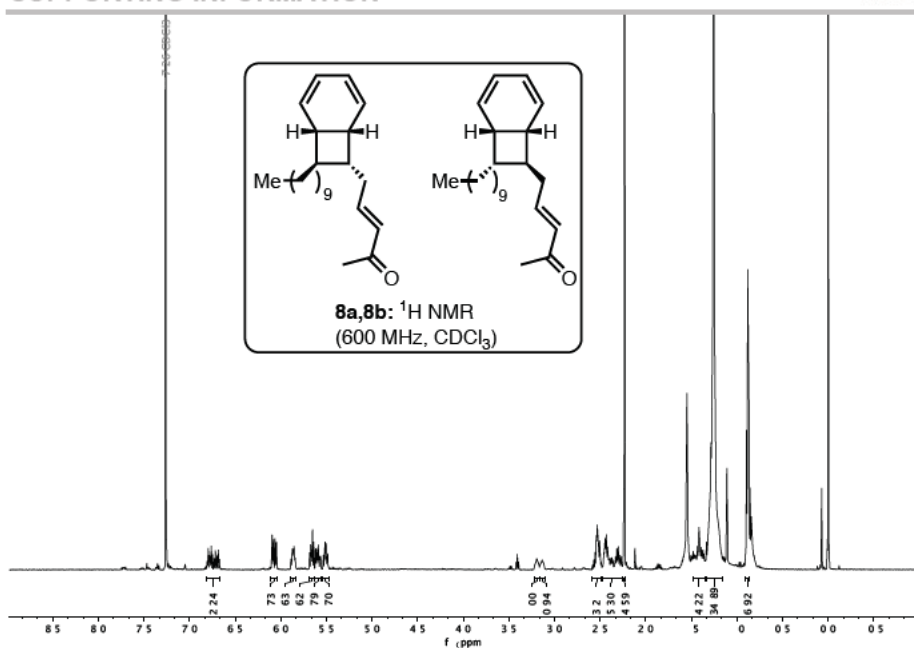
Figure 9: ¹H NMR of **8a,8b**.
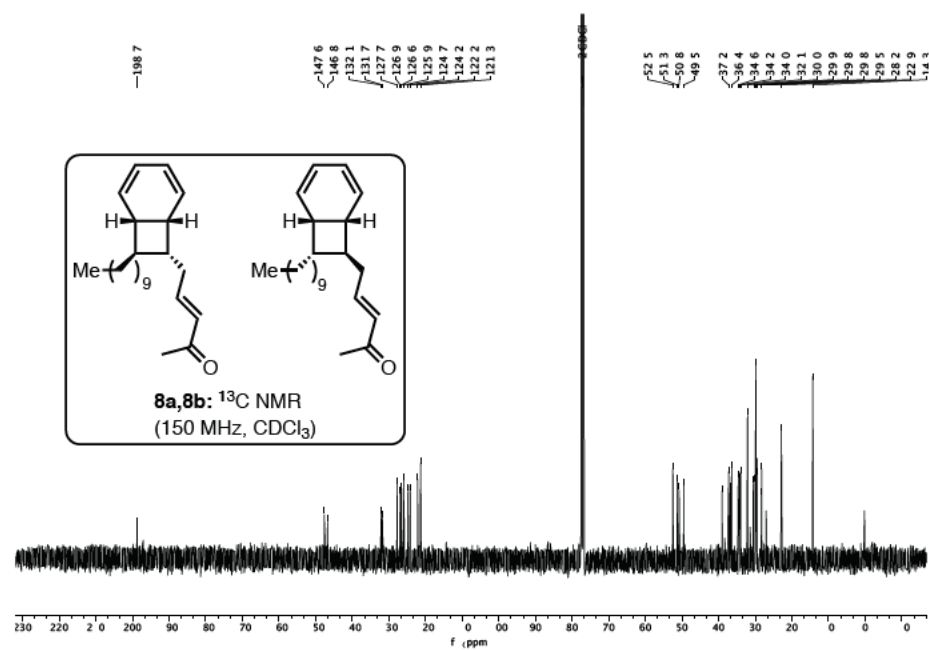
Figure 10: ¹³C NMR of **8a,8b**

13
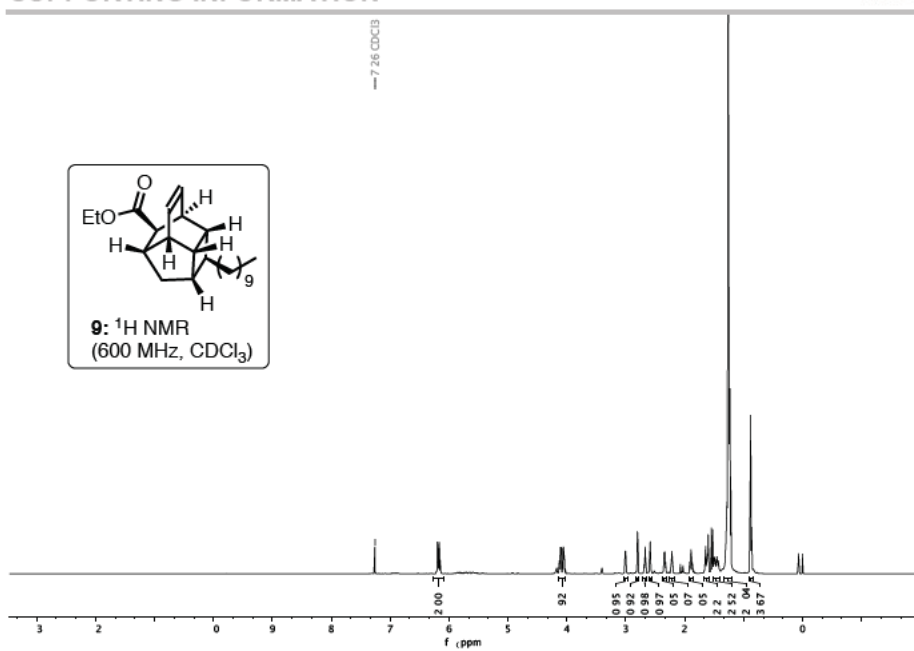
Figure 11: ^{1}H NMR of **9**
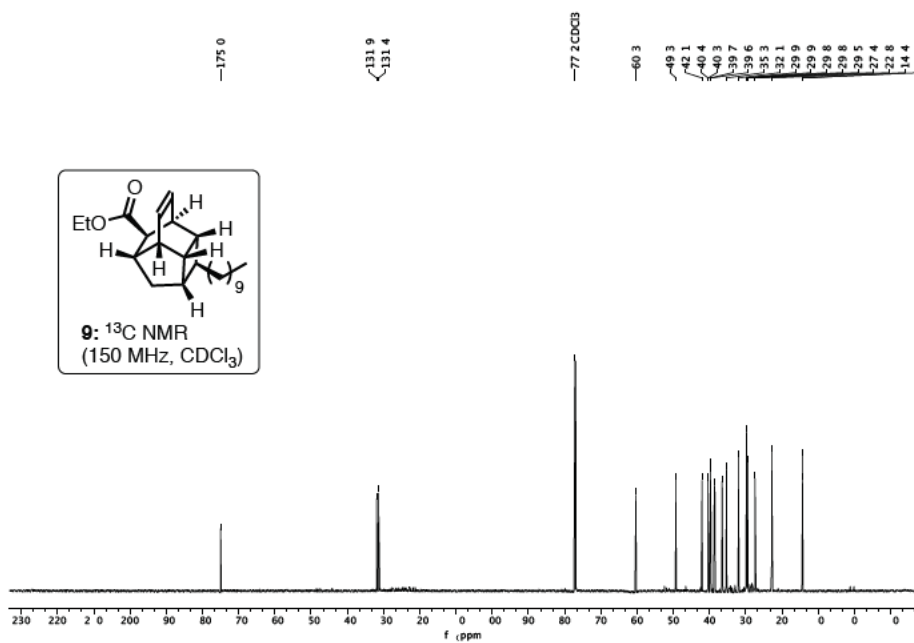
Figure 12: ^{13}C NMR of **9**

14
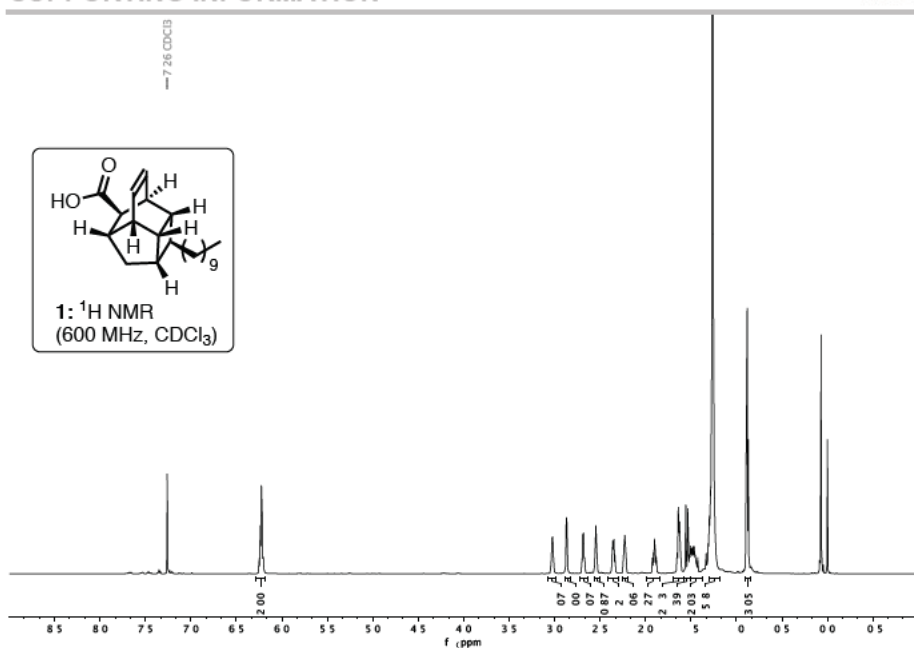
Figure 13: ^{1}H NMR of Endiandric acid J
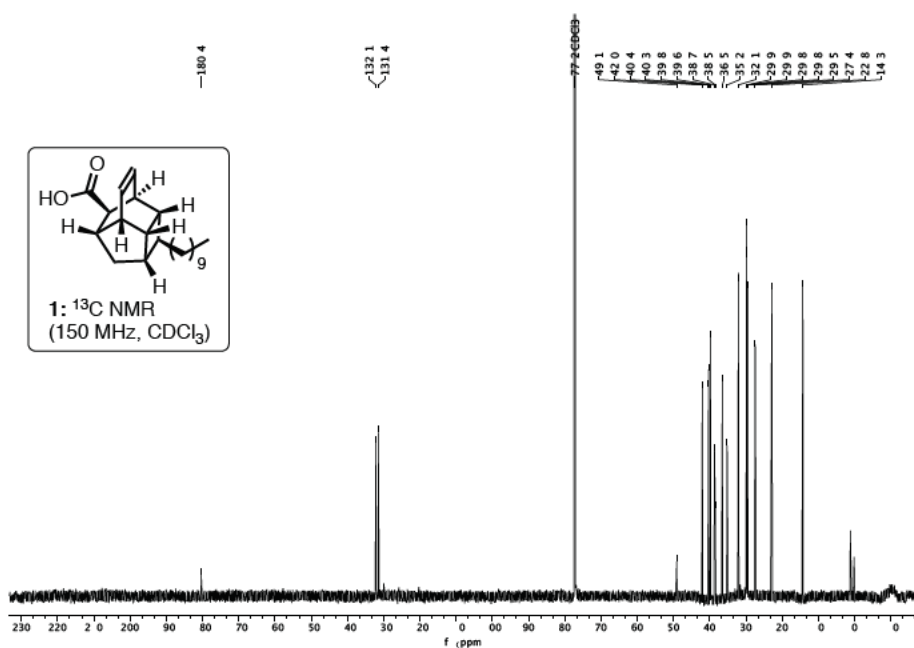
Figure 14: ^{13}C NMR of Endiandric acid J

Figure 15: ¹H NMR of Beilcyclone A

Figure 16: ¹³C NMR of Beilcyclone A

16

Tables of NMR data

Table of ^{1}H and ^{13}C NMR data of natural and synthetic Endiandric acid J (**1**).
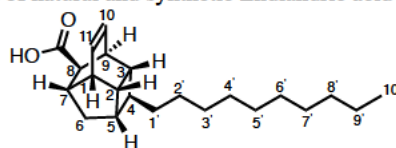
Endiandric Acid J (**1**)

^{1}H NMR of Endiandric acid J		
Assignment	**Synthetic (600 MHz)**	**Natural (400 MHz)**
11	6.19 – 6.26 (1H, m),	6.23 (ddd J = 10.0, 8.0, 2.0 Hz)
10	6.19 – 6.26 (1H, m)	6.23 (ddd, J = 10.0, 8.0, 2.0 Hz)
9	3.02 – 3.00 (1H, m)	3.02 (dt, J = 7.2, 4.8 Hz)
8	2.87 (1H, d, J = 3.8 Hz)	2.87 (d, J = 4.0 Hz)
1	2.65 – 2.71 (1H, m)	2.69 (ddd, J = 7.2, 4.8, 2.0 Hz)
7	2.54 (1H, t, J = 5.2 Hz)	2.54 (t, J = 5.2 Hz)
2	2.34 (1H, dt, J = 8.9, 5.5 Hz)	2.35 (dt, J = 8.4, 5.6 Hz)
5	2.23 (1H, br. t, J = 6.4 Hz)	2.23 (br. t, J = 6.8 Hz)
6	1.89 (1H, ddd, J = 12.9, 7.6, 5.4 Hz)	1.90 (ddd, J = 12.6, 7.6, 5.6 Hz)
3	1.66 – 1.68, (1H, m),	1.61 – 1.66 (m)
4	1.66 – 1.68, (1H, m),	1.61 – 1.66, m
6	1.54 (1H, d, J = 12.7 Hz),	1.54 (d, J = 12.6 Hz)
1'	1.43 – 1.51 (2H, m),	1.43 – 1.50 (m)
2' – 9'	1.26 (16H, m)	1.26 (br. S)
10'	0.88 (3H, t, J = 6.9 Hz)	0.88 (t, J = 6.6 Hz)

^{13}C NMR of Endiandric acid J		
Assignement	**Synthetic**	**Natural**
C=O	180.3	180.1
H-C	132.1	131.9
H-C	131.4	131.3
H-C	49.1	48.9
H-C	42.0	41.8
H-C	40.4	40.1
H-C	40.3	39.4
H-C	39.8	39.6
H-C	39.6	38.5
H-C	38.7	38.2
CH$_2$	36.5	36.3
H-C	35.2	35.0
CH$_2$	32.1	31.9
CH$_2$	29.9	29.4 – 29.7
CH$_2$	29.9	29.4 – 29.7
CH$_2$	29.9	29.4 – 29.7
CH$_2$	29.8	29.4 – 29.7
CH$_2$	29.8	29.4 – 29.7
CH$_2$	29.8	29.4 – 29.7
CH$_2$	29.5	29.4 – 29.7
CH$_2$	27.4	27.3
CH$_2$	22.9	22.7
CH$_3$	14.3	14.1

Table of ^{1}H and ^{13}C NMR data of natural and synthetic Beilcyclone A (2).
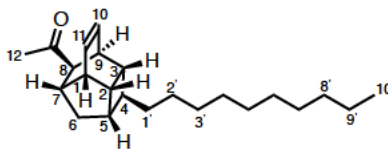
Beilcyclone A (2)

^{1}H NMR of Bilcyclone A		
Assignement	Synthetic (600 MHz)	Natural (600 MHz)
11	6.20 (1H, ddd, J = 8.0. 6.4, 1.0 Hz)	6.20 (ddd, J = 8.0, 6.4, 0.8 Hz)
10	6.11 (1H, ddd, J = 8.0, 6.4, 1.0 Hz)	6.10 (ddd, J = 8.0, 6.0, 1.0 Hz)
9	3.02 (1H, dt, J = 7.3, 4.1 Hz)	3.02 (dt, J = 6.0, 4.0 Hz)
8	2.78 (1H, d, J = 3.6 Hz)	2.78 (d, J = 4.0 Hz)
1 and 7	2.68 − 2.65 (2H, m)	2.68 (m)
		2.66 (m)
2	2.35 (1H, dt, J = 9.8, 5.4 Hz)	2.35 (dt, J = 7.2, 6.0 Hz)
5	2.23 (1H, t, J = 6.3 Hz, 3.5 Hz)	2.23 (br. t, J = 6.0 Hz)
12	2.12 (3H, s)	2.12 (s)
6	1.89 (1H, ddd, J = 12.7, 7.5, 5.2 Hz)	1.89 (ddd, J = 12.8, 7.7, 5.0 Hz)
4 and 3	1.69 − 1.64 (2H, m)	1.64 − 1.70 (m)
6	1.53 − 1.45 (2H, m)	1.52 (m)
1$^{'}$		1.46 (d, J = 12.8 Hz)
2$^{'}$ − 9$^{'}$	1.26 (16H, br. s)	1.27 (br. s)
10$^{'}$	0.88 (3H, t, J = 6.9 Hz)	0.88 (t, J = 6.9 Hz)

^{13}C NMR of Beilcyclone A		
Assignement	**Synthetic**	**Natural**
C=O	209.3	209.2
H-C	132.4	132.3
H-C	130.5	130.3
H-C	57.9	57.8
H-C	42.4	42.2
H-C	40.4	40.3
H-C	40.1	40.2
H-C	40.1	39.9
H-C	39.8	39.6
H-C	38.5	38.3
H-C	37.0	36.9
H-C	36.5	36.3
H-C	35.6	35.5
H-C	32.1	31.9
CH_2	29.9 – 29.5	29.4 − 29.8
$COCH_3$	28.5	28.3
CH_2	27.5	27.3
CH_2	22.8	22.7
CH_3	14.3	14.1

Computational Studies

Calculations were carried out with density functional theory (DFT) using Gaussian 16 (revision A.03).[2] Geometries were optimised in the gas phase at the M06-2X/6-31G(d) level.[3] Stable ground states and transition states were identified by the number of imaginary vibrational frequencies. Zero-point energies and thermal corrections at 333.15 K (**10-13**), 393.15 K (**14-17**) and 1 atm were determined from the unscaled frequencies. The transition states were shown to connect reactants and products using intrinsic reaction coordinate calculations.[4] Single-point energy calculations of the optimised geometries were carried out in the gas phase at the M06-2X/6-311+G(d,p) level and in toluene solvent using the SMD continuum solvent model[5] at the M06-2X/6-31G(d) level. The optimised geometries are given below in Cartesian coordinates and the energies given in units of Hartree. The Gibbs free energy in toluene solution at 333.15 K (**10-13**), and 393.15 K (**14-17**) was calculated as Gsoln = EM06-2X/6-311+G(d,p) + ΔGthermal,M06-2X/6-31G(d) + GM06-2X/6-31G(d),toluene − EM06-2X/6-31G(d). The reaction free energy profiles below were calculated from the relative values of Gsoln for the various species.

Kinetic simulations were performed using the software program *KinTec Explorer* (https://kintekcorp.com).

Figure 17 shows the reaction profile of aldehyde **14**. The calculated transition structure of a thermal Claisen rearrangment in a chair-like conformation is located at 139.8 kJ/mol above the energy of the vinyl ether **17**. This activation barrier is inconsistent with the experimental reaction temperature of 60 °C, but we cannot discount the possibility of hydrogen bonding or transition metal catlaysis under the reaction conditions.
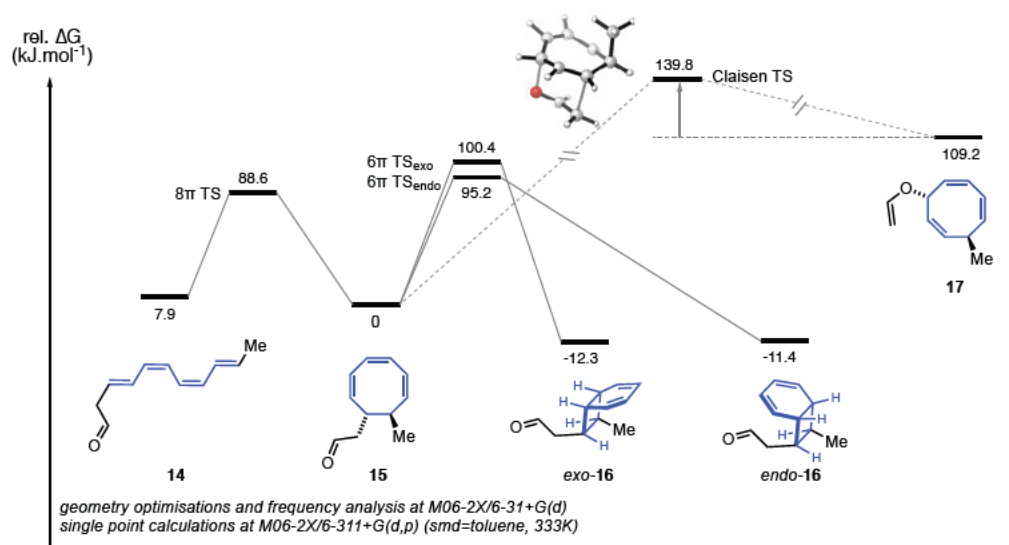
*Figure 17. Computational analysis of the 8π/6π-Claisen rearrangement sequence of vinyl ether **17**.*

Figure 18 shows a kinetic simulation starting from a population oone antipode of *endo*-**16** at 60 °C. Racemisation is predicted within hours, and equillibration between diasteroisomers within ~1.5 days.

21
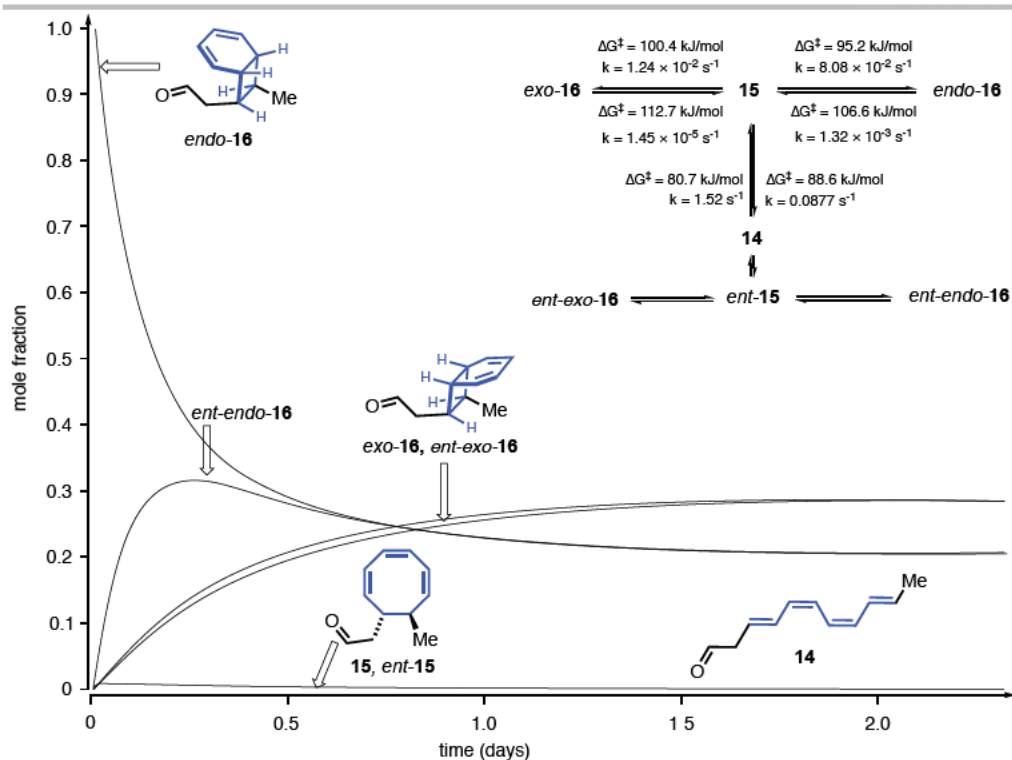
*Figure 18. Kinetic simulation from aldehyde endo-**16** at 333 K.*
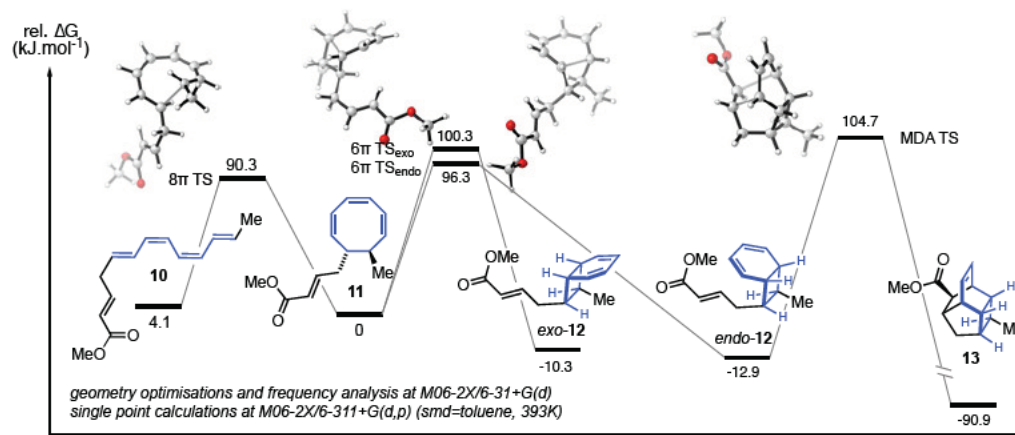
*Figure 19. Computational analysis of the 8π/6π/DA rearrangement sequence of ester **10**.*

Figure 20 shows a kinetic simulation starting from a population oone antipode of *endo*-**12** at 120 °C. Racemisation and equillibration between diasteroisomers is predicted within minutes.
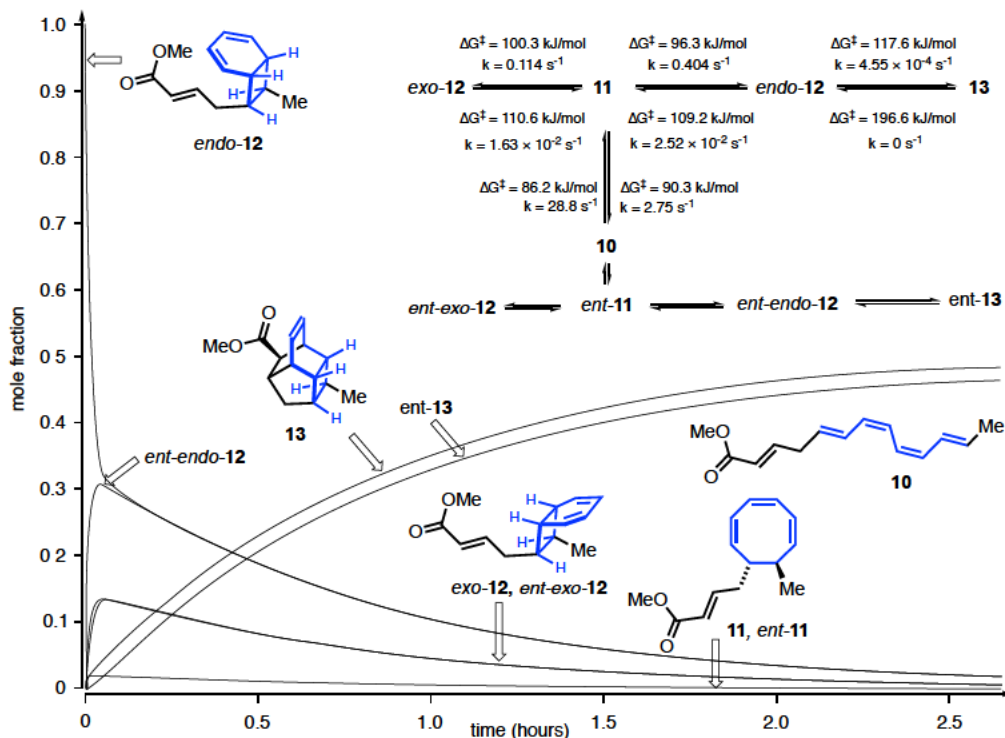
Figure 20. Kinetic simulation of ester endo-**12** at 393 K.
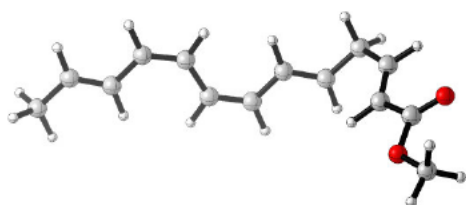
tetraene **10**
M06-2X/6-311+G(d,p) smd toluene
Energy (0K, vacuum) = -694.581874
Gibbs free energy (393K) = -694.381651

C	-1.26637300	-0.72122600	1.10092100
H	-0.96692100	-0.55518700	2.13449700
C	-2.51256200	-0.35306900	0.73692700
H	-3.14129100	0.08875000	1.50533400
C	-3.09164800	-0.49221900	-0.58682800
H	-2.46512600	-0.93224200	-1.35790000

```
C      -0.25385900  -1.32855500   0.25080700
H      -0.50036300  -1.52012400  -0.79217000
C      -4.33950400  -0.12253000  -0.94398400
H      -4.64088200  -0.28732900  -1.97747100
C      -5.35256000   0.48378700  -0.09428300
H      -5.11013800   0.67499000   0.94957800
C       0.96493700  -1.66473800   0.69255500
H       1.22408500  -1.46925300   1.73407200
C      -6.57058500   0.81733900  -0.54100900
H      -6.81164400   0.62506400  -1.58719400
C      -7.64542900   1.44254200   0.29161600
H      -7.31077400   1.59515900   1.32123400
H      -8.54358300   0.81460700   0.31232300
H      -7.94732800   2.41319500  -0.11838600
C       2.03248300  -2.29592200  -0.14896500
H       1.63824400  -2.52785800  -1.14788300
H       2.32631500  -3.26303200   0.28383800
C       3.27579200  -1.46336300  -0.30533100
H       4.14412300  -1.94708800  -0.75111200
C       3.39769800  -0.18374200   0.04793100
H       2.58470200   0.38514800   0.48773700
C       4.68495200   0.51618200  -0.17263800
O       5.68280700   0.02919400  -0.65138300
O       4.61438900   1.79710200   0.23452100
C       5.81363100   2.54532100   0.05498200
H       5.59905000   3.54598400   0.42695600
H       6.08850000   2.57750600  -1.00175500
H       6.63362500   2.09250400   0.61700200
```
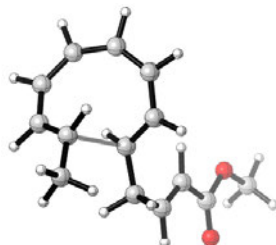

tetraene 10 8pi-TS
M06-2X/6-311+G(d,p) smd toluene
Energy (0K, vacuum) = -694.55896
Gibbs free energy (393K) = -694.34883
imaginary frequency: -348.05

```
C      -3.16987200   0.95789500  -1.56686200
H      -3.43018300   1.20959200  -2.59333800
C      -2.91322400   2.06190500  -0.76199500
H      -3.18169200   2.99624100  -1.25450900
C      -2.43170100   2.30370700   0.55228700
H      -2.64911600   3.32537200   0.86322500
C      -1.72520400   1.60432200   1.52393600
H      -1.65147700   2.12129300   2.47877600
C      -3.16997700  -0.41722400  -1.27493300
```

24

H	-3.20195700	-1.10301500	-2.12187000
C	-3.06020100	-0.95077400	-0.00781300
H	-3.30750700	-0.29615600	0.82023600
C	-1.07601200	0.35818600	1.46909900
H	-0.76024600	-0.07979200	2.41655500
C	-0.88356200	-0.37322700	0.31613900
H	-0.91993100	0.16724300	-0.62339300
C	-3.18055500	-2.42523900	0.25204700
H	-2.58410200	-2.73296100	1.11651700
H	-2.86280400	-3.01170300	-0.61567900
H	-4.22258900	-2.68789900	0.47054900
C	-0.08105000	-1.64420000	0.30948700
H	-0.21405900	-2.18209300	1.25937300
H	-0.45126700	-2.32319900	-0.47031800
C	1.39409400	-1.44048500	0.08774800
H	1.99351200	-2.33609800	-0.07312000
C	2.02819300	-0.26784900	0.07680900
H	1.52201300	0.67903900	0.23504800
C	3.49244200	-0.23594500	-0.15060700
O	4.20127400	-1.19760300	-0.33829200
O	3.95842200	1.02622800	-0.12333700
C	5.36224600	1.14675800	-0.33468500
H	5.63689400	0.74344300	-1.31203900
H	5.91234900	0.60246300	0.43634300
H	5.58089800	2.21225500	-0.28326600

cyclooctatriene 11
M06-2X/6-311+G(d,p) smd toluene
Energy (0K, vacuum) = -694.597663
Gibbs free energy (393K) = -694.383209

C	3.52806600	0.16455800	-0.78005100
H	4.53899000	-0.12860800	-1.06826900
C	3.29169600	1.48414500	-0.83483300
H	4.13635500	2.07436900	-1.19229200
C	2.12851800	2.34055800	-0.55342500
H	2.07394300	3.21019000	-1.20766400
C	1.24728600	2.30950900	0.46134800
H	0.56871400	3.15666200	0.55445600
C	1.12424700	1.27631600	1.48843900
H	0.96574700	1.61987400	2.50940000
C	1.11443700	-0.03792100	1.24144600
H	0.99102100	-0.72353300	2.08047500
C	1.20631400	-0.66977300	-0.12231500
H	0.86969300	0.05835000	-0.87136000

C	2.66090500	-1.02866700	-0.47939100
H	2.63421100	-1.61772200	-1.41132300
C	0.29445600	-1.89966500	-0.21037600
H	0.52226500	-2.60055500	0.60566300
H	0.51113100	-2.45512000	-1.13455200
C	-1.17805600	-1.61826100	-0.18058300
H	-1.83928900	-2.48441900	-0.20465500
C	3.33732400	-1.90654500	0.58373200
H	2.78075400	-2.83373700	0.75275600
H	3.41471700	-1.36682000	1.53223000
H	4.34965400	-2.18049200	0.27079400
C	-1.76029300	-0.41843000	-0.14272300
H	-1.20859700	0.51510400	-0.10595800
C	-3.23952200	-0.33126800	-0.13942100
O	-4.00645700	-1.26607300	-0.16134200
O	-3.64788100	0.95170900	-0.10872000
C	-5.06178200	1.12517200	-0.10487400
H	-5.50294200	0.68586000	-1.00252100
H	-5.23027800	2.20079400	-0.08089200
H	-5.50295200	0.64636100	0.77236100
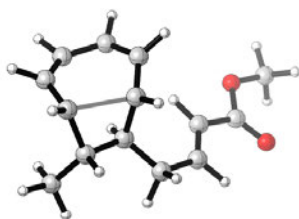
*cyclooctatriene **11** 6pi-exo-TS*
M06-2X/6-311+G(d,p) smd toluene
Energy (0K, vacuum) = -694.559128
Gibbs free energy (393K) = -694.345014
imaginary frequency: -578.11

C	-1.33497900	0.20928700	1.25217300
H	-1.28733000	-0.26186300	2.23635700
C	-0.84582000	1.51281100	1.13515100
H	-0.33712400	1.98292400	1.97487100
C	-1.12957200	2.27993100	0.01257900
H	-0.58041300	3.20325200	-0.15533600
C	-2.31858600	2.11333000	-0.71987700
H	-2.55288800	2.89968400	-1.43404300
C	-3.37901300	1.30447200	-0.31043400
H	-4.36399300	1.74392600	-0.47920800
C	-3.34837700	0.13544900	0.47415700
H	-4.26745500	-0.01825800	1.04781600
C	-2.69934700	-1.17322900	0.02069800
H	-2.88771400	-1.91604600	0.80910500
C	-1.23962900	-0.77767500	0.09319700
H	-0.96561200	-0.23101400	-0.81780800
C	-0.27329300	-1.93656000	0.31683600

```
H     -0.47556400   -2.71777900   -0.43237200
H     -0.49538700   -2.40948100    1.28542900
C      1.19138600   -1.62266900    0.26550800
H      1.87261300   -2.44247600    0.49338400
C     -3.21947600   -1.70633700   -1.30859500
H     -2.73453800   -2.65269300   -1.57315200
H     -3.02427200   -0.97989200   -2.10437300
H     -4.29955100   -1.88200000   -1.26860300
C      1.74468500   -0.44974500   -0.04657900
H      1.16917000    0.43940700   -0.28155900
C      3.22132600   -0.32946300   -0.06842500
O      3.59990200    0.91702900   -0.41115800
O      4.01053400   -1.21104900    0.18204500
C      5.00926600    1.11779100   -0.45814500
H      5.46653600    0.44740600   -1.18952000
H      5.45554300    0.92499500    0.52019400
H      5.15306100    2.15771600   -0.74773900
```


cyclooctatriene 11 6pi-endo-TS
M06-2X/6-311+G(d,p) smd toluene
Energy (0K, vacuum) = -694.559041
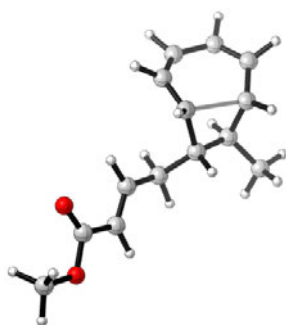Gibbs free energy (393K) = -694.346533
imaginary frequency: -572.51

```
C     -3.15335400    0.50354900    0.96537600
H     -3.15249100    1.02827300    1.92310400
C     -4.27867600   -0.25760400    0.64033500
H     -5.16097200   -0.23266900    1.27741900
C     -4.23461500   -1.18190200   -0.39601300
H     -5.16185100   -1.61576500   -0.76263500
C     -3.04840500   -1.84826000   -0.75106200
H     -3.16317400   -2.70929200   -1.40585900
C     -1.86332600   -1.77469700   -0.01678200
H     -1.34445700   -2.72978900    0.08779100
C     -1.38251700   -0.71683900    0.77849700
H     -0.74059200   -1.05311800    1.59774100
C     -0.98560600    0.65015200    0.21803500
H     -0.56595100    1.23735400    1.04684000
C     -2.35140900    1.20297400   -0.12556400
H     -2.66961400    0.80097700   -1.09485100
C      0.04134500    0.60627800   -0.92357300
H      0.23511700    1.62553900   -1.28009000
```

H	-0.40942600	0.03856500	-1.74960100
C	-2.49539700	2.71910700	-0.12341300
H	-3.53031300	3.01588600	-0.31929500
H	-1.86129400	3.17588700	-0.89105700
H	-2.20090100	3.13328000	0.84776900
C	1.32165700	-0.04903400	-0.51529700
H	1.27589800	-1.09782200	-0.22030900
C	2.50996600	0.55422800	-0.46067000
H	2.65241200	1.59495400	-0.73654600
C	3.70346800	-0.20097400	-0.01510000
O	4.80420300	0.57448400	-0.03842800
O	3.71959500	-1.35973000	0.33015000
C	6.00030000	-0.07880500	0.37690500
H	6.21466000	-0.93107700	-0.27196400
H	5.90281600	-0.43651600	1.40447500
H	6.78915500	0.66826800	0.30325400
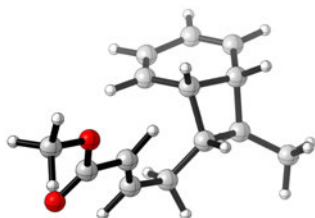
bicyclo[4.2.0]octadiene **12**-*endo*
M06-2X/6-311+G(d,p) smd toluene
Energy (0K, vacuum) = -694.603461
Gibbs free energy (393K) = -694.388117

C	1.20197000	-1.51340800	0.48293300
H	0.23909800	-1.75207600	0.93231600
C	2.30937300	-2.15894200	0.86945500
H	2.25193500	-2.91792700	1.64490500
C	3.61466300	-1.91617200	0.23625200
H	4.44150200	-2.56881300	0.50150300
C	3.77830100	-0.93596600	-0.65941400
H	4.73998100	-0.77567700	-1.14057000
C	1.21119200	-0.47408400	-0.60170600
H	0.57671100	-0.80919600	-1.43248500
C	2.64735700	-0.00661200	-0.97742200
H	2.68591200	0.32978800	-2.02004000
C	0.92355100	0.97642200	-0.10640700
H	0.48785500	1.56389200	-0.92609600
C	2.45002500	1.22082000	-0.04344700
H	2.81432000	0.95872000	0.95850700
C	2.99254300	2.56966600	-0.47521300
H	2.64490400	2.81944400	-1.48405800
H	4.08742700	2.57307800	-0.48445700
H	2.66162000	3.36558900	0.20108100
C	0.13465100	1.19820600	1.17205400
H	0.22928700	2.24946700	1.48219500

H	0.59249200	0.61346100	1.98395700
C	-1.32080400	0.85035300	1.10963800
H	-1.90685200	1.00047100	2.01627200
C	-1.96581900	0.36670000	0.04591900
H	-1.48297800	0.17884800	-0.90761500
C	-3.41344400	0.06571000	0.14085100
O	-4.10483000	0.21258100	1.12177300
O	-3.88637200	-0.40572000	-1.02828300
C	-5.27579100	-0.72185900	-1.02342500
H	-5.48988900	-1.48894200	-0.27577100
H	-5.50198300	-1.08666100	-2.02418500
H	-5.86834900	0.16663700	-0.79379000
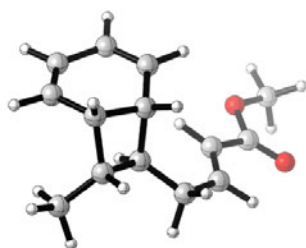
bicyclo[4.2.0]octadiene **12-exo**
M06-2X/6-311+G(d,p) smd toluene
Energy (0K, vacuum) = -694.602865
Gibbs free energy (393K) = -694.387143

C	0.75940200	1.49822100	-0.96373500
H	-0.16627300	1.64788000	-1.51372600
C	1.24480100	2.45354800	-0.16182600
H	0.71874200	3.39620600	-0.04123300
C	2.51998100	2.27389000	0.54741900
H	2.82669300	3.04348400	1.25042000
C	3.32276800	1.23016500	0.30461500
H	4.28877800	1.15852200	0.80130000
C	1.46664000	0.18199400	-1.08234700
C	2.96929900	0.14642400	-0.67393000
C	1.19750800	-0.90403200	0.00197500
H	0.95297700	-0.41284800	0.95324000
C	2.70589900	-1.24328500	-0.02309400
H	2.88456900	-2.02226600	-0.77646700
C	3.38147900	-1.61558400	1.28383500
H	3.20448500	-0.84601300	2.04263100
H	4.46400100	-1.72751500	1.16038600
H	2.98942300	-2.56461200	1.66523700
C	0.22528600	-2.03187800	-0.29036100
H	0.39150100	-2.85250400	0.42516000
H	0.45778200	-2.46290000	-1.27569700
C	-1.23114700	-1.67870600	-0.26105200
H	-1.93282000	-2.46086700	-0.55060000
C	-1.75165800	-0.50291800	0.09499100
H	-1.15203400	0.34831900	0.40147100

29

```
C        -3.22235300  -0.32280600   0.07458200
O        -4.03648800  -1.16077900  -0.23736400
O        -3.56128300   0.92429500   0.45368100
C        -4.96230100   1.18236200   0.46340600
H        -5.38306300   1.04447000  -0.53527800
H        -5.07292900   2.21602300   0.78776600
H        -5.47032200   0.50529200   1.15394900
H         1.32382600  -0.25826700  -2.07607000
H         3.70321500   0.13509000  -1.48989200
```
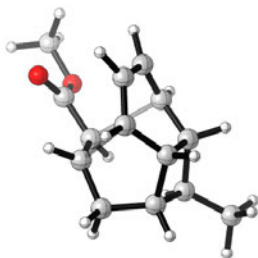

bicyclo[4.2.0]octadiene **12**-*endo IMDA TS*
M06-2X/6-311+G(d,p) smd toluene
Energy (0K, vacuum) = -694.567091
Gibbs free energy (393K) = -694.343315
imaginary frequency: -478.95

```
C         0.77474600   1.88408400  -0.38261800
H         0.99826900   2.84041000   0.08813300
C        -0.27266600   1.81211800  -1.28706700
H        -0.93195800   2.66274800  -1.42966300
C        -0.66344500   0.55284600  -1.77883500
H        -1.62095700   0.45356000  -2.28254600
C        -0.00036100  -0.56802100  -1.31807800
H        -0.40256600  -1.55754600  -1.52881600
C         1.92040100   0.91218200  -0.51095600
H         2.73414700   1.36951500  -1.08259500
C         1.48817200  -0.46738000  -1.07236900
H         1.97459300  -0.72470300  -2.02314800
C         2.38139400   0.23137800   0.80627800
H         3.41860800   0.41186600   1.11022200
C         2.17655300  -1.16016200   0.13522900
H         1.55402900  -1.86051900   0.70073900
C         3.48819100  -1.83700200  -0.23782800
H         4.13178100  -1.14995100  -0.80031700
H         3.31498900  -2.71957600  -0.86236000
H         4.03642900  -2.15164200   0.65616700
C         1.40754400   0.60785900   1.92553300
H         1.73307400   1.54856700   2.38191100
H         1.41567100  -0.15373300   2.71560400
C         0.01966300   0.78069200   1.35183200
H        -0.57097500   1.64502500   1.63702000
C        -0.68513500  -0.31727300   0.88082300
H        -0.35249000  -1.33555700   1.03465700
C        -2.10360800  -0.12744000   0.56372100
```

O	-2.66275500	0.94724100	0.50285600
O	-2.72910300	-1.29374700	0.28489100
C	-4.09532000	-1.15604700	-0.08727900
H	-4.46129900	-2.16685500	-0.26358500
H	-4.18709400	-0.55194900	-0.99390000
H	-4.66614900	-0.67462200	0.71019400
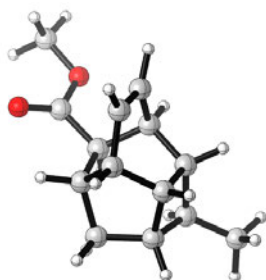
IMDA product 13
M06-2X/6-311+G(d,p) smd toluene
Energy (0K, vacuum) = -694.646924
Gibbs free energy (393K) = -694.417819

C	1.91165300	-0.73632000	0.69906500
H	2.64950300	-1.05897900	1.43580000
C	1.43854300	0.73777000	0.82872000
H	1.77978300	1.26889600	1.72372400
C	2.41270700	-0.42475400	-0.74206400
H	3.43469700	-0.71462800	-1.00510100
C	2.22563900	1.08927700	-0.46210600
H	1.66297800	1.64146000	-1.22557100
C	3.53713200	1.80540500	-0.17338400
H	4.11521000	1.25944600	0.58174800
H	3.35999800	2.81642600	0.20813000
H	4.15320500	1.88160000	-1.07535100
C	1.35913900	-1.07172800	-1.65030100
H	1.69631200	-2.07319600	-1.94210100
H	1.17960500	-0.50354000	-2.57041900
C	-2.10691700	0.01305000	-0.56070900
O	-2.73062500	-0.96472500	-0.89089100
O	-2.70262900	1.15106400	-0.15461900
C	-4.12717200	1.10166900	-0.12511500
H	-4.45225600	2.08263600	0.21851200
H	-4.46578700	0.32119800	0.55996600
H	-4.52328500	0.89152300	-1.12107200
C	0.10071400	-1.20239900	-0.77716400
H	-0.61732400	-1.91769500	-1.18289500
C	-0.59522700	0.15747300	-0.56806000
H	-0.36590500	0.83464000	-1.40085200
C	-0.10648900	0.79058300	0.76818600
H	-0.47352600	1.81517400	0.85573600
C	0.68116200	-1.66827300	0.59515100
H	0.97955200	-2.71938900	0.54009800
C	-0.24408800	-1.38476300	1.74823900

H	-0.54468000	-2.16693000	2.43837600
C	-0.62495700	-0.10921000	1.86510900
H	-1.27309000	0.26396300	2.65195900
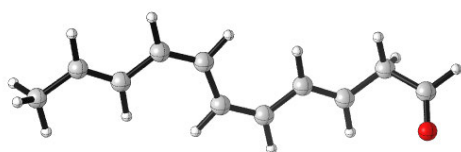
tetraene 14
M06-2X/6-311+G(d,p) smd toluene
Energy (0K, vacuum) = -502.648737
Gibbs free energy (393K) = -502.492141

C	0.59773100	-0.83334900	-0.42156600
H	0.90186600	-1.85632200	-0.63617200
C	-0.71987800	-0.58236100	-0.27353800
H	-1.39800000	-1.42495600	-0.37868700
C	-1.31606700	0.70976500	0.01298600
H	-0.64055400	1.55453500	0.11744800
C	1.68460800	0.12861600	-0.32351300
H	1.43844800	1.16487500	-0.09727900
C	-2.63493100	0.95479500	0.16119300
H	-2.93989200	1.97815200	0.37538100
C	-3.72201400	-0.00715900	0.06711300
H	-3.47955600	-1.04693000	-0.14521500
C	2.96893800	-0.20590300	-0.49777900
H	3.23254500	-1.24099000	-0.70771100
C	-5.00787100	0.33069600	0.23074100
H	-5.24898900	1.37286100	0.44381300
C	-6.15979400	-0.62074900	0.14459800
H	-5.81913300	-1.63666900	-0.07280600
H	-6.86272600	-0.31930100	-0.64054900
H	-6.72460100	-0.64219000	1.08373800
C	4.10725100	0.76083300	-0.41452800
H	3.78896900	1.72976100	-0.00887100
H	4.52008900	0.98139400	-1.41288500
C	5.26986500	0.24928800	0.41021400
H	6.09584700	0.97658500	0.55859500
O	5.34108300	-0.86220500	0.86821000

32
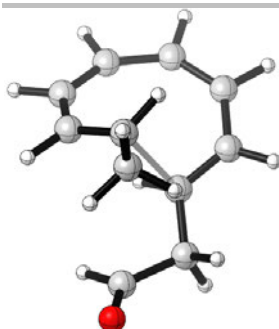
*tetraene **14** 8pi-TS*
M06-2X/6-311+G(d,p) smd toluene
Energy (0K, vacuum) = -502.626711
Gibbs free energy (393K) = -502.461417
imaginary frequency: -348.05

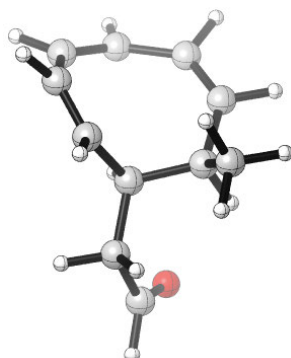|			
C	-3.16987200	0.95789500	-1.56686200
H	-3.43018300	1.20959200	-2.59333800
C	-2.91322400	2.06190500	-0.76199500
H	-3.18169200	2.99624100	-1.25450900
C	-2.43170100	2.30370700	0.55228700
H	-2.64911600	3.32537200	0.86322500
C	-1.72520400	1.60432200	1.52393600
H	-1.65147700	2.12129300	2.47877600
C	-3.16997700	-0.41722400	-1.27493300
H	-3.20195700	-1.10301500	-2.12187000
C	-3.06020100	-0.95077400	-0.00781300
H	-3.30750700	-0.29615600	0.82023600
C	-1.07601200	0.35818600	1.46909900
H	-0.76024600	-0.07979200	2.41655500
C	-0.88356200	-0.37322700	0.31613900
H	-0.91993100	0.16724300	-0.62339300
C	-3.18055500	-2.42523900	0.25204700
H	-2.58410200	-2.73296100	1.11651700
H	-2.86280400	-3.01170300	-0.61567900
H	-4.22258900	-2.68789900	0.47054900
C	-0.08105000	-1.64420000	0.30948700
H	-0.21405900	-2.18209300	1.25937300
H	-0.45126700	-2.32319900	-0.47031800
C	1.39409400	-1.44048500	0.08774800
H	1.99351200	-2.33609800	-0.07312000
C	2.02819300	-0.26784900	0.07680900
H	1.52201300	0.67903900	0.23504800
C	3.49244200	-0.23594500	-0.15060700
O	4.20127400	-1.19760300	-0.33829200
O	3.95842200	1.02622800	-0.12333700
C	5.36224600	1.14675800	-0.33468500
H	5.63689400	0.74344300	-1.31203900
H	5.91234900	0.60246300	0.43634300
H	5.58089800	2.21225500	-0.28326600

cyclooctatriene **15**
M06-2X/6-311+G(d,p) smd toluene
Energy (0K, vacuum) = -502.664644
Gibbs free energy (393K) = -502.495162

C	-0.8102020000	1.7048200000	-0.4296120000
H	-0.7845080000	2.7937720000	-0.4957570000
C	-1.8948000000	1.1384700000	-0.9802260000
H	-2.5797850000	1.8481690000	-1.4455320000
C	-2.3732800000	-0.2430470000	-1.1477430000
H	-2.9346820000	-0.3840910000	-2.0709350000
C	-2.3687730000	-1.2867170000	-0.3005530000
H	-2.9355230000	-2.1674490000	-0.5997660000
C	-1.7208160000	-1.3606050000	1.0078330000
H	-2.2915570000	-1.8317940000	1.8068280000
C	-0.4740470000	-0.9500420000	1.2627690000
H	-0.0894790000	-1.0562080000	2.2778870000
C	0.4760510000	-0.3891580000	0.2404460000
H	0.1733330000	-0.7352910000	-0.7542890000
C	0.4338940000	1.1513060000	0.2106760000
H	1.2689230000	1.4932900000	-0.4178450000
C	1.8901270000	-0.9183570000	0.4985790000
H	1.8656050000	-2.0015620000	0.6892280000
H	2.3405520000	-0.4819100000	1.4014950000
C	2.8484810000	-0.7096710000	-0.6483970000
H	3.8857010000	-1.0629750000	-0.4651060000
O	2.5525000000	-0.2191960000	-1.7097510000
C	0.6107190000	1.7797760000	1.6013060000
H	1.5418980000	1.4574060000	2.0791340000
H	-0.2254240000	1.5101850000	2.2533320000
H	0.6408210000	2.8713780000	1.5288700000

34
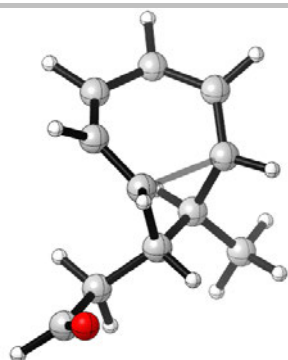
bicyclo[4.2.0]octadiene **15**-*endo*
M06-2X/6-311+G(d,p) smd toluene
Energy (0K, vacuum) = -502.627819
Gibbs free energy (393K) = -502.45891
imaginary frequency: -574.49

|			
C	-1.42753200	0.69328700	0.85223600
H	-1.39313600	1.26718900	1.78069400
C	-2.63010100	0.06652300	0.51708800
H	-3.52448700	0.23933500	1.11313100
C	-2.66807400	-0.91264700	-0.46780200
H	-3.62932000	-1.24597000	-0.85172900
C	-1.56475300	-1.74289600	-0.73465400
H	-1.76646700	-2.61959200	-1.34663300
C	-0.40634000	-1.77735300	0.04409900
H	-0.01962100	-2.78309500	0.22085000
C	0.18052200	-0.74831400	0.80481800
H	0.75146700	-1.11079600	1.66156900
C	0.76738400	0.52600200	0.19513500
H	1.22798900	1.09589700	1.01259900
C	-0.50302400	1.22360200	-0.23734900
H	-0.83658800	0.81140800	-1.19710700
C	1.81671900	0.28524800	-0.88266900
H	2.11996700	1.23038300	-1.35919400
H	1.40199600	-0.34000700	-1.68660500
C	-0.45252400	2.74368000	-0.31978300
H	-1.43245600	3.15642000	-0.57835000
H	0.26436900	3.07425800	-1.07981100
H	-0.14562200	3.17201000	0.64128100
C	3.06629700	-0.38078000	-0.36540000
H	3.83584000	-0.62010600	-1.12964700
O	3.25932900	-0.64818100	0.79557900
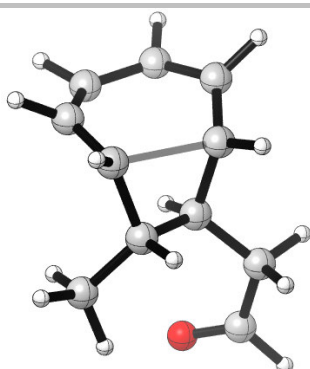
*bicyclo[4.2.0]octadiene **15**-exo*
M06-2X/6-311+G(d,p) smd toluene
Energy (0K, vacuum) = -502.625871
Gibbs free energy (393K) = -502.456922
imaginary frequency: -574.83

| C | -0.73602200 | -0.93321800 | -1.02551200 |
H	-0.54019200	-1.19626100	-2.06747300
C	-1.70409000	-1.66960500	-0.33863500
H	-2.16644000	-2.53878300	-0.80326100
C	-2.21858300	-1.20594800	0.86572400
H	-2.81870300	-1.87107200	1.48197600
C	-2.29890100	0.16599600	1.15923500
H	-2.91290900	0.43537400	2.01572700
C	-2.03320300	1.18145200	0.23892900
H	-2.73008400	2.02005100	0.29300400
C	-1.16295200	1.17465700	-0.86776300
H	-1.48859100	1.84535000	-1.66919500
C	0.35994700	1.06955500	-0.76232100
H	0.75253200	1.11688000	-1.78888600
C	0.47065000	-0.36679800	-0.28940400
H	0.28725200	-0.41159800	0.78913700
C	1.76127200	-1.11374100	-0.60150100
H	2.08981400	-0.93437900	-1.63614400
H	1.60518200	-2.20109000	-0.52945700
C	2.90630600	-0.78066300	0.32342000
H	3.87564800	-1.26045400	0.06951200
O	2.81696300	-0.06707600	1.29162600
C	0.99736800	2.17363400	0.07256700
H	2.08893400	2.11653700	0.04706100
H	0.67772000	2.08556800	1.11542300
H	0.69338400	3.15855800	-0.29887100
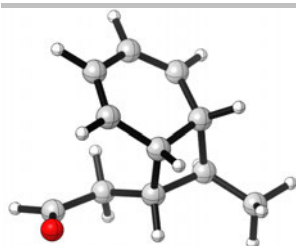
*bicyclo[4.2.0]octadiene **16**-endo*
M06-2X/6-311+G(d,p) smd toluene
Energy (0K, vacuum) = -502.671214
Gibbs free energy (393K) = -502.499491

|			
C	-0.79194300	1.19641500	-1.07019400
H	-1.65209400	1.09971600	-1.72665100
C	-0.64034300	2.27193800	-0.28826500
H	-1.37147000	3.07535600	-0.30726900
C	0.52141500	2.41265200	0.60428500
H	0.54983300	3.26540500	1.27718600
C	1.53546300	1.53939200	0.58323300
H	2.39687600	1.67997300	1.23417500
C	1.56061400	0.35281100	-0.33672300
H	2.42985500	0.42484700	-1.00501000
C	0.19858200	0.07147000	-1.03501600
H	0.34464300	-0.33000400	-2.04193600
C	1.45130800	-1.02378200	0.38062600
H	1.60818400	-0.97601300	1.46639200
C	-0.04349100	-1.10903100	-0.03586900
H	-0.32746200	-2.04757400	-0.52378700
C	2.32377400	-2.10760900	-0.23257800
H	3.38564200	-1.91232300	-0.05072000
H	2.17304300	-2.15547400	-1.31762700
H	2.08064500	-3.09129000	0.18231900
C	-1.01931100	-0.81921600	1.09014400
H	-0.81661600	0.15146800	1.56326500
H	-0.91806900	-1.56798500	1.89052500
C	-2.45743700	-0.82967900	0.63997100
H	-3.20701600	-0.58203900	1.42121100
O	-2.81347300	-1.09577900	-0.48247000

37
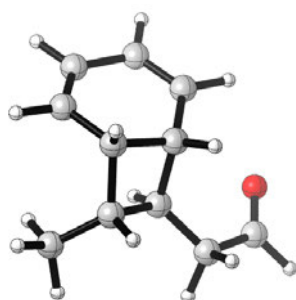
*bicyclo[4.2.0]octadiene **16**-exo*
M06-2X/6-311+G(d,p) smd toluene
Energy (0K, vacuum) = -502.670072
Gibbs free energy (393K) = -502.499858

C	2.37393300	-0.03532000	-0.02076400
H	3.22039500	0.62365400	-0.20601100
C	2.33432700	-1.25206900	-0.57663600
H	3.14399200	-1.57906700	-1.22362200
C	1.24083500	-2.19724400	-0.30726800
H	1.33069700	-3.20817800	-0.69392800
C	0.16601500	-1.83269200	0.39984100
H	-0.64257400	-2.53042000	0.59304900
C	1.30178900	0.46404200	0.90530300
H	1.73755200	0.66332800	1.89266500
C	0.01944200	-0.42115600	0.88262200
H	-0.49699700	-0.38377900	1.84971600
C	0.44790100	1.63732700	0.33813900
H	0.05985900	2.23023500	1.17730700
C	-0.62113500	0.60564000	-0.09357700
H	-0.43974100	0.27739400	-1.12430600
C	1.02756800	2.55500800	-0.72291600
H	1.84476100	3.16593500	-0.32471200
H	0.26002100	3.23488300	-1.10875300
H	1.41915100	1.97204300	-1.56313200
C	-2.07591900	0.98820700	0.08946700
H	-2.26269000	1.33026600	1.11956900
H	-2.35259200	1.83810900	-0.55248600
C	-3.04404200	-0.13414900	-0.18938100
H	-4.11928400	0.12635100	-0.08849900
O	-2.71585400	-1.25329000	-0.49698000
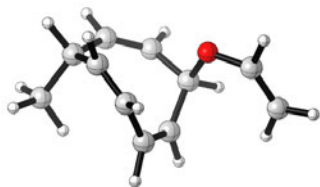
*vinyl ether **17***
M06-2X/6-311+G(d,p) smd toluene
Energy (0K, vacuum) = -502.625837
Gibbs free energy (393K) = -502.453576

C	1.52431300	1.50811600	-0.21502400
H	2.19448300	2.36044900	-0.33299800
C	0.30637100	1.80204300	0.24055200
H	0.09559000	2.85198400	0.43004100
C	-0.86223700	0.87317500	0.49368600
H	-1.61856600	1.44250900	1.05207200
O	-1.43107700	0.55582400	-0.77547300
C	-2.68646700	0.05246600	-0.78346900
H	-3.02220000	-0.06668900	-1.80986400

C	-3.46793300	-0.26414700	0.24848900
H	-4.46504900	-0.63668400	0.05143400
H	-3.15587100	-0.18754900	1.28271100
C	-0.52200800	-0.34665400	1.32463300
H	-0.77893200	-0.27693800	2.38030700
C	0.00771700	-1.47987300	0.85998200
H	0.10828900	-2.32446100	1.54136400
C	0.44696100	-1.67507800	-0.52840400
H	-0.00159700	-2.50514600	-1.07313900
C	1.34303600	-0.90994200	-1.15597900
H	1.54296900	-1.13354400	-2.20209900
C	2.19759400	0.19363100	-0.56172000
H	2.92317700	0.45162500	-1.34280600
C	3.03060500	-0.28812500	0.64415400
H	3.72372400	0.49611700	0.96493300
H	3.61152000	-1.17441600	0.37345300
H	2.38337300	-0.53753300	1.48696700
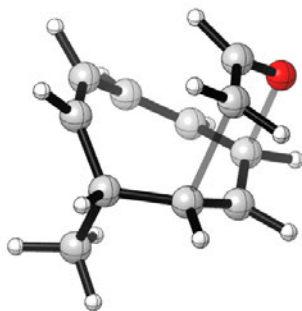
*vinyl ether **17** Claisen rearrangement TS*
M06-2X/6-311+G(d,p) smd toluene
Energy (0K, vacuum) = -502.572019
Gibbs free energy (393K) = -502.400323
imaginary frequency: -537.48

C	0.10432900	-1.40846000	-0.63085500
H	0.06231400	-2.46279900	-0.90431100
C	-0.63239800	-0.59922300	-1.47302600
H	-1.29840800	-1.13100600	-2.14900300
C	-1.03667000	0.73027500	-1.21859200
H	-1.77353900	1.08692100	-1.93273300
O	-2.27906900	0.42445000	0.10486800
C	-1.74831700	-0.24785800	1.06685300
H	-1.33429100	0.31136500	1.91237800
C	-1.48740100	-1.60058600	0.95545900
H	-1.03001700	-2.12911200	1.78879400
H	-2.06316000	-2.19588200	0.25722900
C	-0.20492000	1.86308400	-0.74735000
H	-0.37449500	2.75787700	-1.34380200
C	0.66325300	2.02577100	0.26497300
H	1.05977600	3.03587700	0.36464000
C	1.11075400	1.12598100	1.32927000
H	1.24043200	1.62151400	2.29130200

WILEY-VCH

C	1.39907900	-0.17795400	1.28567300
H	1.68960000	-0.64050000	2.22739700
C	1.41918700	-1.09705900	0.09285600
H	1.76796200	-2.06388100	0.47180300
C	2.44580600	-0.62484700	-0.95504700
H	2.50283000	-1.33605900	-1.78460300
H	3.43716800	-0.53185800	-0.50206200
H	2.15016600	0.34719300	-1.35725100

References

1. F. Del Moro, P. Crotti, V. Di Bussolo, F. Macchia, M. Pineschi, *Org. Lett.* **2003**, *5*, 1971–1974.
2. M. J. Frisch, G. W. Trucks, H. B. Schlegel, G. E. Scuseria, M. A. Robb, J. R. Cheeseman, G. Scalmani, V. Barone, G. A. Petersson, H. Nakatsuji, X. Li, M. Caricato, A. V. Marenich, J. Bloino, B. G. Janesko, R. Gomperts, B. Mennucci, H. P. Hratchian, J. V. Ortiz, A. F. Izmaylov, J. L. Sonnenberg, D. Williams-Young, F. Ding, F. Lipparini, F. Egidi, J. Goings, B. Peng, A. Petrone, T. Henderson, D. Ranasinghe, V. G. Zakrzewski, J. Gao, N. Rega, G. Zheng, W. Liang, M. Hada, M. Ehara, K. Toyota, R. Fukuda, J. Hasegawa, M. Ishida, T. Nakajima, Y. Honda, O. Kitao, H. Nakai, T. Vreven, K. Throssell, J. A. Montgomery, Jr., J. E. Peralta, F. Ogliaro, M. J. Bearpark, J. J. Heyd, E. N. Brothers, K. N. Kudin, V. N. Staroverov, T. A. Keith, R. Kobayashi, J. Normand, K. Raghavachari, A. P. Rendell, J. C. Burant, S. S. Iyengar, J. Tomasi, M. Cossi, J. M. Millam, M. Klene, C. Adamo, R. Cammi, J. W. Ochterski, R. L. Martin, K. Morokuma, O. Farkas, J. B. Foresman, and D. J. Fox, Gaussian, Inc., Wallingford CT, 2016.
3. Y. Zhao, D. Truhlar, Theor. Chem. Acc. 2008, 120, 215.
4. H. P. Hratchian, H. B. Schlegel, J. Chem. Phys. 2004, 120, 9918.
5. A. V. Marenich, C. J. Cramer, D. G. Truhlar, J. Phys. Chem. B 2009, 113, 6378.

Reference

[1]   G. Schröder, J. F. M. Oth, *Angew. Chem, Int. ed.* **1967**, *6*, 414–423.

[2]   S. Ferrer, A. M. Echavarren, *Synth.* **2019**, *51*, 1037–1048.

[3]   A. N. Bismillah, B. M. Chapin, B. A. Hussein, P. R. McGonigal, *Chem. Sci.* **2020**, *11*, 324–332.

[4]   W. von E. Doering, W. R. Roth, *Angew. Chem, Int. ed.* **1963**, *2*, 115–122.

[5]   P. Ahlber, L. D. Harris, S. Winstein, *J. Am. Chem. Soc.* **1970**, *92*, 4454–4456.

[6]   P. Ahlberg, J. B. Grutzner, D. L. Harris, S. Winstein, *J. Am. Chem. Soc.* **1970**, *92*, 3478–3480.

[7]   J. C. Walton, *J. Chem. Soc. Perkin. Trans* **1989**, *2*, 2169–2176.

[8]   L. G. Greifensten, J. B. Lambert, M. J. Broadhurst, L. A. Paquette, *J. Org. Chem.* **1973**, *36*, 1210–1215.

[9]   W. von E. Doering, B. M. Ferrier, E. T. Fossel, J. H. Hartenstein, M. Jones, G. Klumpp, R. M. Rubin, M. Saunders, *Tetrahedron* **1967**, *23*, 3943–3963.

[10]   H. E. Zimmerman, G. L. Grunewald, *J. Am. Chem. Soc.* **1966**, *88*, 183–184.

[11]   G. Schröder, *Chem. Ber.* **1964**, *97*, 3140–3149.

[12]   W. v. E. Doering, W. R. Roth, *Tetrahedron* **1963**, *19*, 715–737.

[13]   G. Schröder, *Angew. Chemie Int. Ed. English* **1963**, *2*, 481–482.

[14]   G. Schröder, *Angew. Chemie* **1963**, *75*, 722–722.

[15]   M. Jones, and L. T. Scott, *J. Am. Chem. Soc.* **1967**, *89*, 150–151.

[16]   K.–H. Pook, W. Kirmse, *Chem. Ber* **1965**, *98*, 4022–4026.

[17]   M. Jones, S. D. Reich, L. T. Scott, *J. Am. Chem. Soc.* **1970**, *92*, 3118–3126.

[18]   S. Masamune, H. Zenda, M. W. N. Nakatsuka, G. Bigam, *J. Am. Chem. Soc* **1968**, *90*, 2727–2728.

[19]   W. von. E. Doering, J. W. Rosenthal, *J. Am. Chem. Soc* **1966**, *88*, 2078–2079.

[20]   J. W. Rosenthal, W. von E. Doering, *Tetrahedron Lett.* **1967**, *4*, 349–350.

[21]   M. Saunders, R. M. Rubin, G. Klumpp, M. Jones, J. H. Harstein, E. T. Fossel, W. von E. Doering, *Tetrahedron* **1967**, *23*, 3943–3963.

[22]   J. Font, F. Lopez, F. Serratosa, *Tetrahedron Lett.* **1972**, *13*, 2589–2590.

[23]   H.–P. Löffler, *Tetrahedron Lett.* **1974**, *15*, 787–788.

[24]   H. P. Löffler, G. Schröder, *Angew. Chemie Int. Ed.* **1968**, *7*, 736–737.

[25]   J. Casas, F. Srratosa, *An. Quim.* **1977**, *73*, 300.

[26]   S. Ferrer, A. M. Echavarren, *Angew. Chemie – Int. Ed.* **2016**, *55*, 11178–11182.

[27] O. Yahiaoui, L. F. Pašteka, B. Judeel, T. Fallon, *Angew. Chemie – Int. Ed.* **2018**, *57*, 2570–2574.

[28] and G.´rard B. Mathieu Achard, Marc Mosrin, Alphonse Tenaglia, *J. Org. Chem.* **2006**, *71*, 2907–2910.

[29] M. Jones, *J. Am. Chem. Soc.* **1967**, *89*, 4236–4238.

[30] M. Jones, S. D. Reich, L. T. Scott, *J. Am. Chem. Soc.* **1970**, *92*, 3118–3126.

[31] J. S. McKechnie, I. C. Paul, *J. Chem. Soc. B Phys. Org.* **1968**, 1445–1452.

[32] A. Allerhand, H. S. Gutowskv, *J. Am. Chem. Soc.* **1965**, *87*, 4092–4096.

[33] M. G. Newton, I. C. Paul, *J. Am. Chem. Soc.* **1966**, *88*, 3161–3162.

[34] R. Aumann, *Angew. Chemie Int. Ed. English* **1970**, *9*, 800–801.

[35] E. Vedjs, *J. Am. Chem. Soc* **1968**, *90*, 4751–4752.

[36] R. Aumann, *Chem. Ber.* **1975**, *108*, 1974–1988.

[37] R. Aumann, *Chem. Ber* **1977**, *110*, 1432–1441.

[38] R. Aumann, *Angew. Chem* **1976**, *88*, 375.

[39] P. Glockner, G. N. Schrauzer, *Angew. Chemie* **1964**, *76*, 498–498.

[40] I. G. K. Reid, I. C. Paul, P. Glockner, G. N. Schrauzer, *J. Am. Chem. Soc.* **1970**, *92*, 4479–4480.

[41] H. P. Löffler, G. Schröder, *Tetrahedron Lett.* **1970**, *24*, 2119–2122.

[42] U. Prange, B. Putze, J. Thio, J. F. M. Oth, G. Schröder, *Chem. Ber.* **1971**, *104*, 3406–3417.

[43] G. Mehta, R. Vidya, P. K. Sharma, E. D. Jemmis, *Tetrahedron Lett.* **2000**, *41*, 2999–3002.

[44] G. Mehta, V. Gagliardini, C. Schaefer, R. Gleiter, *org.* **2004**, *6*, 1617–1620.

[45] G. Mehta, R. Vidya, K. Venkatesan, *Tetrahedron Lett.* **1999**, *40*, 2417–2420.

[46] G. Mehta, R. Vldya, *Tetrahedron Lett.* **1997**, *38*, 4173–4176.

[47] S. Liang, C. H. Lee, S. I. Kozhushkov, D. S. Yufit, J. A. K. Howard, K. Meindl, S. Rühl, C. Yamamoto, Y. Okamoto, P. R. Schreiner, et al., *Chem. – A Eur. J.* **2005**, *11*, 2012–2018.

[48] M. J. Goldstein, S. Tomoda, G. Whittaker, *J. Am. Chem. Soc* **1974**, *96*, 3676–3678.

[49] M. J. Goldstein, T. T. Wenzel, G. Whittaker, S. F. Yates, *J. Am. Chem. Soc* **1982**, *104*, 2669–2671.

[50] S. Kirschner, J. R. Malpass, and L. A. Paquette, *J. Am. Chem. Soc* **1969**, *91*, 3970–3973.

[51] I. Erden, *Tetrahedron Lett.* **1985**, *26*, 5635–5638.

[52] I. Erden, C. J. Gleason, *Tetrahedron Lett.* **2018**, *59*, 284–286.

[53]   G. Schröder, *Chem. Ber.* **1964**, *97*, 3131–3139.

[54]   A. G. Invernizzi, R. Gandolfi, M. Strigazzi, *Tetrahedron* **1974**, *30*, 3717–3722.

[55]   H.–P. Löffler, T. Martini, H. Musso, G. Schröder, *Chem. Ber.* **1970**, *103*, 2109–2113.

[56]   R. Jösel, G. Schröder, *Liebigs Ann. chem.* **1980**, *264*, 1428–1437.

[57]   T. Asaki, K. Kanematsu, N. Okamura, *J. Org. Chem.* **1975**, *40*, 3322–3325.

[58]   O. Schallner, C. Weitmeyer, A. de Meijere, *Chem. Ber.* **1977**, *110*, 1504–1522.

[59]   G. Schröder, R. Merényi, J. F. M. Oth, *Tetrahedron Lett.* **1964**, *5*, 773–777.

[60]   J. M. Oth, R. Merenyi, J. Nielsen, G. Schröder, *Chem. Ber* **1965**, *98*, 3385–3400.

[61]   H.–P. Löffler, G. Schröder, *Chem. Ber.* **1970**, *103*, 2105–2108.

[62]   J. F. M. Oth, E. Machens, H. Röttele, G. Schröder, *Liebigs Ann. chem.* **1971**, *745*, 112–123.

[63]   R. Zeiger, K. Sarma, G. Schröder, *Chem. Ber.* **1986**, *119*, 2889–2894.

[64]   L. A. Paquette, G. H. Birnberg, *J. Org. Chem.* **1975**, *40*, 1709–1713.

[65]   J. F. M. Oth, R. Merenyi, H. Röttele, and G. Schröder, *Tetrahedron Lett.* **1968**, *36*, 3941–3946.

[66]   K. Rebsamen, H. Röttele, G. Schröder, *Chem. Ber.* **1993**, *126*, 1429–1433.

[67]   K. Sarma, W. Witt, G. Schröder, *Chem. Ber.* **1986**, *119*, 2339–2349.

[68]   W. Witt, G. Schröder, *Angew. Chem.* **1979**, *91*, 331–332.

[69]   K. Sarma, G. Schröder, *Chem. Ber* **1984**, *117*, 633–641.

[70]   G. Schröder, W. Witt, *Angew. Chemie Int. Ed. English* **1979**, *18*, 311–312.

[71]   K. Sarma, W. Witt, G. Schröder, *Chem. Ber.* **1983**, *116*, 3800–3812.

[72]   K. Rebsamen, G. Schröder, *Chem. Ber.* **1993**, *126*, 1425–1427.

[73]   K. Rebsamen, G. Schröder, *Chem. Ber* **1993**, *126*, 1419–1423.

[74]   K. Rebsamen, H. Röttele, G. Schröder, *Chem. Ber.* **1993**, *126*, 1429–1433.

[75]   G. Schröder, *Angew. Chemie Int. Ed. English* **1965**, *4*, 695–696.

[76]   W. Grimme, W. Meckel, H. J. Riebel, E. Vogel, *Angew. Chemie – Int. Ed.* **1966**, *5*, 590.

[77]   T. Martini, G. Schröder, *Angew. Chem* **1967**, *79*, 820–821.

[78]   H. Röttele, P. Nikloff, J. F. M. Oth, und G. Schröder, *Chem. Ber.* **1969**, *102*, 3367–3377.

[79]   U. Krüerke, *Angew. Chem. Int. Ed. Engl.* **1967**, *6*, 79.

[80]   R. E. Davis, T. A. Dodds, T. H. Hseu, J. C. Wagnon, T. Devon, J. Tancrede, J. S. McKennis, R. Pettit, *J. Am. Chem. Soc.* **1974**, *96*, 7562–7564.

[81]   A. R. Lippert, J. Kaeobamrung, J. W. Bode, *J. Am. Chem. Soc.* **2006**, *128*, 14738–14739.

[82]   K. K. Larson, M. He, J. F. Teichert, A. Naganawa, J. W. Bode, *Chem. Sci.* **2012**, *3*, 1825.

[83] A. R. Lippert, V. L. Keleshian, J. W. Bode, *Org. Biomol. Chem.* **2009**, *7*, 1529–1532.

[84] O. Yahiaoui, L. F. Pašteka, C. J. Blake, C. G. Newton, T. Fallon, *Org. Lett.* **2019**, *21*, 9574–9578.

[85] H. D. Patel, T.–H. Tran, C. J. Sumby, L. F. Pašteka, T. Fallon, *J. Am. Chem. Soc* **2020**, *142*, 3680–3685.

[86] J. D. Williams, M. Nakano, R. Gérardy, J. A. Rincón, Ó. De Frutos, C. Mateos, J. C. M. Monbaliu, C. O. Kappe, *Org. Process Res. Dev.* **2019**, DOI 10.1021/acs.oprd.8b00375.

[87] L. A. Paquette, T. J. Barton, *J. Am. Chem. Soc* **1967**, *89*, 5480–5481.

[88] J. R. Malpass, G. R. Krow, T. J. Barton, and L. A. Paquette, *J. Am. Chem. Soc* **1969**, *91*, 5296–5306.

[89] J. R. Malpass, L. A. Paquette, *J. Am. Chem. Soc* **1968**, *90*, 7151–7153.

[90] G. R. Krow, L. A. Paquette, *J. Am. Chem. Soc* **1968**, *90*, 7149–7151.

[91] A. R. Lippert, A. Naganawa, V. L. Keleshian, J. W. Bode, *J. Am. Chem. Soc.* **2010**, *132*, 15790–15799.

[92] M. He, J. W. Bode, *Proc. Natl. Acad. Sci. U. S. A.* **2011**, *108*, 14752–14756.

[93] J. F. Teichert, D. Mazunin, J. W. Bode, *J. Am. Chem. Soc.* **2013**, *135*, 11314–11321.

[94] F. M. Oth, R. Merenyi, H. Röttele, and G. Schröder, *Chem. Ber* **1967**, *100*, 3527–3537.

[95] J. Gasteiger, G. E. Gream, R. Huisgen, W. E. Konz, U. Schnegg, *Chem. Ber.* **1971**, *104*, 2412–2419.

[96] O. Yahiaoui, L. F. Pašteka, B. Judeel, T. Fallon, *Angew. Chem, Int. ed.* **2018**, *57*, 2570–2574.

[97] W. Hess, J. Treutwein, G. Hilt, *Synthesis (Stuttg).* **2008**, *22*, 3537–3562.

[98] M. A. Drew, S. Arndt, C. Richardson, M. Rudolph, A. S. K. Hashmi, C. J. T. Hyland, *Chem. Commun.* **2019**, *55*, 13971–13974.

[99] R. S. Cahn, C. Ingold, V. Prelog, *Angew. Chem, Int. ed.* **1966**, *5*, 385–415.

[100] G. Bringmann, A. J. P. Mortimer, P. A. Keller, M. J. Gresser, J. Garner, M. Breuning, *Angew. Chemie – Int. Ed.* **2005**, *44*, 5384–5427.

[101] S. T. Toenjes, J. L. Gustafson, *Future Med. Chem.* **2018**, *10*, 409–422.

[102] Z. Zhang, Y. Wang, T. Nakano, *Molecules* **2016**, *21*, 1–10.

[103] S. Yuki, S. Yoshiaki, H. Daisuke, N. Yuuya, F. Takanori, *Chem. Commun.* **2018**, *54*, 12314–12317.

[104] D. Virieux, N. Sevrain, T. Ayad, J. Pirat, *Helical Phosphorus Derivatives : Synthesis and Applications*, Elsevier Ltd, **2015**.

[105] M. W. Gillick–Healy, E. V. Jennings, H. Müller–Bunz, Y. Ortin, K. Nikitin, D. G.

Gilheany, *Chem. Eur* **2017**, *10*, 2332–2339.

[106] M. He, J. W. Bode, *PNAS* **2011**, *108*, 14752–14756.

[107] M. He, J. W. Bode, *Org. Biomol. Chem.* **2013**, *11*, 1306–1317.

[108] M. He, J. W. Bode, *Org. Biomol. Chem* **2013**, *11*, DOI 10.1039/c2ob26954f.

[109] H. Wu, B. Yang, L. Zhu, R. Lu, G. Li, H. Lu, *Org. Lett.* **2016**, *18*, 5804–5807.

[110] R. Huisgen, A. Dahmen, H. Huber, *J. Am. Chem. Soc.* **1967**, *89*, 7130–7131.

[111] K. C. Nicolaou, N. A. Petasis, R. E. Zipkin, J. Uenishi, *J. Am. Chem. Soc.* **1982**, *104*, 5555–5557.

[112] W. M. Bandaranayake, J. E. Banfield, D. S. C. Black, G. D. Fallon, B. M. Gatehouse, *J.C.S. Chem. Comm.* **1980**, *4*, 162–163.

[113] W. M. Bandaranayake, J. E. Banfield, D. S. C. Black, G. D. Fallon, B. M. Gatehouse, *Aust. J. Chem.* **1981**, *34*, 1655–1667.

[114] J. E. Banfield, D. S. C. Black, S. R. Johns, R. I. Willing, *Aust. J. Chem.* **1982**, *35*, 2247–2256.

[115] W. M. Bandaranayake, J. E. Banfield, D. C. Black, *Aust. J. Chem.* **1982**, *35*, 557–565.

[116] J. E. Banfield, D. S. C. St. Black, S. R. Johns, R. J. Willing, *Aust. J. Chem.* **1982**, *35*, 2247–2256.

[117] J. E. Banfield, D. S. Black, D. J. Collins, B. P. M. Hyland, J. J. Lee, S. R. Pranowo, *Aust. J. Chem.* **1994**, *47*, 587–607.

[118] P.–S. Yang, M.–J. Cheng, C.–F. Peng, J.–J. Chen, I.–S. Chen, *J. Nat. Prod.* **2009**, *72*, 53–58.

[119] M. N. Azmi, C. Gény, A. Leverrier, M. Litaudon, V. Dumontet, N. Birlirakis, F. Guéritte, K. H. Leong, S. N. A. Halim, K. Mohamad, et al., *Molecules* **2014**, *19*, 1732–1747.

[120] A. Leverrier, M. E. T. H. Dau, P. Retailleau, K. Awang, F. Guéritte, M. Litaudon, *Org. Lett.* **2010**, *12*, 3638–3641.

[121] A. Leverrier, K. Awang, F. Guéritte, M. Litaudon, *Phytochemistry* **2011**, *72*, 1443–1452.

[122] K. Kurosawa, K. Takahashi, E. Tsuda, *J. Antibiot. (Tokyo).* **2001**, *54*, 541–547.

[123] K. Takahashi, E. Tsuda, K. Kurosawa, *J. Antibiot. (Tokyo).* **2001**, *54*, 548–553.

[124] M. Cueto, L. D'Croz, J. L. Maté, A. San–Martín, J. Darias, *Org. Lett.* **2005**, *7*, 415–418.

[125] E. Manzo, M. L. Ciavatta, M. Gavagnin, E. Mollo, S. Wahidulla, G. Cimino, *Tetrahedron Lett.* **2005**, *46*, 465–468.

[126] K. C. Nicolaou, N. A. Petasis, J. Uenishi, R. E. Zipkin, *J. Am. Chem. Soc.* **1982**, *104*, 5557–5558.

[127] R. E. Zipkin, J. Uenishi, N. A. Petassi, N. C. Nicolaou, *J. Am. Chem. Soc.* **1982**, *194*, 5557–5558.

[128] K. C. Nicolaou, N. . . Petasis, R. E. Zipkin, *J. Am. Chem. Soc.* **1982**, *104*, 5560–5562.

[129] K. C. Nicolaou, R. E. Zipkin, N. A. Petasis, *J. Am. Chem. Soc.* **1982**, *104*, 5558–5560.

[130] S. L. Drew, A. L. Lawrence, M. S. Sherburn, *Chem. Sci.* **2015**, *6*, 3886–3890.

[131] E. B. Go, S. P. Wetzler, L. J. Kim, A. Y. Chang, D. A. Vosburg, *Tetrahedron* **2016**, *72*, 3790–3794.

[132] O. Robles, F. E. McDonald, *Org. Lett.* **2009**, *11*, 5498–5501.

[133] S. L. Drew, A. L. Lawrence, M. S. Sherburn, *Chem. Sci.* **2015**, *6*, 3886–3890.

[134] S. L. Drew, A. L. Lawrence, M. S. Sherburn, *Angew. Chem, Int. ed.* **2013**, *52*, 4221–4224.

[135] W. A. Chalifoux, R. R. Tykwinski, *C. R. Chim.* **2009**, *12*, 341–358.

[136] W. A. Chalifoux, R. R. Tykwinski, *Nat. Chem.* **2010**, *2*, 967–971.

[137] W. N. Chou, D. L. Clark, J. B. White, *Tetrahedron Lett.* **1991**, *32*, 299–302.

[138] R. Huisgen, A. Dahmen, H. Huber, *J. Am. Chem. Soc.* **1967**, *89*, 7130–7131.

[139] A. Bell, A. Ledwith, D. Laboratories, *J. Chem. Soc.* **1969**, 2719–2720.

[140] D. J. Bellville, D. D. Wirth, N. L. Bauld, *J. Am. Chem. Soc* **1981**, *103*, 718–720.

[141] P. Sharma, D. J. Ritson, J. Burnley, J. E. Moses, *Chem. Commun.* **2011**, *47*, 10605–10607.

[142] J. C. Moore, E. S. Davies, D. A. Walsh, P. Sharma, J. E. Moses, *Chem. Commun* **2014**, *50*, 12523–12525.

[143] S. E. Nigenda, D. M. Schleich, T. Keumi, S. C. Narang, *J. Electrochem. Soc.* **1987**, *134*, 2465–2470.

[144] K. A. Parker, Y.–H. Lim, *J. Am. Chem. Soc.* **2004**, *126*, 15968–15969.

[145] C. M. Beaudry, D. Trauner, *Org. Lett.* **2005**, *7*, 4475–4477.

[146] M. F. Jacobsen, J. E. Moses, R. M. Adlington, J. E. Baldwin, *Org. Lett.* **2005**, *7*, 2473–2476.

[147] J. E. Barbarow, A. K. Miller, D. Trauner, *Org. Lett.* **2005**, *7*, 2901–2903.

[148] M. Suzuki, H. Ohtake, Y. Kameya, N. Hamanaka, R. Noyori, *J. Org. Chem.* **1989**, *54*, 5292–5302.

[149] A. K. Miller, D. Trauner, *Angew. Chem, Int. ed.* **2005**, *13*, 4602–4606.

[150] G. Liang, A. K. Miller, D. Trauner, *Org. Lett.* **2005**, *7*, 819–821.

[151] R. Rodriguez, R. M. Adlington, S. J. Eade, M. W. Walter, J. E. Baldwin, J. E. Moses, *Tetrahedron* **2007**, *63*, 4500–4509.

[152] V. Sofiyev, G. Navarro, D. Trauner, *Org. Lett.* **2008**, *10*, 149–152.

[153] R. L. Grange, M. J. Gallen, H. Schill, J. P. Johns, L. Dong, P. G. Parsons, P. W. Reddell, V. A. Gordon, P. V. Bernhardt, C. M. Williams, *chem. Eur. J.* **2010**, *16*, 8894–8903.

[154] P. S. Engel, *Chem. Rev.* **1980**, *80*, 99–150.

[155] K. C. Nicolaou, N. A. Petasis, in *Strateg. Tactics Org. Synth.* (Ed.: T. Lindberg), Academic Press, **1984**, pp. 155–173.

[156] A. C. Cope, M. Burg, *J. Am. Chem. Soc* **1952**, *74*, 168–172.

[157] W. Reppe, O. Schlichting, K. Klager, T. Toepel, *Justus Liebigs Ann. Chem.* **1948**, *560*, 1–92.

[158] D. A. Bak, K. Conrow, *J. Org. Chem.* **1966**, *31*, 3958–3965.

[159] T. S. Cantrell, *J. Am. Chem. Soc* **1970**, *92*, 5480–5483.

[160] W. Hartmann, H. G. Heine, L. Schrader, *Tetrahedron Lett.* **1974**, *11*, 883–886.

[161] E. Grovenstein, D. V. Rao, J. W. Taylor, *J. Am. Chem. Soc* **1961**, *83*, 1705–1711.

[162] D. Bryce–Smith, J. E. Lodge, *J. Chem. Soc.* **1962**, 2675.

[163] B. E. Job, J. D. Littlehailes, *J. Chem. Soc.* **1968**, 886–889.

[164] M. Ohashi, Y. Tanaka, S. Yamada, *J.C.S. Chem. Comm.* **1976**, *19*, 800.

[165] R. Guo, B. P. Witherspoon, M. K. Brown, *J. Am. Chem. Soc* **2020**, *142*, 5002–5006.

[166] N. J. Line, B. P. Witherspoon, E. N. Hancock, M. K. Brown, *J. Am. Chem. Soc.* **2017**, *139*, 14392–14395.

[167] D. L. Comins, G. M. Green, *Tetrahedron Lett.* **1999**, *40*, 217–218.

[168] D. C. Sanders, A. Marczak, J. L. Melendez, H. Shechter, *J. Org. Chem.* **1987**, *52*, 5622–5624.

[169] L. Echegoyen, J. Nieves, R. Maldonado, A. Alegria, *J. Am. Chem. Soc.* **1984**, *106*, 7692–7695.